Reactivation history of the Carajas and Cinzento strike-slip systems, Amazon, Brazil.

Roberto Vizeu Lima Pinheiro

REACTIVATION HISTORY OF THE CARAJÁS AND CINZENTO STRIKE-SLIP SYSTEMS, AMAZON, BRAZIL.

by

ROBERTO VIZEU LIMA PINHEIRO

A thesis submitted in partial fulfilment of the degree of Doctor of Philosophy at the Department of Geological Sciences, University of Durham.

March 1997

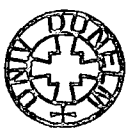

Dedicated to my parents

Cezídio & Maria de Belém Pinheiro

The Itacaiúnas River, the forest and the *Carajás hills*...

Declaration

No part of this thesis has been previously submitted for a degree at this university or any other university. The work described in this thesis is entirely that of the author, except where reference is made to pervious published or unpublished work.

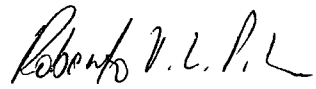

R.V.L.Pinheiro
University of Durham
Department of Geological Sciences
March, 1997

ABSTRACT

The Carajás-Cinzento fault system is centred within the Itacaiúnas Shear Zone, the northern tectonic margin of the Archaean Sul do Pará Granite-Greenstone Terrain of the Amazonian Craton, Brazil. The regional tectonostratigraphy can be subdivided based on the geological relationship of units to the main phase of ductile movements along the Itacaiúnas Shear Zone. A *Basement Assemblage* includes an older group of orthogneisses, migmatites, and granitic to dioritic plutons (Xingu Complex) and a later volcano-sedimentary sequence of ironstones, quartzites, amphibolites and schists (Igarapé Salobo Group). Intense ductile shearing and high grade metamorphism along the Itacaiúnas Shear Zone has led to widespread tectonic interleaving of the gneisses and volcano-sedimentary rocks and has obliterated all traces of the original unconformity between these units. A *Cover Assemblage* is represented by very low-grade volcanic and sedimentary rocks that are inferred to rest unconformably on the Basement Assemblage rocks deformed within the Itacaiúnas Shear Zone. Older clastic, volcanic and ironstone sequences (Igarapé Pojuca & Grão Pará Groups; ca.2.7 Ga) are overlain by a sequence of shallow-water marine to fluvial clastic deposits (Águas Claras Formation). Both Cover and Basement assemblages are intruded by ca.1.8 Ga A-type granitic plutons and basic dykes. All units are unconformably overlain by a thin, localised sequence of polymictic conglomerates (? Gorotire Formation).

During the formation of the upper amphibolite facies within the Itacaiúnas Shear Zone, sub-vertical mylonitic fabrics, generally E-W-trending, were variably developed in the Basement Assemblage rocks. They preserve widespread sinistrally transpressional kinematic indicators. Radiometric dating suggests that the metamorphism and deformation in the shear zones occurred toward the end of the Archaean (ca.2.8 Ga). At least three cycles of brittle-ductile strike-slip reactivation at low metamorphic grades appear to post-date the development of the Itacaiúnas Shear Zone, leading to the formation of the Carajás and Cinzento faults. There is no stratigraphic, structural or sedimentological evidence to suggest that these faults were active during the deposition of the Cover Assemblage sequences. However, as most outcrops of Cover Assemblage rocks are presently localised within bends, branches and offsets of these fault systems it appears that, following their deposition, they were faulted down into dilational jogs formed during an initial phase of brittle dextral movements. The effects of a later episode of brittle-ductile sinistral transpression are widely preserved in both Basement and Cover assemblages, with intense deformation localised in the region of the major fault strands. The 1.8 Ga granites and dykes appear to relate to a regional extensional or dextral transtensional episode recognised in the Middle Proterozoic throughout the Amazon region. There is some circumstantial evidence for further minor fault reactivation during the Phanerozoic, and the region appears to be tectonically active in the present day, as illustrated by the occurrence of recent small-scale earthquakes and hot springs centred along the major fault traces. The influence of the basement architecture and the intensity of later reactivations appears to wane after a time of ca.1.0 Ga following the existence of a weakening effect on a lithospheric-scale with a finite life span, possibly originating in the underlying lower crust and mantle.

There is widespread evidence that the mylonitic fabrics of the Itacaiúnas Shear Zone have controlled the orientation of later structures, including the Carajás and Cinzento fault systems. Long-term fault zone weakening mechanisms are recognised in the region. Brittle fracturing processes have caused increases in fault zone permeabilties allowing extensive ingress of fluids, some of which have caused e.g. gold and copper mineralisation.

ACKNOWLEDGEMENTS

Daring to come abroad to live in England, represents by far the biggest challenge I have had in my life. So the words written in this single volume can never represent all the changes acquired in these four years.

So many people took part in this "fast" period, not only with regards to the subject of this thesis but also about all things that came along during this time. If I could name all, It would probably be a list as long as this volume.

First of all I wish to thank three major organisations that gave the financial support: CAPES (Federal Agency for Post-Graduate Education, Brazil), UFPa (Universidade Federal do Pará) and CVRD (Companhia Vale do Rio Doce) / DOCEGEO (Rio Doce Mineração). They had an almost equal contribution to this research, but CAPES should be mentioned particularly for providing grants to cover University fees and subsistence during the time spent in Durham. I must thank the UFPa, especially the Departamento de Geologia (CG) and FADESP (Fundação de Amparo de Ddesenvolvimento a Pesquisa), for granting me the job license that permitted me to be a PhD candidate in Durham, and for providing essential assistance during the field trips. I am obliged to CVRD-DOCEGEO for their generous financial support of this research during 1993 and 1994, and for the helpful assistance provided by their staff in Carajás and Belém, during and after field trips.

The original idea of this project stems from Dr. João Batista Sena Costa who first aroused my interest in the structural geology of the Carajás region. I want to express here my personal gratitude to him.

I owe a great deal to my helpful companions on field trips, particularly *Werner Truckenbrodt, Afonso Nogueira, Cadú Barros (Conexão Tigre)*, Joel Macambira, Clóvis Maurity, Ronaldo Nascimento, Lúcia Travassos, Cintia and William Neves, from whom I have learned and enjoyed so much. Thanks to Timothy for the English lessons in Brazil, Mônica Marçal for sharing with me her thin sections of the N-4 Mine; José Wilson Ribeiro for helping me with the data from the Cutia Mine, and Juscelino Nézio and Dr. J.B. Siqueira for essential support in the N-4 and Salobo mines respectively. Thanks to Cadú (again); Ana Goes, Anaisse, Odete Silveira, Silvia Souza, Barradas & Yukari, Paulo Alves, for keeping my daily enthusiasm, assurance and jocularity aroused and helping me photos, bibliography, contacts, solving problems at university in Brazil, etc., etc.... I want to thank particularly Ruthléa Bemerguy for her hard work managing my "bureaucratic" and "departmental life" at University in Brazil.

The Graduate Society has to be remembered for all the assistance and support they provided me with.

The list of people from the department in Durham, to whom I want to say "Thanks!" is quite long. It starts with the staff: Prof.Tucker, Dr. Hutton, Dr. Henderson, Prof. Thompson, Dr. Sally Gibson, D. Schofield, D. Stevenson, D. Asbery, Carol, Claire, Jerry, Julie, Karen, Alan and Ron. Dr. G. Larwood is mentioned here in particular for his hard work in reviewing the last drafts of this thesis. To Wayne Bailey, Alun Price, Simon Molyneux, Johnny Imber and Adam Styles I have to thank for almost everything you can imagine concerning my time in the department from "real-life" to the bizarre. They are also responsible for the "improvement" of my spoken English (...no offence!). I have to remember also, Michele, Chris, Ziad, Jo, Toby, Ercan, Simon Russel, A. Ross, J. Jacques, Javier...for the companionship.

I certainly could not have survived without speaking Portuguese...even if it was with that strange accent from Portugal. The friends Luis, João, Rui, Conceição and João Fonseca... gave me an idea that in Portugal everybody is a physicist, pá!.....but some are geophysicists...(My *Cod* !). Brazilians are everywhere in this world, and even in Durham I could not complain about it. I received important support from Affonso and Teresa Brod (especially gastronomic... but also "some" geological advice and road-map orienteering instructions); Mr and Mrs. Marcos & Pascal Sampaio, Fernando, Zé Luis & Márcia, Zé Roberto, Nilson, Ricardo (who reviewed the first drafts of this thesis) Manuel (not from Barcelona..., but from Madrid), Albert and Dimitrius, for the support and company in the lazy hours.

A special thanks to Dr. Richardson (Mike) and Ana Maria for so many conversations, dinners, trips, etc.... Mike was responsible for my "acclimatisation" lasting from the first fifteen minutes after my arrival in Durham, till the last revisions of this thesis....and also some "few" miles running along the trails around Durham in between.

Bob Holdsworth is intentionally the last name on this list...it is impossible to mention everything he became responsible for during my stay in Durham and in my professional life. I have to thank him for all the attention, time spent in the field and during this research as a whole, providing me feedback and confidence in the face of all sorts of questions. Particularly for his friendship and odd sense of humour in so many moments of this project and in my daily life in Durham. It is still difficult to find the words in English to say thank you to him appropriately.

CONTENTS

CHAPTER 1
INTRODUCTION

1.1- THE CARAJÁS REGION

The Carajás region comprises an exceptional set of hills and plateaux over 500m high and surrounded by an extensive lowland area. It is one the most important South American mineral provinces located within the Amazon region in the north of Brazil (Fig.1.1).

A large part of this area (>80%) is covered by the typical dense and humid Amazon rain forest. The remaining territory has been gradually occupied by cattle farms, agricultural fields, mines and timber industries. It is a relatively unexplored area in terms of human settlement and geological knowledge.

The importance of studying the geology of such a remote area is not only the presence of large volumes of ore concentrated in its rocks but embodies a challenge to elucidate the Precambrian history of such a vast unknown territory. This challenge is enhanced by the remarkable geometry of lineaments revealed by remote-sensing in this region (Photo 1.1), and also since the late 1980's by extensive debate on their interpretation and origin.

1.2- BRIEF OBSERVATIONS ABOUT THE GEOGRAPHY OF THE AREA.

The so-called Serra dos Carajás region forms a set of E-W orientated hills and plateaux about 200-600m high. It is surrounded by relatively low land, covering an area of about $25x10^3$ Km^2 in the southeastern Amazon region (Photo 1.1).

The Serra dos Carajás lies in the Equatorial Zone with a climate characterised by high humidity (>80%) and high rainfall (ca. 2000 mm/year), with a dry season lasting from June to October when only ca. 200 mm of rain falls. The temperature varies between 18°C and 35°C almost all year round (Nimer, 1991).

The major rivers in the region are the Itacaiúnas and Parauapebas rivers, both of which are tributaries of the Tocantins river, one the major drainages of the Amazon system (Fig.1.1). These rivers cross the Carajás region from south to north and have been referred to as epigenetic rivers

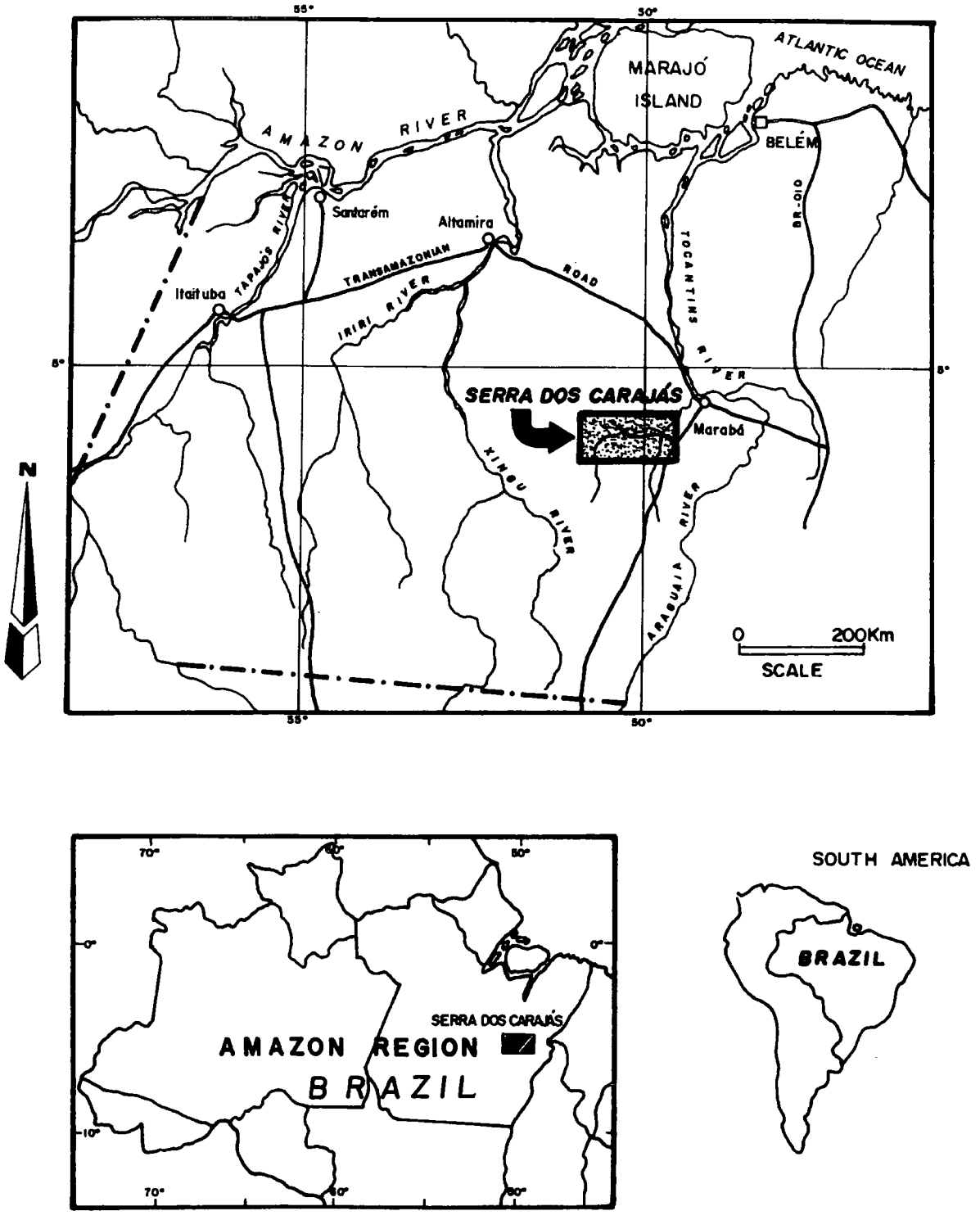

Fig.1.1- Location of the Carajás region in the Amazon region.

Photo 1.1- The studied area in the Carajás region, from LANDSAT image.

(Liandrat, 1972) since they do not seem to be significantly controlled by the strong E-W trend of the relief. They form, as a whole, a relatively dense hydrographic system, composed of numerous 2nd and 3rd order rivers that are responsible mainly for the present relief of the region.

Three major geomorphological units were recognised by Araújo and Maia (1991): (1) the Domain of Sierras and Plateaux, comprising regions elevated between 400m and 700m high corresponding to areas underlain by Archaean volcanic and sedimentary rock sequences. They are also related to major faults and shear zone systems, here named Carajás and Cinzento strike-slip systems. This may explain why these fault systems are displayed so clearly on satellite and radar images (Photo 1.1). (2) the Domain of Hills, corresponding to the sets of isolated hills with an altitude between 300-400m, with areas underlain by older Archaean basement rocks; and (3) the Domain of Mounds representing the remaining areas of lower elevations which are also underlain by basement rocks.

According to Boaventura (1974, in Silva *et al.*,1974) the plateaux represent the remains of a Pliocene exhumation surface named "Planalto Dissecado do Sul do Pará", while the lower hills are equivalent to the so-called "Depressão Periférica do Sul do Pará", a Post-Pliocene peneplain surface. Ab'Sáber (1986) and Gatto (1991) suggested that the entire region has a relatively long history of uplift which probably started at the late Mesozoic - early Tertiary.

During the last two decades, the natural environment in the Carajás region has been considerably disturbed. This has been mainly due to the rapid and disordered colonisation that has continued unabated due to a lack of land occupation laws. The settlement of farms, mining activities and timber industries have also contributed. Most of the local cities are newly established. Their history is closely related to a gold rush which started around 1976 when several gold deposits were discovered in the Serra das Andorinhas, Gradaús and Rio Maria (i.e. the southern region of Carajás), and later in Serra Pelada and its environs.

An area of about 400 thousand hectares, located in the SW of the region, corresponds to the Gorotire-Cateté Indian Reserve where about 270 Xikrin indians live (Vidal, 1986).

Official action to develop the region is evident by the establishment of several agricultural colonies such as the CEDERE's ("Centro de Desenvolvimento Regional"; I, II and III) and from the setting-up of the "Grande

Carajás Project", directed by the CVRD (Companhia Vale do Rio Doce). It is responsible for the management of the mineral resources in the region.

The Carajás mineral resources include voluminous deposits of Fe, Mn, Cu, Au, Ni, Cr, Ag, Mo, Zn, Al, W, Sn and Pd (Fig.1.2). The iron, manganese, copper and gold ores are the most extensively mined deposits. Over 90% of these products are exported to Japan, Germany, USA, South Korea, Italy, France, England, Spain, Austria, China, Turkey and Argentina. The remaining 10% is used in the internal market.

The area studied covers about $18x10^3$ Km^2, delimited by the geographic coordinates 51°10' W - 49°20'W and 5°35'S - 6°35'S. The main geographical features inside this area are the Itacaiúnas and the Parauapebas rivers, and the Northern and Southern Hills. The main settlements are Carajás Village, Parauapebas, and Curionópolis. Several other villages are spread about the region particularly towards the east. The zone between the Itacaiúnas and the Parauapebas river, covering about 75% of the study area, is virtually uninhabited, with very restricted access limited to a few roads connecting mines.

1.3- OBJECTIVES OF RESEARCH AND OUTLINE OF THESIS STRUCTURE.

The main objective of this research is to elucidate the nature and evolution of the regional tectonostratigraphy and structures of the Carajás region.

Chapter 2 introduces a short bibliographical review of the main structures examined in this thesis and defines terms used throughout this work.

Chapter 3 presents a summary review of the geology of Brazil and the regional context of the Carajás region.

Two major structural domains are recognised in the Carajás region: (1) the Carajás Strike-Slip System and; (2) the Cinzento Strike-Slip System. These represent distinct E-W orientated strike-slip fault zones, that also delimit the outcrop of volcanic and sedimentary rocks, separated by zones of the basement rocks, forming the Itacaiúnas Belt (Araújo *et al.*, 1988).

Chapter 4 concentrates on the Carajás Strike-Slip System, emphasising particularly structural data. Six main sections describe the geology of different places studied along this fault system.

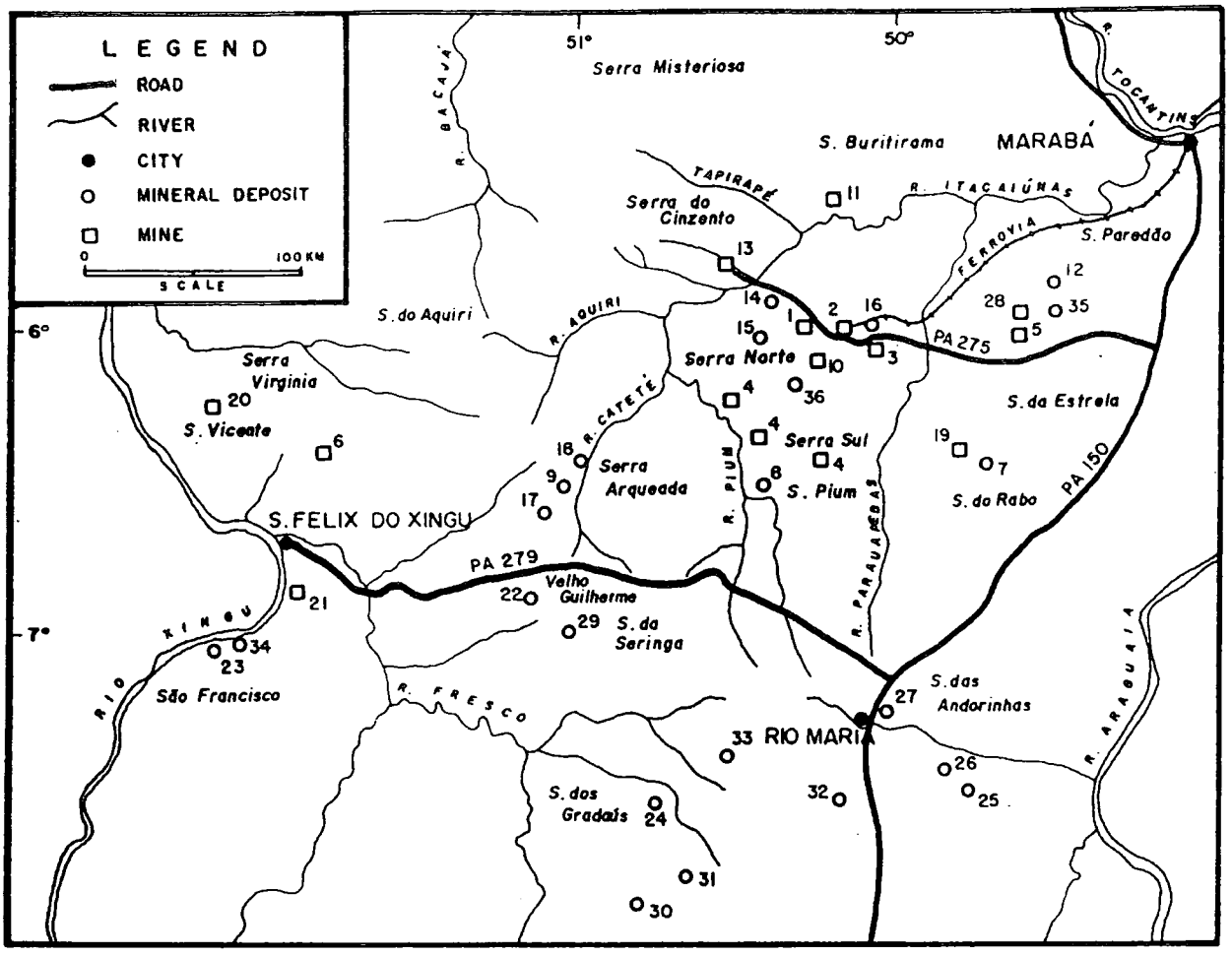

MINERAL RESOURCES

1- Serra Norte-N1/N2/N3	Fe	19-Vermelho	Ni
2-Serra Norte-N4/N3	Fe	20-Antônio Vicente	Sn
3-Serra Norte-N5	Fe	21-Mocambo	Sn
4-Serra Sul-S11	Fe	22-Velho Guilherme	Sn
5-Serra Leste	Fe	23-São Francisco	Sn
6-Serra São Félix	Fe	24-Gradaús	Sn
7-Serra do Rabo	Fe	25-Andorinhas-Babaçu-Mamão	Au
8-Serra do Pium	Fe	26-Andorinhas-Lagoa Seca	Au
9-Serra Arqueada	Fe	27-Rio Maria	Au
10-Azul	Mn	28-Serra Pelada	Au,Pd
11-Buritirama	Mn	29-Rio Branco	Au
12-Sereno	Mn	30-Cumaru	Au
13-Salobo	Cu,Au,Ag,Mo,Fe	31-Macedônia	Au
14-Pojuca	Cu, Zn	32-Pedra Preta	W,Au
15-Bahia	Au, Cu, Ag	33-Cachoeirinha	W, Sn
16-Serra Norte-N5	Al	34-Bom Jardim	W
17-Onça (Carapanã)	Ni	35-Luanga	Cr
18-Puma (Cateté)	Ni	36- Aguas Claras	Au

Fig.1.2- Distribution and location of the main mineral resources existing in the Carajás region (modified after Santos, 1980)

Chapter 5 is focused on the Cinzento Strike-Slip System and follows the same model plan as that for the Carajás Strike-Slip System chapter. Three key areas are examined concerning the structural geology of this strike-slip system.

Data concerning Proterozoic magmatism in the Carajás is given in Chapter 6. Exposures in several plutons and minor intrusions are examined.

The geology of part of the Serra do Paredão area is briefly presented in Chapter 7 emphasising stratigraphical problems concerning some of these rocks.

The final chapter presents a summary and set of conclusions drawn from the work in this thesis.

1.4- METHODOLOGY

Most of the data presented here were collected during two field seasons in the 'dry' seasons of 1993 and 1994, representing more than four months of fieldwork. In addition some of the data concerning the Águas Claras region, Azul Mine and N-4 Mine were collected during several successive short field trips undertaken during 1991 and 1992; those related to the Cotia Mine, presented in the Chapter 5, were obtained during the main field season of the "Projeto Curionópoles" (Departamento de Geologia / UFPa), in 1989. Additional regional information was complimented by material from earlier published geological maps on the region.

The maps used in this work were hand-made by integrating data obtained from the visual interpretation of LANDSAT satellite images in scales 1:1000000, 1:250000 and 1:100000; radar images in 1:250000 and 1:100000 were also used. Maps of the Águas Claras and the N-4 Mine area were also constructed using aerial photos at 1:40000 scale. The remote sensing images were interpreted visually and analysed according to Riverau (1972), Soares and Fiori (1976) and Veneziani and Dos Anjos (1982). Geological information obtained by remote sensing analysis at different scales was adjusted to a final scale by photocopying and fitted to form surveying maps at 1:100000 scale by IBGE (Brazilian Geographical and Statistical Institute) and the Brazilian Army Cartographic Service. The coordinate system shown in detailed-scale maps of the Águas Claras, N-4 Mine and Bahia Mine corresponds to local topographic grids currently used by the mine company.

Data were collected and processed following routine methods of geological mapping for Archaean/Proterozoic deformed terrains (e.g. McClay,

1987; Passchier *et al.*,1990). Bearings of planar structures were recorded and processed following the notation: strike dip/dip quadrant; and for linear structures the notation: plunge angle / azimuth of plunge is used. Stereonets were constructed supported by the software "StereoNet For Windows 2.07" (Ivar Steinsund, 1993).

Most of the sketches and sections presented in the figures were constructed using sequentially mounted field photographs, later reduced by photocopying and adjusted manually to minimise distortions.

Rock samples collected were orientated and later cut in thin sections according to routine methods (e.g. Prior *et al.*,1987). Kinematic indicators were carefully observed both on field and/or thin section within the XZ planes, parallel to linear structures related to displacement. Rock descriptions, names, and textures under the microscope, follow the nomenclature introduced mainly by Bard (1980); Adams *et al.*(1984); Mackenzie and Guilford (1988); Le Maitre *et al.*(1989); Yardley *et al.*(1990) and Mackenzie *et al.*(1995).

CHAPTER 2
DEFINITION OF TERMS AND APPLIED CONCEPTS

The research presented in this thesis examines kilometre-scale strike-slip systems in the Carajás region. In this chapter concepts and terminologies applied in the thesis are briefly discussed.

2.1- STRIKE-SLIP FAULT SYSTEMS

Strike-slip faults have been recognised as fundamental geological features that control the structural architecture of continental margins, island arcs, collision zones, oceanic and continental rift zones and stable cratonic areas (Fig.2.1). Applied rigidly the term *strike-slip fault* refers to structures in which the net slip is parallel to the direction of the fault strike (Beckwith, 1941; Sylvester, 1984; Sylvester, 1988). Strike-slip faults and dip-slip faults are end members of a spectrum in the kinematic classification of faults (Reid *et al.*, 1913), and the nomenclature *oblique-slip* has been used to refer to structures between these two end members (e.g. Spörli, 1980; Ballance and Reading, 1980; Reading, 1980). The terminology strike-slip faults is used throughout this thesis in a general way to refer to faults with predominantly strike-slip movements.

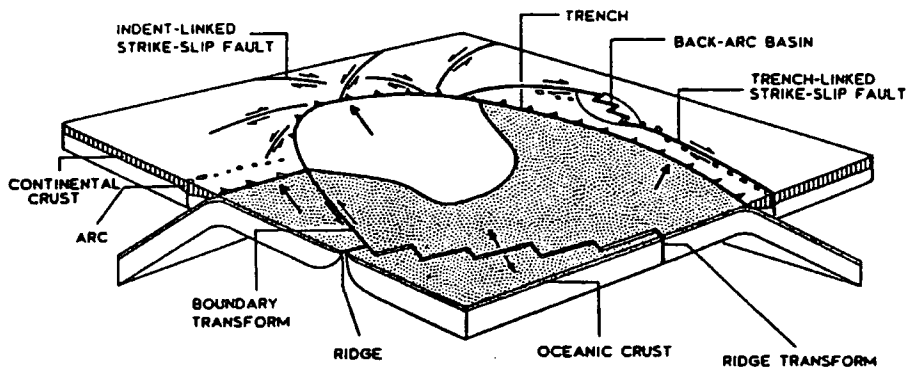

Fig.2.1- Indent-linked and trench-linked strike-slip faults in the plate tectonic context (After Woodcock, 1986).

Transform (Wilson, 1965) and *transcurrent faults* (Geikie, 1905, in Sylvester, 1988) are the two main kinds of strike-slip faults. Transform faults cut the lithosphere forming plate boundaries, whilst transcurrent faults are confined to the crust (Wilson, 1965; Crowell, 1974*a*; Freund, 1974; Reading, 1980; Woodcock, 1987; Sylvester, 1984, 1988; Zolnai, 1991). Their basic geometrical and kinematic features are summarised in the Table I.

TRANSFORM FAULTS *(Wilson, 1965; Freund, 1974)*	**TRANSCURRENT FAULTS** *(Reading,1980;Chritie-Blick and Biddle,1985; Sylvester,1984,1988)*
-they are boundaries between lithospheric plates	-they occur in several geological settings.
-they incorporate lithospheric displacement.	-they affect mostly the upper crust.
-the displacement along the fault planes is accommodated at the end of the faults by several kinds of extensional and contractional features.	-the displacement along their length generally shows progressive change, going to be null at the fault termination. The displacement is a fraction of its size.
-they terminate abruptly in a single and straight plane that can connect a network of belts.	-their terminations are dominated by splay geometry and is frequently bent as a whole.
-the fault is parallel to the direction of extension or shortening at its end.	-the directions of shortening and extension are oblique to the fault strike.
-they offset other structures with an opposite sense of apparent displacement.	-a large number of secondary structures can be associated with their geometry, generally in oblique position in relation to the main faults, both extensional and compressional simultaneously.
-adjacent parallel faults can present opposite sense of displacement.	-parallel faults normally have the same sense of displacement in relation to others parallel to them.
-fault rotation is rare.	-the fault can rotate subsequently during deformation

Table 2-1. Main differences between *transform* and *transcurrent faults.*

Some special types of transcurrent faults can be individualised in different geological settings: *tear faults* or *transverse faults* (Fig.2.2; Sylvester, 1984, 1988); *transfer faults* (Fig.2.2; Gibbs, 1984; Gawthorpe and Hurst, 1993); *indent-linked and trench-linked strike-slip faults* (Fig.2.1; Burker and Sergör, 1986; Woodcock, 1986).

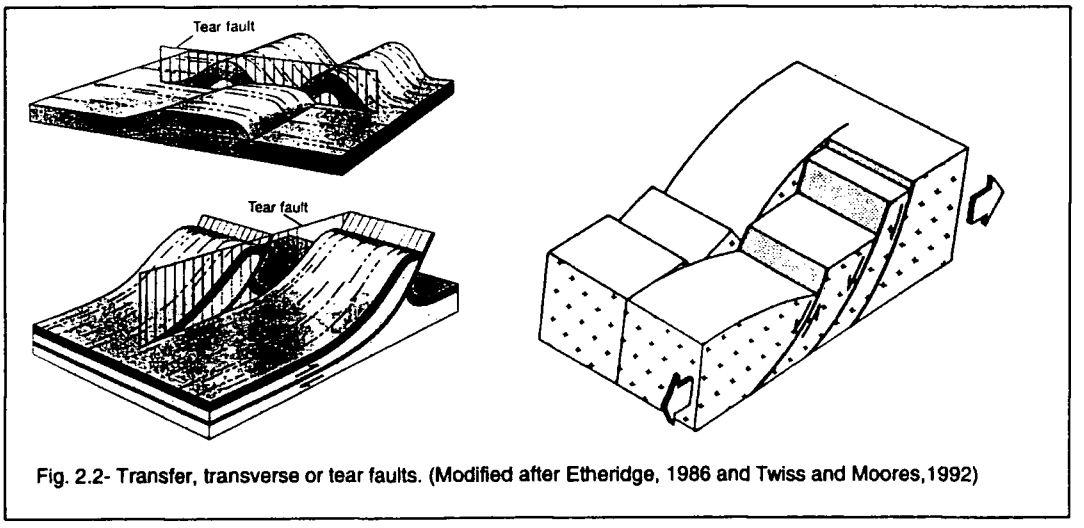

Fig. 2.2- Transfer, transverse or tear faults. (Modified after Etheridge, 1986 and Twiss and Moores,1992)

2.1.1- Geometry and kinematics.

a) Shape. The shape of a strike-slip fault can vary and depends on several factors including the mechanical properties of the rocks present in the region where it occurs. The two main factors controlling fault shape are: (1) the stratigraphical organisation of the host rocks; and (2) the earlier structural history of the region (Crowell, 1974*a*, *b*; Sylvester, 1984).

A strike-slip fault may be expressed as (1) a long single, concave straight or curved plane; (2) a long and narrow set of curved planes in a parallel or en-echelon offset pattern, or (3) by more complex anastomosing patterns composed of several combinations of these fault geometries (e.g. braided geometry, duplexes, etc.). Most strike-slip faults are thought to be steep structures that may link into a flat detachment at depth or down to a steep shear zone (Fig.2.3) which cuts much or all of the continental crust (Kingma, 1958; Segal and Pollard, 1980; Sylvester, 1988; Swanson, 1988).

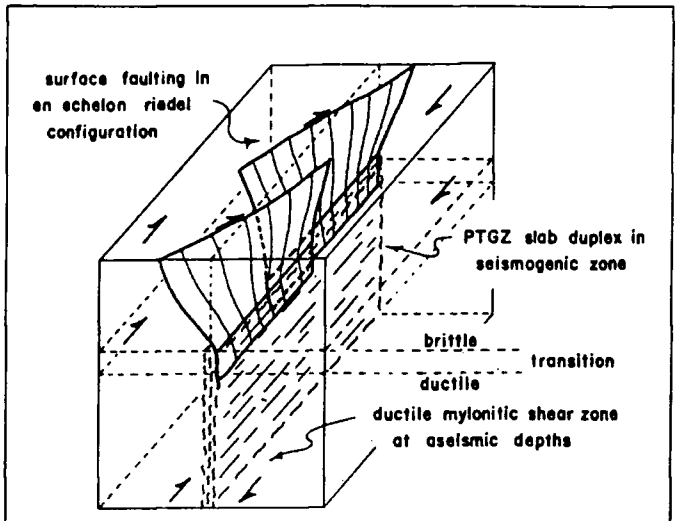

Fig.2.3- En echelon faults that converges to a main steep plane and ductile mylonitic shear zones (After Swanson, 1988).

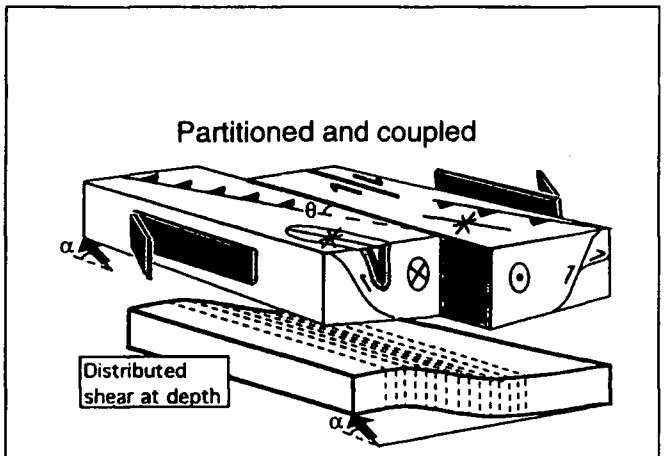

Fig.2.4- Partitioning of discrete strike-slip system in the upper crust controlled by plate motion (After Tikoff and Teyssier, 1994).

On a large scale partitioning of strain may occur in the seismic upper crust coupled to an aseismic shear zone in the lithospheric mantle at depth (Fig.2.4; Molnar, 1992; Tikoff and Teyssier, 1994).

Fault systems can be hundreds of kilometres long, but the same geometric pattern is seen on scales of a few

millimetres to kilometres (Tchalenko, 1970).

A single fault plane may be curviplanar along its strike (Freund, 1971) producing a *ribbon effect* characterised by a twisted plane along the fault (Zolnai, 1991). In this case, the same fault plane can have both normal and reverse displacement in different places.

b) Fault displacements. The determination of the **horizontal displacement** associated with a strike-slip fault depends on the presence of vertical stratigraphic markers or other geological references such as stratigraphical contacts, intrusions (dykes, batholiths), metamorphic isograds, fold-axes, suture zones, juxtaposition of provinces having dissimilarities, and so on (Sylvester, 1988; Zolnai, 1991). Circumstantial evidence may be used to estimate horizontal movements, including: physiographical criteria, geophysical investigations, presence of structural features such as pull apart basins, earthquake analysis or by theoretical and experimental models (Tchalencko and Ambraseys, 1970; Freund, 1974; Woodcock, 1986; Zolnai, 1991).

Strike-slip systems can also produce important **vertical displacements** (Woodcock and Fisher, 1986). These vertical movements are often associated with *bends* and *offsets* along the main fault. The term "porpoising" has been used to describe the mechanism of migration of the deformation, isolating fault lozenges accompanied by uplifts and subsidences along the fault strike (Crowell and Sylvester, 1979). *Convergent strike-slip* or *transpression* (Harland, 1971; Sanderson and Marchini, 1984) refers to a deformation involving horizontal shortening and vertical thickening across a strike-slip fault zone while *divergent strike-slip* or *transtension* produces extension accompanied by vertical thinning (Fig.2.5). Partitioning of strains is common in these settings leading to complex oblique, vertical and horizontal displacements. Transpression and transtension can occur either regionally, reflecting large-scale oblique displacements, or locally in bends or offsets along strike-slip faults.

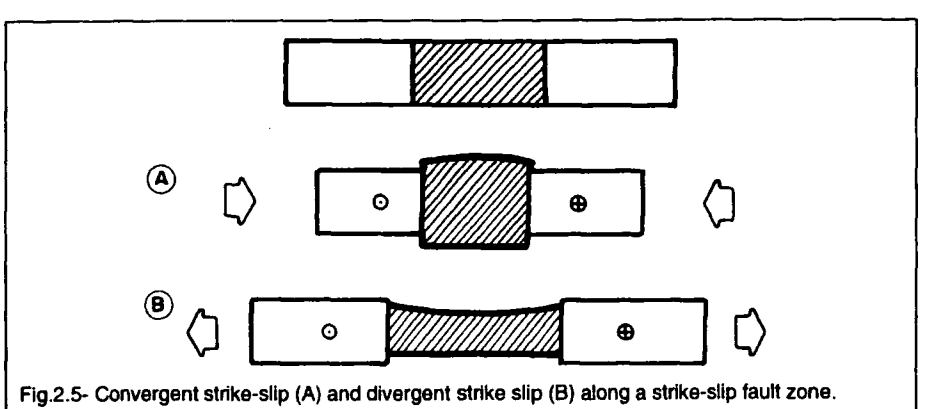

Fig.2.5- Convergent strike-slip (A) and divergent strike slip (B) along a strike-slip fault zone.

c) Related structures. The area of deformation associated with strike-slip faults can be wide and may, as in the case of the San Andreas Fault in California, be up to 1000 km wide (Sylvester, 1988). There are several characteristic structures related to strike-slip systems. The most common are: (1) *single faults*, (2) *secondary faults and fractures*, (3) *horsetail structures*, (4) *folds*, (5) *pull-apart structures;* (6) *wedge-shaped basins*; (7) *duplexes* and (8) *sidewall ripout structures.*

Single faults develop in strike-slip systems where adjacent blocks merely slide by each other, with insignificant differential elevation or subsidence (Crowell, 1979). The occurrence of a single strike-slip fault is rare in nature, but may occur, when the fault is strongly controlled by a pre-existing fracture (Segall and Pollard, 1983; Zolnai, 1991).

Secondary fractures are sets of fractures and faults orientated in several directions that are thought to form at roughly the same time as the movement occurred at the main fault (Chinnery, 1966a; 1966b). They can show a complex pattern, composed of steeply dipping curved fractures that mutually cross-cut, and usually have less movement and depth penetration than the master fault. Together with the major faults, they can form a fault zone that can be from metres to kilometres wide (Fig.2.6).

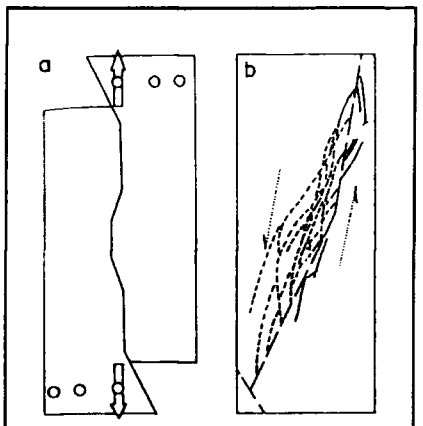

Fig.2.6-a) Single fault; b) Strike-slip fault zone (Modified after Price and Cosgrove, 1994).

The development and nucleation of secondary faults in nature is influenced by several physical and rheological parameters and also by the presence of old structures in a favourable orientation (Segall and Pollard, 1983).

The study of secondary faults has been carried out in various ways: investigation of real fault arrays (Tchalenko 1970; Tchalenko and Ambraseys, 1970); analogue modelling using clay (e.g. Wilcox *et al.*,1973), unconsolidated sand (e.g. Naylor *et al.*,1986), wax (e.g. Oliver, 1987), plasticine (e.g. Freund, 1974), and wet tissue paper (Christie-Blick and Biddle, 1985); experimental deformation of homogeneous rock samples under confining pressure (e.g. Bartlett *et al.*, 1981); analyses of structures produced during earthquakes (e.g. Tchalenko, 1970), and in several theoretical models (e.g. Segall and Pollard, 1980).

Five sets of asymmetric fractures or faults have been associated with major strike-slip systems (Fig.2.7; Tchalenko and Ambraseys, 1970): (1)

synthetic strike-slip faults, or Riedel (R) shears; (2) antithetic strike-slip faults or conjugate Riedel (R') shears; (3) secondary synthetic faults or P shears; (4) tension fractures (T or P'); and (5) faults parallel to the main displacement zone, termed D (or PDZ - Principal Displacement Zone) or Y shears of Bartlett *et al.* (1981). X shears are a sixth and less common type corresponding to symmetrical fractures in relation to R' (Bartlett *et al.*, 1981). Neither the X or P' structures has been documented in nature (Smith and Durney, 1992).

Geological models have shown that the *synthetic strike-slip fractures* (R) and *antithetic strike-slip fractures* (R') are particularly important features in the evolution of strike-slip belts (Wilcox *et al.*, 1973). R fractures have a low-angle orientation in relation to the main fault strike (about 10° to 30°) and show the same sense of displacement as the main zone. R' fractures form a high-angle orientated set (70° to 90°) and have opposite sense of displacement in

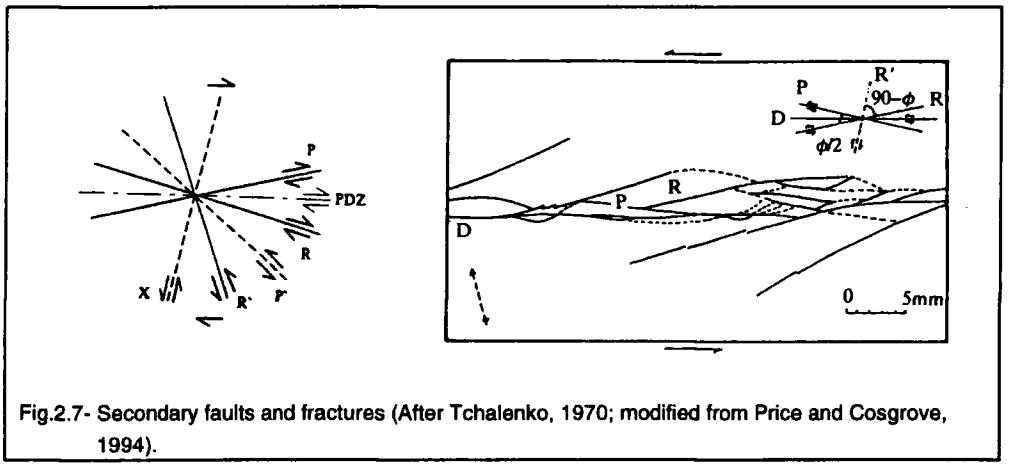

Fig.2.7- Secondary faults and fractures (After Tchalenko, 1970; modified from Price and Cosgrove, 1994).

relation to the main fault. R secondary faults show an angle $\phi/2$, and R', $90°-\phi/2$ where ϕ is the angle of internal friction of the material (Fig.2.7; Tchalenko, 1970). The antithetic faults are thought to develop less commonly in nature, and may occur more often when there is a substantial overlap between adjacent synthetic faults (Keller *et al.*, 1982). The geometry of these faults at depth is not well known but it is generally accepted that they converge into the main plane of displacement at deepest levels of the crust, and may have a helicoid geometry steeping upward.

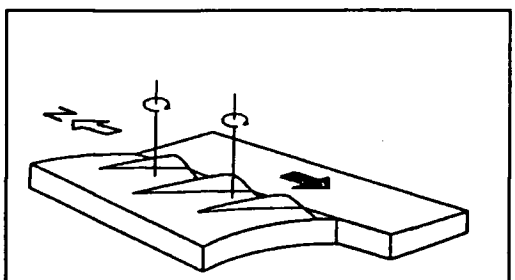

Fig.2.8- Clockwise rotation associated with dextral strike-slip faults. Example of the N Japan (After Kodama *et al.*, 1993).

Blocks delimited by secondary faults are able to rotate during simple shear. A sinistral fault block will rotate

counter clockwise whereas dextral ones rotate clockwise (Wilcox *et al.*, 1973). An example of this relationship was pointed out by Kodama *et al.* (1993) in the north of Japan (Fig.2.8). However the sense of block rotation may be more complex and also be controlled by the spacing, orientation and position of the pole of rotation of these faults (Fig.2.9; Ron *et al.*,1984; Garfunkel and Ron, 1985; Smith and Yamauchi, 1994). Theoretical models developed by Freund (1974) pointed out that R and P secondary faults tend to rotate relatively slowly

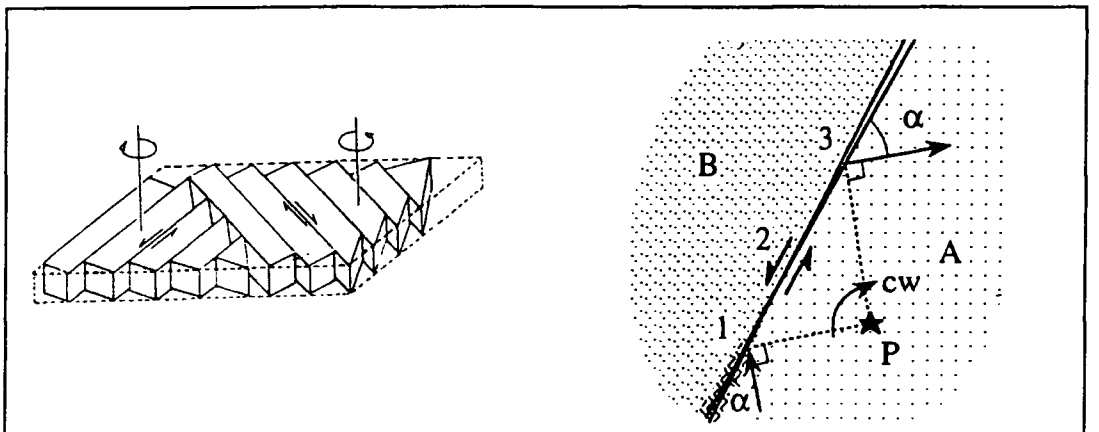

Fig.2.9- The rotation associated to main faults and secondary faults depends on the space, orientation and position of the rotation pole (After Garfunkel and Ron, 1985; Smith and Yamauchi, 1994).

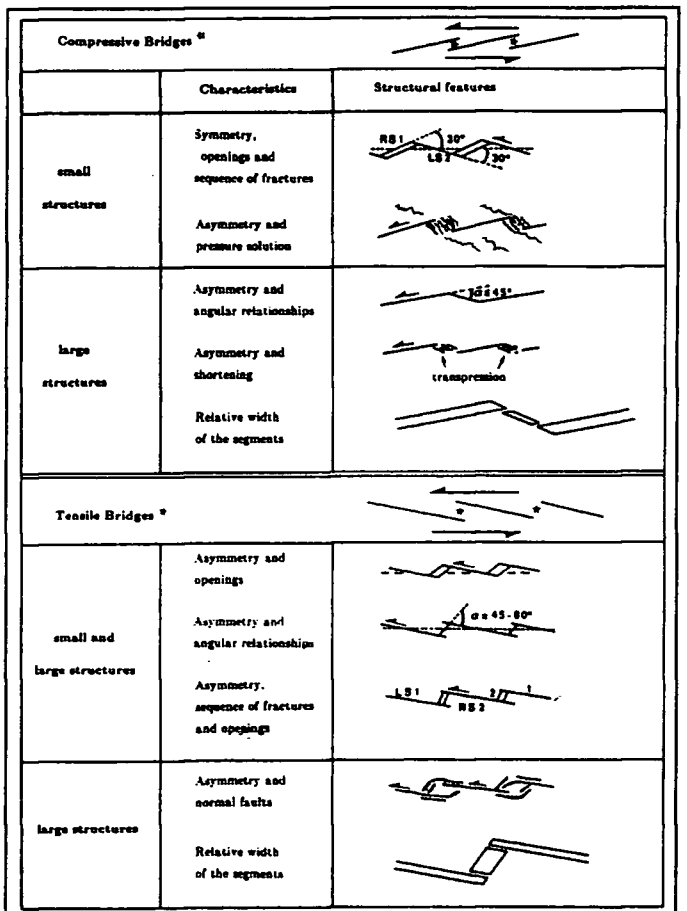

Fig.2.10- Some geometric features in several scales used as criteria for sense of movement in faults (After Gamond, 1987).

(against the shear) whilst the R' rotate more rapidly. These models are in agreement with the observed sense of rotation of similar secondary faults observed in the field (Wilcox *et al.*, 1973).

The asymmetry of secondary faults can be used as an indicator to determine the major displacement sense (e.g. Tchalenko, 1970; Gamond, 1987; Fig.2.10).

Tchalenko (1970) and others have shown by both experimental and field analyses of secondary faults, at different scales, that the Riedel fractures (R

and R') are the first to form during strike-slip simple shear, followed by P shears and other fractures parallel to the strike of the main structure (Y shears).

Horsetail structures are features associated with strike-slip fault terminations. The displacement along a strike-slip fault tends to diminish towards the end of the fault plane. This deformation is accommodated by either bending or splaying towards the fault end, where the displacement is divided between several branches forming a *horsetail structure* (Fig.2.11).

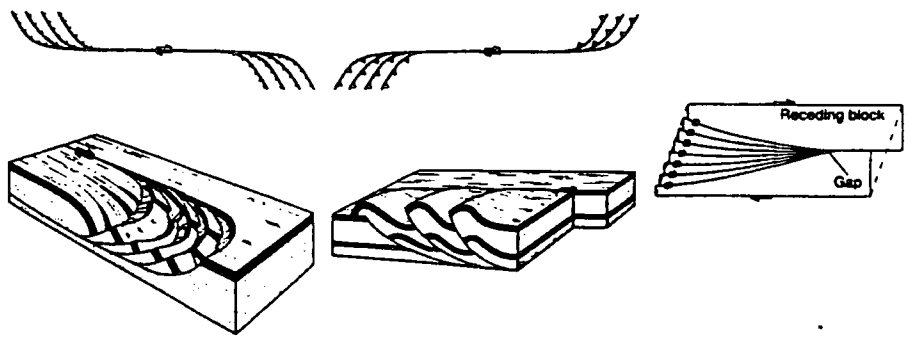

Fig.2.11- Main fractures observed in association to horsetail structures (After Twiss and Moores, 1992).

Woodcock and Fisher (1986) refer to structures developed in the region of strike-slip terminations as imbricate fans and sub-divide them into *leading / trailing extensional* or *contractional imbricated fan* (Fig.2.12).

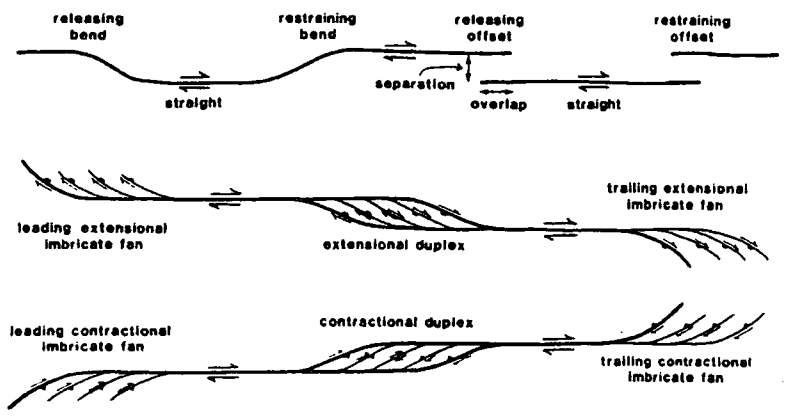

Fig.2.12- Strike-slip duplexes and imbricated fan terminations (After Woodcock and Fisher, 1986).

Regional strike-slip faults are often related to individual **folds** or **fold-swarms**, typically arranged in an en echelon pattern, oblique to the principal direction of shear. These folds, together with other compressional structures formed along strike-slip faults are thought to be produced by local secondary strain field, induced by the simple shearing component (Wilcox *et al.*, 1973; Sylvester, 1988).

The fold-axes of the *en echelon folds* are gradually rotated by continued deformation related to movement along the main fault (Fig.2.13), to eventually become sub-parallel to the fault (Sylvester, 1988; Zolnai, 1991). The axial trace of en echelon folds may be 10° to 35° oblique to the strike of the main fault (Wilcox *et al.*, 1973; Sylvester, 1988), and the sense of obliquity can be used to deduce the overall sense of shear. The angular relationship between fold axes and the principal displacement zone may depend locally on the depth of erosion, as well as the amount of internal rotation within the system. This is due the apparently helicoid shape of the axial surface (Sylvester, 1988), where the fold axial plane twists and flattens upwards (Fig.2.14).

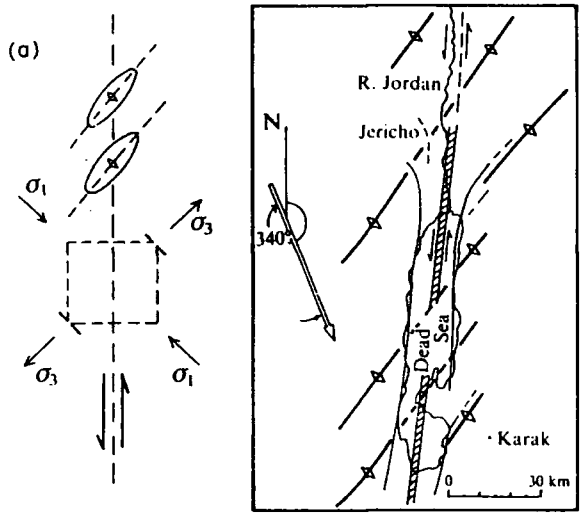

Fig.2.13- The oblique orientation of drag folds in experiments (a) and in the Dead Sea fault (After Price and Cosgrove,1994).

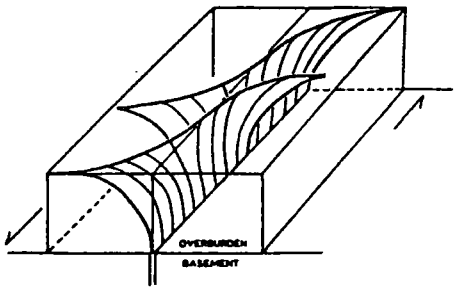

Fig.2.14- Helicoidal form of the axial surfaces in en echelon folds associated to sinistral strike-slip faults (After Sylvester and Smith, 1976)

Other factors which influence the shape and trend of the *en echelon folds* include: (1) convergence of blocks during the fault movement; (2) change in the strike of the fault; (3) large components of vertical displacement; (4) differences in kind and thickness of sediments: and (5) displacement of basement near the folds. (Wilcox *et al.*, 1973).

Folds in which the broadly contemporaneous cleavage cuts across the axial plane are termed **cleavage-transected folds**

(Powell, 1974). Several authors have suggested that these are related to convergent strike-slip systems, i.e. transpression (Sanderson *et al.*, 1980; Soper and Hutton, 1984; Soper, 1986).

The geometric description of the *cleavage-transected folds* uses 3-D angular relations between several imaginary planes, projected simultaneously in a single folded surface transected by cleavage planes (Fig.2.15; Borradaile, 1978; and Johnson, 1991). The two more important angles to describe these folds are the Δ and the **d** angles (Borradaile, 1978). The Δ represents the acute angle between the cleavage plane and the fold axis, and **d** is the angle between the axial plane and the cleavage in the fold profile plane. Negative and positive angles refer to clockwise and anticlockwise senses of transection respectively. A complementary angle **d*** was used by Johnson (1991) to further characterise the geometry of transection, corresponding to the angle between the cleavage and the limb bisector plane trace measured in the fold profile plane. The angle between the axial surface trace and the cleavage trace in map view or in a horizontal plane was been used in field descriptions, represented by the symbol t (e.g. Sanderson *et al.*, 1980) and was named *apparent axial-transection* angle by Johnson (1991).

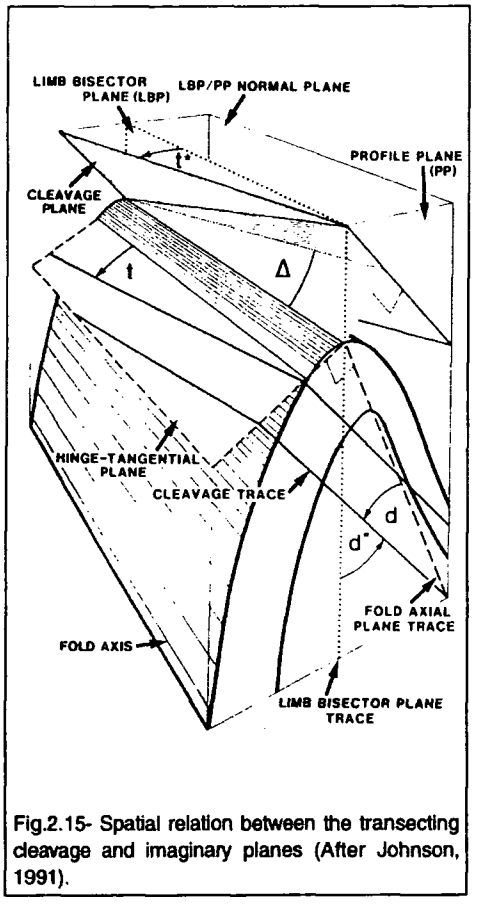

Fig.2.15- Spatial relation between the transecting cleavage and imaginary planes (After Johnson, 1991).

Pull apart structures are formed due to transtension along oblique segments or offsets along strike-slip faults (Burchfield and Stewart, 1966). General terms such as *releasing bends* or *offsets* (Fig.2.16) or **dilational jogs**

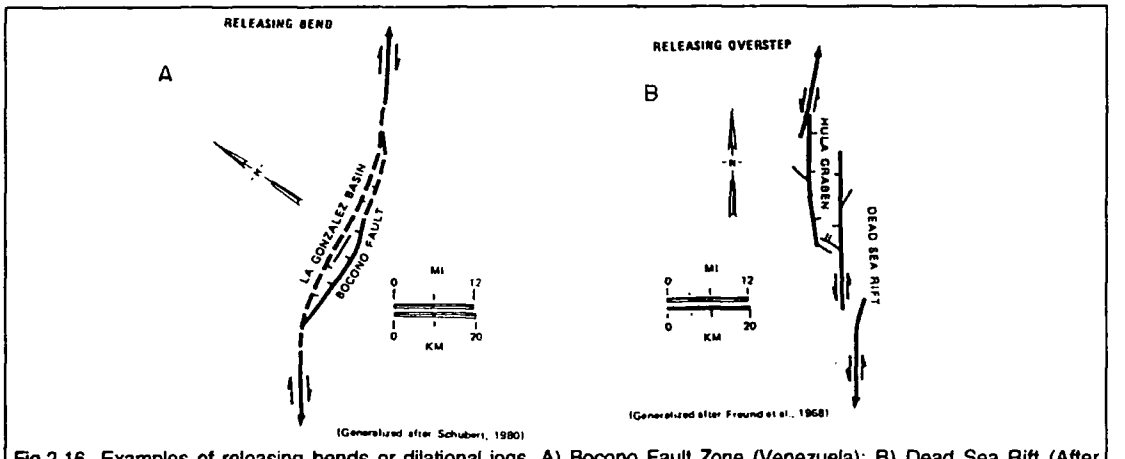

Fig.2.16- Examples of releasing bends or dilational jogs. A) Bocono Fault Zone (Venezuela); B) Dead Sea Rift (After Harding *et al.,1985).*

and **bends** can be used to refer to these structures as a whole (Crowell, 1974*a* and *b*; Woodcock and Fisher, 1986; Sylvester, 1988).

Mann *et al.* (1983) proposed several models to account for the development of *pull apart basins* in *releasing offsets* involving localised lithospheric extension, high heat flow and volcanism (Fig.2.17A). They suggested five different progressive stages in the development of pull apart basins (Fig.2.17B).

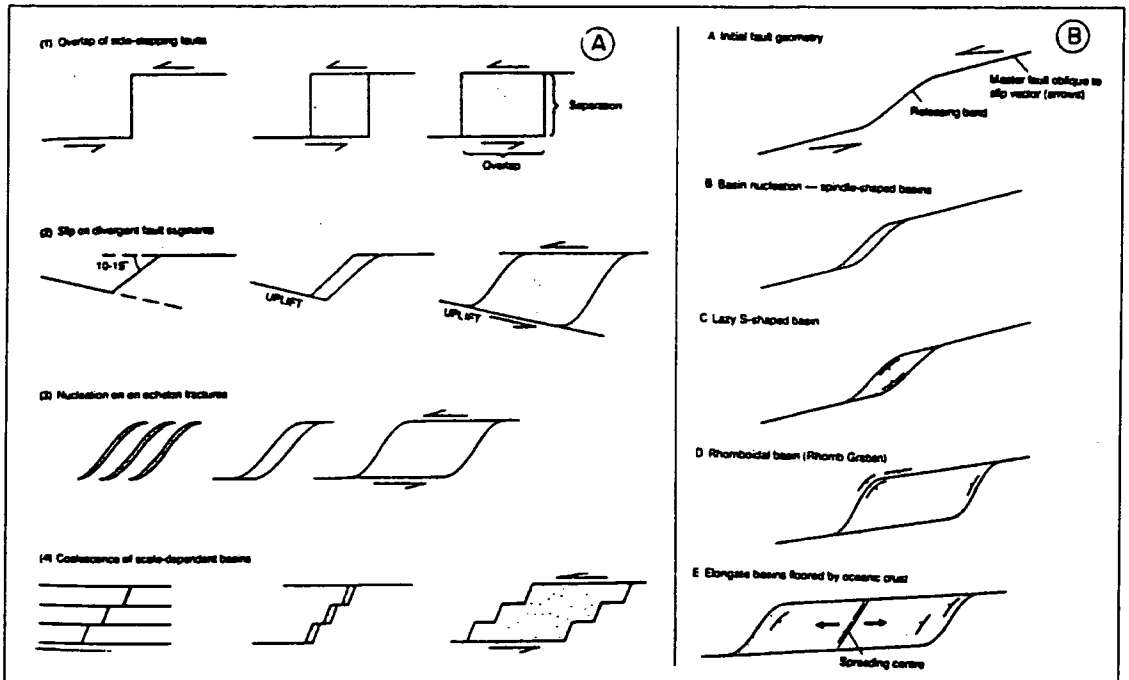

Fig.2.17- Models of development of pull apart basin in releasing offsets (A) and evolution of pull apart basin in a releasing bend (After Mann *et al.*, 1983).

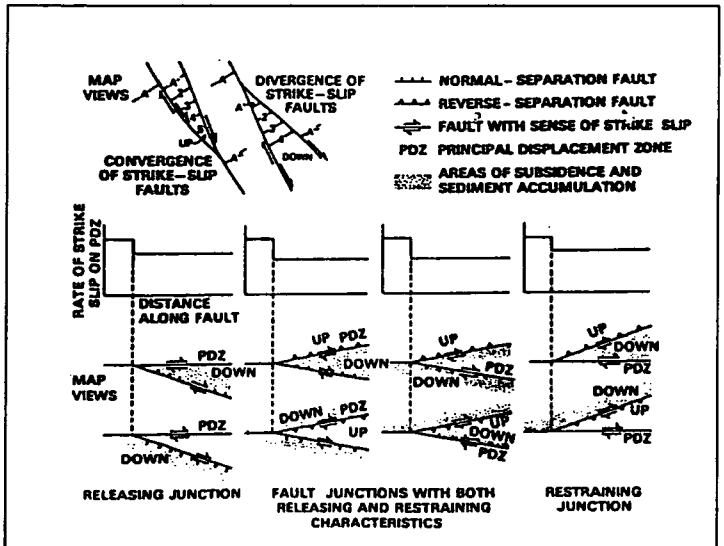

Fig.2.18- Sketch illustrating the relation of the main fault kinematics and uplift or subsidence of blocks in wedge structures (After Christie-Blick and Biddle, 1985).

A special type of pull-apart basin was described and named by Crowell (1974*a*) as a **wedge shape basin**. According to Crowell (1974*a*) such a basin forms due to a tectonic depression formed in places where braided or anastomosing fault zones develop (Fig.2.18).

The peculiar feature of this type of graben is

that in the same structure one of the faults is a reverse fault and the other normal (Crowell. 1974*a*; Christie-Blick and Biddle, 1985).

The term **duplex** refers to a splay of faults that converge both downwards and upwards to a sole fault and to a roof fault respectively. This concept was first applied to thrust systems by Dahlstrom (1970) and later, widely recognised in different tectonic environments, such as extensional regions (Gibbs, 1984) and strike-slip movement zones (Woodcock and Fisher, 1986). *Strike-slip duplexes* form mainly at fault bends or offsets, and their associated extensional or contractional character will be a function of the geometric location of these bends or offsets, in relation to the fault kinematics (Fig.2.12). They may also form by the interaction of sets of secondary faults in different orientations, i.e. R, P, R' and Y(D) shears (Fig.2.19; Woodcock and Fisher, 1986). In 3-dimensions, the faults are thought to link downwards into the principal zone of displacement forming *flower structure* geometries (Fig.2.20).

In transtensional and transpressional settings these are referred to as *negative flower structures* and *positive flower structures* respectively (Harding and Lowell, 1979). Swanson (1989) describes **sidewall ripout structures**, which are arcuate or listric splay faults that cut out asymmetric lenses or elongate slabs of rocks from the sidewalls adjacent to straight planar strike-slip fault surfaces (Swanson, 1989). The geometry

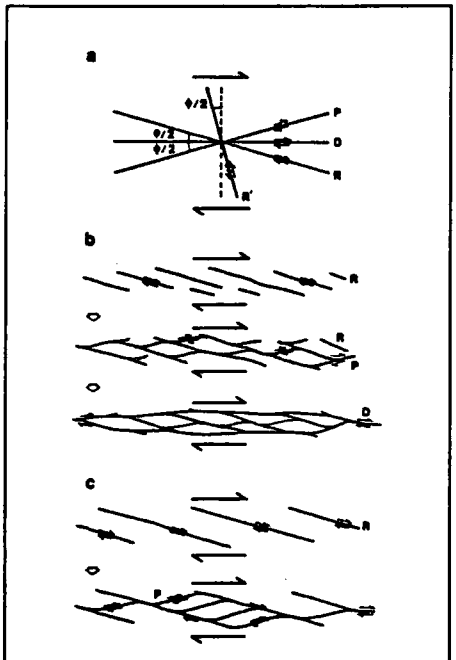

Fig.2.19- Strike-slip duplexes formed by combination of secondary faults (After Woodcock and Fisher, 1986).

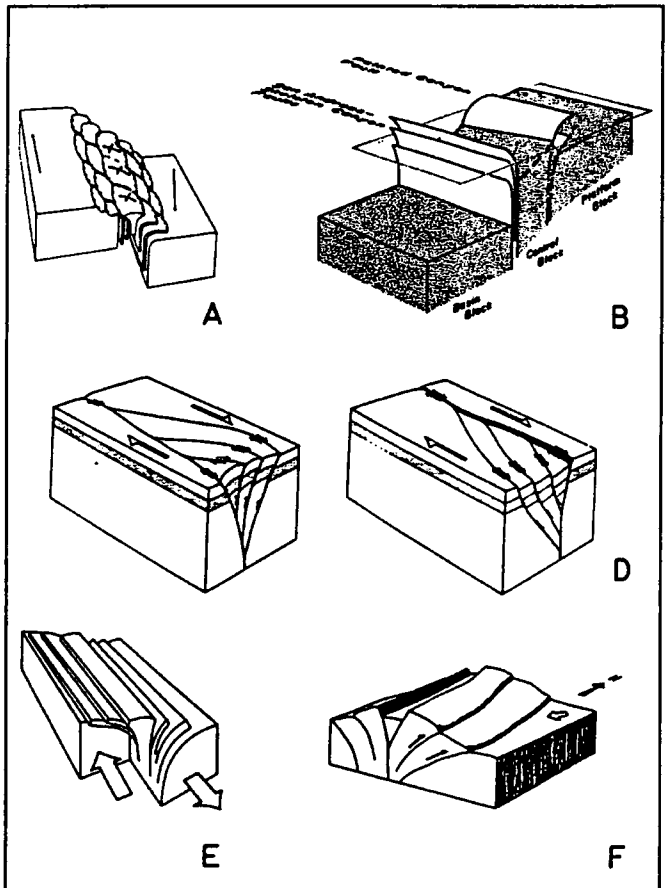

Fig.2.20- Models of positive flower structures (After Sylvester, 1988).

of the structure is mostly controlled by the anisotropy of the host rocks. *Scallop-shaped lens ripouts* developed preferentially in isotropic or weakly anisotropic host rocks, while *elongated slab ripouts* develop in strongly anisotropic host rocks. They form end-members in a spectrum (Fig.2.21).

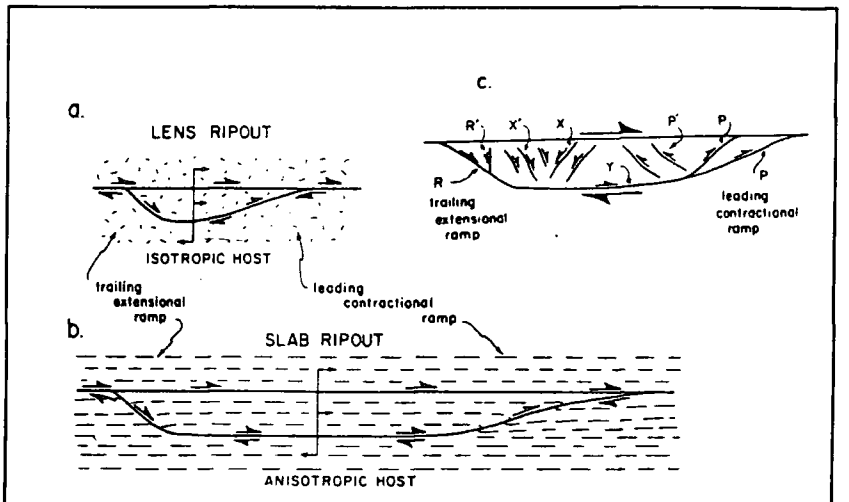

Fig.2.21-Two end-terms of sidewall ripout structures: a) lens ripout; b) slab ripout. c) sidewall ripout shear fracture terminology (After Swanson, 1989).

The double-tapered asymmetric geometry can be described in terms of leading contractional (P fracture), and trailing extensional (R fracture; Fig.2.21). Both converge towards the flat side of the structure at different angles (theoretically 30° and 60° respectively). This asymmetric form can be used as a kinematic indicator (Swanson, 1989). Their origin is attributed to periodic adhesion across the fault due to variations in the coefficient of friction and its effect on slip velocities within the fault walls (Swanson, 1989).

2.1.2 - Sedimentation in strike-slip systems

The main characteristics of deposition associated with strike-slip systems are: high sedimentation rates and abrupt facies changes; the relatively proximity of the source areas; abrupt lateral thickening of sedimentary sequences over short distances, putting in contact facies of different origins such as marginal facies breccias and lacustrine mudstones; abundant unconformities formed due to syn-depositional fault movements; and the presence of local facies representing talus detritus or alluvial fans such as the occurrence of rapidly deposited conglomerates and breccias piled up against faulted basin margins (Miall, 1984; Sylvester, 1988).

As faults move simultaneously with sedimentation, the depocentre tends to migrate and is easily influenced by the longitudinal and lateral basin asymmetry. This can explain the usual asymmetric cross-section observed in both sides of some basins (Christie-Blick and Biddle, 1985). The Ridge Basin in California provides a good example of these characteristics (e.g. Crowell, 1974*a*, and *b*).

The vertical component of motion in strike-slip faults is an important control on the position of source areas. Evidence that sediments are derived from the upthrown side are rare, except where alluvial or submarine fans develop. Palaeocurrents and palaeogeographical evidence from fluvial, deltaic or marine environments more often show sediment transport parallel to the strike-slip fault rather than perpendicular to it (Reading, 1980). Every type of sedimentary facies may be found in strike-slip basins. In a continental setting, the most important initial depositional environment is lacustrine (Ballance and Reading, 1980). If the basin is developed in a coastal region the marine depositional environment may dominate the sedimentation pattern.

2.1.3 - Magmatism in Strike-Slip Systems

Sparse syntectonic magmatic activity is a characteristic of strike-slip systems, except locally in zones of transtension and along trench-linked strike-slip faults which are embedded in the volcanic arc (Sylvester, 1988). The presence of volcanic rocks in strike-slip basins is widely documented and may include lava flows, dykes, sills and other shallow intrusions. These are thought to reflect highly localised, rapid extensional episodes related to the development of these basins (Crowell, 1974*a, and b*). Sedimentation rates are an important control on the development of volcanic assemblages (Mann *et al., 19*83). Thick sediment piles in many basins tend to reduce the heat flow and prevent magmas from reaching the surface. In the Guaymas basin, northern California, for example, the basaltic magma forming the new oceanic basement in the pull apart is intruded as sills rather than extruded as pillow basalt, because of several hundreds of metres of sediments overlying the spreading centre (Mann *et al.,* 1983). Volcanic rocks in continental strike-slip systems are normally alkali basalts and tholeiites, whilst calc-alkaline magmas are typical of strike-slip zones behind arcs and in areas of continental collision.

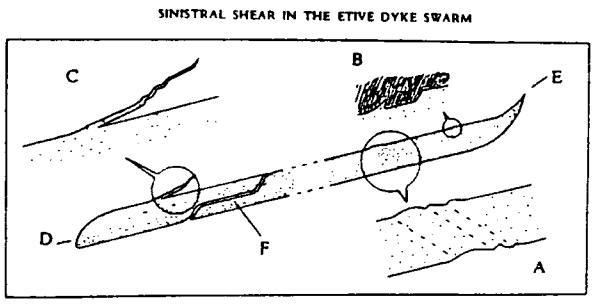

Fig.2.22- Kinematic indicators observed in syntectonic dyke, Scotland (After Morris and Hutton, 1993). See text for details.

Dykes can be emplaced into areas of transtension along strike-slip faults. Segall and Pollard (1980) show that there is a relationship between the geometry of fractures and the preferential emplacement of dykes. Dykes may be emplaced in an oblique en echelon pattern thereby acting as shear sense indicators (e.g. Lisle, 1993). Alternatively asymmetric features of dykes may yield shear sense information (Fig.2.22), e.g. matching contact re-entrants (A), oblique dyke offshoots (B), asymmetric dyke terminations (C, D and E), oblique bridges (F) and also by dating the fault displacements (Morris and Hutton, 1993).

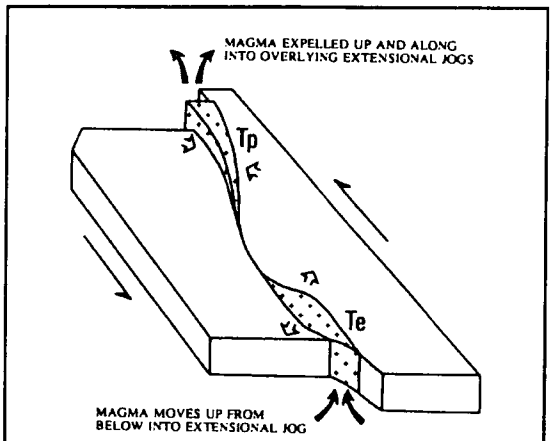

Fig.2.23- Example of the relation between granite emplacement and strike-slip faults (After D'Lemos *et al.*, 1992)

Granite petrogenesis and emplacement may also be related to strike-slip zones (Fig.2.23). The genesis, ascent, siting and emplacement of plutonic rocks, may be closely linked to fault and shear zone deformation processes (Guineberteau *et al.*, 1987; Hutton, 1988*a*; Hutton, 1988*b*; Hutton and Reavy, 1992; D'Lemos *et al.*, 1992).

Hydrothermal deposits are often associated with strike-slip faults. Sibson (1987, 1992 and 1994) has suggested that hydrothermal mineral deposits form along strike-slip faults and occur as follows: (1) brecciation by rapid hydraulic implosion during relatively localised extension at releasing bends, in association with locally reduced fluid pressure; (2) sudden concentrated influx of fluid into the bent zone; (3) delayed slip transfer through the bend simultaneous to the fluid pressure re-equilibrium by diffusion; (4) concentration of hydrothermal mineral deposits in episodic events. Sibson (1996) has suggested that the formation of *mesh structures* in dilational jogs facilitates the flow of large volumes of hydrothermal fluids through fault zones (Fig.2.24). In these cases, the fault zone permeability shows preferential development parallel to fracture

intersections and the σ_2 normal stress; in strike-slip systems, this will generally be orientated sub-vertically.

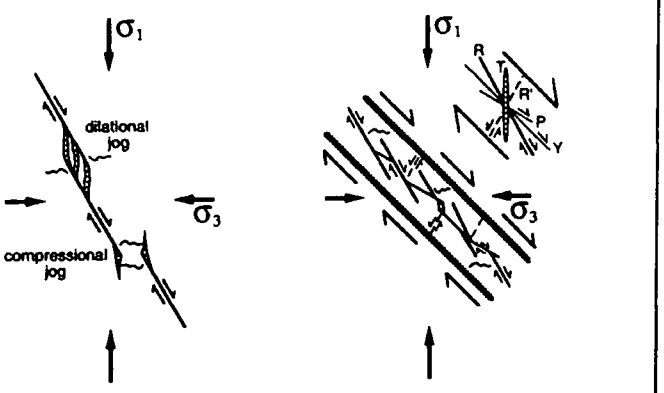

Fig.2.24- The influence of *mesh structures* formed along dilational jogs and the flow of fluids (Modified after Sibson, 1996).

2.2- STRAIN PARTITIONING IN TRANSPRESSION AND TRANSTENSION ZONES.

In the original model of transpression, Sanderson and Marchini (1984; Fig.2.25) considered the strain to be a homogeneous 3-D strain that could be mathematically factorised into a compressional pure shear with vertical thickening (or thinning in case of transtension) and a strike-slip simple shear component (either sinistral or dextral). Subsequent work (e.g. Fossen and Tikoff, 1993; Tikoff and Teyssier, 1994; Teyssier *et al.*, 1995) has shown that two end member types of transpression may be defined: pure shear and wrench dominated transpression (Fig.2.26). The latter setting is characterised by switches in the orientation of the finite extensional axis of the strain ellipsoid and by non-parallelism between these axes and those of the incremental strain ellipsoid (Tikoff and Teyssier, 1994). Several authors (e.g. Jones and Tanner, 1995, Teyssier *et al.*, 1995) suggest that transpressional and transtensional deformations are often partitioned and that the degree of partitioning strongly affects the distribution and nature of strains within a deforming region. In particular, the strike-slip component may be taken-up

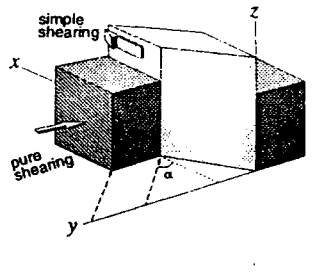

Fig.2.25- Sanderson and Marchini (1984) model to homogeneous transpression.

preferentially by movement along a single strike-slip fault resulting in pure-shear dominated transpressional strains in the adjacent regions of the deforming zone (Fig.2.27). The "switching" of finite strain axes, coupled to the development of strain partitioning can lead to rapid changes in lineation orientations and senses of shear within transpression zones (Fig.2.28; Robin and Cruden, 1994, Holdsworth and Strachan, 1991 and Holdsworth, 1994; Gooldwin and Williams, 1996).

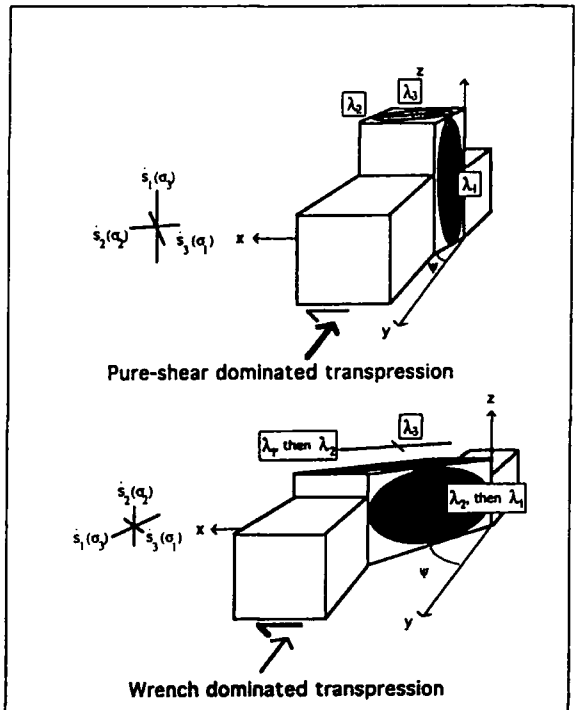

Fig.2.26- The two end-terms of transpression (After Tikoff and Teyssier, 1994).

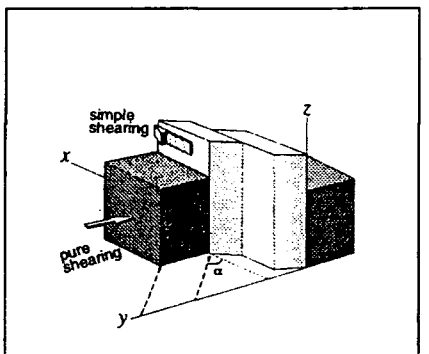

Fig.2.27- Model of partitioned transpression (After Teyssier *et al.*, 1995).

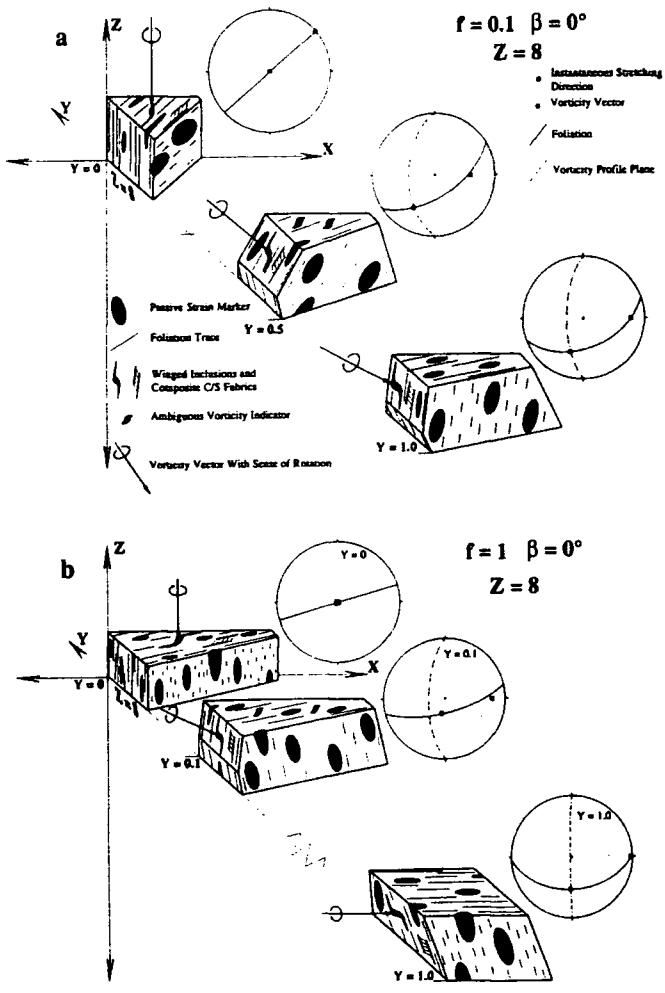

Fig.2.28- Fabric and vorticity pattern predicted by the Robin and Cruden (1994) model for ductile transpressional zones. Z=normalised height; f= component of compression/component of transcurrence ratio; β=orientation of the progressive simple shear direction; Y=normalised zone width (After Robin and Cruden, 1994).

2.3- REACTIVATION

The presence of pre-existing structures influencing the geometry and kinematics of later structures has been a subject of attention for many years (e.g. Hills, 1946; Watterson, 1975; White *et al.*,1986; Butler, 1995). The term *reactivation* as used in this work, follows the definition of Holdsworth *et al.* (1997): "*reactivation...is defined as the accommodation of geologically separable displacement events (interval >1Ma) along pre-existing structures*".

Geometric reactivation is used to refer to cases of reactivation where different senses of relative displacement occur along a particular structure, whilst *kinematic reactivation* is used to describe cases where structures reactivated with similar senses of relative displacement for successive events (Fig.2.29).

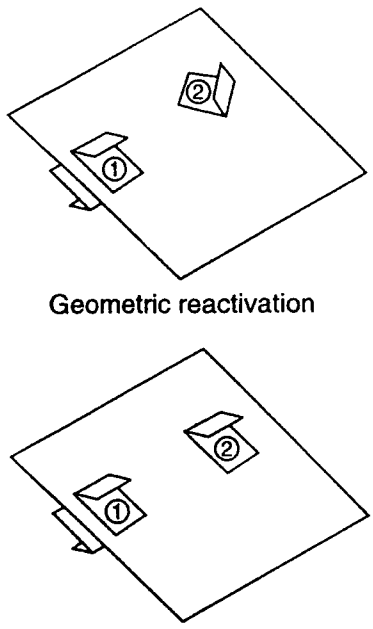

Fig.2.29- Two main types of reactivations (After Holdsworth *et al.*,1997).

Recurrent events refers to shorter term (<1Ma interval) successive displacements which occur along all active faults as part of the seismic cycle (Holdsworth *et al.*, 1997). Reactivation probably occurs because pre-existing structures are weak in the long term relative to the surrounding rocks. When it occurs along regional-scale structures, reactivation many strongly control the extent, orientation and style of younger deformation (Prucha, 1992).

2.4 - OTHER STRUCTURAL TERMINOLOGY.

2.4.1- Folds

Folds are described according to the orientation of their main geometric elements (Fig.2.30; see Fleuty, 1964; in Twiss and Moores, 1992).

The style of the folds can be described according to their cylindricity, symmetry, style of folded surface, style of the folded layer and style of fold multilayer (see Ramsay, 1967; Ramsay and Huber, 1987; Twiss and Moores, 1992).

The term *parasitic fold* (de Sitter, 1958) is used here to describe folds formed at different scales simultaneously in such a way that large folds include smaller-scale folds in their limbs and hinge zones (Fig.2.31). They are supposed to follow the Pumpelly's rule that folds formed in such circumstances have the same style and attitude at all scales (Twiss and Moores, 1992).

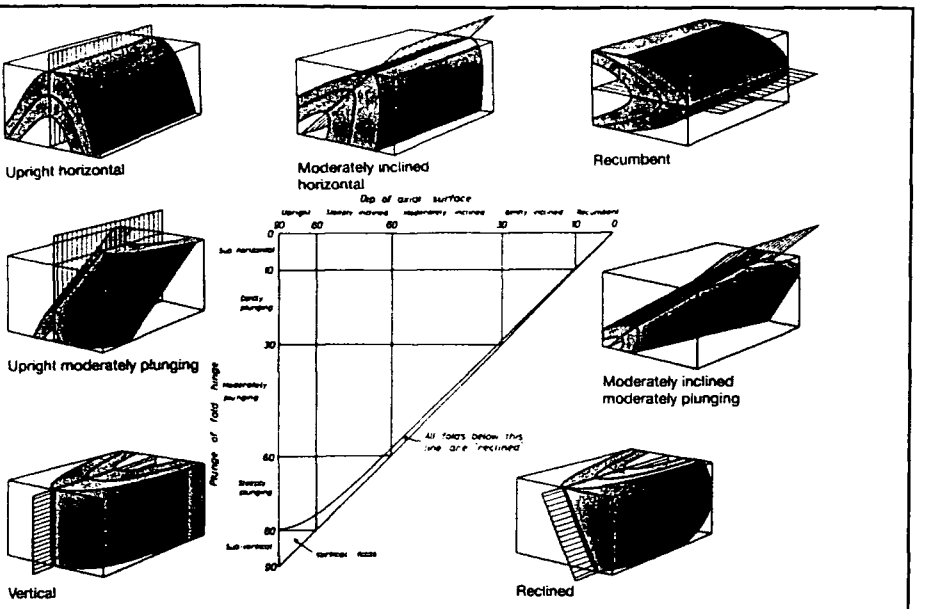

Fig.2.30- Fold classification based on Fleuty (1964: modified after Twiss and Moores, 1992).

The term *fold vergence* is utilised here based on Bell (1981) referring to the direction of sense of fold asymmetry (Fig.2.32), while the *fold facing* concept is based on Shackleton (1957), as the direction normal to the fold axis and along the axial plane, towards the younger beds. These concepts can be used to study the orientation and geometry of complex or major folds (Holdsworth, 1988) who suggested a series of procedures by using stereographic projection.

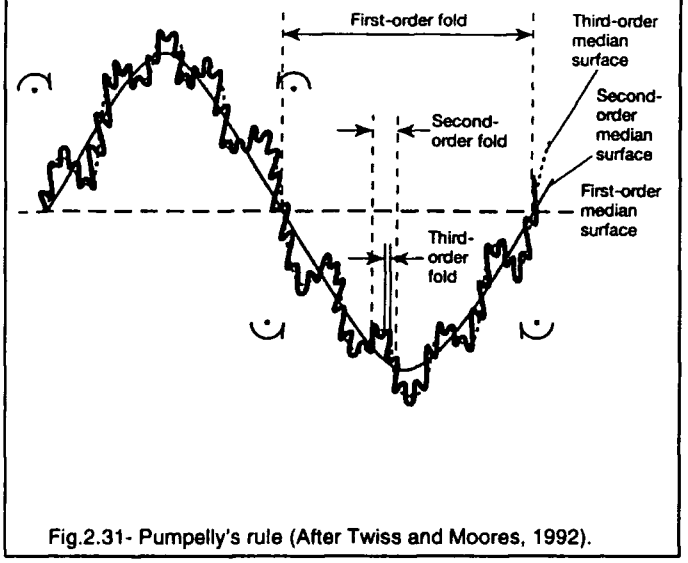

Fig.2.31- Pumpelly's rule (After Twiss and Moores, 1992).

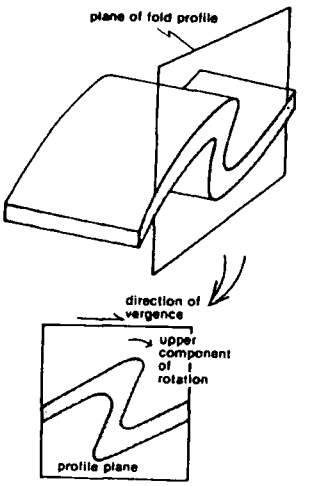

Fig.2.32- Fold vergence (modified after McClay, 1987).

2.4.2- Foliation

The term *foliation* is applied in this thesis to refer to any homogeneously distributed planar structure present in the rocks (Twiss and Moores, 1992). *Cleavage* is used (sensu-stricto) to describe the tendency of the rock to break along surfaces of a specific orientation (Twiss and Moores, 1992). The morphology of both foliations and cleavages in tectonites were described based on the shape and/or arrangement of components of rock. This classification is outlined in Fig.2.33 after Twiss and Moores (1992).

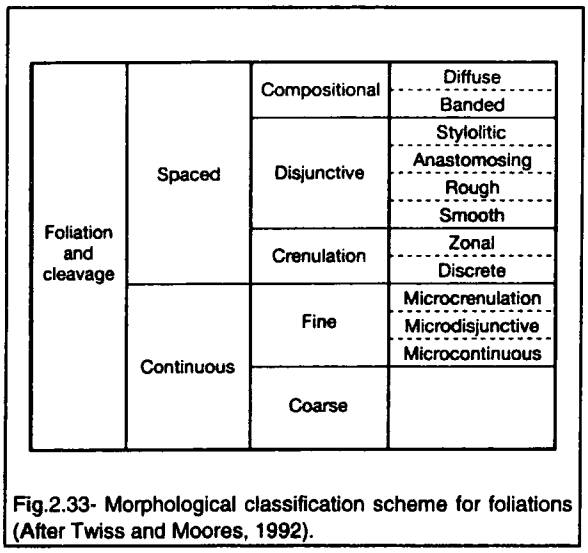

Fig.2.33- Morphological classification scheme for foliations (After Twiss and Moores, 1992).

Any planar tabular feature in the rocks marked mainly by differences in composition is referred to as *banding*. This term is used here to describe such arrangement in both high-grade metamorphic gneisses and in ironstones where the term *layer* was also applied as a synonym.

A special type of cleavage corresponding to a smooth disjunctive foliation present in very fine-grained rocks, affected by low metamorphic grade, particularly in slates is referred to in this thesis as *slaty cleavage*.

In rocks observed in ductile shear zones the nomenclature *S* and *C foliations* is applied here as defined by Berthé *et al.* (1979). The term *mylonitic foliation* is used often in this thesis to refer to the *C-foliation* when the subordinate *S-foliation* is not present or not observed.

2.4.3- Lineation

The main linear features observed in the rocks described here were classified based on their morphological characteristics, according to a scheme introduced by Twiss and Moores (1992) reproduced in Fig.2.34. The term *mineral lineation* is applied in the text describing a preferred orientation of either individually elongated mineral grains or elongated polycrystalline aggregates. Use of the terms *slickenfibers*, *slickensides*, and *slickenlines*, corresponds to the meaning defined by Wise *et al.* (1984).

Lineations in tectonites (surficial or penetrative)	Structural	Discrete	Pebbles Ooids Fossils Alteration spots
		Constructed	Hinge lines Intersections Boudin lines Mullions Structural slickenlines
	Mineral	Polycrystalline	Rods Mineral clusters Mineral slickenlines Nonfibrous overgrowths
		Mineral grain	Acicular habit grains Elongated grains Mineral fibers Fibrous vein filling Slickenfibers Fibrous overgrowths

Fig.2.34- Morphological classification scheme for lineation (After Twiss and Moores, 1992).

2.4.4- Fault and shear zone rocks.

The terminology utilised to describe the products of brittle or ductile deformation (Fig.2.35) along shear zones is based currently on Wise *et al.* (1984). The term *phyllonite* is used in this thesis based on the textural classification suggested by Sibson (1977), i.e. a phyllosilicate-rich mylonite or ultramylonite.

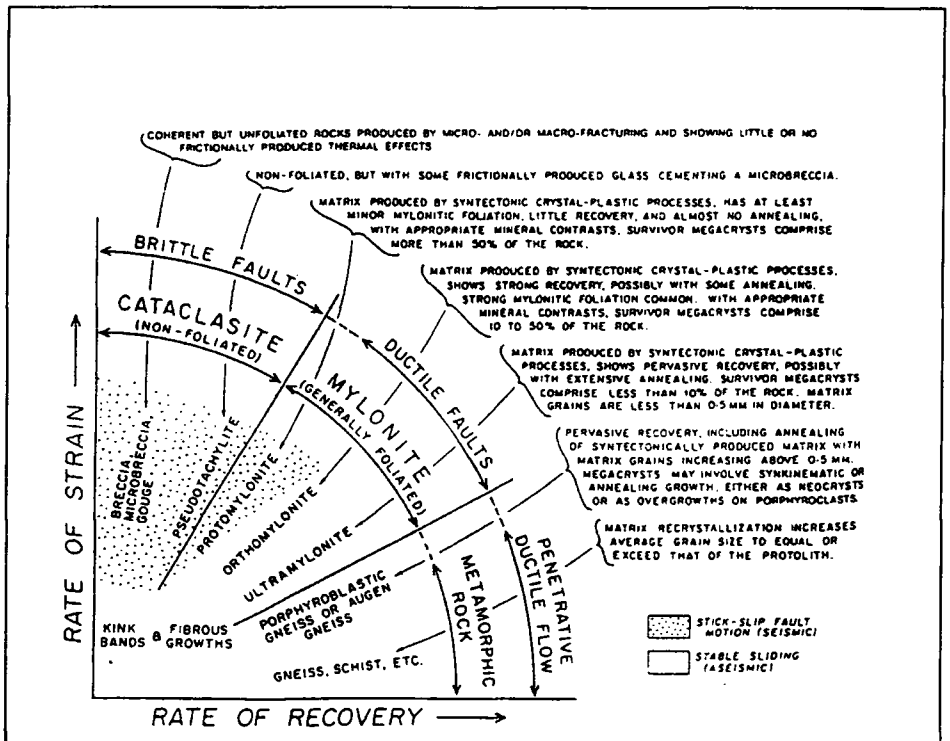

Fig.2.35- Terminology of fault related rocks. Horizontal and vertical scales are variable depending on composition, grain size and fluids (After Wise *et al.*, 1984).

CHAPTER 3
REGIONAL GEOLOGY

3.1- SOUTH AMERICAN GEOLOGY: REGIONAL CONTEXT

Brazil forms a major portion of the **South American Platform** (**SAP**) which comprises mainly Precambrian terrains of granite-gneisse basement and greenstone belts, surrounded by mobile belts that have undergone deformation and associated high- to low-grade metamorphism (Almeida and Hasui, 1984). Volcanic and sedimentary cover sequences of Precambrian to Phanerozoic ages are also present, including thick intracratonic clastic sequences (Fig.3.1).

The **SAP** in Brazil is formed of three main regions of Precambrian rocks, separated geographically by Phanerozoic basins (Fig.3.1): (1) the Guyana Shield, (2) the Brazil Central Shield (or Guaporé Craton); and (3) the Atlantic Shield (Almeida *et al.,* 1976, 1977, 1981). Together, these three shields occupy an area of around 10^6 km^2.

Five stable cratons occur in the **SAP** (Almeida *et al.,* 1976, 1981): (1) the Amazonian Craton, merging the Guyana Shield, the Brazil Central Shield and the small Eastern Paraguay Shield; (2) the São Luís Craton; (3) the São Francisco Craton; (4) the Rio de La Plata Craton, in Uruguay, as well as (5) the small Tandilia and Sierras Australes cratonic areas in Argentina (Fig.3.1). Small areas of basement include (1) the Goiás Central Massif, (2) the Pernambuco-Alagoas Massif and (3) the Guaxupé Massif (Fig.3.1). These cratonic areas and massifs are bordered by fold or mobile belts, of different ages, most of them displaying several overprinting phases of deformation and associated metamorphism; reactivation is a common feature in these belts. The most important belts in the **SAP** are: (1) the Uruaçu and Espinhaço Belt; (2) the Paraguay Araguaia Belt (or Araguaia Fold Belt, Herz *et al.,* 1989); (3) the Brasilia Belt; (4) the Sergipano Belt and (5) the Araçuaí Belt (Fig.3.1). The present work concentrates on an area in the eastern part of the Brazil Central Shield, close to its border with the Araguaia Belt (Fig.3.1).

A series of Archaean to Late Proterozoic volcanic and sedimentary sequences lie unconformably upon both basement and fold belts.

Phanerozoic sedimentary rocks are present in three main depositional sites (Fig.3.1): (1) the Amazon Basin, (2) the Parnaíba Basin; and (3) the

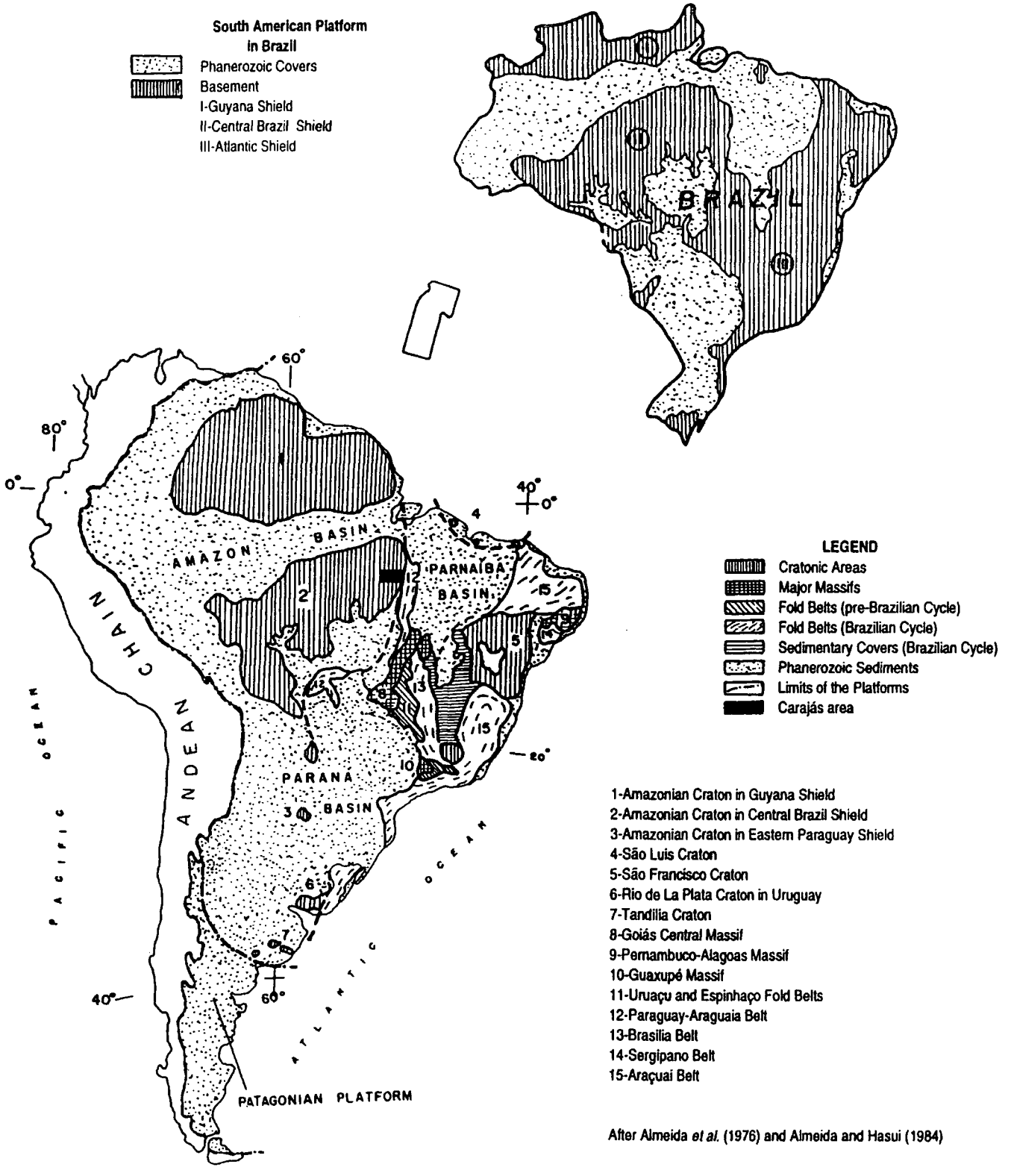

Fig.3.1- The South American Platform and its major geotectonic terrains. It is formed mainly by Precambrian shields and Phanerozoic basins. The three shields present in the Brazilian territory are shown in the top right figure. Carajás lies on the southeastern part of the Amazonian Craton, in the Brazil Central Shield.

Paraná Basin. These extensional intracratonic basins were first established in the Palaeozoic and are bordered by marginal faulted regions that allowed possible 'seaways' between the basins at several times (Petri and Fúlfaro, 1983). The Palaeozoic rocks are obscured in many regions by Post-Jurassic cover sequences laid down in a series of rift and flexural basins related to the opening of the modern Atlantic Ocean.

3.2- REGIONAL GEOTECTONIC UNITS

Since the first use of radiometric dating methods in the 1960s at least five important tectonic cycles have been defined in Brazilian Precambrian geological history (Almeida *et al.*, 1976) and they are generally accepted by most workers (Table 3-I):

ICS/IUGS(1989) subdivision (in Plumb, 1991)	Sub-division currently used in Brazil (Almeida and Hasui, 1984)	Brazilian Tectonic Cycles (Almeida *et al.*, 1976)
Neoproterozoic (1000-650 Ma)	Late Proterozoic (1000-650/570 Ma)	**Brazilian Cycle** (1000-500 Ma)
Mesoproterozoic (1600-1000 Ma)	Middle Proterozoic (ca.1800-1000Ma)	**Uruaçuano Cycle** (>1500-1000 Ma)
Palaeoproterozoic(2500-1600Ma)	Early Proterozoic (2500/1750 Ma)	**Transamazonian Cycle** (2000±200 Ma)
Archaean (>2500 Ma)	Late Archaean (3000-2500 Ma)	**Jequié Cycle** (2700±100 My)
	Early Archaean (>3000 Ma)	**Guriense Cycle** (>3000 My)

Table 3-I- Main tectonic cycles recognised in the Brazilian Precambrian.

It is important to note that the ca.1600Ma boundary between Palaeoproterozoic and Mesoproterozoic as proposed by the ICS/IUGS (1989, in Plumb, 1991) does not fit well in the Brazilian territory, particularly in the Amazonian region where it does not coincide with any important tectonic episode in the Brazilian Precambrian history (Almeida and Hasui, 1984; Neves, 1992). The available data for the Middle Proterozoic rocks in this region suggests that the lower boundary lies around 1900 to 1750 Ma (Neves, 1992).

3.3- REGIONAL STRUCTURAL PROVINCES

Traditionally, ten structural provinces (Fig.3.2a), each with a distinct geological history, are defined in Brazil (Almeida *et al.*, 1977, 1981; Wernick, 1981: Neves, 1992). Three of these, the Rio Branco, the Tapajós and the Amazonian provinces lie in the Amazonian region (Fig.3.2b). Lima (1994) has suggested that the Rio Branco and Tapajós provinces should be merged to create the so-called Amazonian Structural Province and renamed the Amazonian Province of Almeida *et al.* (1977) to Amazonas-Solimões Province. Both the Rio Branco and the Tapajós provinces were subdivided in several subprovinces according to their geological-geochronological affinities (see Fig.3.2b). The area focused on this study is located in the Carajás subprovince, the most eastern terrane, part of he Tapajós Province.

A different approach based on radiometric dating has been proposed by Cordani and Neves (1982). These authors point out that the distribution of distinctive sets of radiometric ages obtained from cratonic rocks can be used to define several mobile belts in the Amazonian Craton (Fig.3.3). This is based on the hypothesis that the tectonic evolution of this area was controlled primarily by episodic crustal accretion during the Precambrian (Cordani *et al.*, 1979; Gibbs and Baron, 1983; Gaudette and Olszewski, 1985; Teixeira *et al.*, 1986; Teixeira *et al.*, 1989; Neves, 1992). The geographical distribution of these provinces is shown in Fig.3.3, and includes the so-called Central Amazonian Province (Archaean) bounded on its northern side by the Maroni-Itacaiúnas Mobile Belt (Early Proterozoic), to the west by the Rio Negro-Juruena magmatic arc (Middle Proterozoic, 1.75-1.50 Ga); and to the south by both the Rondonian and Sunsa mobile belts (Middle Proterozoic). Phanerozoic sediments lie unconformably upon these cratons and mobile belts.

More recently, a rather different model has been proposed by Hasui *et al.* (1984, 1992) as it became apparent that many of the published K-Ar and Rb-Sr isotopic ages used by Cordani *et al.* (1979) were poorly defined isochrons of uncertain significance (Hasui *et al.*, 1984). Especially in the last ten years, more reliable radiometric methods (e.g. U-Pb, Pb-Pb and Sm-Nd) have been used to date Brazilian rocks and the ages obtained suggest that the earlier models should be carefully revised (e.g. Machado *et al.*,1991; Macambira and Lafon, 1994) . The new approach proposed by Hasui *et al.* (1992) is based on these new sets of radiometric ages, integrated to geological and geophysical (mainly gravimetric and magnetometric) data, allowing a series of large crustal blocks to be defined (Fig.3.4). These blocks are bounded by

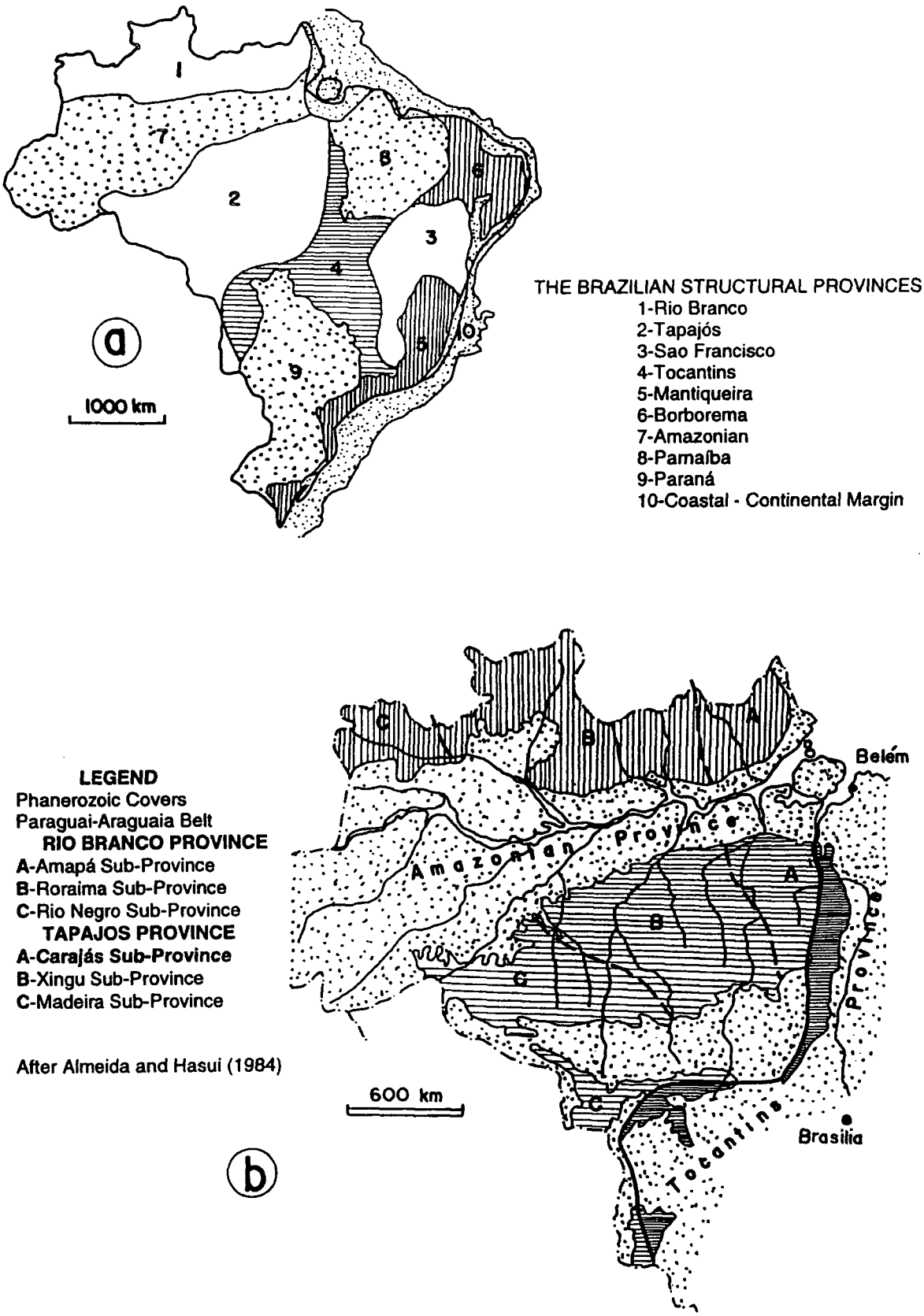

Fig.3.2- a) The Brazilian structural provinces according to Almeida *et al.* (1977, 1981). b) The Rio Branco and the Tapajós provinces in detail.

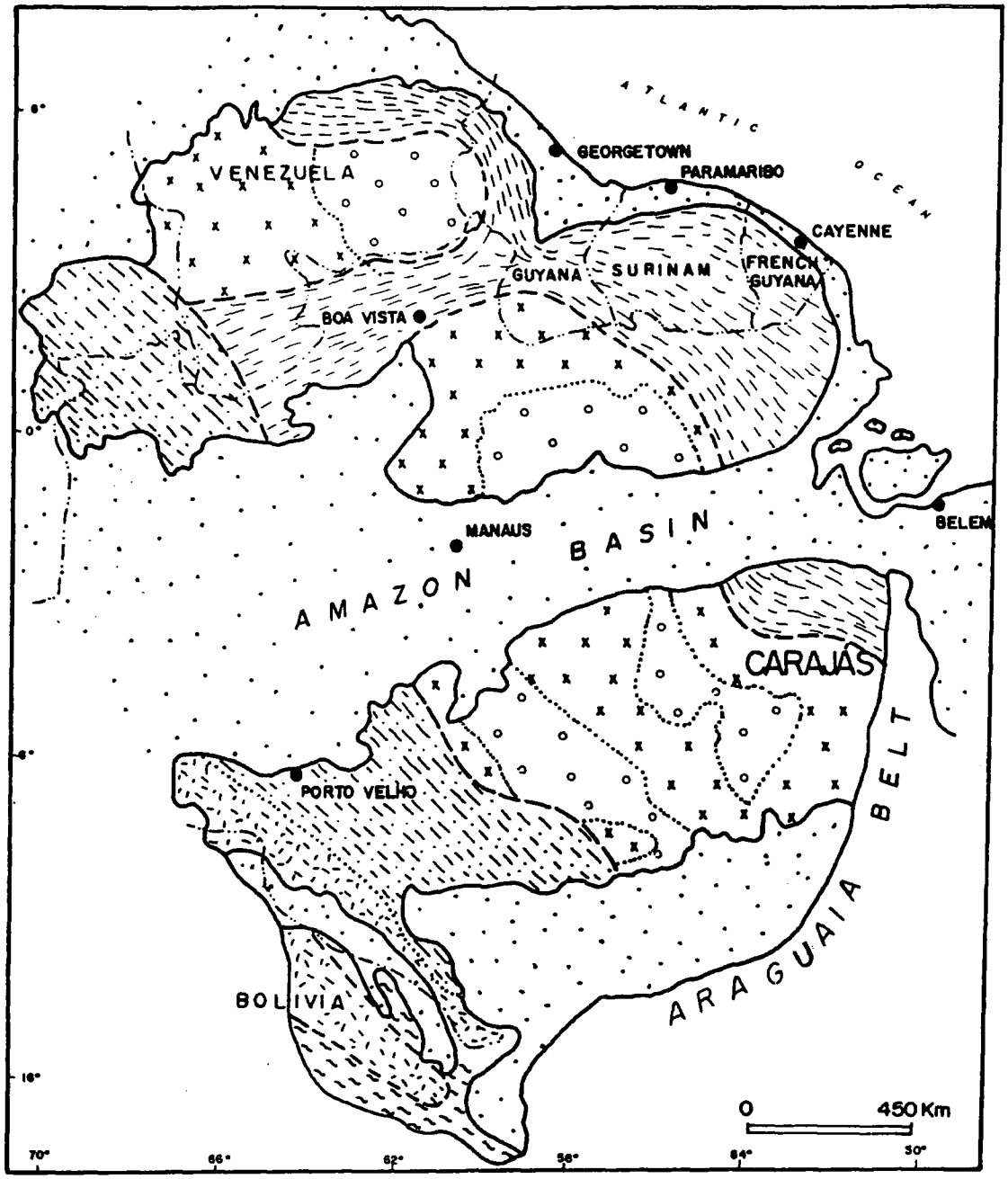

LEGEND

- Central Amazonian Province (>2.5Ga)
- Maroni-Itacaiúnas Mobile Belt (2.25-1.9Ga)
- Rio Negro-Juruena Mobile Belt (1.75-1.5Ga)
- Rondonian Mobile Belt (1.45-1.25Ga)
- Sunsas Mobile Belt (1.1-0.9Ga)
- Phanerozoic Sediments
- Proterozoic Covers

- Transition zone between belts
- Approximate contacts between belts
- National boundaries

After Teixeira *et al.* (1989)

Fig.3.3- The Cordani and Neves (1982) classification of Amazonian geotectonic domains.

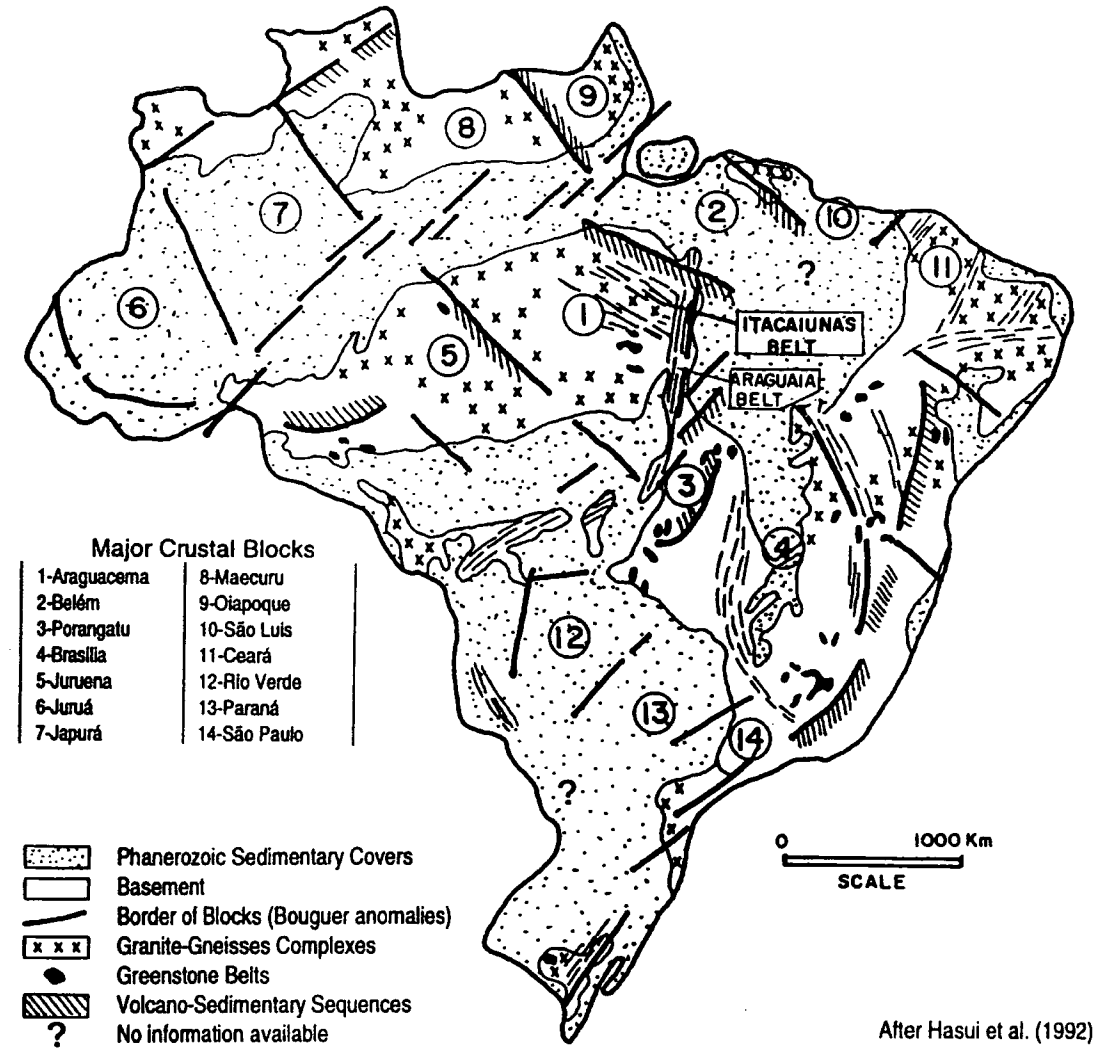

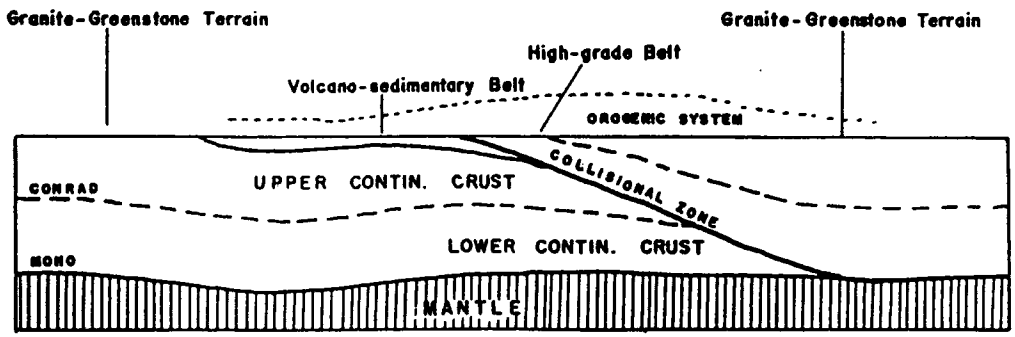

Fig.3.4- Major crustal blocks identified in Brazil by interpretation of geological and geophysical data, according to Hasui *et al.* (1984 and 1992). This model visualises the distribution of volcano-sedimentary belts, high-grade belts (granulites) and granite-greenstone terrains according to a plate tectonic model in which blocks boundaries are interpreted as Himalayan-type collision suture.

major discontinuities interpreted as Himalayan-type collision sutures often with triple junction arrays (Hasui *et al.*, 1984, 1992). In general, the borders of the main recognised blocks define positive gravity anomalies or strongly disturbed magnetic areas and, geologically, well defined linear belts of deformation and metamorphism (Fig.3.4). The nuclei of the crustal blocks are typically formed by both granite-gneiss terrains and greenstone belt sequences whilst border regions comprise zones of high grade rocks (granulites) together with sub-parallel belts of volcano-sedimentary sequences. These reveal a history of accretion of continental sialic terrains that were consolidated in northern Brazil prior to 1.8 Ga (Hasui *et al.*, 1984, 1992). In the Amazonian region, Hasui *et al.* (1984) define the Belém, Araguacema, Juruena and Porangatu blocks (Fig.3.4). The Itacaiúnas Belt, where Carajás is placed, and the Araguaia Belt are located close to the northeastern and eastern borders respectively, of the Araguacema block.

3.4- PREVIOUS WORK ON THE AMAZONIAN CRATON AND CARAJÁS REGION.

3.4.1- LITHOSTRATIGRAPHY AND AGES.

The Archaean rocks of the eastern Amazonian Craton, in the Carajás area, can be subdivided into three main categories (Fig.3.5): (1) High Grade Granite-Gneisses (HGGG); (2) Granite-Greenstone Belts (GGB) and (3) Low Grade Volcano-Sedimentary Supracrustals (LGVSS). All these units are present in the Central Amazonian Province (Cordani and Neves, 1982), forming parts of the Araguacema and Juruena blocks of Hasui *et al.* (1984). The Carajás area lies along the northern border of the Araguacema block close to its contact with the Belém block (Hasui *et al.*, 1984) .

The **High Grade Granite-Gneisses (HGGG)** include the Pium Complex (DOCEGEO, 1988), Xingu Complex (Silva *et al.*, 1974), several deformed and metamorphosed Archaean granitoids and a series of small isolated mafic-ultramafic intrusions (Fig.3.5).

The **Pium Complex** (DOCEGEO, 1988) refers to outcrops of granulites distinguished within the area of the larger Xingu Complex (see below), mainly along the southern part of the Serra dos Carajás region and in the northern

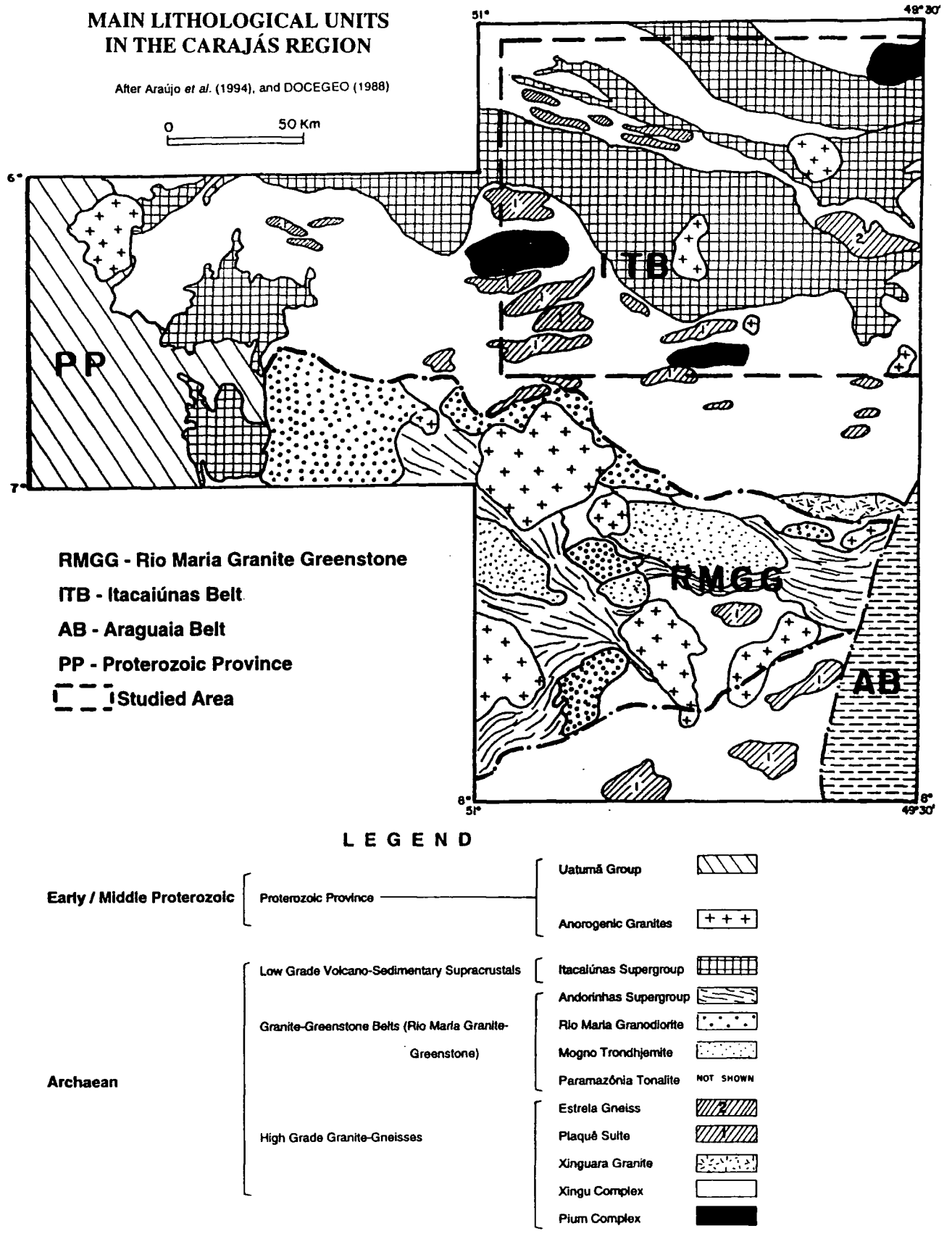

Fig.3.5- Geological map of the southeastern part of the Brazil Central Shield where Carajás is located, showing the distribution of the main lithological units.

part of the granite-greenstone belts (Fig.3.5). A Pb^{207}/Pb^{206} whole rock age of 3050±114 Ma is taken to date the metamorphism of these rocks (Rodrigues *et al.,* 1992). They display various types of contacts with the adjacent Xingu Complex, but most boundaries appear to be concordant within ductile shear zones (Araújo and Maia, 1991).

The **Xingu Complex** is an assemblage of tonalitic gneisses, with trondjhemites, granodiorites, granites and amphibolites (Silva *et al.,* 1974; Hirata *et al.*, 1982). They display a high grade of metamorphism with associated regional migmatization, and preserve evidence of heterogeneous polyphase ductile deformation. The age of the last episode of migmatization in these rocks is thought to be ca.2859±2 Ma (U/Pb in zircon; Machado *et al.*, 1988), whilst ages of 2519±04 Ma (U/Pb in zircon) are thought to indicate later overprinting tectono-thermal events (Machado *et al.*, 1991).

Several Archaean granitoids are recognised within the HGGG. They outcrop as isolated bodies of orthogneisses or deformed granite within the gneisses of the Xingu Complex or in association with the GGBs. One of the most important bodies forms the **Estrela Granite** (Barros, 1991; Araújo and Maia, 1991) outcropping in the eastern part of the Carajás region (Fig.3.5). An Rb/Sr (whole rock) age of 2527±34 Ma, is thought to date the main ductile event responsible for the predominant deformation fabric that overprints these intrusive rocks (Barros *et al.,* 1992*b*).

The **Plaquê Suite** (Araújo *et al.,* 1988) also called "Plaquê Estratóide Granite" by Araújo and Maia (1991) is a further group of small granitoid intrusions delimited within the HGGG (Fig.3.5). It forms several small linear E-W bodies outcropping within the Xingu Complex and is thought to be an example of a granitic rocks emplaced syntectonically during the main ductile deformation that took place in the HGGG (Araújo and Maia, 1991; Jorge João and Araújo, 1992). There are no radiometric age data concerning the emplacement of these rocks but geological mapping points to an Archaean origin (Jorge João and Araújo, 1992).

The **Xinguara Granite** is an isolated body of granodiorites and syenogranites outcropping north of the Rio Maria Granite-Greenstone Terrain (Fig.3.5; see below). It is an Archaean granite showing xenoliths of both the Xingu Complex and Rio Maria Granodiorite (Leite and Dall'Agnol, 1994).

The **Granite-Greenstone Belts (GGB)** are represented by well defined units located mainly in the southeastern region of the Central Brazil Shield, bounded to the north and south by the Xingu Complex and its associated belts (Fig.3.5). These Archaean rocks, in this region, known as the **Rio Maria**

Granite-Greenstone Terrain (Huhn *et al.*, 1988), form several belts of metamorphosed volcano-sedimentary sequences, surrounded by granites and gneisses. It is considered part of the nuclei of the Araguacema block (Hasui *et al.*, 1992; Costa *et al.*, 1995). The main lithostratigraphic units include the Rio Maria Granodiorite, the Mogno Trondhjemite, the Parazônia Tonalite and the Andorinhas Supergroup, a metamorphosed volcano-sedimentary sequence (DOCEGEO, 1988).

The **Rio Maria Granodiorite** forms a batholith of granodiorites and monzogranites intruded into tonalitic gneisses of the Xingu Complex (Fig.3.5; Souza *et al.*, 1990), although most contacts with these rocks presently lie within ductile shear zones (Leite and Dall'Agnol, 1994). U/Pb radiometric ages of 2876+13/-11 Ma (zircon), are thought to correspond to the probable age of intrusion (Macambira and Lancelot, 1992; Macambira and Lafon, 1994).

The **Mogno Trondhjemite** (DOCEGEO, 1988) forms another batholith delimited within the domains of the GGB in the south of Pará State (Fig.3.5). It is characterised by trondhjemites carrying xenoliths of ordinary granodiorite. A Rb-Sr whole rock age of 2880±60 Ma is thought to date its intrusion (Tassinari *et al*, 1987).

The **Paramazônia Tonalite** is another deformed pluton showing evidence of having been intruded into the Rio Maria Granodiorite and in the Mogno Trondhjemite (Pimentel and Machado, 1994).

The volcano-sedimentary sequences associated with the GGB are typified by the **Andorinhas Supergroup** (DOCEGEO, 1988). This unit comprises an interlayed sequence of metavolcanics, metasediments and metamorphosed mafic intrusions, including peridotites with spinifex texture, that underwent greenschist facies metamorphism. The metasediments are typically pelitic schists and quartzites. These rocks were, in part, affected by the deformation responsible for the development of the Itacaiúnas Belt (see below) during the Archaean (Araújo and Maia, 1991). The U/Pb (zircon) isochrons of 2979±5 from felsic rocks present in these sequences have been interpreted as a minimum age of formation (Pimentel and Machado, 1994).

The relative age relationship between the units forming the Rio Maria Granite-Greenstone Terrain are not well defined (Pimentel and Machado, 1994) but it is known that the Xinguara Granite cuts the tonalitic gneisses of the Xingu Complex (Leite and Dall'Agnol, 1994) whist the Rio Maria Granodiorite is thought to form the regional basement to the greenstone belts and that both are cut by the Mogno Trondhjemite (Souza *et al.*, 1990). On the other hand, Costa

et al. (1995) suggest from field evidence that the Mogno Trondhjemite may form part of the greenstone belt basement.

The **Low-Grade Volcanic and Sedimentary Sequences (LGVSS)** are represented in the Central Brazil Shield, along the Carajás region, by the rocks of the **Itacaiúnas Supergroup** and several later sedimentary cover sequences (Fig.3.5). In the Itacaiúnas Belt, they include the **Igarapé Salobo Group**, the **Igarapé Pojuca Group**, the **Grão Pará Group**, the **Igarapé Bahia Group** and the **Buritirama Group** (DOCEGEO, 1988). According to Araújo *et al.* (1988) and supported by several other authors (Araújo and Maia, 1991; Araújo and Costa, 1994; Araújo *et al.*,1992), all these rocks were deposited in a series of small fault-bounded basins related to regional strike-slip movements.

Other sequences include the clastic sedimentary rocks of the **Rio Fresco Group** (Cunha *et al.*,1984; DOCEGEO, 1988) or **Águas Claras Formation** (Araújo and Maia, 1991; Nogueira, 1995), and the **Gorotire Formation** (e.g. Hirata *et al.*, 1982). Almost all of these units were poorly defined in the Carajás region and have been the focus of several controversies (see below).

Several suites of Early to Middle Proterozoic granitic plutons (**anorogenic granites**) cut almost all the rocks of the LGVSS and the older basement (Fig.3.5). These include, the Central Carajás Granite (1880±2 Ma), the Cigano Granite (1883±2 Ma), The Seringa Granite (1710±40 Ma), the Parauari Granite (1902±39 Ma), the Musa Granite (1883±2 Ma), the Jamon Granites (1601±21 Ma) and several other, less important bodies spread along the Brazil Central Shield (Gomes *et al.*, 1975; Dall'Agnol *et al.*, 1986; Machado *et al.*, 1988 and 1991; Macambira *et al.*, 1992).

Rocks younger than the Early Proterozoic are relatively minor in the Carajás region, apart from a kilometre-scale thick sequence of volcanic and sedimentary rocks known as the **Uatumã Group** (Silva *et al.*, 1974). These rocks are thought to be Middle Proterozoic in age, based on tectonic and stratigraphic evidence (Costa *et al.*, 1993*b*; Macambira *et al.*, 1994). They comprise sequences of andesites and rhyolites interbedded with clastic sedimentary rocks occupying an area of around 3500 km^2, located west of the area studied (Fig.3.5), forming the **Proterozoic Province**.

The Palaeozoic is poorly represented in the region with a few outcrops of sedimentary rocks, correlated with the Silurian and Devonian of the Parnaíba Intracratonic Basin, present in a small graben which occur along the eastern and southeastern margin of the shield and the Araguaia Belt. These rocks have

been contradictorily referred to a Precambrian age, correlated to the so-called Rio Fresco Group (e.g. DOCEGEO, 1988).

The Cainozoic is represented by the development of a widespread lateritic crust and by the deposition of alluvial and colluvial sediments. They are associated with the establishment of a Cretaceous peneplain surface, which still strongly influences the present-day topography and drainage patterns (Assad and Beisiegel, 1978; Bemerguy and Costa, 1991).

Since the first geological surveys took place in the Carajás region (e.g. Rêgo, 1933; Barbosa *et al.*, 1966; Knup, 1971), a proliferation of terminology and often controversial proposals have been made with regard to the stratigraphy of the rocks in the area. Figures 3.6 and 3.7 show some of the published stratigraphic sequences in the Carajás area during the 1980s. The flow chart (Fig.3.8) tries to show the complex relationships between the various stratigraphic terminologies proposed for the region, since the reconnaissance of the Grão Pará Group by Rêgo (1933). The lack of consensus concerning names and stratigraphical position of the rocks has become a considerable problem. A detailed discussion of this confusing evolution of nomenclature is not necessary, but some of the major problems will be discussed in section 3.5, in this chapter, and together with a revised stratigraphy which is proposed in Chapter 8.

3.4.2- PREVIOUS TECTONIC MODELS.

The **Itacaiúnas Belt** forms one of the main geotectonic features in the eastern Amazon, covering a large area (ca. $6x10^4$ km^2) in the NE part of the Central Brazil Shield (Fig.3.9). It affects rocks associated with the Xingu and Pium complexes and supracrustals of the Itacaiúnas Supergroup amongst others. It is thought to be an Archaean belt of ductile deformation that is placed to the north of the Rio Maria Granite-Greenstone Terrain according to Araújo *et al.*, (1994), and which follows the general E-W trend. To the east, it is cut by the Late Proterozoic Araguaia Belt (Hasui *et al.*, 1981, in Hasui and Costa, 1990; Araújo and Maia, 1991), whilst to the west, the belt is overlain by Middle Proterozoic volcano-sedimentary sequences (Proterozoic Province). To the north it is covered by Phanerozoic sediments.

Previous workers have subdivided the regional structure of the Itacaiúnas Belt into two domains (Fig.3.9): (1) a set of imbricate thrusts (shear zones), that are associated with (2) large-scale strike-slip structures, both with

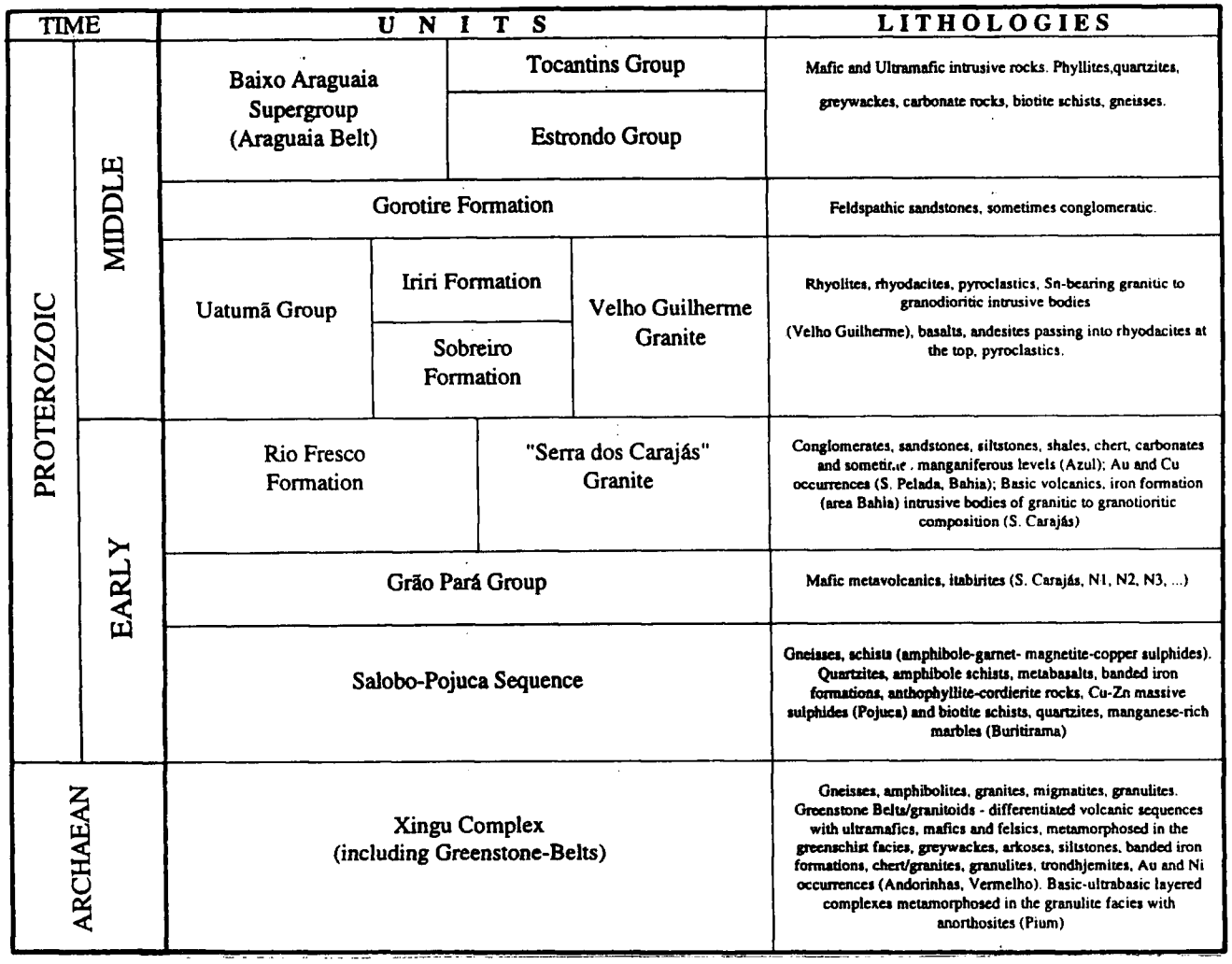

After Hirata *et al.* (1982)

Fig.3.6- An early stratigraphic column proposed by Hirata *et al.* (1982) for the rocks of the Carajás region.

LITHOSTRATIGRAPHIC UNITS OF THE CARAJÁS REGION
(After Meireles *et al.*,1984 ; DOCEGEO,1988 ;Araújo *et al.*,1988)

ERA	PERIOD	MEIRELES *ET AL.* (1984)	DOCEGEO (1988)	ARAÚJO *ET AL.* (1988)
MESOZOIC	JURASSIC	"Santa Inês" Gabro		
PROTEROZOIC	Late		Acid and basic dykes	
PROTEROZOIC	Middle	Uatumã Group: Iriri Formation Sobreiro Formation		
PROTEROZOIC	EARLY	Rio Fresco Formation: "Granito Central de Carajás"	Granites: Carajás, Cigano, and others.	Post-Tectonic Intrusive Granites
PROTEROZOIC	EARLY	Grão Pará Group: Superior Formation Carajás Formation Parauapebas Formation	Santa Inês Gabbro Rio Fresco Group	Post-Tectonic Ultramafic Intrusions
PROTEROZOIC	EARLY	Salobo Pojuca Sequence Estrela Granite	ITACAIÚNAS SUPERGROUP: Estrela Granite	
PROTEROZOIC	EARLY		ITACAIÚNAS SUPERGROUP: Buritirama Group / Igarapé Bahia Group — Sumidouro Formation Grota do Vizinho Formation	Plaquê Suite
ARCHAEAN		XINGU COMPLEX AND GREENSTONE BELTS	ITACAIÚNAS SUPERGROUP: Grão Pará Group — "Paleovulcânica Superior" Formation Carajás Formation Parauapebas Formation	Grão Pará Group: Águas Claras Formation Carajás Formation Parauapebas Formation
ARCHAEAN			ITACAIÚNAS SUPERGROUP: Igarapé Salobo Group / Igarapé Pojuca Group — Cinzento Formation Três Alfa Formation Cascata Gneiss — Corpo Quatro Formation	Sapucaia Group
ARCHAEAN			Luanga / Serra Azul Complex	Estrela Gneiss
ARCHAEAN			Xingu Complex	Xingu and Pium Complex
ARCHAEAN			Andorinhas/ Sa. do Inajá Supergroup: Lagoa Seca/ Rio Preto/Babaçu/ Santa Lúcia Groups — Pium Complex	

Fig.3.7- A comparison of three different stratigraphic proposals for the Carajás area, suggested by different authors, which shows the evolution of ideas during the 1980s.

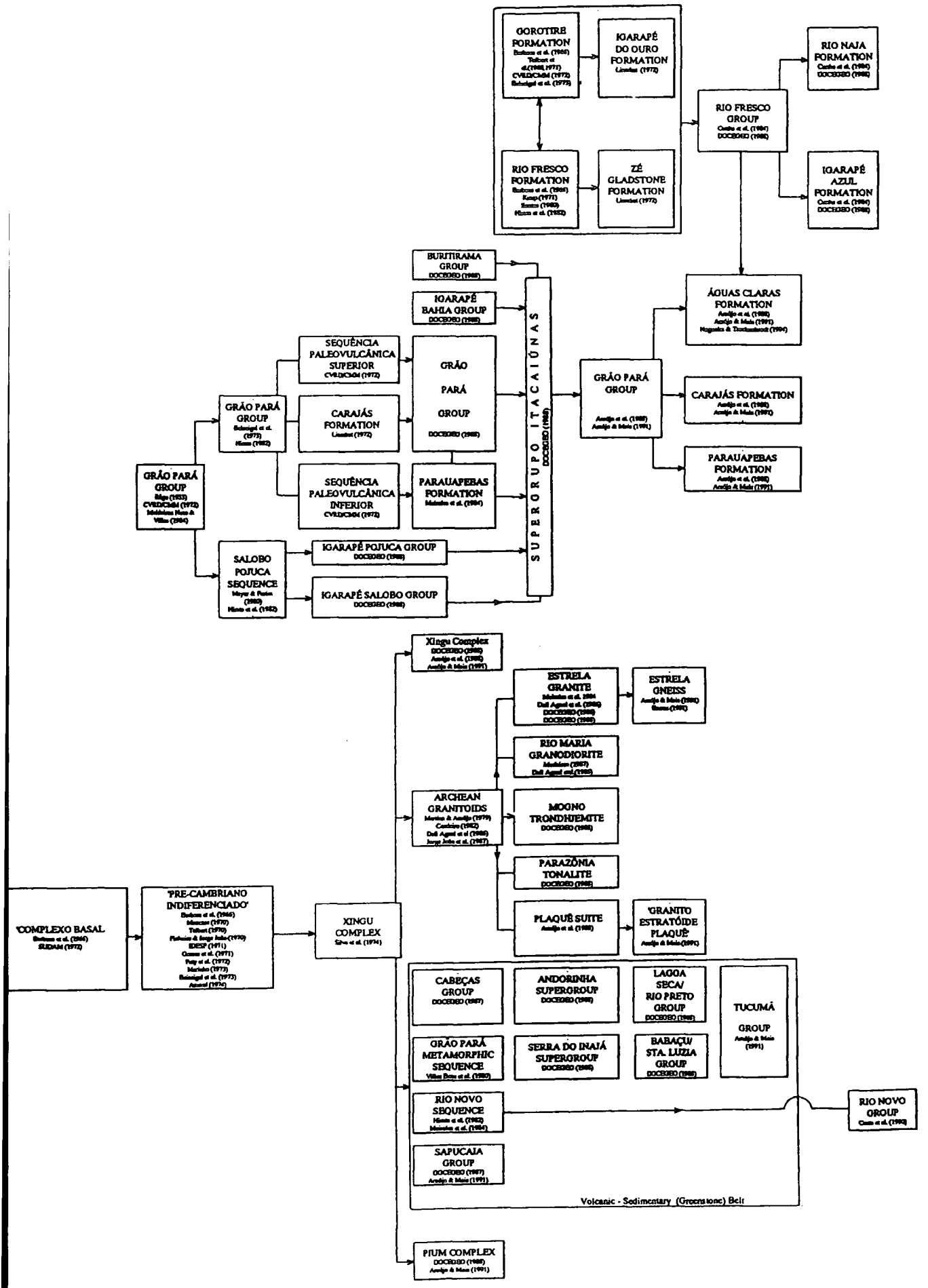

Fig.3.8- See next page.

Fig.3.9 - Flow chart showing the evolution of the names of the main Archaean/Proterozoic units suggested in the Carajás region. The Xingu Complex was first identified as "Complexo Basal" by Barbosa *et al.* (1966) and SUDAM (1972). This unit was referred to as "Pre-Cambriano Indiferenciado" by several authors from 1966 to 1974. In 1974 Silva *et al.* suggested the name Xingu Complex. More detailed mapping allowed separation of smaller sub-units (the Pium Complex, several Archaean Granitoids and granite-greenstone terrains).

The Grão Pará Group was first mentioned by Rêgo (1933). The name was used later by several other authors, and was sub-divided (Beiseigel *et al*, 1973) into three sub-units (Sequência Paleovulcânica Inferior, Carajás Formation and Sequência Paleovulcânica Superior). Meyer and Farias (1980) separated the Salobo-Pojuca Sequence from the Grão Pará Group, and it was later sub-divided into the Igarapé Pojuca Group and the Igarapé Salobo Group, by DOCEGEO (1988). Also in 1988, DOCEGEO replaced the "Sequência Paleovulcânica Inferior", suggesting the name Parauapebas Formation (introduced earlier by Meireles *et al.*, 1984) whilst the Grão Pará Group was used to name the Carajás Formation and the "Sequence Paleovulcânica Superior". New names were suggested to describe newly discovered and apparently different rocks outcropping in the region, such as the Igarapé Bahia Group and the Buritirama Group. All these units were placed in the Itacaiúnas Supergroup (DOCEGEO, 1988). In the same year, Araújo *et al.* (1988) suggested that the rocks called Itacaiúnas Supergroup by DOCEGEO (1988) should be called the Grão Pará Group, which was subdivided into the Parauapebas Formation, the Carajás Formation and the Águas Claras Formation. This proposal was later supported by Araújo and Maia (1991) and by several other authors (e.g. Costa *et al.*,1995). The name Águas Claras Formation replaces the Rio Fresco Group proposed previously by Cunha *et al.* (1984). This unit derives from several earlier names (Gorotire Formation, Barbosa *et al.*,1966; Rio Fresco Formation, Barbosa *et al.*,1966).

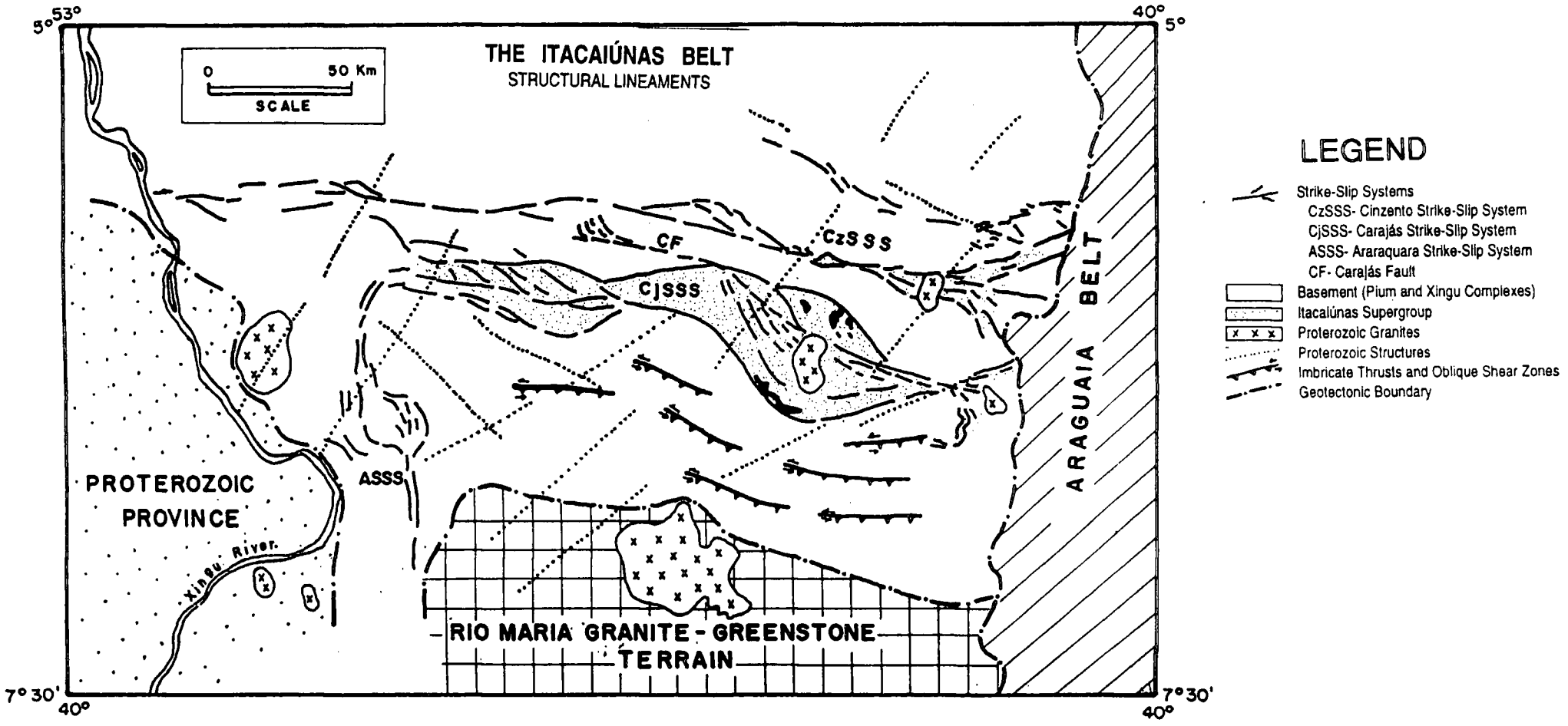

Fig.3.9- Structural map of the Itacaiúnas Belt according to Araújo and Maia (1991); Macambira *et al.* (1994) and Costa *et al.* (1994a). It is limited to E by the Araguaia Belt, to W by the Proterozoic Province and to the S by the Rio Maria Granite-Greenstone Terrain. Three major strike-slip systems are identified along the Itacaiúnas Belt lying to the north and west of the imbricate thrusts. To the north the Itacaiúnas Belt is covered by Phanerozoic sedimentary rocks.

an E-W general trend (Araújo *et al.*, 1988; Araújo and Maia, 1991; Araújo *et al.*,1992; Costa *et al.*, 1994*a*; Costa *et al.*, 1995). The imbricate thrusts (shear zones) are thought to affect mainly rocks of the basement, especially the Xingu and Pium complexes, forming ductile shear zones in which syn-tectonic granitoid emplacement occurs, e.g. the Plaquê Suite (Araújo and Maia, 1991; Jorge João and Araújo, 1992). To the north and west, three strike-slip fault systems cut the basement rocks (Fig.3.9). They are (1) the Carajás Strike-Slip System including the Carajás Fault (Araújo and Maia, 1991; Costa *et al.*, 1994*a*); (2) the Cinzento Strike-Slip System (Costa and Siqueira, 1990; Siqueira and Costa, 1991), both with a general E-W trend, and (3) the Araraquara Strike-Slip System (Macambira *et al.*, 1994; Costa *et al.*, 1994*a*) which cuts the basement in the west of the region, with a N-S trend (Fig.3.9).

According to the published literature, at least two main Archaean tectonic episodes are recognised during the development of these strike-slip systems (Araújo *et al.*, 1988 ; Siqueira, 1990; Araújo and Maia, 1991; Costa *et al.*, 1994*a*; Macambira *et al.*,1994; Costa *et al.*, 1995). The first is thought to be related to a dextral transtensional movement, affecting the basement, producing localised areas of subsidence adjacent to curved and offset segments of the major strike-slip faults. Araújo *et al.* (1988), followed by several other authors, suggested that a number of small separate basins developed, each of which was infilled by volcanic and sedimentary rocks. Subsequent tectonic inversion is thought to have occurred during at least one later phase of sinistral transpressional displacement along the main shear zones, both in the Carajás Strike-Slip System and in the Cinzento Strike-Slip System (Araújo *et al.*, 1988; Costa *et al.*, 1990; Siqueira, 1990; Costa and Siqueira, 1990; Siqueira and Costa, 1991; Araújo and Maia, 1991; Costa *et al.*, 1992; Araújo *et al.*, 1992; Costa *et al.*, 1993*b*; Araújo and Costa, 1994; Macambira *et al.*, 1994; Costa *et al.*, 1995). In the Cinzento Strike Slip System, a later dextral transtension has been proposed and is thought to overprint several later transpressional structures (Costa *et al.*, 1991; Siqueira, 1990; Siqueira and Costa, 1991).

All these episodes of deformation are thought to have been formed during a single oblique collision between the Araguacema and the Belém blocks at the end of the Archaean (Costa *et al.*,1995).

Using radiometric data, Machado *et al.* (1991), suggested ages of 2.77-2.73 Ga and 2.58-2.49 Ga (U-Pb zircon) for two extensional episodes affecting the rocks in the Itacaiúnas Belt. According to these authors the first age interval corresponds to a transtensional reactivation responsible for the deposition and

emplacement of volcanic-sedimentary rocks forming the upper sequence of the Itacaiúnas Supergroup (DOCEGEO, 1988), while the second age refers to a consecutive extensional event that took place along all the Itacaiúnas Belt. The direct correlation between these ages and the model proposed by Araújo *et al.* (1988) Araújo and Maia (1991) is not clear.

The **Carajás Fault** (Silva *et al.*,1974) forms one of the most prominent tectonic feature in the region, trending diagonally across the Carajás Strike-Slip System from NW to SE (Fig.3.9). It has been interpreted as a "P" sinistral shear zone thought to have formed during later displacements within the evolution of the Carajás Strike-Slip System (Gouvêa, 1990; Araújo and Maia, 1991; Costa *et al.*, 1995). A major bend in the Carajás Fault trace, from an E-W to NW-SE direction, has led several authors to postulate the existence of a transpressional duplex located in the central area of the Carajás Strike-Slip System, affecting mainly the sedimentary rocks present in this region (Gouvêa, 1990; Pinheiro *et al.*, 1991). The age of this fault is constrained to lie between 2.6 Ga (age of the mafic dykes cutting clastic sedimentary rocks cut by the fault; Dias *et al.*,1996*a*) and 1.8 Ga (age of the Central Carajás Granite which cuts the fault; Wirth *et al.*,1986).

According to Araújo *et al.* (1988) and Araújo and Maia (1991) fault bend and offset regions in these strike-slip systems are filled with rocks of the Grão Pará Group, formed by three major sequences comprising volcanic rocks (Parauapebas Formation), banded iron formations (Carajás Formation) and clastic sedimentary rocks (Águas Claras Formation). All units are associated with the Carajás Strike-Slip System, and lie unconformably the basement rocks. The results of more recent studies of the Águas Claras Formation suggest that these rocks were not deposited in isolated basins formed during transtension but it is proposed instead that there was just one large basin that originally covered an area much larger than the size of the presently exposed Carajás Strike-Slip System (Nogueira *et al.*, 1992; Nogueira and Truckenbrodt, 1994; Nogueira *et al.*, 1994; Nogueira, 1995; Nogueira *et al.*, 1995; Pinheiro and Holdsworth, 1997*a*). This means that the Grão Pará Group (as proposed by Araújo *et al.*, 1988) would have been laid down in an older, now largely eroded basin, fragments of which are preserved in releasing bends and offsets formed during early dextral displacements along the Carajás Strike-Slip System.

To the west the Carajás Strike-Slip System appears to join onto a N-S set of faults called the Araraquara Strike-Slip System (Macambira *et al.*,1994; Costa *et al.*,1994*a*). This structure is also supposed to be composed of small basins filled with volcanic and sedimentary rocks and the N-S faults have been

interpreted as a set of antithetic structures related to the Carajás Strike-Slip System. They are relatively little studied, however, and their exact significance and structural age are uncertain.

The Cinzento Strike-Slip System (Fig.3.9) lies sub-parallel and to the north of the Carajás Strike-Slip System. It is marked by a supposed strike-slip "horse-tail" structure at its eastern termination, branching from the main E-W sinistral shear zone (Siqueira, 1990; Costa and Siqueira, 1990; Siqueira and Costa, 1991). This region is thought to preserve a complex history of transtensional and transpressional reactivation (Siqueira, 1990). The Cigano Granite (ca.1.8 Ga; Machado *et al.,* 1988) was emplaced along this fault system, cutting the major structures.

The end of the Early Proterozoic, beginning of the Middle Proterozoic is marked in the Carajás region and throughout the Amazonian Craton by an important extensional event responsible for the emplacement of several anorogenic granitic bodies and, dykes together with deposition of clastic sequences (see section 4.7 in the Chapter 4, and Chapter 7). This extension is related to the development of sets of NE-SW- and NW-SE-trending faults (Fig.3.9 and 3.10) which affect both the basement and parts of the supracrustal cover sequences, controlling the deposition of widespread volcanic and sedimentary sequences in grabens, through the Amazonian Craton as shown in Fig.3.10 (Isller *et al.*, 1985; Dall'Agnol *et al.,* 1986; Gonçalez *et al.,* 1988; DOCEGEO, 1988; Costa *et al.,* 1991; Costa and Hasui, 1992; Costa *et al.*,1995). The Uatumã Group which outcrops mainly at the west end of the Itacaíunas Belt is also postulated to be related to the Middle Proterozoic extension (Costa *et al.*,1995).

The main NW-SE faults present in Carajás are thought to be extensional faults forming graben and half-graben, whilst the NE-SW sets show predominantly strike-slip displacements consistent with an origin as transfer faults during a regional NE-SW extension (Costa *et al.,* 1991; Costa and Hasui, 1992). Basic dyke swarms display NE and NW trends and are thought to be related to this same episode, affecting the Amazonian Craton on a regional scale (Sial *et al.*, 1987; Teixeira, 1990).

Basic dykes, mainly tholeiitic dolerites of Permo-Triassic age, are present in the Carajás region and are widespread in the Central Brazil Shield, Guyana Shield and Amazon Basin (Sial *et al.,* 1987; Choudhuri *et al.*, 1990; Oliveira and Tarney, 1990). Their trends appear to be strongly affected by the orientations of pre-existing basement anisotropies.

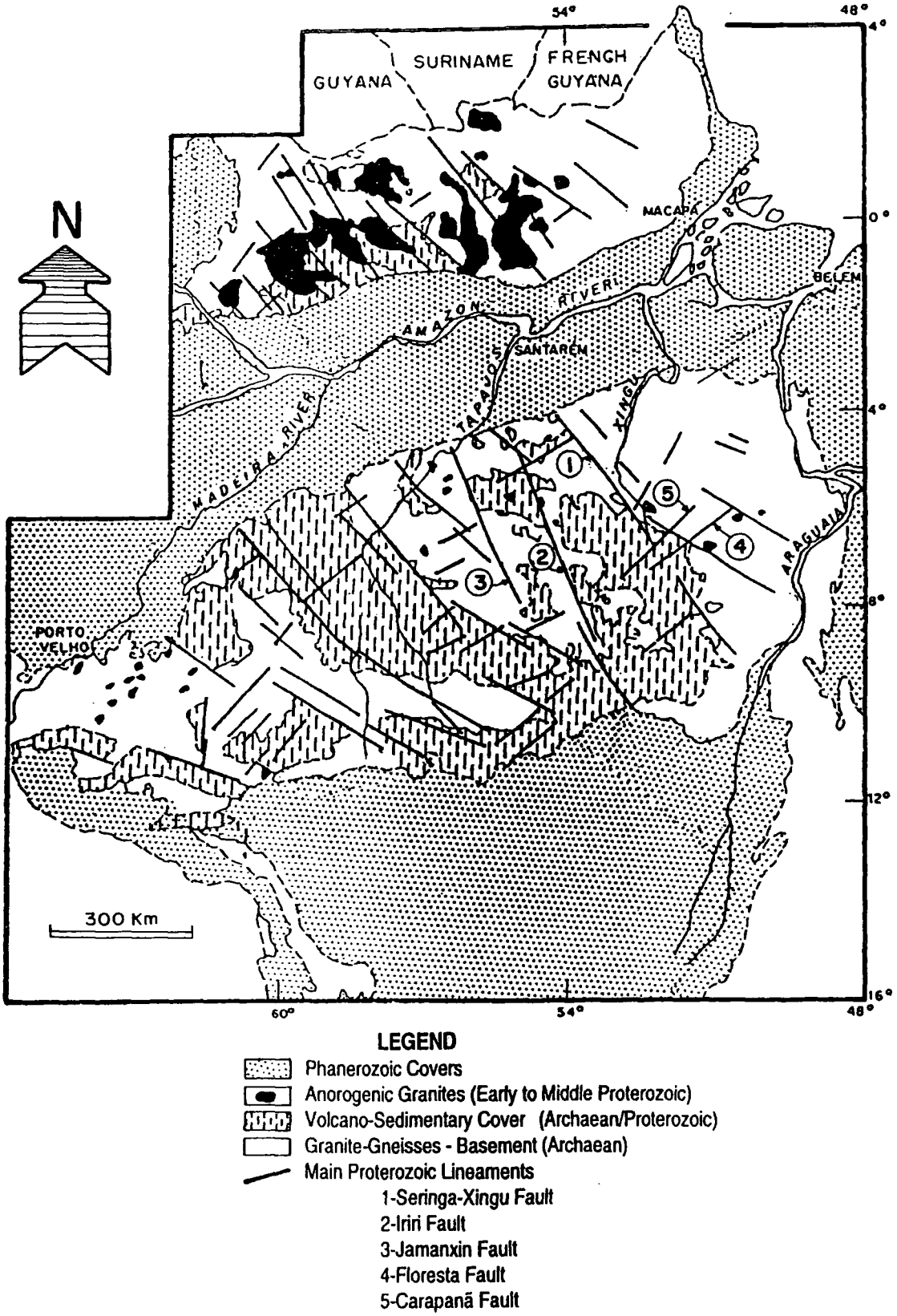

Fig.3.10- Geotectonic map of the Amazonian Craton highlighting the distribution of granite-gneiss rocks, volcano-sedimentary covers and anorogenic granites in contrast with Phanerozoic Covers. The NE-SW Proterozoic lineaments are interpreted as extensional faults whilst those NW-SE are thought to represent transfer faults (after Costa *et al.*, 1991).

According to the existing literature, at least two neotectonic events affected the Amazonian Craton during the Tertiary (Miocene-Pliocene) and Quaternary (Costa *et al.,* 1994*b*). The evidence of these events are rather obscure in Carajás and are the subject of recent studies. Preliminary conclusions point to probable extensional reactivation ("*resurgent tectonics*") of older E-W lineaments during the Tertiary and Quaternary (Costa *et al.,* 1994*b*).

Using seismological data for the Amazonian Region it is possible to identify a set of epicentres (younger than 1990) located along the Carajás region (Fig.3.11). The presence of these seismic zones have been associated with recent reactivation taking place at the border of the Belém and Araguacema blocks (Costa *et al.*,1993*a*).

3.5- A CRITICISM AND DISCUSSION OF PREVIOUS WORK.

The Itacaiúnas Belt (Araújo *et al.,* 1988) is undoubtedly the most important geotectonic feature in the Carajás area. The tectonostratigraphy of this belt is still poorly defined despite the relatively large volume of published works concerning these rocks. Problems have arisen because the criteria used to define stratigraphical units have not been agreed and a proliferation of different names for the same units or the use of the same name for different units has occurred. Furthermore, boundaries of units are often poorly defined or are entirely conjectural. There could be two main explanations for these problems: (1) more than 80% of the rocks are very poorly exposed or hidden by dense rain forest and soil cover; and, (2) the effects of deformation have variably disrupted the stratigraphical sequences and their primary relationships in the region. As new mines, roads and communities are established in the area, more exposures have been revealed.

In many ways, some of the earlier stratigraphical sequences proposed for the Carajás region (e.g. Hirata *et al.,* 1982; Meireles *et al.,* 1984), are both reasonable and objective basic accounts of the relationships between different rock units outcropping in the area. This contrasts sharply with the more complex and confused nomenclature that has arisen subsequently, especially after the end of the 1980s.

The DOCEGEO (1988) lithostratigraphic column (Fig.3.8) reflected an attempt to organize the large volume of information obtained by company geologists working in this region for more than 20 years, and it is still one of the most cited accounts concerning the geology of the Carajás region. The main

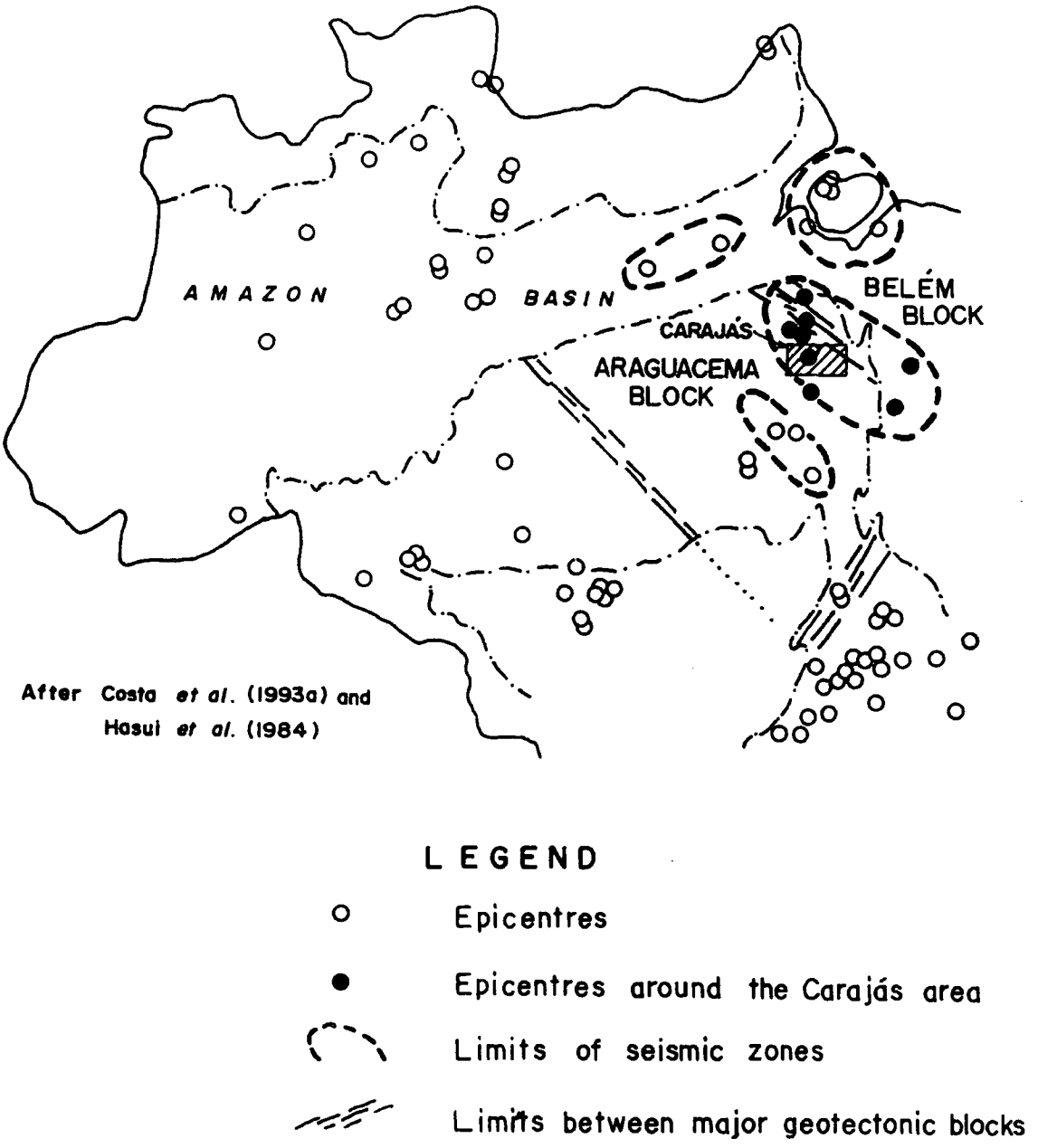

Fig.3.11- Distribution of epicentres of small-scale earthquakes in the Amazonian region. A well defined seismic zone is pointed out around the Carajás area, interpreted as recent movements of the Belém and Araguacema blocks (Data till 1990; after Costa *et al.*,1993a and Hasui *et al.*,1984).

criticisms of these proposals are (1) the apparent lack of any supporting structural data and (2) that it establishes a complex set of new stratigraphic names for units based only on lithological mapping in widely separated and isolated areas where the company has operated its mines. Thus, new names such as "Corpo Quatro Formation", "Buritirama Group", "Igarapé Bahia Group" and so on, reflect more the volume of information collected by the company at various locations and there is little actual attempt to rigorously correlate units to establish a regional stratigraphy.

The stratigraphical sequence proposed by Araújo *et al.* (1988) suggests a rather different account of the Carajás region (Fig.3.7), and was based on the results of a regional mapping project. This sequence (see Fig.3.11) was later recast by Araújo and Maia (1991) and both related the stratigraphy to an oblique-slip tectonic model for the Itacaiúnas Belt. This regional scale model correctly emphasises the strong tectonic influence on the geological evolution and distribution of rock units in the Carajás region, but can be criticised for its lack of detailed stratigraphy and structural data.

Several important facts emerge from these two first attempts at regional correlation of units and events:

1) The temporal and structural relations between the structurally complex component rock units forming the Rio Maria Granite-Greenstone Terrain are not yet known (DOCEGEO, 1988). Their relation to the Xingu Complex is also uncertain. Some advances have been made following accurate radiometric age determinations and detailed geological mapping of rock units of these regions, but there are still many uncertainties (Souza *et al.*,1990; Macambira *et al.*, 1991; Machado *et al.*,1991; Macambira and Lancelot, 1992; Ferreira Jr, 1993; Macambira and Lafon, 1994; Costa *et al.*,1994*a*; Araújo *et al.*,1994).

2) The initially large outcrop area of the Xingu Complex has progressively reduced as new mapping and associated studies have revealed new units and subdivisions. The temporal relationship between most of these subunits is not well established and the solution involves systematic geological mapping supported by isotopic dating.

3) Hutchinson (1979) originally suggested that the sedimentary and volcanic rocks of the Salobo, Pojuca and Grão Pará groups were all different facies of the same volcano-sedimentary sequence. However, in detail, the stratigraphical and structural relationships between the Igarapé Salobo Group / Igarapé Pojuca Group / Igarapé Bahia Group / Grão Pará Group are poorly defined and uncertain. Petrological and geochemical studies by Medeiros Neto

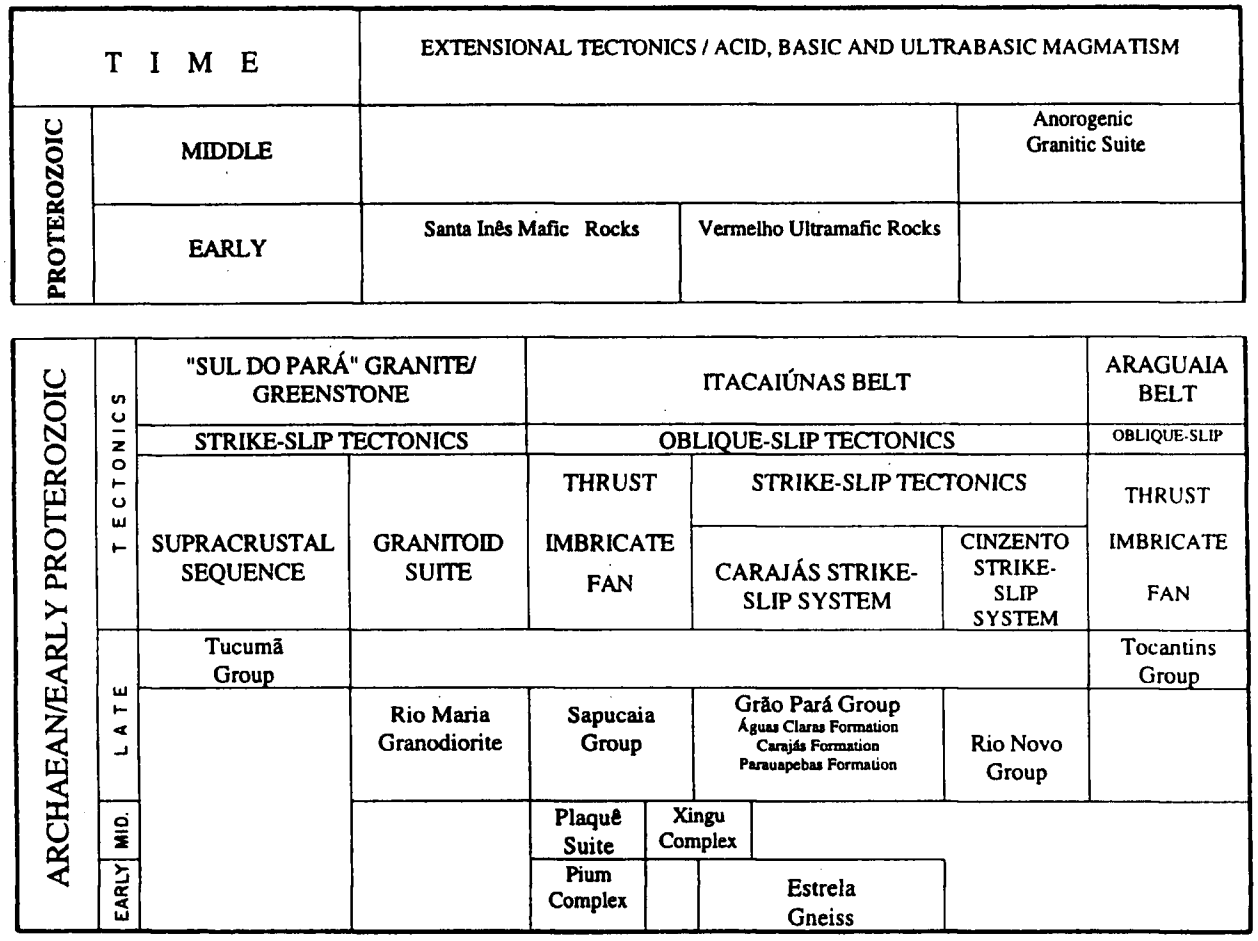

Fig.3.12- Tectonostratigraphic colunm for the Carajás region proposed by Araújo and Maia (1991).

and Villas (1984) and Medeiros Neto (1985) were used to suggest a "lithological similarity" between the "Salobo Sequence" (later called Igarapé Pojuca Group by DOCEGEO, 1988), defined by Hirata *et al.* (1982), and the volcanics of the Grão Pará Group. Ferreira Filho *et al.* (1987) then used geochemical and petrological studies to suggest a correlation between the "Bahia Sequence" (DOCEGEO, 1988) and the Grão Pará Group. Araújo *et al.* (1988) suggested a correlation between all these units assigning all of them to the Grão Pará Group. They used the argument that these units were all affected by the same tectonic event. Lindenmayer and Fyfe (1992), used geochemical analysis (LILE and FeO%) to suggest that the continental tholeiitic basalts of the Parauapebas Formation (Grão Pará Group) and Igarapé Salobo Group, corresponded to the same magmatic event. Conversely Machado *et al.* (1988) correlated the rocks of the Igarapé Salobo Group with parts of the Xingu Complex based on radiometric dating studies. So the problem concerning the similarities and differences between these units still remains.

4) Various sequences of clastic sedimentary rocks are recognised overlying the volcanics and ironstones of the Grão Pará Group and the Xingu Complex basement in several places along the Carajás region (e.g. Tolbert *et al.,* 1968; Knup, 1971; Liandrat, 1972; Beisiegel *et al.,* 1973). Several authors have suggested different names for different clastic sequences or have incorrectly correlated these sequences to distinct units. For example, DOCEGEO (1988) placed all clastic sedimentary rocks present in Carajás into the Early Proterozoic Rio Fresco Group. It is evident that more than one unit is present, according to these earlier studies. Conversely, Araújo *et al.* (1988) referred to these rocks as the Águas Claras Formation, which they considered to be a sub-unit of the Archaean Grão Pará Group. This problem has been clarified more recently by Nogueira *et al.* (1994) and Nogueira *et al.* (1995) who have used detailed stratigraphical and sedimentological studies in association with structural data to study this unit. They showed that the Águas Claras Formation is younger than the Grão Pará Group. Its age is uncertain and it is only constrained by a minimum relative age of the cross-cutting ca.1.8 Ga Central Carajás Granite and an age of ca. 2.6 Ga to sills intruded in this unit (Dias *et al.,*1996*a*).

Other different clastic rocks occur around the region but are not well understood from the sedimentological and stratigraphical point of view.

5) The initial structural studies of Beisiegel *et al.* (1973) suggested that the regional structure in the Carajás region was a single large-scale faulted synclinorium. Based on the interpretation of satellite and radar images, together

with regional-scale fieldwork, Araújo *et al.* (1988) proposed a "flower structure" model to represent the geometry of these rocks. This was based on the development of a series of braided and anastomosing features that are associated with prominent E-W trending lineaments in the Itacaiúnas Belt and supported by an apparent convergence of the planar structures inside the fault system, on a regional scale. The suggested existence of several small basins originally sited along dilational bends and jogs of dextral strike-slip faults (Araújo *et al.,* 1988; Costa and Siqueira, 1990; Araújo and Maia, 1991; Araújo *et al.,* 1992) remains conjectural, whilst Wirth (1986), Nogueira *et al.* (1992), Nogueira *et al.,* (1994) and Nogueira (1995) have shown that for the Grão Pará Group and Águas Claras Formation that there is no petrological or sedimentological evidence to support deposition of these rocks in pull-apart-type basins.

6) Systems of oblique thrusts and reverse shear zones related to the transpressional sinistral episode of tectonic inversion are referred to by several authors as affecting rocks of a large area of both basement and cover rocks (Araújo *et al.,* 1988; Costa and Siqueira, 1990; Araújo and Maia, 1991; Araújo *et al.,* 1992). However their existence has never been conclusively proven by detailed field studies and have been supported only by little data collected sparsely around a large area.

7) The types, distribution, grade and ages of metamorphism affecting the supracrustal sequences are problematic and poorly known. Mineralogical assemblages and textures in the ironstones, sandstones, mudstones and volcanic rocks of the Carajás region are thought by many authors to be indicators of low metamorphic grades. However, the situation is still unclear since later hydrothermal alteration is regionally widespread (Suszynski, 1972; Beisiegel *et al.,* 1973; Macambira *et al.,* 1990). Conversely, supracrustal assemblages from the Salobo region are clearly affected by metamorphism up to upper amphibolite facies (DOCEGEO, 1988; Lindenmayer, 1990). The significance of these differences is unclear even though some supracrustal units of markedly different grade have been stratigraphically correlated by some authors (e.g. Araújo and Maia, 1991).

The foregoing discussion illustrates that some re-organisation of the contradictory and confused nomenclature in the published literature is required. The tectonostratigraphic framework followed in this work is shown in Fig.3.13. This choice will be explained in the subsequent chapters.

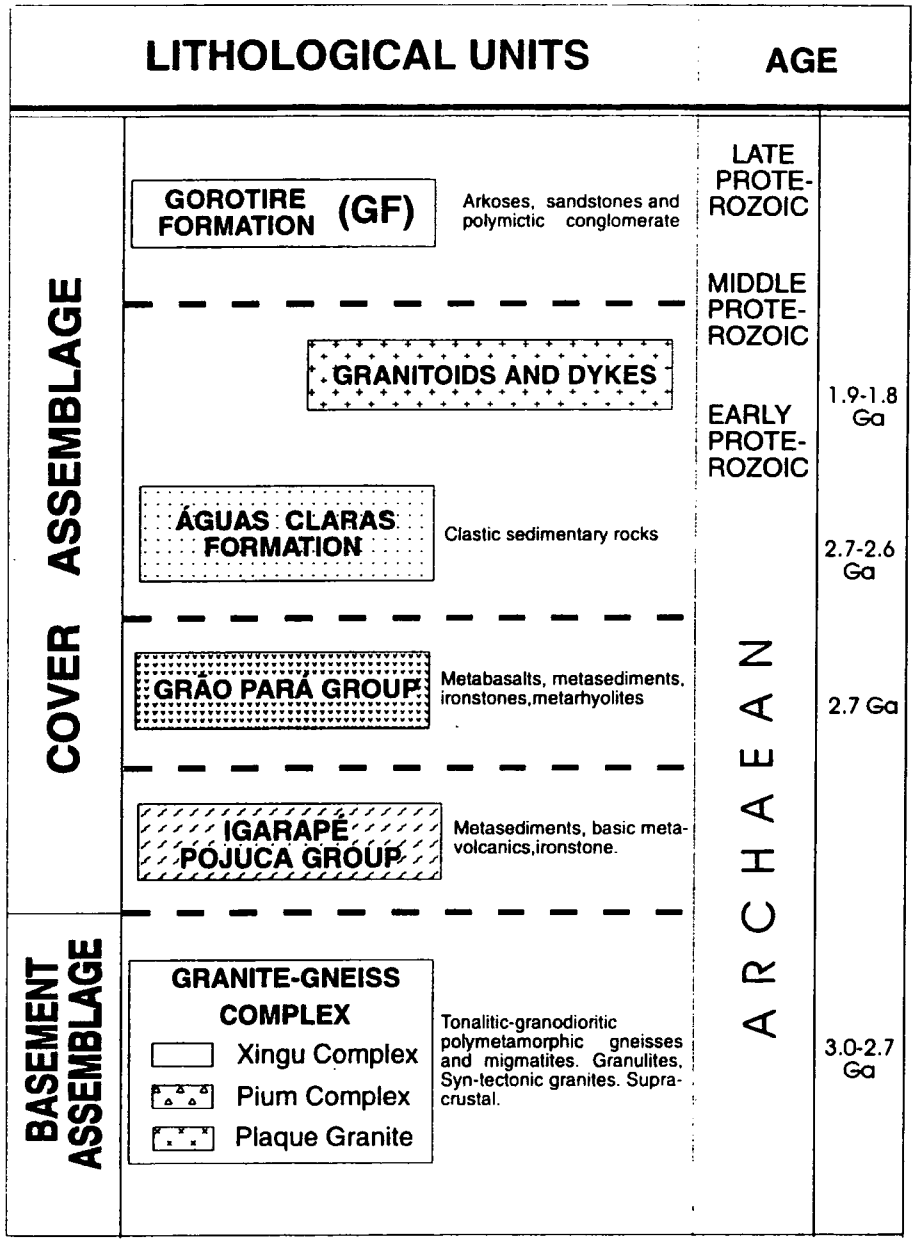

Fig.3.13- Tectonostratigraphic colunm for the Carajás region (modified after Pinheiro and Holdsworth, 1997*a*).

CHAPTER 4
THE CARAJÁS STRIKE-SLIP SYSTEM

INTRODUCTION

The Carajás Strike-Slip System is the largest fault system recognised within the Itacaiúnas Belt with an along-strike length of 180 Km and a width of 60 Km in its central part (Fig.4.1). On satellite and radar images it registers a sigmoidally shaped set of E-W discontinuous, curved and anastomosing lineaments. The Carajás Fault (Fig.4.1) forms the most prominent single fault in the system, although its lateral terminations extend beyond the zone of sigmoidally shaped lineaments, that is referred to here as the *Carajás Structure*. A second set of N-S to NNE-SSW -trending lineaments cross-cut the main sigmoidal structure and are also observed elsewhere outside the structure.

The Carajás Strike-Slip System delimits the outcrop of volcanic and sedimentary sequences that are downfaulted into the Archaean basement granite-gneisses of the region. The age of these supracrustal sequences ranges from Archaean to Middle Proterozoic and they are cut by Middle Proterozoic granitic plutons and mafic dyke swarms.

The data presented here were collected in six key study areas: (1) Águas Claras region; (2) Azul Manganese Mine area; (3) N-4 Iron Mine; (4) Bahia Gold Mine;(5) Itacaiúnas river region; and (6) Serra do Rabo region. Collectively, the geological data from these areas reveal the importance of the Carajás Strike-Slip System in the tectonic history of the Itacaiúnas Belt. In particular, this study shows that the Carajás Strike-Slip System is an example of a regional-scale structure in which the heterogeneous and complex distribution of deformation has been strongly controlled by reactivation of early pre-existing structures in the basement.

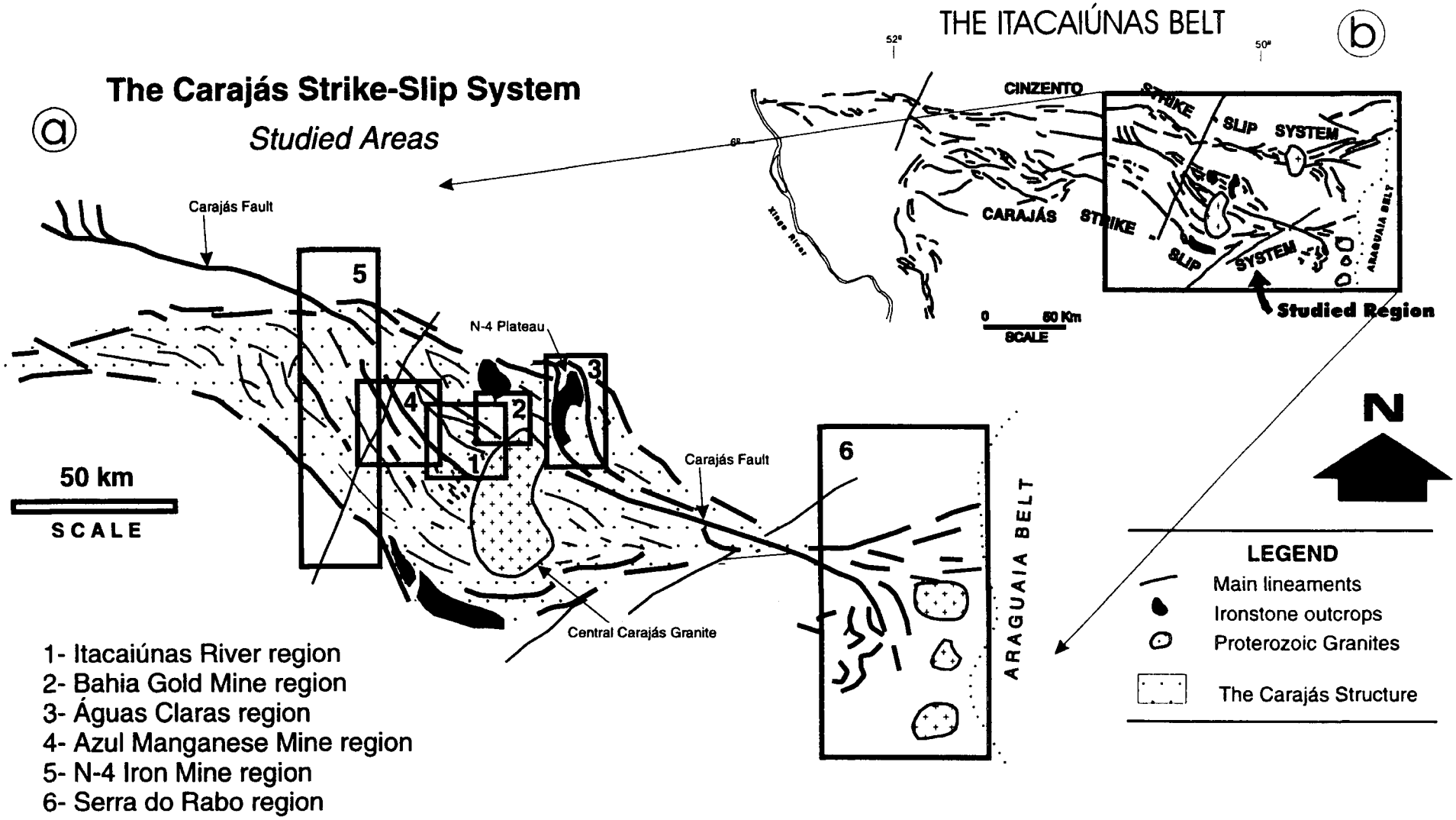

Fig.4.1- Location of the study areas along the eastern part of the Carajás Strike-Slip System.

4.1- THE ÁGUAS CLARAS RIVER REGION

The Águas Claras area is located in the central part of the Carajás Strike-Slip System (Photo 4.1.1). Sequences of sedimentary rocks belonging to the Archaean Águas Claras Formation (Nogueira *et al.*, 1995) outcrop along the road linking the N-4 plateau to the Bahia Mine (Fig.4.1.1). The best exposures occur from approximately 5 Km NE to 4 Km SW from the place where the road cuts the Águas Claras river. This section was studied in detail and will be presented here.

4.1.1- REGIONAL SETTING

The rocks observed in the area are predominantly sandstones and mudstones and are a sequence of marine to fluvial deposits, cut by dyke swarms and sills. They are locally strongly deformed by sets of folds and fractures associated with the Carajás Fault which crosses the area adjacent to the Águas Claras river valley (Fig.4.1.1).

The Águas Claras Formation outcrops in a relatively large area (ca. 900 Km^2) in the central part of the Carajás Strike-Slip System (Photo 4.1.1; Fig.4.1.1). It appears lie unconformably on the volcanics of the Parauapebas Formation and the ironstones of the Carajás Formation, both of which belong to the older Archaean Grão Pará Group (Araújo and Maia, 1991). Actual contacts were not observed in the field.

The Águas Claras Formation is intruded in its central part by the Central Carajás Granite, probably intruded 1880±2 Ma (U/Pb, zircon; Machado *et al.*, 1988), or 1820±49 (U/Pb, zircon; Wirth *et al.*,1986). Xenoliths of sedimentary rocks and a thermal aureole are present and affect rocks of the Águas Claras Formation (e.g. Wirth, 1986; Rios, 1991). Swarms of mafic dykes of uncertain radiometric age (?Middle Proterozoic) cut the sedimentary rocks. Gabbroic sills cut these rocks in the central part of the fault system and yield an age of 2645± 12 Ma (Pb/Pb, zircon; Dias *et al.*, 1996*a*), suggesting that the Águas Claras Formation is of Archaean age.

The present study focuses on the tectonic and structural evolution of this region. Recent information about the lithostratigraphy, sedimentology and petrological aspects to these rocks can be found in Nogueira *et al.* (1992, 1994,

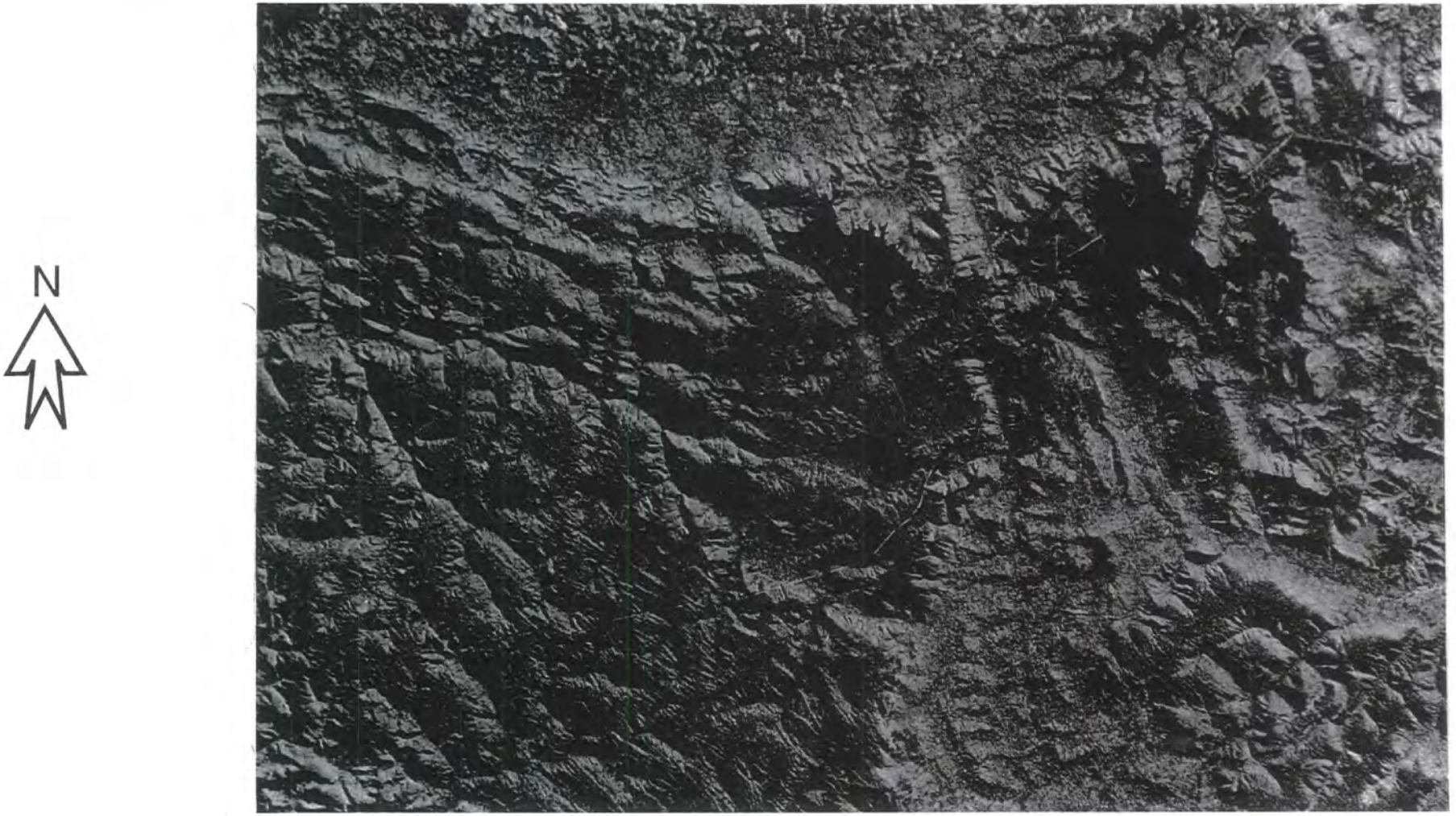

Photo 4.1.1- Satellite image of the central area of the Carajás Strike-Slip System. See Fig.4.1.1.

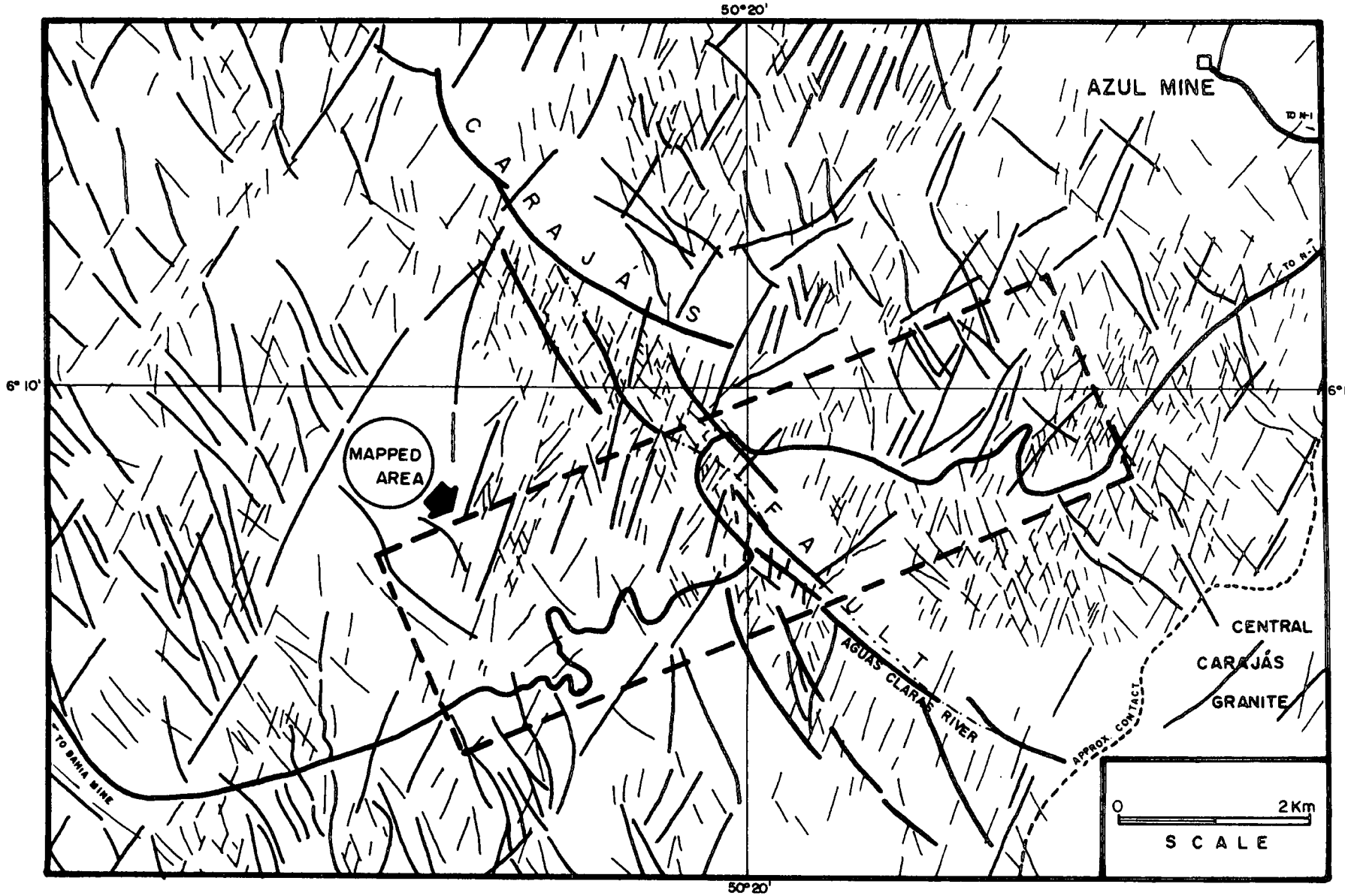

Fig.4.1.1- Map of lineaments interpreted from satellite and radar images from the central area of the Carajás Strike-Slip System. The area studied in this work is marked.

1995), Nogueira and Truckenbrodt (1994), Nogueira (1995), Soares *et al.* (1994) and Truckenbrodt *et al.*(1996).

4.1.2- PREVIOUS WORK

The rocks now recognised as part of the Archaean Águas Claras Formation in this region were first mentioned by Rêgo (1933) who considered them to be part of the Grão Pará Group. Tolbert *et al.* (1968) described these rocks in the Carajás area and referred to them as a "clastic rock sequence". They recognised packages of coarse- to medium-grained quartzitic sandstones interlayered with conglomerates as part of this unit. At that time these rocks were correlated with the Gorotire Formation (Andrade Ramos, 1954), which was thought to be pre-Silurian based on correlation with similar rocks defined by Barbosa *et al.* (1966) along the Xingu river, about 200 Km west of this region.

Knup (1971) described quartz-arenites, arkoses, greywackes and conglomerates, together with siltstones and mudstones, outcropping in the Carajás region. This author assigned the name "Rochas Sedimentares Precambrinas e Eopaleozóicas" to these rocks and mentioned a possible correlation with both the Rio Fresco and Gorotire formations described earlier by Barbosa *et al.* (1966).

Liandrat (1972) referred to two sequences of outcropping sedimentary rocks that were named the Igarapé do Ouro Formation and the Zé Gladstone Formation. The age of these units was thought to be Eo-Paleozoic. A possible correlation of these rocks with the Gorotire, Cubencraquém and Rio Fresco formations was considered. It is important to observe that Liandrat (op.cit.) mapped these units in only a small area (ca.20%) relative to what is today recognised as the Águas Claras Formation. The remaining area was referred to as being covered by the metasedimentary rocks of the so-called Serra dos Carajás Formation (Precambrian).

Limited information concerning the structural geology of these rocks has been published. Beiseigel *et al.* (1973) refer to a large synclinorium in the sedimentary sequence of the central Carajás region. They correlated these rocks to the Gorotire Formation following several other authors.

The Rio Fresco, Cubencraquém and Gorotire formations, described by Barbosa *et al.* (1966) around the Xingu river, became standard units of correlation for almost all the sedimentary cover rocks in the Amazonian Craton

for at least two decades (e.g. Cunha *et al.*,1984; DOCEGEO, 1988). This probably caused many difficulties because these authors did not present an extensive stratigraphical or sedimentological description of the units around the Xingu river.

Sedimentological and petrological studies of the rocks in the Carajás region were presented by Ramos *et al.* (1983), Figueiras and Villas (1984) and Figueiras *et al.* (1987). They suggested a fluvial to lacustrine origin for these rocks, including localised aeolian deposits and suggested that they had undergone a low grade metamorphism.

DOCEGEO (1988), using the name Rio Fresco Group (Early Proterozoic), expanded the area of occurrence of the Rio Fresco Group to include the metasedimentary sequences of the Igarapé Pojuca Group outcropping in the Serra Pelada region (NE from Carajás) and also the sedimentary rocks present in the regions of Rio Maria Granite-Greenstone Belt.

Macambira *et al.* (1990) suggested several new stratigraphical subdivisions of the rocks of the central and northern areas of the Carajás region. They introduced the Igarapé Cigarra Formation, the Igarapé Boa Sorte Formation, both considered to be Archaean in age, and the Azul Formation (Proterozoic) earlier mentioned by DOCEGEO (1988). These proposals were based entirely on lithological data.

A substantial change in the local stratigraphy of the clastic sedimentary sequence in the region was proposed by Araújo *et al.* (1988) and Araújo and Maia (1991). These authors, based on regional mapping, introduced the Águas Claras Formation as a further Archaean tectonostratigraphic unit, referring to a sequence of rocks deposited in a fluvial to lacustrine basin developed during localised transtension along the Carajás Strike-Slip System.

According to Araújo and Maia (1991) the tilted bedding observed in the Águas Claras rocks defines nearly sigmoidal shape of the Carajás Structure in map view. This was interpreted as part of a "positive flower" structure by these authors. Araújo *et al.* (1988) and Araújo and Maia (1991) described systems of ductile shear zones dominated by reverse-oblique kinematics along the region. This deformation, according to these authors was responsible for intensive lithological imbrication and the development of a mylonitic fabric limiting blocks of undeformed rocks.

More recently, Nogueira *et al.* (1992, 1994, and 1995), Nogueira and Truckenbrodt (1994), and Nogueira (1995) have presented the definitive sedimentological and stratigraphical review of the rocks outcropping in the

Águas Claras area. They formally redescribed and redefined the Águas Claras Formation based on sedimentological and structural data.

These authors recognised 22 lithofacies in the Águas Claras Formation, along the central area of the Carajás Strike-Slip System, summing a thickness of about 1500m. The predominant rock-types are sandstones and mudstones, with different grades of lithification, hydrothermal and weathering alterations.

Two members were defined. A Lower Member is represented by mudstones and siltstones related to a marine platform system, whilst an Upper Member of main sandstones and conglomerates represents a fluvial to shallow water littoral deposits. They suggested an Archaean age for this unit and did not find evidence to support the depositional model controlled by transtension as suggested by Araújo *et al.* (1988) and Araújo and Maia (1991). They proposed that the sequences relate to a broader basin whose margins extended beyond the limits of today, an idea later supported by Pinheiro and Holdsworth (1997*a*) based on regional tectonic studies.

Petrological studies of the Águas Claras rocks by Truckenbrodt *et al.* (1996), and Anaisse Jr. and Truckenbrodt (1995) revealed a predominance of quartz-arenites and subarenites, with a post-depositional illitic matrix. Studies of hydrothermal alteration and its relation to the gold/copper ore preserved in veins, mafic dykes and sills cutting the Águas Claras rocks were presented by Soares *et al.* (1994), Barros *et al.* (1994*a*) and Silva (1996).

Dias *et al.* (1996*a*) attributed a Pb^{207}/Pb^{206} (zircon) age of 2645±12 Ma to a sill intrusion into the Águas Claras rocks, corroborating an Archaean age for this unit.

The Carajás Fault is the major structure cutting the Águas Claras rocks from NW to SE with a trace slightly concave towards the NE in map view (Fig.4.1.1). This fault trace is not continuous in large scale and is represented by sets of segments forming an approximately 1-2 Km wide zone of anastomosed lineaments. Several branches diverge from the main fault trace forming sets of concave splays projecting consecutively towards the SW (Pinheiro and Holdsworth, 1997*a*).

4.1.3- DATA FROM SATELLITE IMAGE.

The satellite image reproduced in the Photo 4.1.1 shows that the Águas Claras region is strongly cut by lineaments. Major lineaments are orientated

mostly NW-SE and NNE-SSW. Apparently the NNE-SSW set cross-cut those that are NW-SE.

The NW-SE lineaments are anastomosed displaying two close sub-parallel directions: (1) ca.320° and (2) ca.340° (Fig.4.1.1). These two sub-sets are responsible for a kilometre-scale rhomb-shaped pattern observed in most of the remote-sensing images of this region. The strongest NW-SE anastomosed lineaments observed in this area cross the central part of the area shown in the Fig.4.1.1 (from NW, towards the Central Carajás Granite) distinguished by its oval N-S elongated shape, contrasting finer texture and lighter grey tone in the SE corner of the area (Photo 4.1.1). This lineament develops several branches which diverge from the main NW-SE direction, inflecting towards NNW-SSE.

The NNE-SSW lineaments are straight and some are relatively continuous.

Small lines (<0.7 Km) orientated in a NW-SE and NE-SW direction create a multi-lozenge texture that sets the background of the major lineaments. This pattern is distributed irregularly in the region being more concentrated in the NW and W area of the Central Carajás Granite.

4.1.4- FIELD OBSERVATIONS.

A detailed description of the structures developed in a 7 Km section exposed along the N-4 Mine/ Bahia Mine road crossing the Águas Claras river is presented here from W to E. A series of domains are defined limited by major fault traces observed along the transverse (Figs.4.1.2 and 4.1.3).

4.1.4.1- DOMAIN 1.

This domain corresponds to the first 800m of the section shown in Figs. 4.1.2 (labelled C-D and B) and 4.1.3, starting from its west end. It outcrops for about 2 Km along the road from the top of the first hill in the SW corner of the area (Fig.4.1.2) to the NW-SE valley of a tributary of the Águas Claras river. It includes outcrops of the fluvial deposits (Sequence D), tide-dominated braided deltaic deposits (Sequence C) and storm dominated platform deposits (Sequence B).

The rocks forming sequence D are essentially sandstones and conglomerates with parallel lamination, tabular cross-stratification and trough

THE ÁGUAS CLARAS RIVER AREA

CARAJÁS REGION

GEOLOGICAL MAP

From interpretation of LANDSAT satellite images (1:100000); radar images (1:50000) and topographic map by IBGE-Brazil and the Brazilian Army (Sheet SB-22-Z-A-II, 1:100000). Field data collected in February/90, November/91, February/92 and July/93. Lithostratigraphy based on Nogueira (1995) and Nogueira *et al.*(1995).

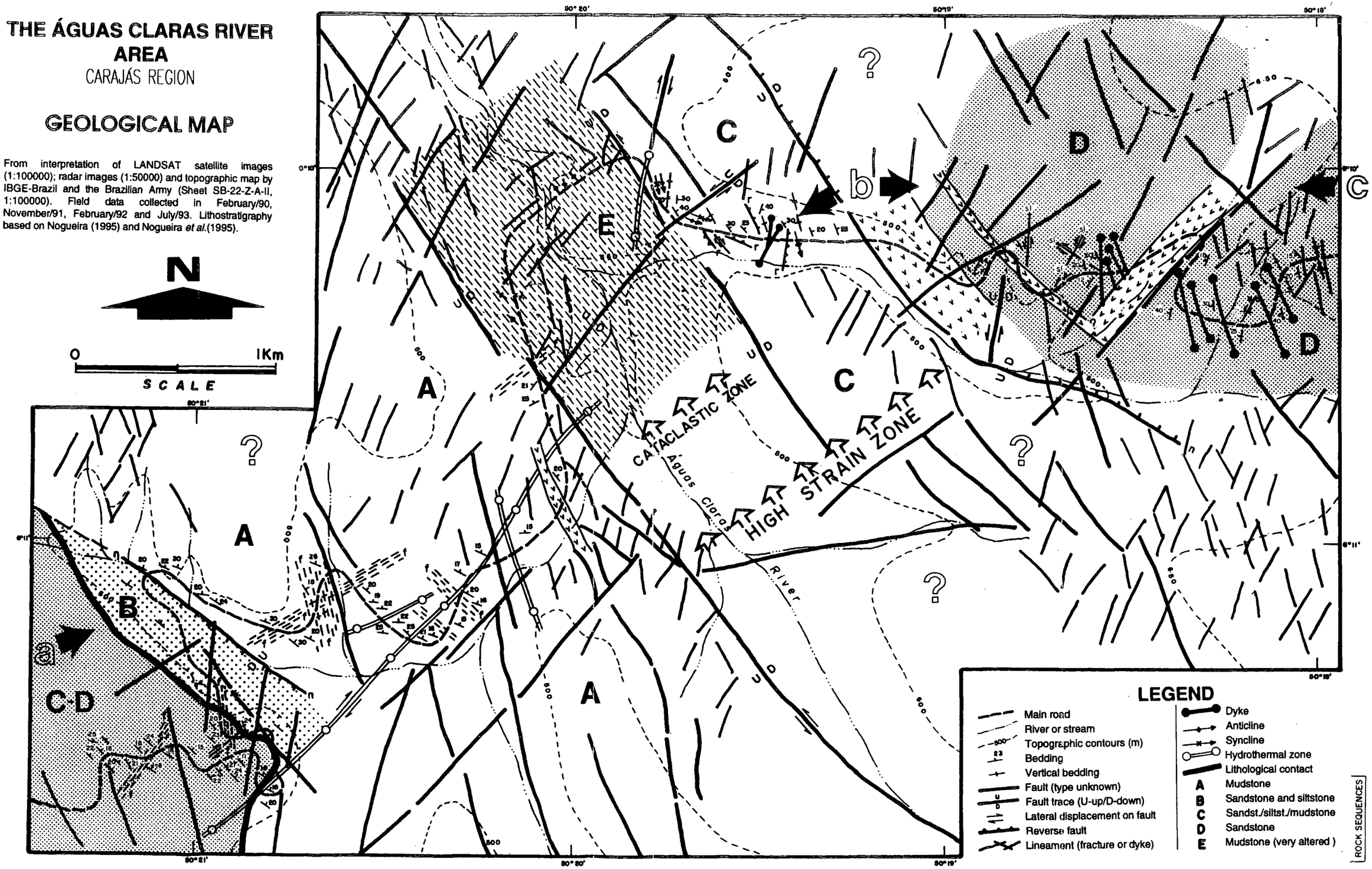

Fig.4.1.2- Geological map of the central region of the Carajás Strike-Slip System, adjacent to the Águas Claras river.

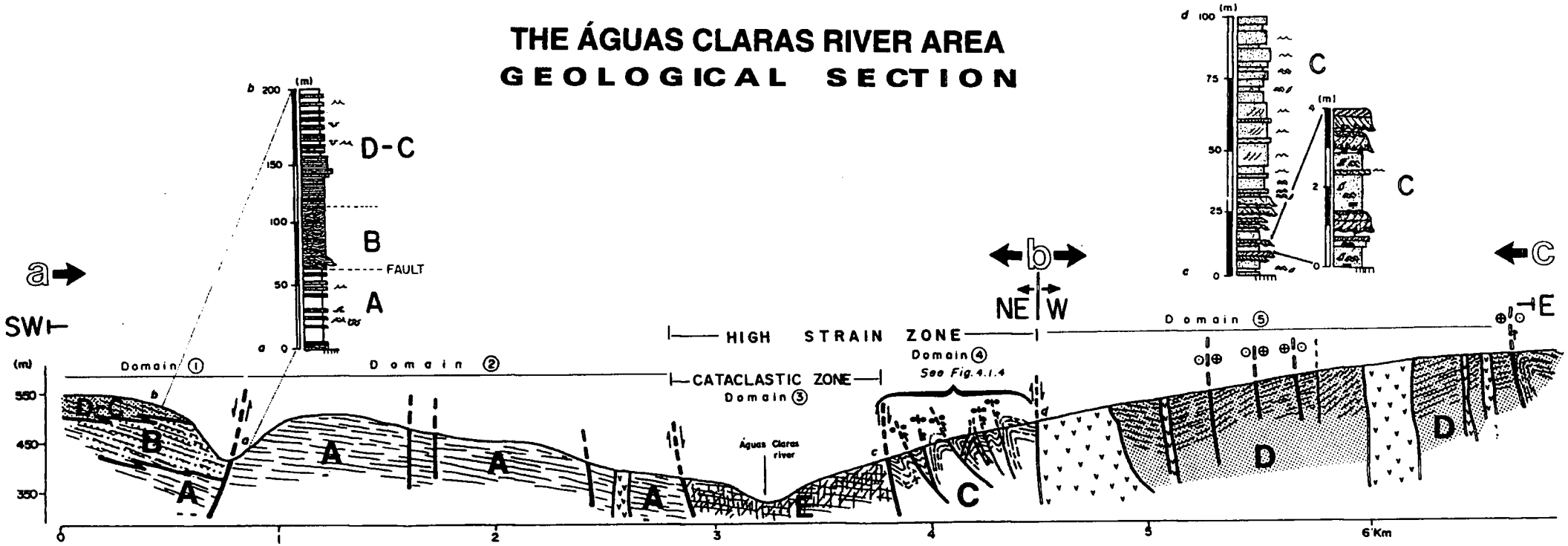

Symbols

- Tabular cross-stratification
- Trough cross-stratification
- Herringbone cross-stratification
- Parallel lamination
- Load cast
- Lenticular bedding
- Wavy bedding
- Convolute lamination
- Symmetric ripple mark
- Ripple mark
- Hummocky cross-bedding

LEGEND

- Strike-slip or oblique-slip fault with dextral displacement
- Strike-slip or oblique-slip fault with sinistral displacement
- Sense of vertical displacement in faults
- Fault (type unknown)
- Dyke
- Mudstone
- Sandstone and siltstone
- Sandstone, siltstone and mudstone
- Sandstone
- Mudstone (with strong hydrothermal alteration)

See Map on Figure 4.1.2

MAIN LITHOFACIES

A - Platformal Deposits (offshore)

B - Platformal Deposits (storm deposits; shoreface)

C - Tidal Deposits (shoreface)

D - Fluvial and Deltaic Deposits (braided system)

E - Cataclastic Rocks

(After Nogueira, 1995; Nogueira *et al.*,1995)

Fig.4.1.3- Geological section to the central part of the Carajás Strike-Slip System. See Fig.4.1.2.

cross-stratification as the main primary structures (Nogueira, 1995). Sequence C is represented by sandstones and mudstone/siltstones (Fig.4.1.3) with parallel lamination, load casts, symmetrical ripples and tabular cross-stratification (Photo 4.1.2). The contact with the overlying sequence D is transitional. Both sequences together have a minimum thickness of about 50 m in this section. These rocks overlie sequence B, a series of platform deposits at least 50m thick (Fig.4.1.3). This is mainly fine to coarse sandstones with swaley cross-stratification, hummocky cross-bedding, symmetrical ripple marks and parallel lamination. This sequence is faulted against sequence A to the NE by a NW-SE normal fault dipping at high angles toward SW (Fig.4.1.3).

Photo 4.1.2- Tabular cross-stratification present in sandstones of the sequence C, outcropping in the Águas Claras region.

The beds in this part of the section strike regularly NW-SE and dip constantly 18°-24° NE (Fig.4.1.2). A few NE-SW and N-S fracture zones cut the rocks in different places, spaced at about 300-500m (Fig.4.1.2), but the rocks are otherwise little deformed.

A sub-vertical hydrothermal zone about 30m thick crosses part of this block, following a NE-SW direction (Fig.4.1.2). This forms an approximately tabular zone in which the rocks become intensely red or yellow white, with a

conspicuous sub-parallel colour zoning following the borders of this feature. Bedding traces inside this zone are virtually absent, apparently obliterated by fluid influx, recrystallization and weathering. The rocks inside the zone are Si-, Fe- and clay-mineral enriched. They are intensely fractured, sometimes with a brecciated texture. Slickensides indicate predominantly dextral displacements along subordinated planes within or at the borders of this zone. Primary gold, copper, tin, tungsten (wolfram), and other ore minerals are reported to be present along some of these zones in this region as gossan deposits (Soares *et al.*, 1994).

4.1.4.2- DOMAIN 2.

This domain corresponds approximately to 2 Km along the section shown in the Fig.4.1.3, and outcrops for 3.4 Km along the road (labelled A in the Fig.4.1.2). It is composed of mudstones and siltstones of sequence A. These rocks were interpreted by Nogueira (1995) and Nogueira *et al.* (1995) as marine, or offshore platform deposits. They represent the lowest stratigraphical level outcropping in the area. The main primary structures present are climbing wave-rippled cross lamination, parallel lamination, ripple marks, swaley cross-stratification and hummocky cross-bedding in storm sand sheets (Photo 4.1.3).

The beds in this area strike regularly NW-SE and dip 15° to 30° NE (Fig.4.1.2), subparallel to those of Domain 1. Very few tectonic structures are present in these rocks except for sets of systematic fractures spaced by about 10 to 50 metres and occasionally normal faults are responsible for localised tilting of the bedding (Photo 4.1.4). The orientation of these fracture sets is predominantly NE-SW, NNW-SSE and also N-S.

A 30m thick dyke orientated NW-SE cuts these rocks in the NE region of this domain (Fig.4.1.2). Hydrothermal zones with thicknesses of about 5-15 m also occur sub-parallel to these dykes or with a NNW-SSE direction (Fig.4.1.2). The apparently continuous hydrothermal zone, described as cutting Domain 1 (see above), also crosses this part of the section from SW to NE.

The NE limit of Domain 2 is marked by a strong NW-SW lineament observed in satellite and radar images (Photo 4.1.1), and also in aerial-photos (Fig.4.1.1), close to the Águas Claras river.

On a regional scale, Domain 2 appears to correspond to an uplifted faulted block with a relatively vertical displacement of at least 200 m

Photo 4.1.3- Typical swaley cross-stratification observed in outcrop of the sequence B.

Photo 4.1.4- Normal faults tilting beds of mudstones, observed along the Domain 2 of the Águas Claras section.

(Fig.4.1.3). This is consistent with the low stratigraphical position of the sedimentary rocks in this domain.

4.1.4.3- DOMAIN 3.

This domain is an approximately 1Km wide zone of cataclastic and altered rocks running nearly parallel to the Águas Claras valley. It follows a NW-SE direction and is delimited by major NW-SE normal-oblique (sinistral) faults (Fig.4.1.2) corresponding to important regional lineaments observed in remote sensing images (Photo 4.1.1).

Few exposures occur in this zone of low lying, flat topography. The rocks are very altered (hydrothermal+weathering) with fractured mudstones or siltstones, quite similar to those observed in the Domain 2 (Sequence A). It is not possible to identify bedding, but a parallel lamination can be observed in less sheared regions. The rocks vary from red to green or white colours, with very hard resistant areas where enrichment by Si and Fe has occurred.

Fractures follow an NW-SE orientation and define a strong disjunctive anastomosing foliation of tectonic origin. In some fracture planes, it is possible to identify slickensides with striations and slickenfibers showing quite variable plunge angles towards both the NW and the SE. In places, a very fine cleavage is developed orientated sub-parallel to the main fault planes, giving them a phyllonitic appearance. Intense shearing has also led to the local development of incohesive cataclastic breccias with fragments that can vary from 5-10cm to millimetres in size. Quartz, and probably other Si-rich minerals, form the matrix in these rocks (10-20%). Most units are strongly transformed by hydrothermal alteration. In hand-samples, it is possible to recognise an intense process of silicification and probably kaolinitization.

4.1.4.4- DOMAIN 4.

This domain is strikingly different from the rest of the section as it preserves numerous folds and fractures as can be seen in Figs.4.1.3 (labelled C) and 4.1.4. The complexity of deformation in this zone is considerable. The domain corresponds to NW-SE orientated blocks of rocks, approximately 800m wide, limited by high-angle normal faults (Figs.4.1.2 and 4.1.3). The SW contact with the highly sheared rocks of Domain 3 is an oblique-slip fault with a

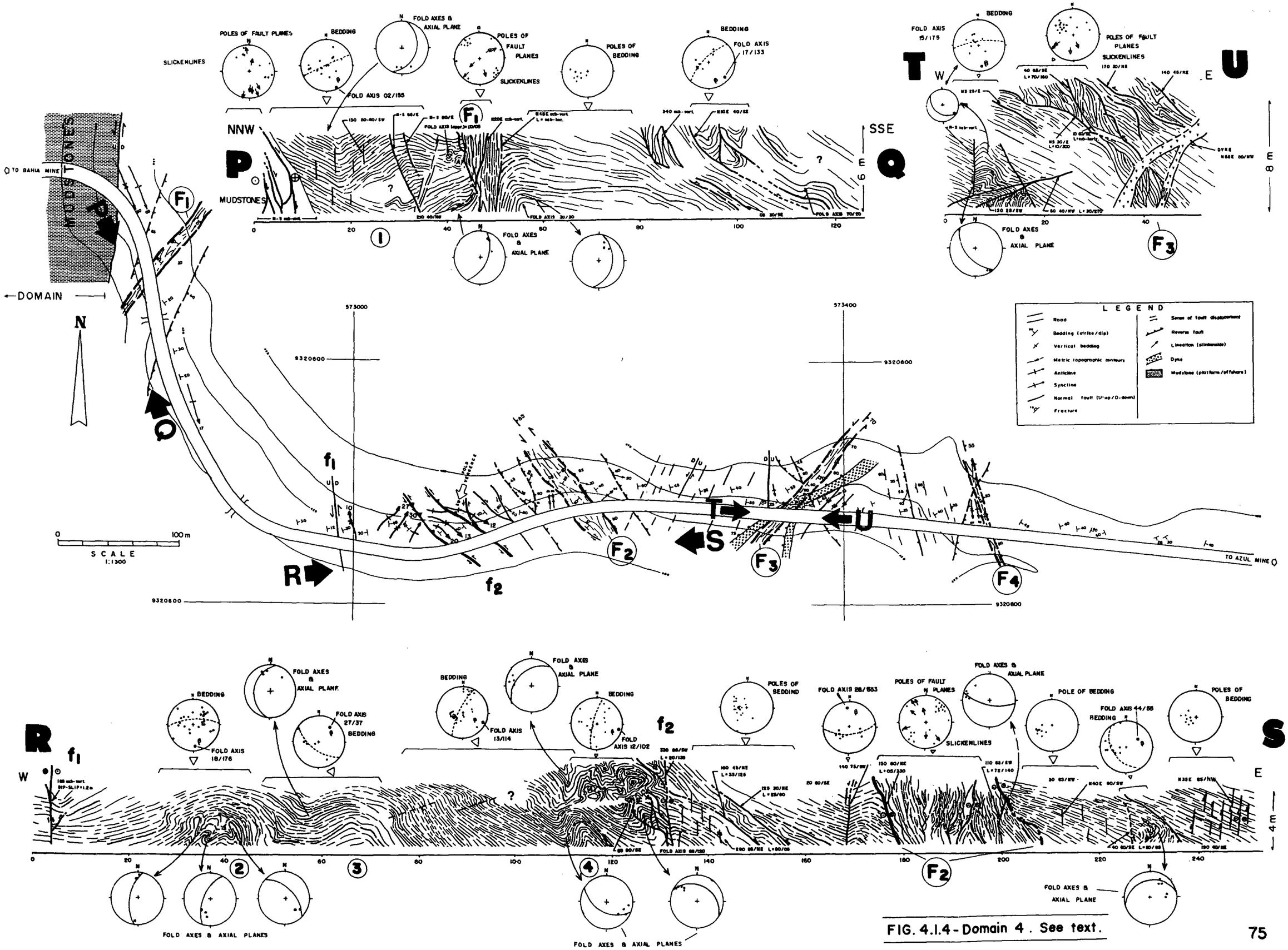

FIG. 4.1.4 - Domain 4 . See text.

predominantly sinistral movement component and a secondary normal displacement. This fault is formed by a zone of imbricated fault planes orientated about N-S to NNW-SSE and dipping steeply W or E. Towards the NE this domain is limited by a NW-SE dyke (Figs. 4.1.2 and 4.1.3).

The rocks are fine to coarse grained sandstones, conglomerates, siltstones and mudstones (Photo 4.1.5) corresponding to sequence C. Several primary structures include tabular cross-stratification, trough cross-stratification, parallel lamination, ripple marks, herringbone cross-stratification (Photo 4.1.6) and tidal bedding.

The bedding in this domain is heterogeneously deformed by folding, faulting and block rotations (Fig.4.1.4). The rocks are also cut by dykes. These tectonic and igneous features will be described below.

a) Folds : Folds occur on several scales and are sometimes associated with reverse or strike-slip faults. Their geometry and style are rather variable and they can show semi-cylindrical, kink and chevron, monoclinal and curvilinear geometries.

A set of four main anticlines and intercalated synclines deform the bedding along the P-Q and R-S sections shown in Fig.4.1.4 (anticlines are labelled 1 to 4). These folds have a wavelength of 10 to 25m and are curvilinear along the total section (Fig.4.1.5). They are cut by several NE-SW and NW-SE faults affecting their continuity in several places. Some of these folds have a complex internal geometry.

On a large scale, these folds are mostly semi-cylindrical to non-cylindrical features with axes plunging <30° N, S, NE or SE (boxes in the Fig.4.1.6). In the exposed cut, they are apparently open to closed structures, slightly asymmetrical verging mainly W or NW, and with a predominantly subrounded or subangular bluntness. Axial surfaces of these folds dip steeply (angles >75°) and strike N-S and NE-SW.

The first structure of this fold train is observed along almost all the P-Q section (labelled 1, Fig.4.1.4) which runs approximately parallel to the axial plane of a ten-metre-scale open anticline plunging about 20°-10° SSE. It is cross-cut perpendicularly by a NE-SW fault zone (labelled F_1, Fig.4.1.4). It is possible to see its hinge region at the upper of the end of the exposure, together with a complimentary syncline to the W.

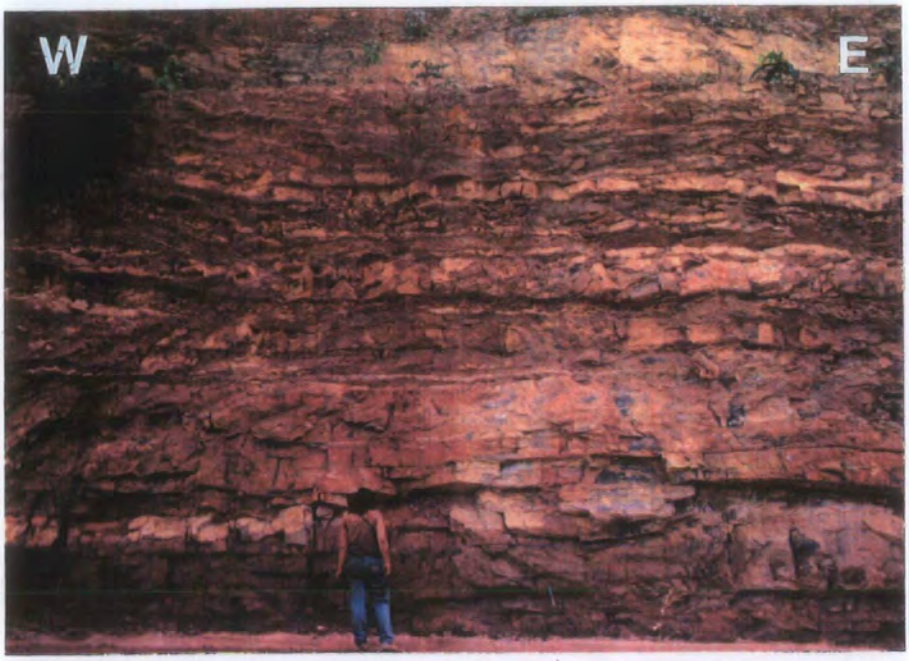

Photo 4.1.5- Part of the outcropping rocks observed in a fold limb along the Domain 4. They are metre-scale beds of mudstones and sandstones interpreted as tidal deposits.

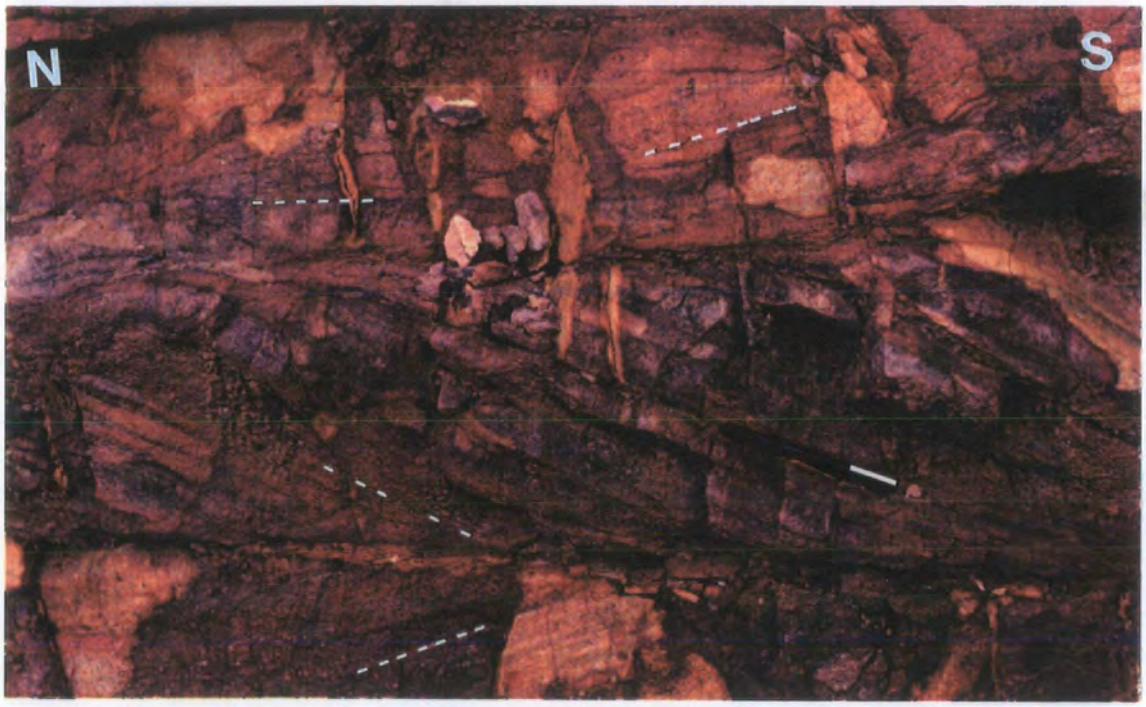

Photo 4.1.6- Typical herringbone cross-stratification observed in the rocks of the Domain 4 along the Águas Claras section.

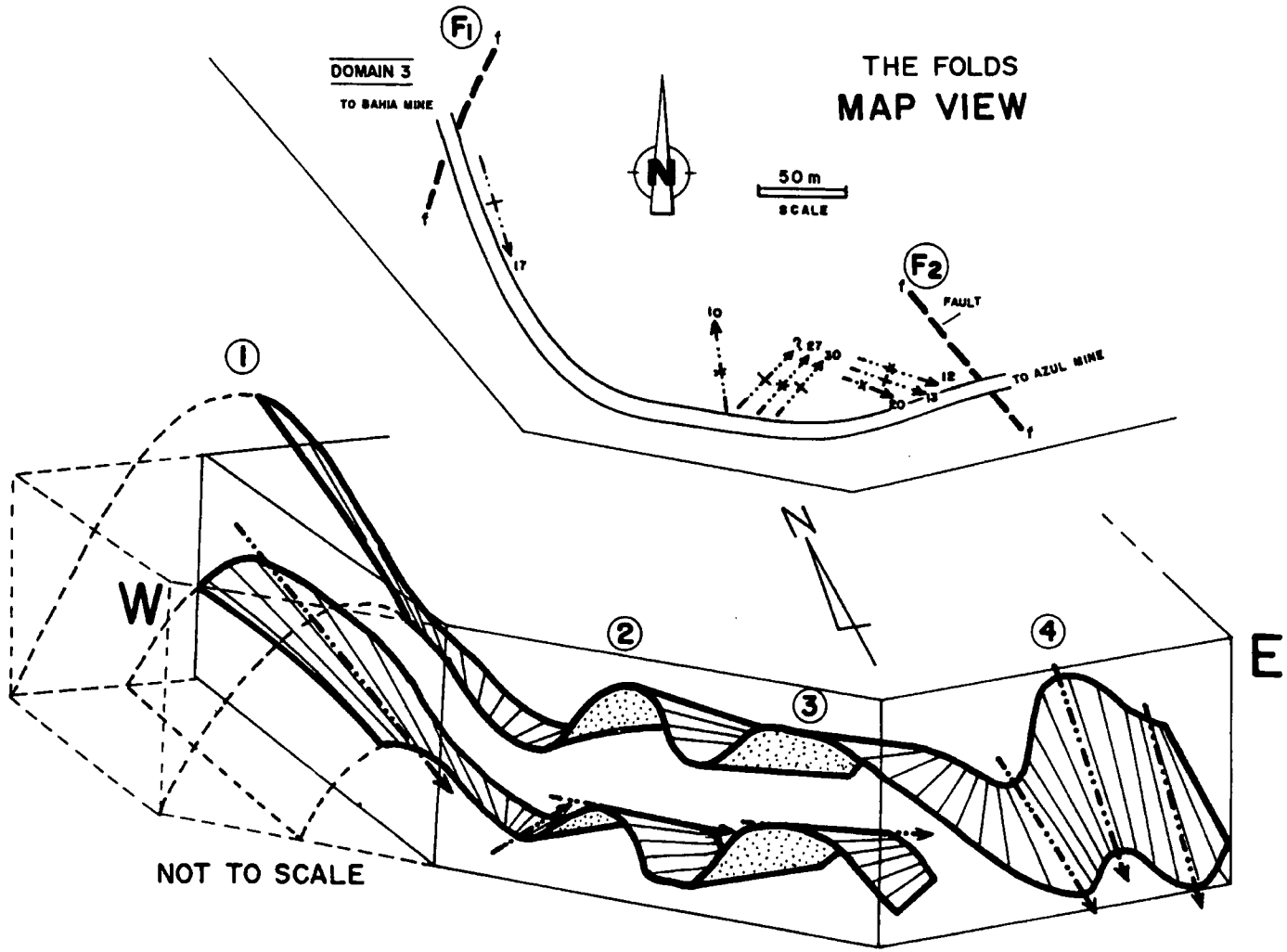

Fig.4.1.5- 3-D representation of the geometry of the curvilinear fold observed in the first 130m of the R-S section (Fig.4.1.4). The arrows in the folded surface represent approximately the fold axis plunge of the folds.

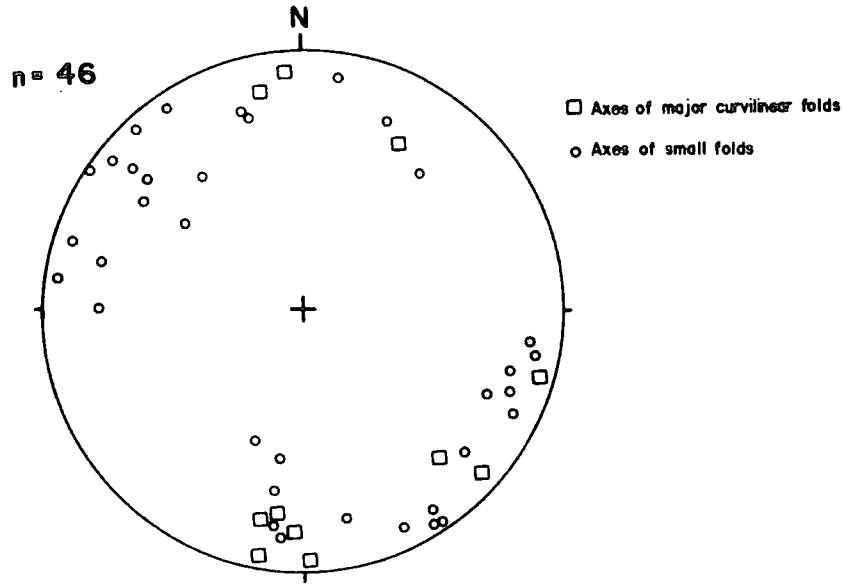

Fig.4.1.6- Stereonet showing the axes of all folds observed in the Domain 4.

This fold continues towards the SE changing gradually in plunge from about 17°S to 10°N in an adjacent gentle to open syncline, with an amplitude of more than 20m. This structure is present in the beginning the R-S section (Figs.4.1.4 and 4.1.5), with its west limb cut by a single normal-sinistral fault (labelled f_1). This synform connects to a pair of ten-metre-scale anticlines (labelled 2 and 3) separated by a synform plunging at 27°-30° NE with N-S striking axial planes dipping 60° to 75° westward. They are observed in the first 80m of the R-S section (Fig.4.1.4). These folds are slightly rounded to sub-rounded in outcrop profile and show a complex geometry in their inner region (see section R-S, Fig.4.1.4 and Photo 4.1.7), to be described in detail later in this section.

The two major anticlines, mentioned above, continue eastward connecting another set of synclines and anticlines plunging 20°-10° SE and with axial planes dipping at about 70° SW (labelled 4 in the Fig.4.1.4 and Photo 4.1.8). They are ten metre-scale asymmetrical folds, verging SW, cross-cut by branches of NW-SE sinistral reverse faults. They are slightly non-cylindrical features, open to close, with a subangular bluntness, and apparently with a relatively thick hinge, between the class 1C and 2 in Ramsay's classification, as observed in the outcrop cut (Photo 4.1.8).

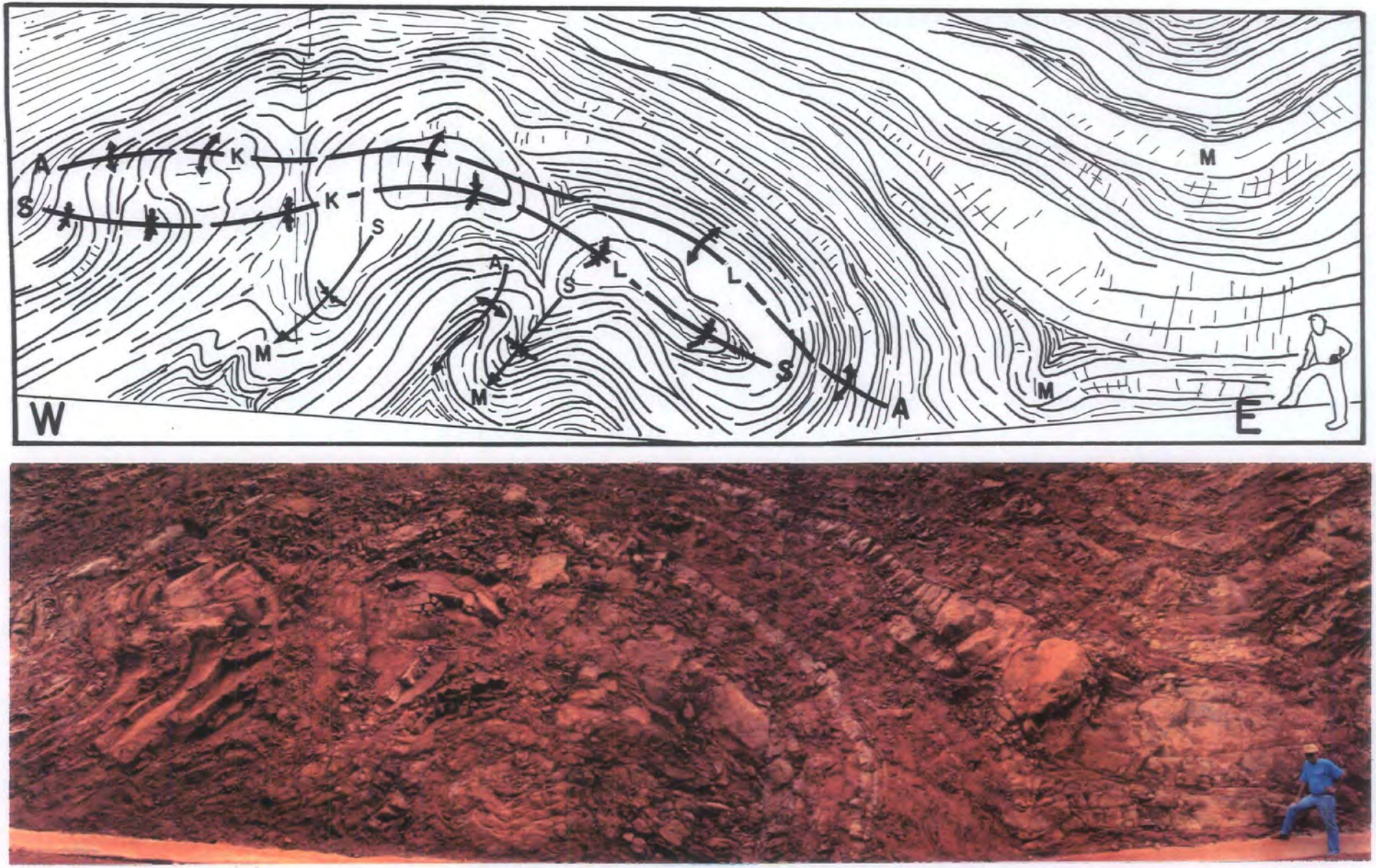

Photo 4.1.7- Complex folds observed in the inner part of decametre-scale curvilinear folds, about 40m from the beginning of the R-S section (labelled 2, Fig.4.1.4). Key: A-anticline; S: syncline; L: folds plunging SE; K: folds plunging NW or sub-horizontal; M: folds plunging south. See Fig.4.1.7 for more information

Photo 4.1.8- Set of approximately cylindrical folds plunging SE with low angle observed at about 120m along the R-S section (Fig.4.1.4). Oblique-slip faults with a NW-SE orientation mark the end of the folds along the outcrop.

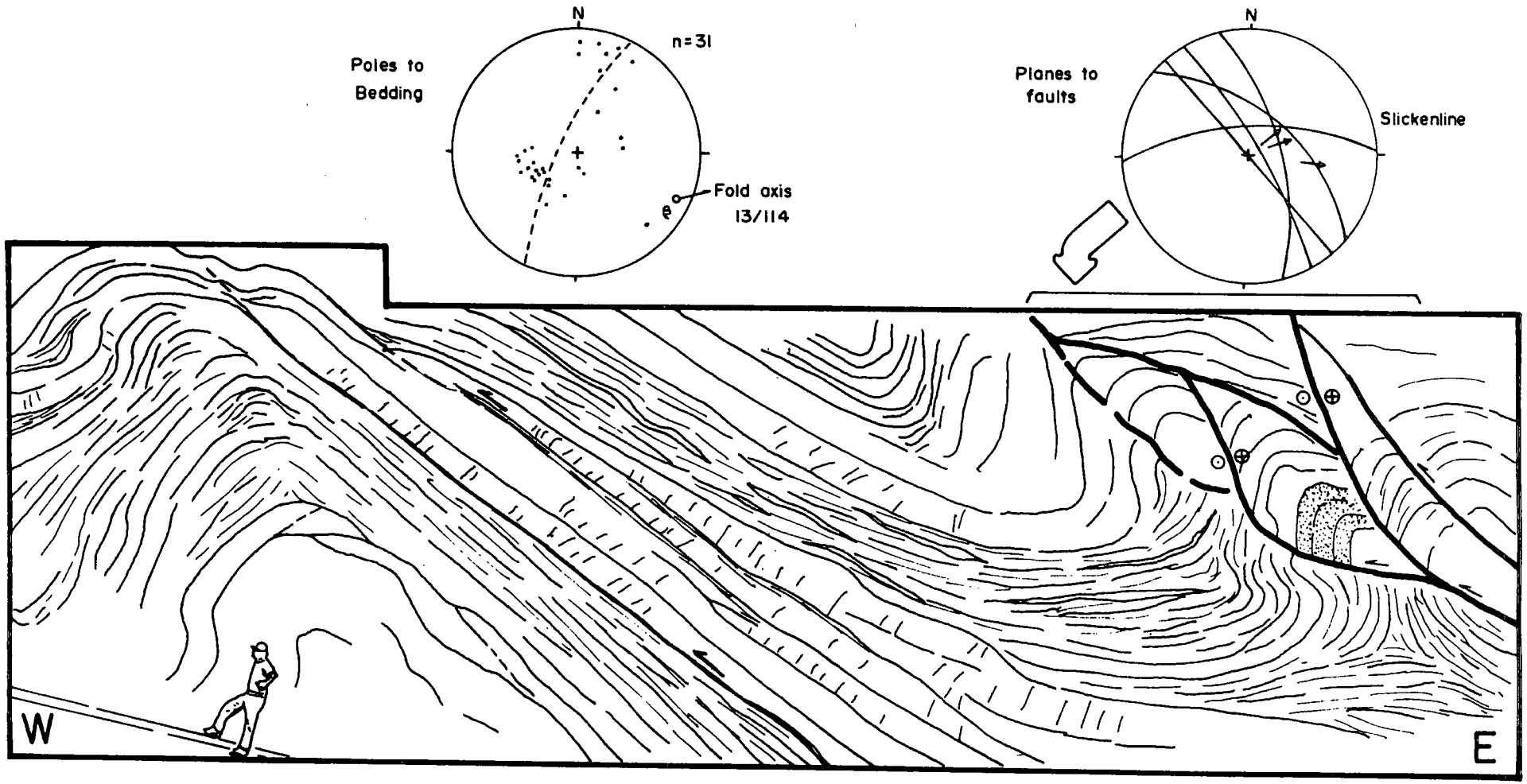

- See Photo 4.1.8 -

These folds are interrupted against a NW-SE steep fault (labelled f_2; Fig.4.1.4) but probably continue for about 40m more beyond this discontinuity, until a major NW-SE fault zone occurs about 180m from the beginning of the R-S section (labelled F_2,.Fig.4.1.4).

The complex geometry present in the inner region of some of these non-cylindrical folds is best exposed in the core of the anticline observed about 40m from the beginning of the R-S section (labelled 2; Fig.4.1.4 and Photo 4.1.7) and also in the folds at the top of the outcrop about 120m along the same section (labelled 4; Fig.4.1.4).

In these folds it is possible to observe a set of parasitic smaller folds, mostly orientated subparallel to the enveloping fold, plunging shallowly S-SE-SW. In the exposed cross-section, the geometrical relationship between the large fold and the small inner folds may be described in terms of complex disharmonic folding. The large-fold is a rounded box fold. The axes of all these folds, gradually become steep southwards and plunge >70°. The pattern observed in the outcrop corresponds to an apparent interference between a dome-like fold plunging SW and NE (K and L, Fig.4.1.7; Photo 4.1.7) with an axial plane striking S, and a set of small semi-cylindrical folds with axes plunging shallowly southwards (M, Fig.4.1.7; Photo 4.1.7) and an axial plane striking about N-S, steeply dipping.

The contours of poles of bedding planes around this complex fold (Fig. 4.1.8a) characterise a typically conical fold with an axis plunging plunging 55° towards 335°. Looking at the distribution of the major pole concentrations observed in the stereonet, it is possible to find three ß axes corresponding approximately to the axes K, L and M obtained from the two interfering folds exposed in the field. Bearings of these axes are plotted in the same stereonet for comparison (K and L= squares; M=small circles).

A stereonet of the complex fold pattern exposed on the top of the outcrop, at about 120m from the beginning of the R-S section, points to a similar arrangement and orientation of this pattern even if the exposure does not give a ready clue in the field on this geometry (Fig.4.1.8b).

It is noteworthy that the thickness of beds involved in these curvilinear folds is remarkably variable. Sandstones show a tendency to be thinned towards the hinge but mudstones tend to be thicker, developing bulbous hinge zones, sometimes forming a localised and discrete slaty cleavage. Often folded beds of sandstone can be thickened towards the hinge by the development of localised conjugate fold sets or arrays of limb thrusts. Millimetre-scale

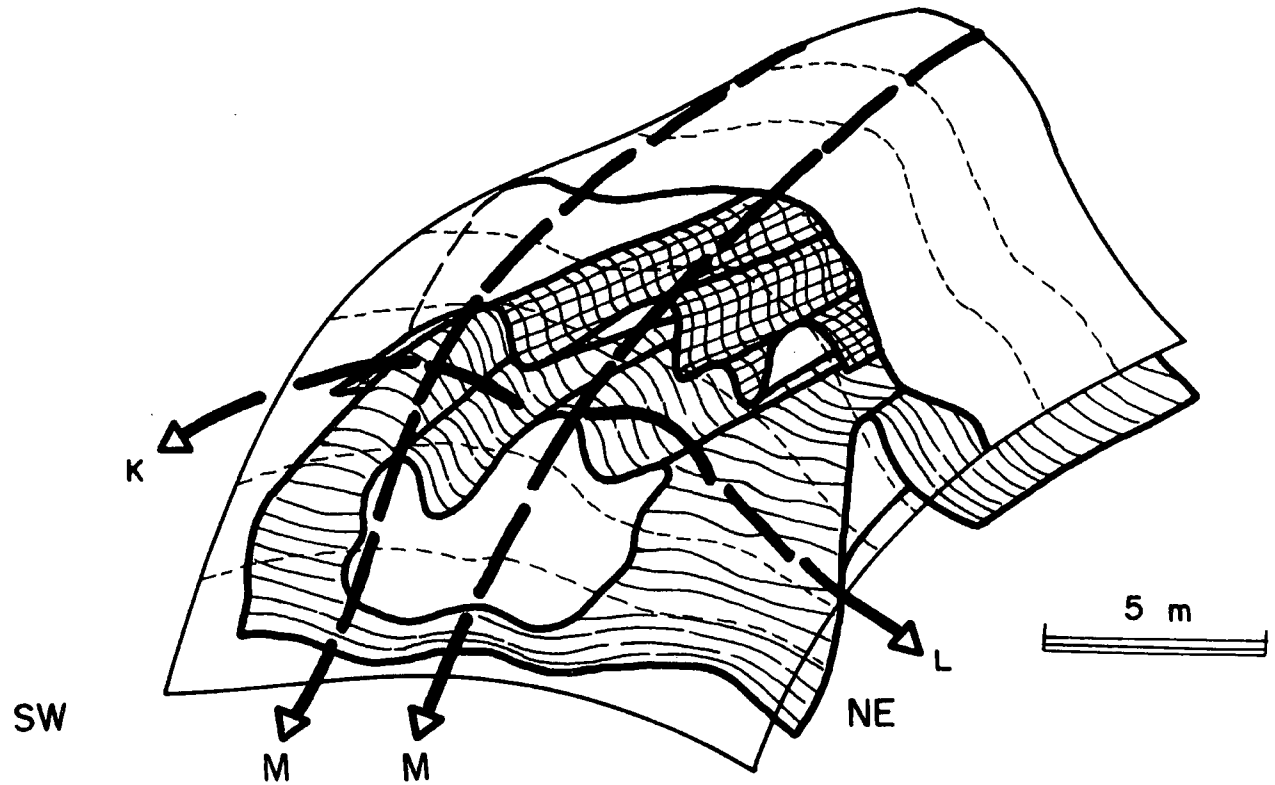

Fig.4.1.7- Non-cylindrical folds observed in the inner part of the anticline labelled 2 in the Fig.4.1.5. Also see Photo 4.1.7.

extension quartz veins are present, forming en-echelon sets particularly in the folded sandstones.

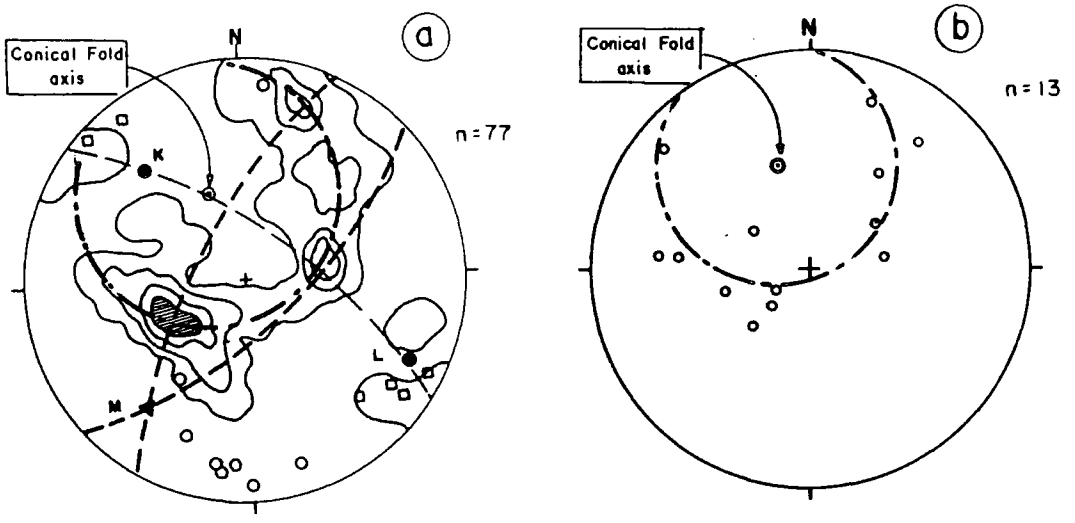

Fig.4.1.8- a) Equal area stereographic projection representing contours (4%, 6.5%, 9% and 12%) of poles to bedding in the folds observed about 40m along the R-S section (labelled 2, Fig.4.1.4). b) Stereonet to fold axes to the folds observed in the top of the outcrop about 120m of the beginning of the R-S section (above fold labelled 4, Fig. 4.1.4).

The rocks exposed at the end of the R-S section and in the T-U section appear not to be affected by the curvilinear folds described above but are also folded in isolated places by kink and chevron folding and centimetre- to metre-scale drag-folds associated with several oblique and reverse faults present in this area (Fig.4.1.4).

Kink and chevron folds are centimetre- to metre-scale and affect the geometry of other folds. They have variable orientations but most have axial planes orientated NW-SE or N-S, similar to the orientation of the oblique-slip faults. The best examples are present in the sections R-S and T-U at about 10m and 170m respectively, from the beginning of these sections (Fig.4.1.4).

An example of kink folding is observed at the beginning of the T-U section (Fig.4.1.4). Its geometry is controlled by sub-vertical N-S, and low-angle NE-SW normal faults. These folds plunge SE with very-low angles (<5°) with axial planes mainly sub-parallel to the conjugate faults (Fig.4.1.4).

Drag-folds are also a very common feature in Domain 4 (Figs. 4.1.2 and 4.1.4). They vary from metre- to centimetre-scale features and are often, but

not always, associated with low-dipping faults and reverse faults widespread in the area.

Small-scale drag-folds are very common in association with faults sub-parallel to zones of steeply dipping NW-SE striking bedding, especially where sandstones are interbedded with mudstones. Occasionally they are present internally in some major folds where shortening has been mechanically transferred to reverse faults. Locally they display variable orientations but mostly plunge NW-SE and have axial planes striking NW-SE or N-S steeply dipping.

Monoclinal folds are directly associated with subvertical strike-slip fault zones striking NW-SE and NE-SW (Photo 4.1.9).

The best example of these open-to-close folds, plunging N-NE or E-NE at low angles (< 25°), is along the P-Q section, 50-60m from the beginning (adjacent to F_1 fault zone; Fig.4.1.4; Photo 4.1.9). At this point the vertical NE-SW striking limbs of the fold are cut by an array of strike-slip faults sometimes accommodated by the bedding planes as slip surfaces or cross-cutting at low angles to produce imbricate zones (see below).

Different metre-scale folds with different geometry from those described can be found commonly in rocks of Domain 4, as observed in the Fig.4.1.4.

They are predominantly asymmetric, verging variably N-NE or NW, open to close with broad or equant aspect ratio, and angular to subangular bluntness. Their orientation is variable, defining upright moderately or moderately inclined and moderately plunging to recumbent folds. Axial planes strike mostly N-S, ENE-WSW or NW-SW dipping steeply. Their axes plunge shallowly (20°-02°) towards NE, SE or W. The fold labelled "2" (Fig.4.1.4) is cut by a NNE fault on its N side (Fig.4.1.4). Fold "3" is cross-cut in both limbs by faults orientated sub-parallel to its axial surface.

The beds observed in many of these folds display significant variations in thickness especially comparing limbs and hinge zones (Photo 4.1.10).

The stereonet in the Fig.4.1.6 shows the axial plunge of the folds present in Domain 4, along the section. They are strongly concentrated in the NW and SE quadrant, plunging with shallow angles.

b) Faults: Most of the faults observed along Domain 4 are *oblique-slip faults* orientated NW-SW, N-S and NE-SW (Fig.4.1.9). The oblique-slip faults display both normal or reverse components, together with consistent sinistral displacements of different magnitudes.

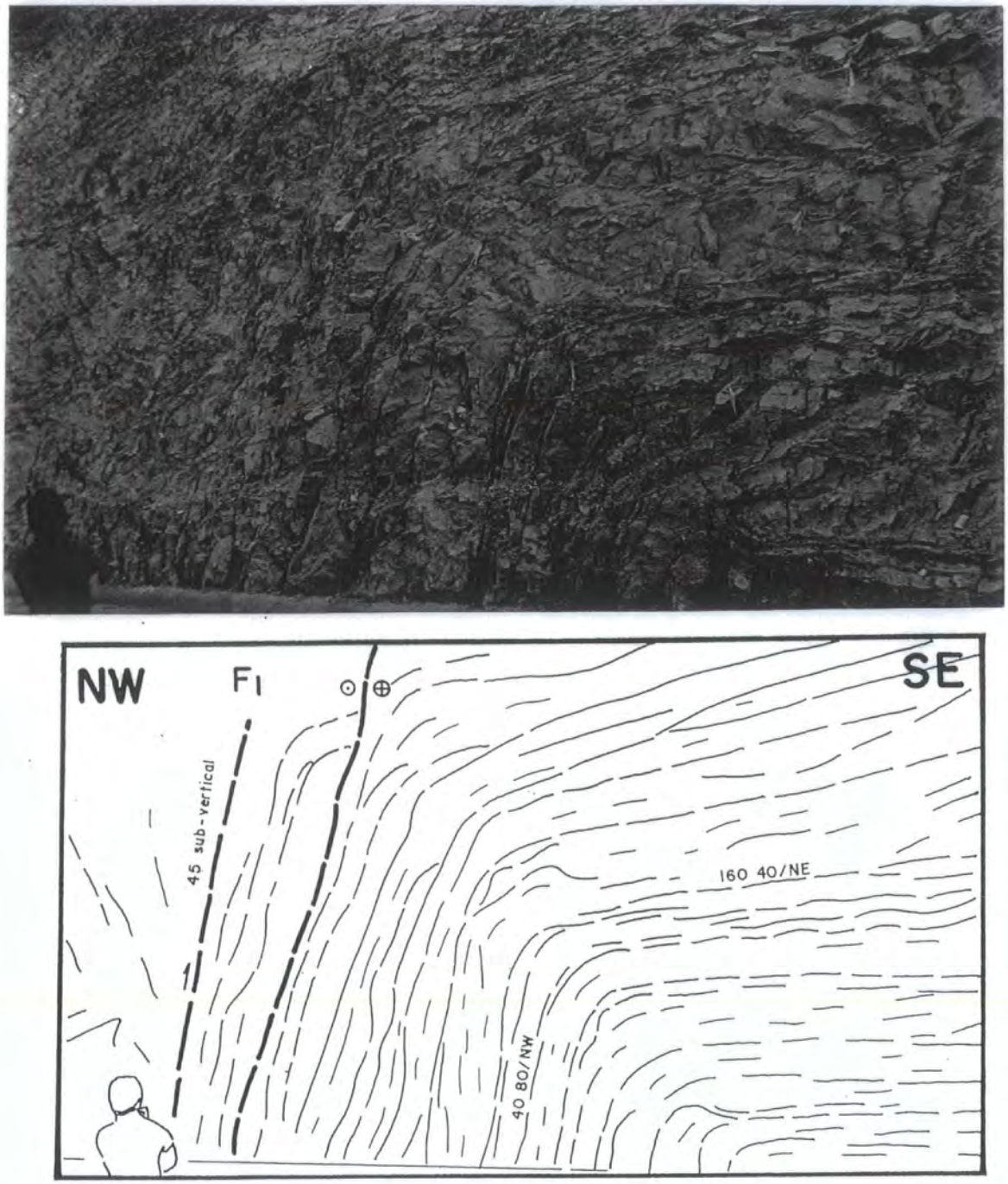

Photo 4.1.9- Decametre-scale monoclinal with a characteristic sub-vertical limb adjacent to the subordinated fault zone (50m along the P-Q section, Fig.4.1.4).

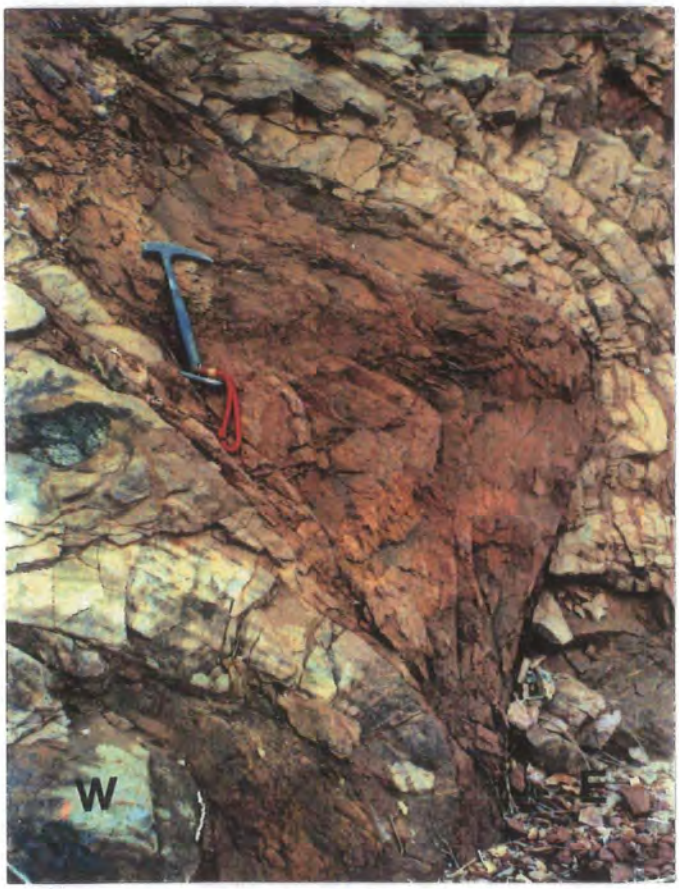

Photo 4.1.10- Hinge region of a recumbent fold observed along the section R-S (Fig.4.1.4).

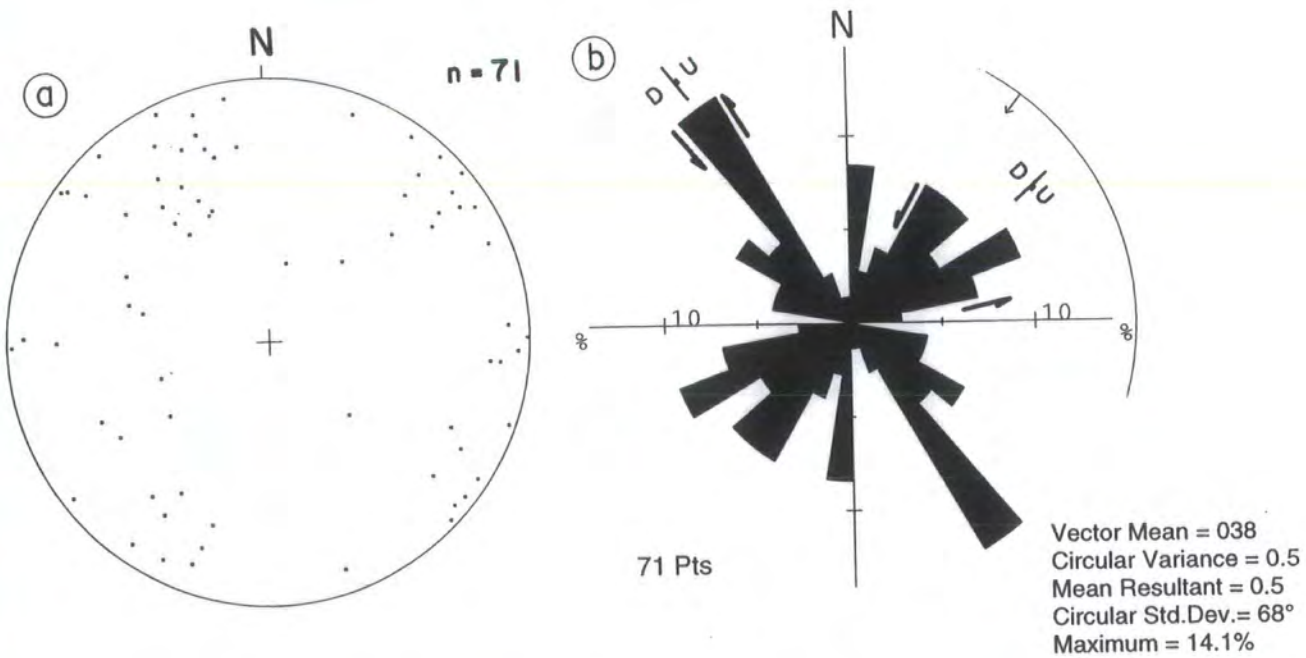

Fig.4.1.9- a) Stereonet representing poles to fractures observed along all the rocks outcropping in the Domain 4. b) Rose diagram showing the orientation of these fractures. Fractures NW-SE have a sinistral displacement associated with a reverse movement (top-to-SW); NE-SW ones are also sinistral with a reverse component (top-to-NW).

On a large scale Domain 4 is cut by at least four major fault zones (labelled F_1 to F_4, Fig.4.1.4), each between 5 and 25m wide. The main characteristics of these fault zones are their association with the vertical limbs of the monoclinal folds (Photos 4.1.9 and 4.1.11), as mentioned above. Intense imbrication is observed along many of these fault zones (Photos 4.1.11 and 4.1.12), with the fault surface crossing obliquely through the bedding and displacing layers within a complex array of anastomosing fault branches (Fig.4.1.10). Small drag-folds deforming the bedding can be observed between fault strands. The orientation of these drag-folds can be rather variable, and may depend on the slip direction of the associated fault (Fig.4.1.10). Folds may plunge at low angles forming synclines or anticlines, or plunge steeply to sub-vertically forming neutral folds.

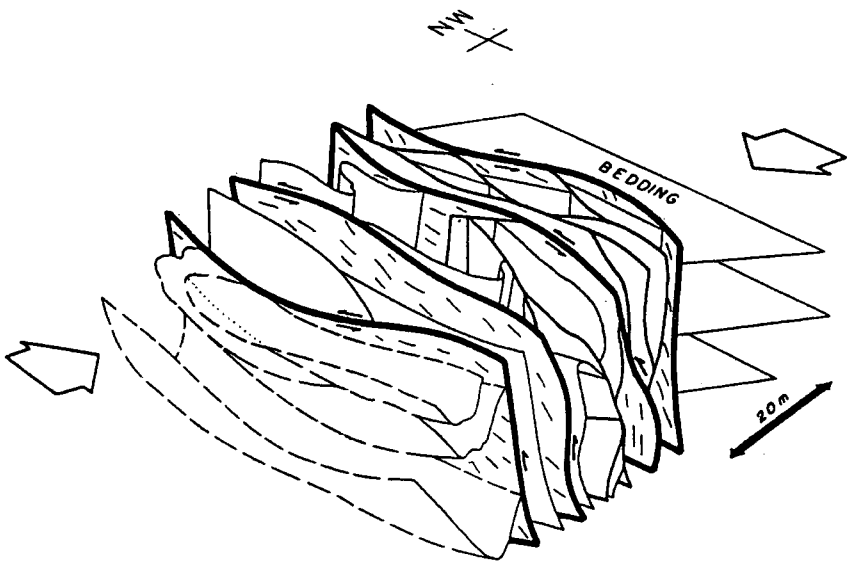

Fig.4.1.10- Diagram illustrating the main features observed inside the main fault zones: sub-vertical bedding, imbrication, small folds with different orientations, strong discordance with bedding outside the fault zone.

Slickenlines along fault planes are mostly at low angles (10°-20°), but steeper orientations are also present (see small stereonets to these faults in Fig.4.1.4). The kinematics of these faults are not easily deduced in the field since kinematic indicators are only sporadically preserved. Slickenfibres are poorly visible in some fault planes, and more than one set may be developed.

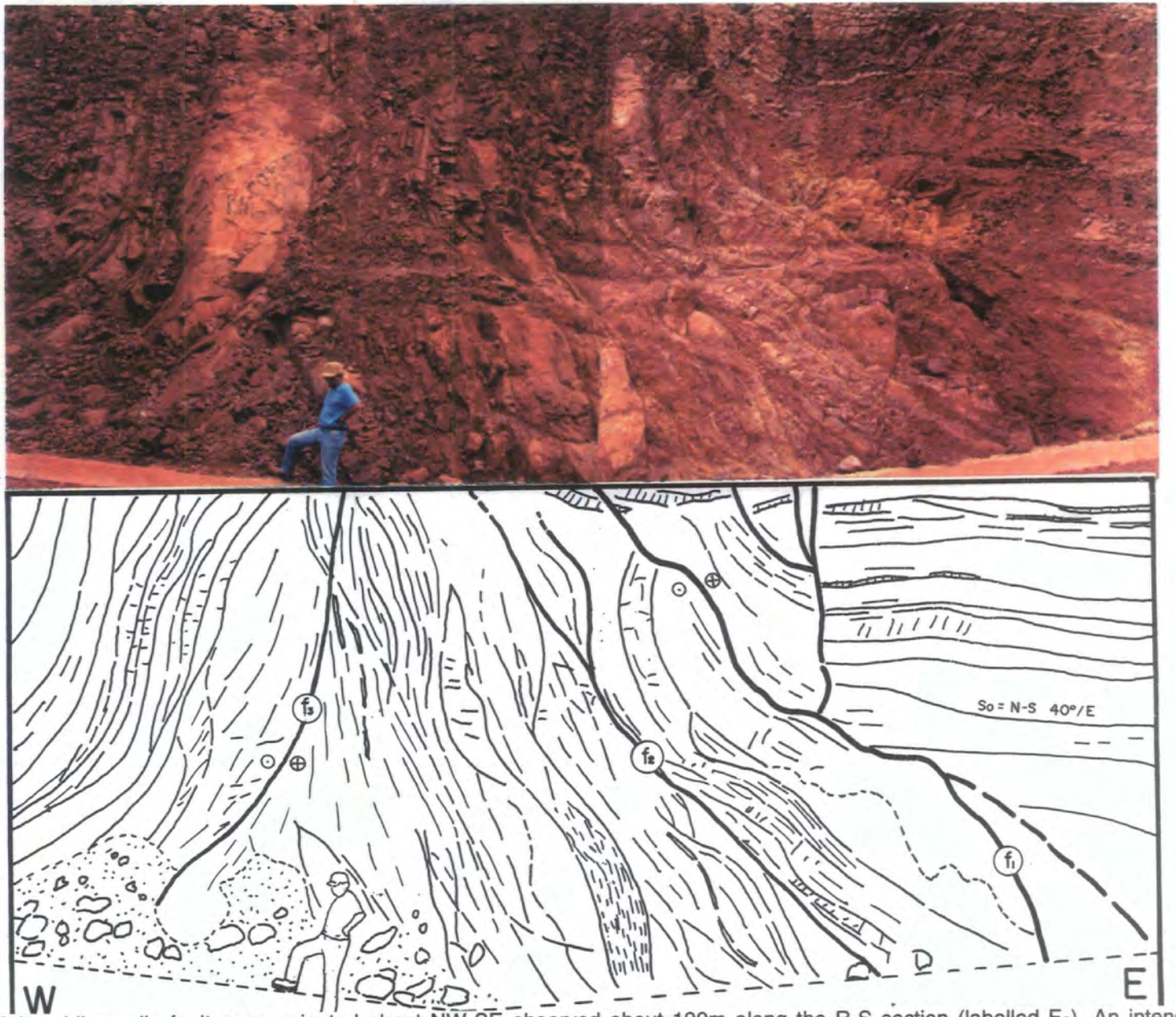

Photo 4.1.11- Major oblique-slip fault zone, oriented about NW-SE observed about 190m along the R-S section (labelled F_2). An intense imbrication is observed inside the fault zone, where the bedding is rotated to the sub-vertical. Note the abrupt relation between this zone and the rocks in the E, out of the zone. f_1= 320° sub-vertical; f_2=300° 80°/NE with slickenlines 45°/130°; f_3=310° 55/SW, slickenlines 40°/120°.

Other slip sense indicators observed include alternating polished and rough facets and secondary fractures following the direction of T-fractures, seen in plan view along some faults. Collectively, these structures suggest a predominance of oblique-sinistral faults with a subordinate high-angle reverse displacement either top-to-SW or top-to-NW. Another important characteristic of these oblique-slip fault zones is marked variations in movement direction along adjacent faults so that strike-slip and reverse faults may occur side-by-side suggesting that kinematic partitioning has occurred.

Photo 4.1.12- The abrupt contact of the fault zone with adjacent undeformed rocks.

The associated monoclinal folds are always developed in the hanging wall fault block. The hinge regions of the monoclines may be partially or totally cut out by the faults (e.g. Photo 4.1.12).

Faults with a predominant *reverse* movement are also common in Domain 4 (Photo 4.1.13). Their orientations are predominantly NW-SE or nearly N-S, dipping 40°-80° NE or E. Fault planes often follow bedding and small scale folds may be developed in adjacent fault blocks. Slickenlines along these faults always show a minor component of strike-slip displacement. Single fault planes are common, but conjugated sets also occur. Excellent examples of these structures can be seen about 150m from the beginning of the section R-S where a set of NW-SE reverse faults dip 30°-45° NE. They are approximately parallel to the bedding and slickenlines plunge about 25°-35° NE.

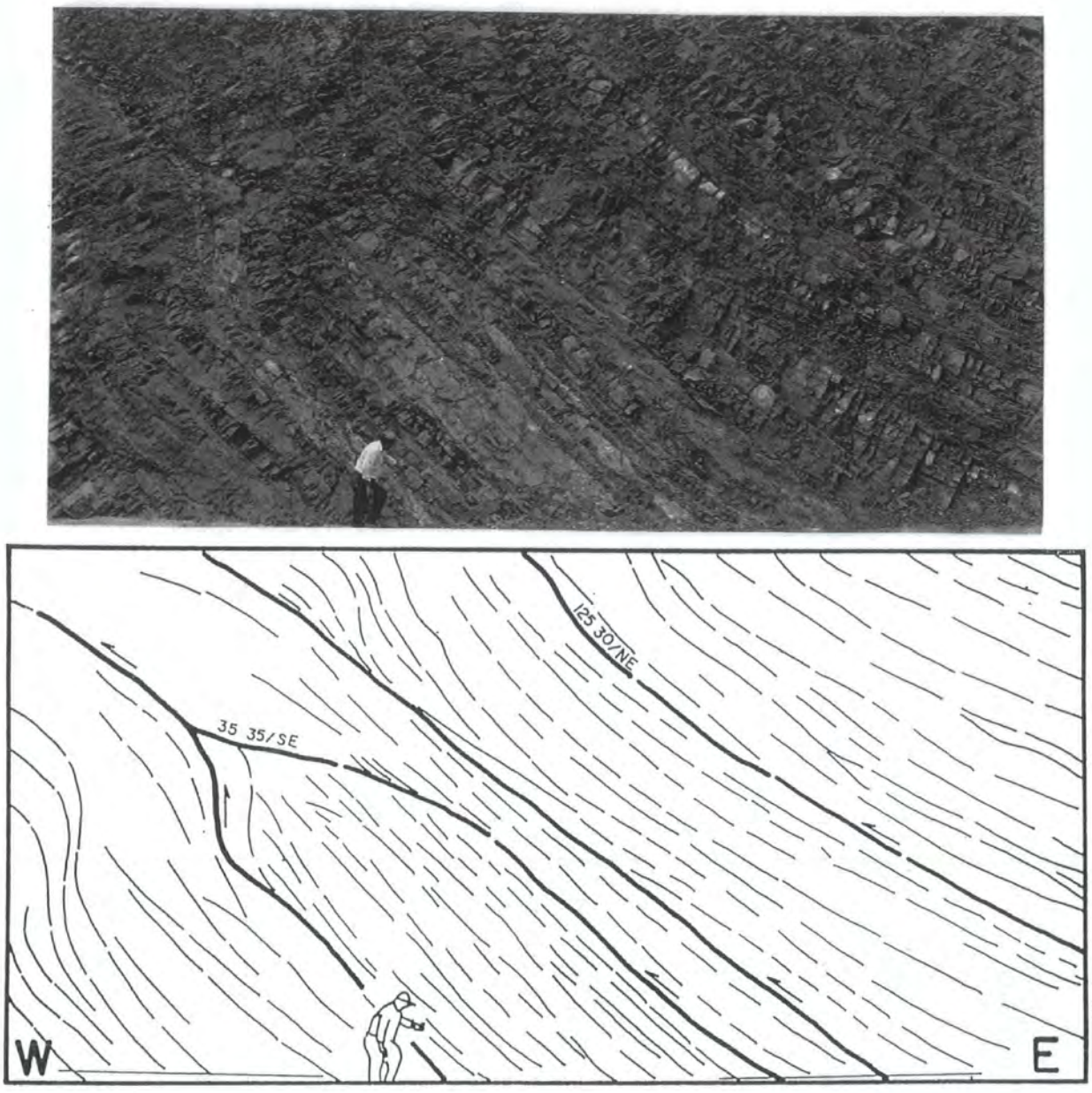

Photo 4.1.13- Set of nearly NE-SW and NW-SE reverse faults sub-parallel to the bedding observed along the R-S section (Fig.4.1.4).

The best example of the occurrence of reverse faults in the oblique-slip fault zones, in association with bedding rotation to the vertical, is along the T-U section where they are orientated NE-SW and NW-SW, dipping NE or SE at about 30°-45°. These faults are responsible for the relatively intense lithological imbrication observed along this fault zone.

Normal faults are subordinate features in Domain 4 and show a small component of strike-slip. Normal faults limit both E and W sides of Domain 4 where they are NW-SE, sub-vertical structures. The displacement along these faults is hard to determine since the complete thickness and the geometry of the sequence C can not be observed. A minimum displacement of 200m can be estimated roughly, taking into consideration the outcropping thickness of the rock sequences (Fig.4.1.3).

Normal faults within Domain 4 are predominantly N-S steeply dipping features, with small (<3m) top to the E displacements in most cases. The best example of these faults is present at the beginning of the R-S section (Figs.4.1.4, labelled f_1), cutting tidal sandstones and mudstones (Photo 4.1.14).

Sets of small normal faults with displacements of decimetres are observed at the end of the R-S section, forming a set of systematic fractures cutting the bedding of the sandstones (Fig.4.1.4).

Steeply-dipping *fractures* are abundant in Domain 4, but are especially widespread from about 160m to the end of the R-S section and all over the rest of the Domain 4 towards the E (Fig.4.1.4). They display mostly N-S, NNE-SSW and NNW-ESE trends. They are systematic, straight to slightly curved features, with a continuity of more than 20m in most cases. Fracture terminations, where observed were mostly straight. Tension fractures are less continuous and are closely associated with folds where they can have a very variable orientation.

c) Dykes: In Domain 4 there is a single, heavily weathered dyke found along the T-U section (Fig.4.1.4). This strikes NE-SW and cross-cuts the NE-SW oblique fault zone. The shape of this dyke in section is bifurcated, with an irregular border and it contains metre-scale slices of the wall-rocks (sandstones) inside the main body.

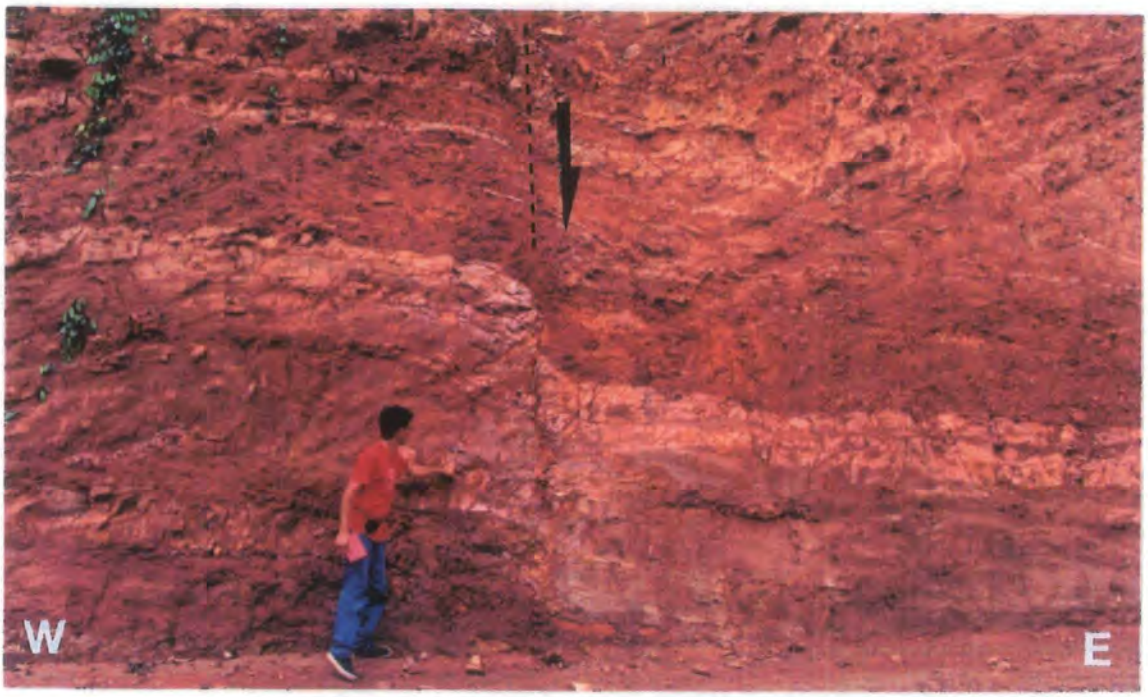

Photo 4.1.14- Small N-S normal fault displacing beds of mudstones and sandstones in the limb of folds present at the beginning of the R-S section (Fig.4.1.4).

4.1.4.5- DOMAIN 5.

Domain 5 corresponds to the rocks in the NE corner of the map in Fig.4.1.2. Sequence D in this domain represents a set of fluvial braided sandstones and conglomerates (Nogueira, 1995). The most common sedimentary structures present in these rocks are tabular cross-stratification, trough cross-stratification and parallel lamination. The sandstones are fine to coarse grained, occasionally associated with small amounts of siltstones and mudstones. The conglomerates are polymictic, with pebbles of quartz and flint with a diameter <1cm, set in a coarse sand matrix. The thickness of beds varies from a few centimetres to < 1m, with remarkable lateral continuity.

Bedding is orientated with mainly NNW-SSW to NE-SW strikes, dipping 20°-40° W.

A dyke swarm with sheets orientated mostly NNW-ESE and secondarily NE-SW and NW-SE is developed widely in this domain (Fig.4.1.2; Photo 4.1.15). They are tabular features, about 1-2 Km spaced and with a thickness ranging from 10m to about 300m. The thicker dykes (>100m) are NE-SW and NW-SE orientated and appear to correspond to regional lineaments observed in satellite images (Photo 4.1.1). An aureole of thermal metamorphism with

variable thickness is always observed in the sandstones where these dykes are emplaced (Photo 4.1.15).

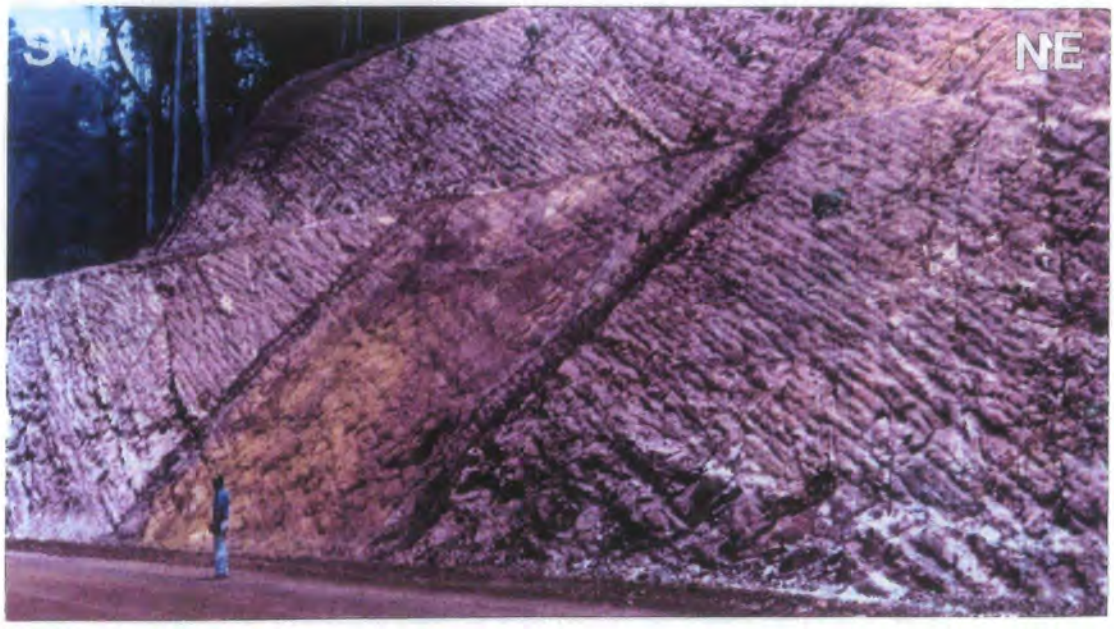

Photo 4.1.15- An example of N-S dyke cutting sandstones in the Domain 5.

Faults and fractures are present in several places in this domain. One of the most important examples occurs at about 700m from the end of the mapped road (Fig.4.1.2) where a sub-vertical oblique fault orientated N-S is associated with a metre-scale monoclinal fold in its hanging wall, similar to those described in Domain 4 (Photo 4.1.16; Fig.4.1.9) This fold is asymmetric, open and angular to sub-angular, with an axial plane striking NNW-SSE, dipping ca. 50° NE. Its axis plunges 30°/N. The beds in the opposite block (foot wall) with an attitude 105° 20°/NE are rotated clockwise (approximately 15°) in relation to those in the hanging wall (240° 19°/NW; Fig.4.1.11). Slickenlines are poorly preserved along the fault plane but are plunging moderately S.

An isolated set of open folds occurs a few hundred metres from the end of this section. It corresponds to rounded, symmetric folds, deforming the trough cross stratification. They plunge shallowly (<10°) N.

Sets of both sinistral and dextral strike-slip faults oriented NE-SW cut the rocks in this domain (Photo 4.1.17; Fig.4.1.2). These faults are apparently responsible for rotations and observed in the bedding along this section adjacent to faults (Fig.4.1.12). The bedding is also deformed adjacent to dyke swarms.

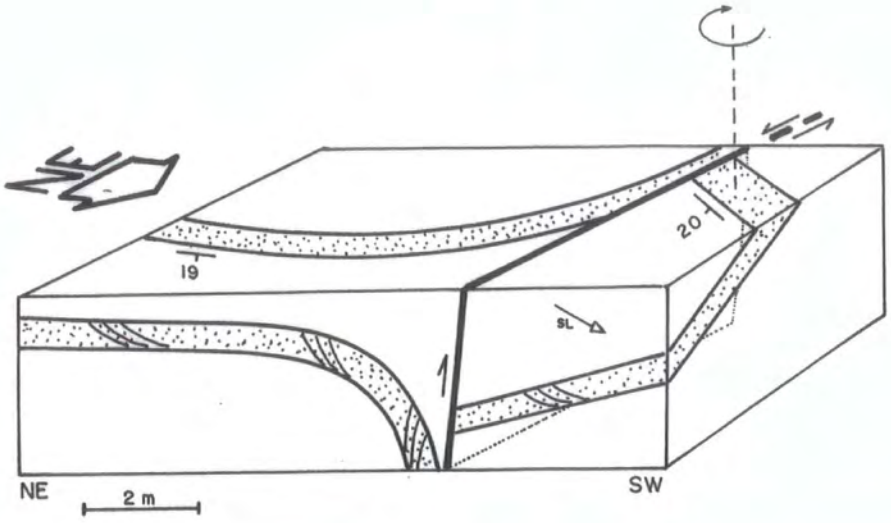

Fig.4.1.11- Diagram illustrating the geometric relation between fault and fold observed in the end of the section along the Domain 5. The footwall block was tilted and rotated clockwise.

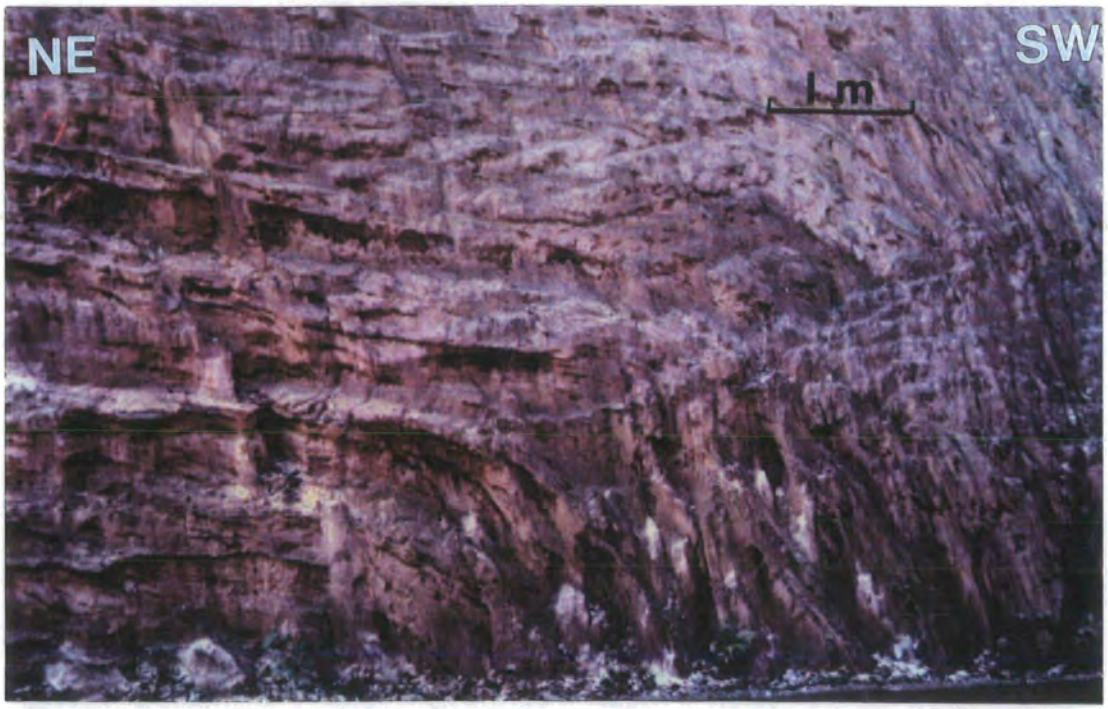

Photo 4.1.16- Monoclinal deforming sandstones observed in the Domain 5. Compare with that on Fig.4.1.12.

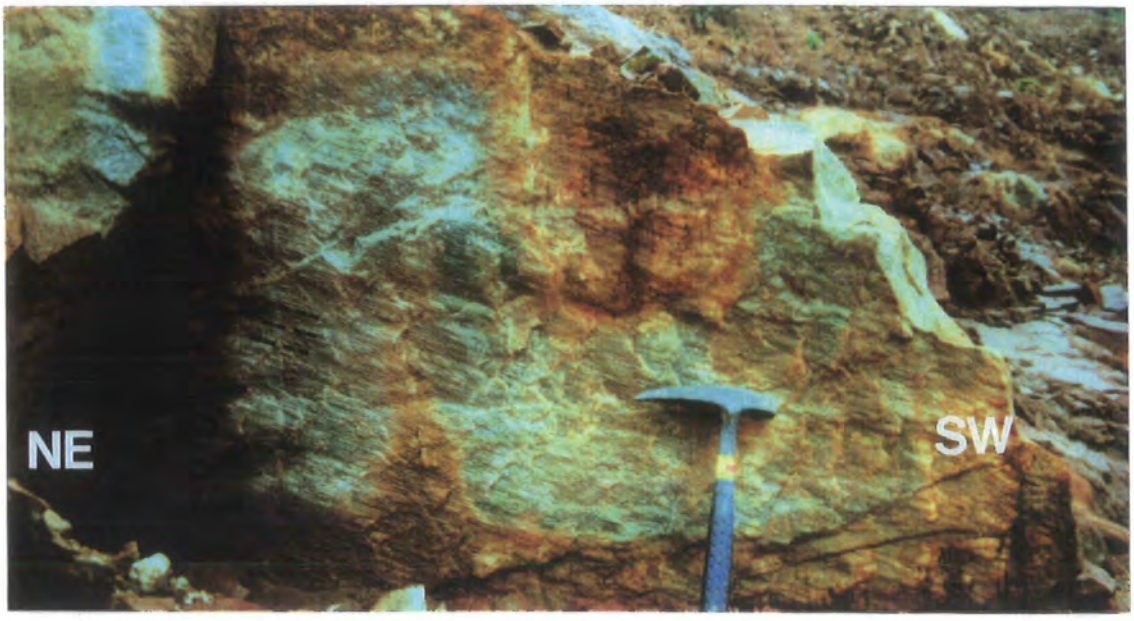

Photo 4.1.17- Slickenside observed along NE-SW strike-slip faults cutting rocks in the Domain 5.

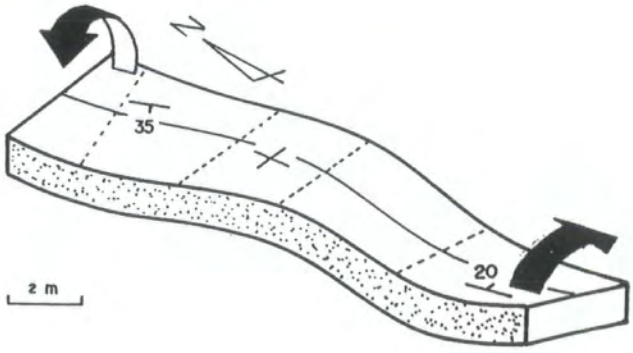

Fig.4.1.12- Torsion-bedding structure observed along the section in the Domain 5.

4.1.5- DISCUSSION

The tectonics observed in the central area of the Carajás Strike-Slip System is dominated by the formation of faulted blocks on a kilometre-scale. They have a rhombo-shaped geometry defined by sets of faults orientated at NW-SE and NE-SW, variably spaced by approximately 1-2 Km (Figs.4.1.2 and 4.1.13). These faults are thought to form the marked lineaments observed with these trends in satellite and radar images (Fig.4.1.1).

Figure 4.1.13 summarises the observed geometry and kinematics of the different domains studied along the road in the Águas Claras River region. On a large-scale there is a predominance of normal and oblique-sinistral strike-slip displacements. The faults are most probably subvertical or with high-dip angles due to the straight to slightly curved traces that their lineaments show on satellite images (Photo 4.1.1; Fig.4.1.1). The vertical displacement of these faults is thought to be a few hundred metres or less considering the exposed thickness of the faulted sedimentary sequences.

The block corresponding to Domain 2 is a horst that was uplifted exposing the lower part of the section (sequence A, offshore deposits). The block corresponding to Domain 5 (Sequence D, fluvial deposits) is the lowest graben of the region studied, whilst the blocks corresponding to domains 1 and 4 are in an intermediate position in relation to the adjacent blocks (Fig.4.1.13).

The intensity and style of deformation within these distinct blocks varies markedly. The bedding in the layers representing domains 1, 2 and 5 (Figs. 4.1.2 and 4.1.3) is affected mainly by fractures with only minor rotation or tilting.

The block defined by Domain 3 (Figs.4.1.2 and 4.1.13) is a region where rocks are very sheared and influenced by hydrothermal alteration and later weathering. It is thought to correspond to a major fault zone or to a very fractured zone where there has been an extensive influx of hydrothermal fluids. The sense of displacement of the probable major fault or faults responsible for the development of this zone is not clear from the poorly exposed structures present.

Domain 4 (Figs.4.1.2 and 4.1.4) is marked by a very high concentration of meso-scale deformational features such as folds and faults strongly contrasting with the adjacent blocks. A complex set of folds, reverse, thrust and sinistral strike-slip faults and normal faults is developed.

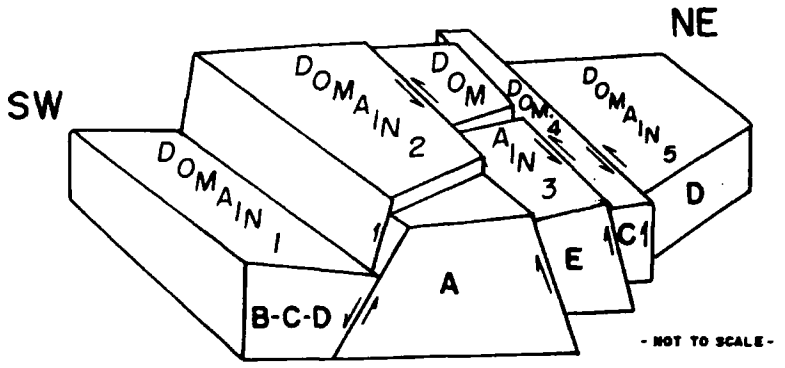

Fig.4.1.13- Sketch representing the orientation and the relative vertical displacement of blocks observed to the central area of the Águas Claras region.

The folds present in this domain are predominantly curvilinear on a large scale forming a train of folds plunging shallowly N, S, NE or SE (Fig.4.1.5). Individual folds in this set are non-cylindrical structures with a conical tendency (Fig.4.1.8). Complex curvilinear outcrop-scale folds are observed in close association with non-cylindrical major folds (Fig.4.1.7). Small folds with different geometry are also present. Kinks/chevron and the monoclinal-folds have nearly the same orientation as the semi-cylindrical and curvilinear structures: axial planes lie close to the NW-SE or N-S orientation and axes plunge towards the N or NE (Fig.4.1.4).

The comparison of these orientations suggests that the folds were mostly formed under similar strain field, but they may not be entirely coeval since they locally refold one another (e.g. Fig.4.1.7). The complex curvilinear geometries are thought to reflect either non-parallelism between bedding and principal strain axes (cf. Treagus and Treagus, 1981) and/or the development of transpression strains, possibly with variable degrees of partitioning (cf. Strachan *et al.*, 1992, Holdsworth, 1994).

The large-scale monoclinal folds are always in the hanging wall of oblique reverse-sinistral fault zones. These fault zones affect partially the sub-vertical limb of the monoclinal folds producing lithological imbrication on different scales. The slickenlines along fault planes show evidence of both reverse and sinistral strike-slip displacement, reflecting a substantial amount of strain partitioning within these fault zones. Oblique-slip displacements are also observed and some fault planes show overprinted slickenlines suggesting a long term history of activity.

Based on the fold-fault relationship observed in the major monoclinal-folds, with their associated faults, it is possible to suggest the following kinematic history involving these features under a transpressional deformational field, illustrated in the Fig.4.1.14: (1) high-angle reverse-sinistral faulting starts obliquely cutting the beds; (2) as the fault increases its vertical movement, the beds in the hanging wall progressively bend against the fault plane, forming a fold projected sub-parallel to the fault; (3) the deformation is gradually propagated towards the footwall, since the fold in the hanging wall has a tendency to lock-up. Sets of curvilinear folds can develop in the footwall resulting from transpression (NE-SW shortening+sinistral strike-slip); (4) Strike-slip kinematics progressively dominate the system and strain hardening projects strike-slip fault towards both footwall and hanging wall. The fault zone becomes wide and the imbrication of the rocks along this zone increases. Some of these monoclinal folds do not reach the stage 4 and a single large fold is formed in front of the fault plane. In outcrop, these folds and faults are observed at a number of levels of depth. Sylvester and Smith (1976) described a very similar set of structures thought to be formed by drag induced by transpression along the Painted Canyon Fault in the San Andreas Fault zone.

The kinks and chevron folds may be related to displacement along individual fault strands. Some kinks affect the limbs of curvilinear folds while others are particularly isolated.

The relationship between the deformation of the high sheared rocks observed in Domain 3 and the deformation that took place in the adjacent Domain 4 is hard to establish with any certainty.

The normal faults delimiting the kilometre-scale blocks are mostly sub-parallel to the oblique reverse-sinistral sets present in the strongly deformed area. There is no clear cross-cutting relationship exposed between these fault sets, but some small scale normal faults cut-across folds and other structures associated with the oblique-slip faults. An example of this relationship is preserved at the beginning of the R-S section where a normal fault is seen cutting the limbs of folds (Fig.4.1.4).

According to Nogueira *et al.* (1992, 1994 and 1995), Nogueira (1995) and Pinheiro and Holdsworth (1997*a*), the clastic sequences present inside the Carajás Structure form a tectonically preserved part of a wider and larger sedimentary basin that dominated the region between ca.2.7/2.8 Ga and 2.6 Ga (age of the gabbroic sills intruded in the Águas Claras Formation, according to Dias *et al.*,1996*a*). A probable regional transtensional episode of deformation has been suggested as being responsible for retaining part of these rocks

inside a dilational jog formed by reactivation of old faults (Pinheiro and Holdsworth, 1997*a*).

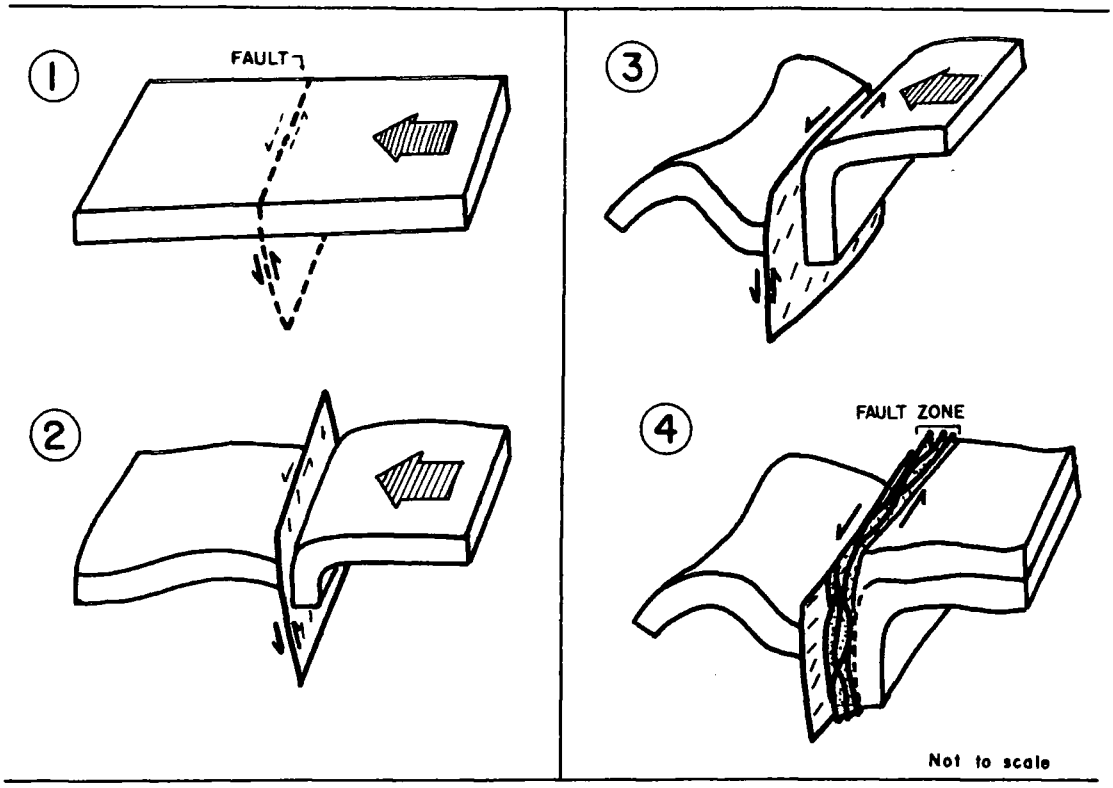

Fig.4.1.14- Simplified evolution of the monoclinal folds and main fault zones: 1) fault is projected cutting the beds; 2) the main reverse component of displacement induces bending of the beds against the fault plane; 3) strain is transferred gradually to the footwall producing folding; 4) strike-slip component of displacement dominates the final stage and propagates faults towards the hanging wall, producing lithological imbrication and partial deformation of the monoclinal fold limbs.

The folds and faults in Domain 4 are consistent with a transpressional episode of deformation. The deformation is limited to a zone sub-parallel to the Carajás Fault and, as it deforms the Águas Claras Formation, it must post-date the transtension responsible for preserving the sedimentary rocks inside the Carajás Structure (<2.6 Ga). It must also pre-date intrusion of the Middle Proterozoic plutons (ca.1.9 Ga) which cross-cut the Carajás Fault.

It is suggested that plutonism and dyke emplacement were related to a later extensional / transtensional episode of deformation. The block-deforming normal faults present in the area are younger than the deformation observed in the rocks of Domain 4 and they are probably associated with this Middle Proterozoic episode.

There is a clear equivalence between the main faults observed on field and lineaments observed in satellite images (Figs.4.1.1 and 4.1.2; Photo 4.1.2). Some of these lineaments correspond to major segments of the Carajás Fault. The structures observed in the section show that the Carajás Fault underwent an important phase of sinistral transpression during its tectonic history, affecting the rocks in relatively narrow zones close to its main fault planes and branches. This is predominantly brittle to brittle-ductile and may have been strongly influenced by the presence of fluids during and after deformation.

The concentration of the deformation in relatively narrow zones can be a response to a high strain rate or the effects of a large scale strain softening where the role of fluids could be essential controlling deformation.

The main geometric characteristics of the Águas Claras section are illustrated in Fig.4.1.15.

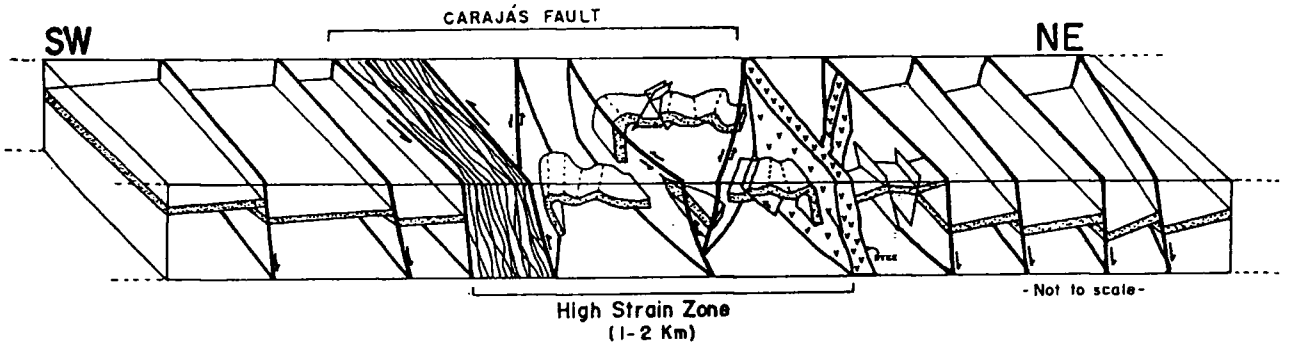

Fig.4.1.15- Sketch summarising the most important geometric characteristics of the area studied in the Águas Claras region. The Carajás Fault produces the most important features observed.

4.1.6- CONCLUSIONS

1) The central region of the Carajás Strike-Slip System is dominated by brittle faulted rocks. A kilometre-scale set of rhomboidal blocks delimited by NW-SE and NE-SW faults is developed with a spacing of about 1-2 Km. The faults are normal and oblique-slip structures with relative and apparent displacements of about 200m or less.

2) Deformation is extremely partitioned into relatively narrow zones a few hundred-metres to 1-2 Km wide. These zones are both limited by and occur along major fault zones, linked splays of the Carajás Fault.

3) Zones of intense deformation are characterised by two different sets of structures: (1) cataclastic zones; and (2) folding-faulting zones. Cataclastic rocks are concentrated in zones about 800m width corresponding to major fault strands associated with secondary branches of the Carajás Fault. Fluid influx is widespread in these zones. Folded and faulted rocks are also present in 1-2 Km wide zones sub-parallel to branches of the Carajás Fault. Deformation in this zone is dominated by transpressional tectonics (sinistral strike-slip + reverse dip-slip kinematics).

4) Transpressional tectonics is thought to be associated with the reactivation of the Carajás Fault during a regional event that took place between ca.2.6 Ga and ca.1.9 Ga.

5) Normal faults controlling the geometry of major blocks are likely to have formed during Middle Proterozoic extension or transtension that took place on a regional scale.

6) Dykes were emplaced along old discontinuities forming swarms visible in satellite and radar images. They can be related to the Middle Proterozoic extension responsible for the normal faulting affecting the region.

4.2- THE AZUL MINE

The Azul manganese deposit in the Carajás region was discovered in September of 1971 by geologists of the Companhia Meridional de Mineração and Companhia Vale do Rio Doce (CVRD). It lies about 15 Km southwest of the N-4 plateau and 13 Km south of the N-1 Camp, in the northern-central part of the Carajás Strike-Slip System (Fig.4.2.1 and Photo 4.2.1).

The Mn-ore in the open cast mine ranges from about 30 to 50% Mn in volume and is hosted in strongly weathered shales and siltstones belonging to the Cover Assemblage. The total volume of the deposit is estimated at around 6×10^7 tons (Silva, 1988). Since its discovery, the stratigraphical position of these rocks has been subject to controversy. The rocks are moderately deformed by folds and faults which have been recognised since the pioneering geological work in the region (e.g. Anderson *et al.*, 1974).

In this section, the geometric and kinematic aspects of deformation in the rocks of the mine are investigated based on detailed structural mapping. The relationship between the deformation observed in the rock and the Carajás Fault is investigated. Regional stratigraphical affinities of the rocks are also discussed.

4.2.1-REGIONAL SETTING

The rocks exposed in the mine are deeply weathered and bedrock is scarcely found.

The Azul Mine lies along the NW-SE trace of the Carajás Fault, about 3 Km NW of the Central Carajás Granite which cuts the fault in the central part of the Carajás Strike-Slip System (Fig.4.2.1 and Photo 4.2.1).

The dominant rocks in the region as a whole are clastic sedimentary rocks belonging to the Águas Claras Formation (Araújo and Maia, 1991; Nogueira *et al.*, 1995), and are cut by gabbro sills ca.2.6 Ga (Dias *et al.*, 1996*a*) and by the intrusive Central Carajás Granite ca.1.8 Ga (Wirth *et al.*, 1986).

The Águas Claras Formation is locally strongly deformed by structures related to the Carajás Fault (Pinheiro *et al.*, 1991; Nogueira *et al.*, 1992; Nogueira, 1995; Pinheiro and Holdsworth, 1997*a*). This deformation is most intense in regions immediately adjacent to the main segments of the Carajás

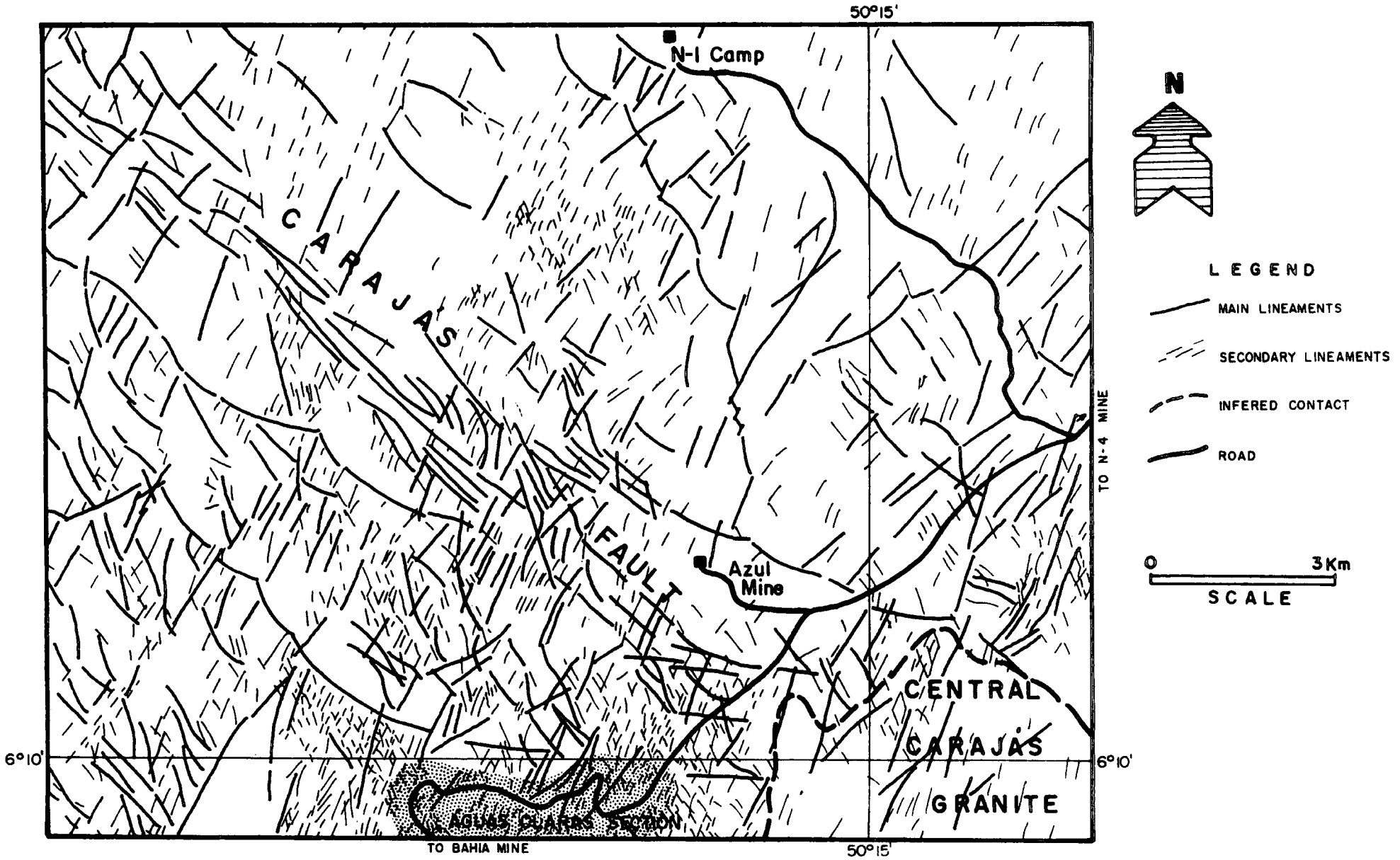

Fig.4.2.1- Map of main lineaments from LANDSAT images from the central area of the Carajás Strike-Slip System.

Photo 4.2.1- LANDSAT image of the central part of the Carajas Strike-Slip System. The white point represents the location of the Azul Mine.

Fault (e.g. see sections 4.1 and 4.3). The Central Carajás Granite cuts the Carajás Fault.

4.2.2- PREVIOUS WORK.

Anderson *et al.* (1974), Valarelli *et al.* (1978) and Bernardelli and Beisiegel (1978) are the most important publications on the geology of the Azul Mine. These authors present a comprehensive description of the rock-types present, their origins and economic potential.

Five major groups of rocks are thought to exist in the mine: (1) a carbon-bearing siltstone and pyrite-rich shales with *Siderocapsaceae pribian* (Lindenmayer, 1993). The unit is about 75m thick, lying around 200m below the surface. Overlying these rocks there is (2) a 17-35m thick, 21-25% manganese-rich shale, associated with a rhodochrosite-bearing limestone (named "Inferior Manganese Ore Unit"). This is followed towards the top by (3) a shale/siltstone 77-79m thick. Covering these rocks is the (4) "Superior Manganese Ore Unit" with about 13-35% of ore hosted in mudstones and shales. Finally (5) a 66m thick crust of deeply weathered mudstones occurs at the top of the succession, with about 6% of Mn-ore (Anderson *et al.,* 1974; Bernardelli and Beisiegel, 1978).

These rocks are E-W striking and have been referred to as the Igarapé Azul Member, a sub-unit of the Rio Fresco Formation (Silva *et al.,* 1974; Anderson *et al.,* 1974; Bernardelli and Beisiegel, 1978; Valarelli *et al.,* 1978; Cunha *et al.,* 1981). Later, Cunha *et al.* (1984) changed the category of the Rio Fresco Formation to 'group' and the rocks of the Azul region became the so-called Igarapé Azul Formation, a unit of the Rio Fresco Group, thought to be of Proterozoic age. This proposal was supported later by several authors (e.g. Meireles *et al.*, 1984).

Gibbs *et al.* (1986), followed by Olszewski *et al.* (1989), Gibbs and Wirth (1990), and Lindenmayer (1993) preferred to correlate the pelitic rocks of the Azul Mine with the upper sequence of the Grão Pará Group. Figueira *et al.* (1987) suggested that correlation of the rocks in the Azul mine with the Rio Fresco Formation or Group is incorrect. Macambira *et al.* (1990) proposed a rather different stratigraphical framework in the region, referring to the rocks from the Azul Mine as Igarapé Boa Sorte Formation, an upper unit of the Grão Pará Group.

Araújo and Maia (1991) suggested a transtensional origin for the clastic sedimentary rocks present inside the Carajás Structure and introduced the term Águas Claras Formation, an upper unit of the Grão Pará Group, Archaean in age, for these rocks. Later Nogueira *et al.* (1995) described this unit according to stratigraphical procedures.

The deformation structures in the Azul Mine have been subject to little study. A set of asymmetric folds, plunging shallowly towards the east or west has been described (Bernardelli and Beisiegel, 1978; Anderson *et al.*,1974), cut by E-W strike-slip faults and N-S dip- or oblique-slip faults (Bernardelli, 1982). Further structural investigations, more specifically in the Azul Mine, were carried out by Marçal (1991) who suggested that the folds and faults were related to the development of a regional divergent strike-slip structure ("flower structure") described by Araújo and Maia (1991).

4.2.3- DATA FROM SATELLITE IMAGE.

Radar images (1:50.000 scale) and LANDSAT images (1:100.000 scale) of the region adjacent to the Azul Mine area (Photo 4.2.1), were interpreted (Fig.4.2.1). An important set of NW-SE lineaments crosses all the area surrounding the mine. Most of these lineaments are slightly curved forming an intricate anastomosing pattern. The Azul Mine lies in the centre of a block delimited by these lineaments. Several more continuous curved lineaments, concave towards the NE, are interlinked to define the Carajás Fault (Photo 4.2.1 and Fig.4.2.1). These features are cut by nearly NNE-SSW to NE-SW shorter and straight lineaments (Fig.4.2.1). Both the NW-SE and the NNE-SSW/NE-SW sets of lineaments correspond to drainage and relief alignments (Photo 4.2.1).

A relatively dense set of very short and fine lines orientated NW-SE and N-SW are observed in the background forming a peculiar lozenge-shaped pattern (Photo 4.2.1; Fig.4.2.1). These lines are strongly concentrated into specific areas such as the western region of the Central Carajás Granite (Photo 4.2.1).

4.2.4- FIELD DATA - STRUCTURAL GEOLOGY OF THE AZUL MINE

a) Lithology and Primary Structures: The rocks outcropping in the Azul Mine are strongly weathered. The manganese ore forms more than 70% of the

outcrop in the mine, whilst the remaining 30% is a red-yellow siltstone and several types of lateritic soils and Mn-Fe-enriched crusts.

Manganese ores in the mine are sub-divided into "superficial deposits" and "sub-superficial deposits" (Bernardelli and Beisiegel, 1978). The "superficial deposits" comprise: (1) manganiferous pisoliths; (2) manganiferous blocks and plaquettes; and (3) manganiferous breccia. Only unit (2) preserves primary structures such as laminations. These deposits are related to the geomorphological evolution of the region and the action of weathering.

"Sub-superficial deposits" rocks maybe partly altered by weathering but still preserve relict structures such as bedding, stratification and folds. According to Valarelli *et al.* (1978), they can be separated into: (1) manganiferous siltstones; (2) grained ore; and (3) massive ore. The grained ore is formed by millimetre-scale grains of ore in a fine matrix, sometimes including millimetre- to centimetre-scale platy fragments (cryptomelane). The massive ore is represented by dense, hard, centimetre-scale fragments of cryptomelane-bearing ore that replace a large volume of the protolithic rocks with their original structures preserved. The grained and massive ores form >50% of the exposed mine walls. Structures, although present, are poorly preserved in these rocks and are not considered further.

The manganiferous siltstones are less altered protolith which is scattered throughout the mine forming well defined packages on tens of metre-scales. The best exposures of these rocks occur in the walls opposite the "Belvedere", in the 528, 532 and 536m levels (Fig.4.2.2). They are light-grey-red finely laminated siltstones and sandy siltstones with Mn grading between 20-30% in volume. They are formed mainly by kaolinite, gibbsite, goethite, illite and quartz, together with Mn-oxides and -hydroxides (Bernardelli and Beisiegel, 1978). Bedding is well preserved, separating layers with 10 to 30 cm of laminated mudstones and siltstones (clay siltstones and sandy siltstones) showing a mean orientation of 133° 30°/SW (Fig.4.2.3B). The lamination is defined by dark-gray to reddish-yellow, millimetre-scale bands of silt and clay with different concentrations of Mn-bearing minerals and ?carbon. Other primary structures present in these rocks include load cast structures (Photo 4.2.2) and hummocky cross-stratification with wavelengths of about 20-40 cm (Photo 4.2.3). According to Nogueira (1995), these rocks were deposited in a marine platform environment with substantial storm activity.

Some contacts between different rocks are very well preserved despite weathering (Photo 4.2.4). The best example is the folded and faulted contact

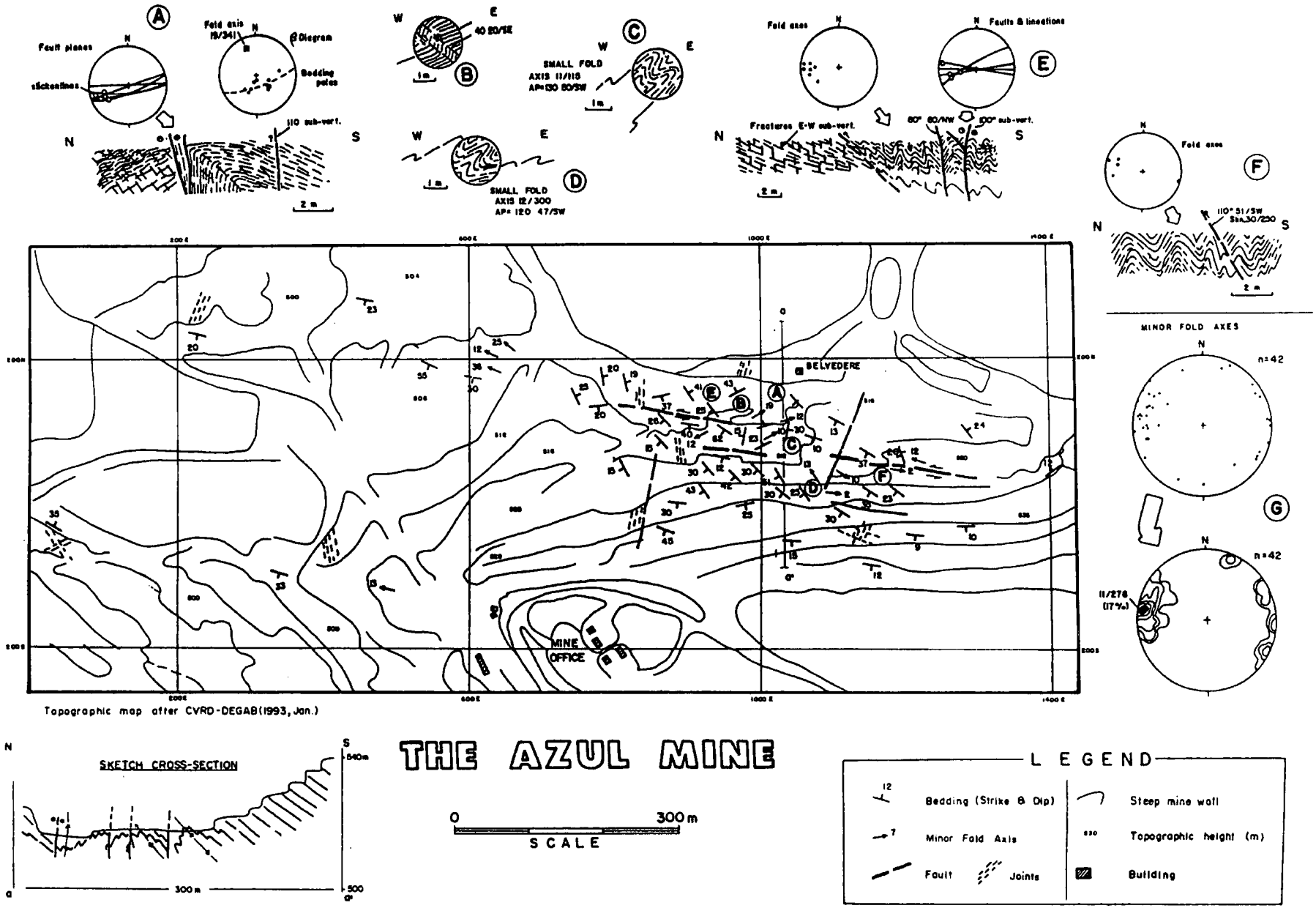

Fig.4.2.2- Map of the Azul Mine showing contours of the mine wall and main orientations of bedding, faults and folds. Locations of the sketches are also shown. Contours intervals on stereonet G (Minor fold axes): 2.3%, 4.8%, 9.5%, 12%, 14.2%, 17%.

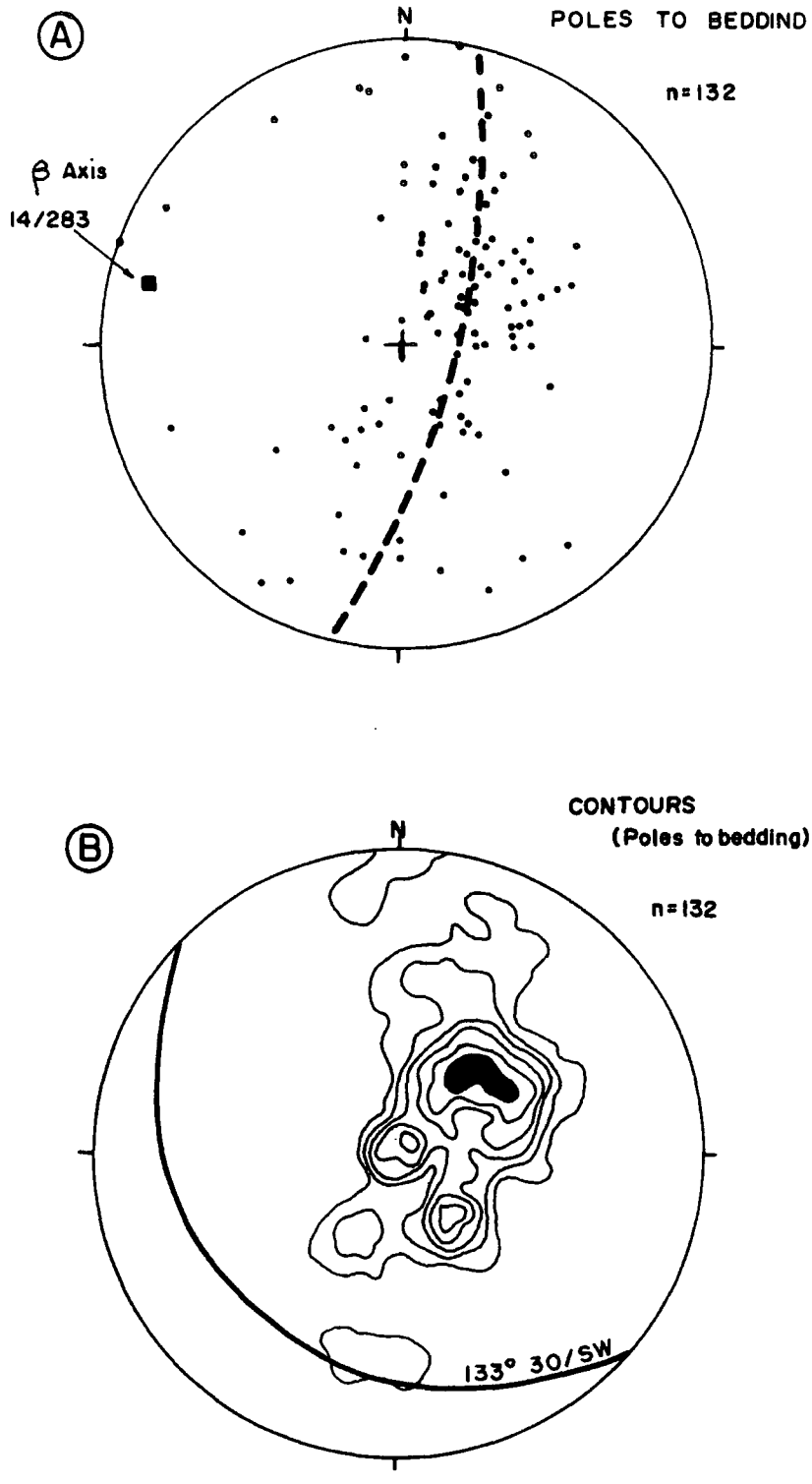

Fig.4.2.3- Stereonets of poles to bedding from the Azul mine. A) The distribution of poles defines a ß-axis to the folded bedding plunging about 14° towards 283°. B) Contours to the poles of bedding in the Azul Mine. An important concentration is observed representing a plane striking 133°, dipping 30° SW (contours: 1.5%, 3.0%, 4.5%, 6.0%, 7.5%, 9.0%, 10.5%, 12.0%).

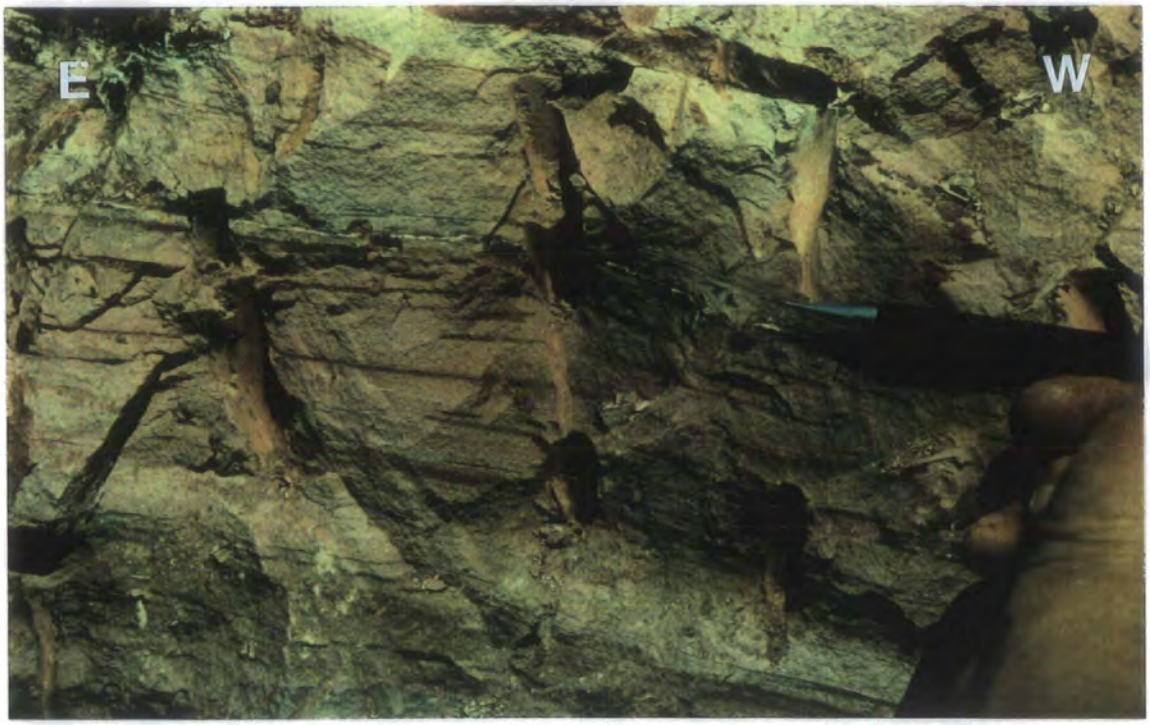

Photo 4.2.2- Load cast observed in the manganiferous siltstones exposed in the south part of the Azul Mine (level 540).

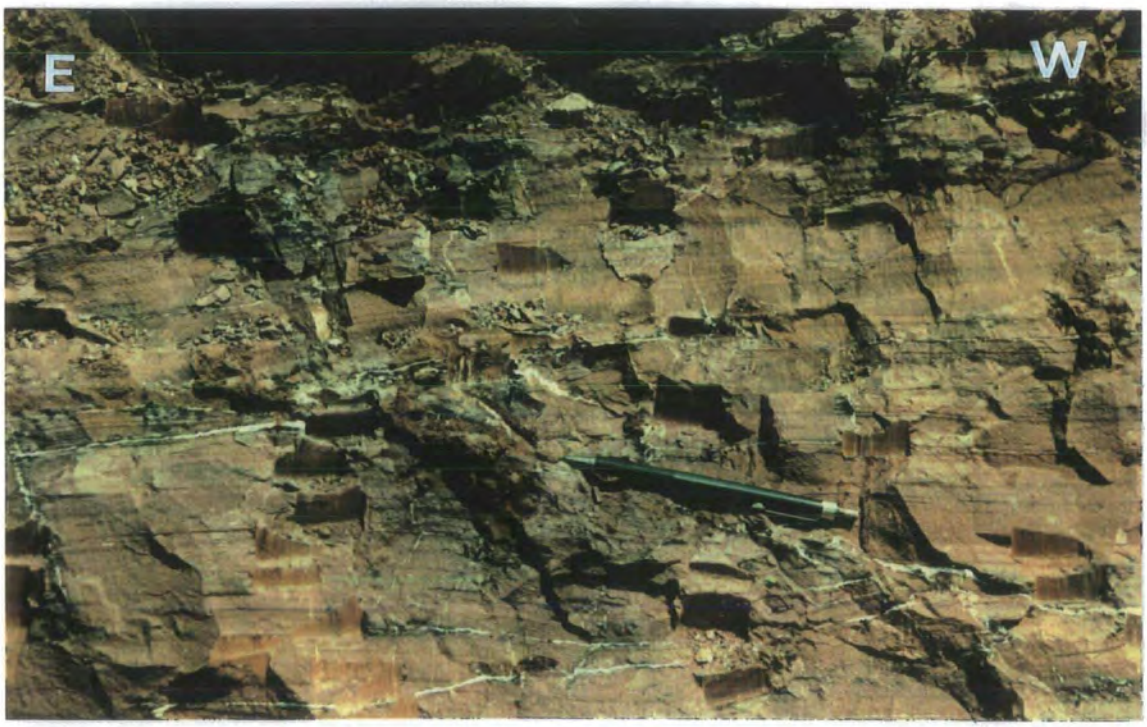

Photo 4.2.3- Hummocky cross-stratification with wavelength of about 30cm observed in the manganiferous siltstones in the south part of the mine (level 540).

between the red siltstones and Mn-rich mudstones and siltstones exposed around the coordinates 960E-100N in the mine (Photo 4.2.4 and Fig.4.2.4).

Photo 4.2.4- Contact between the red manganiferous siltstones and altered Mn-rich mudstones observed in the central area of the mine (coordinates:1000E-050N).

b) Folds: Most of the rocks forming the "Sub-Superficial Deposits" are folded at various scales, intensities and geometries. Centimetre-scale folds affect the primary lamination and also the bedding of the mudstones and siltstones. The poles to bedding observed in the mine as a whole define a ß-axis plunging about 14° towards 283° denoting the orientation of large folds affecting the bedding (Fig.4.2.4A). Two different types of folds can be observed in the mine, according to their shape:

(1) The first group corresponds to centimetre-scale *kinks* and *chevron folds* (Photos 4.2.5 and 4.2.6). These folds plunge shallowly SW and have axial planes striking 40°-50°, dipping 20°-45° NW. Often they occur as isolated asymmetric structures or, more rarely as conjugate sets. Chevron folds are also centimetre-scale structures with axes plunging with a low angle toward the west and axial planes orientated around NE-SW and dipping moderately (<50°) to the SE. A second less usual set of chevron folds is roughly perpendicular to the main one, but few examples of this structure were observed in field.

(2) Small-scale folds are present also as metre-scale structures associated with major classes. These are common, especially between

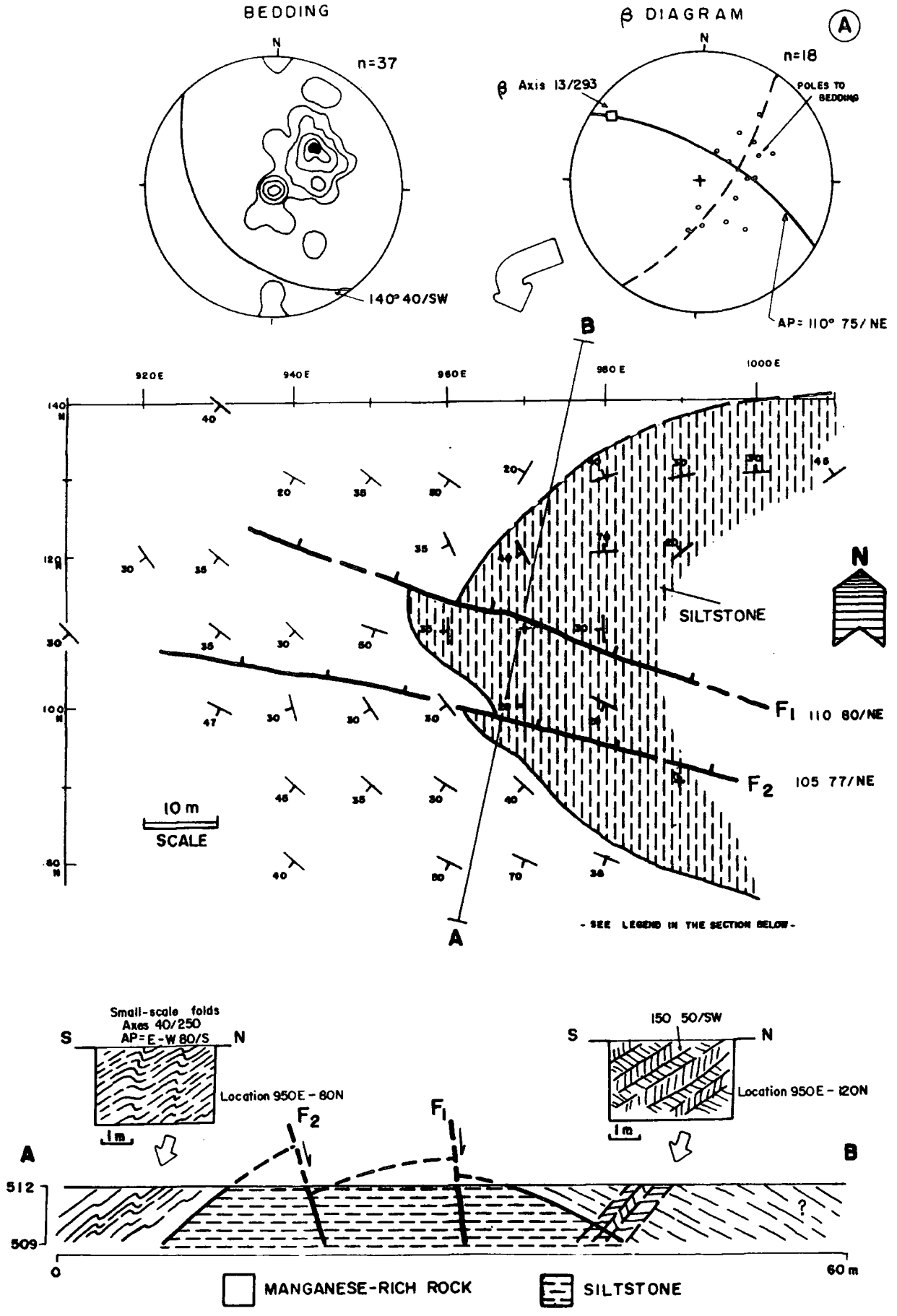

Fig. 4.2.4- Map and geological section of a large-scale folded and faulted lithological contact observed around the coordinates 960E-100N in the Azul Mine. Contours on stereonet of poles of bedding: 2%, 4%, 12%, 18%, 22%.

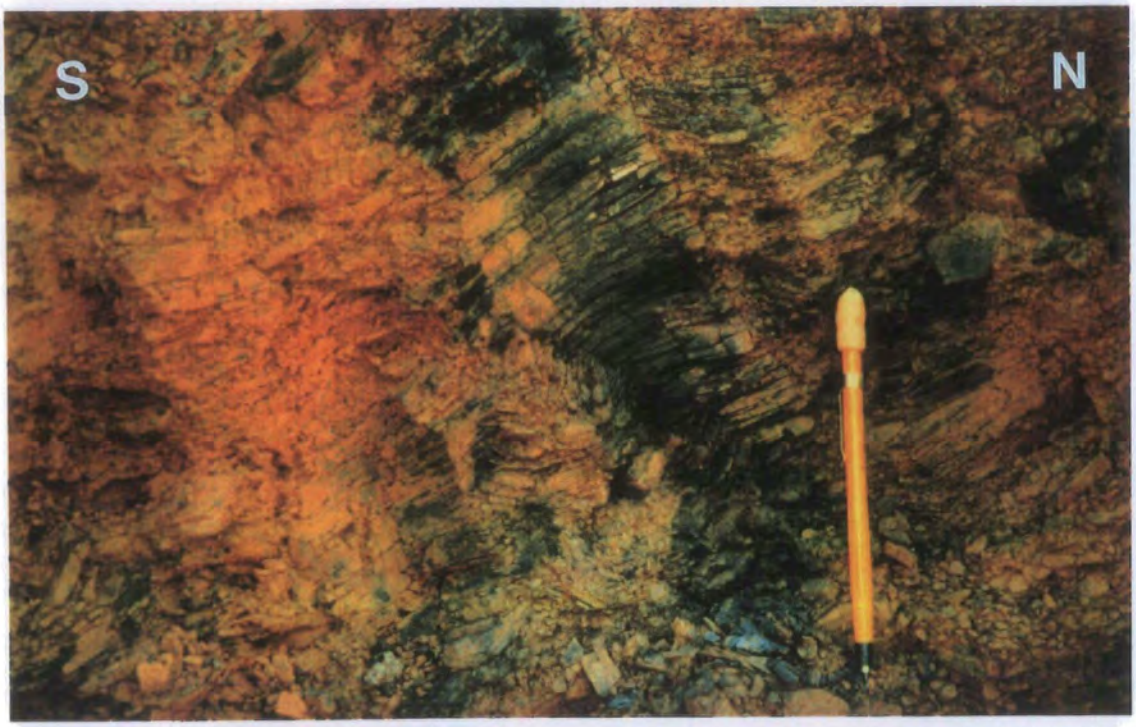

Photo 4.2.5- Centimetre-scale kink bands deforming the primary lamination and bedding of the mudstones.

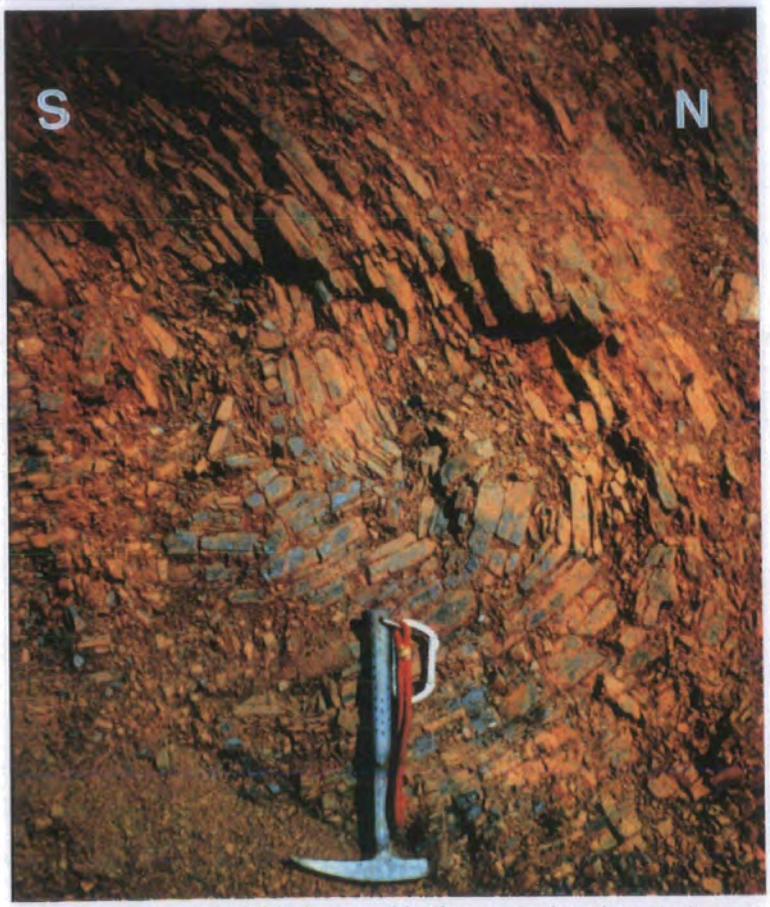

Photo 4.2.6- Example of metre-scale fold observed in the central and central-western area of the Azul Mine.

coordinates 800E-1200E and LT0-200N (Fig.4.2.2). They plunge shallowly (<25°) W or E (Fig.4.2.2 C to F), with axial planes varying from E-W strikes and sub-vertical dips to NW-SE strikes, dipping 30°-50° NE. These third-order folds are open to close, with angular to subangular bluntness.

The fold axes of minor and metre-scale folds, when observed all together, plunge shallowly (0°-30°) in various directions (Fig.2.2.2G) with a mean value of 11°/278°.

Using data from about 60 shafts opened between coordinates 80N-140N and 930E-1050E at a topographic height of 512m (September/94; Fig.4.2.2 and 4.2.4) it was possible to map a broad antiformal structure defined by the concordant contact between a dark-red siltstone and an overlying weathered manganese-rich siltstone (Fig.4.2.4). Stereographic analysis of the folded bedding indicated that this hundred-metre-scale fold plunges 13°/290° (Fig.4.2.4, stereonet on top). The fold axial plane strikes around 110° dipping 75°/NE (Fig.4.2.4, top right). This fold is supposed to be symmetric and is cut by steeply NE dipping normal faults striking 110°. Bedding a few tens of metres west of this fold does not seem to be affected by folding, and is predominantly 140° 40°/SW (Fig.4.2.4, stereonet on top left).

c) Fractures and faults: *Fractures* are often concentrated into prominent zones in the Azul Mine (Fig.4.2.2) but are absent in most areas. Two persistent orientations occur both dipping at high angles (>80°): (1) N-S/NNE-SSW, and (2) close to E-W. The N-S/NNE-SSW set is dominant and can be observed in several places. It is represented by belts of systematically sub-parallel joints with a average spacing of 20 cm. Some lineaments observed both in the field and on air photographs may be related to these joint systems.

Two categories of E-W faults are discernible in the Azul Mine according to their relative motion, although few displacement indicators have been observed. *Sinistral reverse faults* are most common and are closely associated with folds (Fig.4.2.2A and E; Photo 4.2.7). In many places, they show branches, splays and sets of sub-parallel faults in fault zones (Fig.4.2.2A and E). Most are sub-vertical features with low-angle slickenlines, and apparently with centimetre-scale magnitudes of displacement. Reliable piercing points are difficult to define in steep mine walls, especially where strike-slip displacement is predominant. Slickenfiber lineations, striations and ridge-in-groove lineations are rarely preserved due to weathering. A few examples of overprinting slickenlines were observed in some isolated fault planes, displaying oblique-slip displacement, with different pitches.

Oblique-slip normal E-W faults are less common, forming apparently isolated features, sub-parallel to the oblique sinistral-reverse structures (Photo 4.2.8 and Fig.4.2.4).

d) Relationship between folds & faults and between different faults: The faults are observed in most cases adjacent to folds, or in regions between two or more oblique-slip faults (Fig.4.2.2; Photo 4.2.7). Both fault and fold orientations are roughly parallel to the fold axial planes although some folds are slightly oblique to the faults (mainly anticlockwise). Fold zones, in outcrop-scale, often terminate against fault planes.

N-S and NE-SE fractures are shorter in comparison to the apparently more continuous E-W faults as can be observed in the field and also on satellite images where they link into the NW-SE faults. Blocks limited by both E-W and N-S/NE-SW fractures are different structural compartments where folded bedding is heterogeneously distributed and slightly rotated and interrupted against secondary N-S faults (Fig.4.2.2). Most of the E-W faults are cut by the NNE-SSW set but the opposite situation is also observed, mainly on a small-scale. The Carajás Fault forms the major southern limit of the adjacent fault-bounded blocks. The isometric block diagram shown in Fig.4.2.5 roughly illustrates the fold, minor fault and Carajás Fault relationship and geometries.

4.2.5- DISCUSSION

The Azul Mine is located along the Carajás Fault zone and the pattern of deformation observed in its rocks reflects at least in part the kinematic history of this major structure.

According to Nogueira *et al.* (1995) the Águas Claras Formation comprises two members: (1) a Lower Member, including mudstones, siltstones and subordinate sandstones, deposited on a marine platform; and (2) an Upper Member, formed essentially by sandstones deposited in littoral (base of the member) to fluvial (top) facies. The thickness of these rocks in the central part of the Carajás structure is supposed to be >1500m (Nogueira, 1995).

The deeply weathered rocks in the mine are thought to be part of the Lower Member of the Águas Claras Formation (Nogueira *et al.*, 1995). This suggestion is based mainly on the presence of primary structures indicative of marine platform deposits affected by storms (e.g. hummocky cross-stratification, load casts).

Photo 4.2.7- Folds related to near E-W set of sinistral reverse faults (approx. coordinates:900E-100N).

Photo 4.2.8- E-W normal fault with dip-slip displacement of about 2m affecting the contact between Mn-rich mudstones and red siltstones, on top (approx. coordinates: 1150E-000).

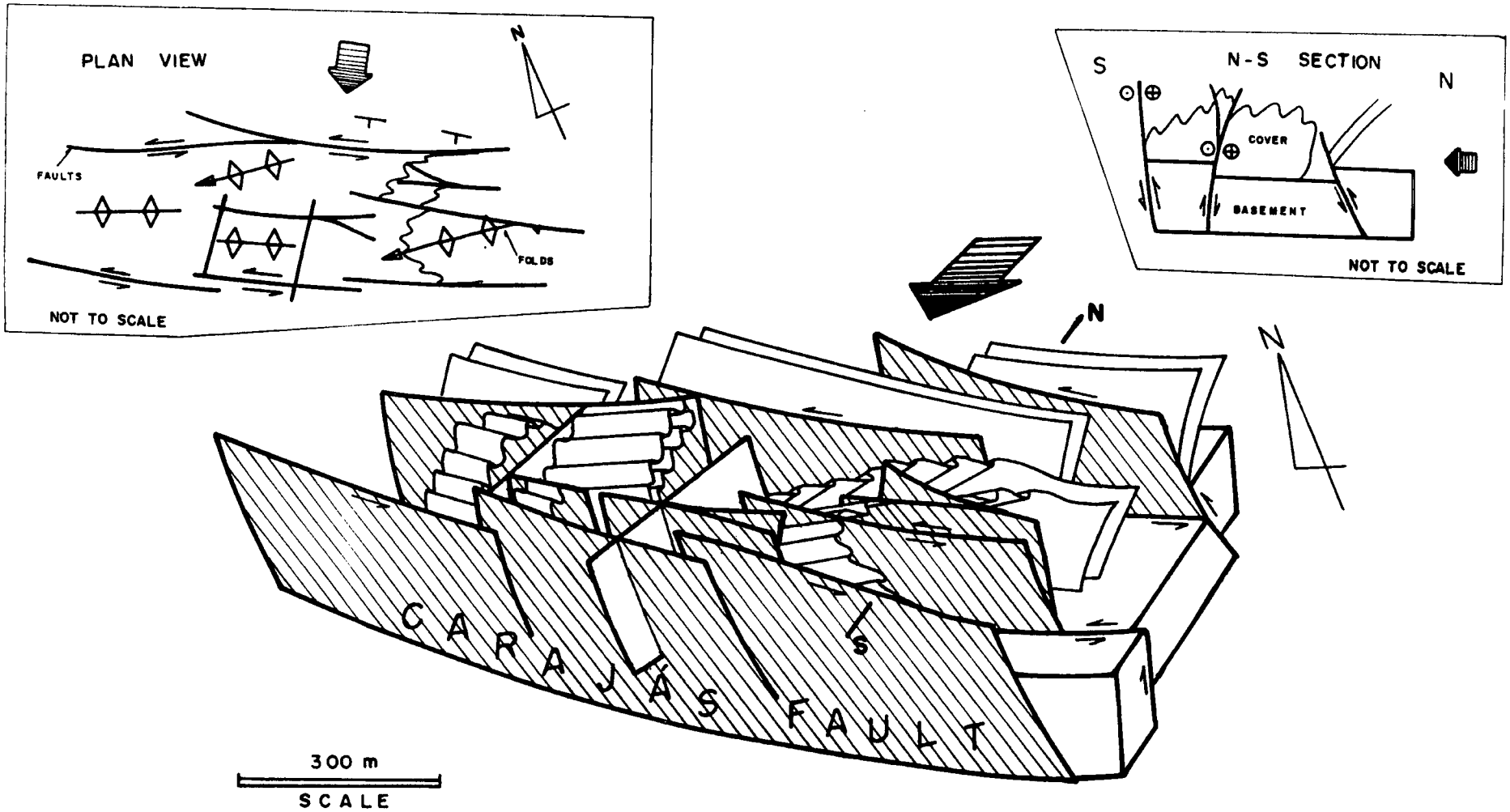

Fig.4.2.5- Block diagram representing the structural geometries in the Azul Mine. The Carajás Fault shown in the sketch is probably southwards, out of the mine and is not observed in the field. Auxiliary figures in the top: plan view (top left) and N-S section (top right).

As discussed in section 4.1 (The Águas Claras Region), outcrops of rocks belonging to the upper part of the Superior Member of the Águas Claras Formation occur no more than 3 Km south of the mine. These two points are separated by the trace of the Carajás Fault. This suggests that the northern block adjacent to the Carajás Fault is uplifted at least 750m relative to the southern one. This estimate is based on the calculated stratigraphical thickness separating the base of the Lower Member and the exposed portion of the Upper Member in the southern fault block.

It is possible to correlate the main sets of lineaments observed on the satellite and radar images with some of the structures seen in the field. The close E-W lineaments correspond to oblique-slip faults with sinistral reverse displacement and also to less common normal faults. The NNE-SSW and NE-SW lineaments are dip-slip faults of uncertain shear-sense, although they seem to cut off the NW-SE set isolating hundred-metre-scale blocks (Fig.4.2.2). The geological interpretation of the dense and fine lozenge-shaped patterns occurring in some regions, as well as the strong NW-SE lineaments, have not been determined from study of the rocks in the Azul Mine.

The area of the mine displays a smooth texture in remotely sensed images consistent with the apparently low density of tectonic structures observed in the field. It lies inside a 5Km x 3Km lozenge-shaped block surrounded by NW-SE faults which swing into an E-W direction. Similar blocks or domains seem to occur on this and other scales throughout the region forming a hierarchy similar to that associated with the Builth Inlie structure in Mid-Wales (Woodcock, 1987) and also with several examples described by Nur *et al.* (1989) in the northern region of Israel and in the Mojave Desert, southern California.

The main E-W faults show two different types of movements: oblique-slip (reverse + sinistral strike-slip) and subordinate normal displacements. There is no evidence to prove that these two conspicuous displacements took place synchronously or even that they were concurrent along the same fault planes.

The regional data suggest that the N-S and NE-SW faults are Middle Proterozoic in age (Costa *et al.*, 1991; Costa and Hasui, 1992), related to the important extensional episode which took place all over the Amazonian Craton (e.g. Neves, 1986; Costa and Hasui, 1991; Neves, 1992). The analysis of the structures in the Azul Mine supports these ideas since the N-S faults cut all other sets which are thought to be Archaean (Araújo and Maia, 1991; Costa *et al.*,1995; Pinheiro and Holdsworth, 1997*a*).

The close association between folding and sinistral reverse faulting is generally consistent with a regime of sinistral transpression. The approximately 100°-280° trend of the folds means that they lie some 30° clockwise of the Carajás Fault (Fig.4.2.6) and although they are almost parallel in the mine, a slight clockwise angle exists between the fold axes and the faults (Fig.4.2.4). This relationship is not compatible with sinistral transpression along the Carajás Fault according to conventional models (e.g. Wilcox *et al.*,1973; Sanderson and Marchini, 1984; Sylvester, 1988). It is, however, compatible with sinistral movements along a regional E-W trending zone (Fig.4.2.6). This may indicate that the folds formed in response to a regional transpression strain prior to sinistral movements along the Carajás and other faults in the region of the Azul Mine. This is in agreement with several early authors who studied the fold-fault relationship in strike-slip systems (e.g. Odonne and Vialon, 1983). It is considered that the fault block containing the folds underwent significant anticlockwise rotations during the propagation of sinistral movements along the Carajás and associated fault strands (Fig.4.2.6). This emphasises that simple clockwise/anticlockwise angular relationship between folds and faults are not always reliable as shear-sense indicators in braided fault zones with complex histories of block rotation and differential uplift. Further rotations of the Azul Mine fault block may also have occurred during later Proterozoic extension along N-S, NE-SW and reactivated E-W fault planes to accommodate NE-SW extension.

4.2.6- CONCLUSIONS

1) The rocks present in the Azul Mine belong to the Archaean Lower Member of the Águas Claras Formation, deposited in a marine platform environment affected by storms.

2) The tectonic structures present in the mine are thought to be related to regional sinistral transpression, apart from an important N-S set of fractures which corresponds to Middle Proterozoic extensional structures.

3) The Carajás Fault in this region is composed of several interlinked anastomosing segments, isolating blocks and distinct tectonic domains. The Azul Mine lies in one of these domains, near to the northeastern margin of the 2Km wide Carajás Fault zone.

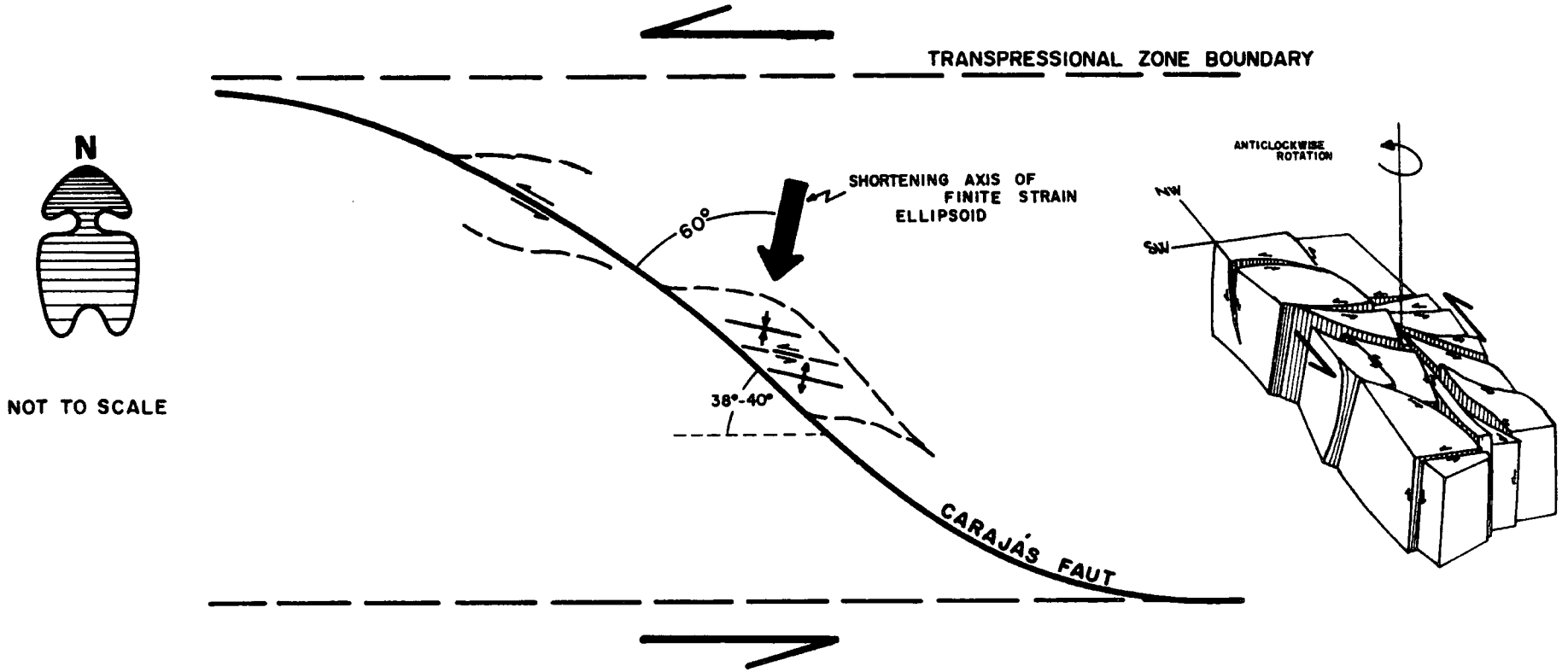

Fig.4.2.6- Sketch summarising the angular relations between some most important structures observed in the Azul Mine and those related to the Carajás Strike-Slip System. The block diagram in the right side represents an idealised picture to the geometry and anticlockwise rotation that probably took place along the Carajás Fault zone. See text for further discussion.

4) The strike-slip displacements along faults are relatively minor. A large (ca.700m) vertical displacement between adjacent blocks across the nearby Carajás Fault is predicted based on offsets in the stratigraphy of the Águas Claras Formation.

5) The fold axes in the mine lie markedly anticlockwise of the Carajás Fault and parallel or slightly anticlockwise of faults in the mine. This may indicate that the folds formed early during sinistral transpression along a broad E-W trending zone of deformation. These structures were then cross-cut by slightly later sinistral faulting along the Carajás Fault and associated structures. Significant anticlockwise fault rotations may have occurred at this time.

6) The E-W oblique-slip faults in the mine were reactivated during the Middle Proterozoic by extension as normal faults.

7) A kinematic model involving transpression with strain partition of discrete slip along multiple segments is invoked to explain the structures present in the rocks of the Azul Mine.

4.3- THE N-4 MINE

The N-4 open cast mine provides the best outcrops of rocks in the north sector of the Carajás Strike-Slip System. In this region the predominant NE-SW trend characterising the N border of the Carajás Structure, changes to a strong N-S direction.

The N-4 plateau, where the mine is situated, is almost 600m high, 10 Km long, with a nearly Z-shape in map view following the general N-S orientation (Photo 4.3.1). It is the fourth of a set of several similar plateaus existing in this region (Fig.4.3.1), controlled by the presence of a thick hard iron-rich crust developed over volcanics and ironstones.

The iron mine lies on the north-eastern branch of the N-4 plateau (Fig.4.3.2a and 4.3.2b) covering an area of around 5 km² and is an open-cast pit about 110 metres deep. The iron ore in the mine has been described as an irregular body, measuring about 4.2 km long, 300 metres wide and about 200 metres thick giving an estimated reserve of around 12 million metric tons, with approximately 66% iron concentration (Araújo and Maia, 1991).

The present study is based on detailed mapping carried out in and around the N-4 Mine and focuses principally on the structural geometry and evolution of the region.

4.3.1- REGIONAL SETTING

The Late Archaean N-4 iron-ore of Serra dos Carajás in the N-4 plateau (Photo 4.3.1 and Fig.4.3.1) forms the largest deposit currently being mined in South America. In common with many other Brazilian ironstones, the rocks display complex patterns of folding and faulting.

The N-4 plateau lies in the north-eastern part of the Carajás Structure where all of the rocks belong to the *Grão Pará Group* (Fig.4.3.1). They are subdivided into two main units: (1) the volcanic rocks of the *Parauapebas Formation* (Meireles *et al.*, 1984) and (2) the ironstones of the Carajás Formation (Beisiegel *et al.*, 1973). The volcanic rocks are a bimodal sequence of basalts, dolerites and rhyolites (Wirth,1986) yielding a U-Pb zircon age of 2759±2 Ma (Machado *et al.*,1991) or 2758±39 Ma (Gibbs *et al.*, 1986) interpreted as dating their intrusion. According to geochemical evidence, these

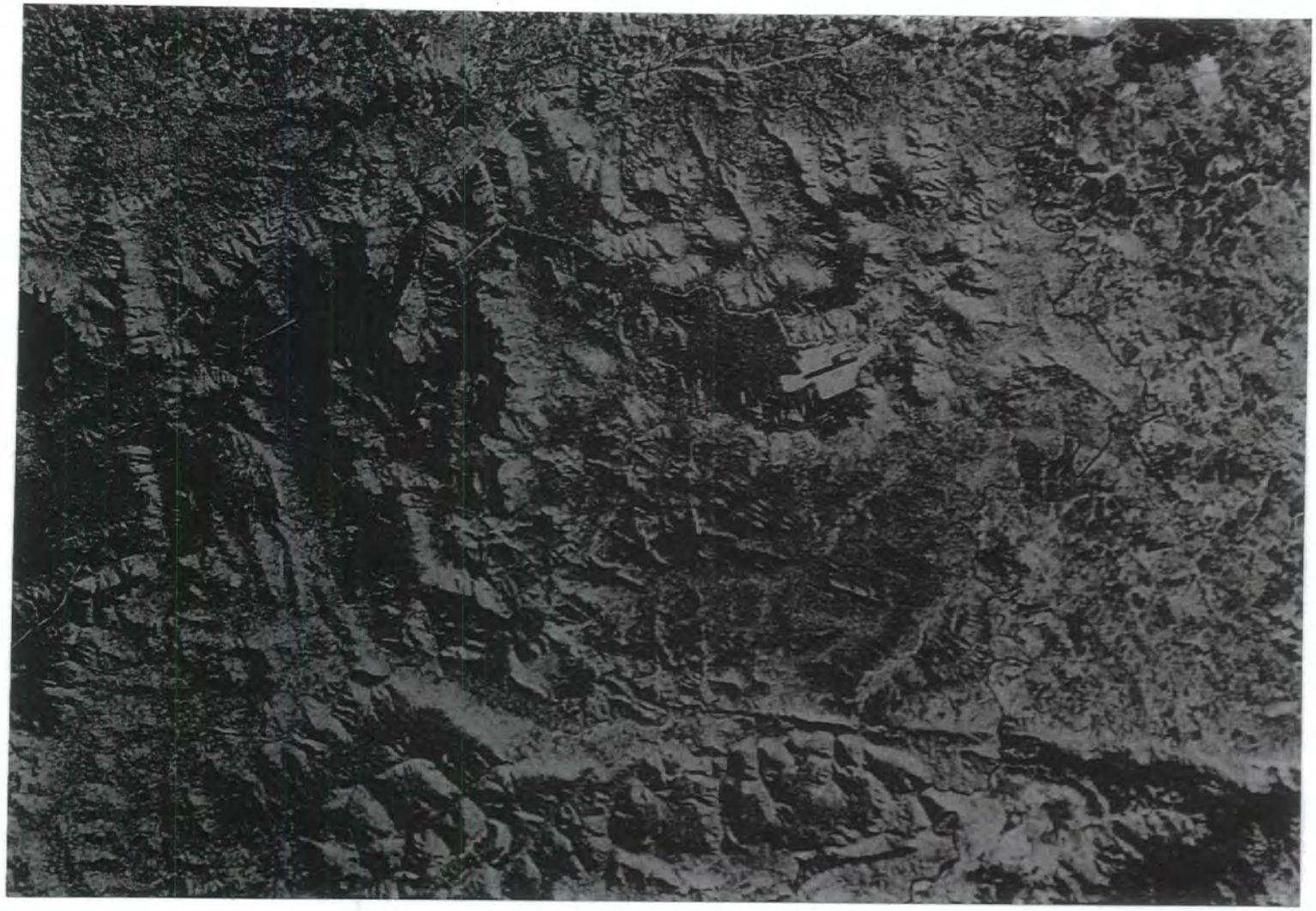

Photo 4.3.1- Satellite image to the NE sector of the Carajás Strike-Slip System showing the N-4 plateau and the nain NW-SE lineaments that converge from close WNW-ESE segment of the Carajás Fault.

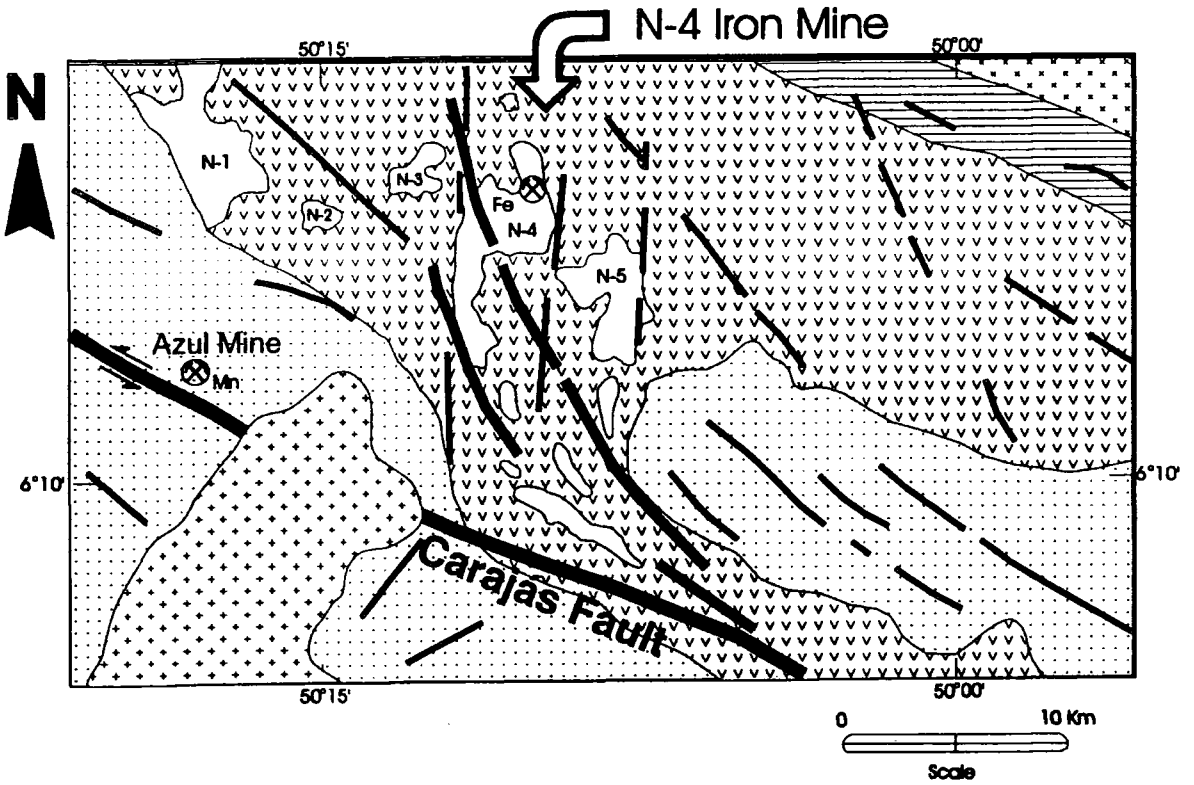

REGIONAL SETTING

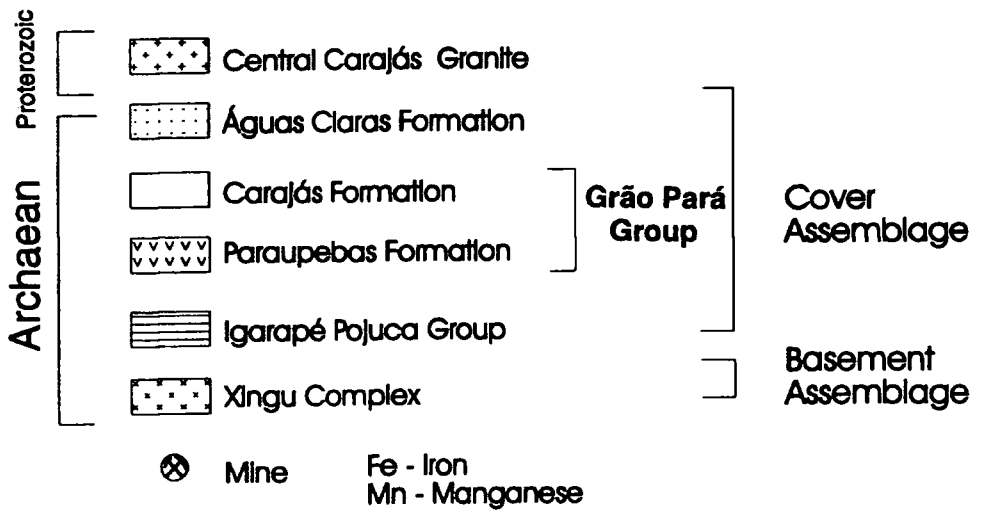

Fig. 4.3.1- Geological map of the region around the N-4 plateau and the N-4 mine along the Grão Pará Group outcropping area (modified after Araujo and Maia, 1991).

volcanics appear to be continental tholeiites (Gibbs and Wirth, 1990; Lindenmayer and Fyfe, 1992). The metamorphism affecting the mafic and felsic volcanic rocks shows characteristics of greenschist facies of low-grade (low pressure and low temperature <500°C) with clear evidence of later hydrothermal reactions (Wirth, 1986; Teixeira and Eggler, 1994). In the region of the N-4 Plateau, units of the Parauapebas Formation are interlayered or tectonically juxtaposed above and below the Carajás Formation (CVRD-CMM, 1972; Beisiegel *et al.*, 1973; Anderson *et al.*, 1974; Araújo *et al.*, 1988).

The Grão Pará Group is overlain in this region by the sedimentary rocks of the Águas Claras Formation which are cut by the Carajás Central Granite (ca.1.8 Ga), outcropping about 5 km SW of the N-4 plateau (Fig.4.3.1). Small apophyses of the Carajás Central Granite outcrop about 3km north of the N-4 plateau (Fig.4.3.1).

The Carajás Fault is the major structure present in this region, crossing the area from NW to SE. Several NNW-SSE fault branches project from the Carajás Fault to the Grão Pará Group forming an uplifted, 6km wide block that separates two regions of the Águas Claras Formation (Fig.4.3.1).

4.3.2- LITHOLOGIES AND PREVIOUS WORK

The ironstones of the Carajás Formation are composed of several different types of iron ore all of which belong to the oxide facies (Tolbert *et al.*, 1971; Beisiegel, 1982, Hoppe *et al.*,1987). The nomenclature used in existing literature on the mine relates mostly to the industrial use or physical properties of the ore. The main types are jaspelite and various types of ore composed of interlayered haematite and silica which are distinguished by their varying hardness, e.g. "soft" haematite, "hard" haematite, etc. (Beisiegel, 1982). Jaspelite comprises alternating layers (2-20mm thick) of very fine crystalline quartz and/or chert bands, with haematite, martite, magnetite and pyrite (Araújo and Maia, 1991; Marçal, 1991). These rocks are cut by centimetre- to millimetre-scale quartz veins sometimes with an irregular distribution associated with the folds developed in this unit. The haematite-dominated rocks are composed of interlayered bands (1-5mm thick) of fine grained haematite and crystalline quartz which are often highly friable. The primary iron-bearing rocks may have been similar to the jaspelites and are thought to have undergone varying degrees of deep equatorial weathering since the Cretaceous forming the other types of ore found in the mine (Beisiegel, 1982). These weathered

rocks are dominant in outcrops (roughly 80% by volume) and show varying degrees of alteration which is responsible for the differences in composition and hardness.

Hoppe *et al.* (1987) named the iron ore of the N-4 mine as "Carajás-type" and did not find similarities with any of those described earlier in the current literature (e.g. Algoma-type, Superior-type; Gross, 1983).

Significant volumes of *basic rock* are emplaced into the ironstones as dykes and other irregular intrusive bodies (5-10% of the mine). It is difficult to assess the original mineralogy as all outcrops of these intrusions are heavily altered by weathering and possibly also by the affects of hydrothermal activity. Two sets of intrusions with different relative ages are distinguished. The first and more common group is folded and deformed by the structures affecting the ironstones, whilst the later set is undeformed. The earlier intrusions were originally emplaced as sill-like bodies (0.5 - 3m thick) lying at low angles to the banding in the ironstones. The later intrusions are generally larger (>20m thick) and irregular in shape, although they tend to follow a N- to NE-trend, with a subordinate group trending SE. None of these intrusions have been dated in the mine, but some probably belong to a Middle Proterozoic suite recognized throughout the Amazonian Craton (Sial *et al.*, 1987; Teixeira, 1990; Costa *et al.*, 1991) or they are intrusions related to the volcanics of the Parauapebas Formation, lying adjacent to the ironstone.

The first detailed published work concerning the structural geology of the rocks of the N-4 mine is that of Ladeira and Cordeiro (1988). They identified three sets of W-SW-plunging folds (B_1-B_3) and associated linear and planar fabrics. Later brittle deformations were thought to be responsible for the development of several joint and fracture sets together with normal faults and zones of brecciation in the ironstone. These authors suggested that the volcanic rocks above and below the ironstone (the "Sequência Paleovulcânica Inferior" and the "Sequência Paleovulcânica Superior" respectively; CVRD-CMM, 1972) could be a single unit repeated by folding or thrusting.

Subsequent work by Marçal (1991) and Marçal *et al.* (1992) has suggested that the compositional banding in the ironstones is a transposed mylonitic foliation formed during intense ductile deformation. Based on fold vergence patterns Marçal *et al.* (op cit) proposed that the ductile fabrics are associated mainly with dextral movements. The northeastern part of the asymmetric N-4 ironstone body has been interpreted as a fault-bounded, gently northwest plunging synform, whilst the western branch of the plateau has been described as a west-dipping homocline (Beiseigel, 1982). These kilometre-

scale folds were thought to be related to postulated N-S-trending dextral faults and shear zones which were active as antithetic structures during regional sinistral transpression along the Carajás-Cinzento fault systems (Araújo and Maia, 1991; Marçal, 1991; Marçal *et al.*, 1992).

More recently Teixeira and Eggler (1994) based on petrological and geochemistry studies, suggested an active continental margin (arc tectonic) setting to the eruption of the Parauapebas Formation.

4.3.3- STRUCTURES OF THE N-4 MINE

4.3.3.1- Carajás Formation

This study has focussed on the very well exposed mine sections that lie on the northeastern side of the N-4 ironstone body (Fig.4.3.2a and 4.3.2b). The benches and exposed walls in the mine provide a series of geological cuts of varied orientation allowing a detailed three-dimensional picture of the structures present to be constructed. Folds and fractures are present on all scales throughout and appear to reflect a somewhat brittle-ductile style of deformation.

a) Nature and origins of compositional banding in the ironstones: The ironstones of the N-4 plateau comprise thin (10-20mm) to very thin (<10mm) interbedded layers and laminae displaying mostly planar parallel forms, with less common examples of wavy parallel, curved parallel and wavy non-parallel forms, according to the classification of Collinson and Thompson (1989).

In thin section, the layers are defined by variations in the relative proportions of haematite, martite and sometimes magnetite, with chert and microcrystalline quartz (Photo 4.3.2). The quartz is predominantly present in cryptocrystalline grains with strong undulose extinction in bands of polygonal aggregates. The contacts between the quartz-iron bands are mainly sharp (Photo 4.3.3) but are, in places, gradational or diffuse (Photo 4.3.3). Top and base of the layers can be easily deduced using the fining upwards criterion (e.g. Photo 4.3.2). When observed in the thicker laminae, quartz grains have straight and 120° triple junction boundaries. These thicker bands of silica-rich minerals may included disseminated crystals of opaque minerals such as magnetite or haematite close to their boundaries with iron-rich laminae (Photo 4.3.4). The iron-rich bands are characteristically grey to black under the microscope, being formed mainly of haematite and magnetite forming compact aggregates with no conspicuous individual crystals. Sigmoidal lenses of chert or jasper may be

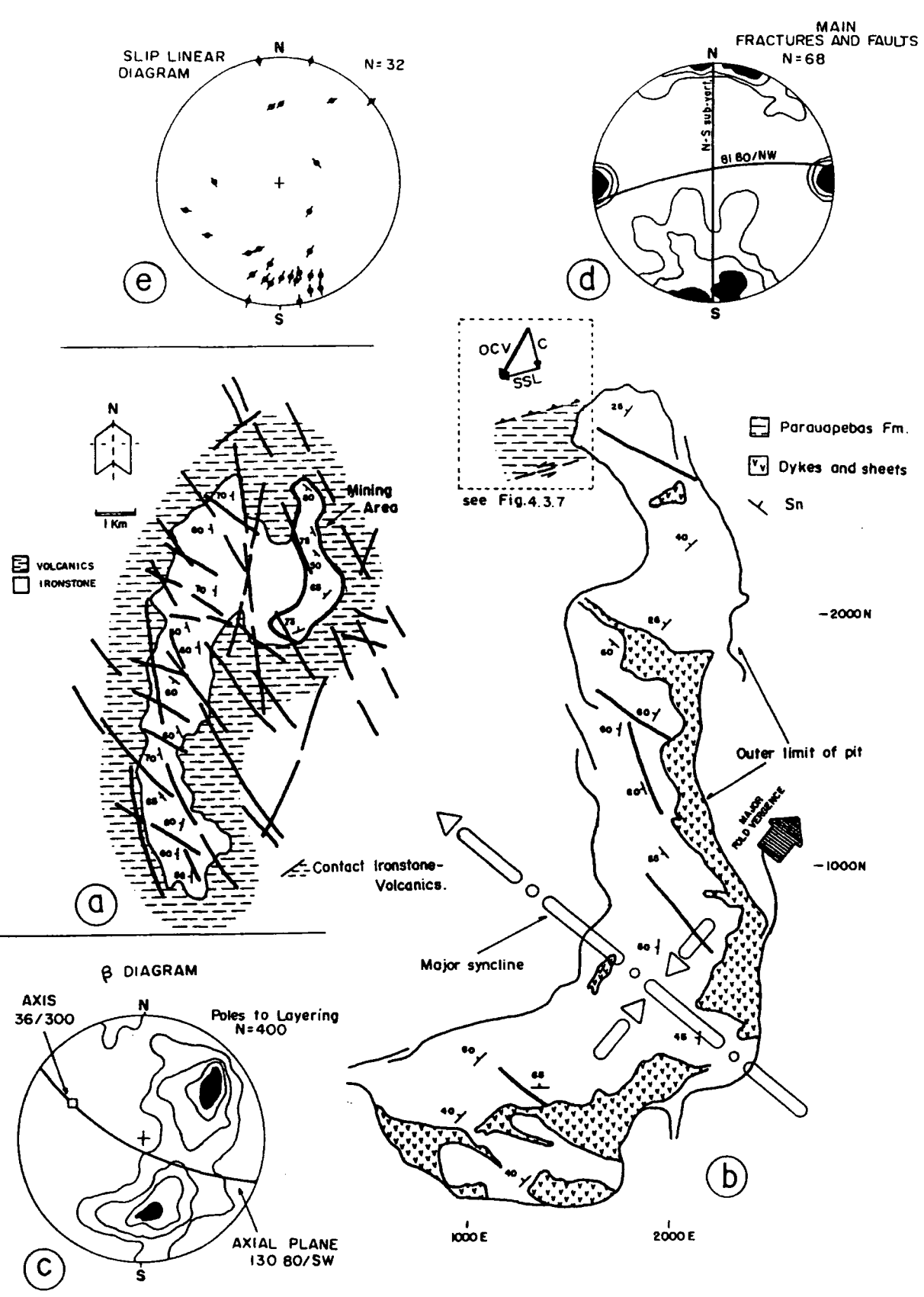

Fig.4.3.2 - The N-4 Mine. (a) Location of the mine in the N-4 plateau; approx. contact ironstone - volcanics;main lineaments and orientation of layering in the ironstone (modified after CVRD, unpublished). (b) Basic intrusions into the folded ironstones (open synform verging NE). The ironstone-volcanics contact shown in the top left is discussed in the text and Fig.4.3.7. (c) Stereonet showing poles to layering in the ironstones (contours: 20%, 15%, 10%, 5%). (d) Stereonet showing concentrations of poles to fractures (contours 20%, 10%, 5%). (e) Stereonet showing slip linear plot to poles of fault planes and directions of slip. E-W fractures show dip-slip to oblique-slip kinematics whilst the N-S set corresponds to oblique- to strike-slip faults.

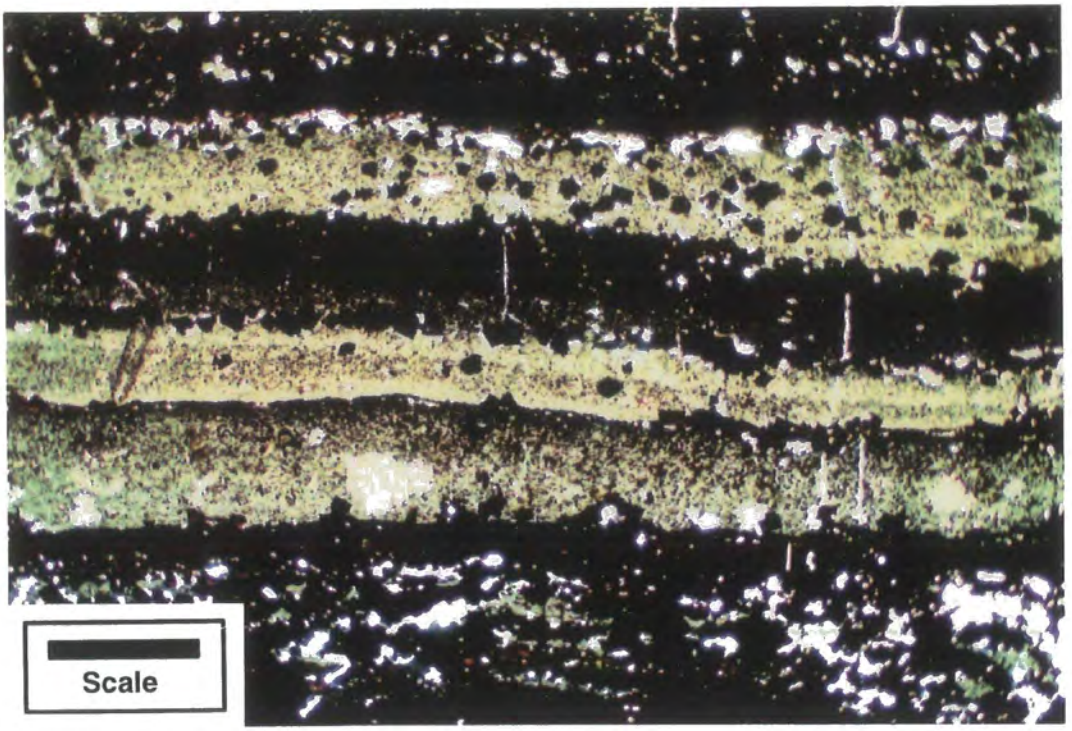

Photo 4.3.2- Photomicrography (XPL) of the Fe-rich (dark brown) - Si-rich (greenish-grey) layers. Graded layers (fining-upwards) is an useful check on way-up. Scale bar= 2mm.

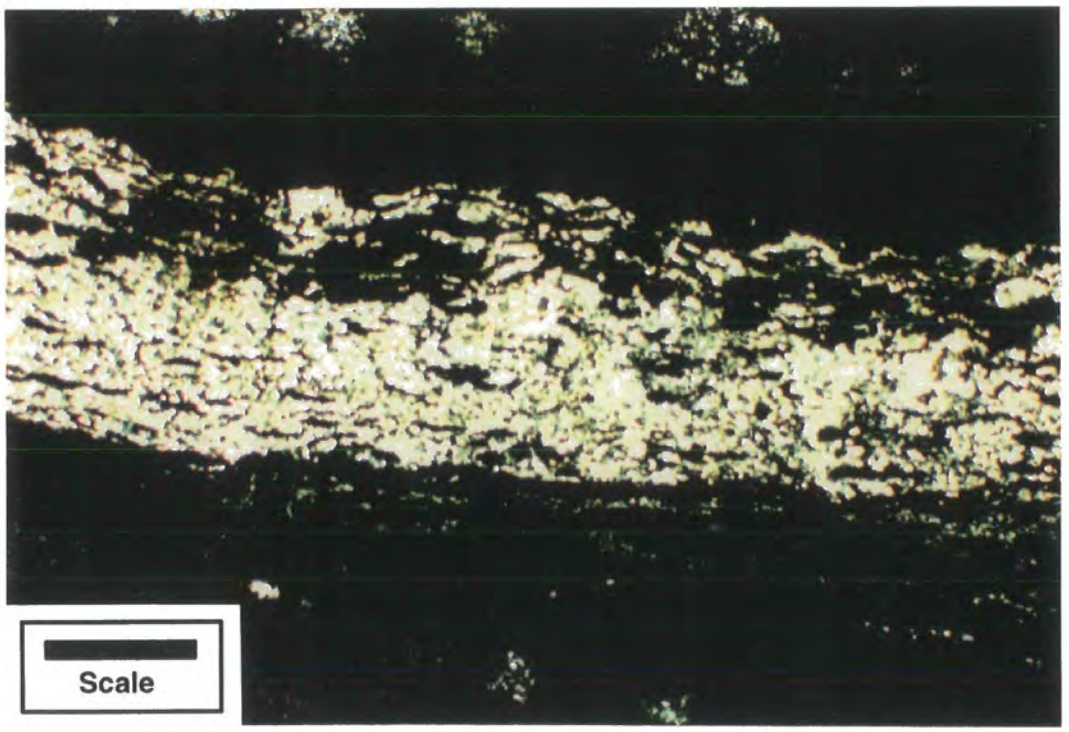

Photo 4.3.3- Si-rich layer of the ironstone under the microscope. The contrasting sharp and diffuse contacts observed in some layers can be carefully used as way-up indicator. XPL - Scale bar= 2mm.

found in these bands (Photo 4.3.5), mostly close to their boundaries with the silica-rich layers, cross-cutting micro-veins of quartz are relatively widespread where the bands are folded (Photo 4.3.6).

Locally, examples of graded bedding and soft-sediment deformation structures (syn-depositional and post-depositional) are preserved (Wirth, 1986; Gibbs and Wirth, 1990; Macambira and Silva, 1994). These observations strongly suggest that the banding is a primary sedimentary layering.

Marçal (1991) has suggested that part of the layering present in the ironstone is tectonic and that it was formed during mylonitisation and metamorphism. This proposal is inconsistent with the evidence for a primary bedded origin cited here and also with metamorphic studies of the ironstones which suggests at most a lower greenschist facies to these rocks if the effects of hydrothermal alteration are ignored (Meireles *et al.*, 1984; Wirth, 1986). Furthermore, pervasive dynamic recrystallisation textures typical of mylonites are not seen in thin section, although minor intracrystalline deformation fabrics (e.g. undulose extinction, sigmoidal lenses) are present in tectonically folded areas of ironstone; these fabrics appear to be uniformly low temperature.

b) Outcrop-scale folds and associated structures: Decametre to hundred metre-wide, NNW-trending belts of millimetre to decimetre-scale folds occur widely in the ironstones and less commonly in the volcanic rocks. Fold styles are typically variable, with wide ranges in interlimb angle (0°-120°), degree of asymmetry, harmony and fold hinge angularity. These fold belts are separated by packages of apparently undeformed strata uniformly dipping between 20°-50° to W and NW in most places (Fig.4.3.2b and Fig.4.3.3).

The predominant group of structures are centimetre- to decametre-scale, open-to-tight folds with variable degrees of hinge-zone bluntness (Fig.4.3.4a and 4.3.4b; Photo 4.3.7). Fold axes are typically periclinal displaying up to 30° of hinge line curvature over distances of 200-300 metres, and individual folds often die-out or branch along plunge defining an irregular *en echelon* pattern (Fig.4.3.4a). The periclinal geometry is also observed in centimetre-scale folds (Photo 4.3.8).Box-fold and polyclinal geometries are common as illustrated by the polydomainal girdle distribution of poles to axial planes (Fig.4.3.4c); note that the pole to the girdle corresponds to the mean fold axis (28°/278°; Fig.4.3.4b and 4.3.4d). In the marginal areas between the fold belts and zones of unfolded rocks, there are often local zones of higher strain (up to 10 metres wide) in which the folds become tight to isoclinal (Fig.4.3.3; Photo 4.3.9). Thus the deformation intensities associated with this dominant set of folds are very

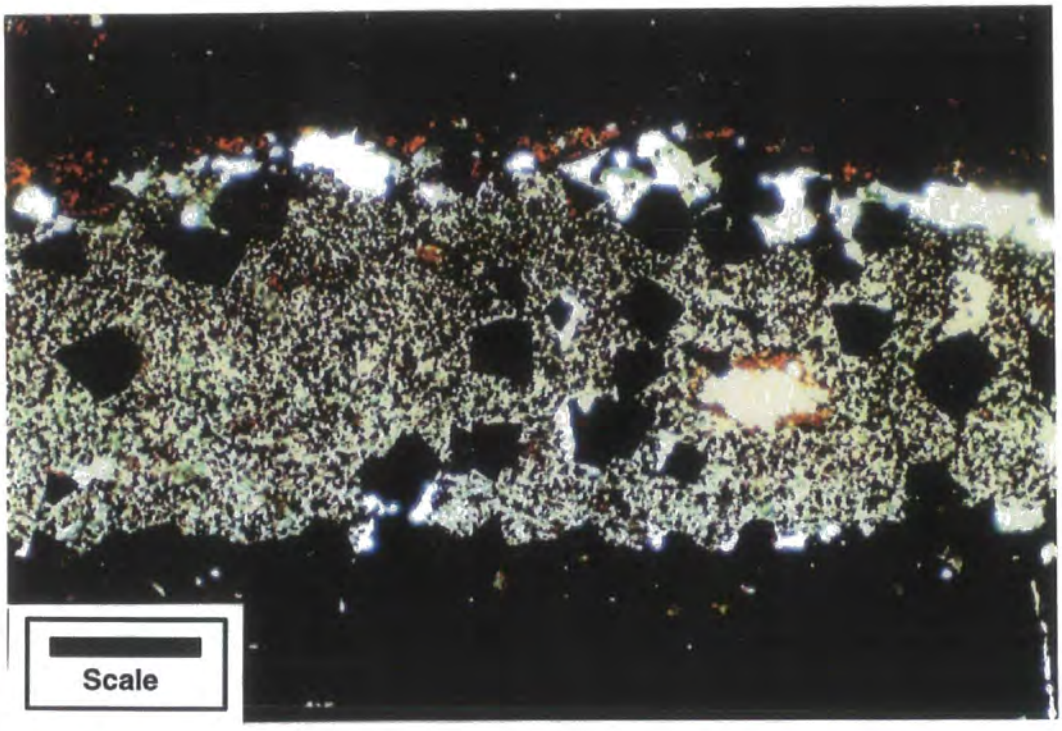

Photo 4.3.4- Euhedral crystals of magnetite disseminated in Si-rich bands. XPL. Scale bar=1.2mm.

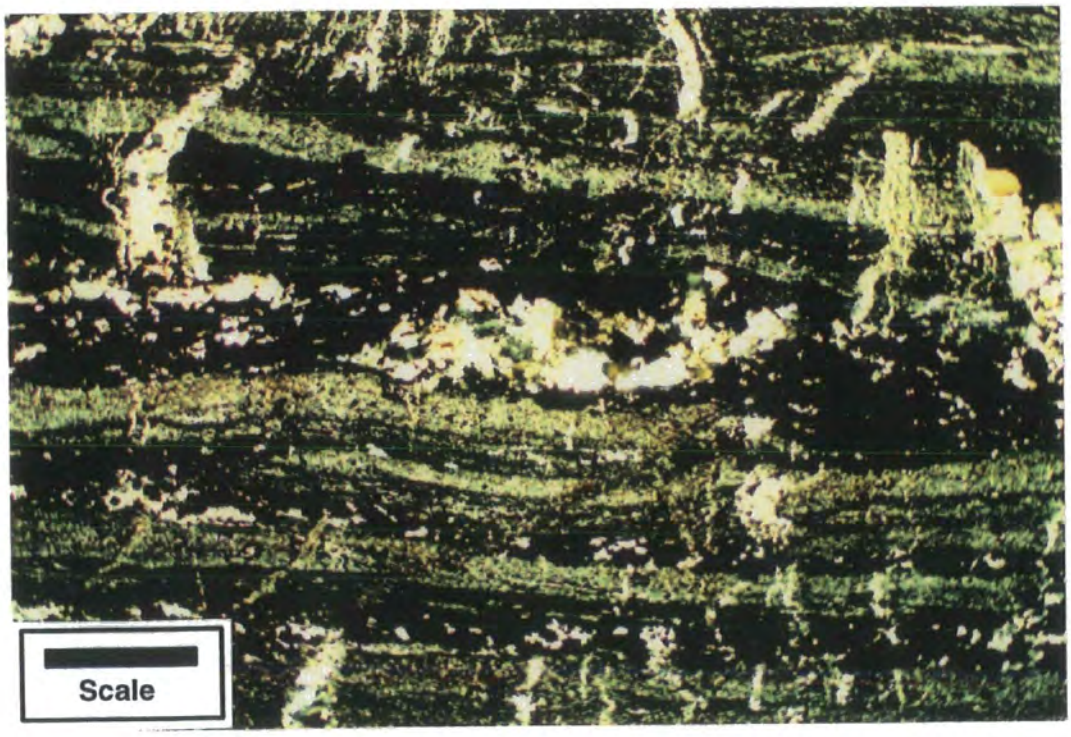

Photo 4.3.5- Sigmoidal lens of quartz and jasper into the Fe-rich band, observed close to centimetre-scale folds in the ironstone (XPL). Scale bar= 2mm.

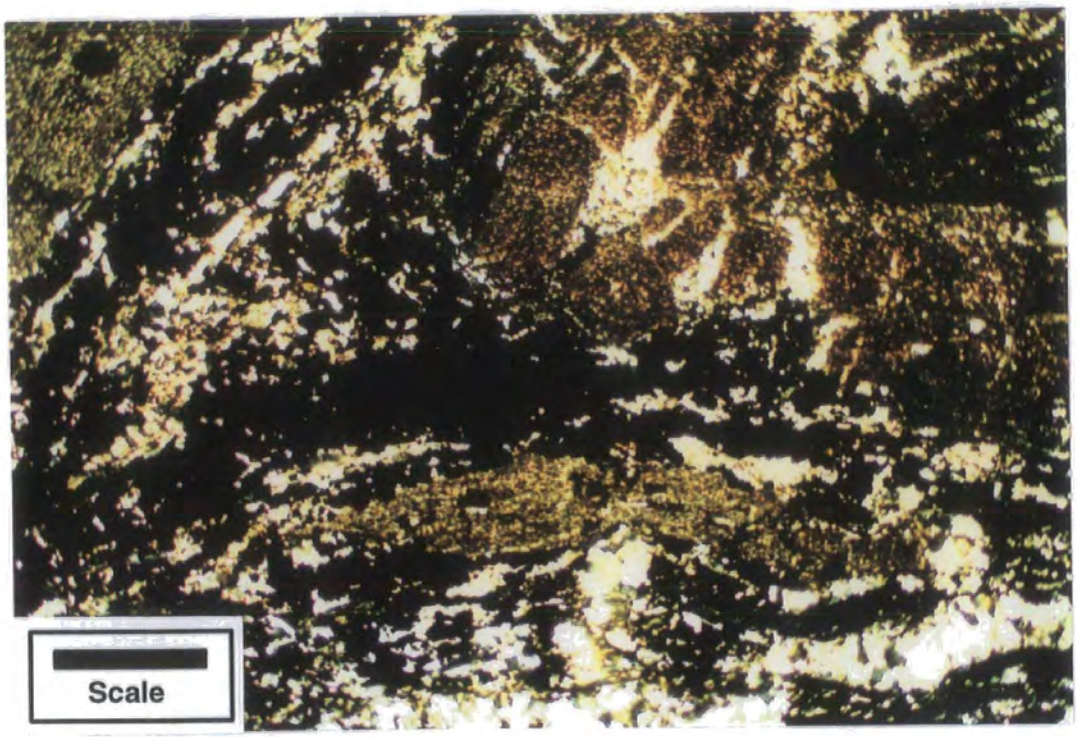

Photo 4.3.6- Millimetre-scale layer fold observed under the microscope. Quartz micro-veins are relatively abundant cutting the folded layers (XPL). Scale bar= 1.6mm.

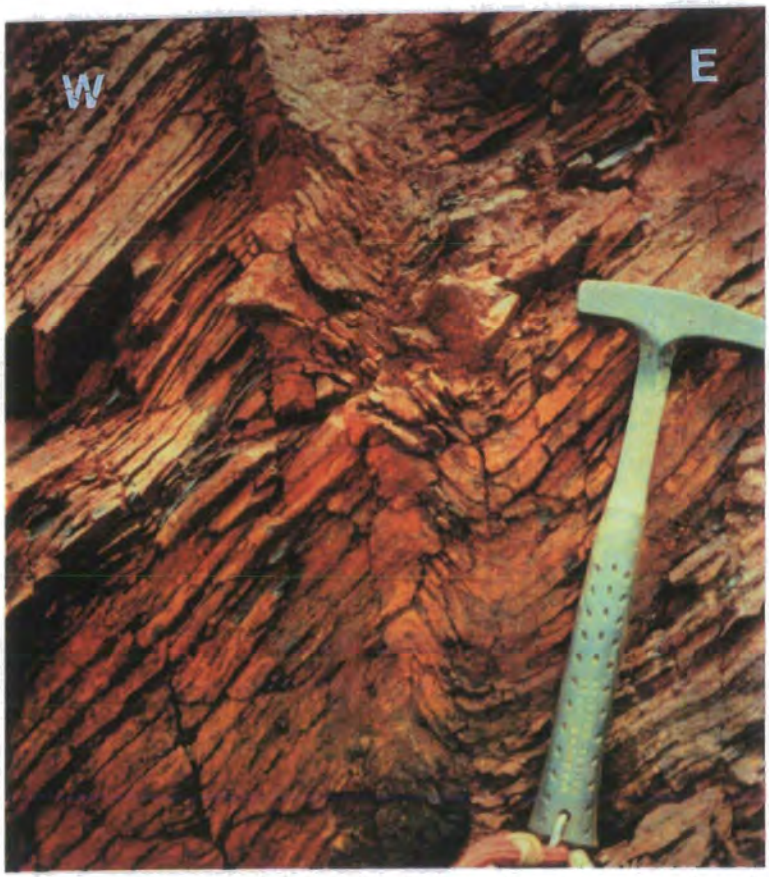

Photo 4.3.7- Centimetre-scale asymmetric ("Z" profile) fold affecting the layers of the ironstones, in the limbs of major decametre-scale, plunging shallowly WNW.

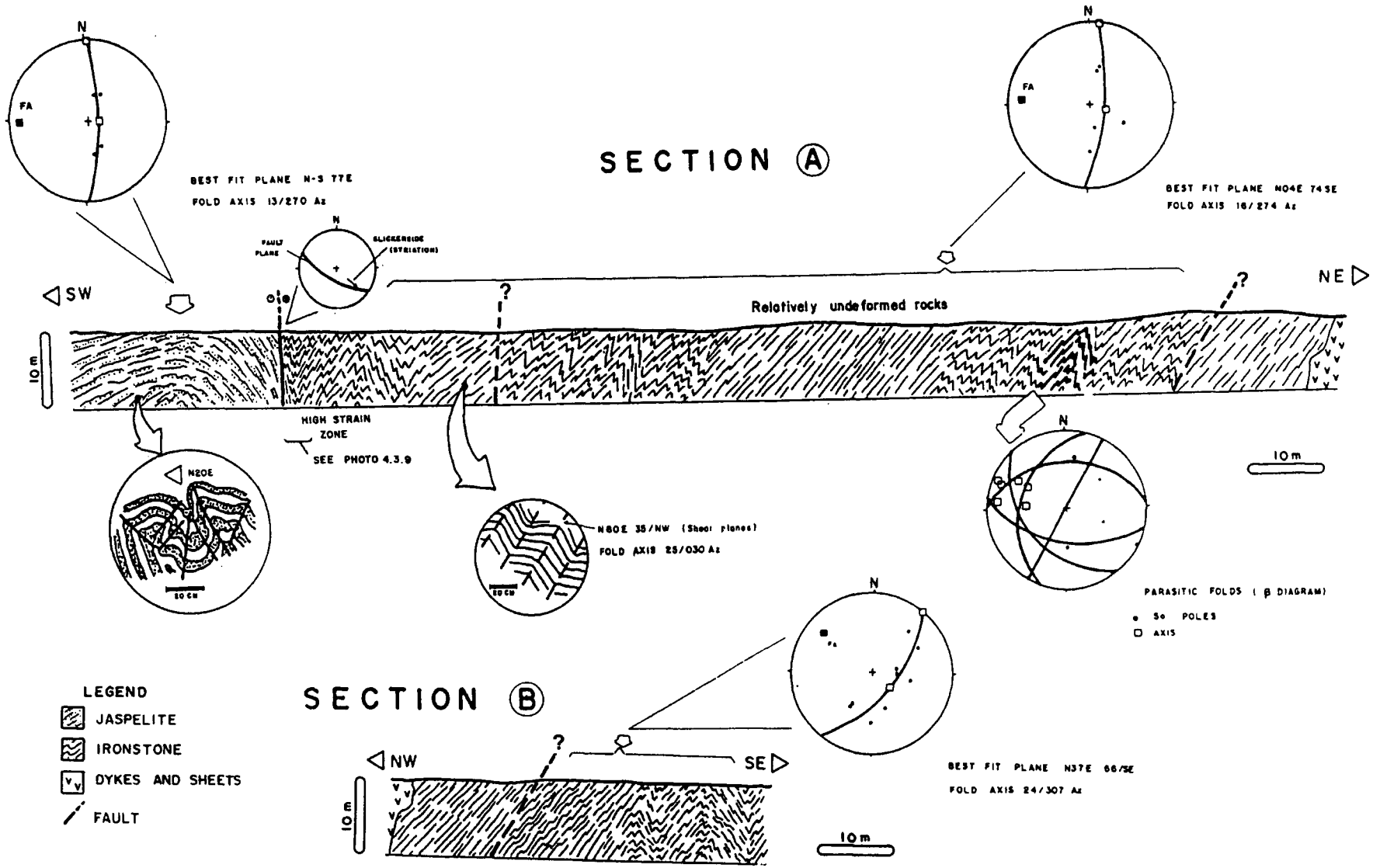

Fig.4.3.3- Schematic geological section representing the rocks on the northern part of the N-4 Mine (see location on Fig.4.2.2b) showing the distribution of different sets of folds and unfolded stratas.

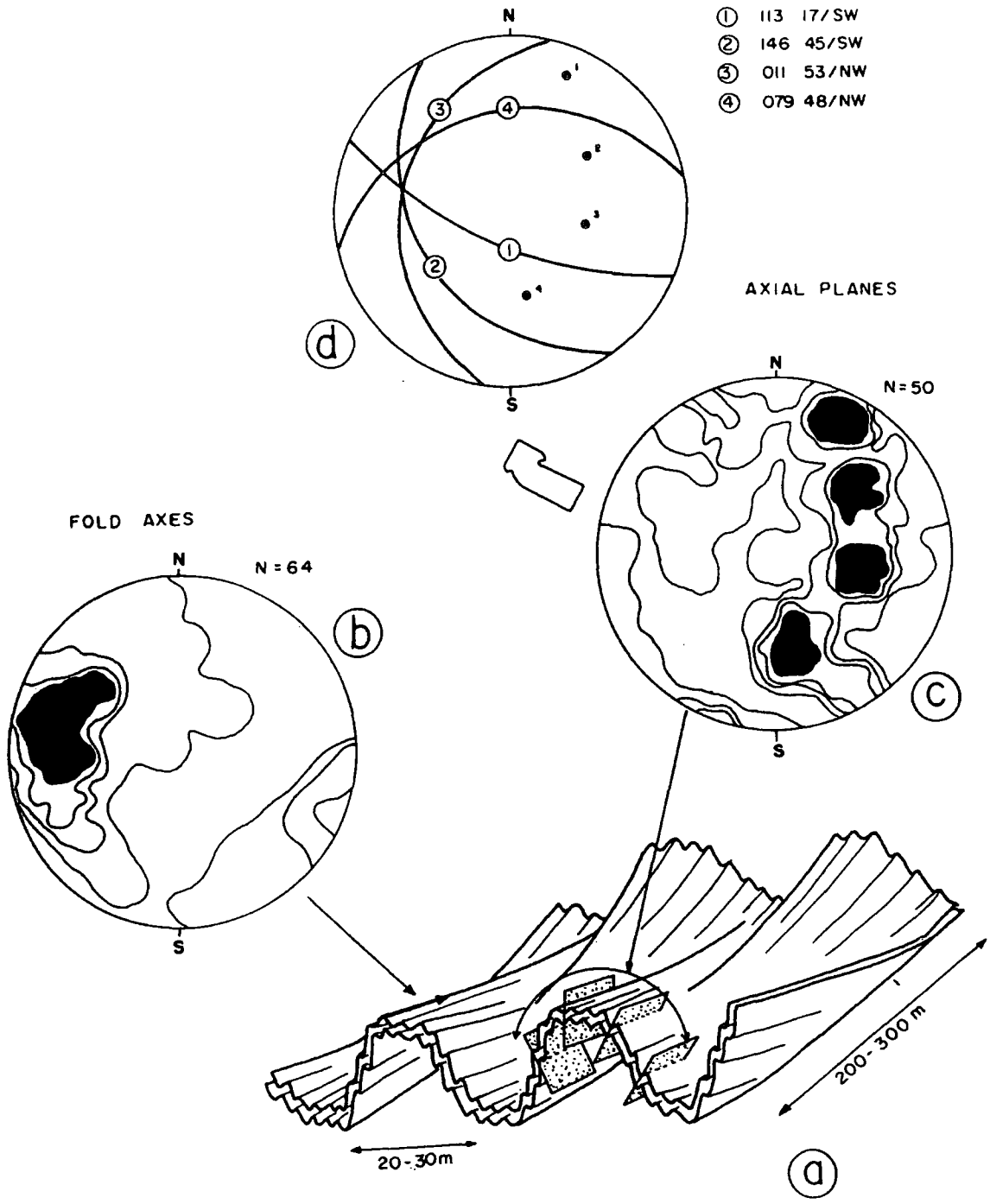

Fig 4.3.4 - Geometry of the predominant set of centimetre to decametre-scale folds in the N-4 Mine. a) 3-D cartoon showing doubly-plunging, polyclinal fold styles in *en echelon* patterns. b) Stereonet showing the distribution of minor fold axes (mean 28°/278°). Contours 20%, 15%, 10%, 5%. c) Distribution of minor fold axial planes showing a polydomainal girdle distribution of poles, in which four main trends are recognized (1 to 4, stereonet "d"). Contours 12%, 10%, 8% and 6%.

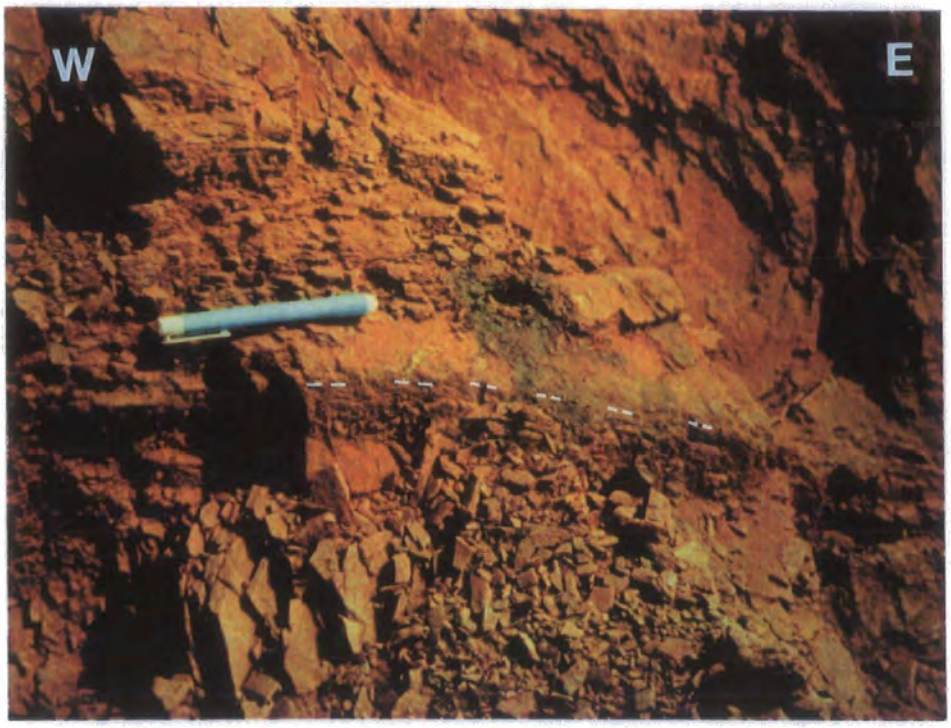

Photo 4.3.8- Crest line culmination observed in centimetre-scale periclinal folds affecting the ironstones in the N-4 Mine (approx. coordinates: 1300N-2100E).

Photo 4.3.9- NW-SE high strain zone characterised by tight to isoclinal folds observed along 4-5m wide zone in the N part of the mine.

variable and suggest that the different styles of folds (B_1 and B_2) identified by Ladeira and Cordeiro (1988) all belong to a single fold group.

Two further subordinate groups of folds are recognized based on differences in style and orientation. A system of kink bands with wavelengths of 0.3-1.0m are developed throughout the mine and are locally seen refolding the main set of folds. The kinks typically plunge shallowly NNE or SSW and occur either as isolated monoclinic kinks (Photo 4.3.10) or as orthorhombic and triclinic conjugate sets (Fig. 4.3.5a, 4.3.5b and 4.3.5c; Photo 4.3.11). Axial planes are variable, but the majority strike NE-SW and dip steeply to either the NW or SE (Fig.4.3.5a, 4.3.5d and 4.3.5e; Photo 4.3.11). The chevron folds are centimetre-scale, showing axes generally plunging shallowly to the NW, with NW-SE to close E-W axial planes dipping moderately to steeply NE or N (Fig.4.3.5f and 4.3.5g and Photo 4.3.12) and are associated with the kinks (Photo 4.3.11). There is no evidence for overprinting of successive tectonic fabrics in the N-4 ironstones. Given the limited development of the later fold sets, there is no compelling reason to assign these structures to separate deformations on a regional scale.

c) Large-scale folding: The variations in strike of the compositional banding within the rocks of the N-4 plateau define a large scale fold pair with a "Z"-shape asymmetry when viewed down-plunge (Fig.4.3.2a and 4.3.2b). These structures are visible on satellite or radar images and poles to banding from the entire region define a fold axis plunging 36° toward 300° (Fig.4.3.2c). The interlimb angles appear to be approximately 100° and the axial plane trends NW, dipping steeply SW.

d) Relationship between folds of different scales: The axes of the large-folds are generally parallel with the axes of the decametre-scale ones (compare Fig. 4.3.2c and 4.3.6b) and this suggests that the latter are parasitic structures of the same age. In detail, however, the orientation and plunge of the outcrop-scale folds show some significant differences (Fig.4.3.6a and 4.3.6b). Such variation probably reflects in part the *en echelon* and branching patterns of the curvilinear fold hinges on both outcrop and hundred-metre scales (cf. Fig.4.3.4a), but they have also significant differences in trend in separate parts of the mine (see small stereonets of fold axes in Fig.4.3.6a). These patterns may have arisen due to small amounts of later rotation of fault-bounded blocks (cf. Marçal *et al.*, 1992), but this could not be demonstrated using field relationships.

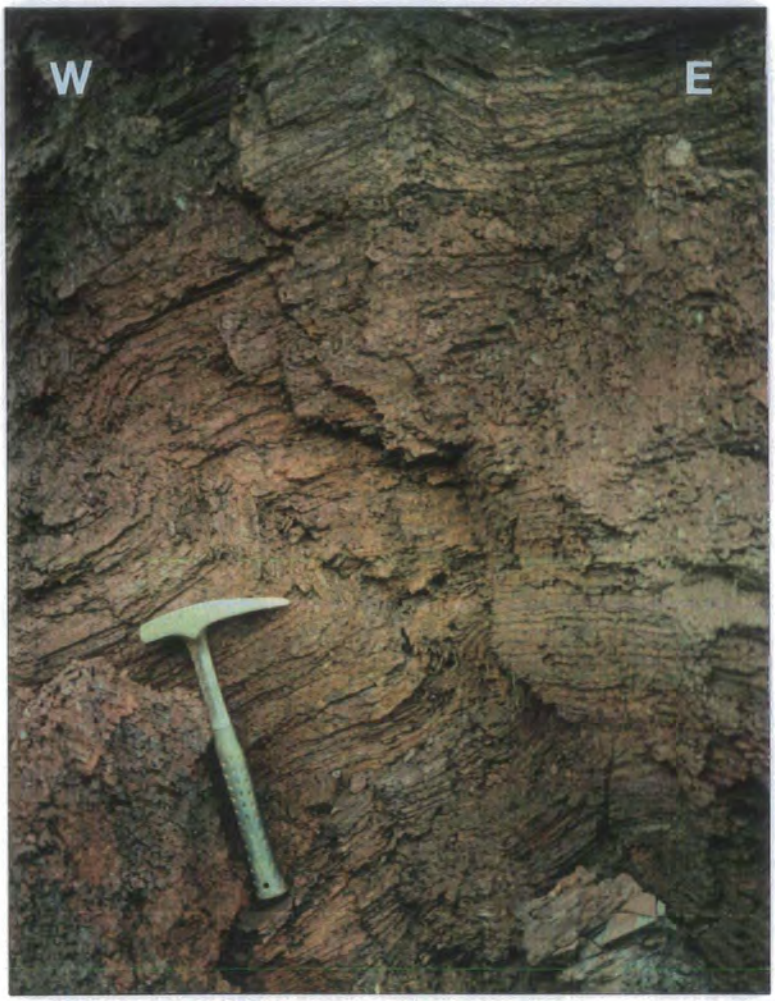

Photo 4.3.10- Example of an isolated orthorhombic kink fold observed in the eastern-central part of the mine (approx. coordinates 950N-2000E).

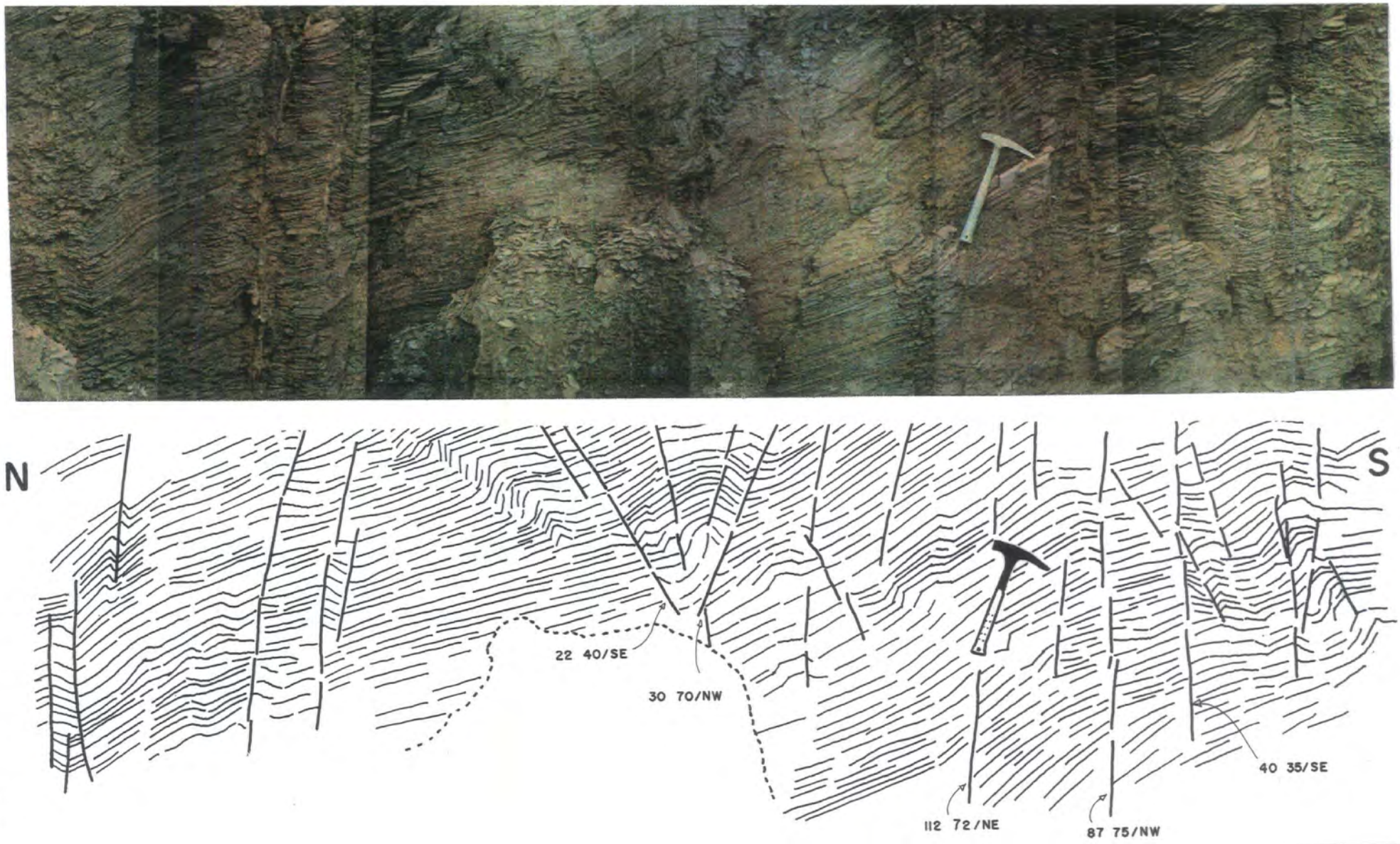

Photo 4.3.11- Kink and chevron folds observed in the NE of the N-4 Mine (approx. coordinates 2200N-2050E). See text for more information

The spatial relationship between the kink and the chevron folds is not entirely clear. The chevron folds appear to be later than the kinks since in many cases it is possible to observe a cross-cutting relationship between them. However they may be related to the same folding event if chevron folds formed where conjugate kink bands intersect (Twiss and Moores, 1992).

e) Brittle faults and lineaments. Most of the faults exposed in the mine are small-scale features with only modest developments of brittle fault rocks apparently reflecting minor amounts of displacement. Two principal minor fault orientations are developed: (1) a set of E- to ENE trending, steeply northerly-dipping fractures and (2) a subordinate group of sub-vertical, N-trending structures (Fig.4.3.2d; Photo 4.3.13). Slickenlines are poorly preserved overall, but the majority (which come mainly from the E-W fault set) suggest dip-slip to oblique-slip movements (Fig.4.3.2e). Senses of movement are often difficult to establish due to a lack of reliable offset marker horizons and brittle shear criteria, but where determined, all faults in this group appear to have compressional offset components. It is important to emphasize that there is relatively little field evidence for significant strike-slip displacements in the N-4 mine area. However, some faults preserve two or more sets of slickenlines, or display curved patterns. In these cases, the later movements tend to produce more shallowly-plunging movement indicators, but these effects may reflect strain partitioning during regional transpression (see below).

On a larger scale, a series of lineaments can be recognized on satellite and radar images (Fig. 4.3.2a; Photo 4.3.1). The majority seem to follow NNW- to NW- trends and do not appear to correspond to either of the dominant sets of fractures recognized in the field. These lineaments more closely correspond in trend to the orientation of the folded and 'not folded' belts of ironstone developed on a scale of hundreds of metres. In several locations (e.g. in the north part of the mine, see section in Fig.4.3.3), intense shear along the boundaries of some folded zones has produced tight to isoclinal folds that partially transpose the banding forming narrow NW-trending zones of intensely foliated rock. In some cases, folded zones are bounded by NW-brittle faults which may follow the trend of earlier high strain zones (Fig.4.3.2b).

The NW-trending lineaments are apparently cross-cut by a more continuous set of N-trending features which probably correspond to the fractures of this trend recognized in the mine (Fig.4.3.2d). These features are very prominent on a regional scale and appear to relate to a regional set of Middle Proterozoic fractures (Costa *et al.*, 1991) thought to post-date most

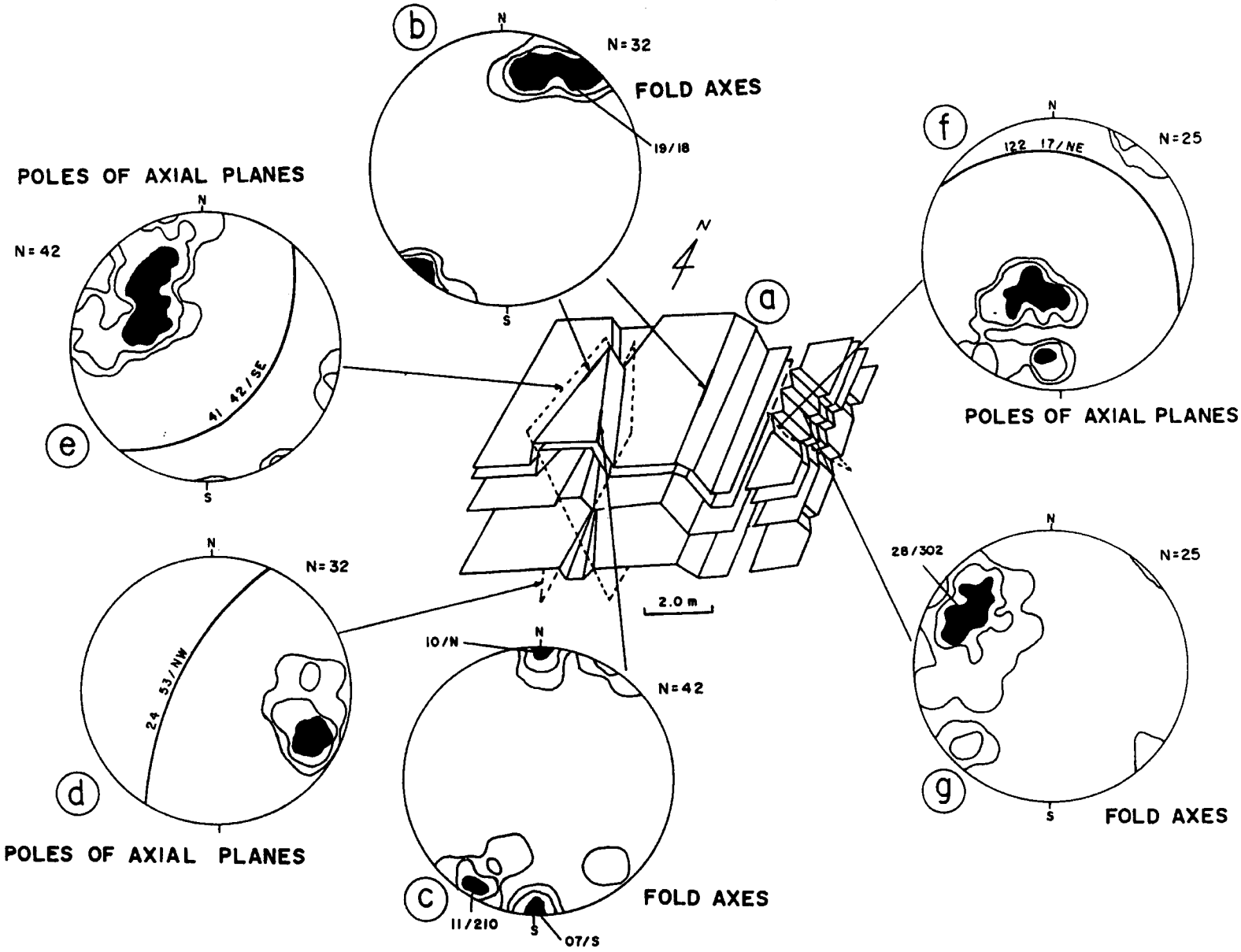

Fig.4.3.5 - a) Three dimensional cartoon illustrating the geometry of the subordinate kink bands and chevron folds. (b) and (c) represent the distribution of kink fold axes. Contours 25%, 15% and 10%. (d) and (e) show poles to axial planes of these folds. Contours 20%, 15% and 10%. f) poles to axial planes of the chevron folds. Contours 20%, 15% and 10%. (g) Chevron fold axes. Contours 25%, 15% and 10%.

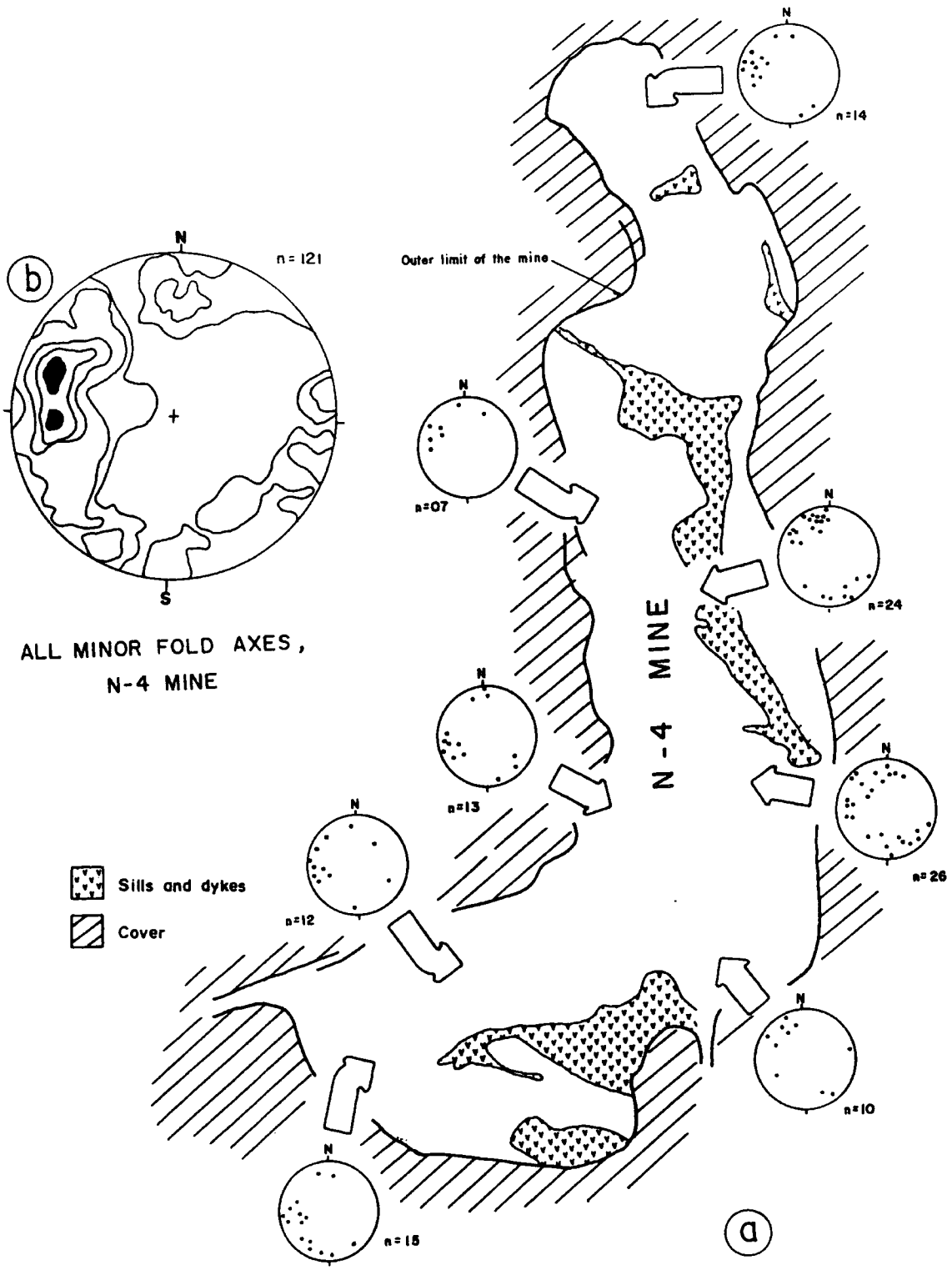

Fig.4.3.6 -a) Distribution and different orientations of minor fold plunges around the N-4 mine. b) Stereonet showing all minor fold axes (mean 35°/275°). Contours 20%, 15%, 10%, 5% and 2.5%.

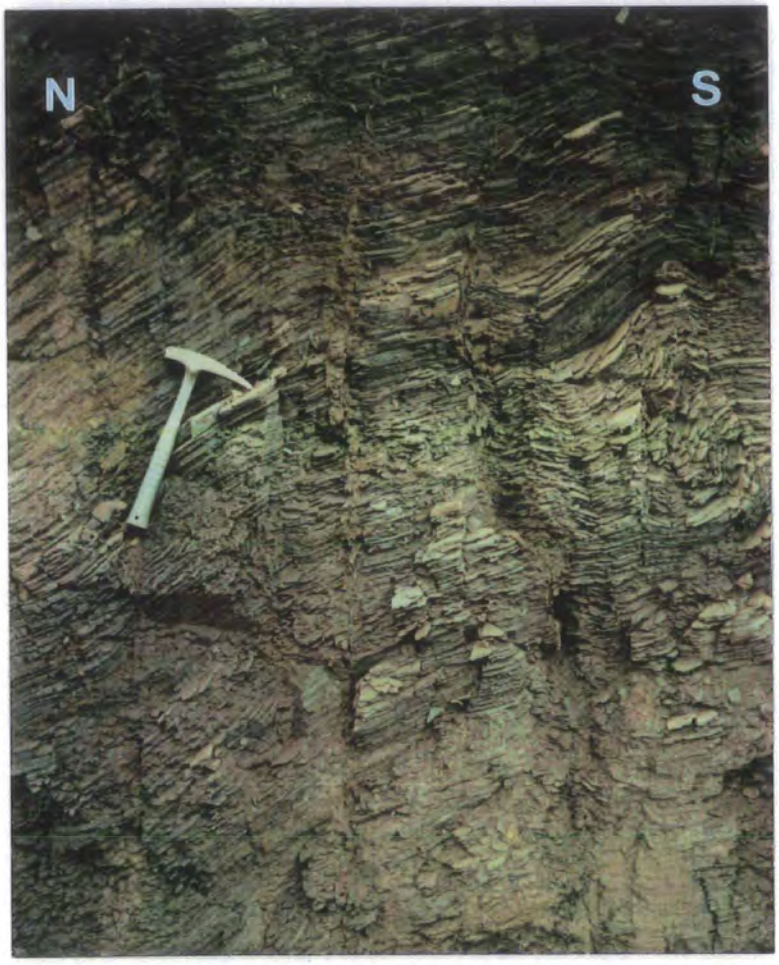

Photo 4.3.12- Set of chevron folds observed in the limbs of decimetre-scale folds (axial plane about E-W dipping sub-vertical). Approx. coordinates: 000-1050E.

movements along the main Carajás Strike-Slip System. No consistent senses of displacement are perceptible on these structures.

A subsidiary set of ENE-trending lineaments is evident on satellite images (Fig.4.3.2a) that may relate to steeply NW-dipping fractures recognized in the field (Fig.4.3.2d), especially those associated with a well exposed set of volcanic - ironstone boundaries (see below).

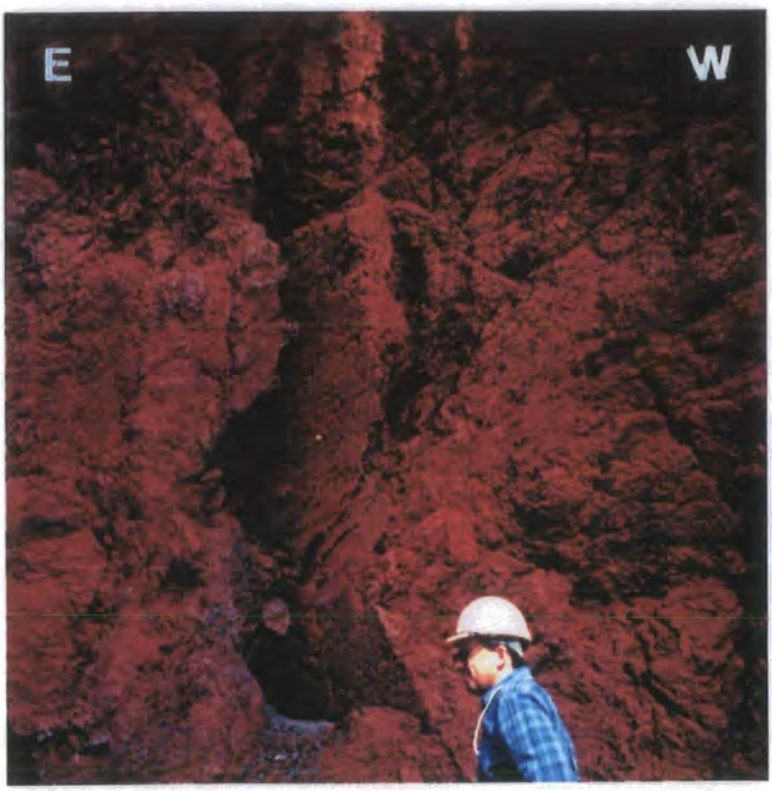

Photo 4.3.13- A steep N-S oblique-slip fault observed in the S part of the mine, cutting the ironstones (approx. coordinates: 0010N-1000E).

4.3.3.2 PARAUAPEBAS FORMATION AND THE CONTACT IRONSTONES-VOLCANICS.

Contacts between ironstones and volcanics are poorly exposed in the region of the N-4 plateau. The volcanic rocks of the Parauapebas Formation comprise a heavily altered sequence of lava flows, tuffs and high-level intrusions of predominantly mafic composition with a subordinate group (10-

15%) of felsic rocks (Gibbs and Wirth, 1990). In general, most of the volcanic sequence is relatively undeformed and shows both conformable and unconformable contacts with the Carajás Formation ironstones. Where conformable, it reflects continued volcanism into the period of early iron deposition (Wirth, 1986). In places where deformation took place, these contacts are disrupted by shearing and folding. The best example of a contact zone is seen in a stream section just outside and to the NW of the mine (Figs.4.3.2a and 4.3.7) where approximately 300m of highly deformed volcanic rocks are interleaved with the ironstones by ENE-trending faults. In the ironstones close to the northern bounding fault, numerous open to tight minor folds are developed on a millimetre to centimetre scale, the majority verging SE (Fig.4.3.7a). These structures are generally fairly angular and the majority are closely associated with small-scale, NNE-dipping reverse faults sub-parallel, or at low angles to the fold axial surfaces. Fold plunges are variable, but the majority plunge shallowly to moderately NE (Fig.4.3.7a). The steeply (ca.80°) NW-dipping bounding fault and associated secondary fractures carry slickensides plunging 55°-60° NE and display brittle shear criteria suggesting sinistral reverse senses of movement.

The volcanics show a much more ductile deformation pattern involving the development of a penetrative cleavage and fine mineral lineation defined by the alignment of dark green phyllosilicates. This fine-grained slaty cleavage strikes E-ENE and dips steeply to moderately NNW, sub-parallel to the northerly faulted contact. Adjacent to this boundary, the mineral lineation plunges 50° NE, sub-parallel to the axes of isolated minor folds of compositional banding and quartz veins. Traced in the continuous exposures about 200m to the south, the plunge of the mineral lineation and minor folds within the more-or-less constantly orientated cleavage planes gradually decreases, until it is sub-parallel to strike. It retains this orientation southwards to the ENE-trending southern bounding fault. The ironstones to the south of this fault display minor folding patterns similar to the ironstones to the north.

The minor fold vergence patterns taken together with the sense of fault movement in the region of the ironstone-volcanic boundary strongly suggest that the deformation relates to larger-scale sinistral transpression. It is proposed that deformation partitioning has occurred in which different parts of the deforming body accommodate strike-slip and compressional strain components of the oblique convergence vector (Fig.4.3.7b). A strain *intensity partitioning* is reflected by the concentration of ductile deformation into the volcanics which contrasts sharply with the lower strain and brittle-ductile structural styles in the

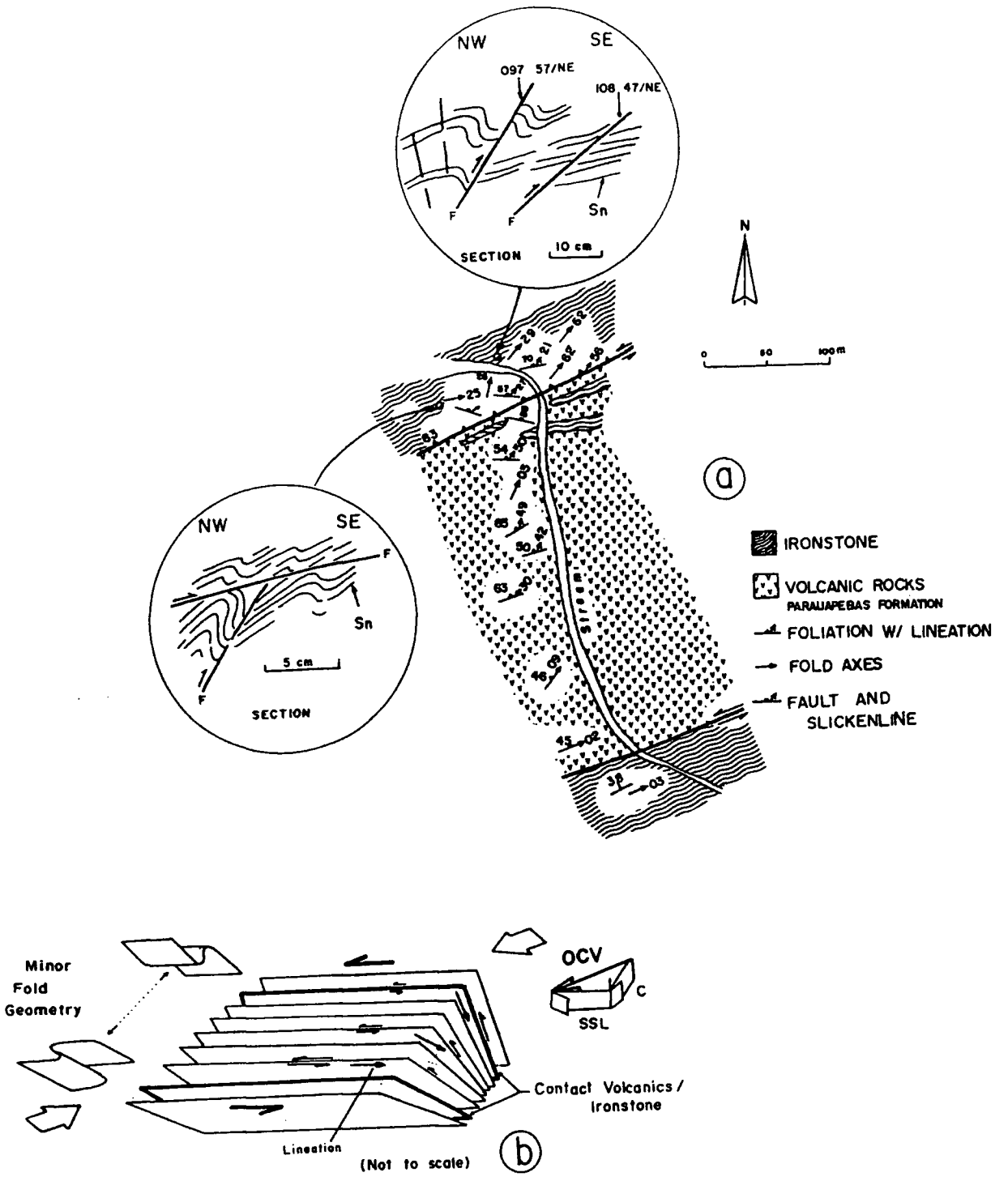

Fig.4.3.7 - a) Structural map of the contact zone between ironstone and the volcanics (for location see Fig.4.3.2). b) Three-dimensional cartoon showing foliation and lineation orientations, minor fold geometries and suggested kinematic partitioning during sinistral transpression (see text for further details).

adjacent ironstones. In addition, the swings in mineral lineation and minor fold plunges strongly suggest that *kinematic partitioning* of strain has also occurred since there is no evidence of overprinting relationships that could indicate polyphase deformation. In this case, the volcanics appear to have focused the strike-slip component which would account for the shallowing of the lineation in these rocks. In contrast, the SE-verging folds in the ironstones preserve evidence of NNW-SSE compression (Fig.4.3.7) and they differ markedly in orientation when compared to the rest of the mine (compare Figs. 4.3.2 and 4.3.7). This difference is thought to reflect strain partitioning localized into the region of the ironstone - volcanic boundary.

4.3.4- DISCUSSION

The ironstones and the subordinated volcanics of the N-4 plateau are significantly more deformed than other bodies of these rock types in the Carajás region. They lie along an uplifted belt of Grão Pará Group rocks that separates two outcrops of the Águas Claras Formation (Fig.4.3.1); elsewhere, these ironstones are peripheral to the main outcrop of younger rocks. Marçal (1991) and Marçal *et al.* (1992) have suggested that the deformation was related in some way to regional sinistral transpression along the Carajás fault system. They propose that the folds were formed due to dextral shear drag along N-S oriented antithetic shear zones and faults.

The field observations of this study suggest that most of the deformation affecting the ironstones can be attributed to a single episode of heterogeneous brittle-ductile folding on all scales. The present outcrop pattern of the N-4 ironstone body reflects the presence of a major shallowly WNW-plunging, NNE-verging fold pair, with a steeply SW-dipping axial surface. These main fold structures appear to be consistent with NE- to NNE-compression and, in the absence of any evidence for steeply plunging folds or N-S-trending dextral shear zones, it is not possible to support the models proposed by Marçal (1991) and Marçal *et al.* (1992). However, the evidence for sinistral transpression associated with the ENE-trending faults and associated zones of shearing along the ironstone - volcanic contacts exposed NW of the N-4 mine supports the more general assertion that the deformation may be related to regional sinistral shear along the Carajás Strike-Slip System. It may be significant that the deformed ironstone body and associated rocks lie adjacent to the central part of a large bend in the Carajás Fault where it swings from an E-W into a

NW-SE trend (Fig.4.3.1). During sinistral shear such a right-hand bend would be expected to form a compressional jog. The strong NW-trend of the fold axial surfaces and fold belts in the area of the N-4 plateau is significantly clockwise of the Carajás Fault (Fig.4.3.1), a feature that is generally consistent with sinistral shear. However, the large scale fold pair in the N-4 mine verges away (to NE) from the Carajás Fault and the present mapping supports the idea that all of the deformation is concentrated in the belt of uplifted Grão Pará rocks that diverges from the main fracture on the northeastern side of the bend (Fig.4.3.1). This implies that the location and trend of the folding could reflect inversion involving a buttressing effect (Butler, 1989; Hayward and Graham, 1989, Deecks and Thomas, 1995) against pre-existing structures which branch onto the main fault at depth. The proposed configuration is shown in Fig. 4.3.8. The geometry of these pre-existing structures may originate in a dilational jog formed during the earlier phase of dextral strike-slip along the Carajás fault system.

Recent work (e.g. Holdsworth and Strachan, 1991; Tikoff and Teyssier, 1994; Teyssier *et al.* 1995) suggests that oblique convergence or transpression zones are typified by strain partitioning. These effects are recognized in the region of the N-4 plateau and appear to be localized adjacent to certain ironstone - volcanic boundaries. This indicates that the partitioning may be controlled by differences in the overall rheological response of these very distinct lithologies during deformation at low metamorphic grades. Furthermore, the non-cylindrical fold styles found in the N-4 Mine with their *en echelon* and branching arrangements are also thought to be consistent with transpression and may also reflect a non-orthogonal relationship between the principal axes of finite strain and the compositional banding in the ironstones on a regional scale prior to folding (cf. Treagus and Treagus, 1981). In such cases, the initial orientation of the fold axes will be determined by the orientation of the longest axis of the sectional ellipse in the plane of the layering and, in general, this will not lie in the bulk XY plane (Flinn, 1962). Depending on the k-value of strain and the degree of original obliquity of the strain axes and the layering, it is possible to produce non-cylindrical, periclinal folds or even folding in two directions which may produce local interference patterns. The presence of chevron and kink folds subordinate to the major structures is also consistent with this hypothesis since the development of symmetric chevron folds or asymmetric kinks depends on whether the direction of shortening is parallel or oblique to layering (Twiss and Moores, 1992).

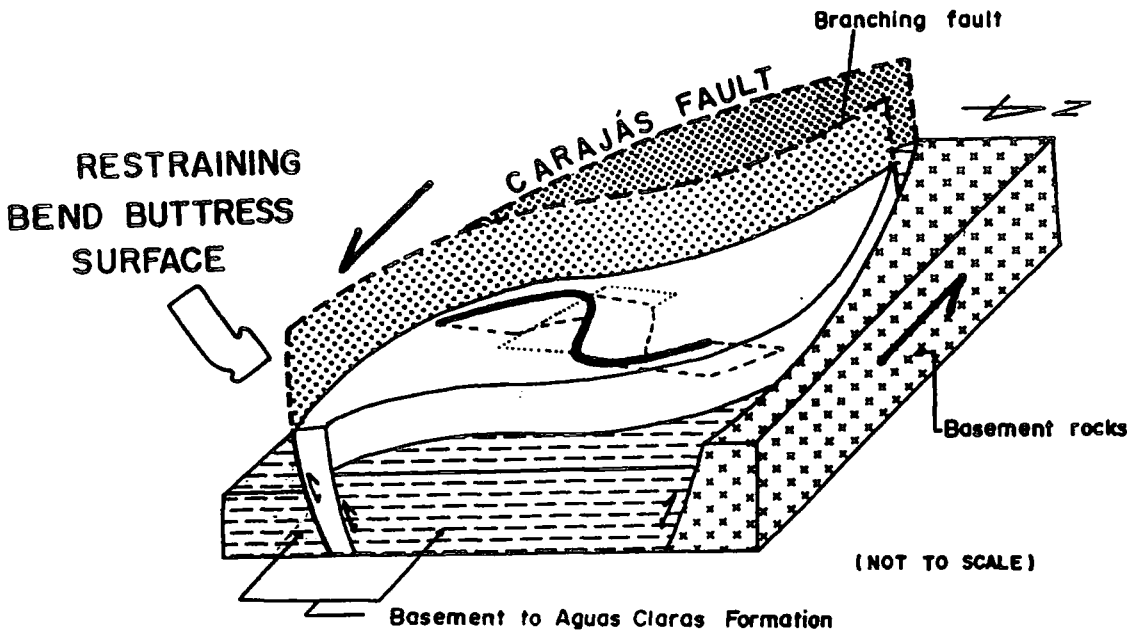

Fig.4.3.8- Schematic block diagram showing the relation between the main structures in the N-4 plateau region and the proposed kinematic model (see text for further details).

In the absence of strain data, it is not possible to investigate these possibilities further, but if it is supposed that the original orientation of bedding in the region of the N-4 plateau lies parallel to the NE border of the Carajás Strike-Slip System (as in the south border of the Carajás Structure), it presumably should strike WNW-ESE, dipping shallowly SSW, before folding (Fig.4.3.9-1). If this assumption is correct it is possible to picture the evolution of the N-4 folding as schematically represented in Figure 4.3.9. The initially unfolded WNW-ESE layers shallowly dipping SW, undergo folding with a gradual clockwise rotation about a vertical axes, as predicted by the Treagus & Treagus (1981) model, and simultaneous rotation of the structures about a horizontal axis increasing the plunge of the folds (Fossen and Tikoff, 1993), -up to a final plunge of 36°. Strike-slip displacements along the Carajás Fault and its fault splays and branches, in close association with the folding, also account for partitioning of the deformation and reactivation. Vertical displacements of blocks coeval with strike-slip motion seem to be associated with buttressing responsible for the final NE vergence of the existing structures.

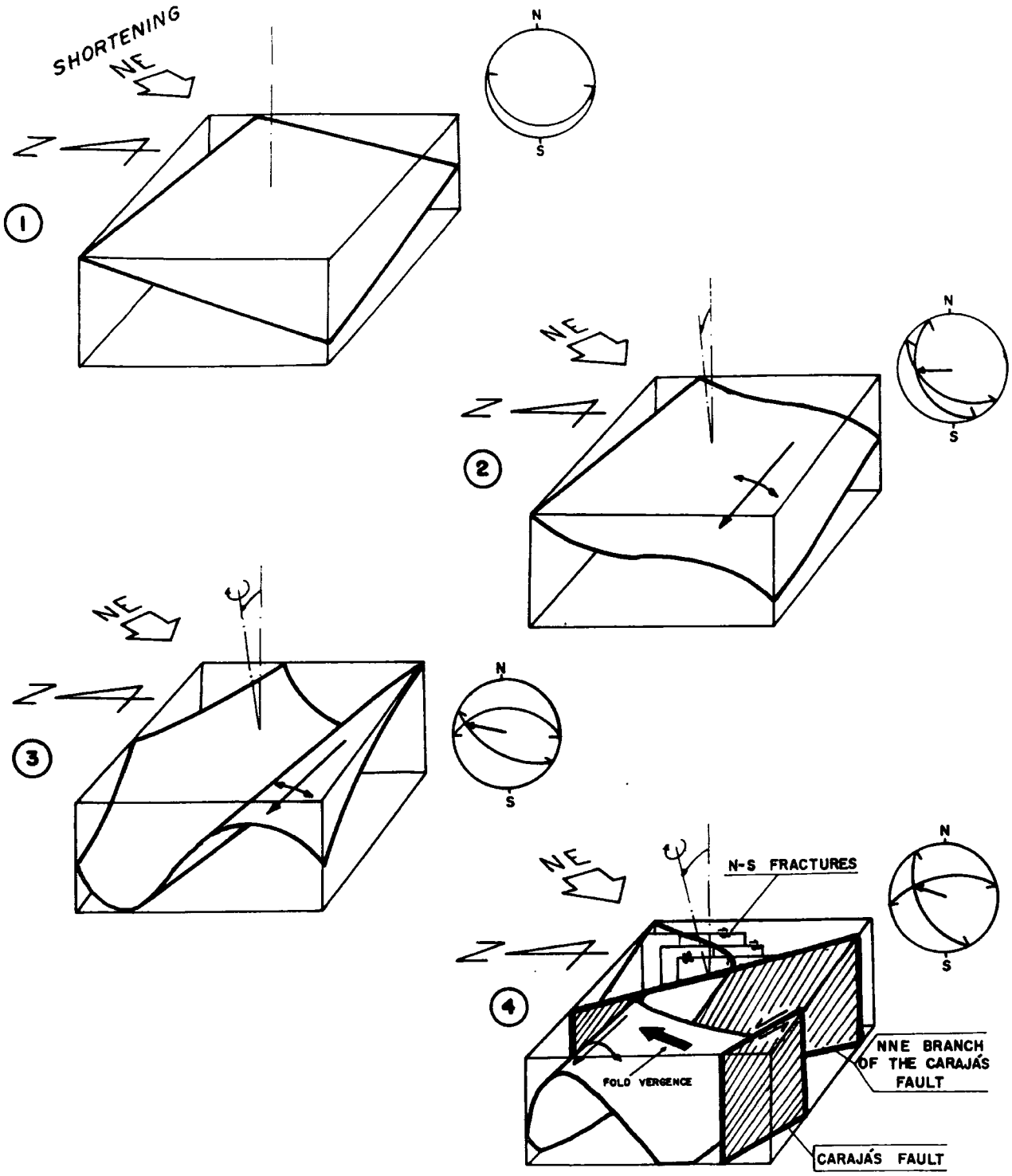

Fig. 4.3.9- Cartoon representing four steps to the probable development of the N-4 Mine kilometre-scale fold, under transpressional deformation, controlled by the Carajás Fault branches.

4.3.5- CONCLUSIONS

1) The ironstones and associated volcanic rocks of the N-4 plateau region lie in a NW-trending deformed belt of Late Archaean Grão Pará Group belonging to the Cover Assemblage. The rocks are all at very low metamorphic grade and, contrary to the assertions of some previous authors (Marçal, 1991; Marçal *et al.*, 1992), there is no evidence for pervasive mylonitisation in the ironstones.

2) Deformation of N-4 ironstones and associated volcanics occurred predominantly during a single phase of brittle-ductile folding reflecting NNE-SSW compression. This deformation has determined the present form of the N-4 ironstone body which now lies in a major shallowly WNW-plunging antiform-synform fold pair with a steeply SW-dipping axial surface. Associated faulting is relatively minor.

3) Many ironstone - volcanic rock contacts are tectonic and display evidence for strain partitioning during sinistral transpression due to differences in the mechanical responses of the two main rock types during deformation.

4) The present observations are consistent with a model in which the principal deformation of the N-4 plateau ironstones and associated rocks occurred due to a localized zone of transpression during sinistral movements (tectonic inversion) along the Carajás fault system. The folding affects an area that lies adjacent to, but separate, from a bend in the Carajás Fault. This suggests that deformation may have occurred due to buttressing against an important pre-existing fault branch of the Carajás Fault in a dilational jog formed during an earlier phase of regional dextral movements (Fig.4.3.8).

5) This example demonstrates that it is necessary to elucidate the geometry and style of structures directly in the field. Interpretations of lineaments from remotely sensed images can be misleading and senses of shear should never be inferred solely from these data. In the case of the N-4 iron mine, it appears that the main set of lineaments are controlled by folding patterns, and only secondarily by faulting.

4.4- THE IGARAPÉ BAHIA REGION

The Igarapé Bahia area preserves an important gold and copper deposit located in rocks of the Cover Assemblage in the central western part of the Carajás Strike-Slip System (Fig.4.4.1; Photo 4.4.1). The rocks in this region are metasediments and metavolcanics which have been correlated with different regional units, in particular with the Archaean Grão Pará Group. There are very few studies of the structural geology in this area and most scientific interest has been focused on petrological and economic studies related to the ore deposits.

In this work, the Igarapé Bahia Gold Mine was the main site used to investigate the structural features and the stratigraphy of the rocks but the research carried out during the field season also explored small outcrops in the surrounding areas, especially along several small new roads. Rocks are generally very poorly exposed.

4.4.1- REGIONAL SETTING.

The metavolcanic and metasedimentary rocks of the Igarapé Bahia area are correlated here with the Archaean rocks of the Igarapé Pojuca Group (DOCEGEO, 1988). This unit was first described as outcropping along both the north and south boundaries of the Carajás Strike-Slip System, unconformably lying on the Xingu Complex (DOCEGEO, 1988). In the Bahia region, the Igarapé Pojuca Group outcrops at an altitude of about 300-500m, when not affected by faults and is covered unconformably by sedimentary rocks of the Águas Claras Formation (Nogueira *et al.*,1995) over 550m. Both units form part of the Cover Assemblage and are extensively affected by hydrothermal alterations (Ferreira Filho and Danni, 1985). An upper 20m thick lateritic crust, formed due to weathering processes, is well developed especially on the top of the plateaus. The tectonic and structural features of the rocks present in this region have never been studied and only very few isolated faults and dykes have been recognised. The main trace of the Carajás Fault lies about 12 Km to the north of the area studied.

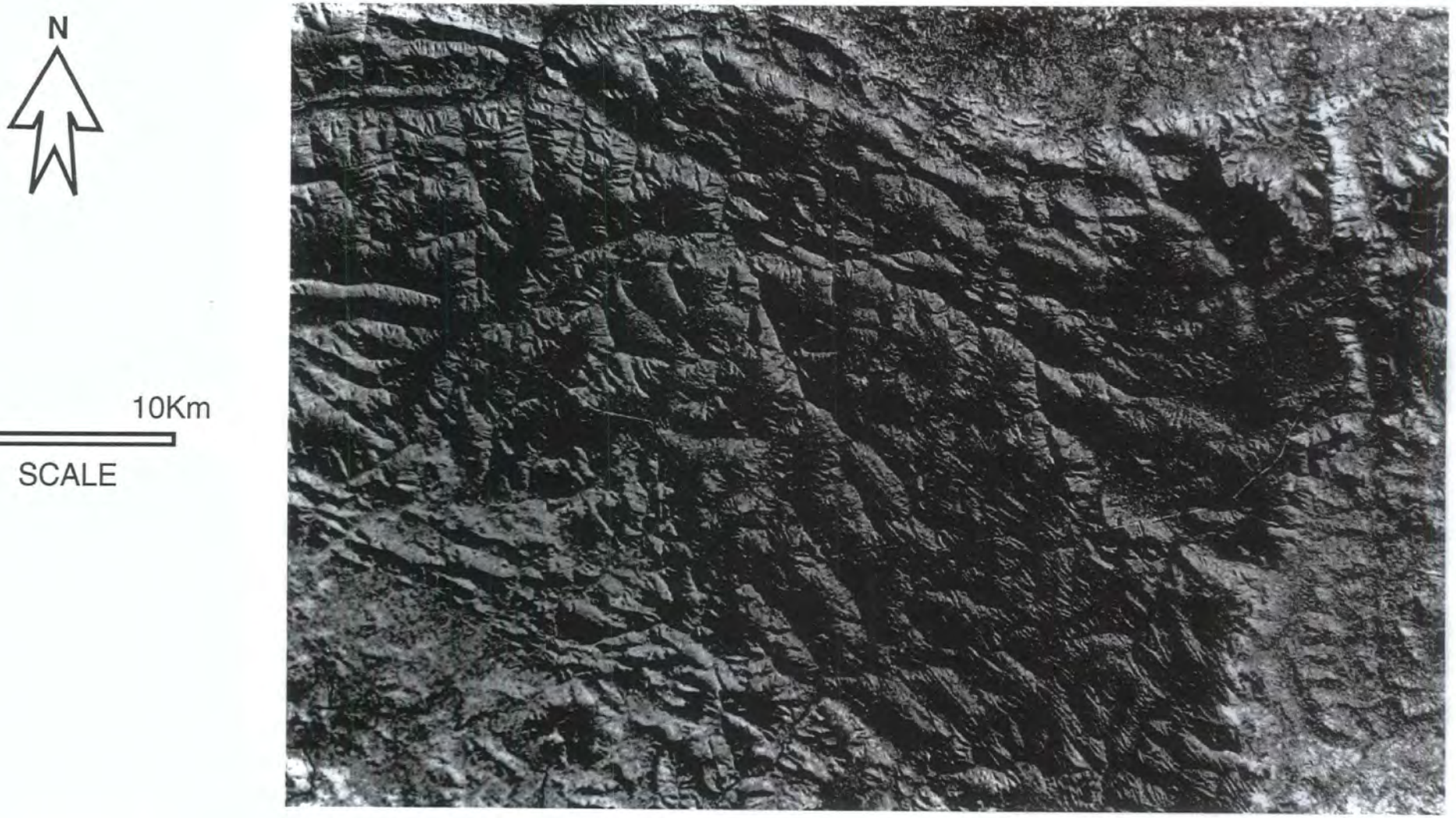

Photo 4.4.1- Satellite image of the W part of the Carajás Structure where the Igarapé Bahia Mine is placed. See Fig.4.4.1.

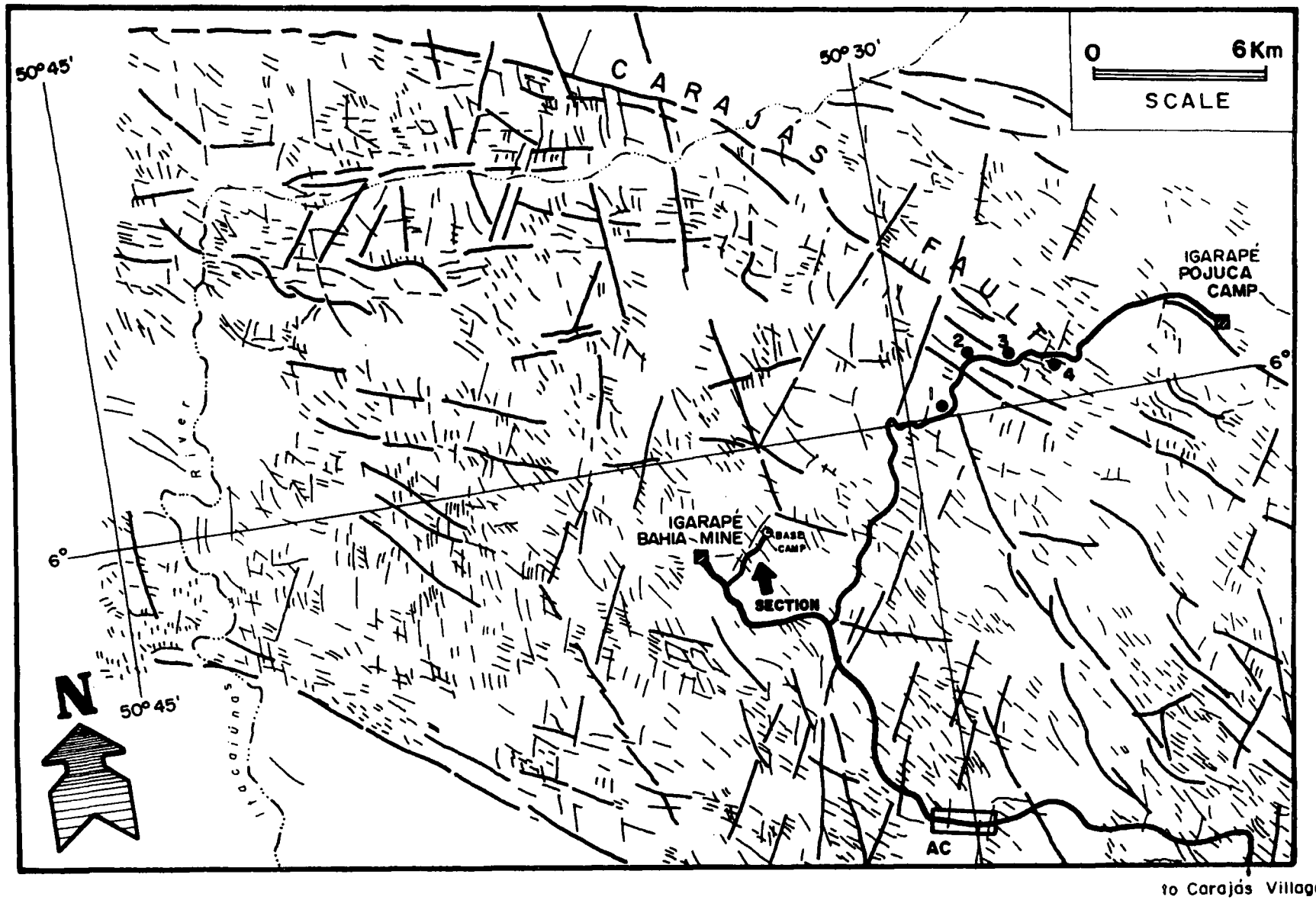

Fig.4.4.1- Location of the Igarapé Bahia area in the central part of the Carajás Strike-Slip System, from LANDSAT image. The lines represent lineaments visualised on 1:100.000 satellite image. Heavy sinuous lines represent roads and the points (1-4) are locations of studied outcrops. The box labelled "AC" represents location of the Águas Claras Formation rocks.

4.4.2- PREVIOUS WORK.

Although it was discovered more than 20 years ago, the first geological descriptions of the "Bahia Prospect" are given in unpublished geological reports by DOCEGEO (Rio Doce Geologia e Mineração S.A.) and in an article by Fonseca *et al.* (1984) summarizing information on the Cu deposit in this area. Fonseca *et al.* (1984) correlated the volcano-sedimentary sequence with the Rio Fresco Formation, thought at that time to be Early Proterozoic (Hirata *et al.*,1982). Using isotopic data, Ferreira Filho *et al.* (1987) have suggested a possible correlation between the Igarapé Bahia rocks and the Later Archaean Grão Pará Group (Wirth *et al.*, 1986). This proposal did not receive significant support from later authors working in the region since most of them preferred to correlate these rocks with the Rio Fresco Formation (e.g. Andrade *et al.*,1991; Zang and Fyfe, 1993) or refer to the "Bahia Sequence" (Althoff *et al.*, 1994). Hutchinson (1979) was the first to suggest, on the basis of petrological data, a correlation between the volcano-sedimentary rocks of the Grão Pará Group and that of the "Salobo-Pojuca Sequence" (Meyer and Farias, 1980). This proposal was later supported by several geological studies developed in Carajás (e.g. Medeiros Neto and Villas, 1984; Lindenmayer, 1990; Araújo and Maia, 1991; Lindenmayer and Fyfe, 1992; Costa *et al.*,1995).

DOCEGEO (1988) refers to the rocks in this region as the Igarapé Bahia Group (Archaean to Early Proterozoic in age),which are subdivided into two distinctive units: (1) the Grota do Vizinho Formation, a basal unit, comprising pelites, sandstones, ironstones, pyroclastic and basic volcanic rocks; and (2) the younger Sumidouro Formation composed of clastic sedimentary rocks, including sandstones, arkoses, and also interlayed volcanic rocks. The contact between these two units was thought to be gradational (DOCEGEO, 1988).

A more detailed description by Ferreira Filho and Danni (1985) of the lithostratigraphy suggests that five lithologic units are present in the region around the Igarapé Bahia Mine. The lowest unit (1) comprises laminated metasediments with subordinate basic volcanics and ironstone, <150m thick. A 100-150m thick (2) sequence of silicic pyroclastics and basic volcanics overlies these rocks, which are in turn overlain by a third unit of metasediments, including ironstones up to 70m thick. These are overlain by (4) 35m of pyroclastic rocks and (5) an upper unit of metasiltstones with fine

intercalated volcanic rocks. Ferreira Filho and Danni (1985) did not assign names or ages for any of these rocks.

The first and second lithological sequences described by Ferreira Filho and Danni (1985) appear to correspond to the Grota do Vizinho Formation, while the third group of rocks should be equivalent to the Sumidouro Formation named by DOCEGEO (1988), even though Ferreira and Danni (op. cit.) refer to an unconformity between the basal volcano-sedimentary rocks and the top clastic sequence.

Araújo and Maia (1991) and Costa *et al.* (1995) adopted the name Grão Pará Group to refer to this sequence, suggesting that all the volcano-sedimentary rocks present in the Carajás Strike-Slip System represent a single sequence laid down in transtensional basins. The detailed geochemical and petrological study of the rocks of the Igarapé Salobo region carried out by Lindenmayer (1990) also suggested that the volcanics of the Grão Pará Group, those of the so-called Igarapé Bahia Group (DOCEGEO,1988) and the amphibolites of the Igarapé Salobo Group (DOCEGEO,1988) are all coeval.

According to Ferreira Filho and Danni (1985) and Sachs *et al.* (1992) the metavolcanic rocks are predominantly spilitic basalts and dolerites forming flows and sills, with preserved primary structures, such as ophitic and subophitic textures, and granophyric intergrowths of quartz and alkali feldspar. Silicic pyroclastics are formed by quartz and feldspar within a fine quartz, sericite and chlorite matrix (Ferreira Filho *et al.,* 1987). Andesites and dacites are also present in smaller quantity, often in the middle part of the sequence (Sachs *et al.,* 1992). Althoff *et al.* (1994) point out that the "Bahia Sequence" comprises 50% metabasalts, 30% metapyroclastics and 30% metasediments. The metamorphism in these rocks is thought to be low-greenschist facies. Although there is intense spilitization and later hydrothermal alteration is responsible for the replacement of most of the primary mineralogy by hydrated minerals such as actinolite, albite, chlorite, epidote, and calcite, in association with copper mineralization (Ferreira Filho and Danni, 1985; Sachs *et al.,* 1992; Althoff *et al.,* 1994). The age of these rocks is Archaean. Rb-Sr isotopic ages of around 2700 Ma and 2577±72 Ma were obtained from granophyric intrusions cutting this sequence (Ferreira Filho *et al.*, 1987). Basaltic dykes cutting the rocks in the north of the area are thought to correlate with those of the Igarapé Salobo region whose intrusion has been dated by Lindenmayer (1990) at 560 Ma (Sachs *et al.,* 1992).

The metasedimentary sequence is formed essentially by metasiltstones and slates with small horizons of ironstones, below and above the metavolcanics (Ferreira Filho and Danni, 1985). Metasandstones are less frequent and can vary from very fine to coarse/microconglomeratic. The metasiltstones are formed mainly by sericite and chlorite, quartz and feldspars. Pyrite and chalcopyrite are finely disseminated in the matrix of these rocks. The slates are cleaved and vary in thickness from a few hundred-metres to a few metres. When metre-scale they are associated with metavolcanic and metasandstones or metasiltstones. They comprise mainly low-grade phyllosilicates such as sericite, chlorite, muscovite, scarce biotite, besides quartz, feldspar and iron oxides (Ferreira Filho and Danni, 1985). The ironstones are less than 2m thick and are often interlayed with clastic metasediments. Their mineralogy is essentially haematite and magnetite together with small proportions of chalcopyrite, bornite, chlorite and quartz (Ferreira Filho and Danni, 1985).

The copper mineralization is thought to have originate from a volcanic-exhalative source in an ocean floor setting, controlled by intense primary hydrothermal activities (Ferreira Filho and Danni, 1985; Ferreira Filho *et al.,* 1987; Althoff *et al.,* 1994). The subordinate quantities of gold, silver, and molybdenum, are thought to be of a similar origin (Ferreira Filho and Danni, 1985, Althoff *et al.,* 1994). They were later remobilized by weathering processes during the development of the lateritic crust which covers all the rocks in the region (Andrade *et al.,* 1991; Zang and Fyfe, 1993).

There is no specific information about the structure of the rocks in the Igarapé Bahia area, except for some general observations in Fonseca *et al.* (1984) which mentions the general N/NW trend of the rocks in this region interpreted as a homoclinal or related to an isocline not mapped. Regional mapping did not pay too much attention to the structural geology in this area (e.g. DOCEGEO, 1988; Araújo and Maia, 1991). Most of the data concerning the deformation of these rocks came from study of supposed correlative units in the Igarapé Pojuca area, about 20 km northeast of the Bahia Mine. These studies suggested that two phases of deformation occurred forming folds, including kink bands, and NE-SW faults (Farias *et al.,* 1984; Medeiros Neto, 1985). Hutchinson (1979) reports the occurrence of "rotated primary structures" in the rocks of the Igarapé Pojuca area thought to indicate local inversion of bedding.

4.4.3- DATA FROM SATELLITE IMAGING.

Visual interpretation of satellite and radar images (Fig.4.4.1; Photo 4.4.1) reveals three sets of major lineaments. A strong NE-SW-trending set is the most conspicuous, represented by very broad 3-6 km long lineaments mainly adjacent to the mine area, and in the region to the east (Fig.4.4.1). A second set, trends N-S and is formed by relatively short lines. Both NE-SW and N-S sets are formed predominantly by straight segments that should reflect high angle structures. Another important set of major lineaments is represented by NW-SE lines that display a close parallelism to the Carajás Fault trace, following the northwestern border of the Carajás Structure. This set of lines often display smooth curved geometries, with an anastomosing pattern, particularly developed to NW and SE of the Bahia mine. A dense and complex network of shorter lines (<1km) cut by the major lineaments fills the background of the satellite images. These small-scale features display predominantly NW-SE and N-S directions, and eventually, close to the Carajás Fault trace in the north, they may follow the E-W bearing. The interaction between them forms small lozenges elongated in the NW-SE direction (Fig.4.4.1; Photo 4.4.1).

4.4.4- FIELD DATA

Most of the data presented here come from two localities: the open-cast Igarapé Bahia Mine and the 300m road section located 2km east from this mine. Additional information was obtained from isolated outcrops along the Igarapé Bahia Mine - Igarapé Pojuca Camp road and along the road linking the mine to the Carajás Village (Fig.4.4.1).

4.4.4.1- THE IGARAPÉ BAHIA MINE

The Igarapé Bahia gold mine (Photo 4.4.2) is located about 20 km east from the Itacaiúnas river, 9 km southwest from the Igarapé Pojuca Camp, and nearly 45 km east of the well-known N-4 plateau (see section 4.3). The mine covers an area of ca. 3.9 x 10^5 km^2 spread along the east boundary of a 650m high plateau surrounded by steep vales. A single road links the mine to the main Carajás village, crossing a dense area of rain forest.

a) Lithology and primary structures: The main characteristic of the rocks exposed in the gold mine is the dark-red colour produced by deep equatorial weathering, which tends to obliterate most of their primary structures and mineralogy. Lateritization is a widespread active process. Fresh rock is obtained only by drilling holes or by examining loose blocks in nearby streams. Added to this troublesome factor, the original unweathered rocks are affected by extensive hydrothermal alteration.

Three different types of weathered rocks can be found in the open-cast mine: (1) laterites; (2) ferruginous rocks; and (3) saprolites. The laterites form the uppermost part of the mine and have been described in detail by Andrade *et al.* (1991) and Zang and Fyfe (1993). The ferruginous rocks comprise only relatively small volume of outcrop (ca.10-20%) in the mine walls. They are distinguished by metre-scale, dark-grey to black pseudo-tabular spots showing sharp to diffuse lateral contacts. Haematite and goethite are the main minerals present in these rocks, though vestiges of centimetre-scale quartz veins and hydrothermal kaolinite may be observed. The textures of these rocks vary from massive to pseudo-foliated or platy-brecciated. These ferruginous rocks may be derived from ironstones or produced by Fe-enrichment during lateritization in brecciated zones (Zang and Fyfe, 1993).

Saprolite is the predominant rock-type present in the mine forming a pervasively foliated rock, with different tones of red or dark-yellow when primarily related to slates or metasandstones, or dark-red to green with white spots when derived from volcanics or sub-volcanics.

The most common primary rock type is a weathered slate or pelite, showing a pervasive slaty cleavage. Under the microscope, these rocks comprise fine-grained aggregates of sericite, chlorite, and kaolinite with few very fine quartz crystals, with a strongly orientated texture. Pseudomorphs of chlorite and ?limonite are found replacing magnetite. The unweathered colour of these rocks seems to be grey so far as it is possible to see in places where the saprolite is less developed. Sub-horizontal hydrothermal kaolinitic veins, 1-5cm thick, are locally common. The total exposed thickness of these rocks in the mine may be estimated as >1200m.

A single outcrop of sandstones 4-8m thick occurs close to the mine's main entrance of the mine (level 640m, in Fig.4.4.2). The rocks show the same reddish colour as the slates and with unclear contacts, but no definite bedding is preserved.

Bedding represents the only primary structure exceptionally found in places where the pelites are less obliterated by weathering and by the later

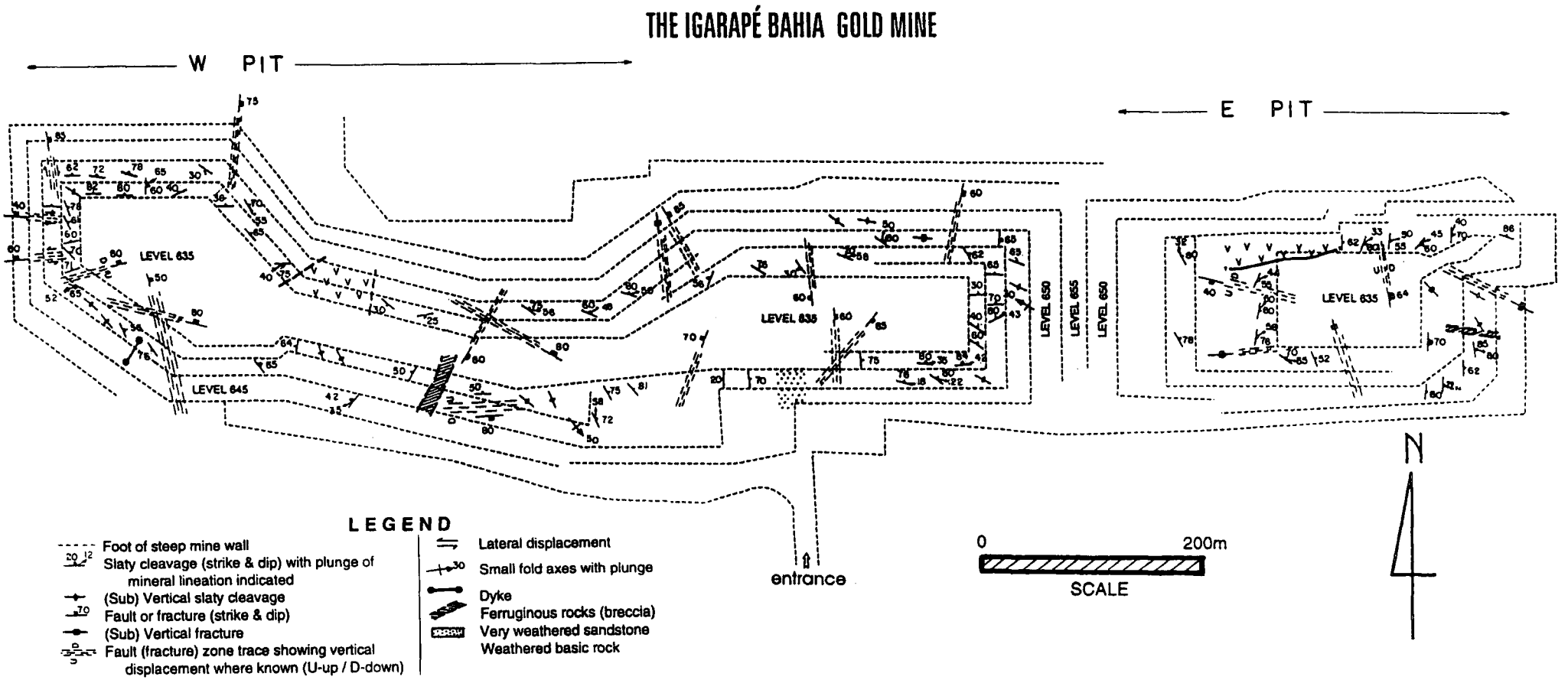

Fig.4.4.2- Map of the Igarapé Bahia Gold Mine showing the main geological and structural features observed.

deformation and metamorphism (Photo 4.4.3). It shows shallow dips towards NE with strikes nearly NW-SE.

Volcanic rocks are strongly altered by weathering and their original mineralogy is almost completely lost. Hydrothermal minerals such as chlorite, epidote and kaolinite are often visible to the naked-eye. Primary structures were not observed in these rocks.

A very altered basic dyke is present in the south wall of the western part of the mine on the 640m level. The dyke trends roughly NE-SW and appears to be an isolated example of a later basic intrusion, examples of which have been widely described in adjacent areas (see section 4.1 and Chapter 6).

b) Slaty cleavage and mineral lineations: Despite the strong weathering alteration, a slaty cleavage and mineral lineation are still preserved in the rocks of the mine.

The slaty cleavage forms a penetrative, smooth, continuous foliation (Photo 4.4.4) mainly defined by fine grains of orientated sericite. It is fairly regular in orientation thoughout the mine (Fig.4.4.2) and is extensively cross-cut by later brittle deformation (Fig.4.4.2). Stereonets of poles to cleavage show a strong 17% concentration maxima representing a mean plane of orientation 152° 75°/NE (Fig.4.4.3A). Local variations in cleavage orientation are more conspicuous in two areas: in the north walls (levels 640m and 645m) of the W pit, and along the eastern side of the E pit, from level 635m to the 645m (Fig.4.4.2). Much of the variation from the main orientation indicated by the stereonet may represent local changes in strike and principally dip of this structure close to later fault/fracture zones (e.g. Photo 4.4.4).

In the few places where bedding is preserved, the slaty cleavage is oblique suggesting that a large scale fold set may exist, but there is insufficient exposure to determine whether any such structures exist in the region of the mine.

Mineral lineation is developed on the surface of the slaty cleavage and is formed by the linear preferred orientation of sericite and elongated clusters of fine quartz grains (Photo 4.4.5). On a stereonet (Fig.4.4.3B), a strong plunge maximum is centred around 63°/077°. A secondary maximum plunges 77°/130° azimuth. Field observations show that in places, a younger 55°/67° lineation overprints an older 50°/140°.

Photo 4.4.2- The Igarapé Bahia Gold Mine (1994), viewed towards the W.

Photo 4.4.3- The primary bedding of the metasedimentary rocks are occasionally preserved, especially in the pelites on the mine. Here, the bedding planes are parallel to the hammer-head.

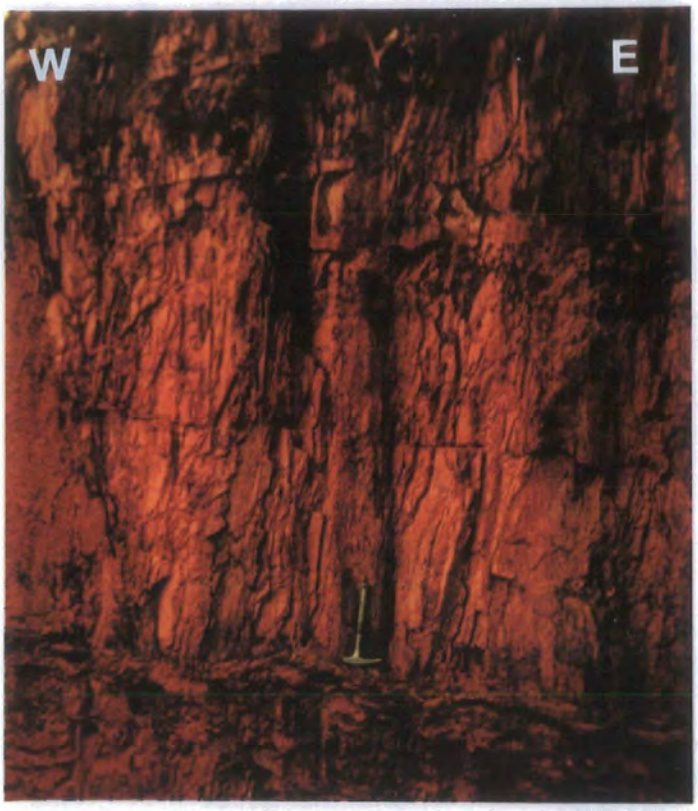

Photo 4.4.4- The steep slaty cleavage cut by sub-vertical small faults on the SW part of the mine.

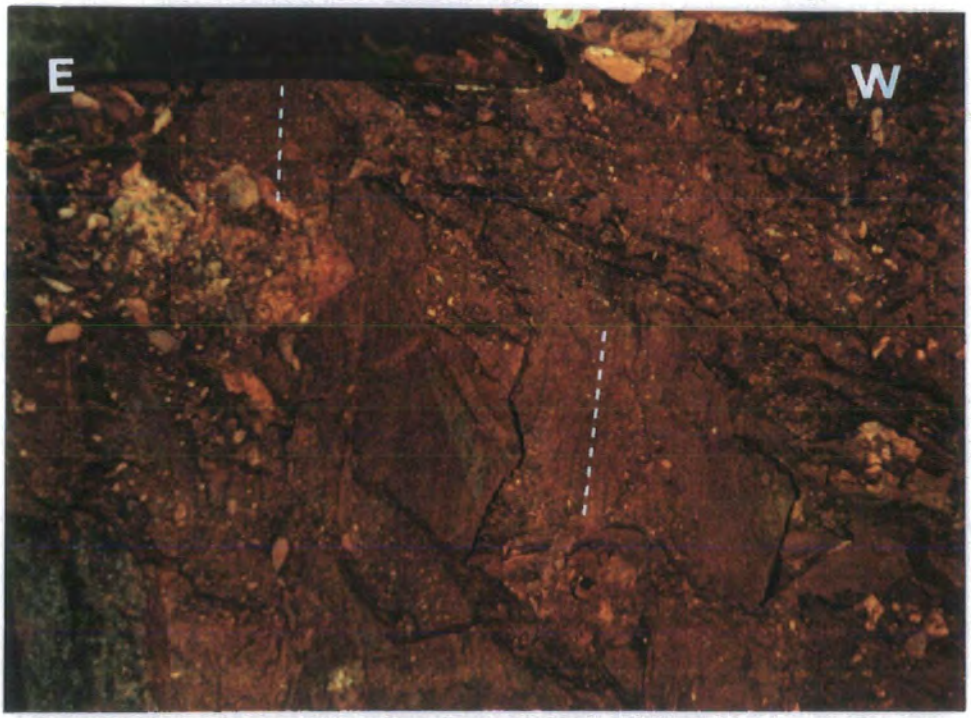

Photo 4.4.5- The mineral lineation printed on the slaty cleavage.

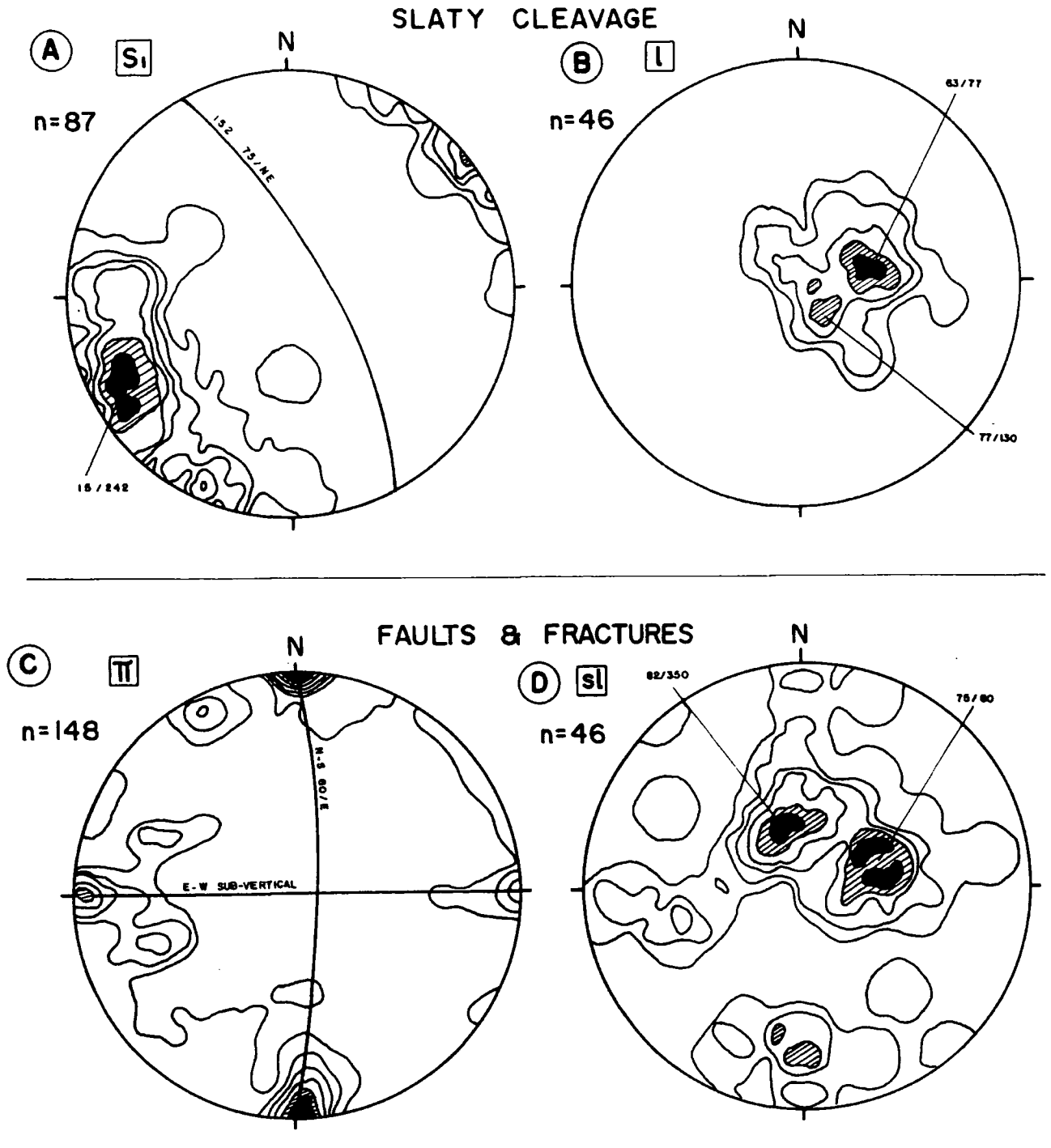

Fig.4.4.3- Equal area stereonets (low hemisphere) of poles to the main tectonic structures observed in the Bahia Mine. (A) S_1, slate cleavage contour diagram (11.5%, 12.5%, 13.5%,15%, 16%, 17%); (B) L, mineral lineation present on the slaty cleavage, contour diagram (2%, 5%, 8.7%, 13%, 17%, 19.5%); (C) p (fracture/ faults planes), contour diagram (1.3%,3%,5.5%, 7.5%, 9.5%, 11.5%, 13.5%, 15.5%, 17.5%, 19.5%). (D) sl (slickenlines fractures), contours of 2%, 4.5%, 6.5%, 8.7%, 11%, 13%, 15.2%.

c) Folds and crenulation cleavage: Folds are uncommon in the mine rocks, especially at outcrop-scales. In a few places the slaty cleavage is folded by centimetre- to metre-scale folds forming isolated chevron structures, with axial surfaces striking NNW-SSE and fold axes plunging nearly 30°-50° towards the ESE and/or WNW (Fig.4.4.2). These folds appear to be related to movements along nearby faults and fractures.

Another group of folds are represented by rare crenulations locally deforming the slaty cleavage. Fold axes plunge steeply NW and are associated with a discrete non-penetrative crenulation cleavage, spaced around 1cm striking N-S and dipping steeply.

d) Fractures and faults: Brittle deformation is widespread in the rocks of the Igarapé Bahia Mine and is focused into an extensive network of fractures and faults (Photo 4.4.6 and 4.4.7). Two main sets of fractures are apparent both in the fold and on a stereographic projection (Fig.4.4.3C). The polar maxima suggest sets of E-W and N-S striking fractures dipping steeply to sub-vertically. The distribution of these structures on maps shows that they are widespread in a mutual cross-cutting relationship, and that no isolated predominance or concentration of any particular set occurs (Fig.4.4.2). Fractures appear to be quasi-continuous features with no obvious terminations. The spacing between them can vary from ten metres to a few centimetres in the same rock type. Where more closely spaced (3-15cm), they can form an apparently disjunctive anastomosing foliation, which locally overprints and obscures earlier structures, and they may be ultimately responsible for the development of a brecciated texture recognized in several regions of the mine.

The displacements associated with the fractures in the mine are difficult to deduce in most cases due to a lack of markers, piercing points or shear-sense indicators. Slickenfibre lineations, striated stepped surfaces, and small sub-horizontal veins cut by fractures provide some information (Photo 4.5.6). Observed displacement magnitudes along fault planes are very rarely determinable and are mainly millimeter-scale to at most 30cm.

A total of 46 of slickenline orientations obtained from fault planes show a dispersed pattern, with two main concentrations plunging 82°/350° and 75°/080° (Fig.4.4.3D). These correspond, respectively to slickenlines associated mainly, but not exclusively, with N-S and E-W fault planes.

Photo 4.4.6- Small N-S striking reverse faults cutting small kaolinitic veins in the NW part of the E pit of the mine.

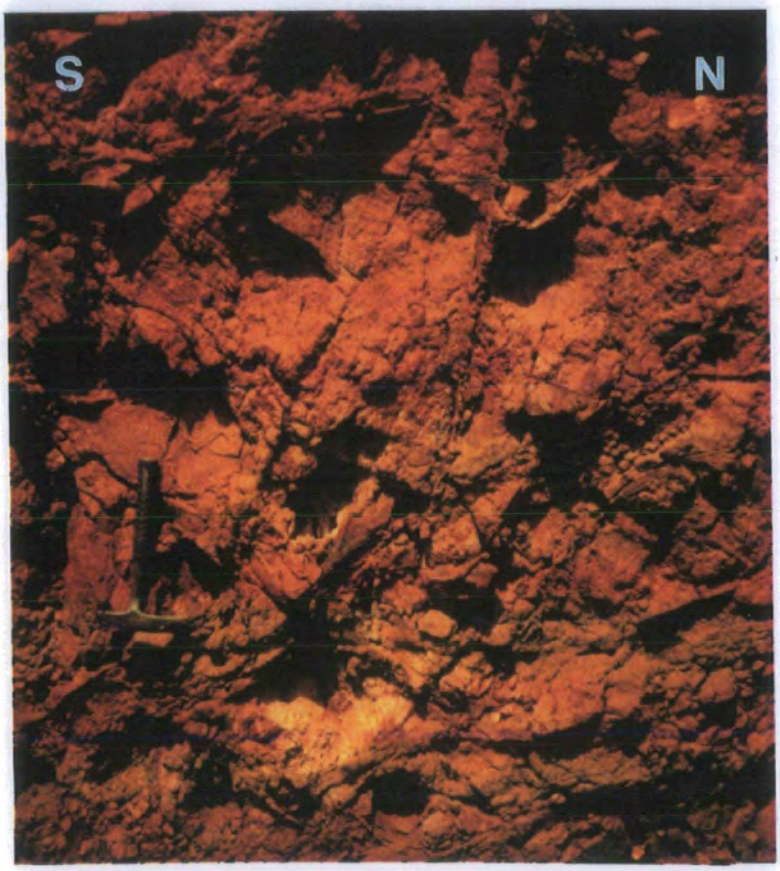

Photo 4.4.7- Continuous to quasi-continuous fractures centimetre-scale to metre-scale spacing typical of the Bahia Mine exposures.

Overprinting slickenlines, mainly striations, are common along several fractures.

4.4.4.2- WORKERS BASE-CAMP ROAD SECTION.

Rocks of the Igarapé Pojuca Group are exposed at several points along the small road linking the main road to a workers base-camp, about 1Km NE of the Igarapé Bahia Mine (Fig.4.4.1). The exposures occur along a 300m section, in 3-5m high road-cuts following a general NNE-SSW direction going up-hill (Fig.4.4.4).

a) Lithology and primary structures: Metavolcanic and metasedimentary rocks outcrop along the road section. They include pelites interbedded with very fine to coarse or microconglomeratic metasandstones, ironstones and basic metavolcanic rocks.

The pelites are red-coloured rocks formed mainly from clay minerals in layers 0.5-2m thick that are often strongly fractured and cut by millimetre-scale quartz veins. Where less weathered, they form grey to yellowish rocks with a smooth cleavage deformed by later crenulations and fractures. Metasandstones occur in metre-scale layers interbedded with pelites. They are rather variable in texture from very fine with a clay matrix to coarse or (ortho)microconglomeratic with millimetre-scale rounded to sub-rounded quartz pebbles. Kaolinite can be observed in the matrix of the microconglomerates. The bedding (So) in the metasediments is well preserved, in the more deformed units of pelites. Ironstones form a minor volume of rocks interbedded in these sequences and are typically dark grey (when less altered) forming apparently discontinuous 10-30cm thick layers. Some confusion may arise concerning the occurrence of the ironstones in this section, since several exposed rocks are Fe-rich due the intense active lateritization affecting the region.

Basic metavolcanic rocks are found in relatively thick layers, often deeply altered by weathering. They seem to lie concordantly with the metasedimentary rocks and are also cut by the penetrative cleavage associated with folding. The original mineralogy of these rocks has been completely destroyed by weathering so that plagioclase crystals are transformed to pseudomorphs of kaolinite. Igneous magnetite may be present but in most cases it is oxidised to more stable iron-bearing minerals. Acid

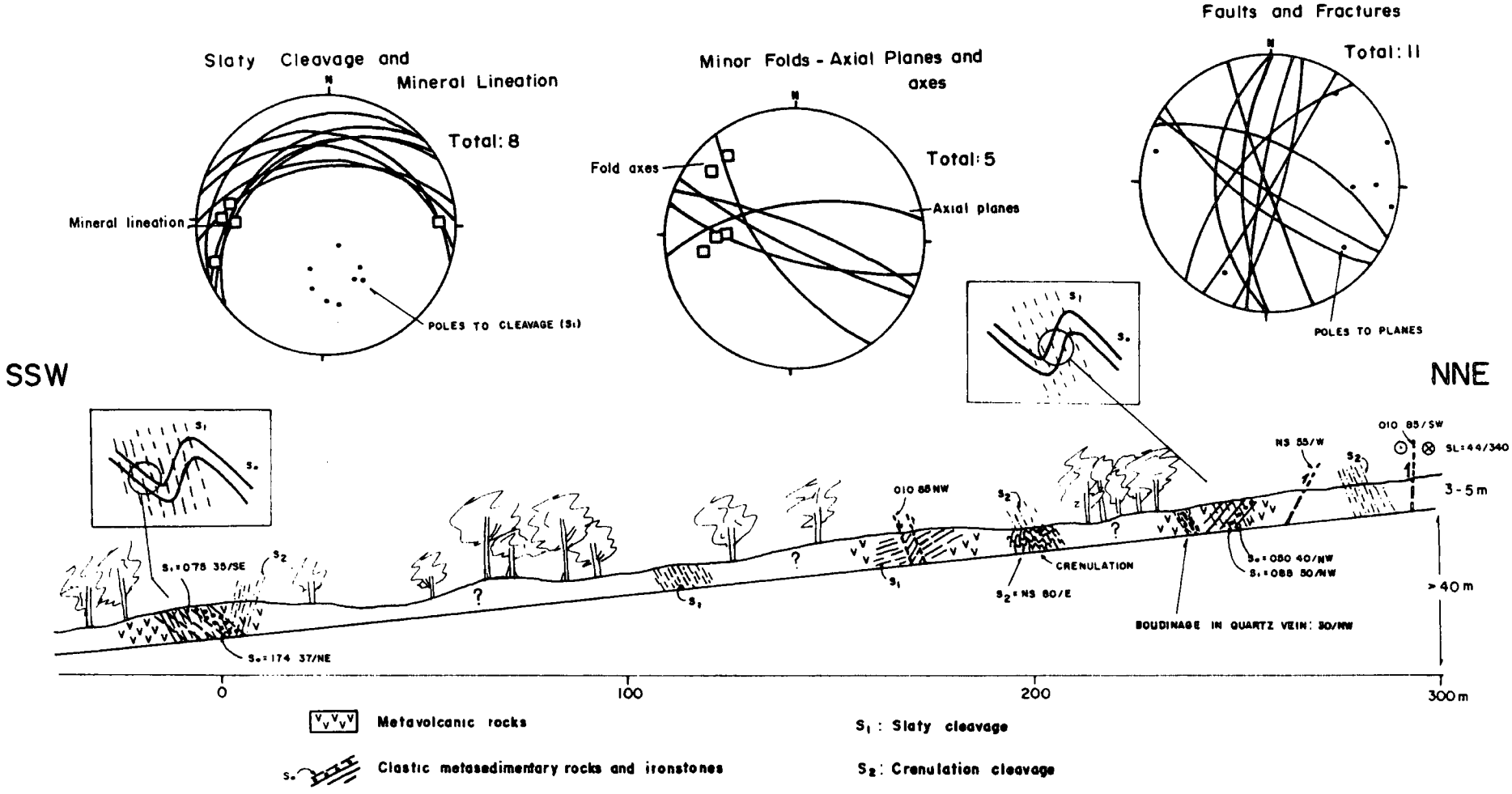

Fig.4.4.4- Sketch section along the Igarapé Bahia Mine - Workers base camp road (see Fig.4.4.1 to location). The scale of representation of structures are enlarged and do not correspond to the section scale. The stereonets show the distribution of the slaty cleavage and mineral lineation, axial planes and axes to minor folds and fractures (from left to right). The cleavage (S_1)-bedding relationships (boxes) suggest that a major synformal closure occurs in the centre of the section, but the exact location of this closure is unknown.

metavolcanics may be present in the section since a relatively high proportion of quartz crystals occurs in some altered volcanics.

b) The slaty cleavage (S_1) and mineral lineation: The most prominent tectonic structure present in the rocks exposed along the road section is a non-penetrative slaty cleavage (S_1) defined by a continuous foliation in the pelites and a weaker fabric in the volcanics and metasandstones (Fig.4.4.4). It displays predominantly E-W strikes, dipping from 30° to 70° N-NW. It cross-cuts the bedding in both clockwise and anticlockwise senses suggesting that a larger-scale synformal fold is present deforming So but there are insufficient exposures to locate the position of this structure. This fold appears to be overturned towards the SW (Fig.4.4.4).

A weak mineral lineation is occasionally present on the surface of the cleavage plunging shallowly W or E (Fig.4.4.4).

c) Folds and crenulation cleavage (S_2): Outcrop-scale folds are represented by kink bands and crenulations (Fig.4.4.4). Kink folds deform the slaty cleavage. They occur in zones up to 3m wide, bounded by reverse faults sub-parallel to the axial surfaces, striking N-S and dipping steeply W. The crenulation cleavage (S_2) also affects the slaty cleavage (S_1) and is not a penetrative structure and is predominantly symmetric (Photo 4.4.8). Associated small-scale folds vary in amplitude from a few millimetres to 2cm. The cleavage strikes mainly N-S, dipping steeply E.

d) Pinch-and-swell structures and boudins: These structures are found in isolated quartz veins conformable with the slaty cleavage (S_1) in the pelites (Fig.4.4.4). The *boudin line* plunging 30° N and boudinage is slightly asymmetric (Photo 4.4.9).

e) Fractures and Faults: The fractures present in the section are predominantly *shear fractures* but few shear-sense indicators are preserved. Most fractures trend N-S dipping steeply W but some are orientated NW-SE, dipping steeply NE or SW (Fig.4.4.4). In a few places, slickenlines are preserved on the fracture planes showing a reverse, oblique-sinistral displacement. Cataclastic features include localized breccias zones up to 1m wide, close to main fractures.

Photo 4.4.8- Symmetric crenulation folds and associated crenulation cleavage (S_2).

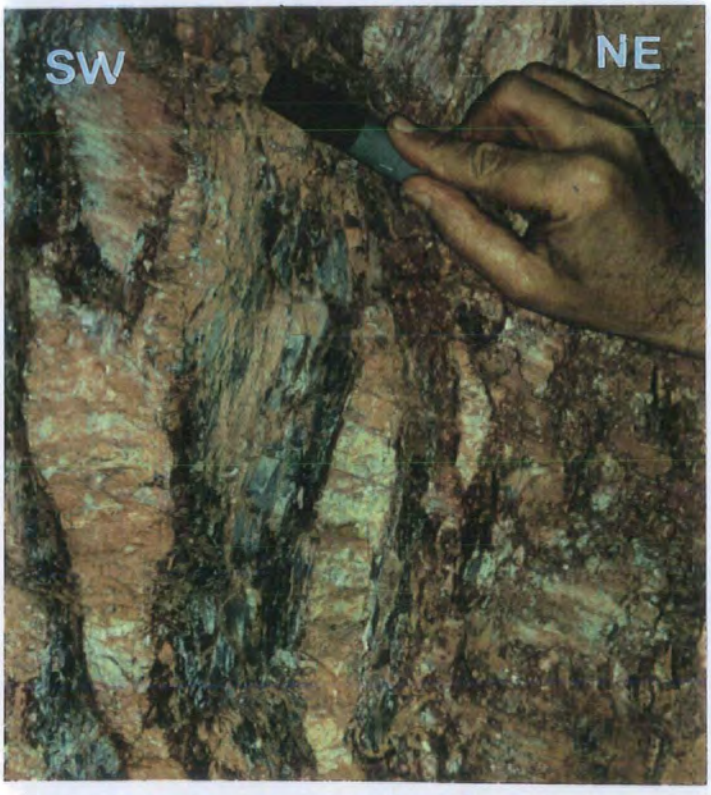

Photo 4.4.9- Asymmetric quartz vein boudin in the pelites of the Igarapé Bahia Mine / Workers base-camp section. This structure is cut locally by strike-slip faults that printed low plunging angle striations in the quartz (top left, parallel to the pen).

4.4.4.3- THE SEDIMENTARY ROCKS OF THE IGARAPÉ BAHIA MINE - CARAJÁS VILLAGE ROAD.

Clastic sedimentary rocks outcrop in several localities along the road from the Igarapé Bahia Mine to the Carajás Village (Fig.4.4.1). They are well exposed in road-cut sections running along the top of the plateau at altitudes between 550-600m.

The rocks in these exposures comprise a sequence of red to white, coarse to medium, moderately to poorly sorted sandstones showing angular to subangular grains, forming layers 1 to 2m thick, with thin (1-5cm) discontinuous horizons of mudstones. The bedding shows a dominant NW-SE strike, dipping shallowly (<20°) NE (Fig.4.4.5). Tabular and trough cross stratifications are the main primary structures present in these rocks together with the bedding (Photo 4.4.10). They may be small-scale (10cm) to large-scale (1m). Microconglomerates form layers <50cm thick associated with the sandstones exhibiting subangular to subrounded quartz pebbles in a grain-supported matrix. The apparent total thickness of the sequences in this section, is estimated as >500m.

Fractures in these rocks show a strong N-S direction dipping at high angles (sub-vertical) or, less abundant, NW-SE orientation (Fig.4.4.5). Joint zones with fractures spaced about 20-30cm and nonsystematic discontinuous joints are also common. Faults with significant displacements were not observed.

A set of cross-cutting dykes are common in these exposures. They are 4 to 7 metres wide, striking N-S and dipping steeply E (Fig.4.4.5). A secondary NW-SE set of dykes is also present. The rocks forming these dykes are fine to very fine, red-weathered basic rocks with frequent millimetre-scale quartz veins and a non-penetrative foliation developed close and parallel to their contacts with the host rocks. Feldspar crystals are completely transformed to kaolinite. The weathering is responsible for a strong zonation sub-parallel to their margins marked by different tones from whitish-yellow to dark-red, being less altered in their central part. Hydrothermal alteration affects these rocks intensely in places and gives them a typical gossan aspect, with a high proportion of Fe-rich minerals and box work ferruginous micro-veins.

Palaeocurrent directions were measured from cross stratifications in the sandstones and point to predominant azimuths toward SW.

Photo 4.4.10- Typical cross stratification in the sandstones outcropping along the Igarapé Bahia Mine - Carajás Village road (see Fig.4.4.1), representing fluvial deposits of the Águas Claras Formation.

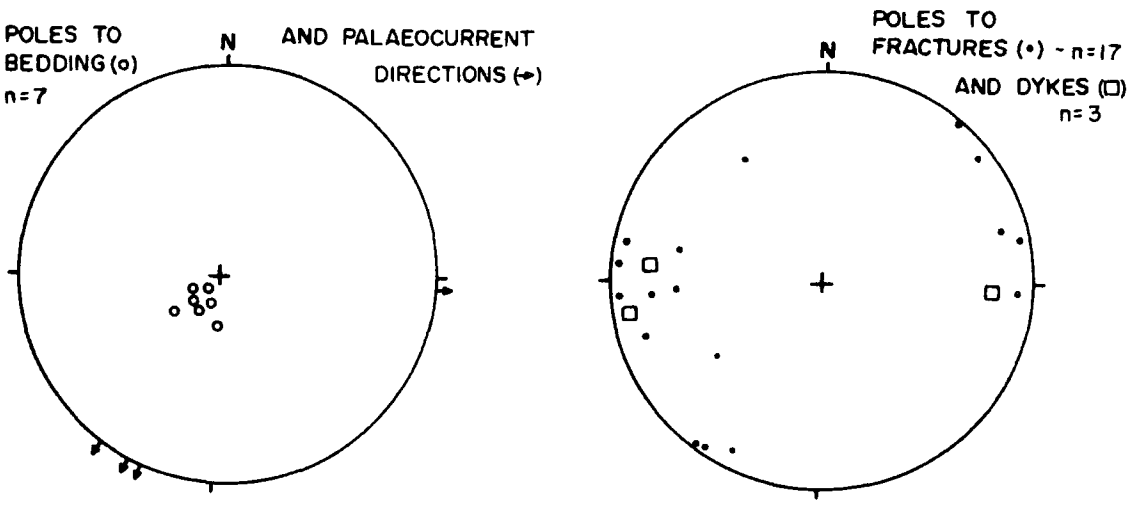

Fig.4.4.5- Stereonets showing poles to bedding, palaeocurrent directions, poles to fractures and poles to dykes observed along the Bahia Mine-Carajás Village road, about 12 Km to the Bahia Mine.

4.4.4.4- OTHER EXPOSURES IN THE REGION.

Outcrops were found in small cuts along the road linking the Igarapé Bahia Mine to the Igarapé Pojuca Camp (localities 1-4, Fig.4.4.1). The rocks in these few locations are poorly exposed since they are close to the soil profile.

At locality 1, intensely weathered, poorly sorted, medium-to-fine grained metasandstones are cut by a set of sub-vertical fractures striking 020 °. Pelites with a well developed slaty cleavage and a characteristic red colour occur at locality 3 (Fig.4.4.1). The cleavage strikes 140° dipping 30° NE. A mineral lineation is present on the cleavage surface, plunging 20°-30° NNE. Decimetre-scale horizons of black pelite, probably carbon-rich units, are present locally interbbeded within the pelites together with 30cm thick layers of E-W striking, sub-vertical fine metasandstones. On the cleavage in the black pelites there is a well developed mineral lineation defined by elongated (?)graphite crystals orientated sub-parallel to strike. Fractures at locality 3 (Fig.4.4.1) are high angle structures orientated preferentially NW-SE and E-W. A crenulation cleavage deforms the early slaty cleavage, striking E-W and dipping 60° S. Metavolcanic rocks occur in a large exposure at locality 2. They are deeply altered by weathering and kaolinite replaces crystals of

feldspar, together with other clay minerals. Metavolcanic units over 10m thick are present also at locality 2. All these rocks are compatible to those found in the Igarapé Bahia Mine.

4.4.5- DISCUSSION

The structure and lithology of the outcropping rocks in the region of the Igarapé Bahia mine fall into two contrasting groups: a presumably lower metavolcano-sedimentary sequence (>2000m thick), folded and metamorphosed to less than low greenschist facies, and an overlying. presumably unconformable clastic sequence of essentially undeformed sedimentary rocks. These rocks may be correlated with rocks of the Igarapé Pojuca Group (DOCEGEO, 1988) and the Águas Claras Formation (Nogueira *et al.*, 1995) respectively.

The penetrative slaty cleavage observed in the low-grade metamorphic rocks seems to correspond to the relatively dense set of short NW-SE and N-S lineaments forming lozenge-shape geometries on satellite images. In the sedimentary cover rocks of the Águas Claras Formation the bedding and dyke swarms follow these orientations also.

The changes in cleavage and bedding relationships observed in the rocks of the Igarapé Pojuca Group, point to the presence of large-scale folds of that may verge SW, with axes plunging with low angle toward the NNW or SE.

The SW-overturning cleavage and associated mineral lineations suggest an important reverse to reverse-sinistral sense of shear (Fig.4.4.6) coeval with low greenschist metamorphism and slaty cleavage formation.

The interpretation of the satellite and field data suggests that the NE-SW and the N-S set of lineaments correspond to sets of predominantly steep normal faults and basic dyke swarms (Fig.4.4.7). In smaller scale, these lineaments may also correspond locally to the crenulation cleavage present in the low angle metamorphic rocks of this area. The relationship between the N-S fault planes and slickenlines suggests that most of these faults had an oblique-slip normal displacement with an additional dextral component (Fig.4.4.7). The steep E-W faults appear to be oblique-slip structures with both dextral-normal and dextral-reverse or sinistral-reverse displacements according to field shear-sense indicators. They may be associated in part,

with movements along the Carajás Fault. The existence of overprinted sets of slickenlines indicates that reactivation has occurred locally.

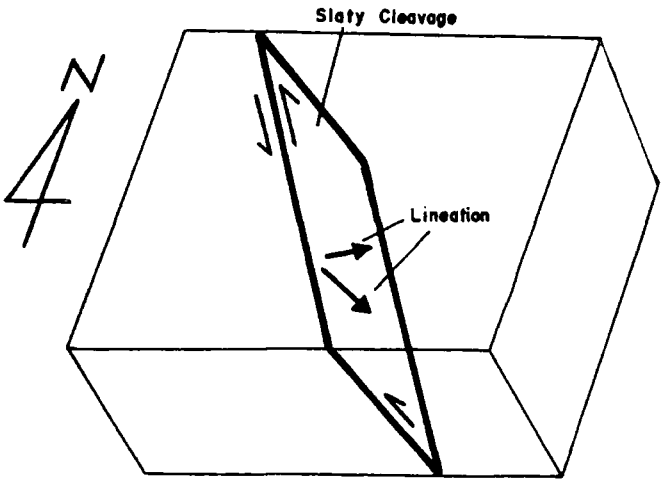

Fig.4.4.6- Diagram representing the geometric relation between the slaty cleavage and the mineral lineation. This arrangement denotes reverse to sinistral-reverse movements during the development of these features.

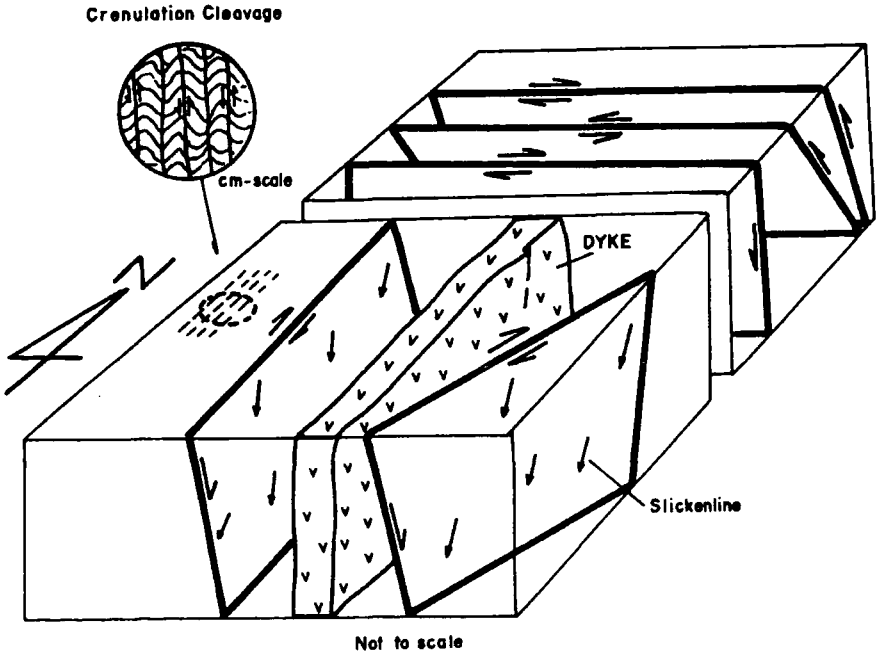

Fig.4.4.7- Sketch showing the orientation and kinematics of the main features observed in the Bahia Mine.

The metamorphism in the rocks of the Igarapé Pojuca Group is low greenschist (Ferreira Filho and Danni, 1985; Sachs *et al.*, 1992; Althoff *et al.*, 1994) but hydrothermal alteration is well recognized as being responsible for the mobilization and concentration of mineralized fluids (Ferreira Filho and Danni, 1985; Sachs *et al.*, 1992; Althoff *et al.*, 1994). The rocks of the Águas Claras Formation show no evidence of metamorphism (Nogueira, 1995; Nogueira *et al.*,1995), but its rocks were affected by hydrothermal alteration (Soares *et al.*,1994; Barros *et al.*,1994*a*), probably at the same time as the Igarapé Pojuca Group rocks. The greenschist facies metamorphic conditions are broadly consistent with the formation of slaty cleavages by a low temperature, fluid-assisted diffusive mass transfer (pressure solution) mechanism (e.g. Weber, 1981; Barker, 1989).

The sedimentary rocks of the Águas Claras Formation in this region, outcrop generally at altitudes above 500m. Cross stratification in the sandstones suggests palaeocurrent directions toward the SW. Nogueira *et al.* (1995) correlated these rocks with the Superior Member of the Águas Claras Formation, deposited in a tidal braided river system prograding to a delta with important tidal influence.

Dykes of basic rocks are found cutting both units. The age of these dykes is unknown, but is supposed to be Archaean to Late Proterozoic based on field observations. Younger dykes, probably Middle Proterozoic and Mesozoic are expected also to be found since there is widespread evidence to suggest extensional episodes of deformation affecting the region during these periods.

In conclusion the separation of the metavolcano-sedimentary rocks (Igarapé Pojuca Group) from the non-metamorphosed sedimentary rocks (Águas Claras Formation) is not as straightforward, as it may seem. Extensive alteration due to weathering and the earlier hydrothermal activities means that these rocks can appear similar in outcrop and hand-specimen. Probably the best and more reliable criterion to distinguish the Igarapé Pojuca Group is the presence of penetrative cleavages and mineral lineations, features entirely absent in the undeformed bedded rocks of the Águas Claras Formation. Folds in the Águas Claras formation, as described in section 4.1 in this thesis, are developed locally, close to the Carajás Fault trace, but there are no associated cleavages present.

4.4.6- CONCLUSIONS

1) Two distinct tectnostratigraphical units are present in the Igarapé Bahia region that are thought to be separated by a non-conformity. The lower unit corresponds to the Igarapé Pojuca Group represented by a low-greenschist volcano-sedimentary sequence. The upper unit is correlated with the clastic sedimentary rocks of the Águas Claras Formation.

2) The Igarapé Pojuca Group displays a strong planar fabric defined by a steeply dipping, NW-SE-trending penetrative slaty cleavage which transposes bedding and shows a steeply plunging mineral lineation. An overprinting lineation gives evidence of localized reactivation probably during reverse to reverse-sinistral displacements. The low-grade metamorphism is thought to be associated with cleavage development.

3) Fractures, faults and dyke swarms cut rocks of both the Igarapé Pojuca Group and the Águas Claras Formation. The N-S and NE-SW sets are predominantly normal faults with a secondary dextral-oblique component. The E-W set is related to normal-dextral, reverse-dextral or reverse-sinistral displacements and shows two sets of overprinting slickenlines. Dykes cutting both the units follow predominantly N-S and NE-SW directions. These structures produce strong lineaments on satellite images.

4) The kinematic complexity of the E-W fractures may relate directly to similar motions along the Carajás Fault.

5) Vertical displacements are controlled by normal faults which are responsible for the occurrence of the Igarapé Pojuca Group at almost the same topographic level as the Águas Claras Formation in this region. These faults also show important components of strike-slip displacement.

4.5- GEOLOGY ALONG THE ITACAIÚNAS RIVER

The Itacaiúnas River, a tributary of the Amazon River, flows NE, forming an important drainage of the Tocantins hydrographic basin. The Itacaiúnas River section exposes one of the most complete geological transverses in the region. It crosses the west end of the Carajás Strike-Slip System, exposing both basement and cover units and it traverses most of the important structural features of the region including the Carajás Fault.

A six-day trip by boat along the river was carried out as part of the present study. In order to maximise access to exposed rocks, it was necessary to make this journey during the dry season when water levels are lowest.

4.5.1- REGIONAL SETTING

In the river section between the Cinzento and the Carajás Strike-Slip System, the rocks of the Xingu Complex (Silva *et. al.,* 1974) are represented by tonalitic gneisses, granodiorites and granites showing very variable intensities of deformation. They have undergone amphibolite facies metamorphism, are locally migmatized and strongly mylonitized (DOCEGEO, 1988; Siqueira, 1990; Araújo and Maia, 1991). Later hydrothermal alteration is also reported to be widespread (Araújo and Maia, 1991). A kilometre-scale zone of lensoid granulites, correlated with the Pium Complex (Hirata *et al.*,1982; DOCEGEO, 1988), follows the strong E-W foliation in the granitic rocks. Syn-tectonic granitic plutons known as the Plaquê Suite (Araújo *et al.,* 1988; Araújo and Maia, 1991) are also present forming concordant, elongated bodies into the Xingu Complex rocks.

The rocks exposed inside the Carajás Structure, along the river section, comprise volcanic and sedimentary rocks of uncertain stratigraphy and structures. The basic volcanic rocks outcropping around both the north and south borders of the Carajás Structure have been correlated to the Grão Pará Group (Silva *et al.,* 1974; Hirata *et al.,* 1982; DOCEGEO, 1988). There are no specific descriptions of the volcanic rocks of the Itacaiúnas River, and only Hirata *et al.* (1982) mentioned metadiorites formed by actinolite, plagioclase and quartz, with ophitic texture preserved, as a common rock-type present along the Aquiri River, a tributary of the Itacaiúnas. Gabbros are mentioned as

exposed along the Pernambuco River, but they are not described as associated with the Grão Pará Group, and have an uncertain age.

The slates and metasedimentary rocks exposed along the Itacaiúnas River have been correlated with different stratigraphical units. They were considered initially to be part of the Grão Pará Group (e.g. Knup, 1971; Hutchinson, 1979) in association with the volcanics. Hirata *et al.* (1982) and Meireles *et al.* (1984) correlated them with the Rio Fresco Formation (Barbosa *et al.,* 1966), while DOCEGEO (1988) called them the "Rio Fresco Group" (Cunha *et al.,* 1984). Most recently, Araújo and Maia (1991) redefined the Grão Pará Group incorporating the rocks earlier associated with the Pojuca, Bahia, and Rio Fresco groups. According to Araújo and Maia (1991) the Grão Pará Group is subdivided into: (1) the oldest Parauapebas Formation (Meireles *et al.,* 1984) basic and acid metavolcanic rocks; (2) the Carajás Formation ironstones, and (3) the youngest Águas Claras Formation clastic metasedimentary rocks. According to these authors, the metabasic rocks present in the Itacaiúnas River section should be correlated with the Parauapebas Formation and the metasedimentary rocks with the Águas Claras Formation.

4.5.2- PREVIOUS WORK.

Very few previous studies refer to the geology along the Itacaiúnas River. The first comments were made by Barbosa *et al.* (1966) who referred to "Precambrian rocks" in the region. During the 1960s and 1970s, when the Carajás region started to attract geological attention, due the discovery of iron and manganese, several surveys were carried out along the main rivers by mining companies, but few data were published.

Liandrat (1972) published the first article specifically about the rocks of the Itacaiúnas and the Parauapebas rivers (the latter is the most important tributary of the Itacaiúnas River crossing the Carajás area about 50Km to the east). He mentioned the "Embasamento Cristalino" comprising Precambrian gneisses and granitoids with amphibolites and quartzites and also the "Serra dos Carajás Formation" including quartzites, ironstones, sericite-schists, slates and basic rocks. He also referred to steeply dipping beds in the central Carajás region and suggested that mylonitization of the basement rocks was responsible for significant retrogression of high grade assemblages.

In the 1980s mineral prospecting by DOCEGEO and CVRD led to the publication of several maps of the region (e.g. Hirata *et al.* 1982; DOCEGEO,

1988). These data were then discussed and interpreted in subsequent published papers.

Hirata *et al.* (1982) referred to the Xingu Complex as the basement rocks, formed by gneisses, granites and amphibolites, outcropping along the Itacaiúnas River and mentioned the presence of gabbros and diorites in the Pernambuco and Aquiri rivers respectively, thought to be part of the Grão Pará Group (arguably Proterozoic).

Araújo *et al.* (1988) and Araújo and Maia (1991) showed basically the same lithological distribution suggested by DOCEGEO (1988) but referred to the Carajás Structure as a "positive flower structure" controlled by sets of ductile shear zones.

4.5.3- DATA FROM SATELLITE IMAGING.

Photo 4.5.1 and Figs. 4.5.1 and 4.5.2 show the Itacaiúnas River cutting the west part of the Carajás Structure as viewed from LANDSAT satellite image.

An analysis of this area reveals a predominance of strongly curved and discontinuous E-W and WNW-ESE lineaments cut by sets of N-S and NNW-SSE lines. The longest and deepest of these lineaments corresponds to the Carajás Fault observed with an E-W direction following part of the north border of this major structure, inflecting gradually to WNW-ENE towards the central part of the Carajás Structure southeastwards. The lineaments produce a polygonal pattern if observed together.

The Itacaiúnas River traverses the Carajás Structure from south to north, being epigenetic drainage, following only partly the main E-W lineaments. It cuts three different zones with distinctive textures and patterns visible in the satellite image. The first zone, labelled I in Fig.4.5.1 is a light-grey, slightly rough area with darker arborescent spots that dominate the upstream region of the river. In contact to the N of this zone is a distinct short and long E-W curved zone marked by a coarse rough texture dominated by asymmetric northward concave relief features. This zone, labelled II in Fig.4.5.1, dissipates gradually westwards. Zone III is a dominant area in the central part of the Carajás Structure and may be distinguished by a dark-grey tone and very-coarse rough texture. This zone is in lateral contact, westwards, with a smooth medium-grey area, labelled IV in Fig.4.5.1. Zone V has a contrasting texture and colour area inside the zone III representing a striped texture defined by fine and continuous

Photo 4.5.1- Satellite image for the western part of the Carajas Strike-Slip System crrossed by the Itacaiunas River.

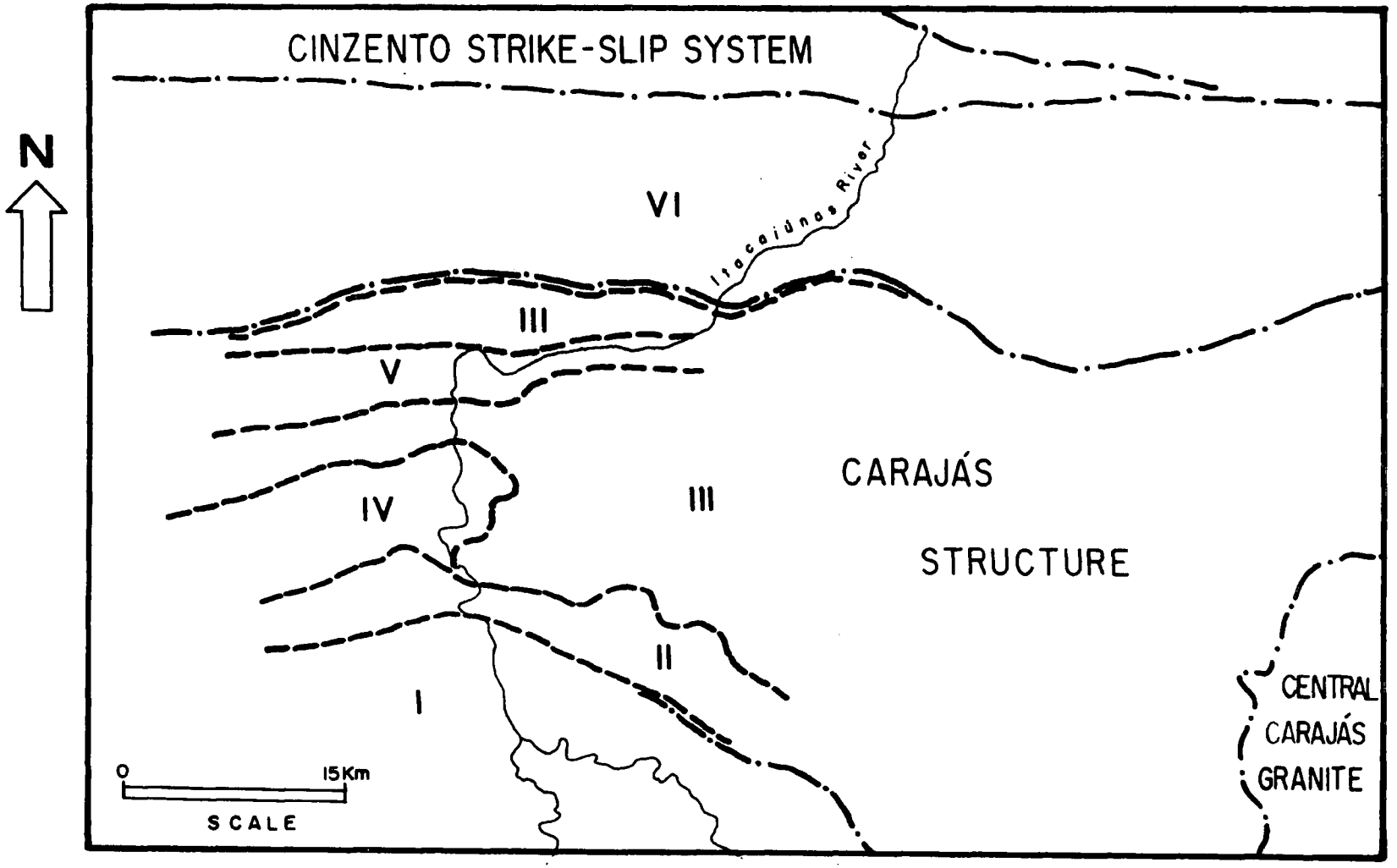

Fig.4.5.1- Interpretation of the different textural and tonal zones observed in the satellite image of the Itacaiúnas River region. See text for discussion and also compare with Photo 4.5.1.

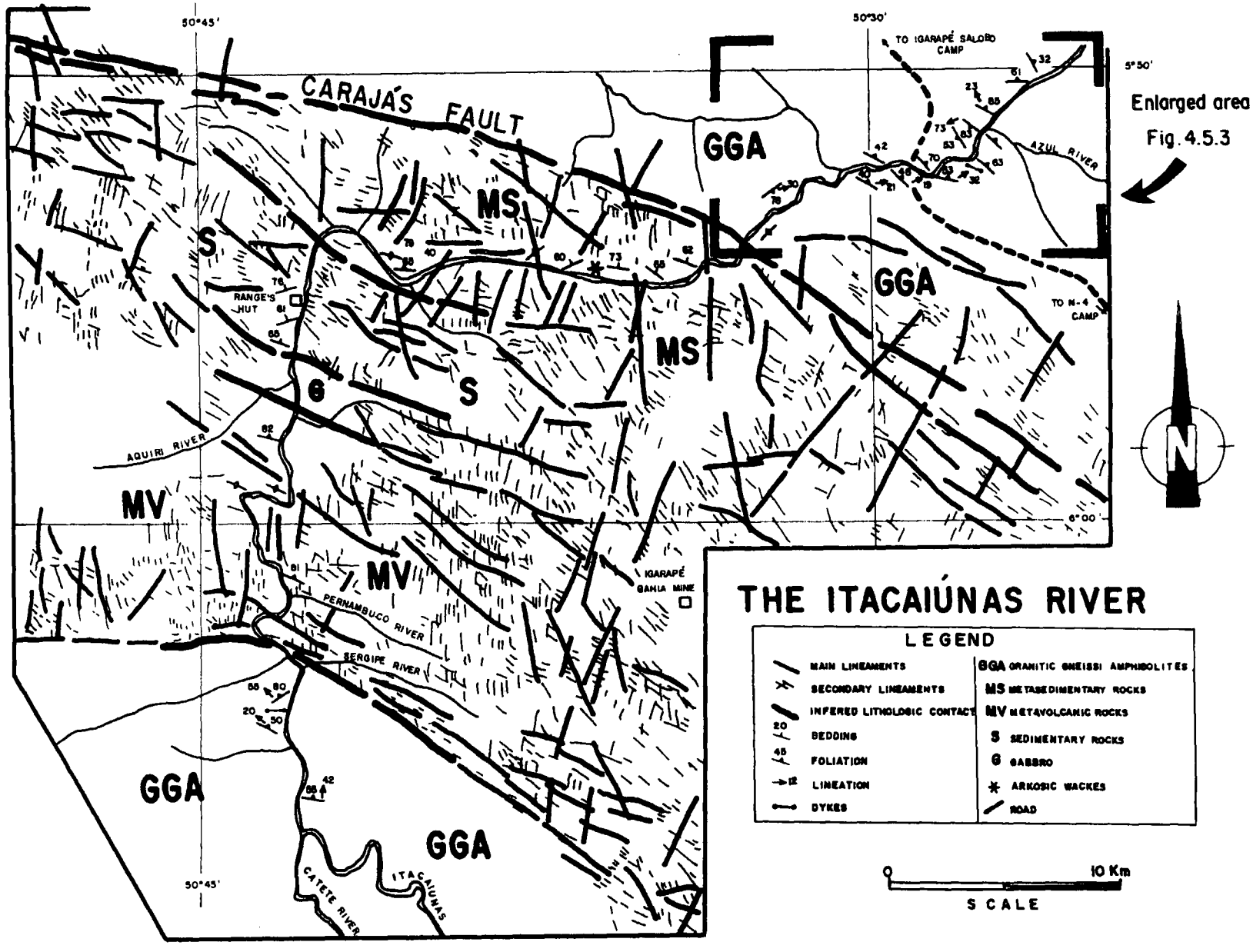

Fig.4.5.2- Map of lineaments in the western part of the Carajás Strike-Slip System from satellite image interpretation. Domains of different lithologies observed along the Itacaiúnas River are correlated to tectonostratigraphic units. The boxed area on the top right is shown in detail-scale on Fig.4.5.3.

curved lines, following the eastwards inflexion of the river close to the N border of the structure. The zone VI corresponds to a large area outside the northern part of the Carajás Structure marked by a fine craggy texture. This zone is in contact with the Cinzento Strike-Slip System towards the north.

4.5.4- FIELD OBSERVATIONS.

Six main types of rocks are exposed along the Itacaiúnas River, from about 3km downstream of the mouth of the Azul River to close to the Cateté River (Fig.4.5.2): (1) gneisses, granitoids and amphibolites (GGA); (2) metasedimentary rocks (MS); (3) metavolcanic rocks (MV); (4) sedimentary rocks (S); (5) gabbroic rocks (G) and (6) dykes and veins. These groups of rocks show particular petrological and structural features that allow correlation to distinctive stratigraphical units.

4.5.4.1 GRANITOIDS, GNEISSES AND AMPHIBOLITES (GGA)

a) Lithology: These are the best exposed rock types along the river. They occur both to the north and south of the Carajás Structure (Fig.4.5.2). *Granitic rocks* are predominant, including granodiorites, granites and tonalites. They are light-grey to yellowish if lightly weathered, and vary from a medium to fine granoblastic or hypidiomorphic-granular texture when less deformed (protomylonites); mylonitic to ultramylonitic types are also present. Banded or *gneissic rocks* including migmatites form a relatively small volume of material (<10%). The granitic rocks are essentially composed of plagioclase (mostly albite), quartz, biotite, microcline, biotite, hornblende and scarce muscovite, apatite and zircon, together with secondary minerals such as chlorite (after hornblende), epidote and calcite. Protomylonites and mylonites, concentrated in relatively large shear zones (>1Km wide), display the same mineralogy. The deformation in the mylonitic rocks is specially marked on the quartz grains when they show a xenoblastic texture, strong undulose extinction, polycrystalline aggregates, sub-grains and new grain growth and development of granoblastic-polygonal structures (Photo 4.5.2). Crystals of plagioclase may be deformed locally by distortion of the crystal lattice (Photo 4.5.3). Ultramylonites are characterized by ultra-fine grain size and lack of porphyroclasts due to complete dynamic recrystallisation (Photo 4.5.4). S-C fabrics are common in

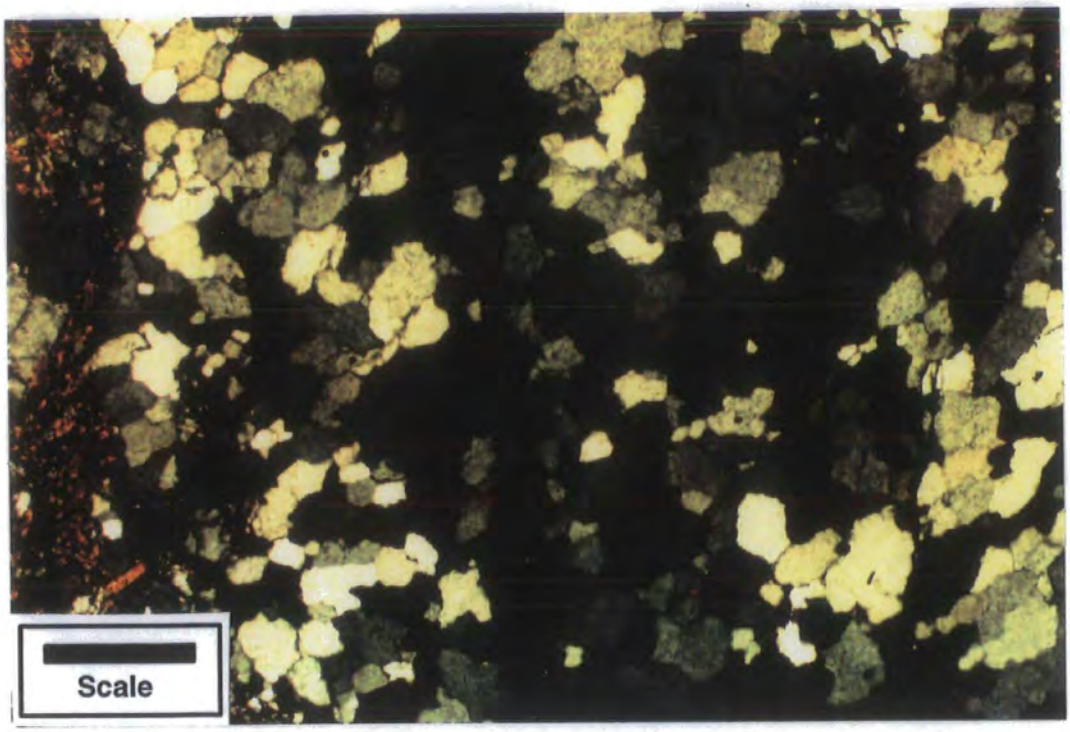

Photo 4.5.2- Granoblastic-polygonal aggregate of quartz in the granodiorites. Note the irregular to straight grain boundaries. Crystals with strong undulose extinction are also associated with these rocks (XPL). Scale bar= 1mm.

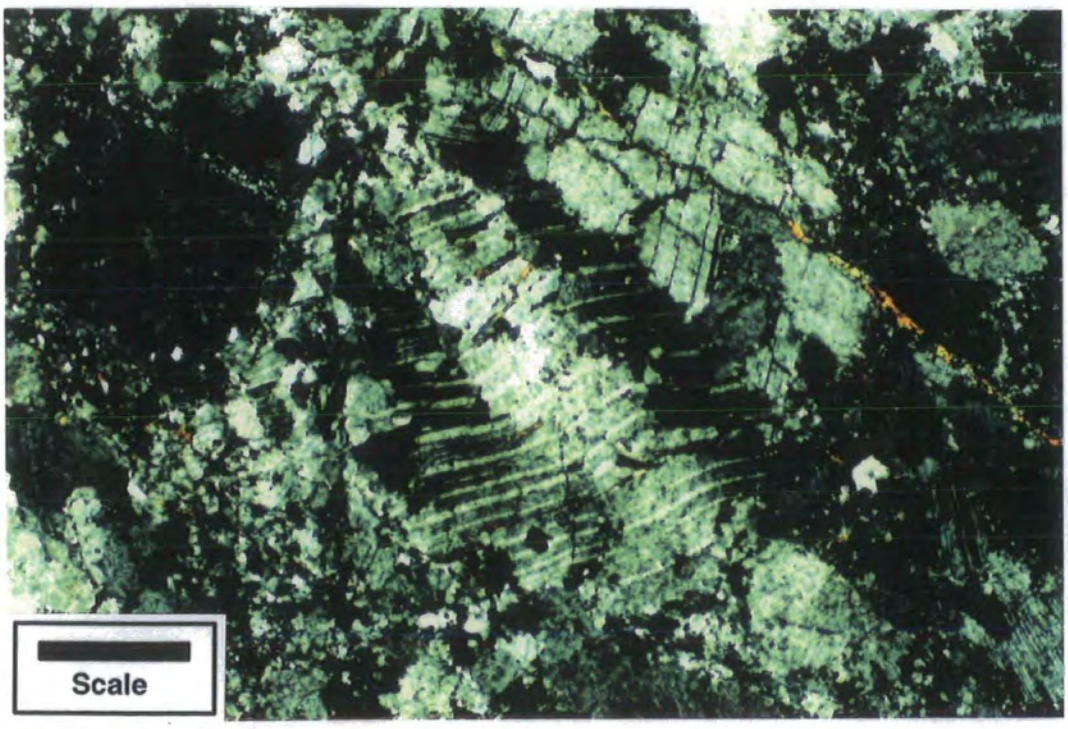

Photo 4.5.3- Kink in a plagioclase crystal observed in protomylonites from Zone 2. (XPL). Scale bar= 0.3mm.

both mylonites and ultramylonites and, together with σ-type porphyroclasts of plagioclase, consistently indicate sinistral senses of shear (Photo 4.5.5).

The metamorphism in these rocks has reached the amphibolite facies (quartz + plagioclase + biotite + hornblende + microcline). This is in agreement with several earlier studies carried out on in these rocks (Macambira *et al.*,1990; Araújo and Maia, 1991; Machado *et al.*,1991; Siqueira, 1990). According to Araújo and Maia (1991) the strong alteration observed in the biotite and hornblende to chlorite is an indication of retrogression diaphtoresis to greenschist grade.

Amphibolites are present in relatively small volume (<5%). Lensoid amphibolite bodies are a few metres to tens of metres wide mostly concordant (NW-SE) to the foliation in the host granitoids (Fig.4.5.3 and also Fig.4.5.5A). The contact with the granitoids may be marked by discrete oblique shear zones, as can be seen about 2km downstream from the mouth of the Azul River (Fig.4.5.2). These amphibolites are strongly foliated, dark-greenish to grey, formed essentially by hornblende (>70%) and plagioclase plus epidote, chlorite and opaques. These rocks are often exposed in weathered zones.

b) Structures: At outcrop a mylonitic foliation is defined by the preferred orientation of quartz, feldspars, amphibole and biotite. In weakly foliated rocks, the mafic minerals are the best field indicators of this structure. Under the microscope quartz forms single highly elongate grains (ribbon-quartz) or fine-grained recrystallized granoblastic-polygonal aggregates. The lineation is not as easy to identify in the field especially in weakly deformed granitoids or coarse grained rocks. In general, it is defined by elongation of quartz grains.

Five distinct zones each with different intensities of mylonitization and orientations of the foliation and lineation were observed in the gneisses outcropping along the section of the river which was studied (Fig.4.5.3). These zones suggest that a complex kinematic partitioning of deformation may affect a relatively large area of the basement.

Zone 1 covers the rocks outcropping from the northern limit of the Carajás structure to about the Cinzento River (Fig.4.5.3). The rocks along this area are medium to coarse granitoids showing a weak mylonitic foliation that strikes NE-SW, dipping with high angles (>75°) toward SE. Isolated examples of the stretching lineation plunge30° NE.

A few hundred metres downstream of the Cinzento River, the granitoids become gradually more deformed and the mylonitic foliation intensifies forming

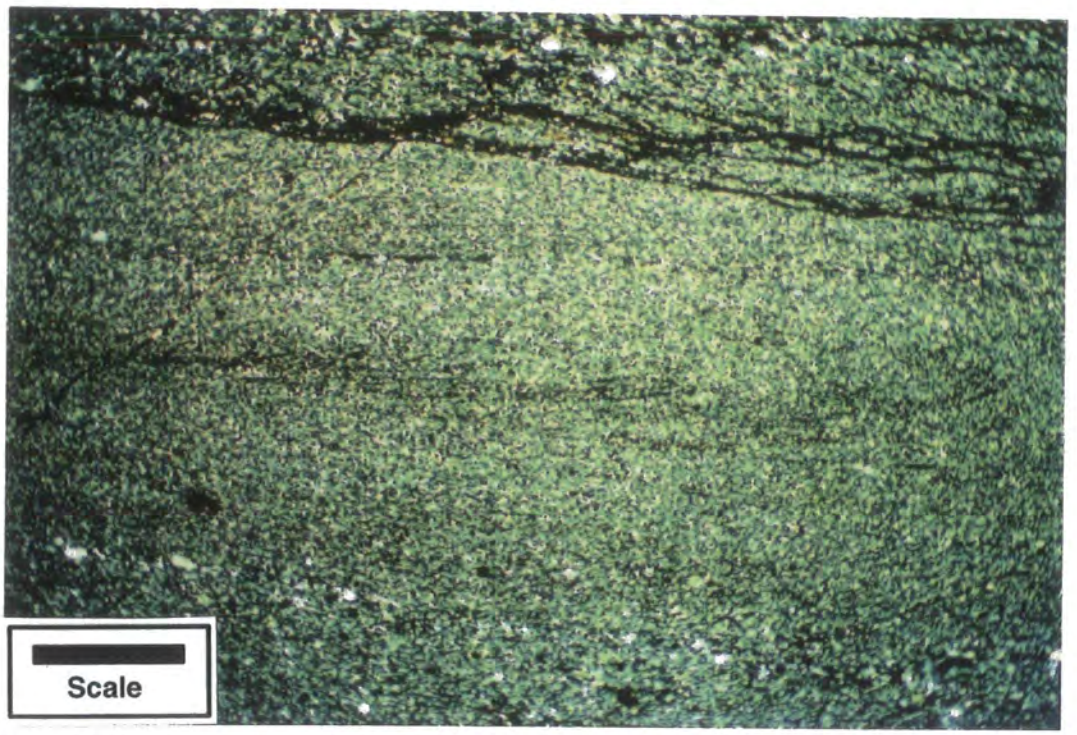

Photo 4.5.4- Typical ultramylonitic present in the Zone 4. The ultra-fine grain size is formed essentially by quartz and feldspar (XPL). Scale bar= 1.6mm.

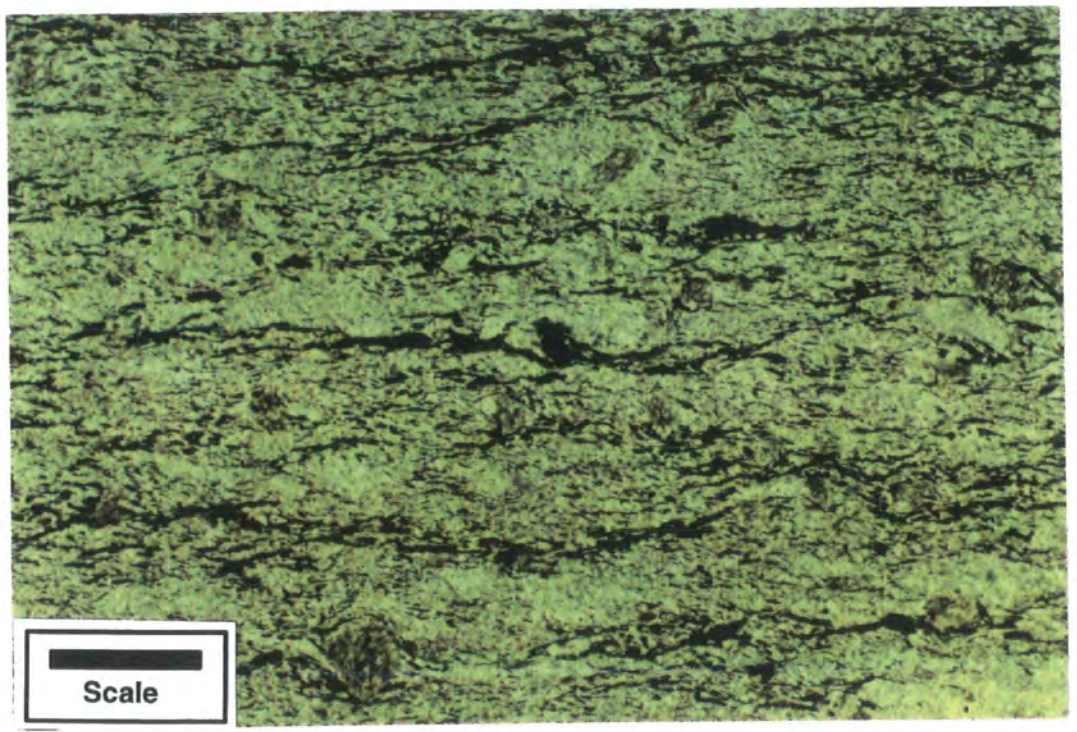

Photo 5.5.5- S-C fabric observed in association with ultramylonites from Zone 4. The small δ-type porphyroclasts of plagioclase, together with the S-C fabric suggest a sinistral kinematics associated with the shear zones on Zone 4 (PPL). Scale bar= 0.16mm.

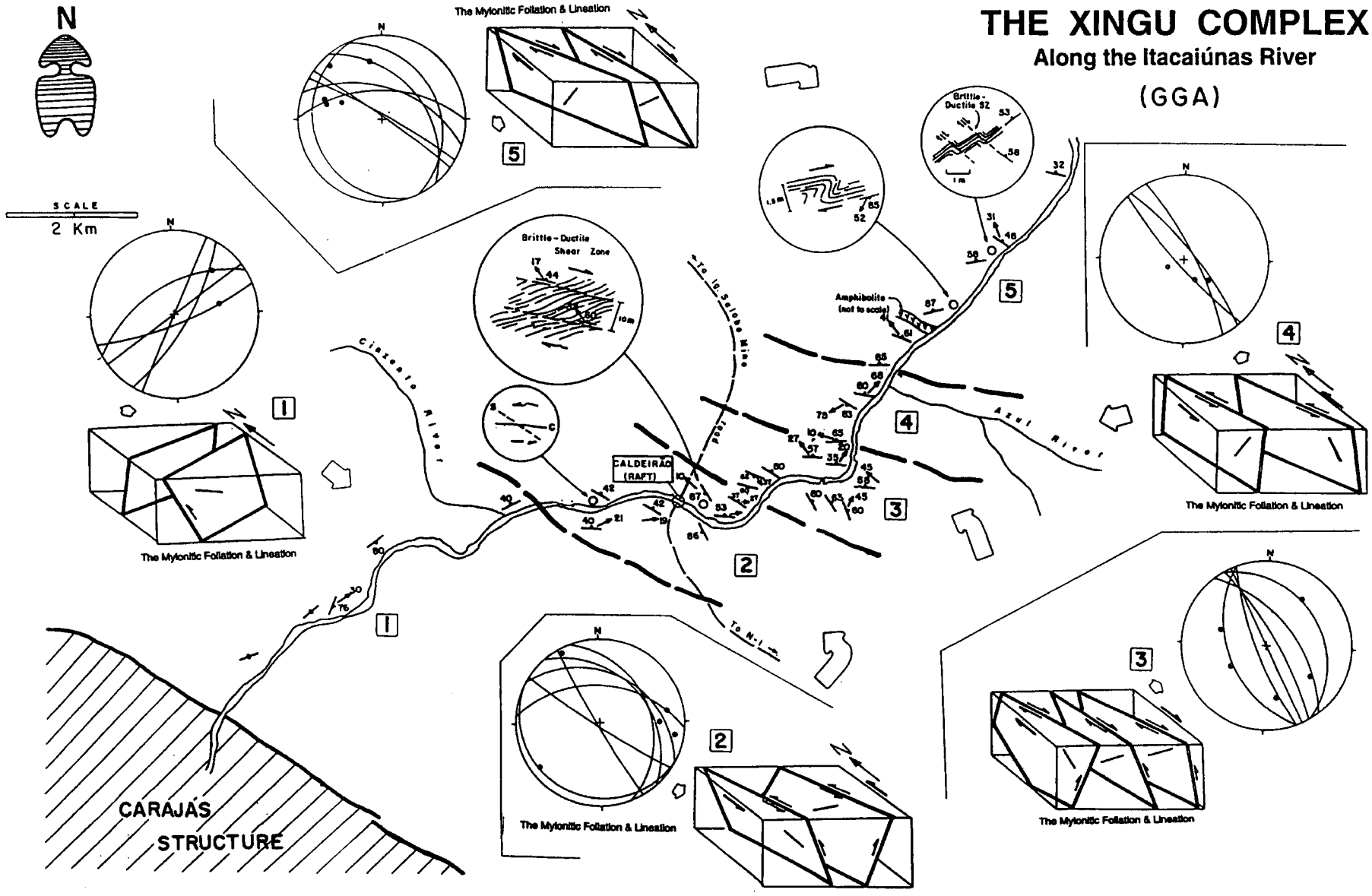

Fig. 4.5.3- Detailed map of the rocks outcropping on the NE border of the Carajás Structure, along the Itacaiúnas River. Five distinctive zones with different geometric and kinematic patterns were mapped (see text for further information).

Zone 2 (Fig.4.5.3). The mylonitic foliation swings clockwise into a NW-SE or N-S direction, dipping 40°-80° toward both NE and SW. The stretching lineation shows two slightly different orientations: in NE-dipping planes the lineation plunges at low angles (25°) towards the east, whist in planes dipping SW they plunge at low angles (ca. 10°) to the NNW. A discrete S-fabric may be found orientated clockwise to the main foliation (C), suggesting a sinistral sense of movement together with a component of reverse motion.

In *Zone 3*, the mylonitic foliation is still striking NW-SE, dipping between 50° to 80° toward NE and SW (Fig.4.5.3). The stretching lineation plunges 20°-40° towards both the west and SE. This zone is dominated by high strain ductile rocks developed along shear zones with a dextral-reverse sense of motion. The main shear-sense indicators are asymmetric folds and S-C fabrics.

Zone 4 extends a few hundred metres downstream of the mouth of the Azul River (Fig.4.5.3). In this zone, high strain granitoids and ultramylonites (Photo 4.5.4) are found in discrete shear zones <200m across. The mylonitic foliation is still orientated NW-SE, but dips >80° toward NE or SW. The stretching lineation is plunging around 60°-70° SE defining oblique shear zones with both reverse and sinistral components of movement.

In *Zone 5* (Fig.4.5.3), the rocks become gradually less deformed. The weak foliation strikes NW-SE, dipping 60°-30° NE. The weak stretching lineation plunges 30°-40° NW and, together with a few kinematic indicators (e.g. asymmetric folds observed about 2Km downstream from the mouth of the Azul River; Fig.4.5.3) suggest a dextral-reverse sense of shear.

Further outcrops of very similar basement rocks occur in the southern part of the Itacaiúnas River section, between the Cateté River and the Carajás Structure (Fig.4.5.2). Here the mylonitic foliation displays at least two main strike directions: NE-SW and NW-SE. The stretching lineation plunges variably (20° to 80°) NW.

Collectively the mylonitic foliation in the granitoid gneisses, outcropping along the Itacaiúnas River, shows a relatively scattered distribution with significant concentration around the orientation of 134° 37°/NE (Fig.4.5.4a). Stretching lineations (Fig.4.5.4b) are very variable in orientation with two diffused concentrations which are centred around the east and west quadrants respectively, plunging variably (Fig.4.5.4b).

Two main sets of brittle-ductile shear zones are observed cutting the granitoids and amphibolites of the basement. They offset the mylonitic foliation, quartz veins and leucocratic segregation veins (Photo 4.5.6). The more common set of shear-zones trends NW-SE displaying dextral displacements

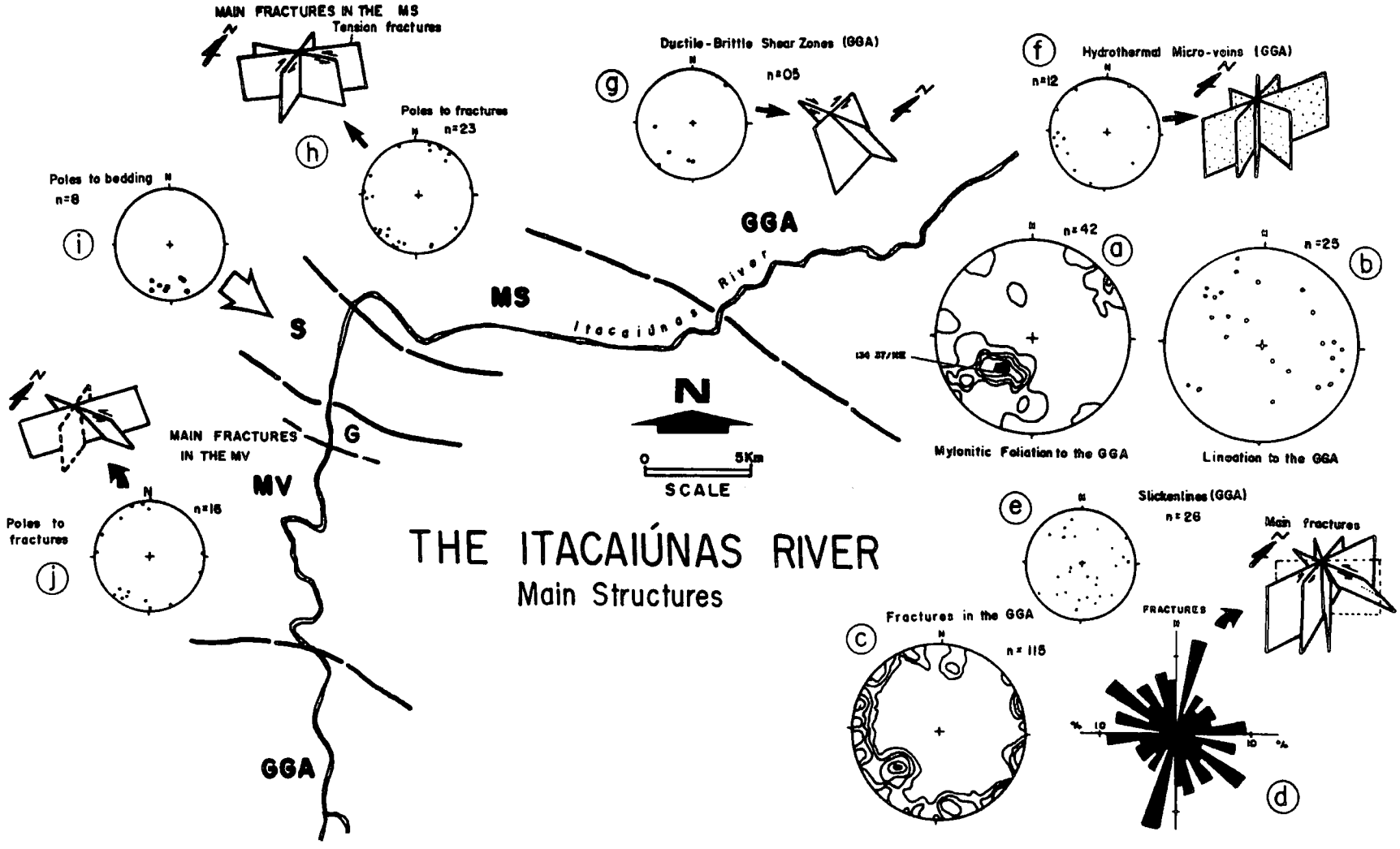

Fig. 4.5.4- Structural data of the main tectonic features observed on the different zones mapped along the Itacaiúnas River. GGA (Granite-Gneiss-Amphibolite): a) Stereonet to 42 bearings of mylonitic foliation (contours: 7%, 12%, 17%, 20%, 22%, 24%); b) Stereonet to 25 stretching lineations observed in association to the mylonitic foliation; c) Contours distribution to 115 poles to fractures planes (contours: 4%, 5%, 7%, 9%, and 10%); d) Rose diagram representing directions of the observed fractures; e) Stereonet to 26 bearings of slickenlines observed in the fracture surfaces; f) Distribution of hydrothermal micro-veins on a stereonet; g) Stereonet showing the orientation of brittle-ductile shear zones observed in the rocks of the GGA. h) Fracture observed in the metasedimentary (MS) rocks of the section. i) Bedding to the sandstones (S). j) Fractures observed in the metavolcanic (MV) rocks. Slickenlines in the fractures of the MS and MV plunges 30 40/E. h).

(Fig.4.5.4g). Generally they form multiple sets separated by >5m and most show apparent displacements of around a few centimetres. A mineral slickenline lineation, observed on the shear plane, plunges obliquely at low angles (<20°). This suggests an important strike-slip component of displacement. When these shear zones cut the mylonitic foliation at high angles they can form metre-scale chevron folds as can be seen on the left river margin, about 3.5 km downstream from the mouth of the Azul River. A second important set of brittle-ductile shear zones trends N-S to NNE-SSW with predominantly dextral displacement of around 10-20 cm. These occur mainly in the region between the Cateté River and the Carajás Structure.

The rocks of the basement are intensively cut by several sets of brittle structures (Fig.4.5.4d). The most obvious set trend NNE-SSW and NW-SE dipping 60°-90° NE (Fig.4.5.4c and d). A few display slickenlines (Fig.4.5.4e) consistent with both sinistral and dextral oblique displacements. A more accurate kinematics study is not possible since few outcrops expose fracture surfaces for direct study.

Another important set of fractures trends in a NNE/NE direction (Fig.4.5.4c and d) and where slickenlines found are preserved in the fracture surfaces, an oblique-dextral or -sinistral displacement is suggested.

Less than 10% of the fractures observed in the field are filled with hydrothermal veins (Fig.4.5.4f), quartz, leucosome or dykes. These are discussed below.

4.5.4.2- METASEDIMENTARY (MS).

a) Lithology: *Metasedimentary* rocks are present in almost all the area inside the Carajás Structure (labelled MS in the Fig.4.5.2), between the mouth of the Sergipe River and about 5km upstream at Caldeirão (the place where the river crosses the road linking the Igarapé Pojuca Camp to the N-1 Plateau; Fig.4.5.2).

They are represented by quartzites, metasandstones and slates forming beds 1-2m thick, orientated NW-SE, dipping steeply NE, (Photo 4.5.7). The quartzites are relatively pure, white to yellow rocks varying from fine, well sorted to medium or poorly sorted sediments. Darker coloured metasandstones are interbedded with quartzites comprising quartz (>90%), actinolite, muscovite, sericite and clay mineral matrix (Photo 4.5.8). Quartz grains in these rocks are sub-rounded to sub-angular and in many places are overprinted by a millimetre

Photo 4.4.6- NW-SE sinistral brittle-ductile shear zone developed in a granitoid of the Xingu Complex displacing leucocratic veins.

Photo 4.5.7- Layers of quartzites, NW-SE oriented, dipping around 60/NE. These rocks are supposed to be part of the Igarapé Pojuca Group.

spaced rough foliation of tectonic origin. Interbedded *slates* are red coloured, very poorly exposed and heavily altered by weathering. A slaty cleavage is the main structure present in these rocks lying at low angles to bedding. Exposures of these rocks display strong ferruginous weathering that may give them the appearance of foliated ironstones.

b) Structures: The *foliation* is best developed in the slates and fine grained quartzites. In the slates, it is a continuous fine cleavage defined by the alignment of sericite and quartz grains. In the quartzites, this structure is represented by an anastomosing to rough disjunctive foliation defined by a weak to strong orientation of elongated quartz crystals. When observed in the metavolcanics this structure forms a weak rough disjunctive foliation, defined by a diffuse alignment of plagioclase. Foliations strike NW-SE to NE-SW, dipping at high angles to sub-vertical. A *lineation* is developed locally in the slates but is poorly preserved due to weathering alteration. In the few places where it was observed it plunges moderately NE.

No large-scale *folds* were found associated with the slaty cleavage based on cleavage-bedding relationships. Later small-scale folds are locally preserved deforming the cleavage in the slates. They are typically kink and chevron folds on the scale of <1m. Axial surfaces strike around 120° dipping 050° /NE and fold hinges plunge about 40° W. Another 10 cm scale set of folds is observed also deforming the slaty cleavage in the slates. They are symmetric, close to tight folds with axial surfaces orientated 105°, dipping 58° NE, and axis plunging around 40° towards 100°.

Fractures are relatively common and most strike NW-SE dipping with high angles NE or SW (Fig.4.5.4h). They have a predominant sinistral movement. N-S fractures are also present, dipping with high angles towards the east, with dextral kinematics (Fig. 4.5.4h).

4.5.4.3- METAVOLCANIC ROCKS (MV).

a)Lithology: *Metavolcanics* are represented by a relatively large volume of rocks that are well exposed between the mouth of the Aquiri and Sergipe rivers (labelled MV in the Fig.4.5.2). They are represented by basic rocks, mostly basalts and dolerites, forming sills and flows (Photo 4.5.9). They comprise mainly plagioclase and hornblende with an ophitic to subophitic texture. Millimetre-scale (<0.5mm) vesicles and amygdales are often found in the

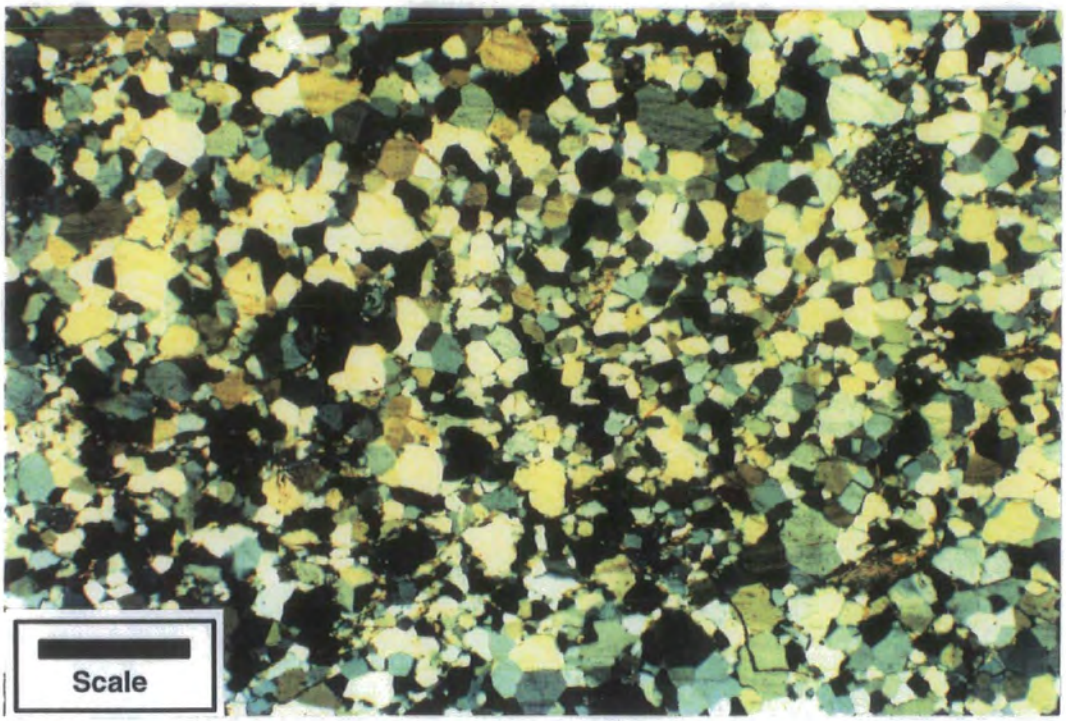

Photo 4.5.8- When observed in thin-section, the quartzites of the Igarapé Pojuca Group show a polygonal texture. A weak spaced rough foliation can be observed (XPL). Scale bar= 0.8mm.

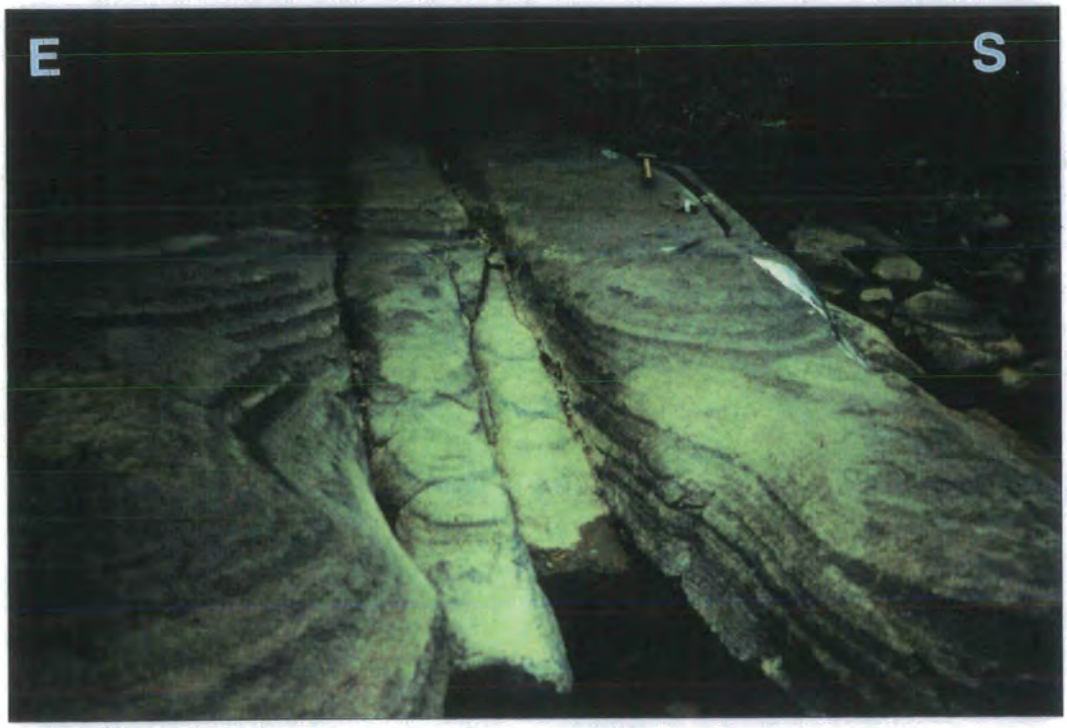

Photo 4.5.9- Massif outcrop of basalts correlated to the Grão Pará Group rocks.

outcropping rocks and allow possible sill and flow margins to be defined. There is a weak to very weak tectonic foliation in these rocks. The metamorphism in these basalts is supposed to be low greenschist grade according to several authors (e.g. DOCEGEO, 1988), but due to the small number of samples studied and the intense alteration of these rocks during weathering it was not possible to describe here any characteristic mineral paragenesis.

b) Structures: A non-penetrative *foliation* is present in most of the volcanic rocks observed along the river. This foliation corresponds to a spaced disjunctive rough foliation defined by few orientated hornblende crystals. This foliation is more evident in rocks with fine texture, but it may be absent in several places.

A relatively large number of *fractures* are found associated with these rocks. Main sets vary from NE-SW and NW-SW. N-S fractures have mostly dextral displacements while those in the NE-SW quadrant are mostly tension fractures (Figs.4.5.4j). The NE-SW set is parallel to a set of quartz veins cutting these rocks. Slickenlines are very scarce along the fracture planes but the few observed suggesting oblique slip displacements along these structures.

4.5.4.4- SEDIMENTARY ROCKS (S).

a) Lithology; A 5km strip of sedimentary rocks outcrops along the Itacaiúnas River (labelled S in the Fig.4.5.2). Exposures occur 2.5 Km both north and south from the Ranger's Hut ("Posto Avançado Itacaiúnas"). Rocks in this area are predominantly bedded *sandstones* arranged in 0.5-1 m layers (Photo 4.5.10). The sandstones are *quartz arenites* and comprise quartz (95%), sericite, muscovite and kaolinite. They are medium to coarse grained, with subrounded to rounded, moderately-sorted quartz grains.

Loose blocks of a distinctive purplish grey sandstone are common in the region where the river runs E-W inside the Carajás Structure (labelled with "*" Fig.4.5.2). This rock is a coarse to medium, less commonly microconglomeratic, poorly-sorted sediment, with angular to sub-rounded grains. It comprises quartz (35%), feldspar (30%), rock fragments (<5%) and a very fine matrix with clay-minerals and quartz (<20%; Photo 4.5.11). Kaolinite is most often associated with feldspar alteration and sometimes can represent >40% of the rock. It is an *arkosic wacke* according to the classification schemes of Dott (1964) and Pettijohn *et al.* (1972).

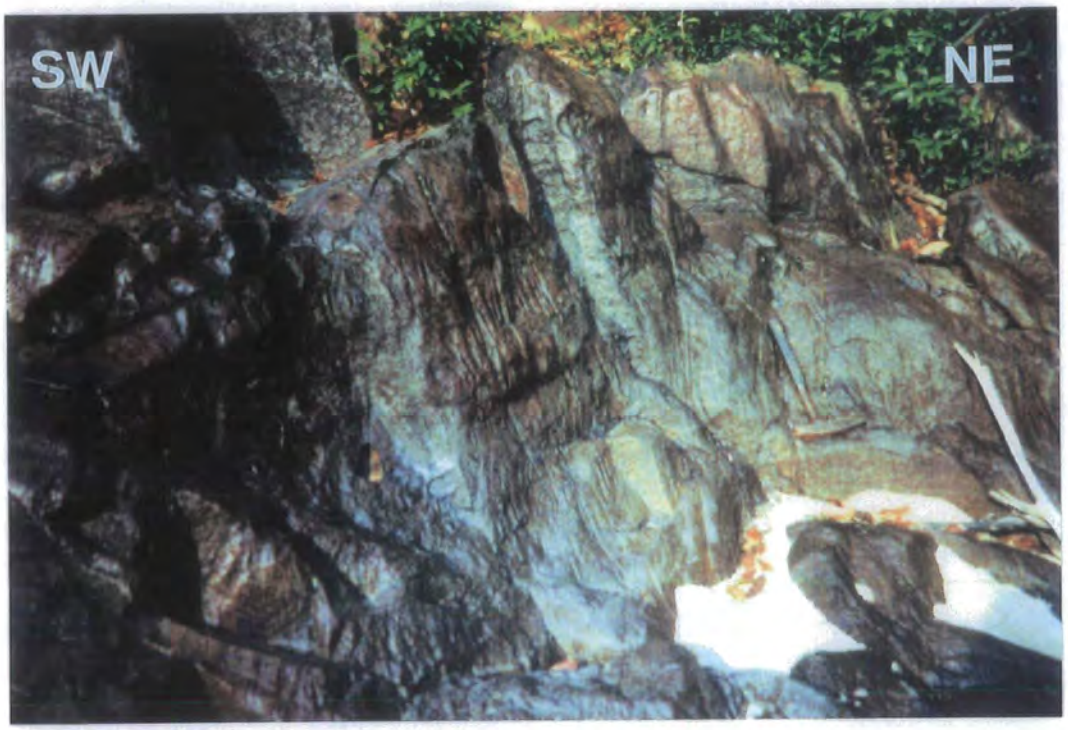

Photo 4.5.10- The sandstones of the Águas Claras Formation outcropping in the Itacaiúnas River. Note the high dip angles of the bedding.

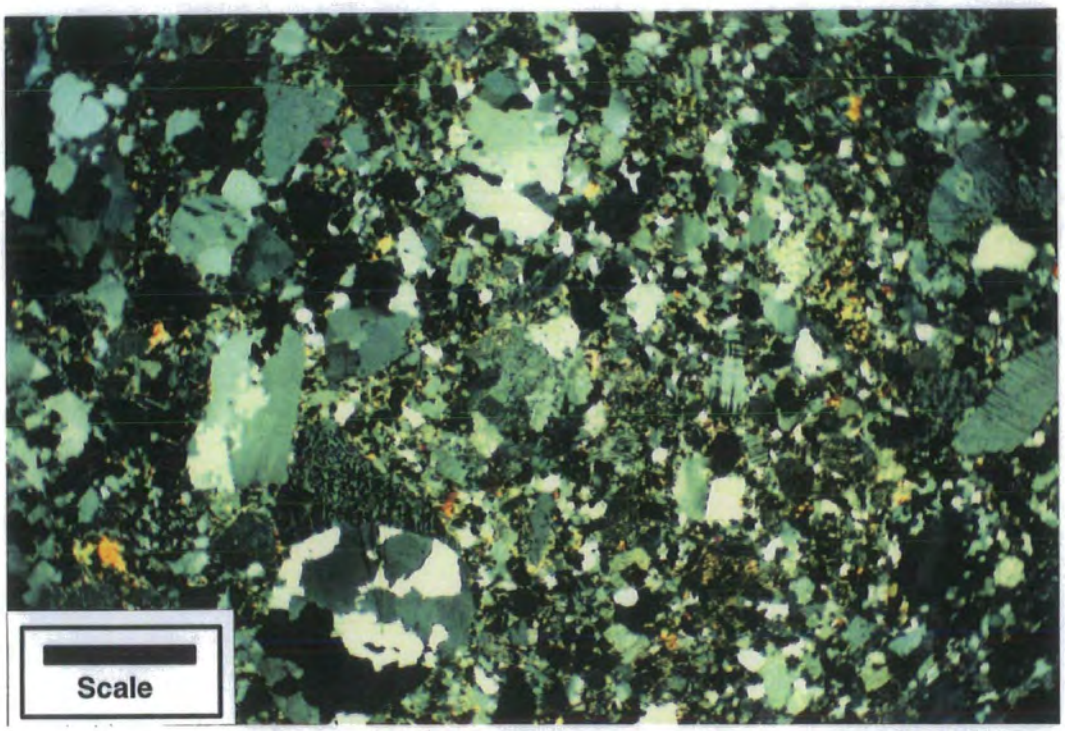

Photo 4.5.11- Arkosic wacke found in lose blocks spread over the Igarapé Pojuca Group rocks. This immature rock is supposed to be part of the Gorotire Formation (Mid-Early Proterozoic). XPL. Scale bar= 1.8mm.

b) Structures: Both trough and tabular metre-scale *cross-bedding* are common primary structures in the quartz arenites. The transport direction indicated by the trough cross-bedding appears to be towards the SE according to examples preserved in three localities. The bedding is systematically orientated WNW-ESE, dipping around 65°-80° towards the north (Fig.4.5.4i). These rocks are locally cut by steeply-dipping N-S and NW-SE fractures. They are otherwise undeformed and are unaffected by regional metamorphism.

Planar cross-beds are the only sedimentary structure observed in the arkosic wackes. The stratigraphical relationship of these sandstones to the adjacent slates and metasedimentary rocks is unclear since it does not outcrop in situ.

4.5.4.5- GABBROS (G).

Gabbroic rocks are found in association with the metavolcanics, outcropping as a large body (>1km) adjacent to the mouth of the Aquiri River (labelled G in the Fig.4.5.2). They are coarse-grained, grey to dark-grey rocks (colour index M>50%) with a well developed hypidiomorphic or subheuhedral granular fabric composed of plagioclase (andesine) hornblende and perthite intergrowths (Photo 4.5.12). These rocks show no evidence of having undergone metamorphism or deformation.

This rock is exposed in massive outcrops and only few fractures NW-SE and N-S were observed. These fractures are sometimes concentrated in 20m wide zones.

4.5.4.6- DYKES AND VEINS.

Dykes of unmetamorphosed basic rocks of uncertain age are intruded concordant or discordant to the fabrics of the granitoids (Fig.4.5.5B and 4.5.5C). They are 30 cm to metre-scale wide (<3m) and are sub-vertical or steeply inclined (>75°). Their directions can be rather variable around the NNE-SSW trend and also E-W. Massive *dolerite dykes* cutting the mylonitic fabric are the dominant type, generally <2-3m wide, with fairly planar walls. The E-W set may include dykes with a fairly irregular geometry showing several cusp-shaped grooves and stubs (Rickwood, 1990) filled with granitic leucosome

(Fig.4.5.5B) as can be observed about 2 km upstream from the mouth of the Sergipe River (Photo 4.5.13).

Quartz veins are mostly centimetre-scale features (around 2-3cm thick) and lie both concordant and discordant to the mylonitic fabric.

Important *leucocratic veins* are found associated with the granitoid rocks. They vary in shape from reasonably tabular to strongly erratic in discontinuous layers. Their thicknesses are mainly 2cm to 20cm, and when more extensively developed, they can give a migmatitic aspect to portions of the granitoids.

Some fractures are filled with *hydrothermal micro-veins* (Fig.4.5.4f) as observed in the GGA zone. They are associated mainly with N-S fractures, but occur also along NE-SW and NW-SE fractures. The width of these micro-veins is <1.0cm and their infill is a very fine black to dark-grey material formed mainly by tourmaline in euhedral crystals (>70%) in association with chlorite, microcline, quartz (<5%) and sericite (Photo 4.5.14).

4.5.5- DISCUSSION

The present study has identified six different groups of rocks outcropping along the studied section of the Itacaiúnas River. (1) Granitoids and amphibolites which occupy the largest area of the section and outcrop outside the Carajás structure, are correlated here with the Archaean *Xingu Complex.* This correlation is based on close similarities in lithology, metamorphic grade and styles of deformation. The Xingu Complex area corresponds to the domains of the zones I and VI in Fig.4.5.1.

(2) Metasedimentary rocks including quartzites, psamites and slates, outcrop inside the Carajás Structure from about 2 Km downstream from the Ranger's Hut to the north contact with the basement (Fig.4.5.2). These rocks are correlated with the Archaean *Igarapé Pojuca Group.* They display a weak to penetrative cleavage or foliation, and low greenschist metamorphic grade. The fabrics of these rocks are often characterised by fine grained recrystallized textures and changes in cleavage/bedding relationships suggesting that these rocks are folded on several scales. Folding of the cleavage in the slates indicates at least one later episode of brittle-ductile deformation. They correspond in map view, approximately to Zones III and V (Fig.4.5.1). They are very similar to the rocks outcropping in the Igarapé Bahia region, a few kilometres eastwards (see section 4.4 in this Chapter), and also to the rocks

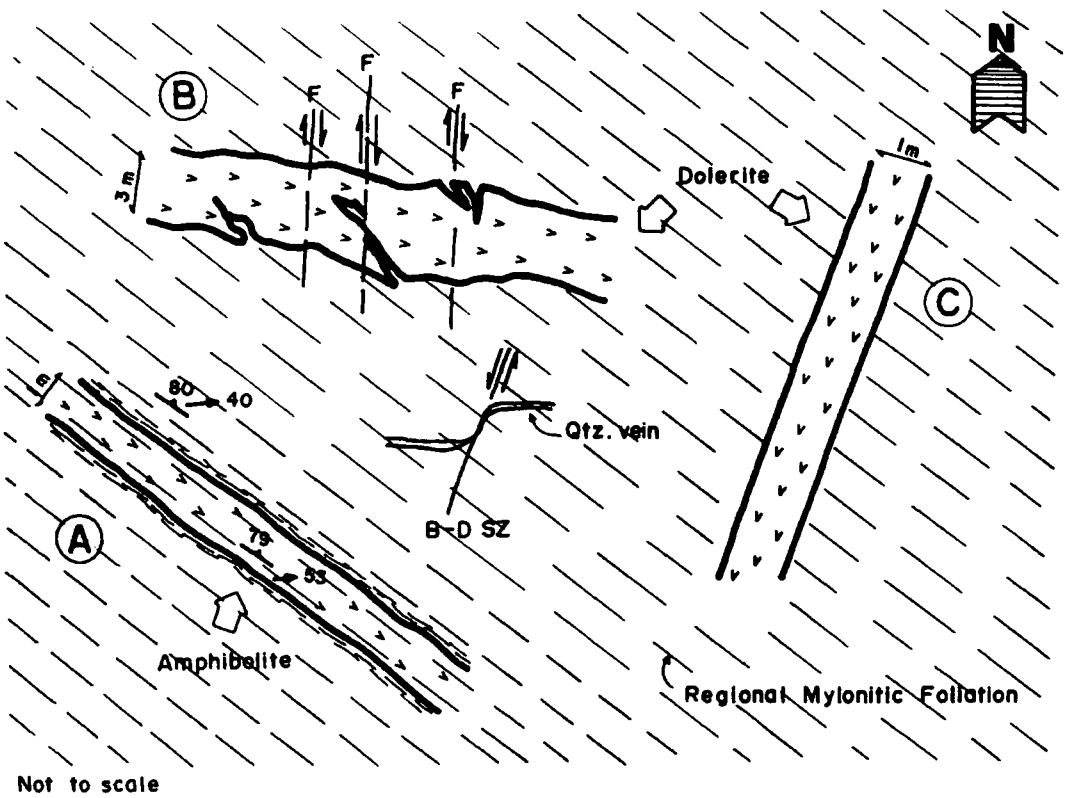

Fig. 4.5.5- Three sets of dykes are present in the Xingu Complex rocks. A- concordant, foliated amphibolitic dykes (shear zone concentrated on the borders); B- approximately E-W dolerite dykes, not foliated, cut by set of N-S faults; C- close NNE-SSW to N-S tabular dolerite dykes, not foliated.

Photo 4.5.12- Hypidiomorphic fabric observed in the coarse-grained gabbro outcropping around the Aquiri River mouth (XPL). Scale bar= 1.8mm.

Photo 4.5.13- A E-W 3m wide doleritic dyke cutting rocks of the Xingu Complex.

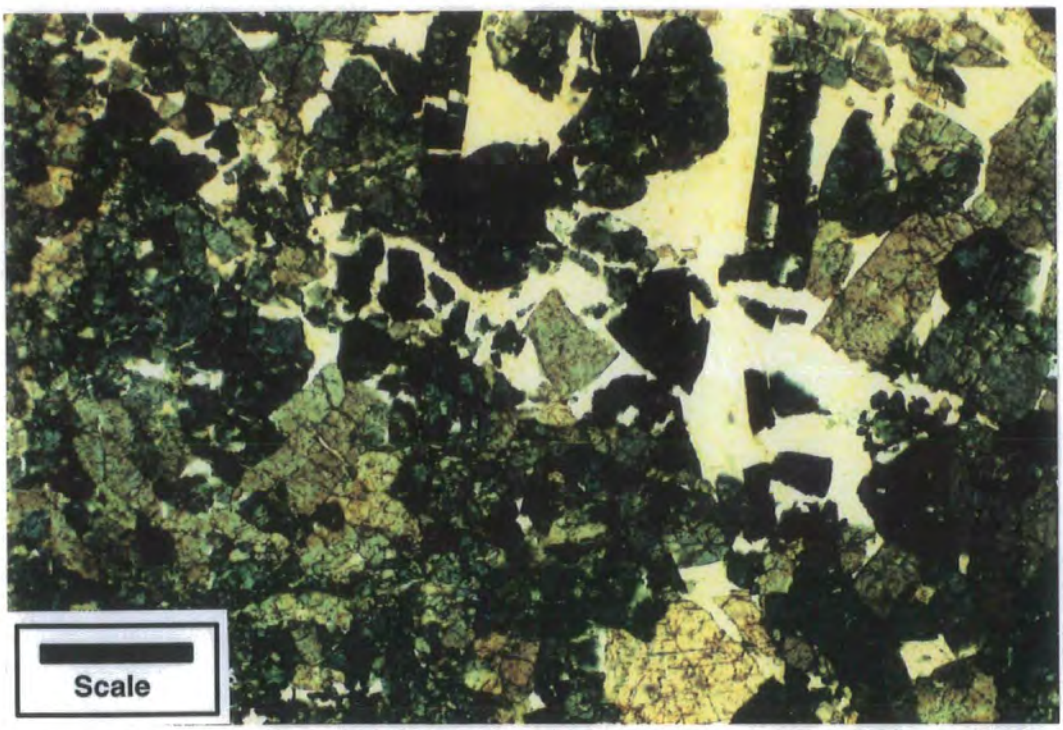

Photo 4.5.14- Microphotograph of the hydrothermal micro-veins observed predominantly on the granitoids of the Xingu Complex (XPL). Scale bar= 0.4mm.

observed in the Serra Pelada region, in the E part of the Cinzento Strike-Slip System (see Chapter 6).

The (3) metavolcanic rocks (metabasalts) outcrop along the river between the mouths of the Sergipe and the Aquiri rivers (Fig.4.5.2). These rocks show evidence of being heterogeneously deformed by low to very-low temperature brittle-ductile shear zones that produced a weak cleavage visible in some hand specimens. In terms of both petrology and structural aspects these rocks are very similar to the *Grão Pará Group.* The correlation with this Archaean unit is highly likely, and is supported here, but there is a possibility that the rocks are from the Igarapé Pojuca Group, since their field characteristics are not very well established and that it was not possible, directly in the field, to observe any contacts with adjacent rocks. For further discussion, see section 4.6, in this Chapter (The Serra do Rabo Region).

The metavolcanic rocks outcrop area corresponds approximately to zones IV and II in the satellite image (Fig.4.5.1).

Sedimentary rocks, particularly the sandstones, could be separated into two quite different types on the basis of compositional and textural maturity: (4) quartz arenite and (5) arkosic wacke. The quartz arenites adjacent to the Ranger's Hut, are predominantly medium to coarse grained rocks, and formed essentially by subrounded to rounded quartz grains, with <10% of matrix. They resemble closely the quartz arenites of the Archaean *Águas Claras Formation.* Despite the lack of extensive outcrops which would better expose primary structures, the presence of trough and tabular cross-bedding suggests a correlation with the fluvial deposits of the upper sequence of this unit (Nogueira, 1995). These rocks were rotated close to the sub-vertical position as observed by the high dip-angles measured by their bedding in this region (>65°; Fig.4.5.2).

The purplish grey arkosic wackes observed in several loose blocks are correlated here with the *Gorotire Formation* (Andrade Ramos, 1954). The textural and mineralogical immaturity of this rock, formed from badly sorted sub-angular grains of quartz, feldspars and rock fragments, do not support its correlation with the Águas Claras Formation as defined by Nogueira *et al.* (1995). The planar cross-bedding is the only sedimentary structure observed and suggests a fluvial origin but more data is needed to understand its derivation. Therefore this rock may be part of the Gorotire Formation earlier defined by Barbosa *et al.* (1966). This unit has been mentioned as being present in the Carajás region by several authors (e.g. Toubert *et al.*,1971;

CVRD/CMM, 1972; Beiseigel *et al.*,1973; Hirata *et al.*,1982). This suggestion is discussed further in the Section 4.6 at the end of this Chapter.

The area of occurrence of the Águas Claras Formation rocks corresponds approximately with Zone III described in the Fig.4.5.1.

(6) Gabbros outcrop extensively around the mouth of the Aquiri River (labelled G in the Fig.4.5.2). They represent a stratigraphical problem since they do not seem to be related to the basalts correlated here with the Archaean Grão Pará Group. The contact between these rocks was not observed. They are undeformed isotropic rocks showing a characteristic coarse-grained plutonic texture in contrast with the basalts that show a weak foliation of tectonic origin. These gabbroic rocks are interpreted here as later intrusions which postdate the Grão Pará Group. Their age and regional stratigraphical position are uncertain. They may be equivalent to metagabbros forming sills cutting the Águas Claras Formation for which Dias *et al.* (1996*a*) have obtained a Pb^{206}/Pb^{207} zircon age of 2645±12 Ma. Similar rocks are also present in the Igarapé Bahia area and have been previously described as being part of the Grão Pará Group (Wirth, 1986). Araújo and Maia (1991) consider them to be low grade metamorphosed rocks and suggested the name "Máficas Santa Inês" for these rocks, with a probable Proterozoic age, supporting DOCEGEO (1988). These authors do not reject the possibility of a relationship between these rocks with the ca.1.8Ga magmatism associated with the beginning of the Middle Proterozoic extension. These affect all the Amazonian Craton.

The granitoids and amphibolites, correlated to the Xingu Complex, are mylonitic rocks associated with major sinistral-oblique shear zones. Zones of high strain are defined by ultramylonites or subordinated mylonites with strong fabrics in relation to associated less deformed rocks. Heterogeneity and partitioning of deformation are responsible for the complex kinematics registered in the rocks of this unit (Fig.4.5.3). The foliation shows an overall NW-SE trend, dipping moderately to steeply NE. Deformation is heterogeneous, but it is possible to define five domains in which similar fabric intensity, orientation and kinematic pattern are developed. Lineation orientations are highly variable, even within single domains. Both sinistral and dextral shear senses are developed, often with one sense dominant in certain domains; all examples display a significant component of top-to-the-SW (i.e. reverse) movement. It is not possible to determine any overprinted relationship or evidence that these dextral and sinistral shears form conjugated arrays. The occurrence of complex foliation and lineation pattern is consistent with a transpressional regime (e.g. Fossen and Tikoff, 1993; Robin and Cruden, 1994)

and, regionally, sinistral shear sense indicators are dominant. The age of this deformation and metamorphism has been given as ca. 2.8 Ga (e.g. Machado *et al.*, 1991) but a longer and more complex history is predicted according to the observed data.

The rocks exposed within the Carajás structure show a dominant NE dip (Fig.4.5.2). The main contacts between the different units appear to be faults which are inferred by the stratigraphical distribution of the rocks (Fig.4.5.6) and by the interpreted lineaments from satellite images (Photo 4.5.1 and Fig. 4.5.2). These lineaments are easily correlated with the location of these inferred faulted-boundaries (Fig.4.5.2).

The tectonostratigraphical arrangement suggests important vertical displacements of the fault-bounded blocks inside the Carajás Structure. All the rocks inside de Carajás Strike-Slip System were down-faulted in relation to the Xingu Complex. The northeastern block, inside the structure, apparently has been relatively more uplifted to expose rocks of the Igarapé Pojuca Group adjacent to those of the Águas Claras Formation immediately to the south (Figs.4.5.2 and 4.5.6). The gabbroic intrusion observed in the S/SW block, inside the Carajás Structure, is emplaced along the contact between the Águas Claras Formation and the metavolcanics of the Grão Pará Group.

This geometric arrangement in uplifted and down-faulted blocks inside similar strike-slip structures is known worldwide and has been referred to by several authors (e.g. Freund, 1970 and 1971; Crowell, 1974*a*; Ballance and Reading, 1980; Eyal and Eyal, 1986; Woodcock, 1986 and 1987; Neugebauer, 1994: Peacock and Sanderson, 1995).

The high dipping angle observed to both tectonic and sedimentary planar structures present inside the Carajás Structure cannot be explained by the same mechanism responsible for the vertical displacement along the high angle normal faults observed.

The Carajás Fault is thought to form the NE border of the Carajás Structure and is interpreted to be a steeply SW-dipping structure. This fault is thought to have significant sinistral movements based on slikenside lineations and shear senses indicators observed along NW-SE fault planes close to the inferred fault trace. As demonstrated in other areas studied inside the Carajás Structure, cut by the Carajás Fault (e.g. Águas Claras, Azul, N-4), an important component of oblique convergence is responsible for the development of several tectonic features close to the fault trace. The data observed in the Itacaiúnas River section, strongly suggest that the sub-vertical geometry of the rocks inside the Carajás Structure resulted from transpression related to an

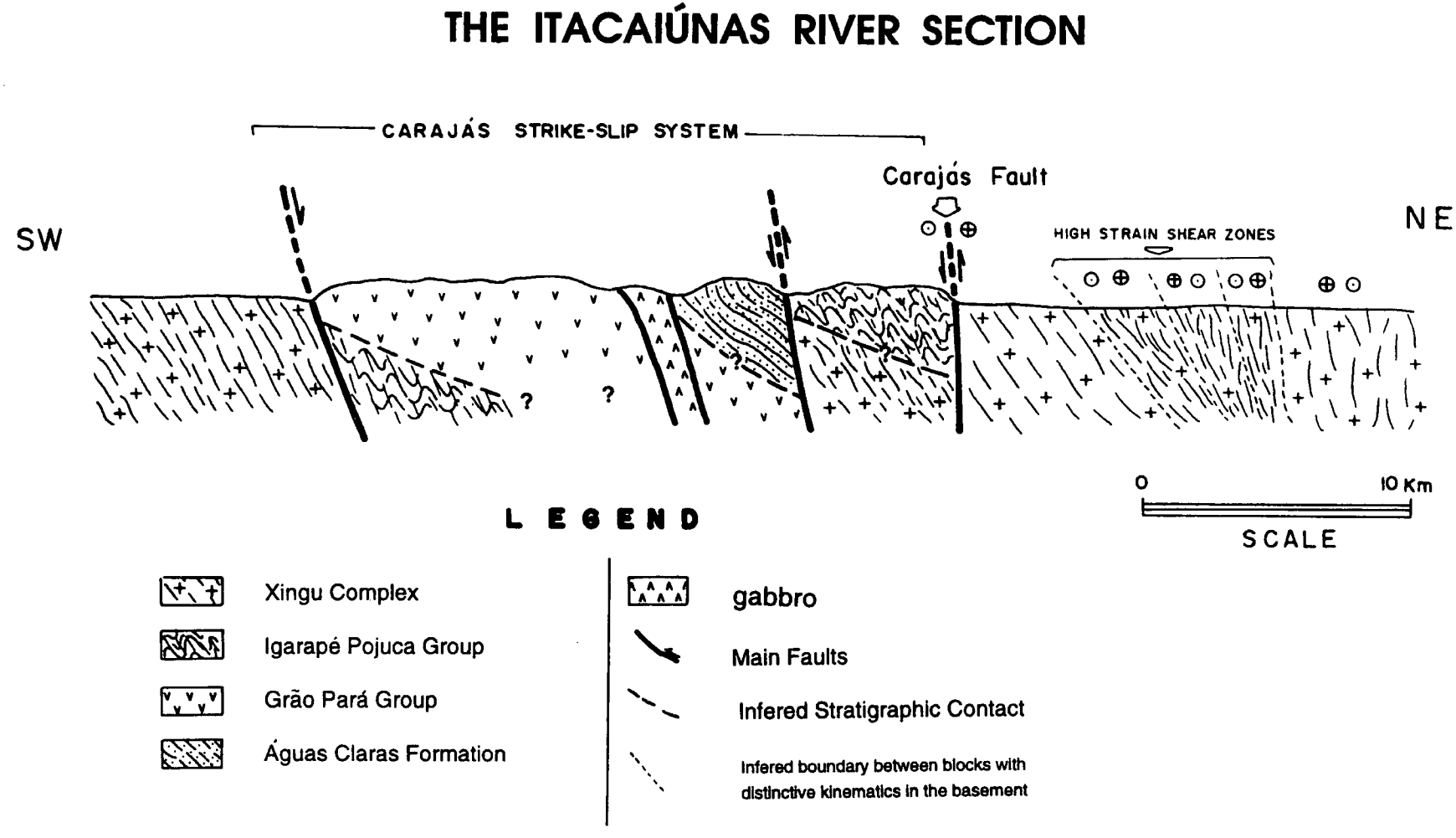

Fig. 4.5.6- Sketch geological section representing the boundaries between the different tectonostratigraphic units based on information from the Itacaiúnas River (see text for further discussion).

important episode of deformation associated with the Carajás Fault kinematics. The probable age of this event should be estimated as later than ca.2.6 Ga (age of gabbroic sills intruded in the Águas Claras Formation according to Dias *et al.*,1996*a*) and earlier than ca.1.9 Ga, since the intrusion age of the Central Carajás Granite, cutting the Carajás Fault a few kilometres to the east of the Itacaiúnas River, is ca.1880±2 Ma (Wirth *et al.*,1986; Machado *et al.*,1991). There is no field evidence to determine the chronological relationship between this event and the extension (or transtension) responsible for the vertical displacement of the block inside the Carajás Structure. This extensional (transtensional) episode could be earlier or later than the Carajás Fault transpression. If it was later, it is related to the extension associated with the subsidence of the rocks inside the Carajás Structure as a whole that should have happened after the deposition of the Águas Claras Formation, intruded by ca.2.6 Ga gabbroic rocks (Dias *et al.*, op.cit.). The other possibility is that it could be related to the Middle Proterozoic extension registered by the plutonic intrusions (see Chapter 7 in this thesis).

Fractures and faults trend mainly NW-SE or N-S/NNE-SSW. The NW-SE trend is sub-parallel to the main direction of the tectonic foliations in both the basement and cover rocks (Fig.4.5.4a,c). The N-S fractures host most of the basic dykes, and cut those dykes concordant to the NW-SE foliation. Brittle-ductile shear zones are also orientated around NW-SE and NNE-SSW. These data strongly suggest a long history of reactivation of older structures during different episodes of deformation that took place in the region.

4.5.6- CONCLUSIONS

1) Six different tectonostratigraphic units outcrop along the Itacaiúnas River section: (1) the Xingu Complex, is the basement, formed by granitoids that had undergone amphibolite metamorphism and deformed by ductile shear zones; (2) the Igarapé Pojuca Group quartzites, metasandstones and slates with low greenschist metamorphism and showing a brittle-ductile fabric; (3) the Grão Pará Group metavolcanics including metabasalts that had undergone low greenschist metamorphic grade; (4) the Águas Claras Formation fluvial sandstones; (5) the Gorotire Formation arkosic wackes. Gabbroic rocks intrude the metabasalts of the Grão Pará Group. They have an uncertain stratigraphic position. All the tectonostratigraphical units identified are probably separated by unconformities.

2) The distribution of the rocks is controlled by shear zones (in the Xingu Complex) and faults (Igarapé Pojuca Group, Grão Pará Group and Águas Claras Formation). The shear zones affecting the basement rocks are kilometre-scale, predominantly reverse-oblique with kinematics partition controlling the distribution of dextral- and sinistral- reverse shear zones (Fig.4.5.3). The deformation along these high temperature ductile shear zones is rather heterogeneous it being possible to identify high strain zones in contrast to very low strain zones. The fault-boundaries between the different tectonostratigraphic units are normal, with high dipping angle and subordinated sinistral displacements, arranged in an imbricate fan (Fig.4.5.6). Vertical displacements are responsible for putting rocks with different ages side by side on the surface level. The original stratigraphical position of the units is not possible to determine since they were partly affected later by transpression during sinistral kinematics of the Carajás Fault.

3) The fault movement responsible for the significant rotation towards the vertical, observed in most of the planar structures adjacent to the Carajás Fault trace, is supposed to have happened between ca. 2.6 Ga (minimum age for sills intruded in the Águas Claras Formation; Dias *et al.*,1996*a*) and ca.1.8-1.9 Ga (age of the Central Carajás Granite; Wirth *et al,* 1986; Machado *et al.*,1991). This episode of transpressional reactivation is related to the main reactivation of the Carajás Fault.

4) The mylonitic fabric printed in the basement rocks exerts a strong influence on the development of later NW-SE structures. N-S structures are related to later regional episodes of deformation that took place in all the Amazonian Craton at the end of the Early Proterozoic- beginning of the Middle Proterozoic.

4.6- THE SERRA DO RABO REGION

The region east of the Parauapebas River forms a relatively lowland area with a large number of secondary and even small roads. Outcrops are easier to find as rain forest has been replaced by grazing land.

The geology of this area is dominated by the basement rocks with several gneisses and granitoids (Xingu Complex), together with volcanic and sedimentary rocks all intruded by Proterozoic granites and undated gabbros. The Estrela Complex Granite (ca.2.5 Ga), occupies a relatively large area in the region, emplaced into both the Xingu Complex and Igarapé Pojuca Group rocks (Fig.4.6.1). The termination of the Carajás Fault is one of the most important structures present in the area (Fi.4.6.2 and Photo 4.6.1).

4.6.1- REGIONAL SETTING

The basement granites and gneisses of the Archaean Xingu Complex form an irregular E-W trending zone separating the supracrustal rocks of the Cinzento Strike-Slip System (to the north) from those of the Carajás Strike-Slip System (in the south). The Xingu Complex also outcrops in regions between branches of the Carajás Fault, which extend eastwards before being cut by the Araguaia Belt. Similar basement rocks occur also in the large area south of the Carajás Strike-Slip System (see Fig.3.9, Chapter 3- Regional Geology).

The Estrela Granite Complex outcrops in a large area along the north part of the Carajás Fault splay (see Figs. 4.6.1 and 4.6.2) and is formed by monzogranites gneisses and pegmatites deformed by ductile shear zones (Barros, 1991; Oliveira,1991). It displays intrusive contacts with amphibolites and ironstones of the Igarapé Pojuca Group, and with amphibolites and gneisses of the Xingu Complex (Barros and Dall'Agnol,1993).

The Plaquê Suite forms another set of granites identified in the area of the Xingu Complex (Fig.4.6.1). They are muscovite-biotite leucogranites forming E-W oriented, elongate bodies, sub-parallel to the trend of the Xingu Complex rocks into which they are emplaced (Araújo and Maia, 1991). They are deformed by shear zones and are thought to be generated and emplaced coevally with the main episode of ductile shear registered in the basement rocks (Jorge João and Araújo, 1992).

THE SERRA DO RABO REGION - Lithological Map

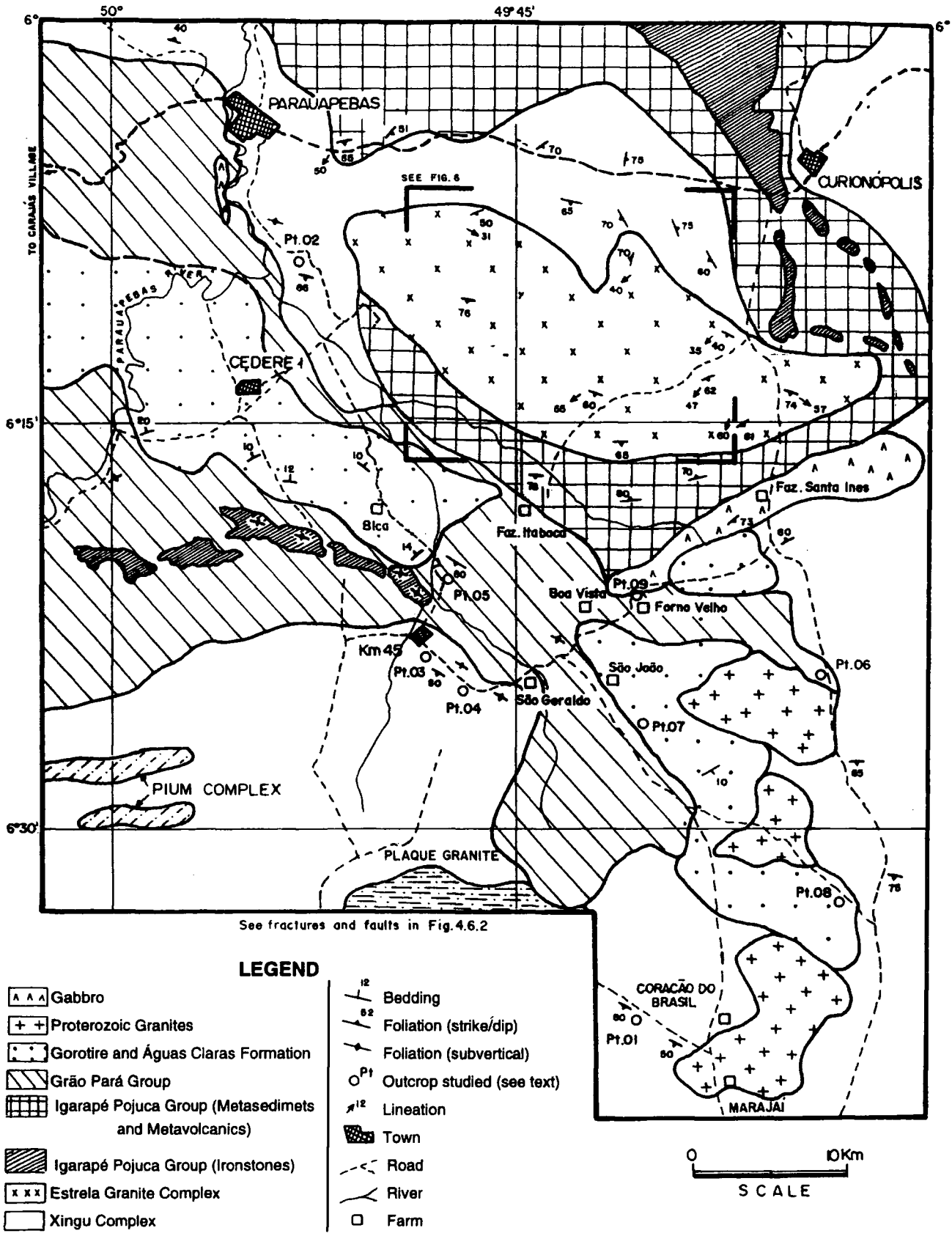

Fig.4.6.1- Lithological map of the Serra do Rabo region. The points shown on the map are explained in the text.

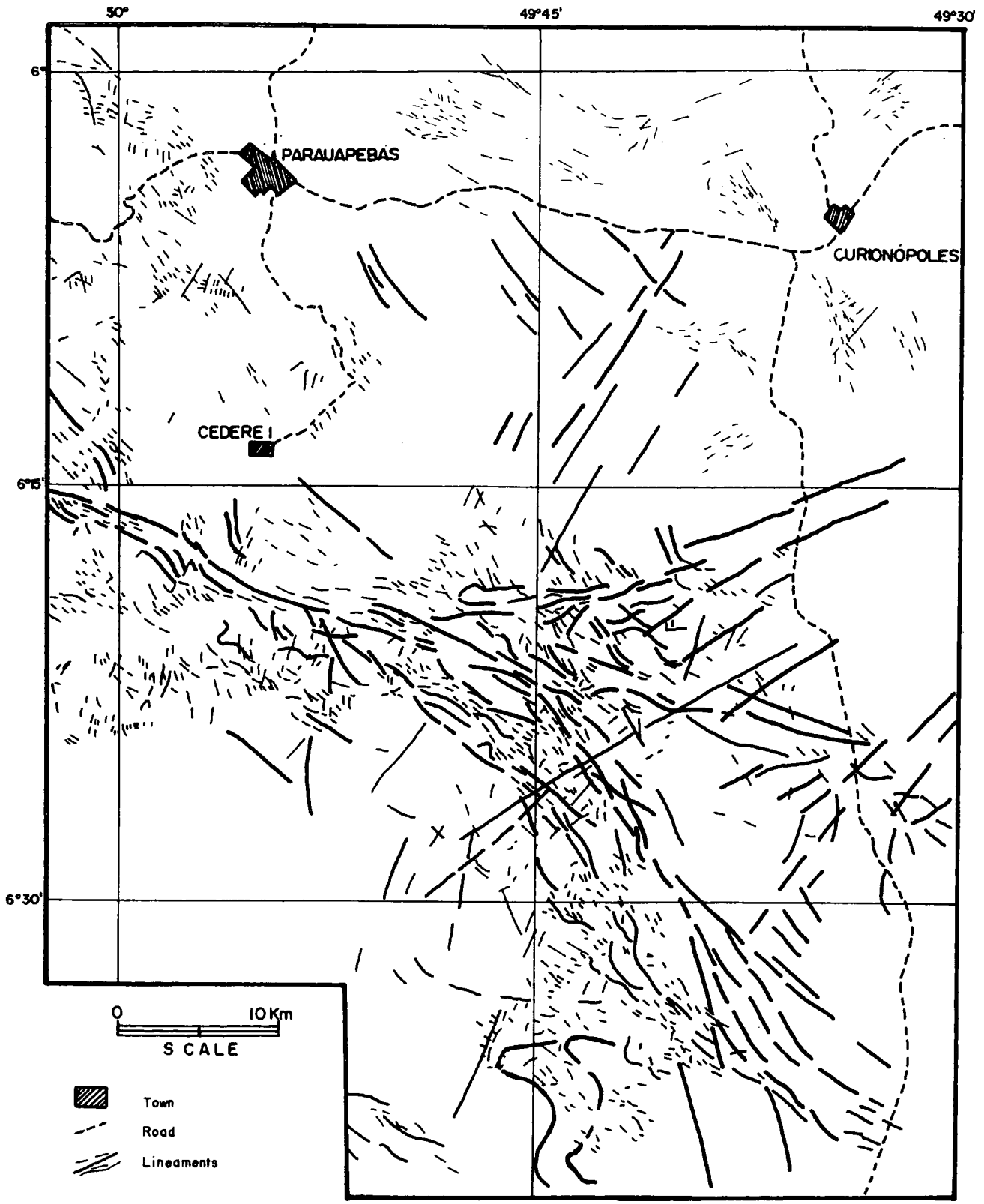

Fig.4.6.2- Map of main lineaments observed in satellite images of the Serra do Rabo region.

Photo 4.6.1- Satellite image of the Serra do Rabo region. The stronger lineaments correspond to the east Carajas Fault termination.

Ultramafic rocks, transformed by greenschist metamorphism, belonging to the Sapucaia Group (Araújo and Maia, 1991) or Andorinhas Supergroup (DOCEGEO,1988; see Fig.3.5, Chapter 3- Regional Geology) are found in a few lens-shaped bodies in the Serra do Rabo region (Araújo and Maia, 1991). They are correlated with the Archaean greenstone belts sequences well exposed in the Rio Maria region, about 70 Km to the south of Carajás (see Fig.3.5, Chapter 3).

The northern area of the Serra do Rabo region is dominated by amphibolites, schists, ironstones, quartzites and metasedimentary rocks, outcropping in E-W and N-S orientated lens-shaped bodies (Meireles *et al.*,1984; Costa *et al.*,1990; Araújo and Maia, 1991). They display greenschist and amphibolite metamorphic grades (Araújo and Maia, 1991) and are correlated here with the Archaean Igarapé Pojuca Group (see section 5.3, Chapter 5). A widespread mylonitic fabric has been reported as being associated with these rocks (e.g. Costa *et al.*,1990; Matta and Teixeira, 1990; Araújo and Maia, 1991) They outcrop along the eastern termination of the Cinzento Strike-Slip System, in the so-called Serra Pelada horse-tail structure (Costa and Siqueira, 1990).

The central part of the Serra do Rabo region is formed by sequences of volcanics and ironstones belonging to the Grão Pará Group, Igarapé Pojuca Group, and clastic rocks of the Águas Claras Formation (Meireles *et al.*,1984; Wirth, 1986; Nogueira *et al.*,1995; Fig.4.6.1). The volcanics are mostly tholeiitic basalts and acid volcanics that have undergone very low to high grade greenschist metamorphism (cf. Meireles *et al.*,1984; Araújo and Maia, 1991). Contacts between these rocks and the adjacent rocks of the Xingu Complex are both tectonic and unconformable.

The distribution of both the Grão Pará Group and the Águas Claras Formation are strongly controlled by the main lineaments of the Carajás Strike-Slip System (Fig.4.6.1). In the Serra do Rabo region, these cover rocks are deformed within the Carajás Fault termination which forms the most important local structure (Fig.4.6.2).

Proterozoic granites (see Chapter 6) are present as several plutons outcropping in the eastern region of the Carajás Fault termination intruding both Xingu Complex and Grão Pará Group rocks (Araújo and Maia, 1991). The age of these granites is supposed to be around ca.1.8 Ga by correlation with similar plutons outcropping in the region (e.g. the Cigano Granite, Central Carajás Granite).

Immature clastic sedimentary rocks are present in several places in the inner part of the Carajás Strike-Slip System overlying the Xingu Complex. They are thought to belong to the Gorotire Formation.

Probably the youngest rocks in the region are represented by grabbroic intrusions (age unknown), outcropping in NE-SW and N-S orientated bodies. These rocks are leucogabbros and anorthosites intruded into the Grão Pará Group and Xingu Complex (Meireles *et al.*,1984; Matta and Teixeira, 1990). DOCEGEO (1988) dated these rocks as Early Proterozoic, while Meireles *et al.*(1984) suggested a Jurassic age for them, and named them Santa Inês Gabbro.

4.6.2- PREVIOUS WORK.

The area has been the subject of geological research since the Carajás region became a target for ore exploration, at the beginning of the 1970's (e.g. Beisiegel *et al.*,1973).

Silva *et al.* (1974) first recognised the importance of the strong lineaments forming the eastern termination of the Carajás Fault in the Serra do Rabo area. They described the rocks in this region as schists and volcanics, folded in synclines and anticlines.

Meireles *et al.* (1984) introduced most of the main stratigraphical units and interpreted some of the structures present in the region. They recognised the Xingu Complex, the "Salobo-Pojuca Sequence" (Hirata *et al.*, 1982), the Grão Pará Group, the sedimentary sequence referred to by them as the Rio Fresco Formation (Barbosa *et al.*,1966), the Cigano Granite, and the Estrela Granite (see Fig.3.7, Chapter 3). Dykes and volcanic rocks present in the western and central part of the area were thought to be part of the Uatumã Group, according to Caputo *et al.* (1971) who compared these rocks with similar units outcropping in the Xingu and Uatumã rivers. The ironstones, ultramafics and mafics that underwent greenschist facies, outcropping in the north of the area, were correlated with the "Rio Novo Sequence" defined by Hirata *et al.* (1982) as part of a greenstone belt thought to be present in the Serra Pelada region.

Meireles *et al.* (1984) divided the ironstones and volcanic rocks of the Grão Pará Group into the Carajás Formation and Parauapebas Formation respectively. They noted some differences in the geochemical composition, metamorphic grade and style of deformation between the ironstones of the

Carajás Formation and those associated to the so-called "Salobo-Pojuca Sequence".

The Estrela Granite was initially correlated with the "Serra dos Carajás-type granites" (Meireles *et al.*,1984), but the deformed characteristics of the former pluton suggests that it is earlier (Dall'Agnol *et al.*, 1986). Hence some authors (e.g. Araújo *et al.*,1988) refer to this unit as "Estrela Gneiss".

The sedimentary sequence, initially correlated with the Rio Fresco Group, was named the Águas Claras Formation by Araújo and Maia (1991). These authors suggested a tectonic model for the region in which a large scale flower structure geometry was developed during regional sinistral transpression. These rocks were later studied by Nogueira *et al.* (1995).

In 1990, detailed mapping by Costa *et al.* (1990) led them to reintroduce the name Rio Novo Group to refer to the mafics, ultramafics, ironstones and quartzites outcropping in the north part of this area. The Estrela Granite at that time was considered to be part of the Xingu Complex rocks deformed by E-W and NE-SW ductile oblique-slip shear zones forming a positive flower structure. The greenschist metamorphism developed in these rocks was thought to be coeval with the regional sinistral transpression responsible for the development of the main structures (Araújo *et al.*, 1988; Araújo and Maia, 1991).

The SE contact between amphibolites and schists and the Estrela Granite was studied by Oliveira (1991) and Oliveira and Costa (1992). They refer to a hundred-metre-scale flower structure defined by two ductile shear zones along the contacts.

Geochemical data concerning the Estrela Granite were first introduced by Araújo and Maia (1991) who demonstrated that the syenogranitic trend in this rock contrasts with the Xingu Complex rocks which show a large variation in composition. Barros (1991), Barros *et al.* (1992*a* and *b*), Barros and Dall'Agnol (1993) and Barros *et al.* (1997) published both geological and geochemical information about the Estrela Granite and referred to it as an example of deformed Archaean A-type monzogranite. The age of this batholith is thought to be the same as that of the Old Salobo Granite (Igarapé Salobo region; 2573±2 Ma, U/Pb-zircon; Machado *et al.*,1991). This correlation was based on a Rb/Sr (whole rock) age of 2527±2 Ma obtained from the Estrela Granite by Barros *et al.* (1992*b*) and supported by the structural similarities between these two rocks.

A different set of granites, termed the Plaquê Suite, are not dated although they have been interpreted as being formed during the main ductile

shear event that took place in the Itacaiúnas Belt around 2.8 Ga (e.g. Machado *et al.*,1991; Araújo and Maia, 1991; Jorge João and Araújo, 1992).

The Araguaia Belt cuts the Itacaiúnas Belt, and outcrops about 15-20 Km east of the Serra do Rabo. The adjacent outcropping rocks correspond to slates and phyllites from the Tocantins Group (Middle Proterozoic; Herz *et al.*,1989).

4.6.3- LITHOLOGIES AND STRUCTURES.

4.6.3.1- THE GRANITOIDS AND GNEISSES.

At least three main groups of granitoids are present in the Serra do Rabo region, all Archaean in age: Those of Xingu Complex; the Plaquê Suite; and the Estrela Granite Complex (Fig.4.6.1).

a) The Xingu Complex granitoids and gneisses. The granitoid rocks are mostly coarse to medium-grained tonalites and granodiorites variably deformed by ductile shears that took place around 2.8-2.7 Ga in the Itacaiúnas Shear Zone. They vary from isotropic granites, through to protomylonites and ultramylonites, including granitic gneisses and migmatites, with a heterogeneous distribution. These different rock-types have a basic mineralogy of quartz, feldspar (plagioclase-andesine and/or microcline-perthite), biotite and hornblende, plus opaque minerals, zircon, apatite, chlorite; and muscovite, sericite and calcite as accessories. The quartz is fine to medium-grained (0.06 to 0.7 mm) and occurs mostly in xenomorphic crystals or as diffuse sub-grains formed due to recovery, or display undulose extinction and ribbon-shapes when in bands in gneisses. The feldspar can be enclosed by biotite and hornblende phenocrystals, but it is more common as small (ca. 0.10 mm) anhedral crystals associated with aggregates of hornblende and quartz. Kink bands are often observed deforming plagioclase crystals. The hornblende crystals are rather variable in size (0.36-0.07 mm) and almost always show evidence of later alteration to chlorite. Fine crystals of biotite and hornblende form strongly orientated grains that can define the S-foliation observed hand-sample scale. More isotropic granites show a weak, discrete foliation marked often by the orientation of the hornblende, biotite, and ribbon quartz crystals. The gneisses of the Xingu Complex are subordinate rock-types and frequently are associated with migmatites. They have a tonalitic or granitic composition, in which bands of quartz and feldspar are interlayered with bands of biotite and hornblende.

Biotite is the main mafic mineral, with hornblende found in very low percentages. The thickness of the layers can vary from 0.5 cm to more than 2.5 cm, but 1.5 cm thick are the most prevalent.

The orientation of the foliation in the granitoids and gneisses of the Xingu Complex outcropping in the area, is rather variable (Fig. 4.6.1 and 4.6.3). Their general trend varies between WNW-ESE and N-S but NW-SE trends are predominant. They dip mainly at high angles (>65°) toward NE or SW. Where strongly mylonitised the rocks become banded displaying anastomosing patterns, folds and transposition fabrics. Augen gneisses are common. S-C foliations are present in both the protomylonitic and mylonitic granitoids, and asymmetric porphyroclasts of K-feldspars, and asymmetrical folds are also observed. Kinematic indicators at various scales (micro- and macro-scale), point to a predominant sinistral sense of shear although dextral kinematic indicators are also common at outcrop-scales.

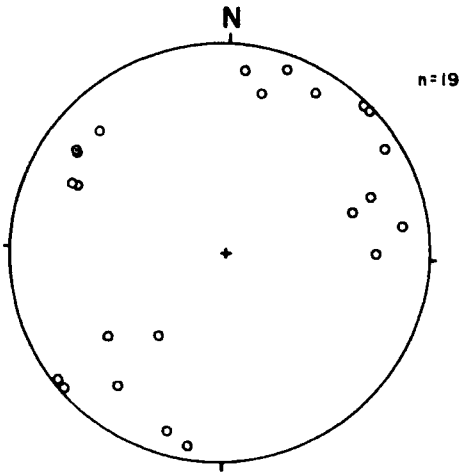

Fig.4.6.3- Stereonet representing poles to foliation in the Xingu Complex, outcropping in the Serra do Rabo region.

The metamorphic grade is predominantly amphibolite facies represented by a mineral assemblage quartz + plagioclase + microcline + biotite + hornblende. Later retrograde metamorphism is probably associated with hydrothermal alteration and is characterised by the presence of an epidote + muscovite (after feldspar and biotite) + biotite + chlorite (after hornblende) mineral assemblage.

Quartz veins and quartzo-feldspar veins are relatively abundant in association with granitic rocks. They can be 2-20 cm wide and are always deformed by ductile, ductile-brittle, and/or brittle deformation.

Fig.4.6.3 illustrates the main features observed in an exposure of a granitoid of the Xingu Complex, in contact with quartzite, located about 3 Km west of Coração do Brasil Farm (Pt.01 on Fig.4.6.1). The coarse-grained granodioritic rock preserves a strong S-C fabric. The C surface is orientated about 112° dipping steeply NE and SW, while the S foliation strikes 090°, with sub-vertical dips, denoting a dextral non-coaxial ductile shear (Fig.4.6.4). Both S and C foliations are defined by brown biotite and hornblende, but quartz aggregates are associated also with these surfaces. The quartzite in abrupt-concordant contact with the granitoid is a coarse-grained, dark-grey to green rock formed by quartz (>90%), chlorite and plagioclase. It is an L-S tectonite with foliation orientated 129/83 NE and a lineation defined by acicular quartz crystals plunging about 52° towards 225° (Fig.4.6.4). The contact between this rock the granitoid is approximately straight and sub-parallel with the foliation in both rocks (Fig.4.6.5A). Quartz veins were observed in both rocks are 5 to 10 cm wide, most of them are orientated NW-SE (Fig.4.6.4).

Two brittle-ductile to brittle sets of shear zones cut across both the mylonitic foliation and quartz veins: (1) NNE-SSW and, (2) NE-SW shear zones (Fig.4.6.5B). Both sets cut the foliation in a brittle-ductile manner, 'brittlely' offset quartz veins and display dextral displacements. The NNE-SSW brittle shears also cut the granitoid/quartzite contact showing a dextral displacement (Fig.4.6.4).

Another set of fractures, some with dextral displacement, are developed sub-parallel to the main ductile mylonitic fabric observed both in the granitoids and quartzite. They are orientated about 110°-115° dipping around 50°-90° towards SW (Fig.4.6.4).

Based on these data it is possible to establish the following chronology of events (see bottom of Fig.4.6.5):

1) Development of the mylonitic foliation during ductile dextral shear.
2) Development of the NNE-SSW dextral brittle-ductile shear zones, affecting the early mylonitic foliation.
3) Quartz vein injection, followed by NE-SW dextral brittle-ductile shear, cutting simultaneously the mylonitic foliation and the quartz veins.
4) Reactivation of the NNE-SSW shear planes by dextral brittle shear cutting the early mylonitic foliation, the quartz veins and the contact granitoids/quartzite.

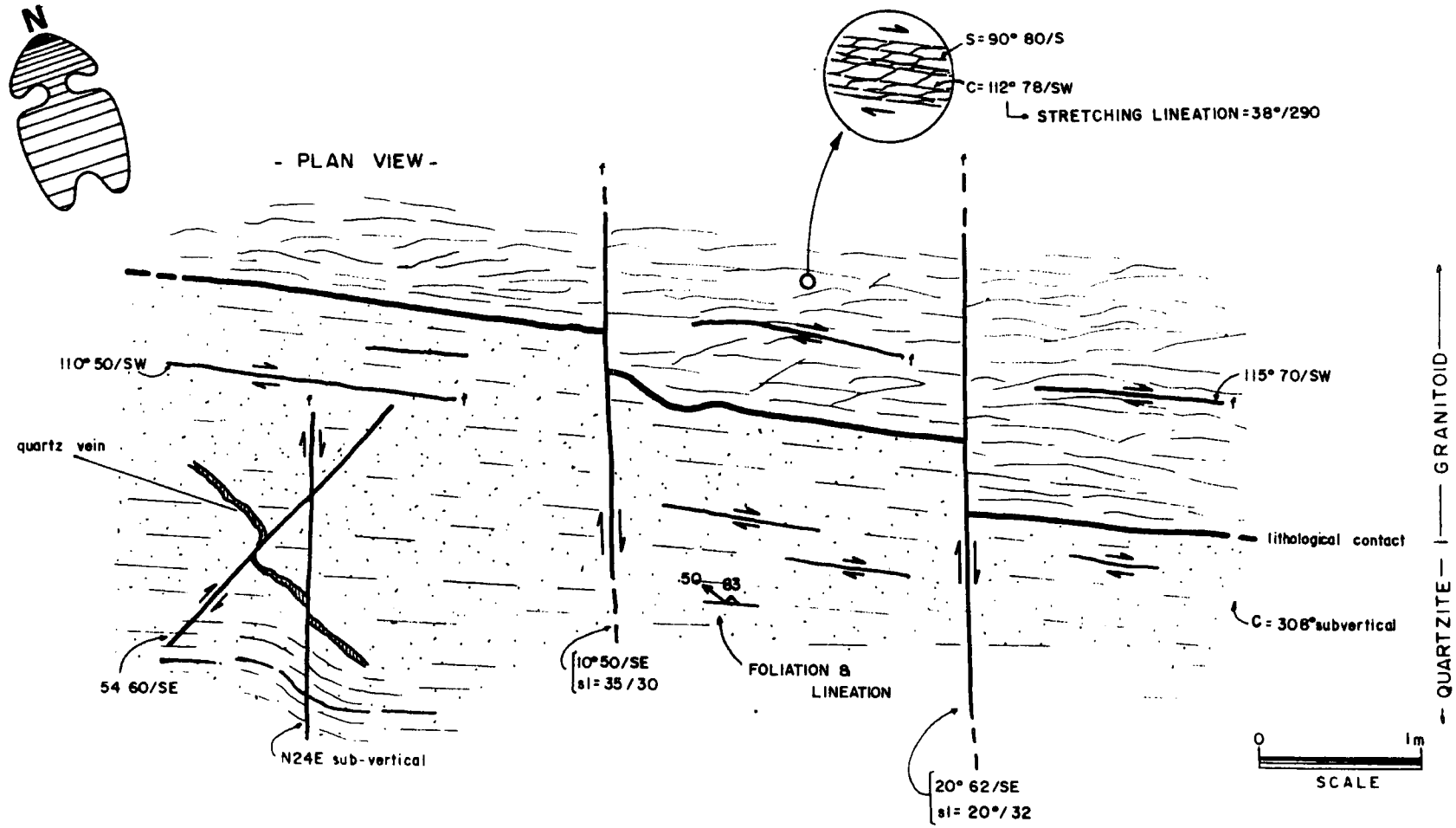

Fig.4.6.4- Faulted contact between quartzites and granitoids of the Xingu Complex observed in the Pt.01 (Fig.4.6.1). Several episodes of brittle-ductile deformation affect the early mylonitic fabric (c). The lines labelled with a "f" correspond to faults.

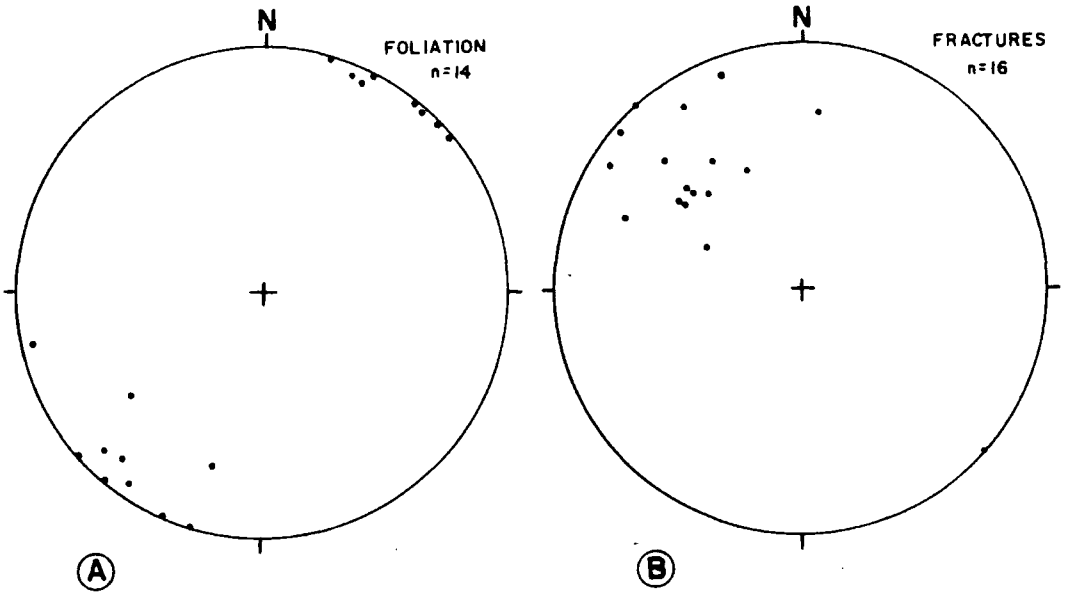

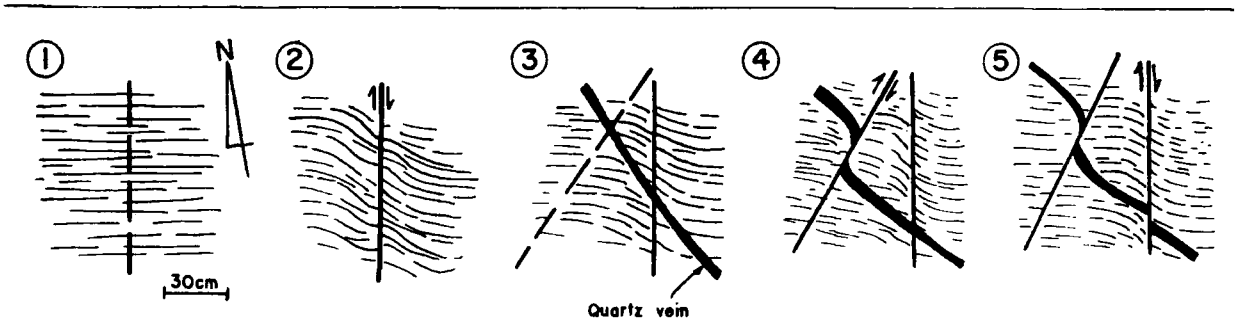

Fig.4.6.5- A) The mylonitic foliation from granitoids and quartzites. B) Main set of fractures in the same outcrop excluding those sub-parallel to the foliation. Below A and B: a set of figures illustrating the sequence of shear zones development and reactivations in relation to quartz veins injection (see text for details).

There are no suitable data, from this outcrop, to indicate the temporal relationship between the development of the 110°-115° set of fractures, sub-parallel to the mylonitic foliation and the other structures.

Apparently the same NNE-SSW, or N-S set of fractures, is present in the Xingu Complex rocks in different places, suggesting it is a regional structural feature. Major lineaments observed in satellite images support the regional importance of these fractures (Fig.4.6.2).

In another outcrop found about 9 km south of Parauapebas, on the hillsides close to the road linking this city to the CEDERE I village (marked as Pt.02 on Fig.4.6.1), a fine-grained granitic rock, varying from granodiorite to tonalite, is found together with localised migmatitic (quartzo-feldspar) veins (Fig.4.6.6). Later millimetre-scale quartz veins cut this rock in several directions. A sub-vertical fine mylonitic foliation is observed, defined in hand-samples by orientated crystals of biotite, following the 120°-140° direction. A stretching lineation is apparently present plunging at a very low angle, following the strike of the foliation. Ultramylonitic portions are observed towards the north in poorly exposed, discrete bands, concordant with the adjacent mylonites and protomylonite fabrics.

The quartzo-feldspathic veins cut obliquely across the early mylonitic fabrics (Fig.4.6.6). They are formed by opaque white to yellowish quartz (>80%) and K-feldspar (?), in folded veins that are from 2-3 cm to 30 cm wide (Photo 4.6.2), cut by later fractures and faults (Photo 4.6.3). En echelon fracture arrays are developed in one of these veins (Fig.4.6.6; Photo 4.6.4). These dilational fissures are filled by dark grey hydrothermal material (quartz + chlorite + epidote), with different orientations in different limbs of the folded vein (070° and 120° in the right and left limb respectively). Some of these veins are cut by N-S fractures with sinistral displacements of a few centimetres (<10 cm; Photo 4.6.3) along which small (<8 cm) pull-aparts are developed (Fig.4.6.6) filled with hydrothermal material similar to the tension gashes in the main veins. Later E-W fractures cut these N-S fractures lying sub-parallel to the mylonitic fabric displaying both apparent sinistral and dextral displacements; these appear to be small normal faults (Fig.4.6.6; Photo 4.6.5).

Taking the deformation patterns displayed by the veins it is possible to suggest that progressive coaxial pure shear was mainly responsible for their folding under brittle-ductile conditions (Fig.4.6.6, boxes A to C on the bottom). The arrows represented in box A in the Fig.4.6.2, indicate the hypothetical orientation of the principal axes of incremental extensional and contractional strain during deformation.

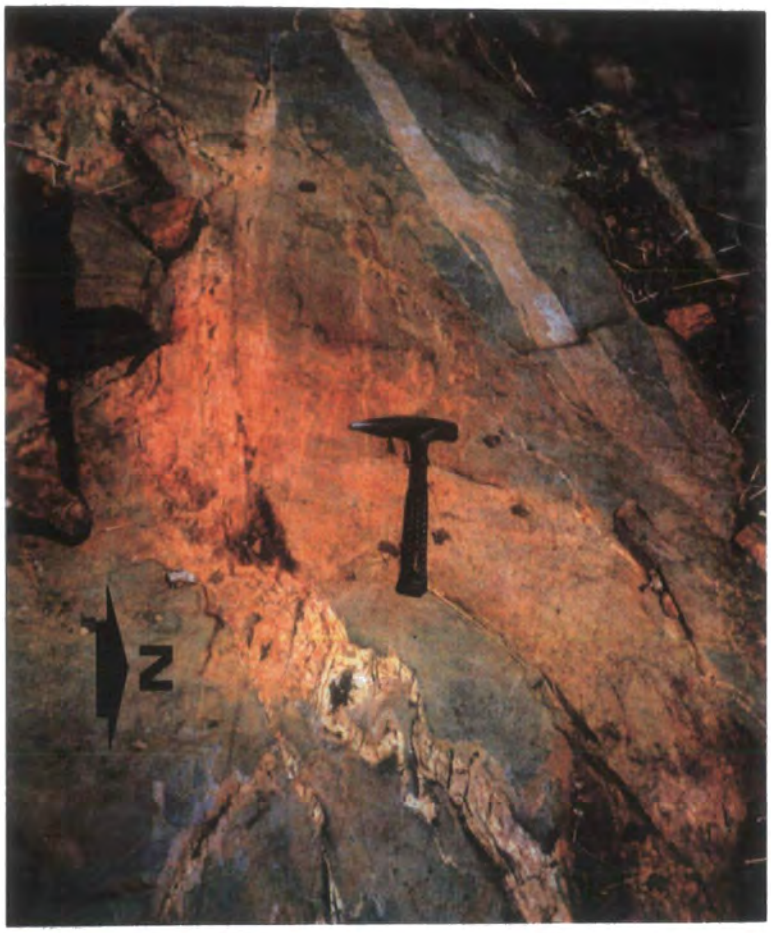

Photo 4.6.2- Faulted quartzo-feldspatic veins observed in the granitoids of the Xingu Complex (Pt.02, Fig. 4.6.1). See Fig. 4.6.3.

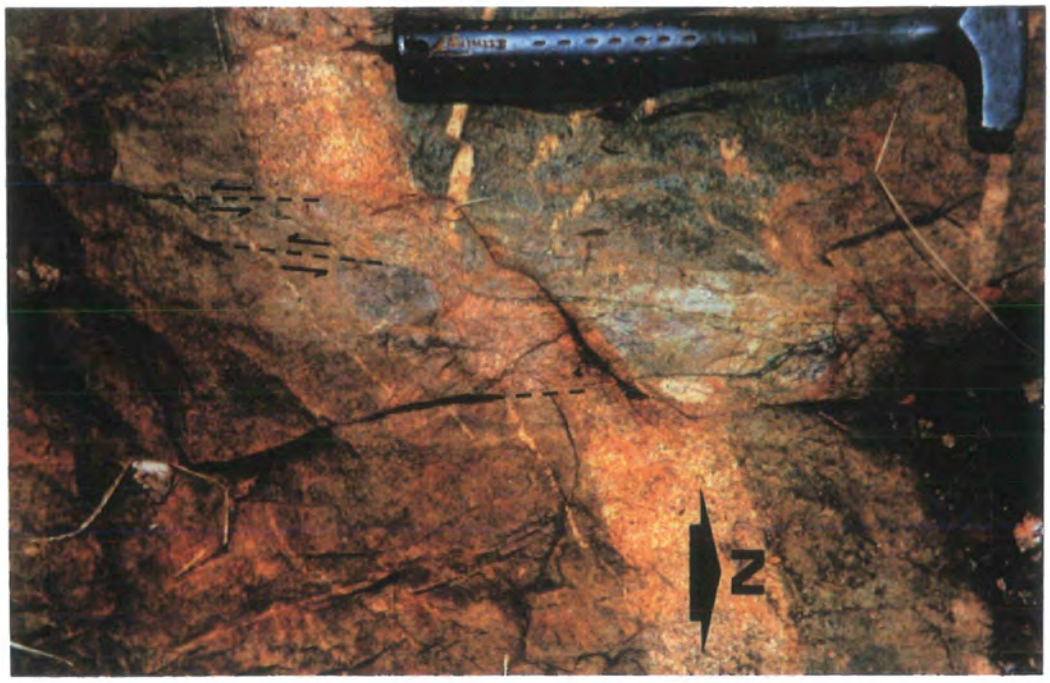

Photo 4.6.3- Faults and fractures cutting the quartzo-feldspatic veins. See Fig.4.6.3 and Photo 4.6.2).

Photo 4.6.4- Tension gashes observed into folded quartzo-feldspathic veins. See Fig.4.6.3 and Photo 4.6.2).

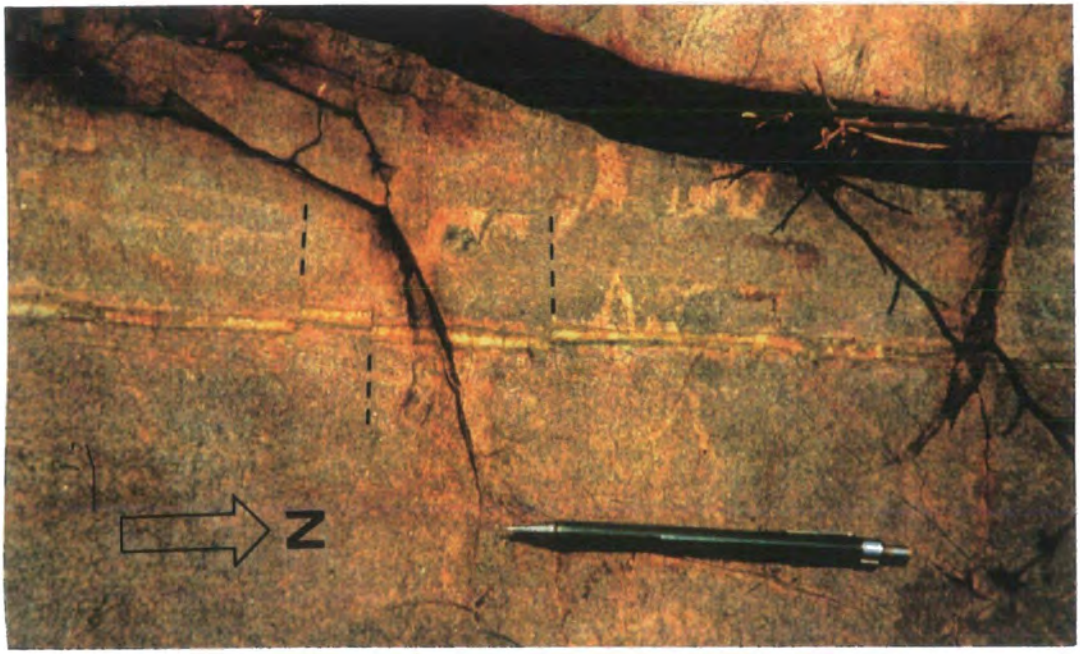

Photo 4.6.5- E-W small faults cutting hydrothermal veins filled with quartz + chlorite + epidote. See Fig.4.6.3 and Photo 4.6.2).

b) The Plaquê Suite: The Archaean granitic rocks referred to as the Plaquê Suite (Araújo and Maia, 1991), were found in a few localities during the present survey (e.g. points Pt.03 and Pt.04 on Fig.4.6.1). They display strong mylonitic fabrics, are typically red-pink in colour and carry biotite and/or muscovite.

The blastomylonitic granites are formed essentially from microcline+plagioclase+quartz+biotite and hornblende, muscovite, chlorite, zircon and opaque minerals in minor amounts. Feldspar (microcline) often forms common σ-type porphyroclasts which together with discrete S-C-C' fabrics, suggest ductile sinistral displacements (Photo 4.6.6). Biotite and quartz are the main minerals responsible for both the S- and C-foliations present in the rock. The biotite is a brown to dark-green type, forming relatively large strong oriented crystals (ca. 1cm or more). Muscovite and sericite are present in very fine crystals dispersed in the feldspars as a secondary mineral. The C-foliation is oriented about 130° and is defined by the trails of the biotite and σ-type feldspar crystals. A C' fabric (e.g. Ponce de Leon and Choukroune, 1980) or extensional crenulation cleavage (Platt, 1984), is a discrete surface disturbing the S-C fabrics, orientated about 105° (Photo 4.6.6). The development of this set of foliations (S-C-C') seems to be non-penetrative, being particularly well developed in places in these rocks. The dominant texture is formed by symmetric porphyroclasts of feldspars and elongate quartz crystals. Evidence of dynamic recrystallisation is best observed in the quartz grains showing serrated or sutured crystal boundaries, recrystallized subgrains in aggregates and new grains.

A stretching lineation is not well developed in most of these rocks although a few examples within C-surfaces are defined by the orientation of the biotite and quartz, plunging with moderate angles towards the east.

A few isolated quartz veins orientated 047 57/SE with a thickness of about 5-10 cm are observed. Pegmatites are also scarce and E-W oriented, dipping 60° S. Fractures are mostly NE-SW dipping with variable angles SE. Slickenlines in these fractures point to mainly strike-slip displacements, plunging at low angles (04° to 19°). Some sinistral offsets are preserved.

A later spaced set of fractures is observed cutting the rock and their early structures, oriented 105°/ 82°SW. These are related to later brittle episodes of deformation affecting the region (Fig.4.6.2).

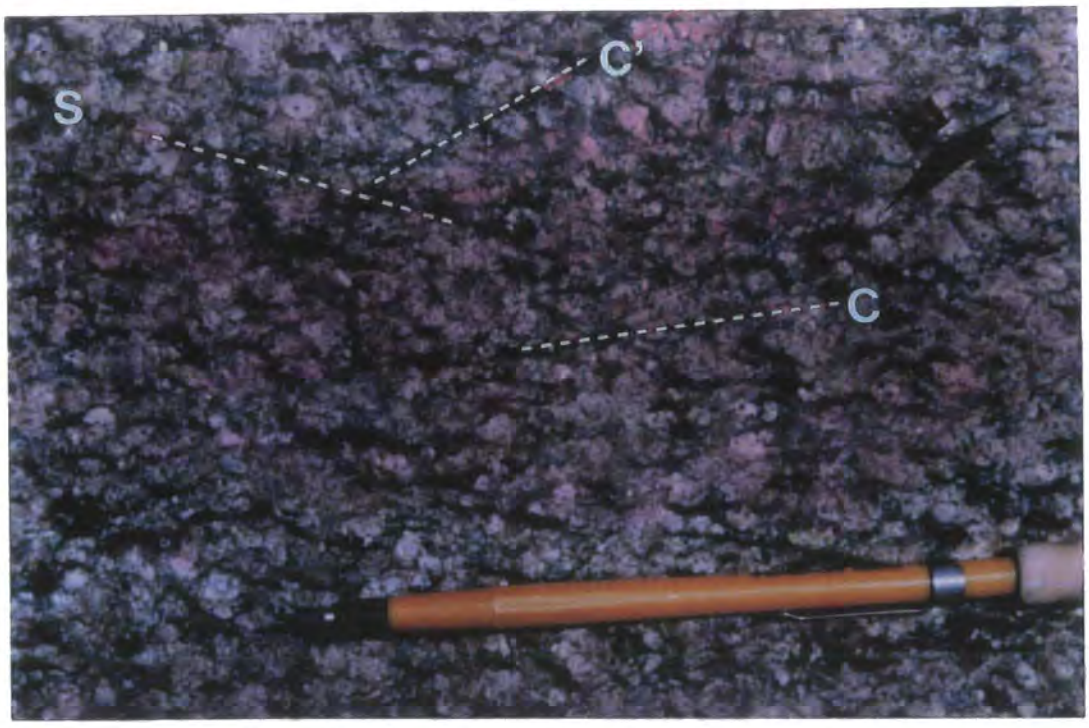

Photo 4.6.6- S-C-C' fabrics in blastomylonites of the Plaque Suite (S= oriented about 160°; C= 130°; C'= 110°). Location: Pt.03 and Pt.04, Fig.4.61).

c) The Estrela Granite Complex: The rocks forming the Estrela Granite Complex are dominantly monzogranites (Barros and Dall'Agnol,1993). In the field, there are also granodiorites, tonalites and granites cut by several pegmatites, leucosomes and quartz veins, outcropping in a relatively large area (about 300 Km^2) southwest of Curionópolis (Fig.4.6.1). The elliptical pluton, elongate in an E-W direction, is relatively well exposed and the forms shown in maps in Fig,4.6.1 and Fig.4.6.7 are based on Araújo and Maia (1991) and Barros (1991) respectively.

The wall-rocks are mostly a sequence of amphibolites and ironstones belonging to the Igarapé Pojuca Group which forms relatively narrow zones within the Xingu Complex, along the NNE, S and SW borders of the pluton. Tonalitic gneisses from the Xingu Complex outcrop in the N and NW contacts. Elongate, orientated xenoliths of amphibolites, sub-parallel to the main fabric, and also cordierite schists, have been mapped in different places in the granite (Fig.4.6.7; Barros,1991; Barros and Dall'Agnol,1993). Thermal metamorphism has been identified affecting the amphibolites from the wall-rocks forming quartz-biotite-cordierite hornfels (Barros, 1991).

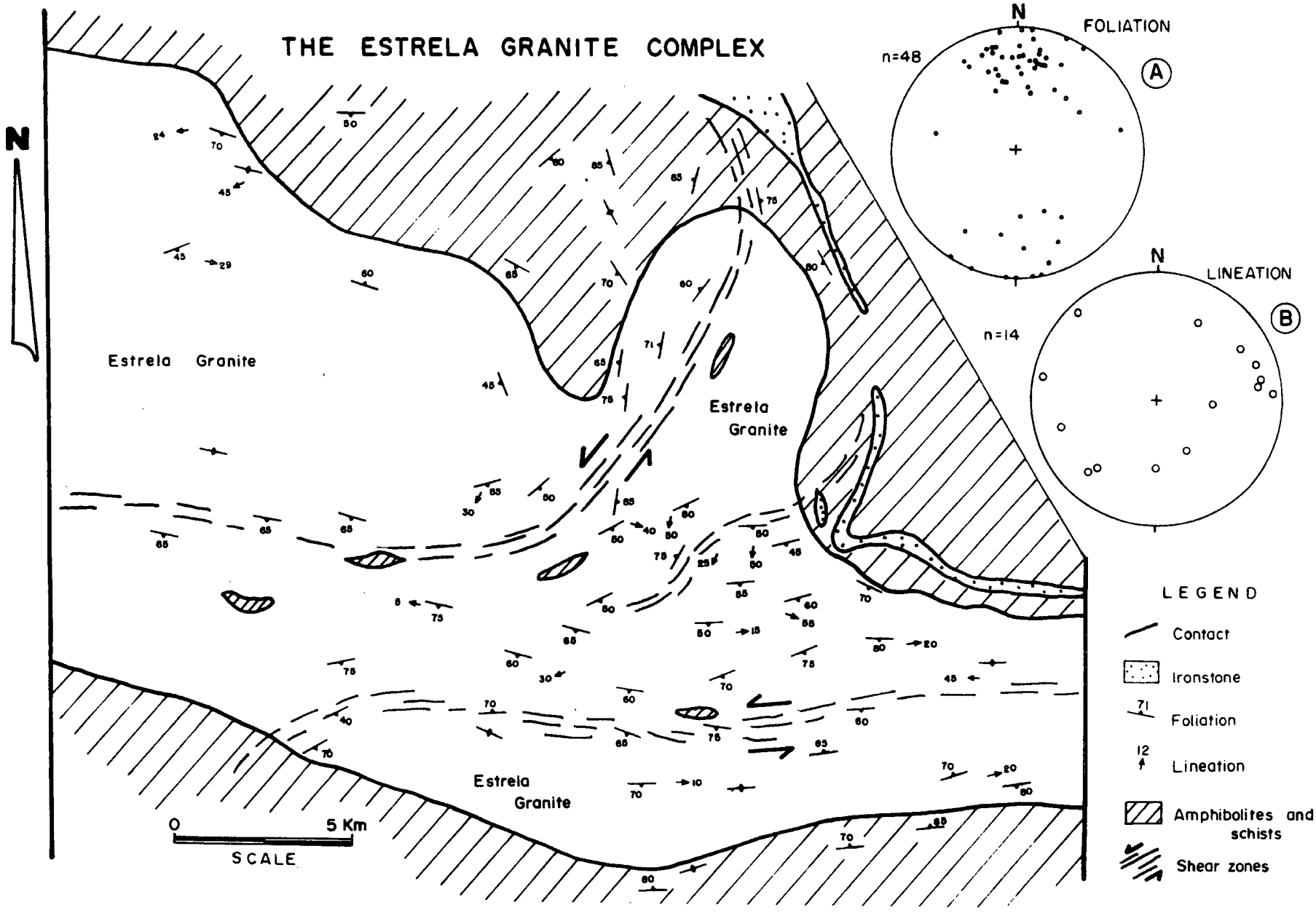

Fig.4.6.7- The central part of the Estrela Granite according to Barros (1991) and Barros and Dall'Agnol (1993). See more detailed location in the Fig. 4.6.1.

The Estrela Granite is affected by ductile deformation to produce a foliation which has been identified as a pervasive regional structure in these rocks (Barros, 1991; Barros and Dall'Agnol,1993). Two anastomosing ductile oblique (sinistral-compressional) shear zones have been mapped by Barros (1991) and Costa *et al.* (1991) crossing the pluton in E-W and NE-SW directions (Fig.4.6.7). Rocks within these shear zones range from protomylonites to mylonites (Barros and Dall'Agnol, 1993). Gneissic rocks are also present showing centimetre-scale alternating quartzo-feldspathic and mafic (biotite and hornblende) bands.

The Estrela Granite is thought to have undergone amphibolite facies metamorphism, with temperatures above 500°-550°C based on metamorphic paragenesis and the characteristics of deformational features observed at meso- to micro-scales (Barros,1991; Barros and Dall'Agnol,1993). Dolerite dykes and gabbros, both inside and outside the pluton, are later intrusions.

Localities visited along the eastern and central part of this granitic body, revealed mainly foliated monzogranites and granodiorites (Photo 4.6.7). These rocks are mostly medium to coarse grained, with hornblende as the common mafic mineral, although these are very variable in concentration from place to place. Pegmatite and quartz veins are also frequent, varying from 4-5 cm to >15 cm wide, displaying both concordant (Photo 4.6.7) and discordant relations to the foliation. Discontinuous leucosome veins are also present up to 30 cm long and a few centimetres thick, concordant with the ductile foliation. Ptygmatic folds of the leucosomes have been reported by Barros (1991) and were widely observed in the field. Transposed folds are also common features observed in both quartz (Photo 4.6.8) and leucosome veins.

The foliation varies from a weak preferred orientation of biotite and/or amphibole to a strong planar fabric, including S-C foliations, banding and crystal plastic strain fabrics. Ductile flow indicators such as S-C fabrics, shear bands, asymmetric intrafolial folds, and rotation of crystals, suggest a predominance of sinistral movements. In the field, S-C textures and anticlockwise asymmetries of folded quartz veins are the most common kinematic indicators. Both microscopic and macroscopic sense indicators are relatively scarce probably due the high temperature during deformation (Barros, 1991).

The map in Fig.4.6.7, reproduced and modified from Barros (1991) and Barros and Dall'Agnol (1993), shows the available data concerning the foliation in the Estrela Granite and its adjacent wall-rocks. Data collected during the present study are shown in Figs.4.6.1 and 4.6.8. These data suggest a general

Photo 4.6.7- Foliated granodiorite cut by pegmatite veins (sub-parallel to the foliation), later cut obliquely by set of fractures (south part of the pluton).

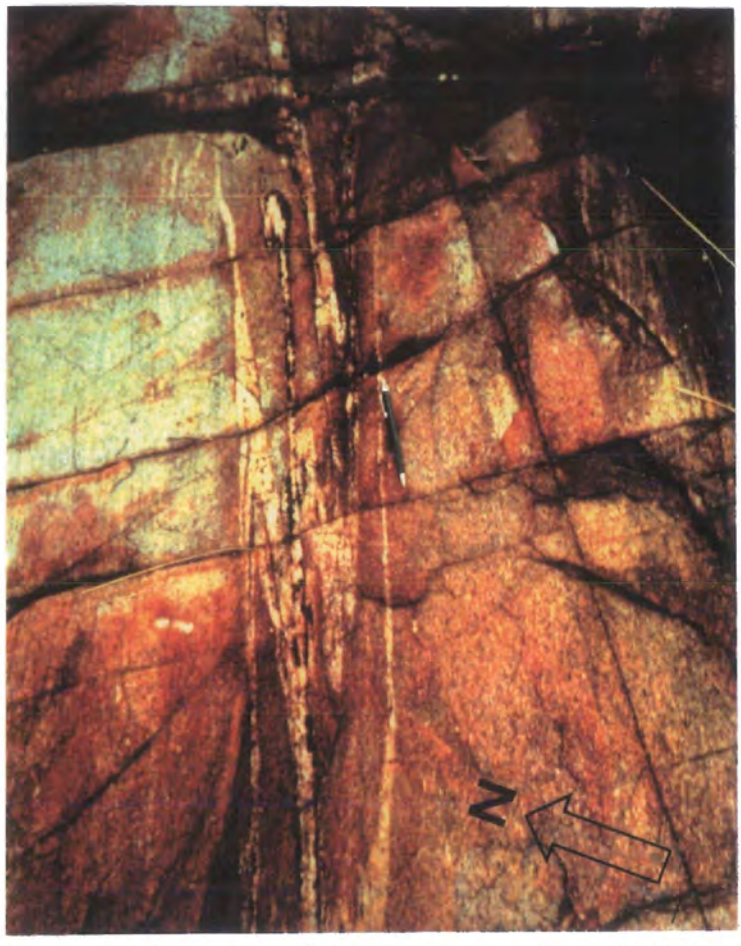

Photo.4.6.8- Transposed folds, sub-parallel to the foliation observed in the Estrela Granite rocks (south portion) formed during a sinistral displacement.

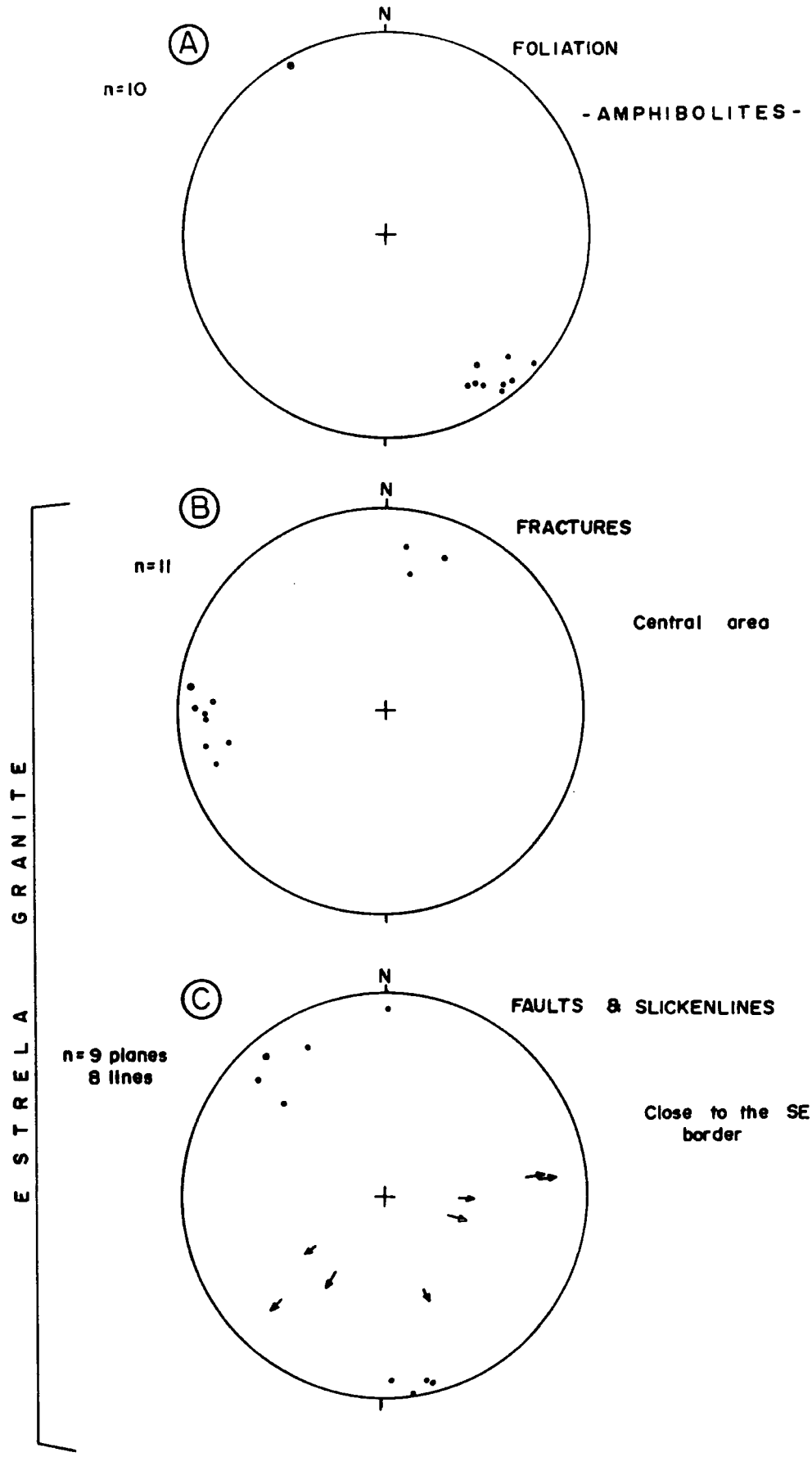

Fig.4.6.8- Stereonets of foliation in the wall rocks (A), fractures (B) and faults and slickenlines (C) around the central portion and borders of the Estrela Granite.

E-W to ESE-WNW trending foliation dipping variably S, or less commonly, N (Figs. 4.6.1 and 4.6.7; stereonets A on the top right). In the N-S offshoot from the granite in the central-north part of the body, the foliation deflects significantly into a N-S direction, dipping W, following the orientation of the nearby contact (Figs 4.6.1 and 4.6.7). The lineation plunges rather variably from low to high angles in different directions, but low angles are more frequent (Fig.4.6.7, stereonet B). The oblique relationship of the foliation and lineation observed in several places, suggests that sinistral shears are associated with a small reverse component.

There is a mylonitic foliation in the wall rocks which is sub-parallel to the pluton margins, dipping N in the south and S in the north region. Around the northern margin, the foliation is more irregular, locally following the N-S direction of the contacts dipping SW and NE.

Fractures and faults occur throughout the pluton (Fig.4.6.8B and C). Barros (1991) suggested mainly strike-slip displacements along most of the faults observed. Slickenlines observed in some of these structures suggest mainly oblique-slip displacements. Faults orientated about NE-SW have slickenlines plunging SW while those trending N-S have lines plunging both NNE and SSE at angles around 30°-50°.

The local influence of major brittle structures can be responsible for the predominance of related sets of fractures and faults. The stereonet in Fig.4.6.8C, for example, shows poles to faults and slickenlines observed in outcrops close to the SE margin of the pluton. A predominance of NE-SW fractures is clearly demonstrated in this diagram. These structures lie sub-parallel to the main lineaments observed in Fig.4.6.2, (i.e. the SE border of this area). Another stereonet representing poles to fractures observed in Pt.4 (Fig.4.6.1), around the central zone of the massif, shows two distinctive concentrations of poles denoting the predominance of both N-S and E-W structures (Fig.4.6.8B).

A set of millimetre spaced fractures may be observed following approximately the N-S direction in several places in the north and central areas of the pluton. It is not a penetrative structure and pervades a 10m wide zone cutting the earlier ductile fabrics.

At least two different generations of quartz veins are preserved. One set lies sub-parallel to the ductile foliation (ca. 060°-100°/ 70° S) and are locally deformed together with the foliation. Some can develop a similar foliation (pre- to syn-deformation), while others are clearly later, cutting obliquely the pre-existing fabrics. This second group of veins can follow several different

directions, but those trending NE seem to be the more common. N-S faults can displace both sinistraly and dextraly quartz veins and pegmatites.

4.6.3.2- AMPHIBOLITES AND SCHISTS (IGARAPÉ POJUCA GROUP).

Amphibolites and schists are present in various parts of the Serra do Rabo area. They have several different compositions and are associated with distinctive deformational histories. They outcrop mainly along the northern region associated with the Igarapé Pojuca Group and in a narrow (<3 Km wide) belt around the south and the northeastern contact zones of the Estrela Granite.

The amphibolites in the northern area are associated with ironstones, quartzites, metavolcanics, and muscovite-schists in smaller proportions. In the south they are associated mainly with garnetiferous hornblende schists with centimetre-scale, slightly asymmetrical porphyroclasts (Photo 4.6.9). These clasts are surrounded by a quartz-biotite-amphibole foliated matrix, denoting mainly sinistral senses of shear.

The amphibolites are green to grey, fine to medium-coarse rocks with a strong foliation defined by the alignment of hornblende which forms about 85% of the rock, and subordinate plagioclase (An_{42}; about 15-20%). Quartz, pyroxene, chlorite, malachite and chalcopyrite are also present as accessories or secondary minerals. The plagioclase is very often altered to aggregates of fine grained epidote. As they are heterogeneously deformed it is possible to find lens-shape blocks of less-deformed rocks that acquire characteristics of the mafic igneous protolith (Oliveira, 1991).

The mylonitic foliation in the amphibolites, south of the Estrela Granite, forms an anastomosing fabric, orientated NE-SW dipping NW (Fig.4.6.8A). It is defined by hornblende in a nematoblastic texture. These rocks gradually become more rich in quartz and develop porphyroclasts of garnet up to 1-2 cm across (Photos 4.6.9 and 4.6.10). The concentrations of the porphyroclasts are variable, defining bands >2m wide. The mylonitic foliation in the garnetiferous schists is defined by ribbon-quartz and plagioclase, or secondarily by amphibole and/or mica (biotite) fish, and also aggregates of quartz sub-grains which, in association to other kinematic indicators, denote a sinistral flow. These data agree with those shown by Oliveira (1991) concerning these rocks.

The stretching lineation defined by aligned, acicular grains of biotite or quartz plunges from about 30° N-NE, to sub-vertical.

Photo 4.6.9- Slight asymmetrical garnet porphyroclasts in the schists observed in association to amphibolites in the south of the Estrela Granite pluton. A set of sinistral faults are displayed parallel to the main foliation.

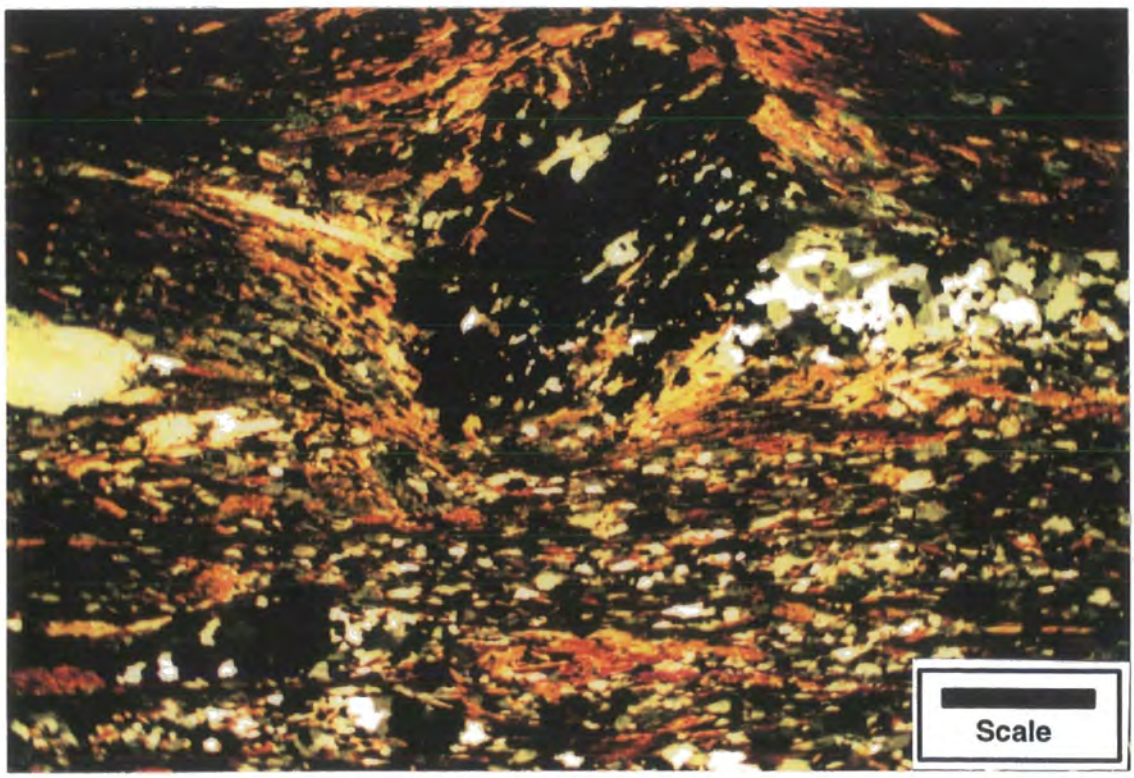

Photo 4.6.10- Rotational phorphyroclast of garnet in the schists present in the south of the Estrela Granite Complex, correlated with amphibolites of the Igarapé Pojuca Group. XPL, Scale bar= 2.1mm.

Kinematic indicators observed in outcrops of the amphibolites and quartz-garnet-schists from the south of the Estrela Granite strongly suggest a predominant oblique sinistral shear with a top-to-the-NW movement.

Later brittle-ductile shear zones are developed reactivating the early mylonitic fabrics. A mineral lineation defined by quartz plunges 0°-20° towards 45°. The shear zones are mainly sinistral based on the development of asymmetric, isoclinal neutral folds deforming the mylonitic foliation. These plunge 70°-90° towards both the NE and the SW, with sub-vertical axial planes orientated NE-SW (Photo 4.6.11). The stretching lineation in the mylonitic foliation is also folded, reinforcing the view that these low-temperature shear zones are chronologically later than the main ductile shear episode.

Another very important later episode of reactivation associated with the earlier mylonitic fabric is indicated by the presence of closely spaced (20-30 cm) sinistral strike-slip faults arranged sub-parallel to this fabric. They cross cut millimetre-scale quartz veins and display centimetre-scale (5-10 cm) offsets (Photo 4.6.9).

Later extensional fractures cut the rocks in several directions, but are predominantly orientated 010°-020°/ 40° SW and 080°/ 60 NW.

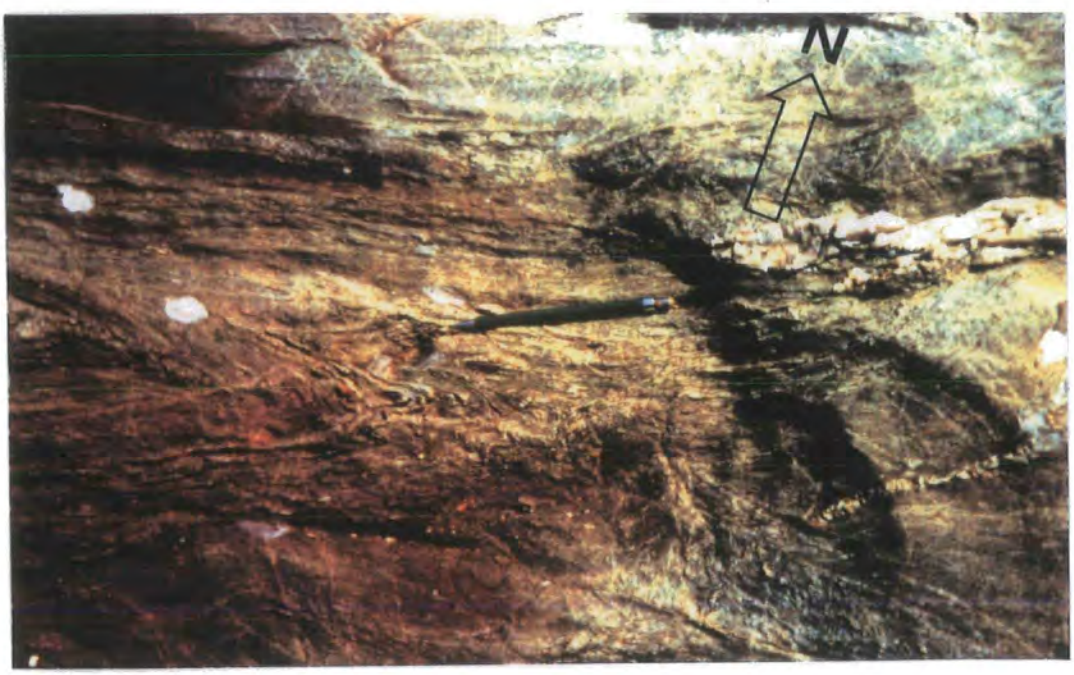

Photo 4.6.11- Asymmetric neutral fold deforming the mylonitic foliation adjacent to a brittle-ductile shear zone in the amphibolites of the Igarapé Pojuca Group outcropping S of the Estrela Granite Complex.

4.6.3.3- IRONSTONES (IGARAPÉ POJUCA AND GRÃO PARÁ GROUPS).

The ironstones are mostly banded iron formations outcropping along the main hills above 200m forming the Serra do Rabo and as relatively small lens-shaped bodies in the northern part of the area. They are associated with amphibolites of the Igarapé Pojuca Group and granitoids and gneisses of the Xingu Complex. They are red to yellow-grey rocks with millimetre- to centimetre-scale bands of quartz alternating with iron-rich bands (mainly haematite-martite, and magnetite together with other opaque minerals, such as specularite (Araújo and Maia, 1991).

Two different types of ironstone can be distinguished based on the predominance of brittle or ductile structures. (1) Those preserving more brittle and primary features are predominant in the south and in places along the Carajás Fault termination (Figs.4.6.1 and 4.6.2). They are similar to the ironstones of the Grão Pará Group outcropping in the N-4 Mine (see section 4.3 in this chapter). (2) Those showing ductile structures are often found in the north sector, between Curionópolis and Parauapebas cities (Fig.4.6.1). These are thought to belong to the Igarapé Pojuca Group.

In the hills south of the CEDERE I village, the layering in the ironstones strikes E-W to NW-SE, dipping steeply (>80°) N and S, following the general trend of features observed on satellite and radar images (Figs.4.6.1 and 4.6.2). The rocks there are formed by white quartz in millimetre- to centimetre-scale (<1.5cm) bands interlayered with grey to red-grey bands of iron-rich minerals (Photo 4.6.12). These bands can be continuous with lengths of more than 1 m, but discontinuous bands are more common. Some parts of the rock are iron-rich with quartz bands effectively absent in hand-sample scale, but always with the primary lamination well preserved. Banding typically anastomoses and is cut by fractures and folded into kink bands on various scales (Photo 4.6.13). Microfaults with displacements of about 0.5- 4.0 mm cut the banding in several directions. These microfaults are sub-parallel to a large number of millimetre-scale quartz veins that are sometimes folded, obliquely cutting the banding.

The ironstones, observed mainly in the north of the region, show widespread evidence of ductile deformation. The mineral assemblage in these rocks is formed essentially by quartz and haematite plus magnetite. Compositional banding is mostly discontinuous and primary structures are preserved only locally (Photo 4.6.14). Quartz-rich bands comprise very fine to microcrystalline grains (0.05-0.30mm) displaying sharp to diffuse contacts with the iron-rich bands (Photo 4.6.14). Quartz crystals are strongly orientated

Photo 4.6.12- Typical ironstone outcropping in the Serra do Paredão region. Shear zone cut the rock, sub-parallel to the banding. A small scale fold is associated to the shear zone with dextral displacement (outcrop south of the Bica; see Fig.4.6.1).

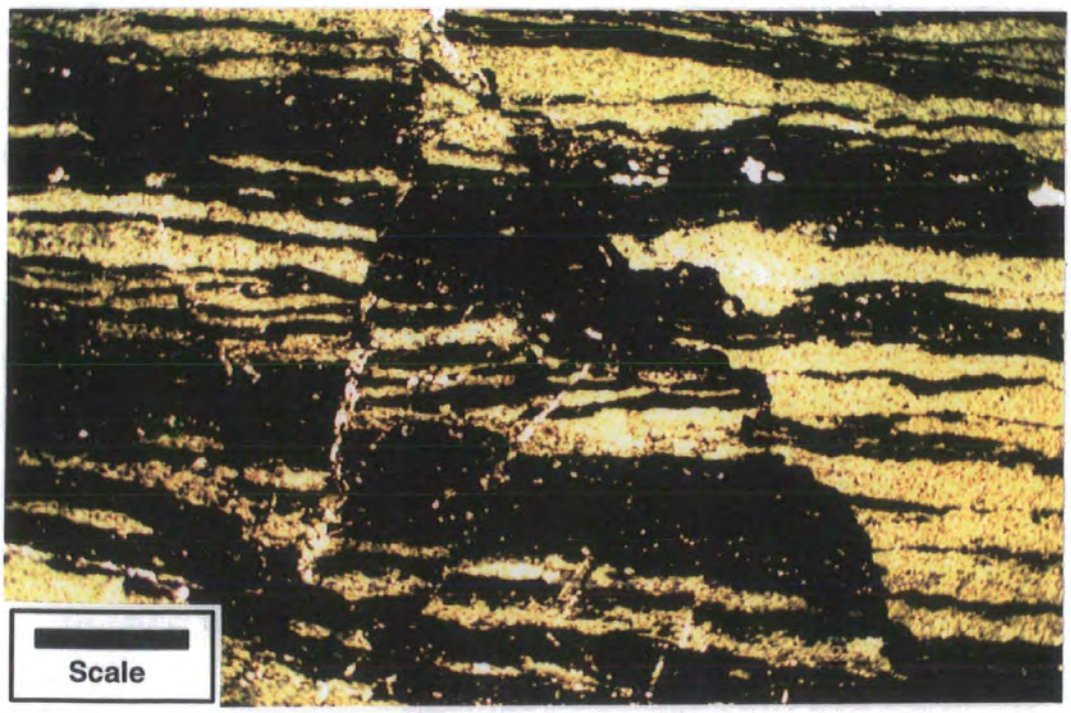

Photo 4.6.13- Kink bands in microscopic- scale deforming the banding of the ironstones (sample from outcrop at S of CEDERE I village; see Fig. 4.6.1). PPL, Scale bar=3mm.

defining a penetrative foliation with local development of ribbon crystals. The iron-rich bands are formed by red to dark-brown opaque minerals forming long braided, anastomosing or spindle-shaped mineral aggregates with very fine isolated crystals of quartz (ca. 0.10 mm). Quartz bands may display pinch-and-swell (millimetre-scale) structures, gently to open millimetre-scale folds, S-C fabrics, and shear bands. Recrystallisation is widespread in quartz bands where very fine sub-prismatic crystals show both irregular boundaries and granoblastic-polygonal aggregates, with incipient development of sub-grains. Quartz crystals may also show a strong undulose extinction.

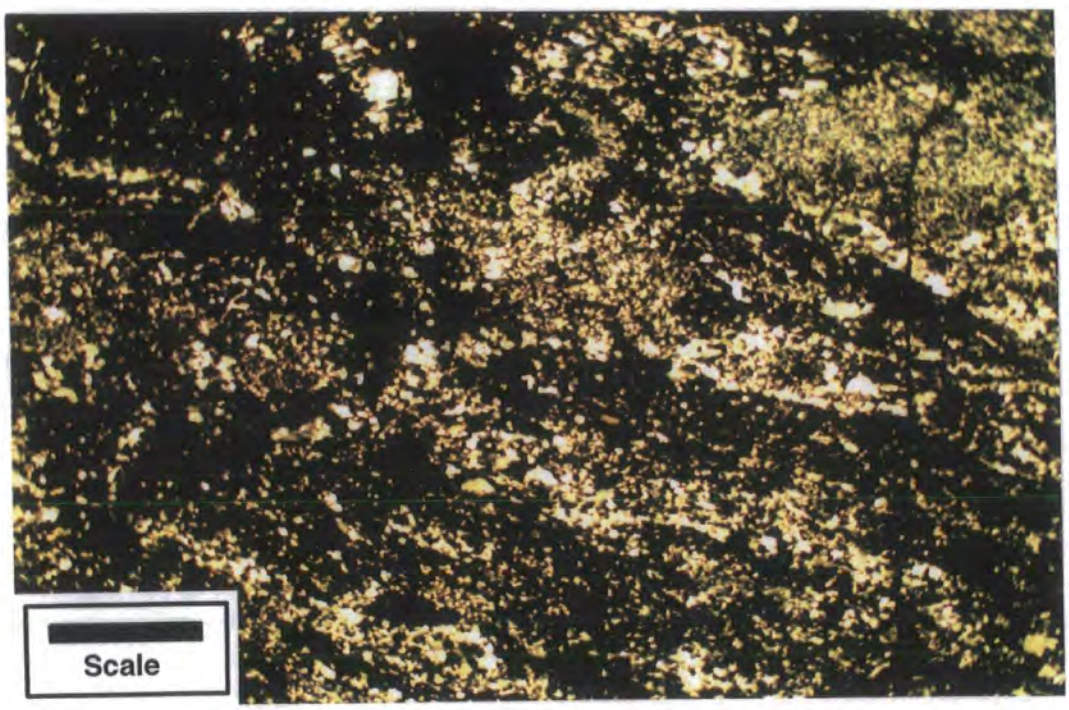

Photo 4.6.14- Photomicrography of the banding in deformed ironstones of the Igarapé Pojuca Group. The contact between Fe-rich and Mn-rich bands is diffuse with crystals strongly oriented (outcropping S of Bica; see Fig.4.6.1). XPL, Scale bar=3mm.

Ductile-brittle to brittle structures are also common. Centimetre-scale drag-folds are often associated with both sub-parallel and oblique ductile-brittle shear zones cutting the original banding (Photo 4.6.12). Most concordant shears are sinistral.

Widespread faults and microfaults show displacements which can vary from 0.5-10 cm. Most are orientated NW-SE, N-S and NE-SW, with sub-horizontal slickenlines. The N-S and NE-SW sets frequently display white

quartz forming centimetre- to millimetre-scale veins. Tension gashes indicate sinistral displacement along the 130°-150° direction. Millimetre-scale pull-apart structures are observed along small fractures, filled by quartz, indicating dextral displacement along NE-SW planes.

A more accurate map showing the correct distribution of these rocks is required to best understand the exact relationship between these two different sequences.

Ironstones also outcrop as N-S kilometre-scale lensoid bands bordering the NE area of the Estrela Granite, associated with volcanics, in contact with the Xingu Complex rocks (Fig.4.6.1). They are associated with amphibolites and schists (Barros,1991; Fig.4.6.7) thought to belong to the Igarapé Pojuca Group.

4.6.3.4- VOLCANICS (IGARAPÉ POJUCA AND GRÃO PARÁ GROUPS).

Volcanic rocks cover a large area in the Serra do Rabo region but few outcrops were found since these rocks are relatively susceptible to weathering. They cover the areas to the south, southwest and west of Parauapebas in the NW corner of the map shown in the Fig.4.6.1, and extend SE, along the Carajás Fault termination, contouring the southern margin of the Carajás Strike-Slip System.

They are closely associated with ironstone lenses and may occur in contact with amphibolites and schists of the Igarapé Pojuca Group, or with gneiss and granitoids of the Xingu Complex. In the central part of the Carajás Strike-Slip System they are covered by clastic sedimentary rocks of the Gorotire and Águas Claras formations. None of these contacts were observed in the field.

The best outcrops of these rocks occur along the road linking Parauapebas and Carajás villages. A few outcrops of volcanic rocks were also observed along several roads south of Parauapebas around São Geraldo, Forno Velho and Santa Inês farms (Fig.4.6.1).

Two types of volcanics occur in the area W of Parauapebas: (1) basic volcanics and (2) acid volcanics. (1) The basic volcanic rocks are mostly fine- to very fine-grained (sometimes vitreous or glassy) basalts, that are isotropic to weakly foliated; amygdaloidal and porphyritic types occur locally. They comprise pyroxene (augite?), biotite, plagioclase (An_{27}-An_{35}) and quartz. Zircon and tourmaline are common accessories. These minerals very often are deeply

altered to secondary chlorite, epidote, zeolites, muscovite, albite, calcite and tremolite-actinolite, illustrating the strong importance of later hydrothermal processes. Glassy and amorphous material may be found in association with both primary and secondary mineralogies. The most common textural type comprises isolated plagioclase phenocrysts set in a fine to very fine matrix composed by pyroxene, plagioclase and secondary minerals. An ophitic or sub-ophitic texture is sometimes present. Secondary minerals and quartz are also important components filling small cavities, amygdales, and microfractures.

(2) Acid volcanics are subordinate to the basic rocks and include rhyolites and rhyodacites. They comprise quartz (in bipyramidal crystals), plagioclase (An_{40} - andesine), hornblende, and rare biotite, with accessories: zircon, epidote, and opaques. Secondary alteration is widespread with higher percentages of zeolites and chlorite occurring compared to the basic rocks, and including occurrences of scapolite. Porphyritic textures are common. Tuffs and other pyroclastic rocks are also thought to be present in places, e.g. in cuttings along the Carajás Airport - Parauapebas road. More details about the petrography and petrology of these rocks is given in Wirth (1986).

Two different types of foliation occur in the volcanics of the Serra do Rabo region. Volcanic rocks associated with ironstones with ductile fabrics (Igarapé Pojuca Group) are pervaded by a mylonitic foliation. Those associated with the ironstones of the Grão Pará Group show little or no fabric.

An outcrop along the road between the places called "Bica" and "Km 45" in the central-south area of the region (Pt.05; Fig.4.6.1 and Fig.4.6.9) shows the relationship between the ironstones and volcanics of the Igarapé Pojuca Group. Along the road-cut an approximately 50m thick unit of ironstone is interbedded with the volcanics and phyllonites, cut by a NW-SE fault zone. The ironstone shows a predominantly sub-vertical banding, sub-parallel to the foliation present in the adjacent rocks. The volcanics in this outcrop are very weathered, with a red to white colour. They display relict igneous textures with tabular prismatic plagioclase in phenocrysts and subordinate small quartz grains; the rocks are extremely altered by weathering. The occurrence of quartz suggests an acid to intermediate volcanic rock. A weak foliation is present, orientated about 120°/ 70° SW defined by aligned clay-minerals and altered plagioclase crystals. Two sets of 20-30cm spaced fractures are orientated sub-parallel to the foliation (NW-SE) dipping at high angles NE and SW). Striations plunge mainly at low angles (<20°).

Two distinct fault zones lie close to the SW contact between the volcanics and the ironstones. They are about 10m wide and are formed by

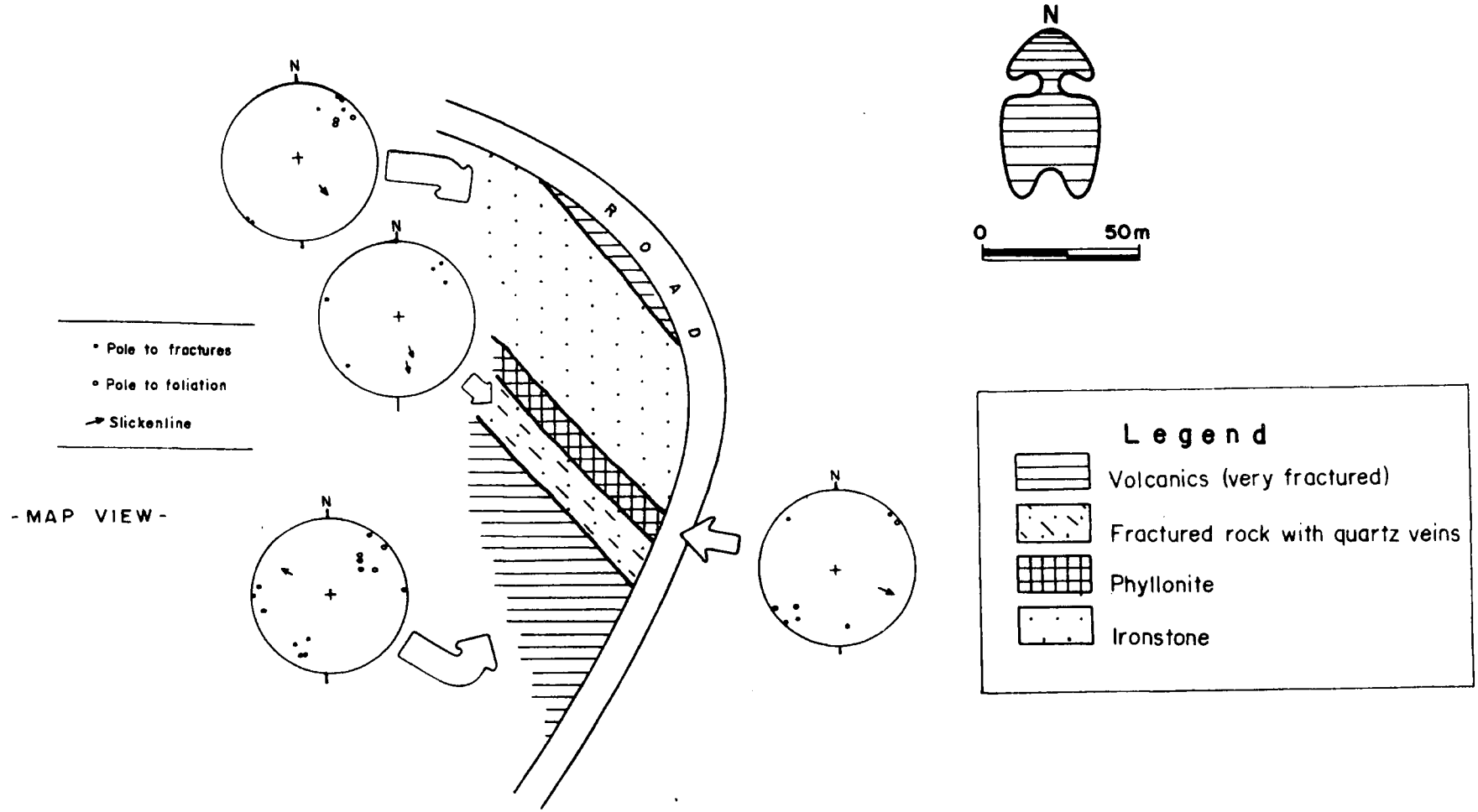

Fig. 4.6.9- Map of a road-cut in the south of the Carajás Strike-Slip System (Pt.06 on Fig.4.6.1) showing a sequence of volcanics interlayered with ironstones cut by a fault zone characterised by phyllonites and fractured rocks. Stereonets show orientation of mylonitic foliation and fractures with slickenlines present in these rocks.

phyllonites and cataclasites separated by an abrupt contact. The phyllonites are dark-red in colour and are deeply affected by weathering, showing a shallow disjunctive foliation formed by aligned phyllosilicates and quartz (Photo 4.6.15). The foliation is strongly disrupted by quartz veins which invade the cleavage domains sometimes forming ocellar structures 1-2cm across. The main foliation follows the general NW-SE orientation dipping steeply (>85°) to NE or SW. Discrete fractures are observed sub-parallel to the main foliation.

A unit of very fractured rock, about 12m wide occurs adjacent to the phyllonites. This rock is a light-yellow white, quartz-rich cataclasite containing millimetre- to centimetre-scale angular clasts of quartz and white millimetre-scale aggregates of phyllosilicate. An anastomosing millimetre-spaced cleavage pervades this rock, sometimes showing a red colour due to the percolation of iron-rich solutions during weathering, forming film-like precipitations. The orientation of the planar structures present in this fault zone is also concordant with the adjacent structures, trending NW-SE. Few lineations observed in the planes of the cataclastic foliation plunge with low angle towards the SE.

The structural trend in these rocks is also seen on a map-scale by the alignment of the hills and several sub-parallel lineaments observed in satellite images (Fig.4.6.2). Some of them are interpreted as faults, or lithological contacts, in the termination of the Carajás Fault.

Very altered volcanic rocks occur in a road-cut about 12 km south of the Santa Inês Farm, on the top of an approximately 50m high hill, ENE-SSW orientated (Pt.06 on Fig.4.6.1). This outcrop shows a grey - red, fine to very fine grained volcanic rock, cut by several fractures and faults (Fig.4.6.10). Blocks of a dark-grey basalt and quartz veins can be found in the hillsides. The basalt show a fine igneous texture with phenocrysts of plagioclase in a very fine to vitreous matrix. There is no evidence of fabrics or other structures preserved.

In the southern part of this outcrop it is possible to distinguish two tabular layers of different rocks, orientated E-W, dipping 50° N (Fig.4.6.10). The lower unit has a thickness of about 4m, and is formed by a yellowish fine rock extremely altered by both hydrothermal and weathering processes. The mineralogy is mainly quartz (>40%) and clay minerals. This rock is strongly fractured with the main fractures orientated sub-parallel to the contacts (080°/ 50° NW) but other sets are also found, particularly those with N-S trend (see stereonet on Fig.4.6.10 and Photos 4.6.16 and 17). Quartz veins in this rock are centimetre-scale features that are discontinuous and sub-parallel to these fractures. The southern contact of this rock with the altered volcanics is a strike-slip fault orientated 082°/52° NW (striations plunging 10°/76°). The rock within

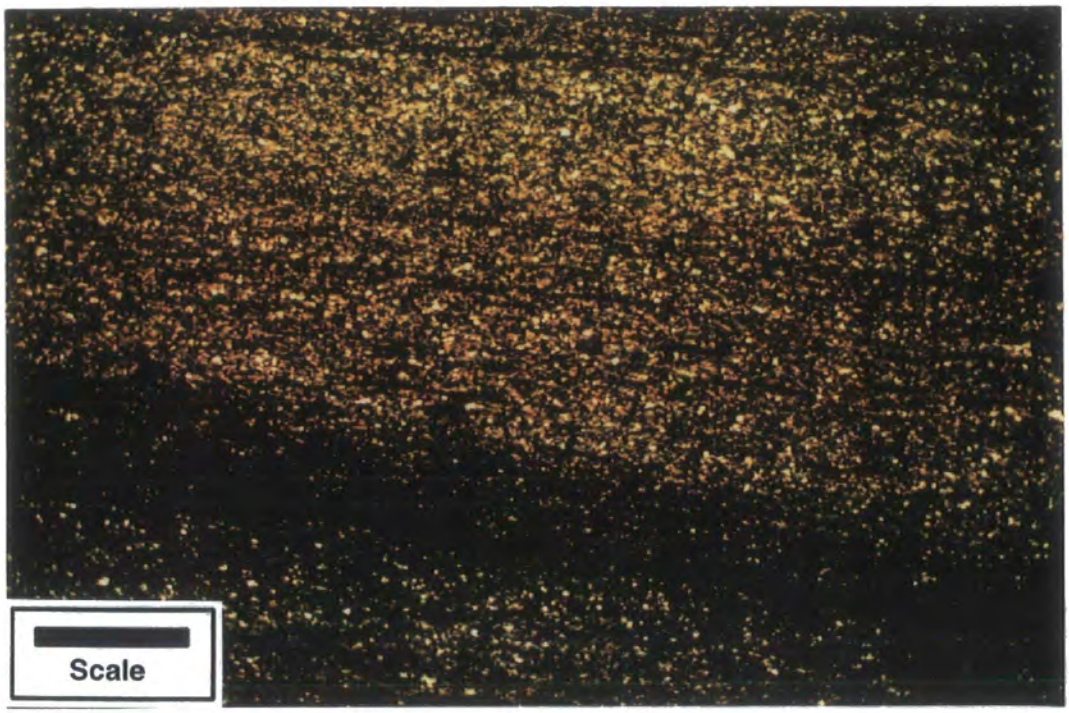

Photo 4.6.15- Photomicrography of phyllonites developed in an about 5m wide zone of deformation cutting the volcanic rocks in the Serra do Rabo region. (Pt.05, Fig.4.6.1 and Fig.4.6.8). XPL, Scale bar= 1.2mm.

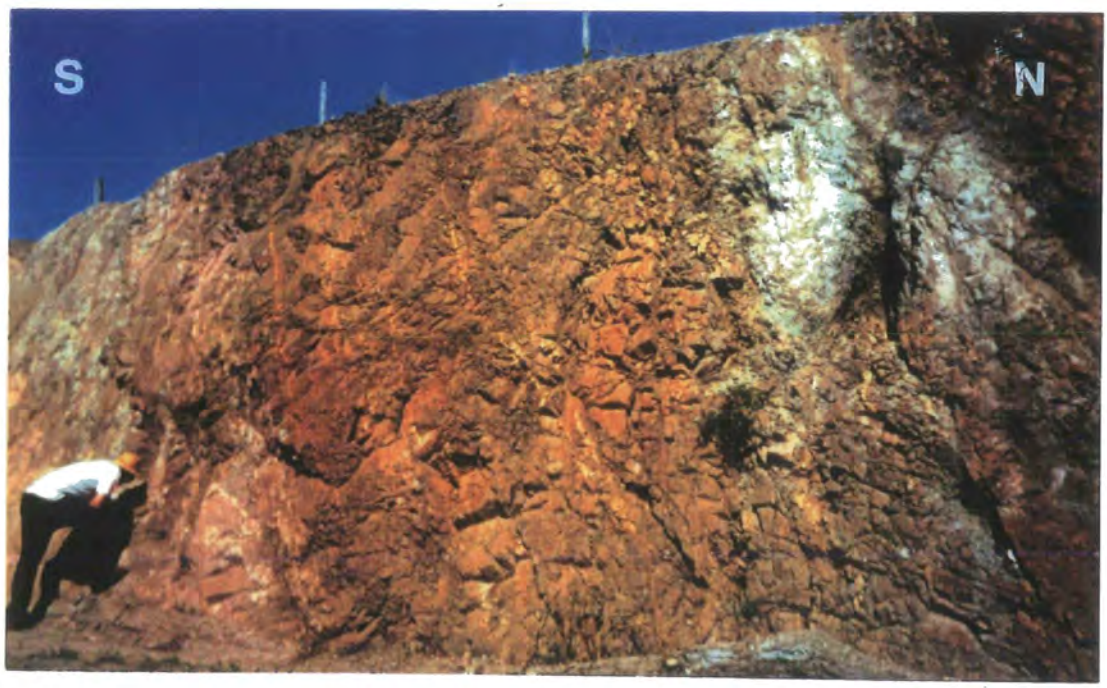

Photo 4.6.16- Zone of alteration and intense fracturing within the volcanic rocks outcropping in the region along the Carajás Fault zone (Pt.06, Fig.4.6.1).

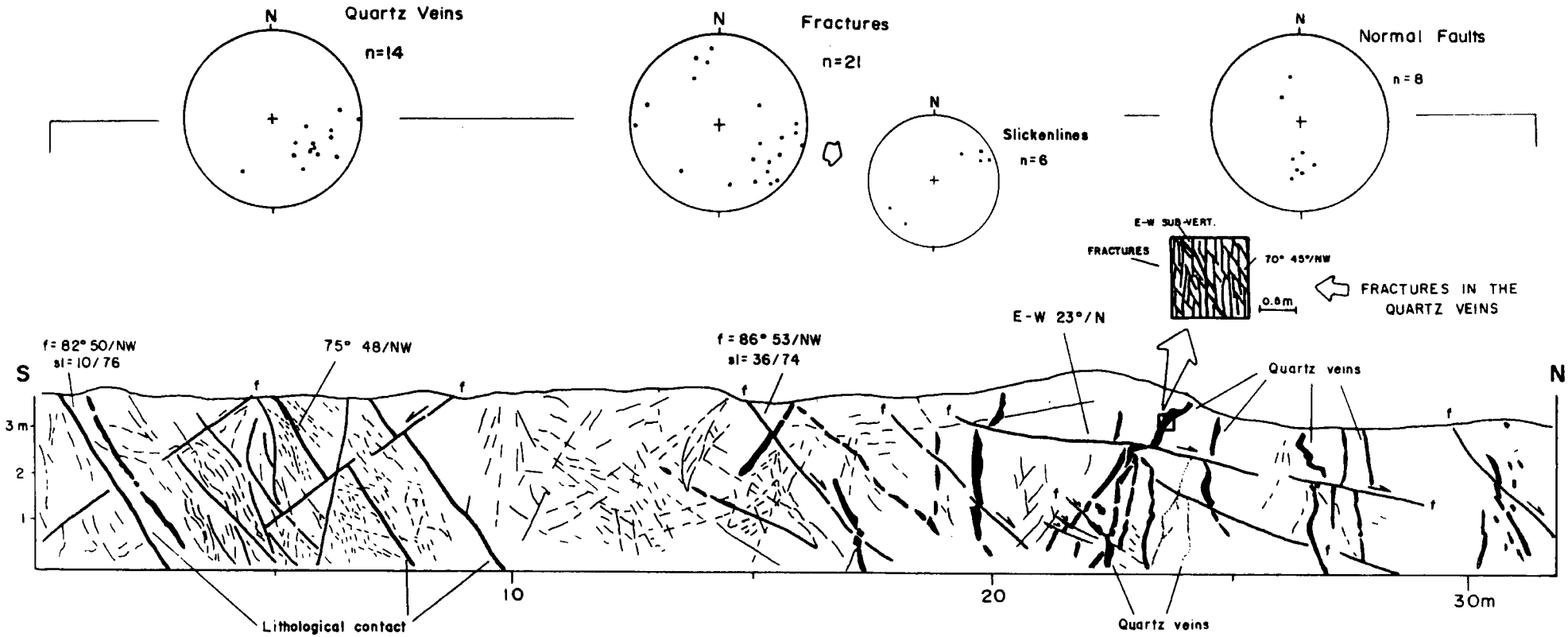

Fig.4.6.10- Sketch section representing altered volcanics intensively cut by faults (f) and quartz veins (in heavy-black) observed in Pt.06 (Fig. 4.6.1). Fine lines represent primary structures preserved.

the fault zone is very fractured and altered with a distinctive white colour and essentially kaolinitic with fine quartz grains and also cut by small quartz veins (Fig.4.6.10).

Quartz veins and micro-veins are strongly orientated NE-SW dipping between about 30° and 90° (see stereonet on Fig.4.6.10), and pervade all rocks. They are from a few centimetres (>1cm) to about 20 cm thick. Fractures in the quartz veins are centimetre-spaced and orientated roughly 090°/ 80 N and S; 070°/ 45° NW; and N-S sub-vertical (see stereonet on Fig.4.6.10).

A later set of low angle normal faults cuts both lithological contacts, strike-slip faults and quartz veins (Fig.4.6.10). These faults are orientated E-W, dipping 40°-20° N and S, although those dipping toward N are dominant (see stereonet on Fig.4.6.10). They displace quartz veins at least 30cm, and offset lithological contacts 0.5m. Striations suggest normal movements with a small component of strike-slip.

4.6.3.5- SANDSTONES AND CONGLOMERATES

The occurrence of sandstones and conglomerates in the SE part of the Serra do Rabo region was first recognised by DOCEGEO (1988).

During this work, two rather different types of sandstones were found on the Serra do Rabo area. One type is sericitic quartz arenites and sublitharenites associated with marine, transitional and fluvial facies belonging to the Archaean Águas Claras Formation (Nogueira, 1995; Truckenbrodt *et al.*,1996). The other, an unusual and little known type in the current literature, is arkosic wackes and arkoses correlated in this work with those belonging to the Gorotire Formation.

The sandstones, similar to those of the Águas Claras Formation (Pt.07 in the Fig.4.6.1), correspond to a sequence of yellow-red fine-grained sandstones in 30-40 cm beds, together with oligomictic paraconglomerates with rounded quartz pebbles (<1cm diameter) dispersed in a fine to very-fine sandy matrix. The sandstones are very poorly sorted, in which fine to very-fine quartz grains (>85-90%), and muscovite (>5% in volume), support rounded to angular grains of quartz and rock fragments with diameter between 0.5mm to 3mm, making up around 1 to 5% of the rock. A variant of this rock type occurs as blocks adjacent Pt.07 (Fig.4.6.1), displaying a very-fine sandy to silty matrix. This rock is yellow-green, containing rock fragments similar to the rocks described above. Small voids (<1mm) in this rock are filled by micro-drusy quartz impregnated by Fe-rich solutions.

The sandstones thought to belong to the Gorotire Formation are mostly purple arkosic wackes to arkoses with medium to coarse grain sizes, that are moderately- to poorly-sorted, with quartz around 30-35%, feldspar with almost the same proportion of quartz, and rock fragments summing above 5%. Matrix varies from 5% to about 20% in different layers.

Excellent in-situ outcrops of the Gorotire Formation arkosic rocks occur east of the Parauapebas River around the CEDERE I village, and at several points along the SE region of the Serra do Rabo where it is relatively well exposed, for example, around de São João Farm and to the NE of Forno Velho Farm.

Bedding in the sandstones of the Gorotire Formation around the CEDERE I village, is orientated NE-SW and NW-SE, dipping at low angles (<14°) N (Photo 4.6.18). In this area, they clearly unconformably overlie deformed rocks of the Grão Pará Group, but the contacts are not exposed. Blocks of these purple arkoses with cross stratification are also present in a small area, between the ironstones of the Grão Pará Group and gabbros, NE of Forno Velho Farm.

A quite different facies associated with these arkosic wackes and arkoses comprises purple lithified polymictic, grain-supported conglomerates with pebbles and boulders of several rocks: volcanics, granites (both isotropic and foliated), gneisses, schists, amphibolites, pegmatites, banded ironstone, chert, Mn-ore fragments, quartz veins and quartzites (Photo 4.6.19). These pebbles and boulders can vary from 2-3cm to >30cm in diameter. They are mostly rounded or subrounded with pebbles in spherical to oblate and even bladed shapes, depending of their parental rock type. The matrix is formed by granules and coarse to very coarse particles of rock fragments (>70%), quartz, feldspar and traces of clay minerals (?kaolinite). Small proportions of cement (<5%) are observed and pores are almost absent. The thickness of beds showing different proportions pebbles or boulders and matrix can vary from 0.3m to 3.0m. Thicker layers have bigger boulders while thinner layer have predominantly granules and very-coarse lithic sand particles, forming a very poorly sorted sandstone. The bedding observed in an excellent outcrop in a quarry (Pt.08 in Fig.4.6.1, known as "Jazida do Romário") displays a NE-SW strike, dipping 30°-40° SE.

Tectonic structures in both sandstones and conglomerates are largely absent. Fractures can be found few localities but in general the rocks are relatively free of faults. Sets of NW-SE fractures are present in some outcrops, spaced a few centimetres to 3-4m apart. There are no offsets along these

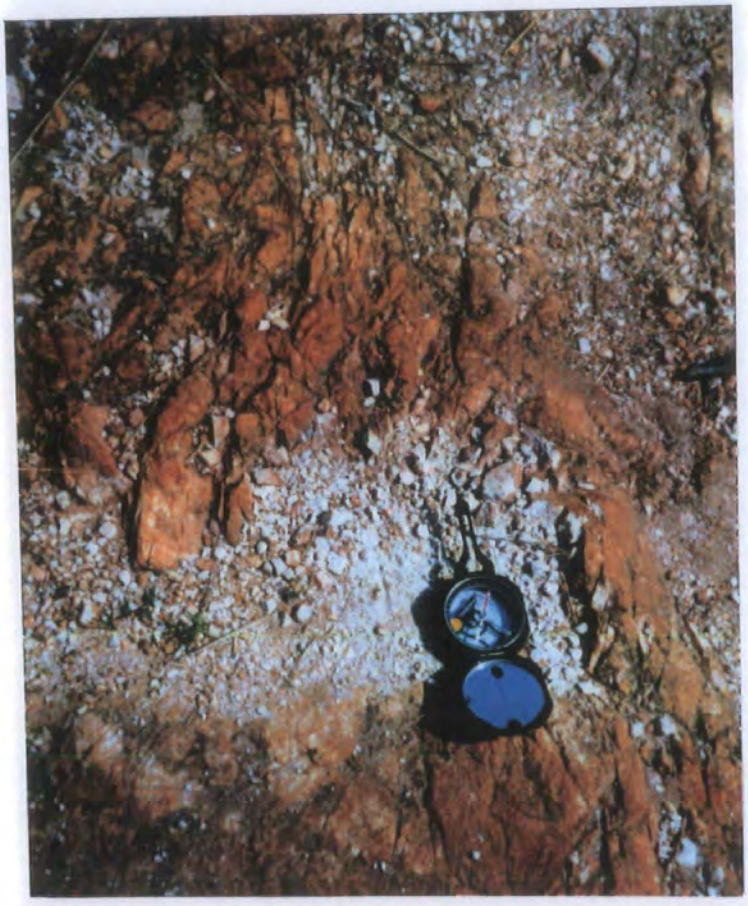

Photo 4.6.17- Intense fracturing in zones cutting the volcanic rocks along the branches of the Carajás Fault. Quartz veins are massive and abundant (Pt.06, Fig. 4.6.1).

Photo 4.6.18- Immature sandstones of the Gorotire Formation. Trough cross-bedding in 10-20cm sub-horizontal sets form the main primary structures present in these rocks. Outcrop located about 2 km SE of the Bica (see map on Fig.4.6.1).

fractures. Some are filled by hydrothermal material consisting of concentrations of fine-grained epidote and quartz.

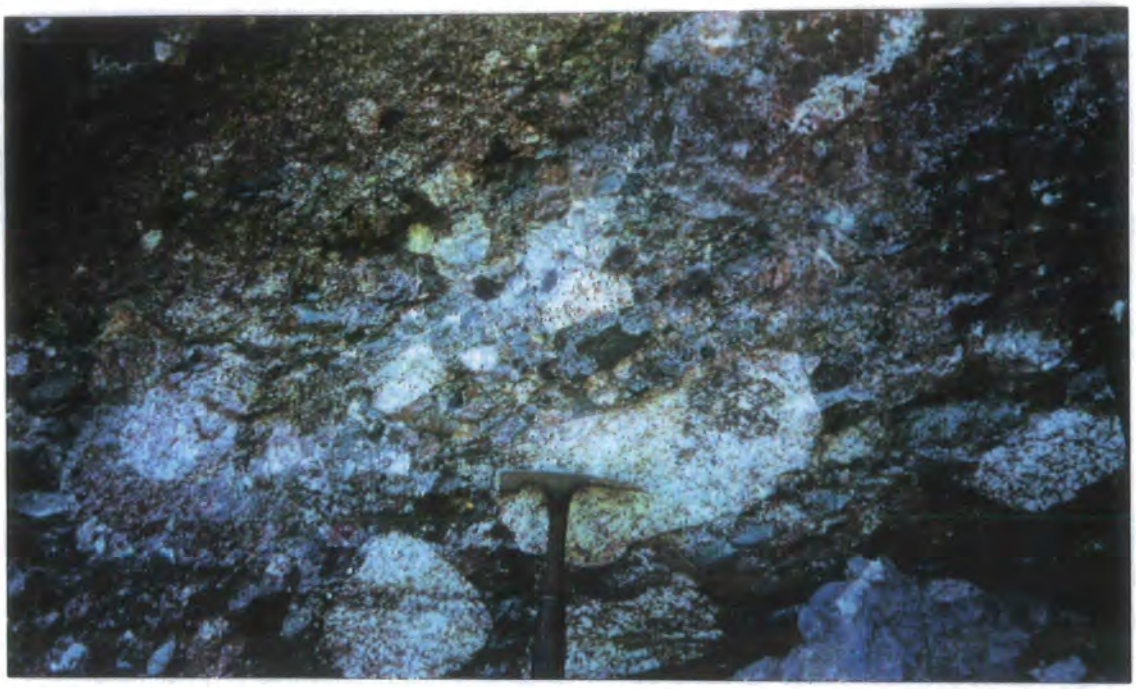

Photo 4.6.19- Polymictic conglomerate with pebbles and boulders of several lithologies (Gorotire Formation). Note the presence of the bedding separating different layers (Pt.08, Fig.4.6.1).

4.6.3.6- GABBROS

Two major units of gabbroic rocks occur in the Serra do Paredão region (Fig.4.6.1). The most important lies adjacent to the Santa Inês Farm, about 20 Km south of Curionópolis. Another is a small intrusion about 3Km south of Parauapebas, along the Parauapebas River.

The intrusion outcropping around Santa Inês Farm (Fig.4.6.1), forms an approximately NE-SW elongate body, 20 Km long and 2 Km wide (Araújo and Maia, 1991). It is emplaced along the contact between garnetiferous quartz-schists of the Igarapé Pojuca Group, and granitoids of the Xingu Complex to the SE. Part of this rock is also in contact with volcanics of the Grão Pará Group in the SW. They are probably partly covered by clastic sedimentary rocks. DOCEGEO (1988) was the first to map this intrusion in the Serra do Rabo region.

This gabbro corresponds to a medium to coarse dark greenish-grey rock, formed by plagioclase (ca. 50%), pyroxene (40%), and K-feldspar, olivine, quartz, biotite, chlorite, sericite, iddingsite and opaques in small percentages. The plagioclase occurs as euhedral crystals with size varying from <0.4mm to porphyritic ones that can be >5.0mm (1.0-2.0mm in average). Their composition can vary between andesine and labradorite (An_{50}). Sericite is a common secondary mineral in plagioclase grains. The pyroxene (?augite) appears in anhedral to subhedral crystals with sizes ranging from 0.4mm to 6.0mm, some with a distinct Carlsbad twinning or compositional zoning. Brown biotite is very often observed as a secondary mineral partly replacing the borders of pyroxene crystals. A light chloritization may be observed in both pyroxene and biotite. Quartz displays granophyric textures in association with a few K-feldspar crystals observed between plagioclase crystals.

The gabbro outcropping in the Parauapebas River is 3Km by 500m wide body, orientated N-S, intruded into the volcanic rocks of the Grão Pará Group (Fig.4.6.1). It was first mentioned by Matta and Teixeira (1990) who referred to two textural types: gabbro and microgabbro. Their mineralogy is very similar to the gabbros observed at the Santa Inês Farm outcrop, but olivine occurs in disseminated aggregates, giving evidence of marginal corrosion. Most olivine crystals are altered to iddingsite.

There is no evidence of metamorphic reactions or deformation in these rocks. In those gabbros outcropping around the Santa Inês Farm, a very weak foliation is defined by an alignment of plagioclase crystals. Araújo and Maia (1991) suggest a correlation of these rocks with those of the Grão Pará Group.

4.6.3.7.- THE CARAJÁS FAULT

The main lineaments observed on satellite and radar images of the Serra do Rabo region around the E termination of the Carajás Fault are shown in Fig.4.6.2. Three sets of lineaments are recognised trending NE-SW, WNW-ESE and NW-SE. These sets of structures converge in a main NW-SE segment towards the W of the region. NE-SW and N-S lineaments tend to cross other sets probably reflecting later development or kinematic activity. A well developed set of curved lineaments occurs in the SW of the main NW-SE branch of the Carajás Fault termination (Fig.4.6.2). This feature may indicate kilometre-scale folds, but there are no field data to confirm this hypothesis.

The Carajás Fault termination is poorly exposed in the field but its presence is indicated locally by sub-vertical bedding in the ironstone units and sub-concordant cataclastic fabrics adjacent to denser zones of lineaments (e.g. Pt.05, Fig.4.6.1). Slickenlines along subsidiary fault planes and fractures associated with this major fault, are relatively scarce. Where found they suggest a predominant strike-slip displacement, but oblique-slip indicators are also frequent (Pt.05; Pt.06).

Voluminous quartz veins are orientated parallel to the trend of the Carajás Fault branches, especially adjacent to their terminations in the east. Examples of these veins are exposed in outcrops at Pt.06 and Pt.09 (Fig.4.6.1). The latter locality is close to Fomo Velho Farm where veins vary from millimetres to 20 cm in thickness. They are densely concentrated in a very altered rock where only quartz and a yellow-white clay-mineral are present (Photo 4.6.20). The veins are orientated about 145°/ 80° NE or SW. They are strongly fractured. Faults sub-parallel to the veins, carry weakly preserved slickenlines with low (<20°) plunges, cutting both the quartz veins and the altered rocks (Photo 4.6.20). The presence of quartz veins with prismatic drusy crystals is common (Photo 4.6.21).

4.6.4- DISCUSSION.

The present study has examined relatively few outcrops in the Serra do Rabo region but some comments regarding both the lithological distribution and stratigraphy of the rocks as described by previous authors are worthwhile.

-Xingu Complex rocks: The variably deformed granitoids of the Xingu Complex preserve asymmetric folds, K-feldspar porphyroclasts and S-C fabrics, suggesting mainly sinistral ductile shear kinematics, with a small component of reverse flow. This episode of deformation has been recognised widely in the Carajás region and is related here to deformation along the Itacaiúnas Shear Zone, ca.2.8 Ga. This has been suggested by many authors (e.g. Machado *et al.*, 1991; Costa *et al.*, 1995).

These rocks have undergone amphibolite facies regional metamorphism preserving a typical assemblage of amphibole + quartz + plagioclase + microcline + biotite. At least one episode of retrograde metamorphism, associated with hydrothermal alteration, is associated with a later assemblage

Photo 4.6.20- Altered rock densely cut by quartz veins and fractures observed in Pt.09 (Fig.4.6.1), along a branch of the Carajás Fault termination.

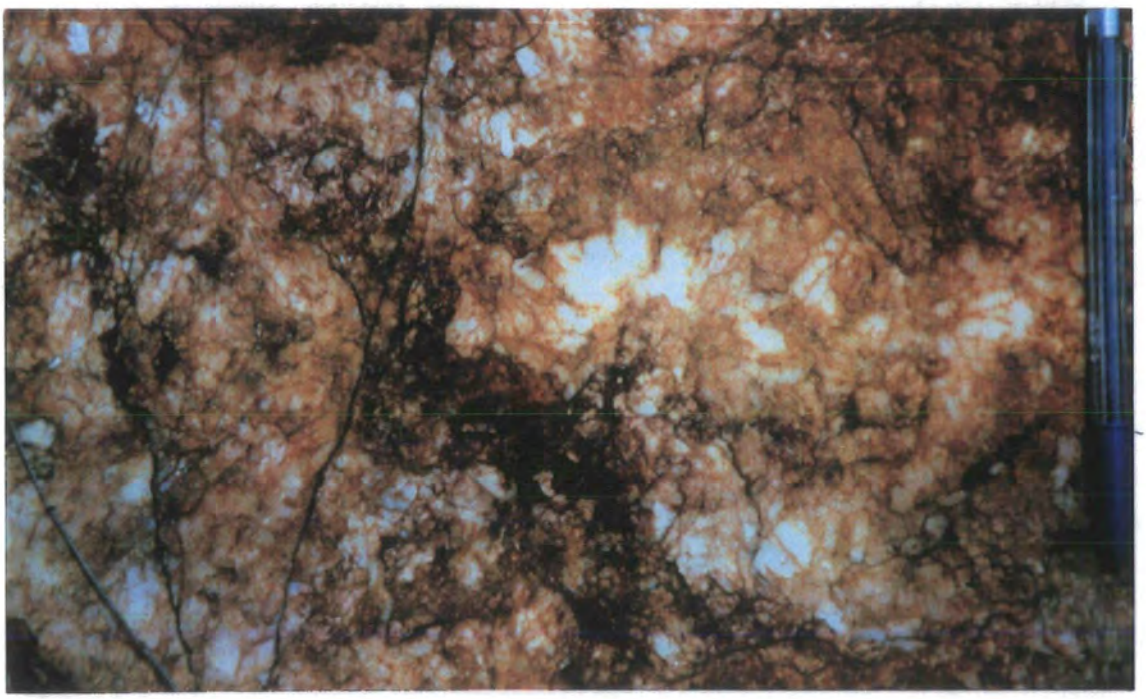

Photo 4.6.21- Quartz vein with prismatic crystals indicating opening of voids during fluid injection related to the Carajás Fault in the Serra do Rabo region (Pt.09, Fig. 4.6.1).

of epidote + chlorite + muscovite, found variably developed throughout these rocks.

The mylonitic foliation (S), observed as a pervasive structure, is predominantly NW-SE orientated, dipping at high angles. This fabric is associated with a poorly developed stretching lineation which has a somewhat variable orientation. Several later phases of deformation cross-cut or reactivate the earlier mylonitic fabrics. Based on the data observed in some outcrops it is possible to propose the following relative chronology of deformation:

1- Earlier development of the mylonitic fabrics accompanied by dynamic recrystallisation at high temperatures (Itacaiúnas Shear Zone).
2- High temperature veins, including quartz and quartzo-feldspar leucosomes injected and deformed both by non-coaxial and coaxial ductile and brittle-ductile deformation. Non-coaxial deformation was predominately sinistral, while the coaxial invokes N-S shortening and E-W extension along the regional foliation.
3- Local N-S brittle-ductile structures developed with mostly dextral displacements.
4- Later quartz veining took place, along N-S and NNW-SSE directions. These veins were later displaced dextrally by NE-SW brittle-ductile shear zones.
5- An important N-S fracturing reactivated early N-S discontinuities and formed new fractures; dextral offsets are more common.

At least two sets of E-W fractures, sub-parallel to the mylonitic foliation were developed, but their relationship to other fracturing events can not be defined due to the lack of features cross-cutting other structures. One occurs in almost all mylonite outcrops, which are sub-parallel to the main foliation while a second set, with a characteristic low angle dip and normal displacement is observed in close association with the Carajás Fault termination. This last set seems to be later in relation to the first as can be observed at the Pt.06 (Fig.4.6.1).

- ***Estrela Granite Complex:*** The shape of the pluton is poorly known although it appears to be slightly elongate and concordant with the regional structures, including the Carajás Fault termination. It intrudes in the Xingu Complex and the Igarapé Pojuca Group rocks producing a quartz-biotite-cordierite hornfels aureole (Barros, 1991).

A pervasive steeply-dipping ductile deformation fabric in the granitic rocks is mainly E-W orientated, dipping S or less frequently N. This orientation is concordant with the orientation of the foliation in the country rock. Mutual shear zones were developed both inside the pluton and in the country rocks (cf. Costa *et al.*, 1991), which show predominantly oblique sinistral kinematics with components of top to the S reverse flow. Changes in the foliation trend close to the N border and may reflect a forceful emplacement mechanism adjacent to the N-S apophisis mapped in the central-north portion of the pluton.

These features are consistent with, though not diagnostic, of syntectonic granite emplacement relative to the main ductile episode of regional transpressional deformation which took place ca. 2.8 Ga, forming the Itacaiúnas Shear Zone. The problem of space creation along oblique or compressional shear zones has been considered to be of lesser importance during granite emplacement since sheets can intrude along foliation weaknesses rather than being controlled by stress field, following a non-Andersonian behaviour (Hutton, 1988*b*; 1992). Similar mechanisms have been reported in the emplacement of several syntectonic granites especially in oblique to strike-slip shear zones (e.g. Main Donegal granite, Ireland - Hutton, 1988*b*; Ox Mountains, western Ireland - McCaffrey, 1992; Armorican Massif, NW France - D'Lemos *et al.*,1992).

The age of this granite is thought to be 2527±34 Ma (Rb-Sr, whole rock; Barros *et al.* 1992*a*). This has been correlated with the age of a similar foliated granite named the Old Salobo Granite (Lindenmayer, 1990) outcropping in the Igarapé Salobo region, that which dated as 2573±2 Ma (U/Pb, zircon; Machado *et al.*, 1991). Conversely, an age of 2859±2 Ma has been related to a major episode of migmatization and deformation in the Xingu Complex rocks (Lindenmayer, 1990; Machado *et al.*, 1991; Lafon and Macambira, 1992). This age has been attributed to the main episode of deformation and metamorphism, including a regional episode of sinistral transpression in the basement discussed in the present work. As the Estrela Granite Complex rocks were emplaced syntectonically into the Itacaiúnas Shear Zone (ca.2.5 Ga) as proposed by Barros (1991), this suggests that the ductile deformation took place for more than ca.300 Ma, or that at least two episodes of reactivation occurred, as proposed by Machado *et al.* (1991).

-Ironstones, volcanics and gabbroic rocks: Two different groups of volcanics and ironstones are found in the Serra do Rabo region. Essentially they are distinguished by the following characteristics described in the Table 4.6.1.

Type I	Type II
1-few primary structures preserved	1-abundant primary structures
2-penetrative foliation	2-non-penetrative foliation
3-steeply-dipping planar fabrics with constant orientation	3-planar fabrics variable in orientation
4-S-C fabrics common	4-S-C fabrics rare
5-penetrative high to moderate temperature mylonitic fabrics with ultramylonites often present	5-low temperature fabrics - non-penetrative, restricted to narrow zones, protomylonites often present
6-often deformed by several later episodes of brittle-ductile and brittle deformation	6-deformed mainly by brittle-ductile and brittle deformation
7-strong to moderate recrystallisation	7-moderate to absent recrystallisation
8-medium to low metamorphic grade including hydrothermal alteration	8-medium to very low metamorphic grade. Hydrothermal alteration predominant

Table 4.6.1- Main characteristics of the ironstones in the Serra do Rabo region.

Type I rocks are correlated with the Igarapé Pojuca Group (e.g. DOCEGEO, 1988) while Type II rocks are correlated with the Grão Pará Group (e.g. Wirth *et al.*, 1986). The contact relationships and distribution of these two sets of rocks are difficult to establish in the Serra do Rabo area. This problem is most obvious in the volcanic rocks since probably at least part of the Grão Pará Group volcanic rocks are emplaced into rocks of the Igarapé Pojuca Group as irregular 3D bodies such as sills, flows, laccoliths, etc. Cross-cutting relationships between these units were not observed in the field and their original geometry is unclear in part due to later deformation. The majority of authors refer to the contact as transitional, with the two units representing different facies of just one sequence (e.g. Hutchinson, 1979; Hirata *et al.*, 1982; DOCEGEO, 1988; Araújo and Maia, 1991; Costa *et al.*,1995). A more recent idea has been proposed by Barros (*personal communication*) that admits the possibility that the Igarapé Pojuca Group represents a thermal alteration of the Grão Pará rocks due the emplacement of granites ca. 2.5 Ga. A similar idea was proposed by Lindenmayer *et al.* (1994*a*) the rocks in the Salobo region.

Dykes and small gabbroic bodies were later emplaced into both volcanic sequences. The Santa Inês Gabbro is the best example of one of these later intrusions whose age, stratigraphical position and distribution in the area is rather speculative.

-Sandstones and conglomerates: Two different sequences of clastic rocks are present in the region. According to the present field observations and data published by Nogueira *et al.* (1995) the main differences between these sequences are summarised in Table 4.6.2.

Águas Claras Formation	Gorotire Formation
1-textural and compositional maturity is common.	1-rocks commonly of very low compositional and textural maturity
2-predominantly (sericitic) quartz arenites, sublitharenites and shales	2-predominantly arkosic wackes, arkoses and polymictic conglomerates or fanglomerates.
3- platform, littoral and distal braided fluvial deposits.	3- braided fluvial to alluvial channels and piedmont zone deposits.
4-May be deformed by folding, faulting and bedding rotations	4- undeformed, sub-horizontal beds
5-wide distribution (>1300 Km^2)in the central region of the Carajás structure	5-widespread in the region. Map distribution not know precisely but apparently more confined outcrop (<200Km^2)
6-cut by ca. 1.8 Ga granitic plutons and dykes	6-adjacent to the granitic plutons, apparently not intruded in the sequence (?)(see 8 below)
7-cut by ca. 2.6 Ga gabbroic sills	7-sills or dykes not observed
8- monomictic conglomerates with quartz pebbles	8-shows pebbles and boulders of several types of rocks including granites similar to those with ca. 1.8 Ga in age

Table 4.6.2- Differences between the Águas Claras and Gorotire rocks.

The Gorotire Formation comprises two main facies in the Serra do Rabo region. The proximal facies is a purplish polymictic conglomerate observed in several localities mainly to the SE of the Serra do Rabo region and exposed in the quarry known as "Jazida do Romário", about 12 Km SE from São João Farm. Isolated blocks of these rocks are found also in the area south of the Carajás region (Geol. Anselmo Soares, *personal communication*). They comprise centimetre- to metre-scale beds of polymictic conglomerates with rounded to sub-rounded pebbles and boulders of several rock types set in a coarse to very-coarse matrix. The relative proportions of rock fragments, quartz, feldspar and clay minerals indicate a tendency to a coarse lithic greywacke composition for these rocks. The only primary structure preserved corresponds to the bedding separating different strata with different sizes of pebbles and boulders. Palaeocurrents measured from pebble imbrication indicate transport from NE to SW. This facies is interpreted as being deposited in alluvial fans. Its thickness is difficult to evaluate, but it is possible to estimate as at least >35m from the outcrop in the "Jazida do Romário".

The distal sequence is represented by purplish sandstones covering an area of about 200 Km^2 along the E side of the Parauapebas River, in the central part of the Carajás structure. Other good outcrops occur along the E and SE area of the Serra do Rabo region. They are mostly medium to coarse arkosic wackes displaying a characteristic trough cross-bedding in centimetre to metre thick sub-horizontal beds. This distal facies can be interpreted as being

related to braided system channels. Its thickness can be estimated to be >30m, as measured in outcrops in the SE area of the Serra do Rabo region.

The spatial relationship between these two facies were not observed directly, but field surveys suggest that they are laterally transitional with the conglomerates probably overlapping partly the fluvial sandstones. This idea is illustrated in the Fig.4.6.11.

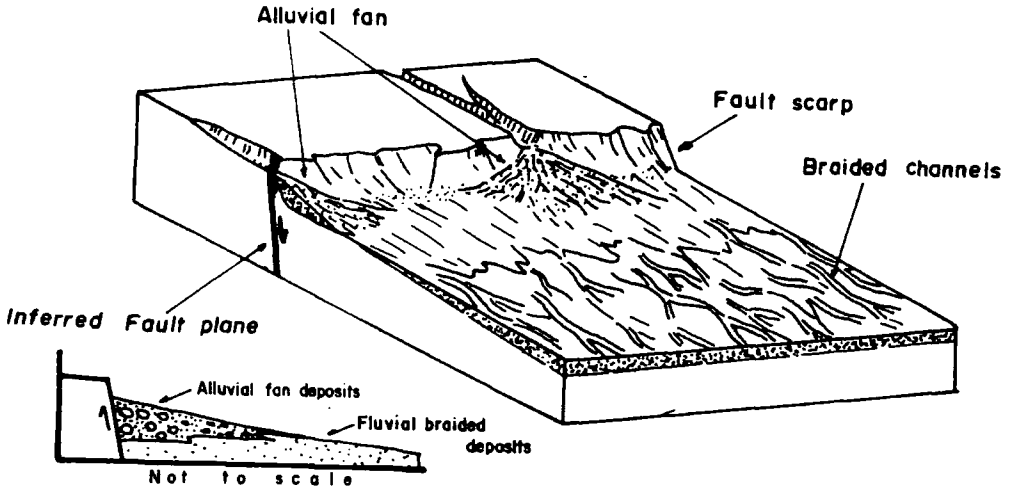

Fig.4.6.11- Cartoon representing the geometry and distribution of the alluvial fan and braided channel facies interpreted in the Gorotire Formation of the Serra do Rabo region.

The sedimentological features of these two facies strongly suggest significant tectonic activity coeval with deposition. Reactivation of parts of the Carajás Fault System may well have controlled deposition.

The age of the Gorotire Formation rocks outcropping in Carajás is uncertain. Earlier authors suggest ages extending from Pre-Silurian (Beiseigel *et al.*,1973) to Middle Proterozoic (Hirata *et al.*,1982) but most authors did not separate these rocks from those of the older Águas Claras Formation or consider them part of the Rio Fresco Formation or Group (e.g. DOCEGEO, 1988; Araújo and Maia, 1991).

Field observations suggest that the Gorotire Formation is younger than 1.8 Ga based on the assumption that these rocks were not observed being cut by the Early-Middle Proterozoic plutons, and that they carry pebbles very similar to those granites. It is important to emphasise that these assumptions need to be more accurately examined due to the resemblance, in hand samples, between some granites from the basement and those of the Middle Proterozoic

suite. In addition, the apparent lack of cross-cutting relationships with the Proterozoic granites may also reflect a lack of sufficient mapping in the region. Nevertheless, on the basis of the existing evidence, the present author suggests a Middle Proterozoic age of deposition.

4.6.5- CONCLUSIONS

1. The Xingu Complex rocks in the Serra do Rabo area are pervasively deformed by sinistral transpressional movements along the Itacaiúnas Shear Zone (ca. 2.8 Ga).

2. Metamorphism affecting the granitoids of the Xingu Complex, the Plaquê Suite rocks, the amphibolites, ironstones and volcanics of the Igarapé Pojuca Group, and the granites and gneisses of the Estrela Granite Complex varies from medium to high grade. It is a high temperature metamorphism, coeval with development of mylonitic fabrics. This episode was followed by at least one later regional episode of retrograde hydrothermal alteration.

3. The syntectonic emplacement of the Plaquê Suite granites (Araújo *et al.*, 1988) is supported but more studies are necessary to reinforce this view.

4. The Estrela Granite Complex may have been intruded syntectonically in relation to later episodes of deformation along the Itacaiúnas Shear Zone (Barros, 1991). A sinistral-reverse oblique-slip transpressional regime is thought to be dominant during emplacement.

5. The suggested intrusion age of ca. 2.5 Ga for the Estrela Granite Complex implies that deformation in the Itacaiúnas Shear Zone took place during at least 300 Ma either as a continuous episode or as separated reactivation events.

6. Later reactivation of the early mylonitic fabrics, by brittle-ductile and brittle, coaxial and non-coaxial deformations, is accompanied by folding, fracturing and quartz vein injections. Sinistral fabrics are predominant, associated with non-coaxial strain, while coaxial deformation took place locally with shortening axes orientated E-W. Brittle reactivation of early mylonitic fabrics is associated with the development of mainly sinistral faults.

7. The schists, metavolcanics, ironstones and metasedimentary rocks in the northern area of the region, are most like part of the Archaean Igarapé Pojuca Group, rather than being related to greenstone sequences as suggested by some previous workers.

8. Rocks belonging to both the Igarapé Pojuca Group and Grão Pará Group are recognised in the Serra do Rabo region. They are lithologically similar comprising mainly ironstones and volcanics sequences. They are distinguished on the basis that rocks of the Igarapé Pojuca Group have generally undergone higher grades of metamorphism, with mylonitic fabrics being dominant whilst the lower grade Grão Pará Group often preserves primary structures. On this basis, the Grão Pará Group is presumed to overlie the Igarapé Pojuca Group, although this relationship was not observed directly in the field. The exact distribution of these two rock groups is uncertain and requires a programme of systematic mapping in the Serra do Rabo region.

9. Two different sequences of sedimentary rocks, thought to be of different ages, are present in the region: the Águas Claras (Archaean) and the Gorotire (Proterozoic) formations.

10. The Gorotire Formation is composed of proximal and distal facies thought to be associated with alluvial fans and braided system channels respectively.

12. The distribution, stratigraphical position, sedimentological and petrological characteristics of the rocks of the Gorotire Formation suggest a close relationship between their deposition and reactivation of parts of the Carajás Fault, during the Proterozoic. This event is probably later than the emplacement of the Proterozoic granites at 1.8 Ga as pebbles of similar rocks are found within the conglomerates of the Gorotire Formation. Further work is needed to confirm this hypothesis.

SUMMARY

TECTONOSTRATIGRAPHY

The rocks present in the Carajás Strike-Slip System range from variable mylonites, granites and high grade gneisses of the Archaean Xingu Complex to unmetamorphosed and little-deformed immature clastic rocks of the Middle-Proterozoic Gorotire Formation (Figs.S4.1 and S4.2). Two major sets of rocks can be identified based on the characteristics of metamorphism and deformation preserved in the rocks: (1) the Basement Assemblage and (2) the Cover Assemblage (Fig.S4.2).

The Basement Assemblage is the structurally lower, older set of outcropping rocks, represented mainly by the tonalitic-granodioritic, polymetamorphic gneisses and migmatites of the Xingu Complex and the Plaquê Granite. They outcrop along the Itacaiúnas River and in the Serra do Rabo region. The age of the main metamorphic phase (amphibolite facies) affecting these rocks, according to Machado *et al.* (1991) is ca. 2.8 Ga, coeval with ductile deformation and mylonitisation, forming the Itacaiúnas Shear Zone.

The Cover Assemblage is represented by volcanic and sedimentary sequences of different ages and origins preserved inside a series of dilational jogs and bends along faults of the Carajás Strike-Slip System. The lowest, the Igarapé Pojuca Group, comprises metasedimentary (slates, schists, ironstones) and metavolcanic rocks as seen, for example, in the Igarapé Bahia area and around the Estrela Granite in the Serra do Rabo region. The age of these rocks is not precisely determined, but their position relative to other units of known ages in the field strongly suggests they are Archaean. A predominant low greenschist metamorphism is observed in the Igarapé Pojuca rocks but higher grades may occur in this unit around the Estrela Granite. Although contacts are not exposed, they are thought to lie unconformably on rocks of the Basement Assemblage and underlie rocks of the Grão Pará Group. This conclusion is based mainly on differences in metamorphic grade and deformation characteristics.

The Grão Pará Group comprises volcanics (Parauapebas Formation) and ironstones (Carajás Formation). The age of these rocks is thought to be ca. 2.7 Ga (Wirth *et al.*, 1986 and Machado *et al.*, 1991). The contact between the

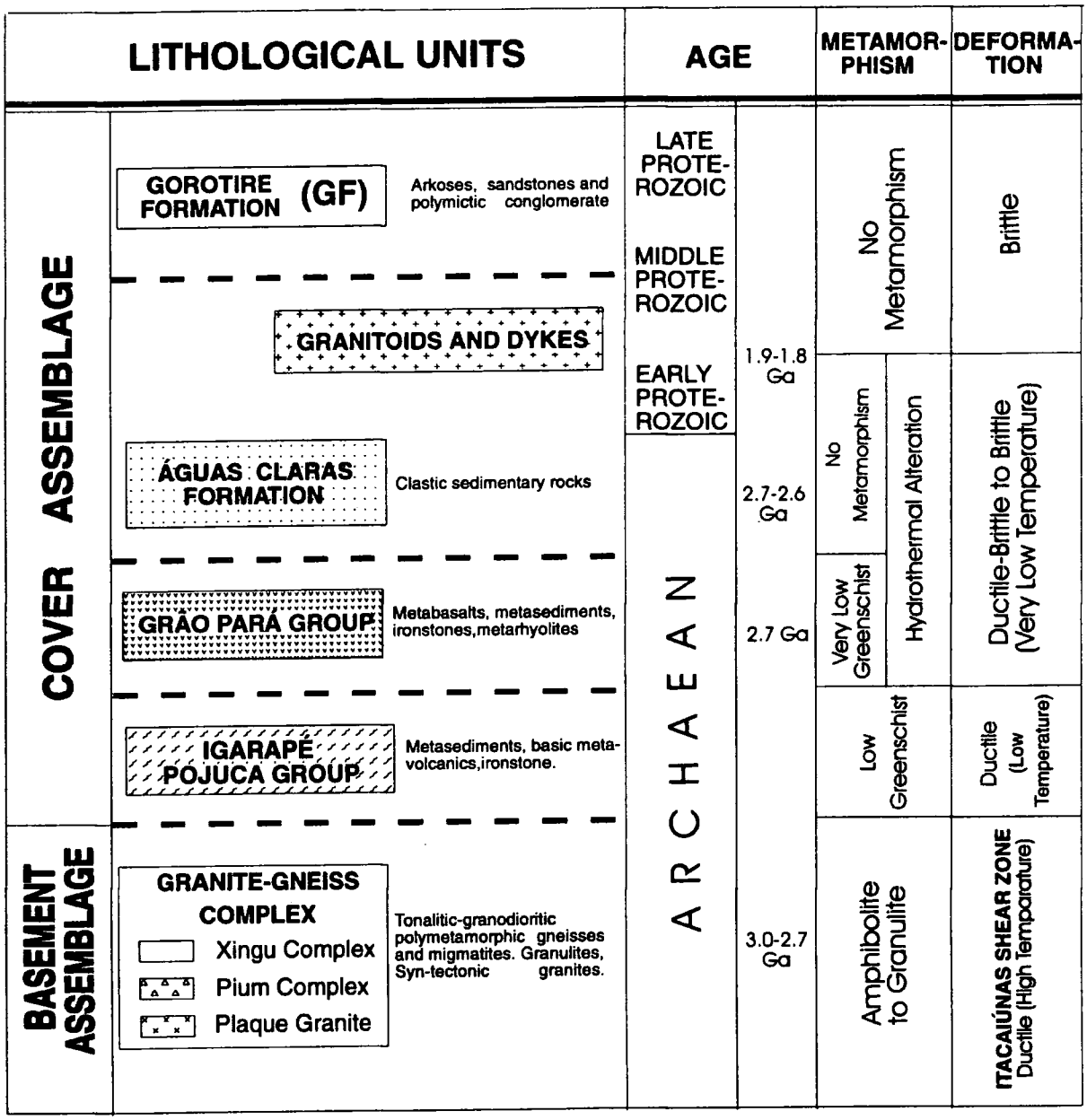

Fig.S4.1- Simplified tectonostratigraphic column for the Carajás region. See map in Fig.S4.2.

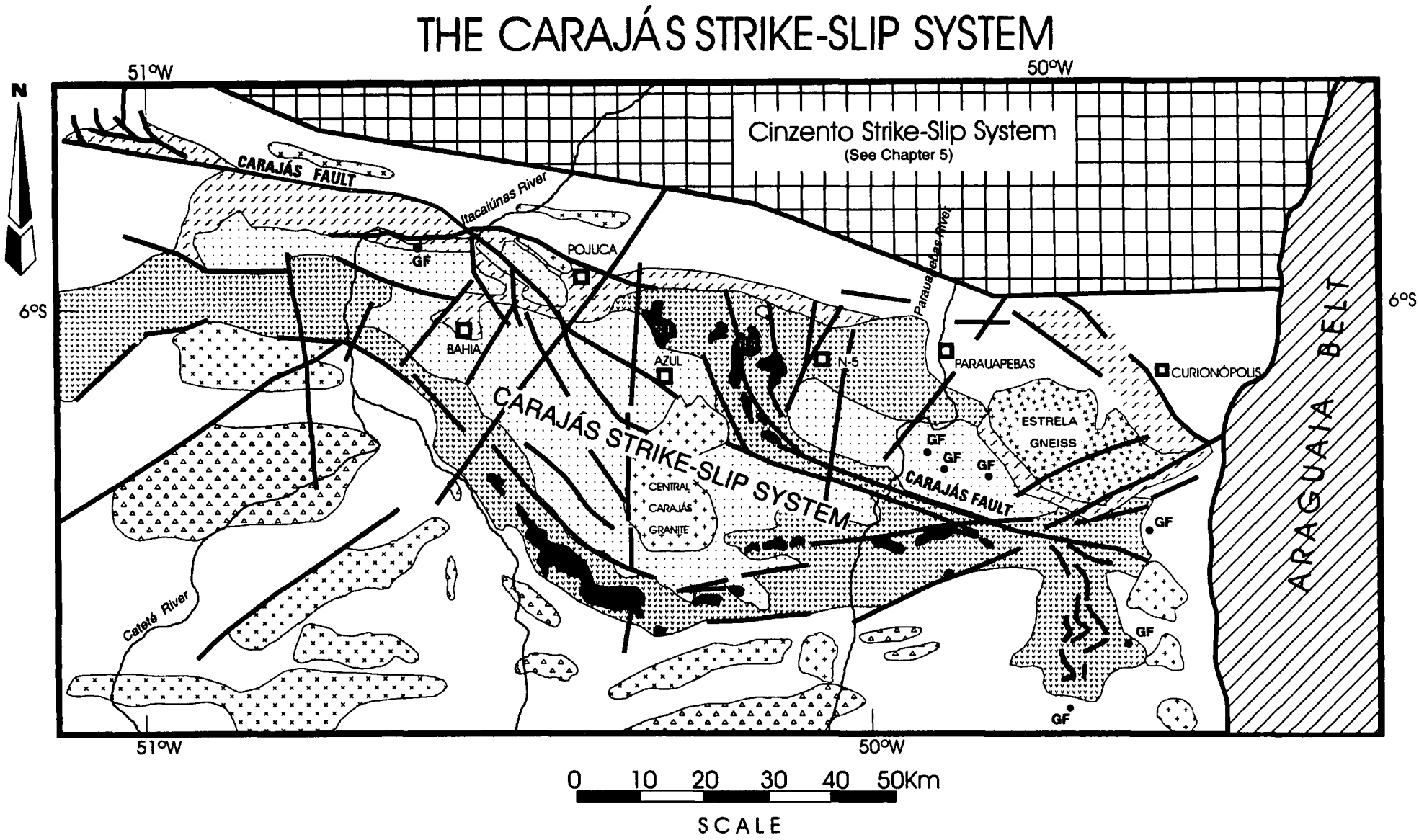

Fig.S4.2- Simplified geological map of the Carajás Strike-Slip System showing the distribution of the main tectonostratigraphic units and tectonic lineaments. See Fig.S4.1 for key to ornaments (modified after DOCEGEO, 1988; Araujo and Maia, 1991; Barros, 1991; Macambira *et al.*,1994)..

volcanics and the ironstones is supposed to be both transitional and locally discordant, in different places, although it is not well exposed in the field. Both units are exposed around the N-4 plateau region where the volcanics are faulted against ironstones, whilst elsewhere, the two units are interlayered. The lack of lateral continuity within the Grão Pará Group sequence appears to be an important characteristic. They are not preserved in the Bahia Mine area where Águas Claras Formation rocks are thought to lie unconformably on the Igarapé Pojuca Group (Fig.S4.1).

Rocks of the Grão Pará Group are affected by hydrothermal alteration and have undergone brittle to ductile-brittle deformation at very low temperatures. The distinction between volcanics of this unit and those of the Igarapé Pojuca Group is difficult to make since the low greenschist metamorphism did not produce significantly distinctive mineral assemblages to allow confident differentiation between these two rock units in the field. Probably the only useful field criteria are the presence of slates, schists and other metasedimentary units in association with the metavolcanics in the Igarapé Pojuca Group. However, the criteria may not be reliable since some basic material associated with the Grão Pará Group is clearly intrusive and may be emplaced at several stratigraphical levels in the regional sequences including metasedimentary rocks of the Igarapé Pojuca Group.

The Águas Claras Formation forms a sedimentary sequence which overlies the volcanics and ironstones of the Grão Pará and the Igarapé Pojuca groups (Fig.S4.2). The age of this unit is thought to be younger than 2759±2 Ma and older than 2645±12 Ma based on dating respectively of the underlying Grão Pará Group and gabbroic rocks intruded as sills into the sedimentary rocks. The deposition of the Águas Claras Formation took place in a large regional basin dominated by platform to fluvial environments which was strongly influenced by tides (Nogueira, 1995). The contact between these rocks and the Grão Pará Group was not observed in the field but it is presumed to be an unconformity since the Grão Pará rocks are widely deformed by folding, especially in the ironstones, adjacent to undeformed, tilted rocks of the Águas Claras Formation, as can be seen around the N-4 and N-1 plateau. They also lie unconformably on the metavolcanics and metasedimentary rocks of the Igarapé Pojuca Group as seen in the Bahia Mine region (Fig.S4.1). Metamorphism in the Águas Claras Formation is not recognised, but hydrothermal alteration and diagenetic effects have been recognised in the Águas Claras area (Soares *et al.*,1994). Sills with an age of about 2.6 Ga are intruded in relatively large volumes, based on drill-hole data, and are a later

phase of gabbroic magmatism. This magmatism may be related to the transtensional event responsible for the subsidence of the Águas Claras Formation inside the dilational jog where it is preserved. Dykes cutting the Águas Claras Formation may be related to the same event or to a regional phase of Middle Proterozoic extension.

Granitoids with intrusion ages of about 1.8-1.9 Ga are intruded into the Xingu Complex, Igarapé Pojuca Group, Grão Pará Group and the Águas Claras Formation. They are present in the central area of the Carajás Strike-Slip System (Central Carajás Granite), in the NW border of this fault system (Itacaiúnas Granite) and in several relatively unknown plutons along the Serra do Rabo region (Fig.S4.1). These plutons are further discussed in chapter 6.

The Gorotire Formation is the uppermost unit present in the Carajás Strike-Slip System, represented by immature sandstones and arkosic rocks that were previously included in the Águas Claras Formation. They are here placed in a separate unit as they are significantly different from the other sedimentary rocks that outcrop in the region. They are undeformed, and are not ever significantly tilted. They are probably younger than the 1.8 Ga -granitoids since they carry pebbles and boulders of rocks very similar to the granites and also pebbles of the Xingu Complex, Igarapé Salobo, Igarapé Pojuca and Grão Pará groups, and also those of the Águas Claras Formation. They are thought to lie unconformably on rocks of the Xingu Complex and Águas Claras Formation. They may have dominated a large area of the central-E region of the Carajás Strike-Slip System.

STRUCTURAL GEOLOGY

The dominant mylonitic fabric present in the Xingu Complex rocks developed during a major sinistral transpressional episode, appears to have been responsible for the development of the Itacaiúnas Shear Zone - a broad ductile system of linked strike-slip and thrust-dominated shear zones. This shear zone is supposed to have existed at least since 2.8 Ga and appears to have been active until about 2.5 Ga, when the Estrela Granite was syn-tectonically emplaced and deformed (Machado *et al.*, 1988, 1991). The deformation during this high temperature ductile event was strongly partitioned on both regional- and small-scales. Sinistral and reverse shear sense indicators are dominant overall. The occurrence of complex foliation and lineation patterns associated with this deformation is consistent with a transpressional regime.

The rocks of the Igarapé Pojuca Group were deformed during low temperature ductile deformation forming pervasive slaty cleavage developed coevally with regional folding observed in these rocks. The age of this episode must be between ca. 2.8 Ga and ca. 2.7 Ga before the deposition of the Grão Pará rocks. These rocks are separated from the adjacent rocks by unconformities. Shear sense indicators suggest that deformation was a transpression coeval with low greenschist metamorphism affecting slates and quartzites outcropping in the Itacaiúnas River and in the Bahia Mine area. The regional extent and significance of this event is unclear.

The sigmoidally-shaped dilational jog forms the most prominent feature of the otherwise E-W trending Carajás Strike-slip System developed within the Itacaiúnas Belt (Fig.S4.1). It is thought to have been developed during an initial phase of dextral transtension forming a new set of faults that reactivated the mylonitic fabrics present in the underlying basement rocks of the Xingu Complex. This structure must have been formed after ca. 2.7 Ga and before ca. 2.6 Ga. Part of the Archaean Igarapé Pojuca, Grão Pará groups and the Águas Claras Formation is preserved inside this dilational jog structure. Evidence for this transtensional episode is indicated by the presence of normal faults, and probably by the emplacement of gabbroic sills intruded in the Águas Claras Formation.

Many of the faults forming the Carajás Strike-Slip System display sinistral strike-slip and reverse kinematic components, and appear to have been reactivated by transpression during the period 2.6-1.9 Ga. The effects of the transpressional event are localised along narrow brittle-ductile high strain zones adjacent to faults in the Carajás Strike-Slip System, including the Carajás Fault. Fluids may have played an important role during reactivation inducing strain softening and kinematic partitioning. Deformation associated with the transpressional event can be observed for example along the central area of the Águas Claras section, in the Azul Mine area and in the N-4 Mine region.

The well known Middle Proterozoic (1.8-1.0 Ga) regional extensional episode that affected most of the Amazonian Craton appears to have caused minor transtensional reactivation of major fault strands in the Carajás Strike-Slip System. These events facilitated granite pluton emplacement into dilational jogs or in voids created by rotation of fault blocks ca. 1.8 Ga. A slightly earlier phase of mafic dykes may also be related to this extension. This Middle Proterozoic extension was also responsible for the development of cross-cutting N-S and NNE-SSW sets of fractures, and also possibly fault-controlled deposition of the Gorotire Formation, mainly in the Serra do Rabo area.

The most important general characteristic of the faults forming the Carajás Strike-Slip System is their reactivated nature. Early normal faults developed during the first episode of transtension were subsequently reactivated and tectonically inverted during alternating episodes of transpression and transtension that took place in the region during the next 1.0 Ga. As a result, faulting has determined both the present distribution of younger Cover Assemblage rocks and also has localised much of the deformation along local fault strands and within compressional restraining bends.

CHAPTER 5

THE CINZENTO STRIKE-SLIP SYSTEM

INTRODUCTION

The Cinzento Strike-Slip System is defined by a discrete set of lineaments lying about 10 km north of the Carajás Strike-Slip System and separated from it by outcrops of granitoids of the Xingu Complex (Fig.5.II.1). The lineaments follow a general WNW-ESE orientation, extending for about 180 km, and are cut by the Late Proterozoic Araguaia Belt to the E.

The geometry of the Cinzento Strike-Slip System is superficially typical of strike-slip fault zones. At its western end there is a 70 km long 12 km wide scallop-shaped geometry with lineaments concave toward the S (Fig.5.II.1a). E of this the 40 km segment between the Itacaiúnas and Parauapebas rivers comprises a narrow zone of lineaments (ca. 3 km wide) in which small (3x5 km) rhombohedral structures are developed (Fig.5.II.1a). The remaining lineaments to the E form a divergent splay of lines similar to a "horse-tail" strike-slip termination. The width of this structure at its E end is > 40 km (Fig.5.II.1a and b).

The Cigano Granite (ca. 1.8 Ga) is intruded into the central eastern part of this fault system (Fig.5.II.1a), while the Estrela Granite (ca.2.5 Ga) borders the southern termination of the "horse-tail" structure to the E (see Chapter 4, section 4.6).

The Cinzento Strike-Slip System is associated with high grade metasedimentary rocks of the Archaean Igarapé Salobo Group, in the western sector and medium to low metamorphic rocks of the Archaean Igarapé Pojuca Group. Ultramafic rocks are also associated with the Igarapé Pojuca Group. All these rocks are believed to post-date the surrounding basement gneisses of the Xingu Complex.

Three areas were selected for study in this fault system, from W to E (Fig.5.II.1): (1) Salobo region; (2) Cururu area; and (3) Serra Pelada region. The southern part of this major structure is also discussed in Chapter 4, section 4.6 (The Serra do Rabo region).

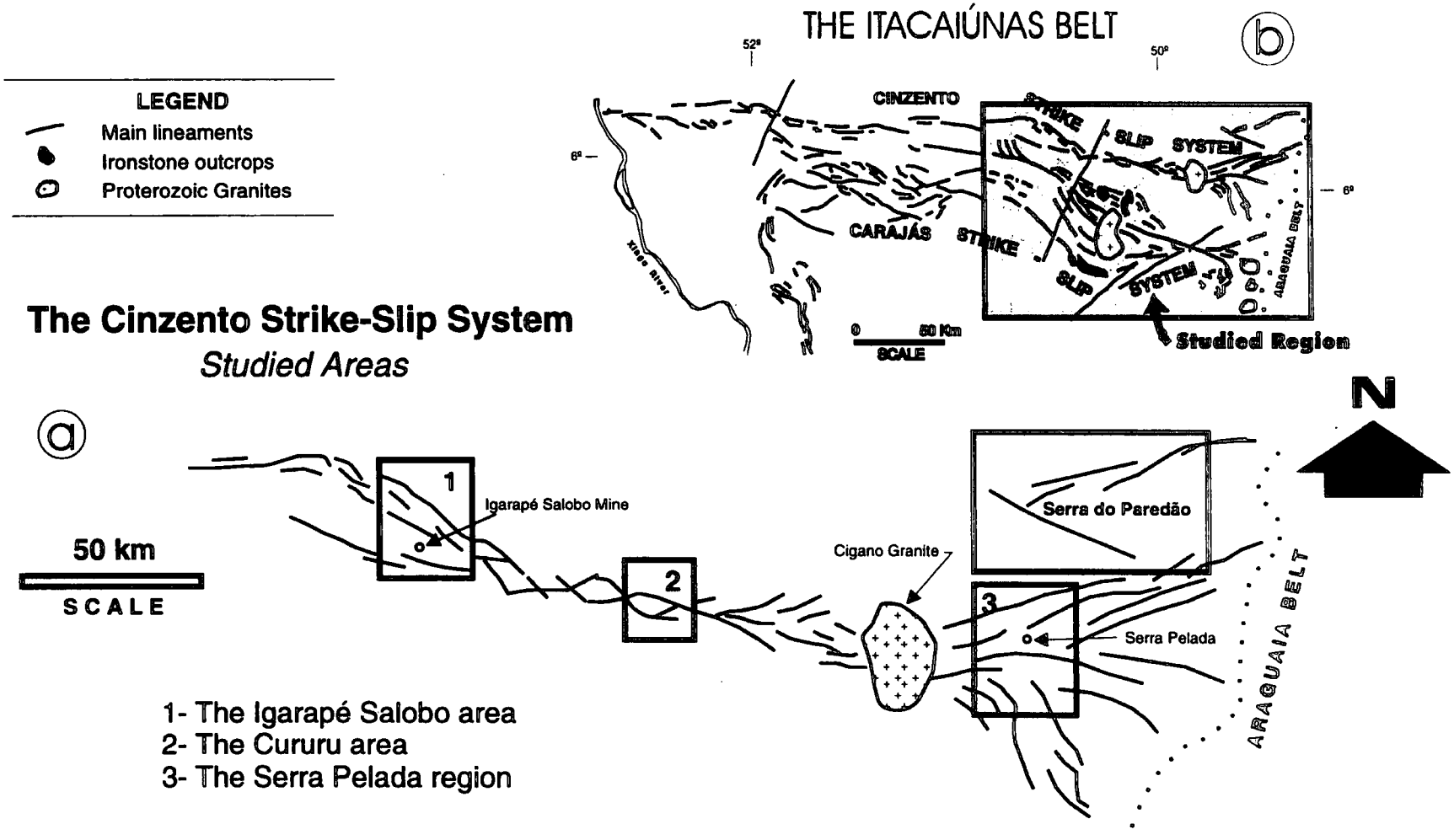

Fig.5.II.1- a) Location of the areas studied in the Cinzento Strike-Slip System. The figure (b) shows the Cinzento Strike-Slip System in the regional context.

5.1- THE SALOBO REGION

The Salobo region lies at the western termination of the Cinzento Strike-Slip System, comprising a kilometre-scale scallop-shaped structure thought to be fault-bounded.

Much of the data presented below comes from published works since exposures in the region are now largely inaccessible. Previous extensive mining activity in the area during the 1980's and beginning of the 1990's revealed numerous exposures and mining borehole cores were collected. These are described mainly by Lindenmayer (1990), Siqueira (1990) and Machado *et al.* (1991). Structural data from these publications is reappraised and re-interpreted here. Satellite images of the region are also re-interpreted.

5.1.1- PREVIOUS WORK

The Salobo region became a target for study in 1977 when important copper deposits were discovered in the 3-Alfa area by geologists from the DOCEGEO/ CVRD. Several works were published focusing on rocks from the ore mine, located in the central-south area (e.g. Hutchinson, 1979; Meyer, 1980; Meyer and Farias, 1980; Farias and Saueressig, 1982; Vieira *et al.*1988). Few regional data were published, due to the lack of access.

The rocks of the Xingu Complex were recognised as the oldest in the Salobo region, comprising tonalitic gneisses, granitoids and migmatites which have undergone amphibolite to granulite metamorphism (Silva *et al.*,1974; Hirata, 1982). The age of the regional metamorphism and migmatization affecting these rocks was dated by Machado *et al.* (1988) at around 2859±2 Ma.

Rocks belonging to the Igarapé Salobo Group were first described by DOCEGEO (1988) as comprising quartzites, schists, ironstones, gneisses and amphibolites whose outcrop was restricted to the Salobo structure. The rocks were subdivided into three formations based on lithology: (1) the "Cascata Gneiss"; (2) the 3-Alfa Formation; and (3) the Cinzento Formation (from base to top). The age of the Igarapé Salobo Group rocks was thought to be Archaean

and Machado *et al.* (1988) obtained an U/Pb (zircon) radiometric age of 2851±4 Ma from gneisses of this unit, and 2761±3 Ma thought to date the metamorphism in amphibolites outcropping in the northern of the region. Consequently these authors considered a possible correlation of these rocks with the Xingu Complex, and suggested that they have undergone metamorphism coeval with the emplacement of basic rocks of the Grão Pará Group (2759±2 Ma, U/Pb in zircon; Machado *et al.*, 1988).

The copper ore in the 3-Alfa Mine is thought to have been emplaced into a sub-vertical sequence of schists, continuous for about 3km across the strike and 80 km along strike, orientated WNW-ESE (Vieira *et al.*, 1988). Petrological studies revealed five different types of schists related to the Cu-ore, together with ironstones, metabasic rocks, gneisses and granites, (Vieira *et al.*,1988). All these rocks, apart from the Middle Proterozoic anorogenic granites intruded in this sequence, were metamorphosed to amphibolite facies and later retrogressed to greenschist (DOCEGEO, 1988; Siqueira,1990).

Ductile and brittle-ductile oblique shear zones were recognised as being responsible for the main NW-SE orientation of the rocks (e.g. Vieira *et al.*, 1988; DOCEGEO, 1988; Siqueira, 1990), with predominantly sinistral senses of shear (Vieira *et al.* 1988; Siqueira, 1990).

Siqueira (1990), Costa and Siqueira (1990) and Siqueira and Costa (1991) published regional and detailed data concerning the structural geology of the Salobo region. Lindenmayer (1990), Lindenmayer *et al.* (1994*a* and *b*) and Lindenmayer and Laux (1994) examined the geochemistry and petrology of the rocks in the area. These data are discussed below.

5.1.2- A RE-INTERPRETATION OF THE SALOBO REGION.

Based on interpretation of digital LANDSAT (1:25000) and radar images (1:100000) together with aerial-photos (1:30000) and field data, Siqueira (1990) published the only geological map of the area (Fig.5.1.1). Nine lithological units are recognised associated with either the Xingu Complex or the Igarapé Salobo Group. Geographically, the rocks are arranged into relatively narrow long strips orientated sub-parallel to the WNW-ESE, NW-SE and E-W lineaments which define the kilometre-scale scallop-shaped structure, concave southwards

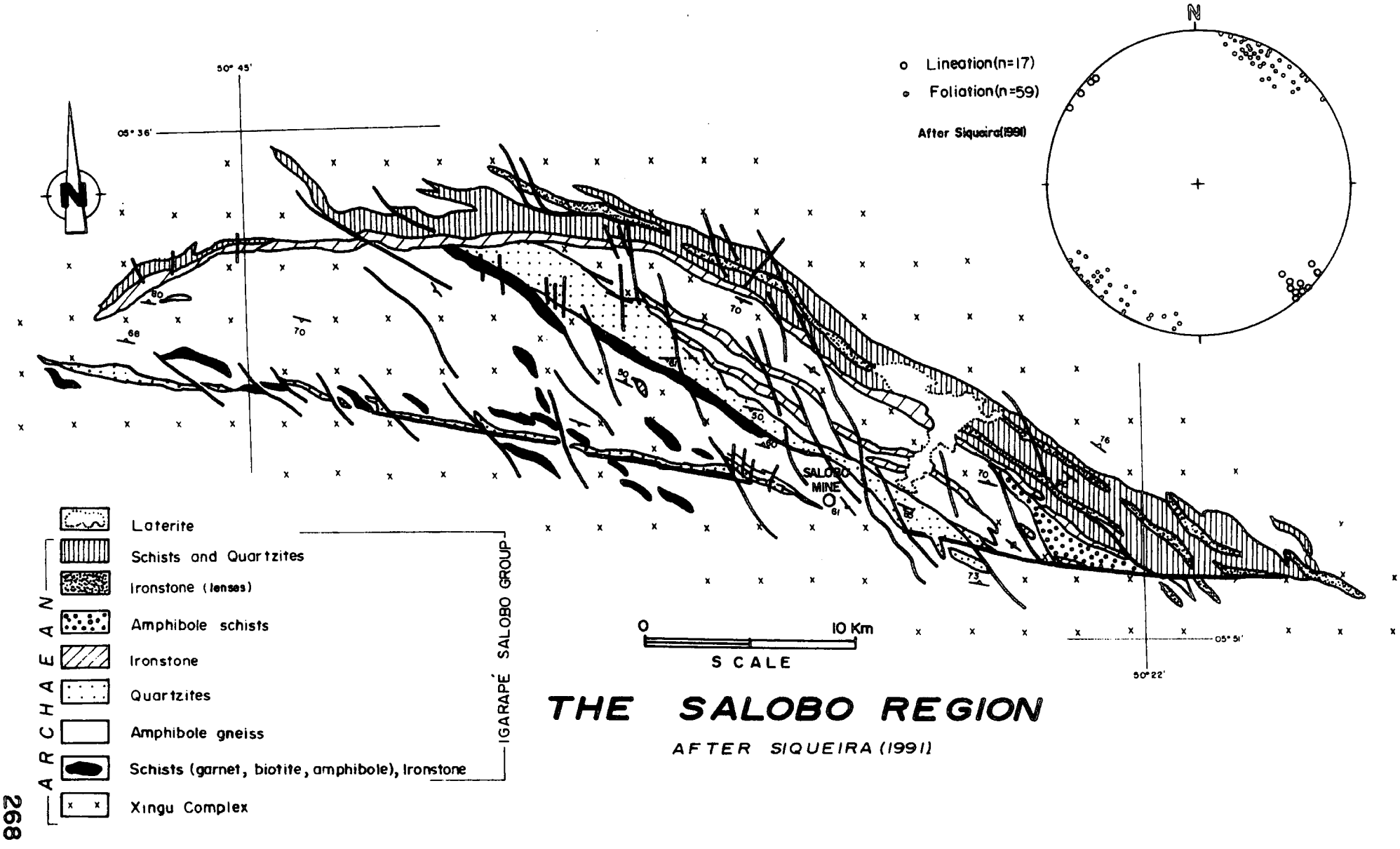

Fig.5.1.1- Geological map of the Salobo region, based on Siqueira (1991). The stereonet in the right top corner represents poles to foliation and lineation from the shear zones observed in the region (after Siqueira, op.cit.).

(Fig.5.1.1). These lithological bands are cut by several NNW-SSE faults and fractures with distinct offsets.

Siqueira (1990) suggested that the most important tectonic structures are ductile shear zones related to prominent strike-slip displacements. They are orientated NW-SE, NNE-SSW and NE-SW, cutting the regional lineaments defining a major curved shear zone in the north, which converges towards a straight WNW-ESE shear zone, in the south.

The mylonitic foliation is strongly orientated NW-SE to WNW-ESE whilst the mineral lineation plunges predominantly at low angles, sub-parallel to the strike of the foliation (Fig.5.1.1, top right). Kinematic indicators observed in the sheared rocks include S-C foliations, asymmetric intrafolial folds (outcrop- and thin-section-scale), sheath folds and δ-type porphyroclasts. According to Siqueira (1990), they indicate predominantly sinistral senses of movement. During the present research petrographic observations on the quartzites outcropping in the adjacent mine area, confirmed the presence of high temperature mylonitic fabric. This myonitic episode is probably coeval with the amphibolite metamorphic grade, since sillimanite is found composing the fabric. Intense ductile deformation is indicated by transposition features preserved on an outcrop-scale affecting both the banding in the ironstones and gneisses, and the foliation in the schists on a large-scale.

Fig.5.1.2 shows the lineament map presented by Siqueira (1990). He suggested that the lineaments are ductile shear zones cut by R, P, R' and Y-D fractures, formed during sinistral and secondary extensional displacement. Thus, Siqueira (1990) interpreted the Salobo structure as an extensional duplex related to a major sinistral strike-slip shear system. The main episode of deformation was thought to be coeval with mineralogical transformations associated with retrograde metamorphism from amphibolite to greenschist facies due to hydrothermal alterations. A kinematic model was proposed, visualising initial transtension, followed by transpression and later transtension. Siqueira (op cit) also referred to the possibility of older rocks having been re-worked by the main sinistral strike-slip shear event.

According to Lindemayer (1990) the metamorphism affecting the rocks in the Salobo region corresponds to a pyroxene hornfels facies followed by two episodes of hydrothermal alteration at amphibolite and greenschist grades (Siqueira, 1990), in partial agreenment with Machado *et al.* (1988 and 1991),

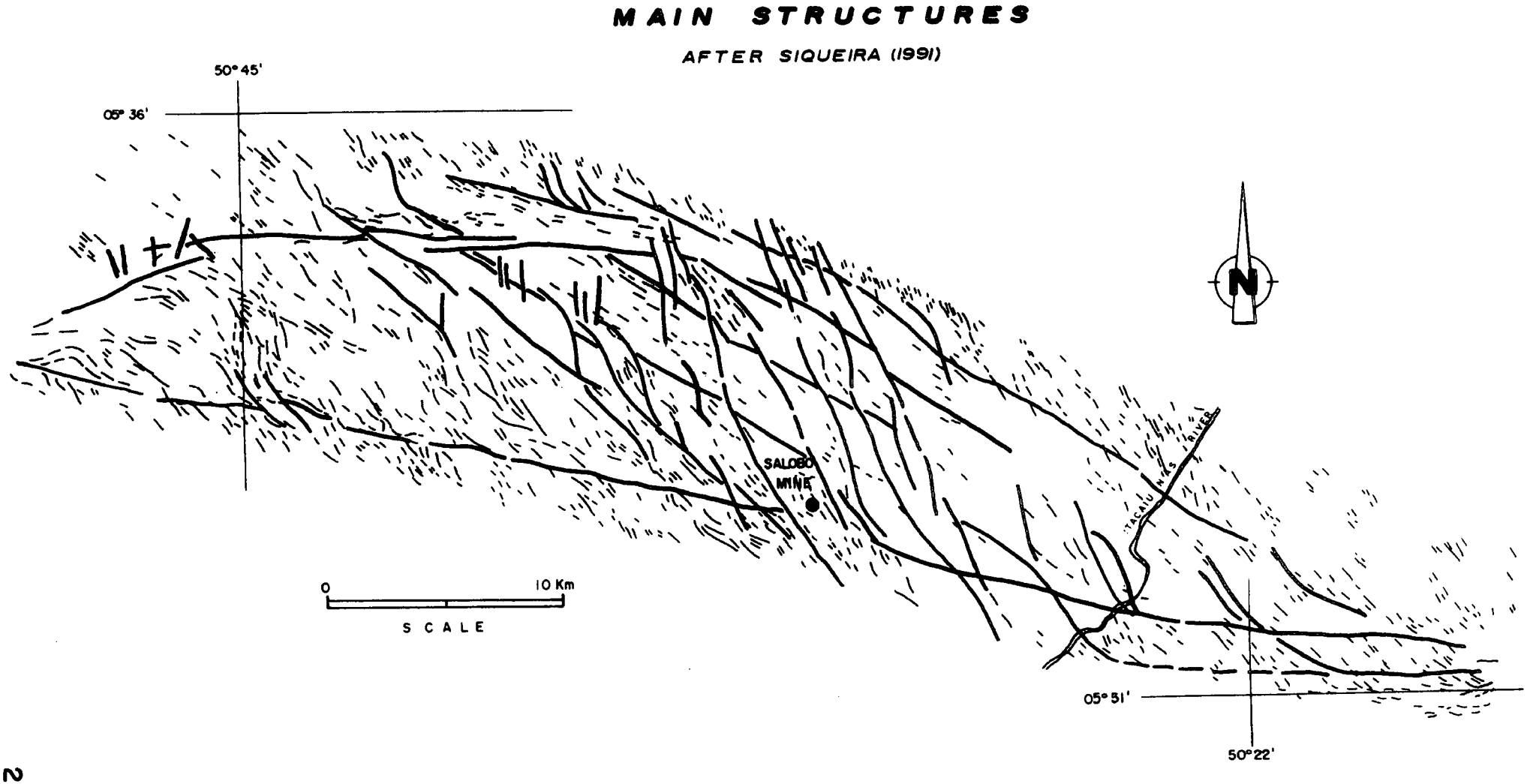

Fig.5.1.2- Structural map of the Salobo region from interpretation of satellite and radar images in different scales (after Siqueira, 1991).

referred to a regional metamorphism at amphibolite grade, followed by hydrothermal alterations at greenschist grade.

Two granitoids, of different ages, were studied in detail by Lindenmayer (1990). They were named Old Salobo Granite (see Chapter 4, section 4.6) and Young Salobo Granite (see Chapter 6). Their radiometric ages are 2573±2 Ma (U-Pb, zircon; Machado *et al.*,1988) and 1880±80 Ma (Rb-Sr; Cordani, 1980), respectively and both sets of data are thought to date intrusion. The Old Salobo Granite is deformed by ductile shear zones, developing a mylonitic fabric. It outcrops in the Salobo Base Camp but it has not been mapped. The Young Salobo Granite does not outcrop but is found in several drill cores. It is interpreted as a sill-like intrusion, 50m thick, covering more than 1300m^2, emplaced close to the contact between the basement rocks and the ironstones in the south of the region. It is basically an undeformed quartz-syenite (Lindenmayer *et al.*,1994*a*).

Machado *et al.* (1998, 1991) carried out geochronological studies in the Salobo region and recognised the following events listed in the Table 5.1.1:

AGE:	INTERPRETED EVENT:
2851±4 Ma (U/Pb, zircon)	Age of the migmatites of the Xingu Complex
2761±3 Ma (U/Pb, zircon)	Metamorphism of the Xingu Complex
2758 Ma (U/Pb, zircon)	Intrusion of granitic veins into the Xingu Complex
2573±2 Ma (U/Pb, zircon)	Emplacement of the Old Salobo Granite
2573-2551 Ma	Shearing of the Igarapé Salobo Group
2497±5 Ma (U/Pb, titanite)	Metasomatic event
1874-1883 (U/Pb, zircon)	Emplacement of the Young Salobo Granite
1880±80 Ma (Rb/Sr, whole rock)[1]	
553±32 Ma (K/Ar, whole rock)[1]	Emplacement of dolerite dykes

[1]Cordani (1980)

Table 5.1.1- Summary of the main geochronological data to the Salobo region rocks.

A new lineament interpretation for the Salobo region is presented in Fig.5.1.3. This map was made by visual analyses of LANDSAT image (Photo 5.1.1), at 1:100000 scale. This map, if compared to that of Fig.5.1.2 (Siqueira,1990) shows some important differences. In particular strong lineaments orientated NNW-SSE, observed in the earlier interpretation, are absent and are replaced by a mainly N-S trending set (Fig.5.1.3).

5.1.3- DISCUSSION

The lineaments observed in satellite images, (Figs.5.1.2 and 5.1.3; Photo 5.1.1) comprise two different sets of lines: (1) short, curved ones orientated mostly NW-SE, and (2) longer, more continuous lineaments which consistently cut the short ones. The first set was correlated by Siqueira (1990) with the mylonitic foliation, but clearly they lie beyond the domain formed by the major lineaments which define the regional structure. These long and continuous lineaments are almost certainly brittle structures, overprinting with a regionally sub-parallel orientation, the earlier ductile fabrics. This suggests that they are a later episode of deformation, even though both ductile and brittle structures show evidence for sinistral movements. Thus the idea that the Salobo structure is a strike-slip duplex formed by ductile deformation, as suggested by Siqueira (1990), is not supported here. The major structure observed in several remote sensing images is thought instead to be defined by brittle structures which have overprinted, and to some extent reactivated, earlier ductile fabrics.

It is further suggested that the Salobo structure formed as a brittle sidewall ripout feature. It appears to have an intermediate geometry between a typical sidewall lens ripout and a sidewall slab ripout as defined by Swanson (1989). The structure has a characteristic leading contractional ramp arranged in the eastern part of the area and a trailing extensional ramp in the west. The dominant flat side of the structure is orientated WNW-ESE, with a length of approximately 70 km. As suggested by Swanson (1989) the asymmetric shape can be used as a kinematic indicator. The movement follows the direction of displacement of the wallrocks on the opposite side of the main fault surface. This arrangement, applied to the Salobo sidewall ripout, suggests a sinistral sense of brittle fault displacement.

Photo 5.1.1- Satellite image of the Salobo region, in the W end of the Cinzento Strike-Slip System.

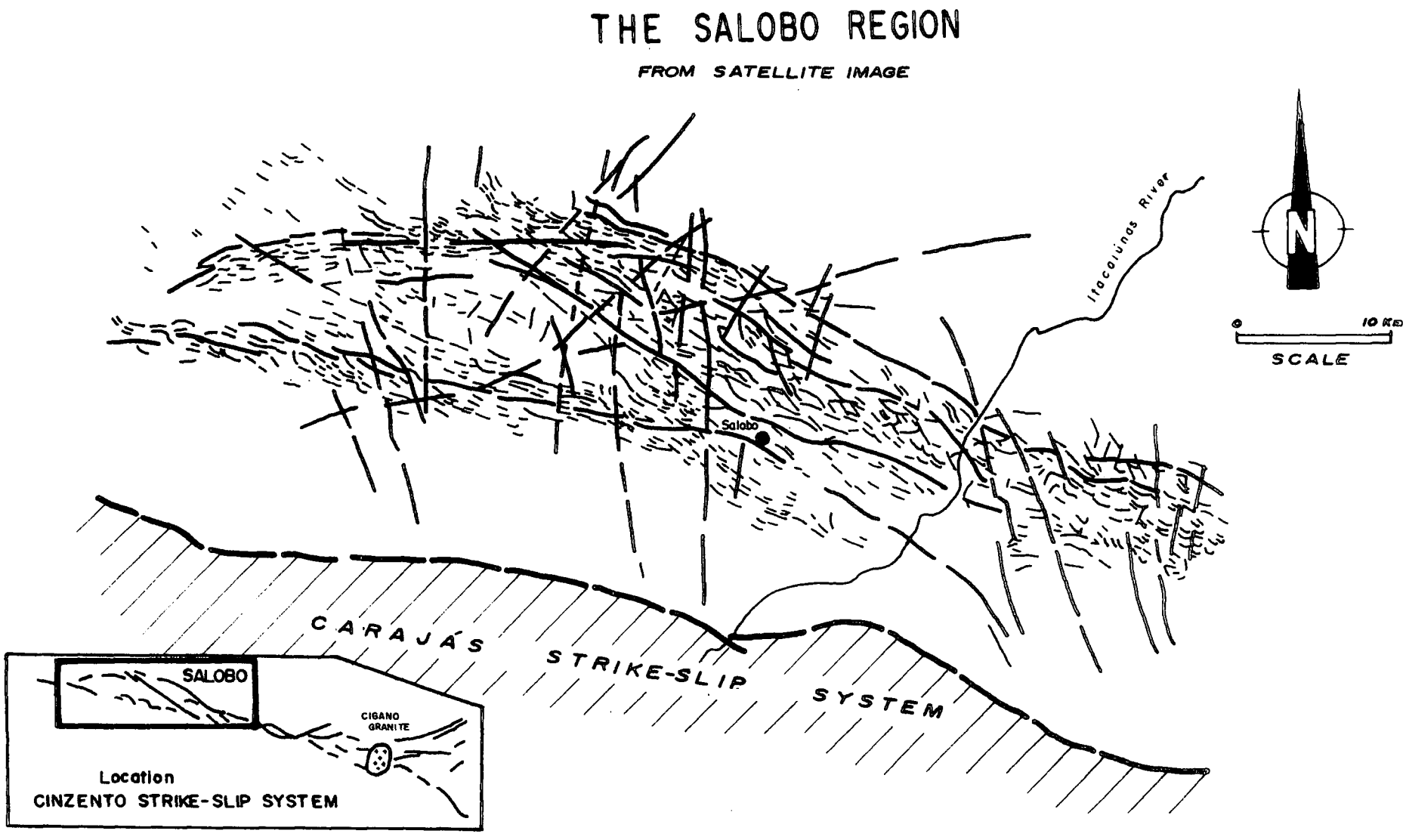

Fig.5.1.3- Map of lineaments to the Salobo region from satellite images.

Using shear fracture terminology (Swanson, 1989), it is suggested that a major P-fracture, orientated NW-SE, divides the Salobo structure into two distinct structural and lithological compartments. The NE sector is dominated by schists, quartzites, ironstones and amphibolites, representing the Igarapé Salobo Group, together with slices of the Xingu Complex rocks (Siqueira, 1990). The orientation of the rocks inside this block follows a NW-SE direction, dipping steeply towards both the NE and SW. Most rock units preserve mylonitic fabrics orientated sub-parallel to their contacts (NW-SE), or E-W, with low-angle mineral or stretching lineations, that, together with shear criteria suggest sinistral-normal kinematics (Siqueira, 1990). In contrast, the SW block is dominated by rocks of the Xingu Complex rocks, which are also affected by steeply-dipping sinistral-normal ductile deformation fabrics.

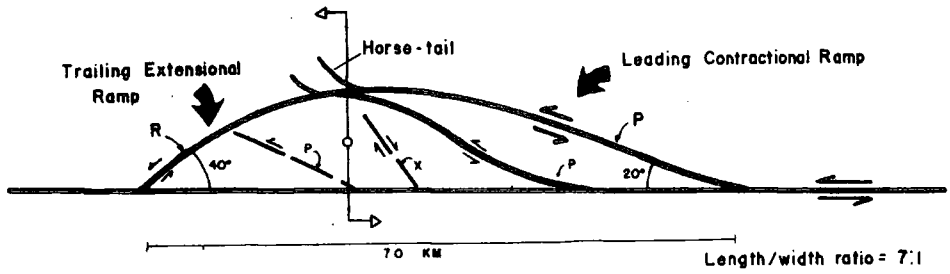

Fig.5.1.4- Sketch representing the Salobo sidewall ripout (not to scale).

The length/width ratio of the Salobo sidewall ripout is about 7:1. The angle between the faults in the leading contractional ramp and the dominant planar fault trace is about 20°, whilst that between the faults in the trailing extensional ramp and the dominant planar fault is about 38°-40° (Fig.5.1.4). Using the length of the structure, and following the theoretical models of Swanson (1989), a maximum of 7 km of displacement is most likely to be associated with this structure.

Secondary features observed in the Salobo sidewall ripout structure include horse-tail terminations projecting NW from the northern superior border of the structure (Fig.5.1.4). It is suggested, therefore that there were at least two main episodes of deformation affecting the rocks in the Salobo region. The first ductile event, produced a widespread mylonitic fabric and the probable lithological imbrication described by Siqueira (1990). The age of this episode, from the data published by Machado *et al.* (1988, 1991), lies somewhere between 2851±4 Ma, the probable age of the last migmatization taking place in the region and 2761±3 Ma, coeval to the age of amphibolite facies metamorphism. The second episode is a brittle deformation overprinting in a sub-parallel geometry the earlier structures, and this led to the development of the sidewall ripout structure. The age of the second event, is more difficult to constrain due to a lack of radiometric data. It is possible only to suggest that this deformation took place at some time between ca.2.5 Ga (age of shearing affecting the Old Salobo Granite reported by Machado, 1991) and ca.1.9 Ga (intrusion of the Young Salobo Granite). This episode was probably associated with one of the hydrothermal events described by Lindenmayer (1990), and may be responsible for later metamorphic alteration observed in the rocks of this region.

It has been shown in different parts of this work that sets of N-S and NNE-SSW fractures are widespread all over the Carajás region. Earlier authors have interpreted these fractures as Riedel fractures related to sets of strike-slip systems (e.g. Siqueira, 1990, in the Salobo region; Araújo and Maia (1991) in the Carajás Strike-Slip System; Marçal, 1991 in the N-4 Plateau). These lineaments are here considered to be unrelated to the development of any strike-slip system, because they clearly cut all the features associated with the system and also occur far from the domain of these structures (e.g. see Fig.5.1.3 and Photo 5.1.1). As is further discussed in Chapter 6, they may be associated with a regional extensional episode of deformation taking place in the Amazon Craton as a whole during the Proterozoic.

5.1.4- CONCLUSIONS

1) The large-scale scallop-shaped structure in the Salobo region is here interpreted as a sidewall ripout feature, developed sub-parallel to an earlier

ductile fabric present in the rocks of the region. It is intermediate between a sidewall slab ripout and a sidewall lens ripout as defined by Swanson (1989).

2) The asymmetric shape of the structure suggests a sinistral sense of shear during brittle faulting.

3) The earlier mylonitic fabrics are also associated with sinistral displacements thought to have occurred synchronously with high temperature amphibolite facies assemblage. The retrograde greenschist metamorphism reported by Siqueira (1990) as overprinting this amphibolite facies assemblage may be associated with some of the later reactivation episodes of deformation. The significance and regional extent of these mylonitic fabrics are uncertain, although they appear to extent beyond the boundaries of the Salobo structure.

4) Three main episodes of deformation are recognised in the region: (1) an early ductile deformation responsible for the development of the mylonitic and migmatitic fabrics, thought to be about 2851±4 / 2761±3 Ma; (2) a brittle deformation responsible for the development of the sidewall ripout (ca. 2.5 to 1.9 Ga); (3) development of N-S to NE-SW fractures (Middle Proterozoic ?).

5.2- THE CURURÚ AREA

The Cururú area is located in the middle part of the Cinzento Strike-Slip System and corresponds to a kilometre-scale rhomb-shaped structure, which occurs where the faults trend approximately E-W (Fig .5.2.1. and Photo 5.2.1). The rocks exposed in this region are predominantly quartzites, metasandstones, slates, ironstones and basic rocks which have undergone greenschist metamorphism.

The data presented here were collected from galleries in an amethyst mine located near to the NNW margin of the Cinzento Strike-Slip System (Fig.5.2.1).

5.2.1- PREVIOUS WORK AND GEOLOGICAL SETTING.

There are no publications specifically concerned with the rocks of the Cururú region. Regional interpretations carried out by Costa and Siqueira (1990) and Siqueira (1990) using satellite images describe the so-called "Cururú Compressional Duplex" as representing a kilometre-scale rhomb-shaped structure. They refer briefly to the lithologies present and to their mainly greenschist metamorphic grade. They also mention the presence of localised breccias, cataclasites, protomylonites and mylonites associated with some of the main lineaments.

Costa and Siqueira (1990) and Siqueira (1990) suggested that the Cururú structure formed because of the interaction of P and Y/D shear zones, from an inverted transtensional pull-apart structure deformed during a later transpressional episode responsible also for an early amphibolite facies metamorphism of these rocks. A later transtensional deformation, associated with retrograde metamorphism and hydrothermal alteration, is referred to as the last main tectonic episode related to the Cinzento Strike-Slip System, affecting the rocks in the Cururu area.

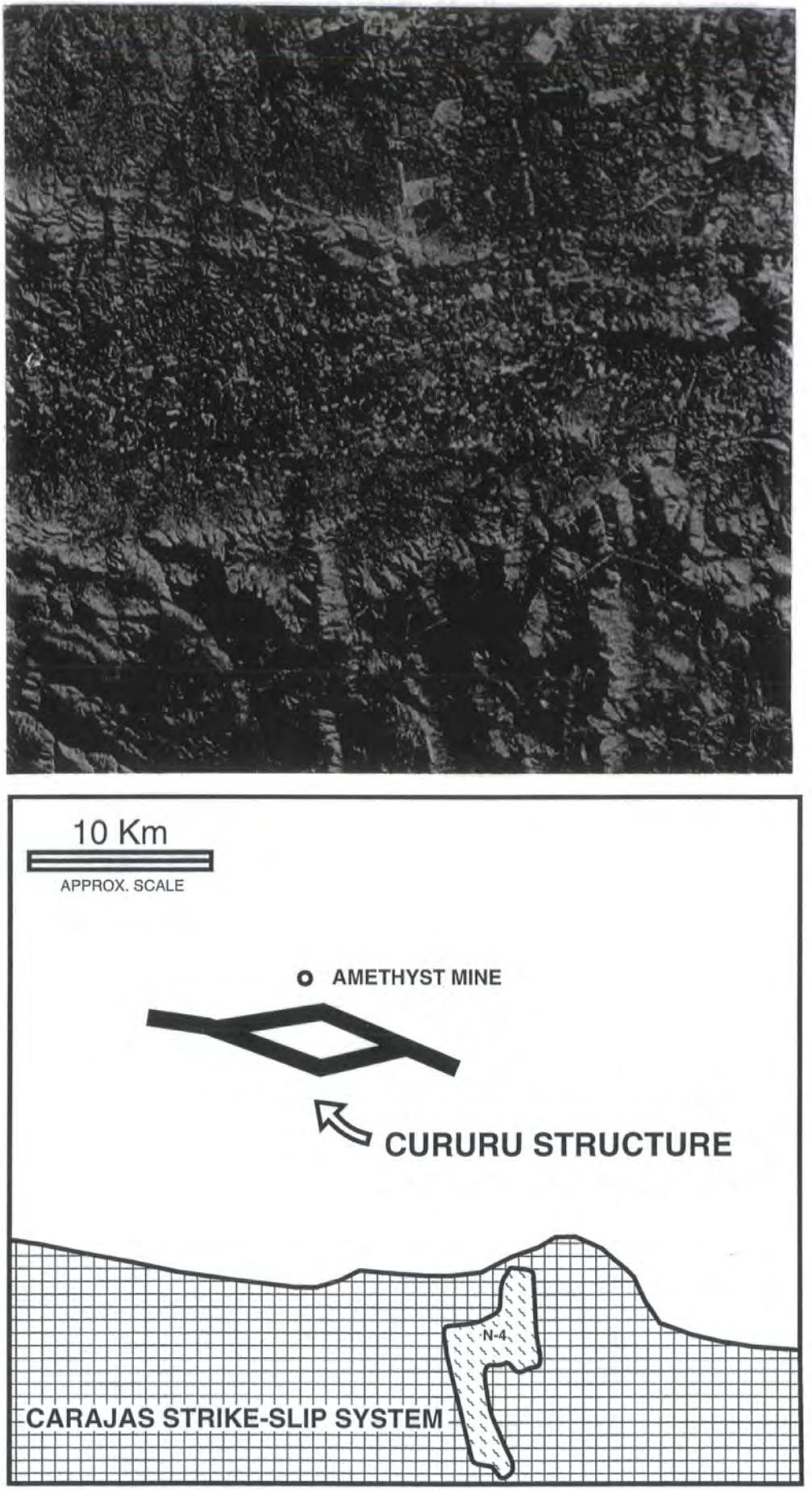

Photo 5.2.1- Satellite image of the Cururu region. The sketch below shows some references to locate the structure (approximately in the same scale of the photo).

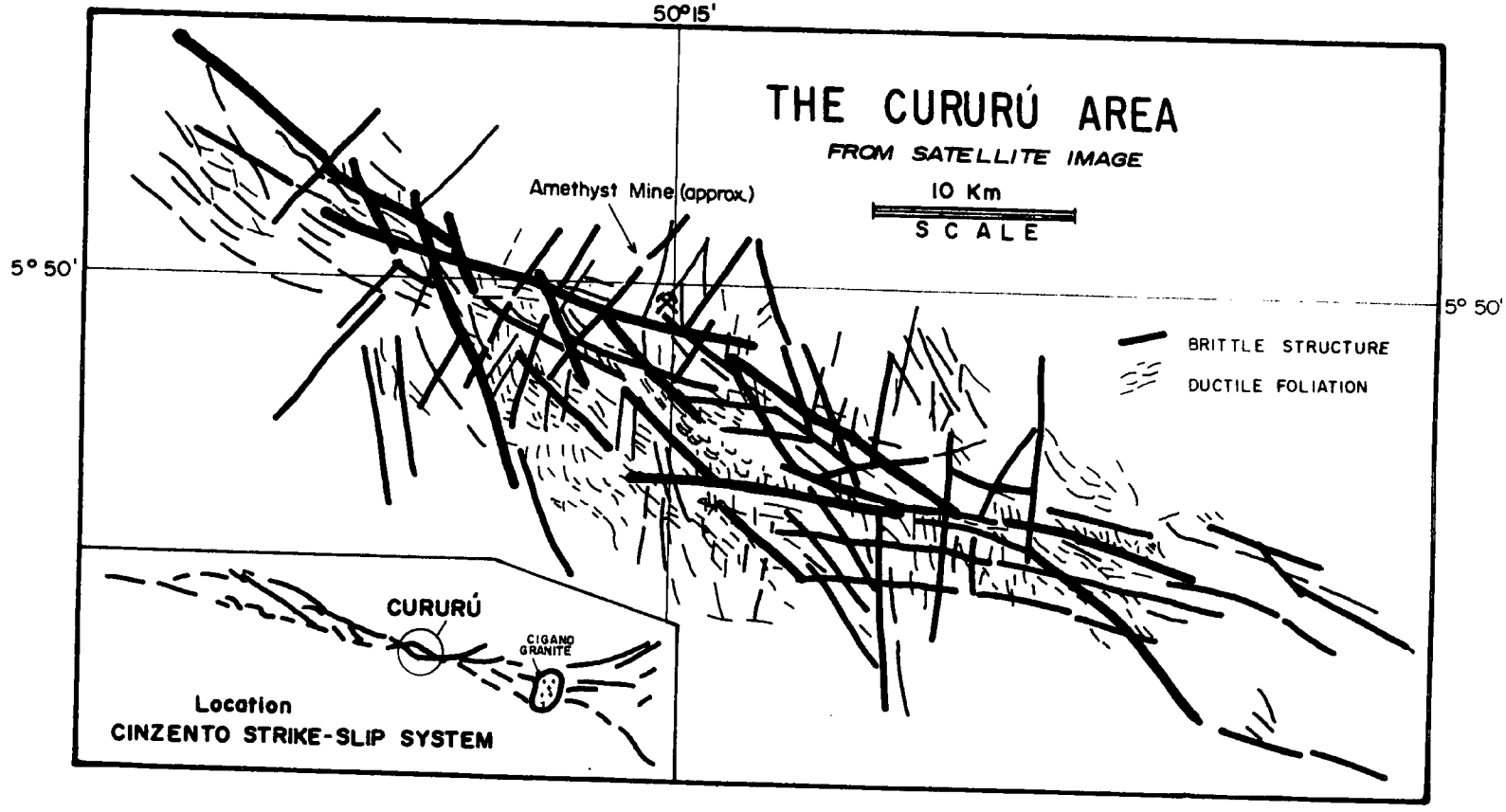

Fig.5.2.1- Main lineaments observed in the Cururu region from satellite images.

5.2.2- THE REGION ON SATELLITE IMAGE.

Major structures observed in satellite and radar images of the Cururú area are characterised by strong, discontinuous lineaments orientated NW-SE (Photo 5.2.1 and Fig.5.2.1). Small rhomb-shaped structures(ca. 4 km) are formed by the intersection of E-W and NW-SE segments. These structures are cut by sets of N-S and NNE-SSW lineaments. The lateral limits of these lineaments are diffuse (Photo 5.2.1 and Fig.5.2.1).

5.2.3- THE AMETHYST MINE

The Amethyst Mine is known in the region as "Zé Miranda´s Garimpo". It is located about 20 Km north of the N-4 plateau and only 23 Km east of the Itacaiúnas River (Photo 5.2.1). Access is via secondary roads running northwards from Parauapebas and from the N-4 Mine. A small runway allows access by air.

The mine comprises about 410m of rudimentary galleries interlinked with several vertical shafts, more than 80m deep. It lies near the edge of a 200m hill (Fig.5.2.2), and an opencast pit with small galleries is also developed along its southern slopes (Fig.5.2.3).

The rocks exposed in the galleries and mine shafts are mainly fine to coarse white to red quartzites arranged in inclined layers varying between 10-15cm to more than 80 cm thick. They are relatively pure, formed essentially by quartz, with variable small proportions of muscovite and sericite. They vary from very hard to slightly friable rocks.

Under the microscope, these rocks are orthoquartzites: muscovite/sericite quartzites comprising quartz (>95%), muscovite/sericite in variable percentage (<5%) and opaque minerals. The quartz forms slightly elongated anhedral crystals varying from 0.7mm to 0.05mm, with strong to moderate undulose extinction (Photo 5.2.2). The elongated quartz crystals, that in a few places forming ribboned crystals, define a penetrative, grain-shaped foliation (Photo 5.2.2). Fluid inclusions are obliquely oriented relative to this foliation and are visible in most crystals. The contacts between the quartz crystals, with variable

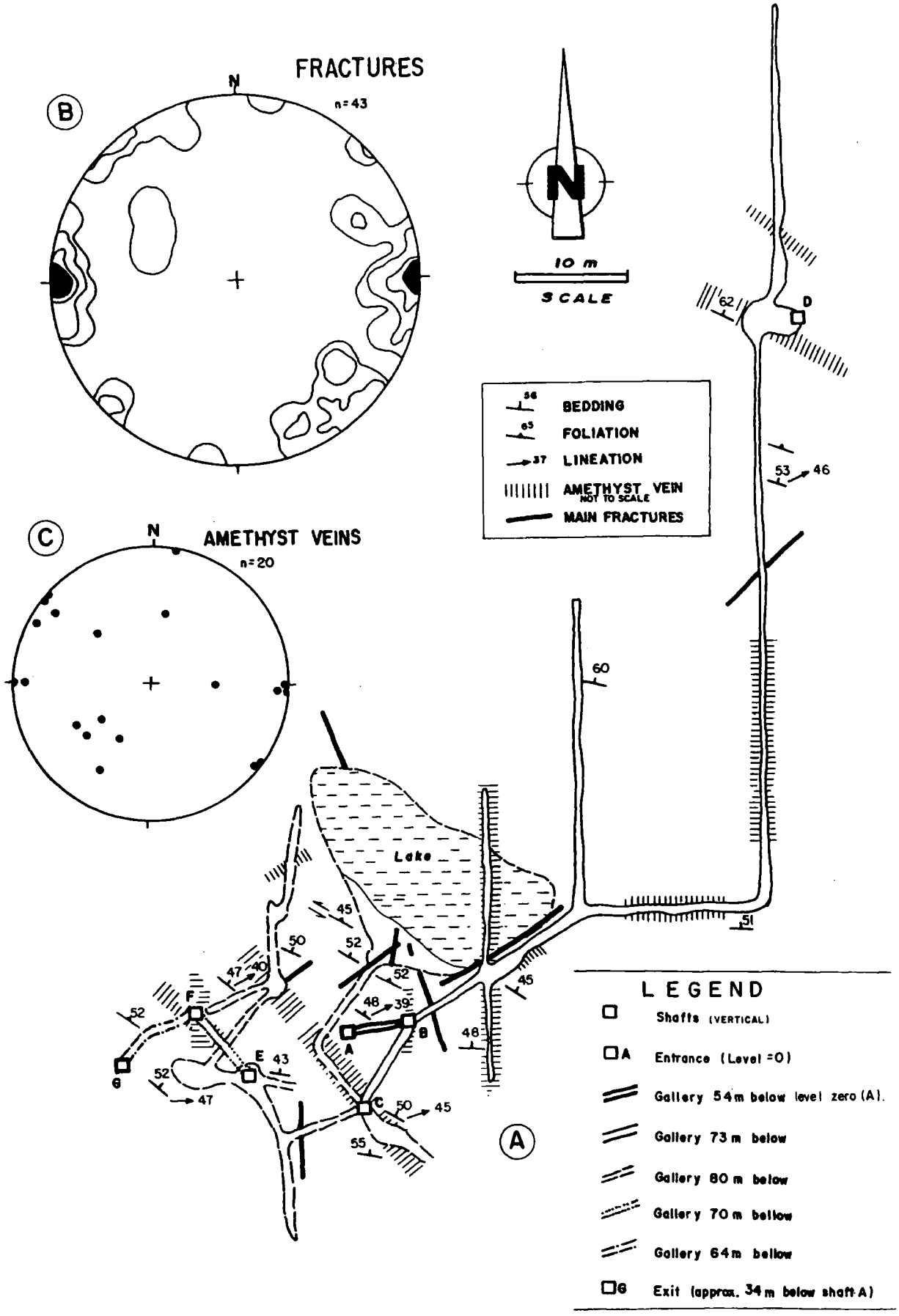

Fig.5.2.2- (A) Map of the shafts and galleries in the Amethyst Mine of the Cururu region. (B) Stereonets showing pole to fractures (contours 4.6/ 9.3/ 14.0/ and 18.6%), including fractures observed in the shafts shown in Fig.5.2.3; (C) poles to amethyst veins.

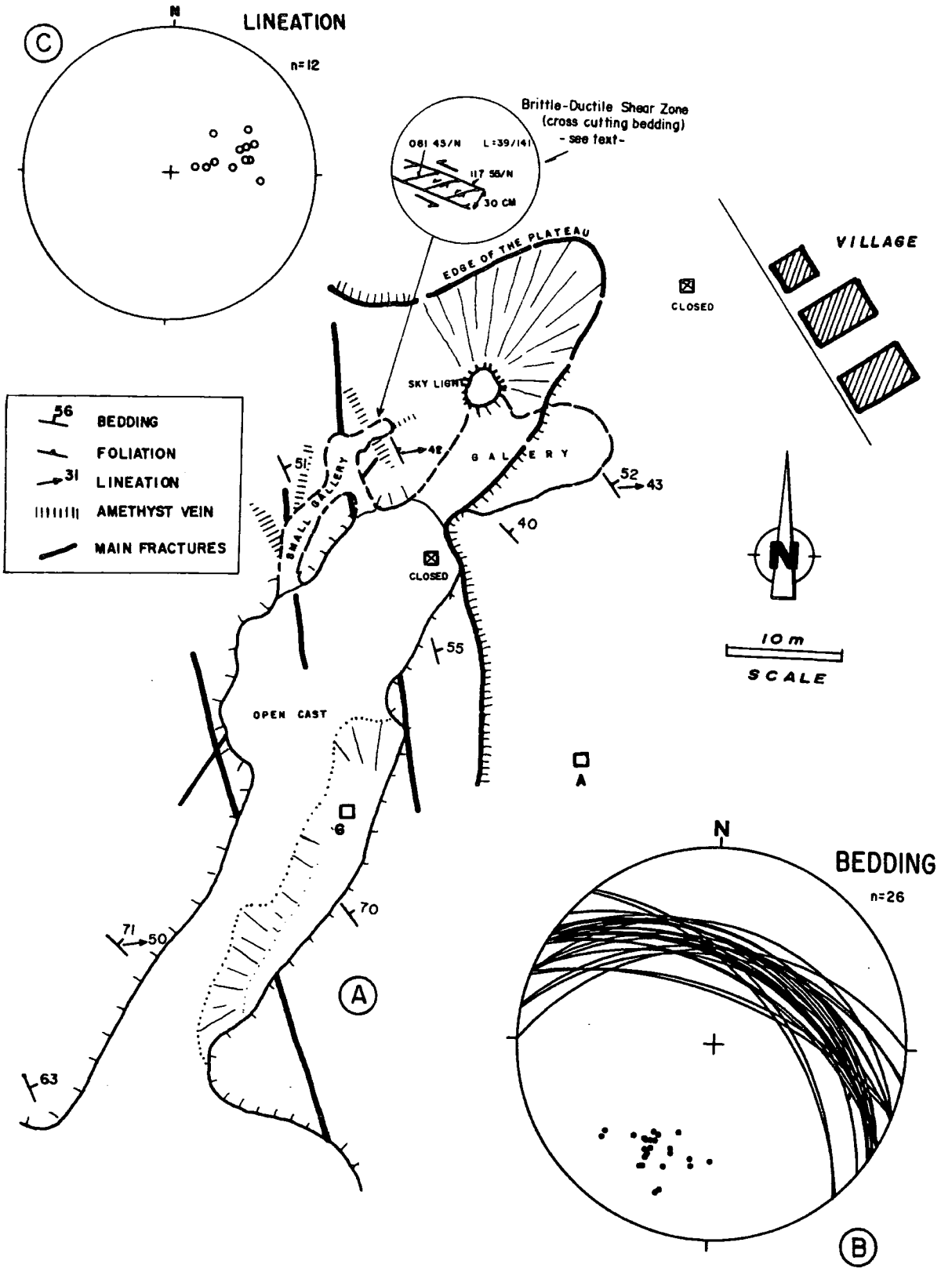

Fig.5.2.3- (A) Map of the open cast pit and small galleries excavated on the southern border of the plateau in the Amethyst mine area. Shafts A and G are also located on Fig.5.2.2. Stereonets represent (B) poles and planes to bedding - including those measured in the galleries on Fig. 5.2.2 - and (C) lineations.

grain shapes, are curved and irregular, serrated, and sometimes straight in triple-junctions (Photo 5.2.2). Sub-grains are common and new grains are present in subordinate amounts. The texture of these rocks is mostly heterogranoblastic-polygonal to grano-lepidoblastic and mylonitic (Photo 5.2.2). Muscovite and sericite form very fine crystals (<0.2mm), constituting aligned discontinuous aggregates arranged around quartz grain boundaries (Photo 5.2.2).

Subordinate metasandstones are interlayered with the quartzites forming red to yellow-red layers displaing a more friable and foliated aspect. These rocks have predominantly subrounded to subangular, quartz grains (Photo 5.2.3) varying in size from 0.8mm to 0.1mm (medium to very fine) and are poorly sorted. The quartz accounts for about 50-60% of the rock, the remainder being formed by a very fine sericitic matrix. This micaceous matrix is itself strongly altered by weathering and shows a weak orientation sometimes forming a spaced rough foliation. These rocks could be classified as quartz-wackes but it is difficult to tell whether the matrix is primary or derived from low grade metamorphism and/or hydrothermal reactions affecting primary feldspar. Cross-bedding and other primary features were not observed.

The bedding in the mine region consistently strikes WNW-ESE, dipping 40°-60° N-NE (Fig.5.2.2 and 5.2.3). A spaced disjunctive or rough to moderately rough foliation is seen under the microscope orientated consistently parallel to the bedding, especially in the fine quartzite and metasandstones. A mineral lineation defined by slightly elongate quartz crystals, occurs within the foliation. The plunge of this lineation is about 50°- 80° ENE/E (Fig.5.2.2 and 5.2.3c).

An S-C fabric is developed in parts of the quartzites which consistently indicates sinistral senses of shear.

Small-scale shear zones, up to 10-30cm across, lie subparallel to the bedding and foliation (Fig.5.2.4). Internally the shear zone rocks are green-brown coloured, and are marked by a strongly spaced disjunctive foliation anastomosing to a moderately rough foliation, defined by the orientation of muscovite and sericite (Photo 5.2.4). Secondary shear band fabrics trend NW-SE, cutting across the foliation at low angles. Quartz has undergone intense grain size reduction during dynamic recrystalisation in these shear zones (Photo 5.2.5). Small crystals (<0.05mm) of tourmaline and epidote cross cut and therefore post date the foliation defined by sericite and elongated quartz grain aggregates (Photo 5.2.6). These rocks can be defined as ultramylonites. Hydrothermal alterations played an important role affecting these rocks along

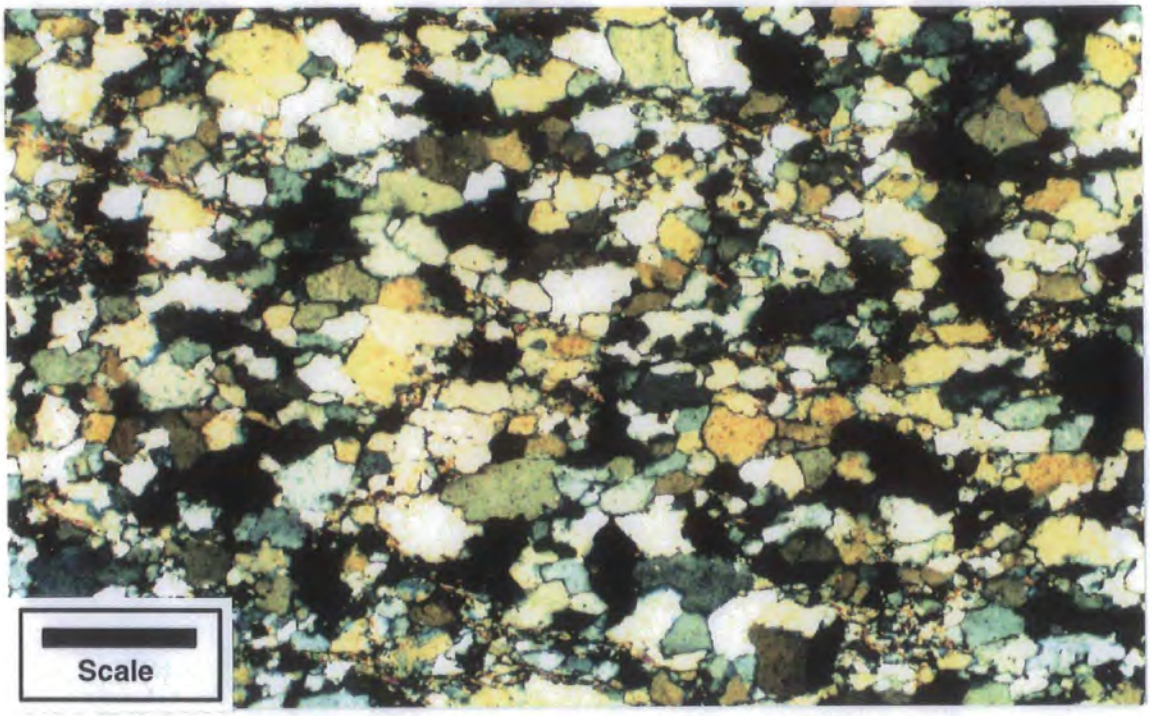

Photo 5.2.2- Photomicrograph of the orthoquartzite observed in the Amethyst Mine (sample from shaft B; Fig.5.2.2). Scale bar = 0.6mm; XPL.

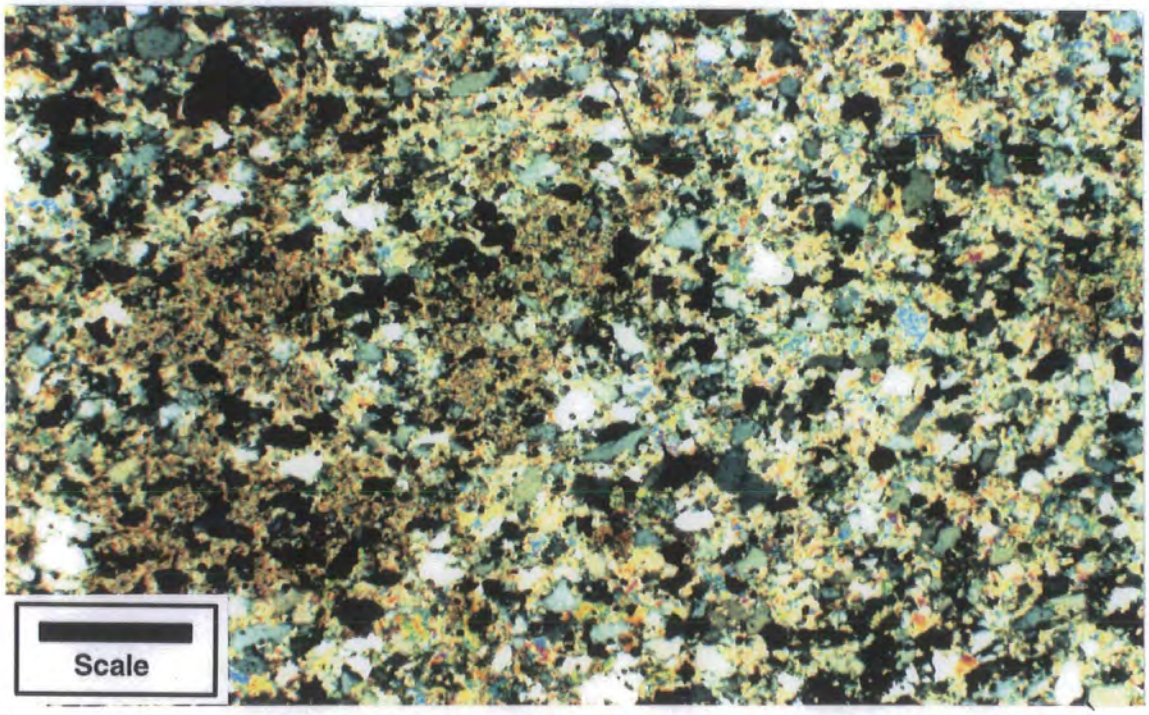

Photo 5.2.3- Metasandstone under the microscope (sample from the gallery between the shaft C and the lake; Fig.5.2.2). See text for comments. Scale bar= 1.0 mm; XPL.

Photo 5.2.4- Ductile shear zone, parallel to bedding, observed in a small gallery close to the lake, in the Amethyst Mine.

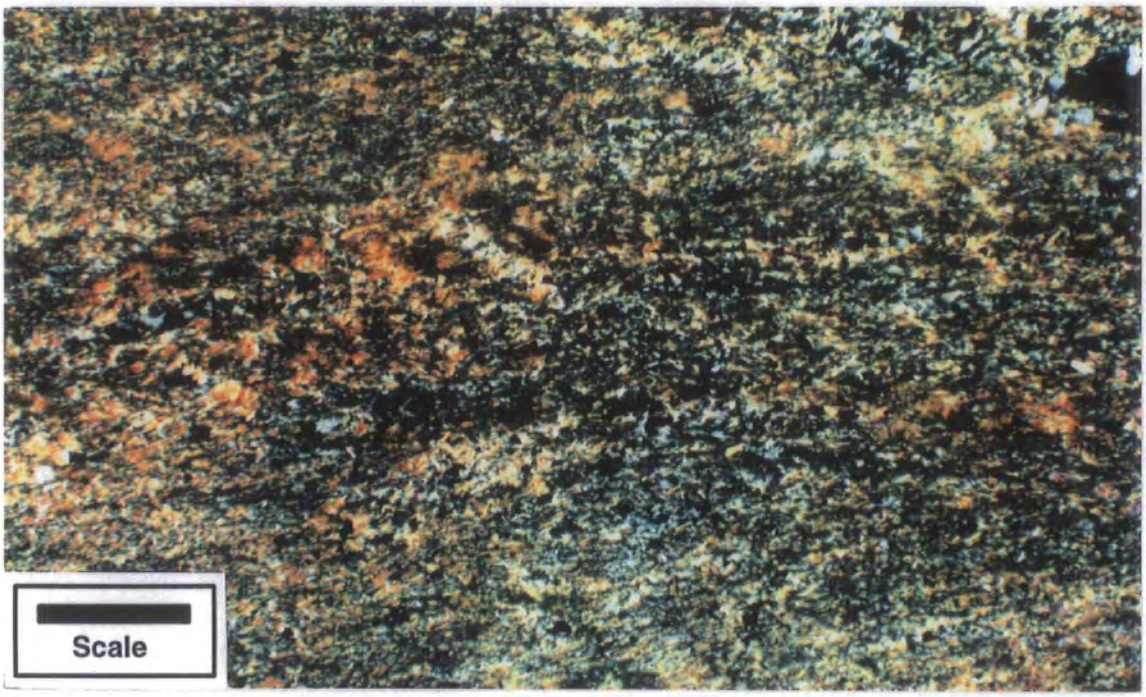

Photo 5.2.5- Ultramylonite observed along WNW-ESE shear zones cutting the quartzites of the Amethyst Mine. Scale bar=0.5mm, XPL.

Photo 5.2.6- Crystals of tourmaline and epidote are present in shear zones cutting the rocks of the mine. Scale bar= 0.5mm, XPL.

these zones. Small scale asymmetric anastomosing shear lenses, inside the shear zones, indicate an up-to-SW and sinistral sense of shear. Some centimetre-scale brittle-ductile shear zones cross cut bedding and foliation. These structures are orientated NW-SE dipping NE, with conjugate shears indicating sinistral movements. The best examples of these structures occur at the northern end of the small gallery dug out of the walls of the open cast mine along the border of the plateau (see detail in the upper part of Fig.5.2.3).

The rocks in the Cururú area are relatively strongly fractured. The fractures are variably spaced by a few metres to tens of metres, and are both extension and shear fractures. They display predominantly N-S and NE-SW sub-vertical orientations (Fig.5.2.2B and 5.2.3 and 5.2.4). Shear sense along faults is difficult to define due to a lack of reliable kinematic indicators and offset markers. Small displacements (<1cm are observed along a few N-S fractures cutting the bedding at high angles. More important fault zones observed in the walls of the mine are shown in Figs.5.2.2 and 5.2.3).

Amethyst veins are found in three more important directions: NW-SE dipping 40°-50° NE, sub-parallel to bedding; N-S sub-vertical; and NE-SW sub-vertical (Fig.5.2.2A, C; 5.2.3 and 5.3.4; Photo 5.2.7). Both the thickness and continuity of these veins is rather variable. Mostly they are 30cm to 2m wide and some are continuous 20-30m along strike (Photo 5.2.7). Many amethyst bodies are linear structures formed along bedding-fracture intersections, especially N-S fractures. These linear bodies plunge 40°-50° N. Sub-vertical bodies are also observed in association with the intersection between sub-vertical sets of fractures (Photo 5.2.8). These are also slightly elongated according to the direction of one or the other fracture planes. The most important veins are emplaced along the bedding (Photo 5.2.9). The infills of the amethyst veins display characteristically drusy growth, with kaolinite infills.

It is worth mentioning that several hot springs occur around the amethyst mine area (Photo 5.2.10). The temperature of the water can reach 40°C, according to local information, contrasting with the 25°-29°C observed in most rivers in the area (Santos, 1986).

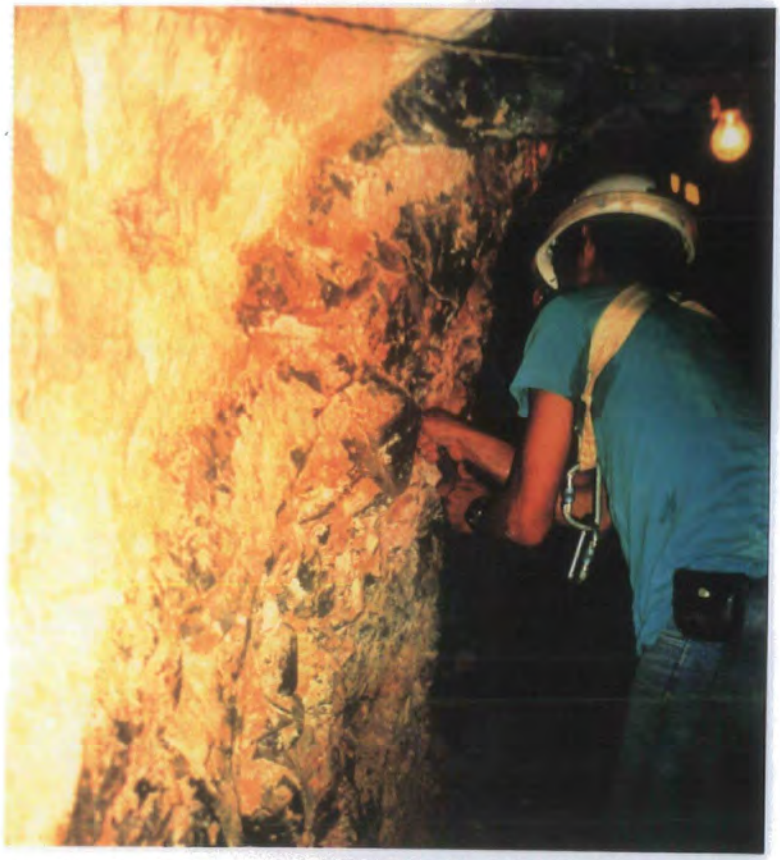

Photo 5.2.7- Amethyst vein following the N-S direction. See text for comments.

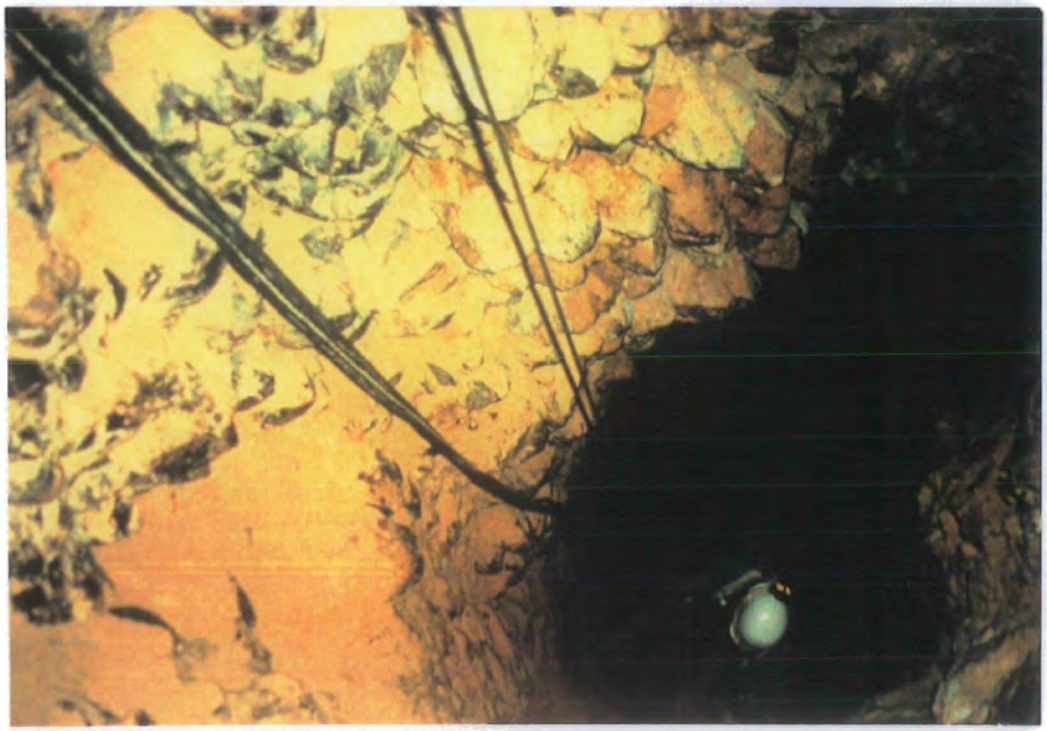

Photo 5.2.8- Amethyst vein observed along shaft B in the mine (see Fig.5.2.2). This vein is approximately elongate along the intersection of bedding and N-S fractures, forming a sub-vertical linear vein.

Photo 5.2.9- Amethyst vein following bedding. The white material is kaolinite.

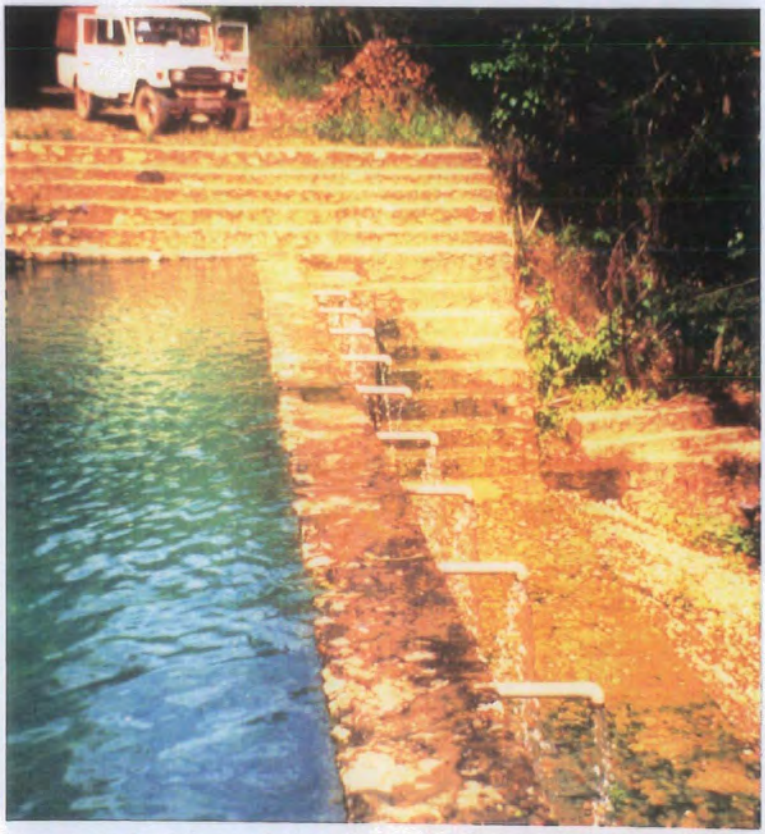

Photo 5.2.10- Hot pool derived from a hot spring in the Cururu region (ca. 600m SE from the mine)

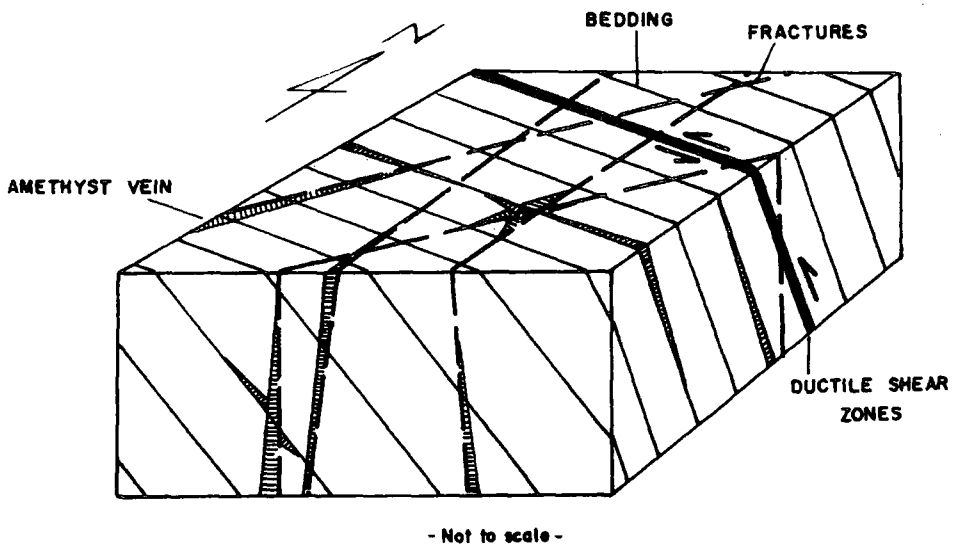

Fig.5.2.4- Block diagram summarising the main planar structures observed in the Cururu area.

5.2.4- DISCUSSION

The quartzites and metasandstones in the Amethyst Mine are a well defined low grade metamorphic sequence described by several previous authors (e.g. Costa *et al.*,1990, Costa and Siqueira, 1990; Lab, 1992). They are here considered to be part of the Archaean Igarapé Pojuca Group, based on their probable correlation with similar quartzites associated with slates along the Serra Pelada region (see next section). Similar units occur also along the northern border of the Carajás Strike-Slip System and in the Bahia Mine area. The dynamic recrystalisation textures in quartz, associated with the mylonitic fabric are consistent with deformation at a low metamorphic grade. Hydrothermal alteration produced widespread sericitization and kaolinitization in these rocks, particularly in fractures and ultramylonitic shear zones. The formation of hydrothermal sericite, epidote and tourmaline post-dates deformation.

The strong NW-SE trend observed in almost all the rocks (bedding, foliation, shear zones, fractures) may explain the presence and orientation of the small lineaments observed in satellite images bounded by major NW-SE

lineaments and, cut by N-S and NNE-SSW features. The mine lies close to the northern border of the main set of lineaments defining this part of the Cinzento Strike-Slip System (Fig.5.2.1). A close analysis of the small lineaments observed to the south and elsewhere in this structure strongly suggests that the bedding is probably also dipping N and NW as well (Photo 5.2.1).

The E-plunging mineral lineation and asymmetric shear criteria indicate a predominantly sinistral reverse sense of displacement. The reverse component of displacement is top-to-WNW in the shear zones observed in the Amethyst Mine area.

In satellite images, two sets of lineament orientated about 100° and 145°-150° intersect to form lozenge-shaped features trending NW-SE (Fig.5.2.1). They display an en echelon arrangement relative to the general 120° trend of the Cinzento Strike-Slip System. Few faults were observed in the mine area in these orientations; most are N-S sub-vertical features and are here suggested to correspond to the later fracture sets seen on the satellite images.

It is here suggested that the so-called Cururú structure corresponds to a set of duplexes formed by the intersection of brittle R (E-W) and P (WNW-ESE) fractures (e.g. Woodcock and Fisher, 1986; Smith and Durney, 1992; Smith, 1993). This conclusion differs from that of Costa and Siqueira (1990) who suggested that it is a symmetric, divergent, compressional structure, defined by P and Y(D) ductile shear zones. These different conclusions arise because there is no geological evidence suggesting that the large scale Cururu structure is in any way linked to the ductile phase of sinistral transpression and low temperature greenschist metamorphism seen in the amethyst mine area. In common with other areas along the Cinzento Strike-Slip System, it is proposed that the discrete structures seen in satellite images formed during and after brittle phases of deformation.

The divergent symmetric geometry proposed by Costa and Siqueira (1990) does not appear to exist. The general structural orientation is WNW-ENE dipping NE. This orientation extends beyond the boundaries of the structure observed in the satellite images both to the N and S. As lineaments are mostly straight they may represent steep faults.

The metasedimentary rocks outcropping around the Amethyst Mine also beyond the limits of the Cururu structure, are continuous along the Cinzento Strike-Slip System towards the Serra Pelada and Salobo regions. This suggests that these rocks are remnants of a broad zone of rocks whose depositional

history may have little direct relation to the geometry of the Cinzento Strike-Slip System. These rocks, after deposition, were then deformed and metamorphosed under low temperature greenschist facies conditions. The ductile shear zones with ultramylonites and the brittle-ductile shear zones were probably formed during this early deformational event coeval with metamorphism.

The N-S lineaments observed in satellite images, are thought to be later structures cutting all the rocks in the region. Their probable Middle Proterozoic age is discussed in Chapter 6.

The N-S fractures and NW-SE bedding appear to control the development of the amethyst veins. These veins may relate to a late extensional episode of deformation of Middle Proterozoic or it is conceivable that they are related to the break up of Gondwana during the Mesozoic. The N-S orientation of the main amethyst veins may be related to dilational jogs formed during the reactivation of the strike-slip duplexes during dextral transtension in the Middle Proterozoic or later (Willis and Tosdal, 1992; Fig.5.2.5). The mechanism of emplacement of the veins may be related to models of epithermal fault-hosted mineralization associated with seismogenic regimes along dilational jogs, as discussed by Sibson (1991, 1994 and 1996).

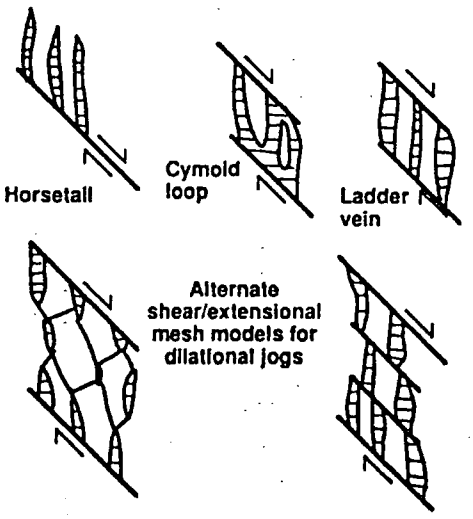

Fig.5.2.5- Models of ore veins filling dextral extensional jogs (after Willis and Tosdal, 1992).

5.2.5- CONCLUSIONS

1) Rocks outcropping in the Cururú region belong to part of the Igarapé Pojuca Group probably of an Archaean age. They were subjected to low temperature greenschist metamorphism and were deformed in a ductile to brittle-ductile manner. An oblique sinistral-reverse sense of shear (top-to-SW) is associated with this event.

2) The quartzites outcropping in the Amethyst Mine and their associated deformation structures are correlated with similar features in the Serra do Sereno area and Bahia Mine regions.

3) The major structures observed on satellite images of the Cururú region are a set of transtensional duplex lineaments formed from linked P and R fractures, cutting the Igarapé Pojuca rocks. The orientation of these major structures may have been strongly controlled by the early ductile fabrics. This episode of transtension occurred after the deposition, deformation and metamorphism of the Igarapé Pojuca rocks.

4) Largely post-tectonic amethyst veins are controlled by the orientation and intersections of NW-SE bedding and N-S fractures. These features may be Middle Proterozoic or younger and, until dated, their age remains conjectural.

5) The occurrence of hot springs in the area suggests that the Cinzento Strike-Slip System may still be active and that the Cururu structure corresponds to a dilational jog (cf. hot springs elsewhere associated with strike-slip fault zones; e.g. Sibson, 1992; 1994).

5.3- THE SERRA PELADA REGION

The Serra Pelada region forms the E part of the Cinzento Strike-Slip System and corresponds to a splay of oblique-slip faults in a typical "horse tail" fault termination zone.

The area is dominated by low grade metamorphic rocks belonging to the Cover Assemblage enclosed within dilational jogs and surrounded by Basement Assemblage rocks. These rocks are intruded by Middle Proterozoic granitic rocks and cut in the east by the Araguaia Belt (Brazilian Orogeny).

The Serra Pelada region is one of the most important gold provinces of the Amazonian Craton. Several mines occur in the region and offer the best exposures in the area. As there is also a dense network of roads, this area is geologically well known (Fig.5.3.1).

This section presents detailed data from three localities: (1) Serra Pelada Gold Mine; (2) Cutia Mine and (3) a quartzite quarry in the Serra do Sereno area (Fig.5.3.1 and 5.3.2). Further information concerning the rocks of the Basement Assemblage is discussed in Chapter 7.

5.3.1- PREVIOUS WORK

The first geological maps of the Serra Pelada region were produced during the mineral prospecting surveys of CVRD/CMM and DOCEGEO (unpublished) during the 1970's.

Meireles and Teixeira (1982), Meireles *et al.* (1982) and Silva (1984) recognised the Archaean Xingu Complex rocks which are gneisses, amphibolites and migmatites. These rocks were described as forming the basement in the region together with an infolded greenstone belt sequence named "Seqüência Rio Novo" (Hirata *et al.*, 1982). This greenstone belt comprises chlorite schists, talc schists, metaperidotites, metapyroxenites, gabbros, diorites, metacherts and banded iron formations which underwent greenschist facies metamorphism.

According to Hirata *et al.* (1982) the Early Proterozoic Grão Pará Group rocks are represented by ironstones unconformably overlying rocks of the Xingu Complex and Rio Novo Sequence. They suggested that these rocks were

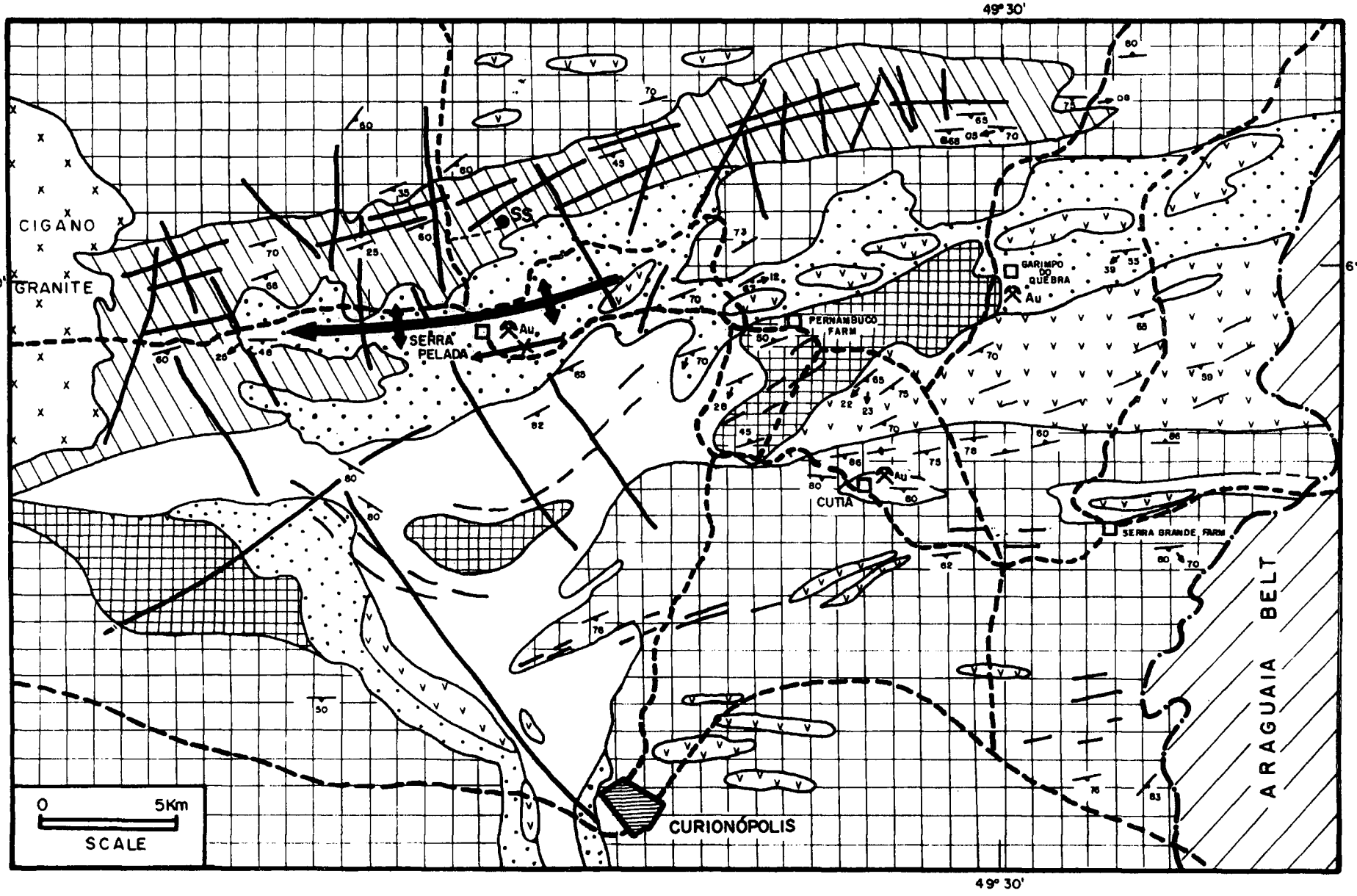

Fig.5.3.1- Geological map of the Serra Pelada region, after Lab (1993) and Jorge João *et al.*, (1982), with new data arising from the present study (see key to the ornaments next page).

LEGEND TO FIG. 5.3.1

Rocks

- Araguaia Belt (Brasiliano Orogeny)
- Cigano Granite
- Quartzites
- Metasedimentary sequence (Sandstones and slates)
- Ironstone
- Metavolcanic rocks
- Mafic-Ultramafic rocks

IGARAPÉ POJUCA GROUP

- Xingu Complex

- Foliation
- Lineation
- Main lineaments
- Road
- Mine
- Farm or small village
- City

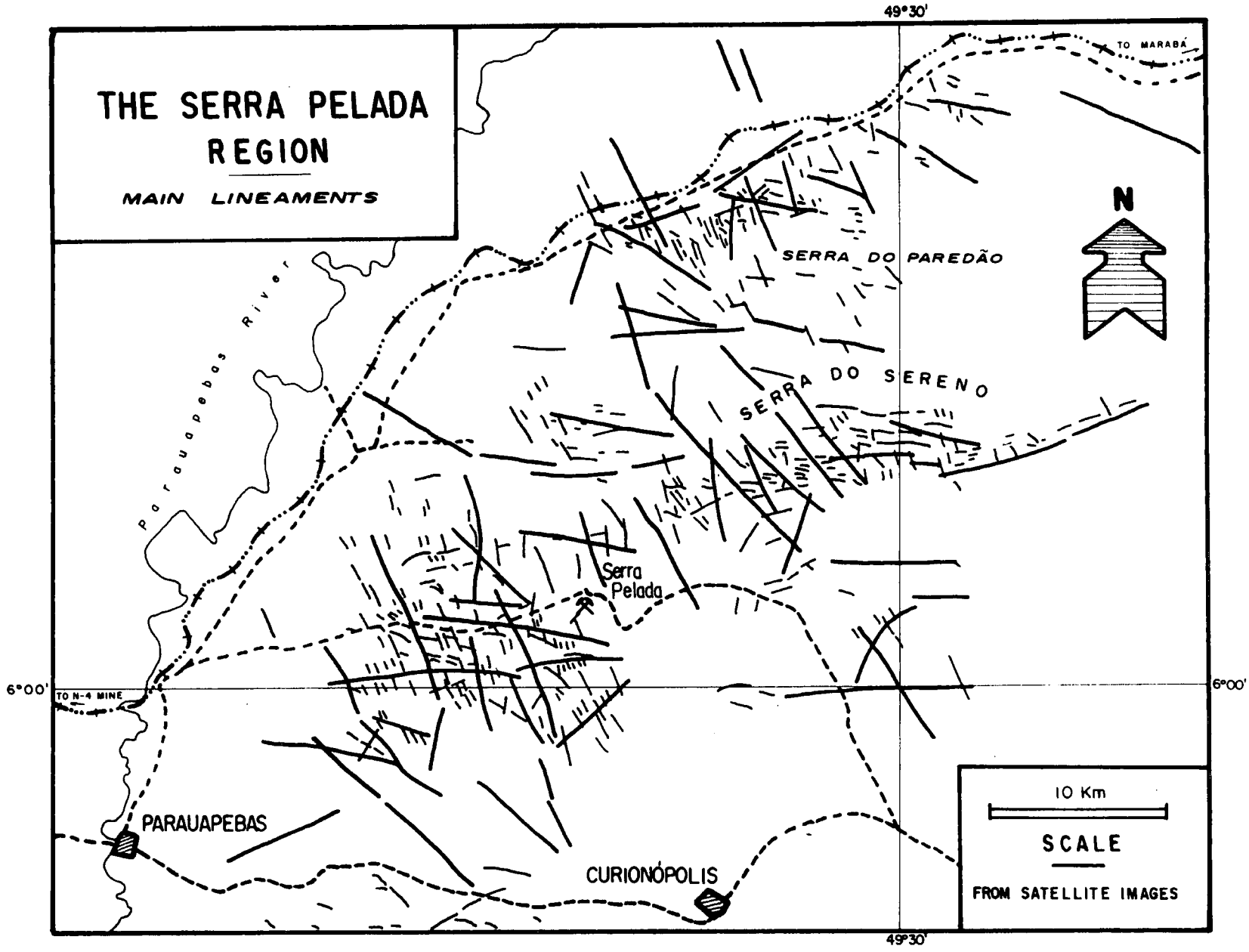

Fig.5.3.2- Map of main lineaments on the Serra Pelada region, from satellite images.

overlain in turn by the clastic rocks of the Rio Fresco Formation. Gabbros, intruded around 198 Ma (Rb/Sr, whole rock); were reported by Meireles and Teixeira (1982) to be the youngest rocks in the region, emplaced as NW-SE dykes.

Meireles and Teixeira (1982) were the first workers to refer to folded rocks in the region. Kilometre-scale structures were thought to control the distribution of metasandstones and pelites in the Serra do Sereno and Serra Pelada areas. They were described as moderately inclined folds, plunging westwards.

Jorge João *et al.* (1982) suggested that the low grade sedimentary rocks in the Serra Pelada area be termed the Serra Pelada Formation. According to Jorge João *et al.* (1982) the Serra Pelada region is cut by sets of Jurassic-Cretaceous dolerite dykes.

The mafic and ultramafic rocks were studied by Suita and Nilson (1988) who referred to them as the "Complexo Ultramáfico Diferenciado Luanga" (Luanga Mafic and Ultramafic Complex), separating them from the Rio Novo Sequence. They established that these ultramafic rocks were emplaced during volcanic activity, at shallow levels, and agreed with the idea that they are part of a greenstone belt. The age of the zircons in leuconorites in this sequence, according to Machado *et al.* (1988) is about 2763±6 Ma (U/Pb). This age has been interpreted as the age of intrusion of this sequence.

In its regional scale synthesis DOCEGEO (1988) reinforced the concept of a greenstone belt sequence infolded into the Xingu Complex rocks in the Serra Pelada region. They included this sequence in the Andorinhas Supergroup, stratigraphically linked to the rocks outcropping in the Rio Maria Granite-Greenstone Terrain, about 200 Km south of the Itacaiúnas Belt. They also introduced the term Buritirama Group to refer to the sedimentary rocks outcropping in the Serra do Buritirama region, about 20 Km north of the Serra Pelada. The metasedimentary rocks outcropping in the Serra Pelada area were assigned to the Rio Fresco Group (Cunha *et al.*, 1984).

Costa *et al.* (1990), followed by Lab (1992) and Lab and Costa (1992), presented detailed geological maps of the Serra Pelada area and locations to the south (Curionópolis region). They used the term Rio Novo Group to refer to the whole metasedimentary, volcanic and ultramafic sequence present in the Serra Pelada region, merging the previously defined rocks of the Grão Pará Group, the Rio Novo Sequence and the Rio Fresco Group. This approach was based on a tectonostratigraphic proposal, which stated that the rocks in the Serra Pelada area were deposited in isolated pull-apart basins infilled by a

single volcano-sedimentary sequence with associated mafic and ultramafic rocks and plutons. The deposition and emplacement of these rocks were thought to be related to an Archaean transtensional episode of deformation that took place all over the region forming different basins. These basins were then inverted by transpression responsible for lithological imbrication, deformation and metamorphism. A later episode of deformation was thought to be responsible for the development of Riedel shear fractures with N-S and NE-SW main directions.

The similar ages of the ultramafics of the Complex Mafic Ultramafic Luanga (2763±6 Ma - U/Pb, zircon; Machado *et al.*,1988), thought to be intruded in the Rio Novo rocks, and the Grão Pará Group rocks (2758±78 Ma - U/Pb, zircon; Wirth *et al*, 1986), was used by Araújo and Maia (1991) to consider them part of the same unit.

5.3.2- REGIONAL GEOLOGICAL SETTING

The Xingu Complex outcrops in a relatively large area north and south of the Cinzento Strike-Slip System (Fig.5.3.1). Similar rocks also occur in an ENE-WSW-trending domain, 1-2 Km wide and 10-12 Km long, inside the domain of the Igarapé Pojuca rocks (Fig.5.3.1).

The Xingu Complex rocks in the southern area are mostly tonalitic to granodioritic gneisses with subordinate amphibolites (Costa *et al.,* 1990). The intensity of the mylonitic foliation is variable, producing ultramylonites to protomylonites. The metamorphic grade in these rocks is thought to be high temperature amphibolite facies allowing localised development of migmatitic fabrics (Araújo and Maia, 1990). At least one important hydrothermal alteration is recognised and is thought to have occurred under greenschist facies metamorphic conditions (e.g. DOCEGEO, 1988; Araújo and Maia, 1990).

The high grade rocks to the north are mostly tonalitic gneisses and amphibolites showing variable grades of ductile deformation (Lab, 1992). Granitoids with biotite, amphibole and garnet are subordinate rock types, and are associated with high grade biotite schists. The fabric observed in these rocks has a strong E-W orientation on a regional scale.

Rocks belonging to the Igarapé Pojuca Group are predominantly quartzites, metasandstones, pelites (slates and metasiltstones), ironstones, and mafic and ultramafic rocks, including dunites, peridotites and pyroxenites which have been metamorphosed to greenschist grade (Meireles *et al.*,1982; Lab,

1992) and/or to low amphibolite facies (e.g. Costa *et al.*,1990). The age of intrusion of the ultramafic rocks is thought to be 2763±6 Ma (U/Pb, zircon) according to Machado *et al.*(1988, 1991).

Shear zones developed mainly along major lithological contacts (Lab, 1992) are considered to relate to a regional transpressional episode of deformation, coeval with greenschist metamorphism (Lab, 1992). Oblique sinistral-reverse shear senses are thought to be the dominant displacements during this event (Costa *et al.*, 1990; Lab, 1992). These main E-W structures appear to be cut by secondary sets of N-S, and NNE-SSW shear zones displaying predominantly dextral displacements based on analyses of c-axes in quartz (Lab, 1992).

5.3.3- THE SERRA PELADA AREA

The Serra Pelada gold mine is located in the central-western part of the Cinzento Strike-Slip System, about 30 Km north of Curionópolis (Fig.5.3.1). Most of the rocks studied here are exposed in the quarry of the open cast mine and also in a few small outcrops along the roads in the northern part of the area. The area lies in a region of pelites and other metasediments which are in contact with quartzites, ironstones, ultramafics and basement gneisses (Fig.5.3.1).

Metasandstones in the area comprise white-red fine- to medium-grained rocks of quartzitic or arkosic composition. Polymictic conglomerates are reported to be present locally in association with metasandstones, containing pebbles of quartz, metasandstone and ironstone (Meireles *et al.*, 1982), but they were not observed during this study. The arkoses are composed of quartz, plagioclase and rock fragments set in a fine grained matrix of quartz, plagioclase, microcline, carbonates, muscovite, biotite, epidote and opaques (Lab, 1992).

In the area of the mine there are also reddish slates and metasiltstones. These rocks are strongly laminated, with beds of about 15-20cm, in which some primary structures such as climbing-wavy bedding, ripple-marks, and *flaser* bedding are preserved (Jorge João *et al.*, 1982). Under the microscope, these rocks are composed of quartz and clay-minerals. The gold is predominantly associated with siltstones altered by hydrothermal fluids in this area (Jorge João *et al.*,1982).

A slaty cleavage is developed in these rocks, normally oblique to the bedding. Cataclastic breccias with fragments of pelites up to 10 cm across occur along N-S to NNE-SSW-trending fault zones.

The bedding in the mine is folded into asymmetric, metre-scale, close to isoclinal folds, representing class 2 or 1C in the Ramsay's fold classification, with an angular to subangular bluntness (Fig.5.3.3; Photo 5.3.1). Small scale parasitic folds are common deforming metre-scale folds which on hundred-metre-scale define major folds (Fig.5.3.3).

The folds plunge mainly SW, WSW with axial planes striking NW-SE, dipping at low angles (<30°) SW. The fold axes have a mean plunge of 33°/ 247° defining a girdle corresponding to the mean axial plane (Fig.5.3.4). In general these structures are reclined to moderately inclined folds, verging southwest (Fig.5.3.4). Field observations of facing directions in areas where primary younging evidence is preserved are consistently upwards and NNW (Fig.5.3.4).

Overall, the structures appear to lie on the inverted limb of a major reclined fold facing N (upwards) with axis plunging SW-WSW (Fig.5.3.4).

Two distinct non-penetrative foliations cut the folded bedding. The most pervasive (S_1) forms a fine to very fine continuous to micro-spaced foliation defined by the alignment of phyllosilicates (sericite and kaolinite), with very fine quartz crystals slightly flattened in microlithons (Photo 5.3.1). The cleavage strikes NNW-SSE, dipping <40° SW (Fig.5.3.5a). This trend is slightly clockwise of the axial planes (Photo 5.3.2). On the stereonet a clockwise transection of 16 ° is apparent (Fig.5.3.5b).

It is also possible to determine the Δ and **d** angles (Borradaile, 1978) from measurements made on individual folds (Table 5.3.1).

Fold Axis	Axial Planes	Cleavage	*Facing* (upwards)	Sense of rotation	Δ	**d**
40/250	120 20/SW	145 26/SW	16/152	clockwise	10^{o}	08^{o}
20/262	131 40/SW	154 35/SW	08/145	?	14^{o}	14^{o}
32/210	128 20/SW	139 30/SW	12/160	clockwise	04^{o}	06^{o}
40/198	110 30/SW	131 45/SW	17/164	clockwise	03^{o}	16^{o}
25/265	120 27/SW	132 20/SW	20/168	?	10^{o}	08^{o}
30/205	155 21/SW	148 30/SW	17/182	?	04^{o}	02^{o}
43/210	170 40/SW	007 45/NW	23/163	clockwise	14^{o}	11^{o}

Table 5.3.1 - Fold axis plunge, orientation of the axial plane, cleavage and facing directions of seven folds studied in the field. The angles Δ and **d** were calculated following Borradaile (1978).

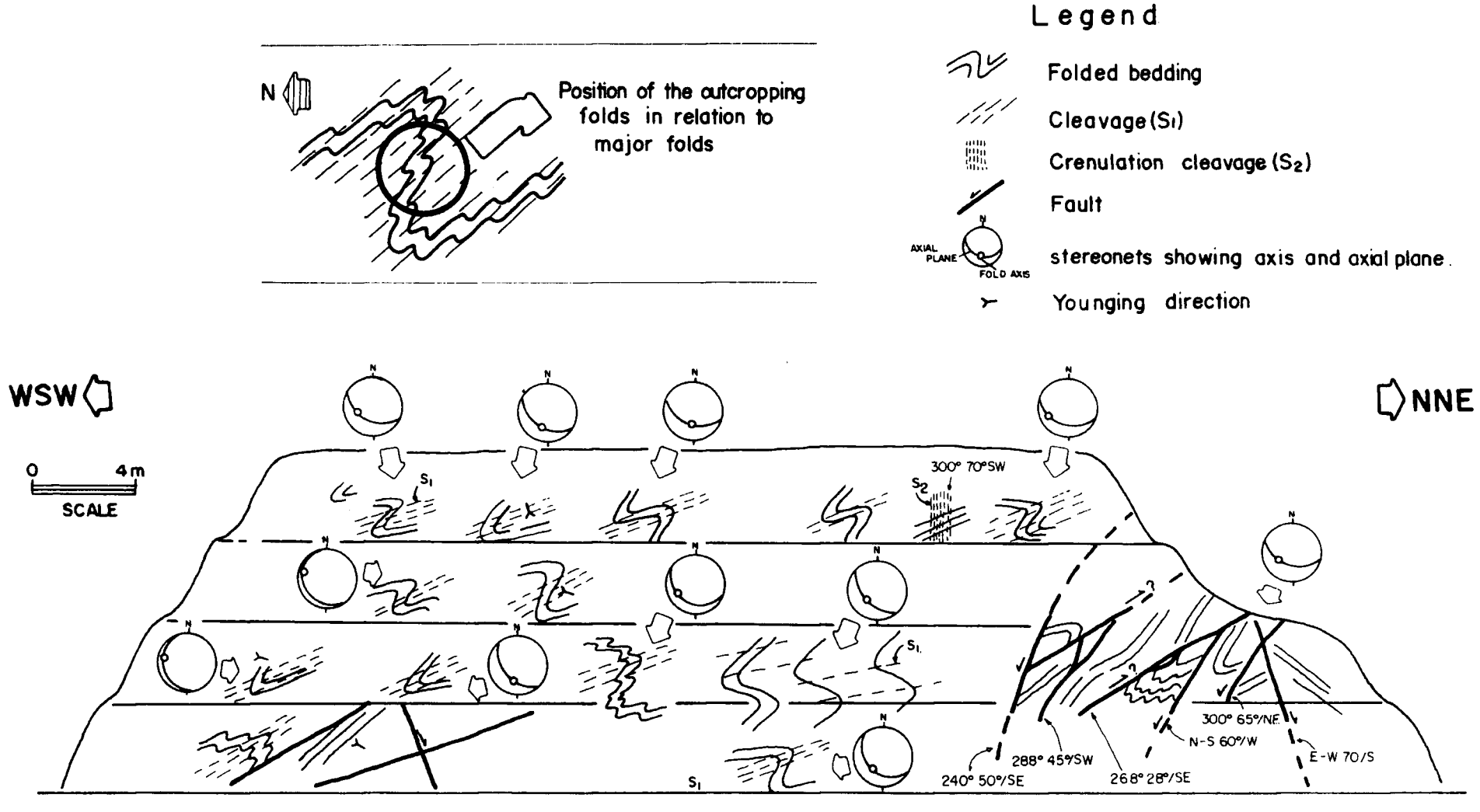

Fig.5.3.3- Sketch of the southern edge of the Serra Pelada mine.

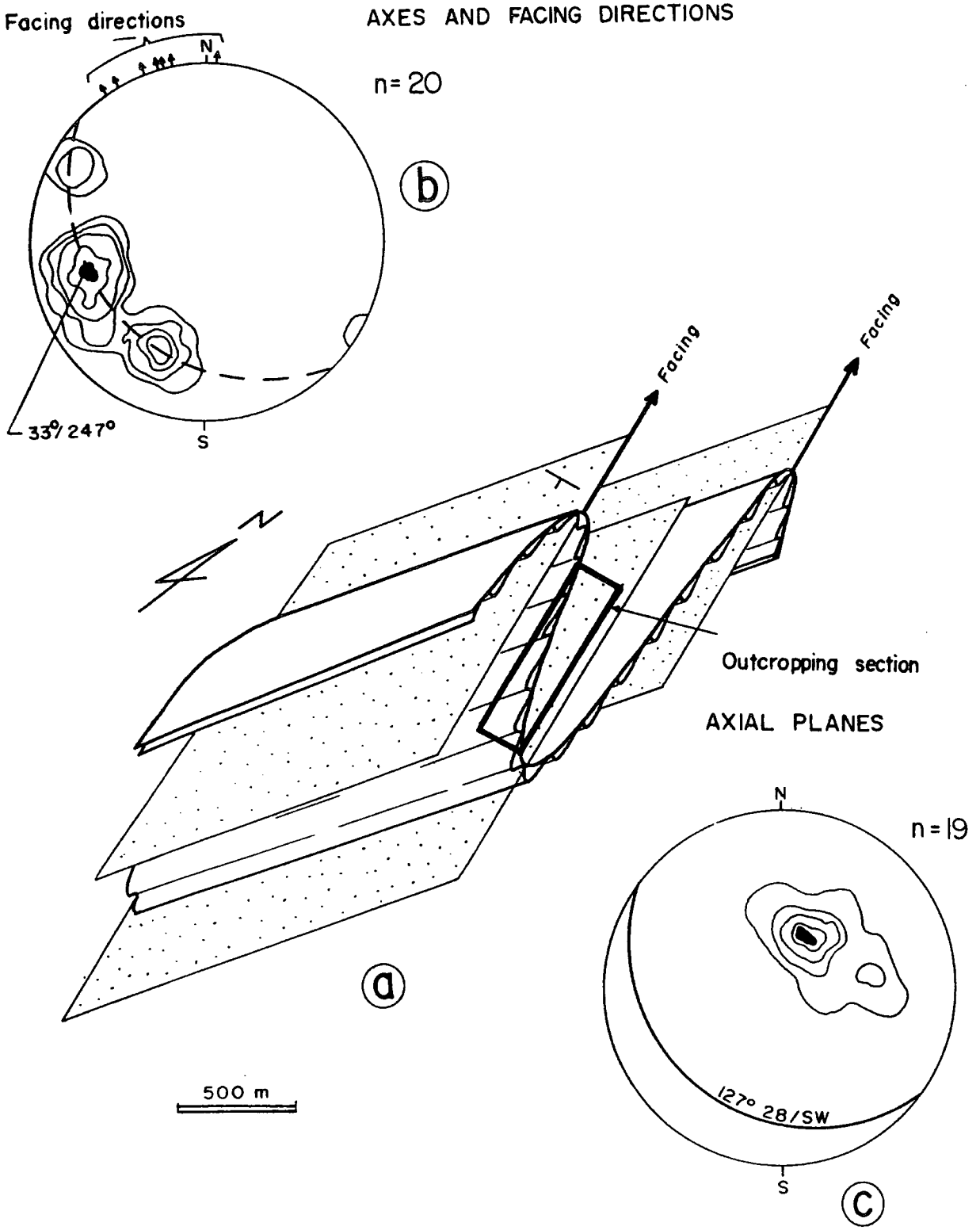

Fig.5.3.4- (a) Diagram showing the simplified geometry and orientation of the major folds present in the Serra Pelada area. (b) Stereonet showing minor fold axis and facing directions of these folds. (c) Stereonet showing poles to axial planes. See text for details.

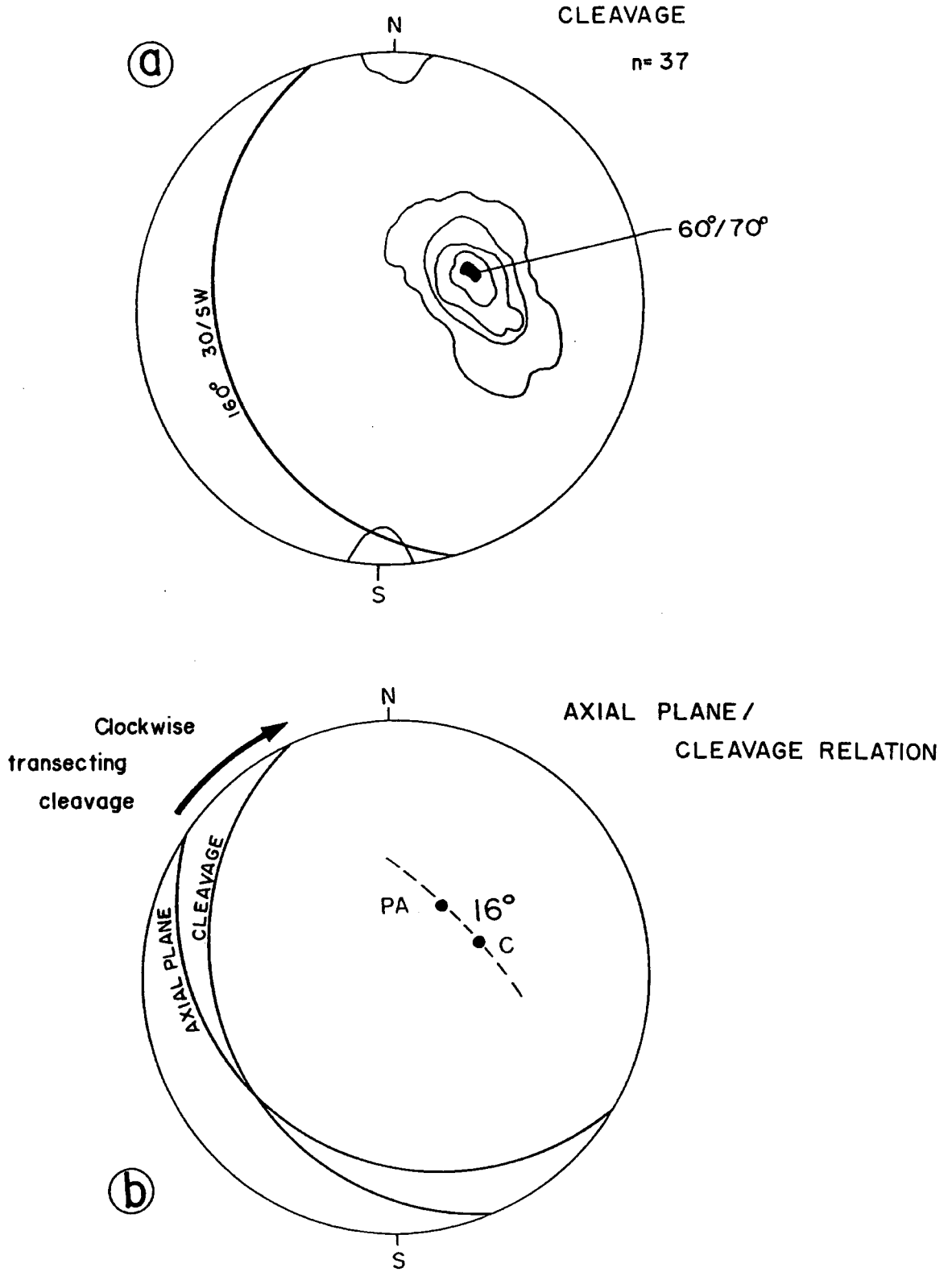

Fig.5.3.5- (a) Poles to cleavage (S_1). Contours representing 2/4/6/8/10%. (b) Stereonet showing the mean axial plane and cleavage. An angle of about 16° separates these planes.

Photo 5.3.1- Metre-scale, close to isoclinal fold, deforming the bedding of the slates in the Serra Pelada mine.

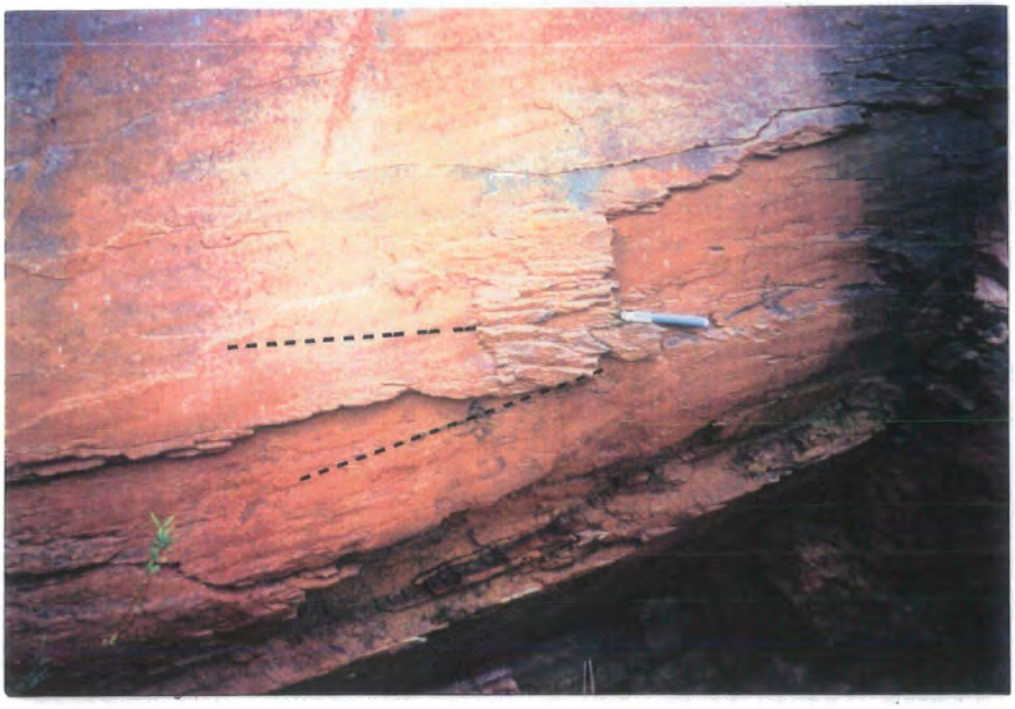

Photo 5.3.2- Hinge of the fold showing the cleavage obliquely transecting the fold hinge in the Serra Pelada mine.

A second later foliation, S_2, corresponds to a discrete crenulation cleavage, with a spacing of a few millimetres (3-5mm). This cleavage occurs in zones up to 3m wide, orientated mainly in NW-SE and NE-SW directions, dipping >70° SW and SE respectively (Photo 5.3.3).

The only linear feature seen in the field is an intersection lineation produced by the slaty cleavage and bedding.

The few fractures observed in outcrops are mostly normal faults concentrated into zones 50-100m long, with a spacing of 5-10m (Fig.5.3.3). They show apparent displacements of 5-10cm, cutting the folds (Photo 5.3.4). Their trend is variable NE-SW to NW-SE, dipping moderately (40°-50°) S. N-S normal faults dipping >80° W are also present but are infrequent.

Reverse faults (Photo 5.3.5) generally lie sub-parallel to bedding and are most obvious where they cut quartz veins obliquely orientated to bedding. They show apparent displacements of about 10-15 cm. Slickenlines were not found along these faults.

Centimetre-scale quartz veins are common filling extension fractures in fold limbs. They are mainly sub-horizontal or form fan-like arrays near to fold hinges.

5.3.4- THE CUTIA MINE AREA

The Cutia mine lies 15 Km NE of Curionópolis (Fig.5.3.1). It was discovered in 1989 by pan-miners and became an important gold mine during 1989-1990. It lies in a lens-shaped outcrop of very altered amphibolites, enfolded in gneisses and granitoids of the Xingu Complex (Fig.5.3.1). Deformation, hydrothermal alteration and weathering are responsible for the very intense modification of both textures and mineralogies of the original rocks. Little has been published about this mine apart from a brief reference in Lab (1992).

The rocks outcropping in the mine are highly banded with various weathered colours (reds, white, purples, greens, browns, grey and black). Lenses of kaolinite in the darker rocks, are reported by miners to contain the highest ore concentrations. All rocks are friable, with some portions being harder due to quartz and/or iron impregnation. Their texture varies from foliated

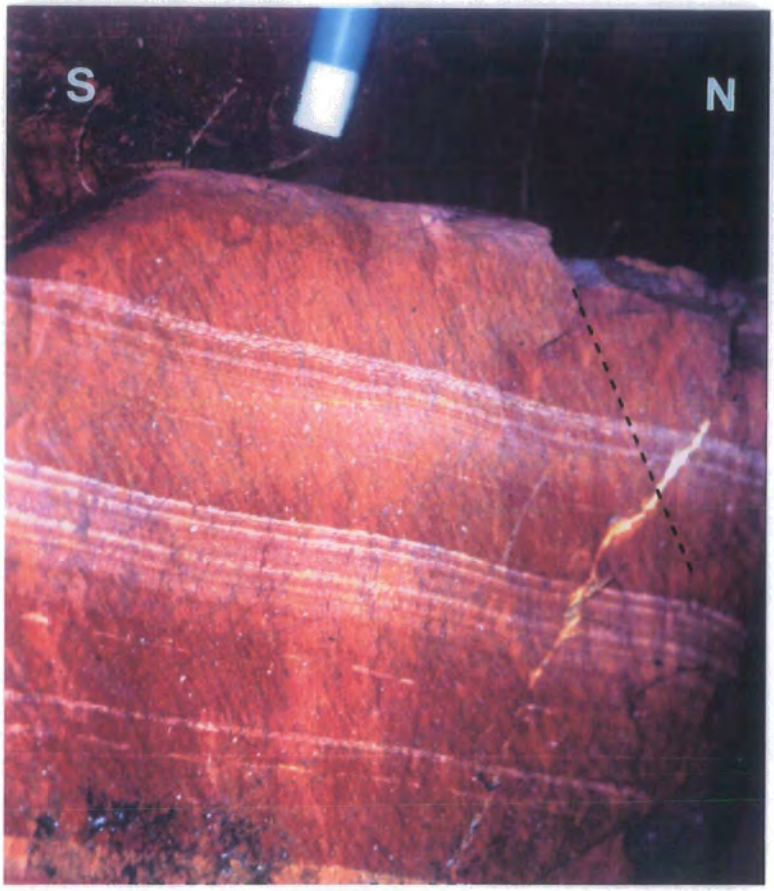

Photo 5.3.3- A crenulation cleavage (S_2) cutting the laminated mudstones in the Serra Pelada mine.

Photo 5.3.4- Normal faults cutting mudstones in the Serra Pelada mine.

Photo 5.3.5- Low-angle reverse fault sub-parallel to bedding in the Serra Pelada mine.

to fine to medium-coarse granular with high porosity and low density. Very fractured or sheared rocks have cataclastic and phyllonitic texture (Photo 5.3.6). The spatial distribution of rocks with different textures and colours follows the trend of the foliation. White quartz veins are abundant filling extensional fractures with drusy infills or in deformed veins parallel to the local foliation (Photo 5.3.7). Drusy veins may contain very fine dark crystals of haematite filling gaps between quartz crystals. Gold is also reported to be secondarily associated with these veins, according to local miners.

The foliation comprises both a fine continuous to moderately rough cleavage and a spaced disjunctive anastomosing cleavage. The former resembles a slaty cleavage in places. They are both subparallel following a E-W to ENE-WSW trend, dipping >50° S (Fig.5.3.6a). Some foliations are orientated NW-SE dipping at high angles NE (Fig 5.3.6a). The disjunctive anastomosing cleavage clearly overprints and locally obliterates the earlier sub-parallel fine continuous cleavage.

A weak mineral lineation is present in the continuous foliation planes plunging generally moderately S to E (Fig.5.3.6b).

Some lens-shaped quartz veins sub-parallel to the foliation are slightly asymmetric, suggesting a sinistral sense of shear. En echelon arrays of quartz veins also strongly suggest sinistral displacements along planes subparallel to the foliation.

Fractures are abundant, most cutting the rocks sub-parallel or orthogonally to the main foliation (Photo 5.3.6). They display spacing varying from a few metres (<2m) to a few centimetres (5 cm).

Faults are predominantly normal displacements dipping steeply E and S (Fig.5.3.6c). Striations observed on these fault planes plunge steeply E or W orientated along the central area of the stereonet (Fig.5.3.6d). E-W trending faults also display secondary strike-slip components of displacement, both dextral and sinistral.

Dolerite dykes are observed cutting the rocks adjacent to the mine. One of these dykes is oriented N-S dipping steeply (>80°) both E and W.

5.3.5- THE SERRA DO SERENO AREA

The Serra do Sereno forms a set of E-W orientated hills located NE of the Serra Pelada Mine (Fig.5.3.2). A sequence of low grade metasedimentary

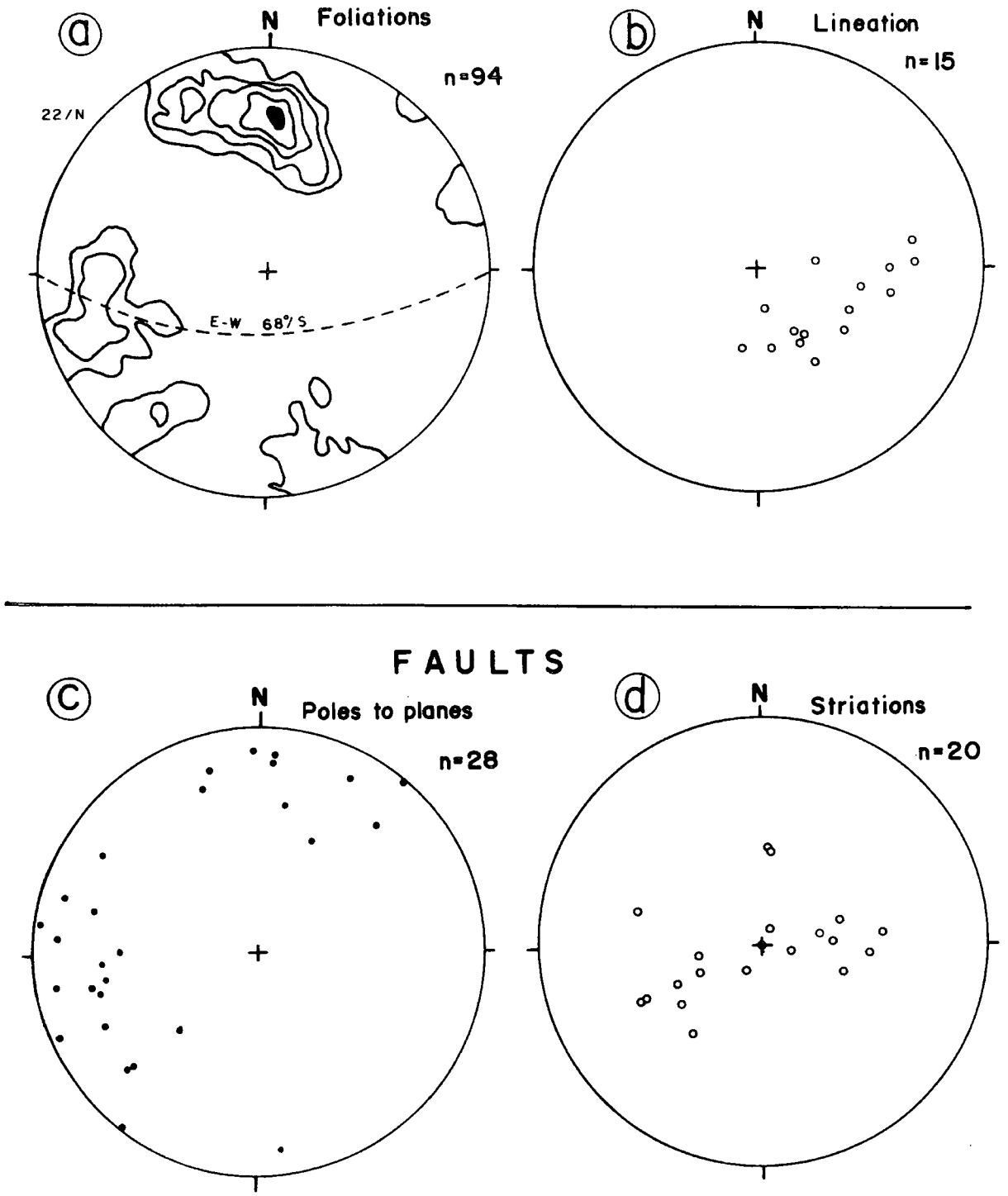

Fig.5.3.6- (a) Poles of foliation observed in the Cutia Mine. The main orientation is shown by the dashed line (counters: 3.2/5.3/7.5/9.5/11.7%). (b) Plots of lineations observed on the foliation surface. (c) Poles to planes of faults observed in the mine. (d) Orientation of striations observed on the fault planes in the Cutia Mine.

rocks are exposed in a quarry located about 5 Km from the Serra Pelada mine (marked as 'SS' on Fig.5.3.1). This quarry was mapped in detail (Fig.5.3.7).

The rocks are pelites, interlayered sandstones and siltstones and quartzites.

The pelites are red-yellow rocks, bedded on a scale of 20- 40 cm, with a total thickness of 17 m in the northern part of the quarry (Fig.5.3.7). The bedding is orientated NE-SW dipping 30°-35° SE, and is cut by a discrete, fine continuous cleavage orientated NNE-SSW dipping 60°-65° SE. A weak slickenline lineation in cleavage planes plunges at low angles (<20°) SW. A later crenulation cleavage is orientated roughly NNE-SSW dipping moderately E. Associated crenulations plunge 35° SSW (Fig.5.3.7).

Three main sets of sub-vertical faults cut these rocks, orientated N-S, NW-SE and close to E-W (Fig.5.3.7). Slickensides indicate mainly dextral displacements. The NW-SE faults consistently displace those trending E-W, and develop drag-folds in adjacent beds.

Above these rocks, in concordant contact, is a 150m thick succession of low grade sandstones, siltstones and quartzites interlayered on a scale of 10 to 50 cm (Photo 5.3.8). The bedding in these rocks strikes NE-SW, dipping 40°-70 ° SE (Fig.5.3.7). Right way up cross-stratification within sandstone beds indicates a probable palaeocurrent direction towards about 110°. A cleavage runs oblique to bedding, striking NNE-SSW, and dipping 50° SE (Fig.5.3.7). The intersection between bedding and cleavage plunges 65° / 115°.

A massive unit of fine to coarse grained quartzites overlies the rocks described above. They are mostly bedded on a scale of 1-2m, and the bedding defines a gentle fold plunging about 12° NE (Fig.5.3.7). These rocks are densely fractured with at least three main sets of fractures developed, orientated N-S, NW-SE, and E-W (Photo 5.3.9). The N-S fractures are the most abundant and locally obliterate bedding.

5.3.6- DISCUSSION

The data from the Serra Pelada area suggests that the major structures in the region are a series of kilometre- to hundred-metre scale folds, overturned towards the N-NE, with axes plunging SW. The major folds are slightly curvilinear since their axes define a girdle corresponding to the mean axial plane (Fig.5.3.6). These conclusions are generally consistent with the findings of Meireles and Teixeira (1982) and Meireles *et al.* (1982) who referred to a set

Photo 5.3.6- Typical rock exposure in the Cutia Mine. A slaty cleavage is overprinted by a sub-parallel disjunctive anastomosing cleavage and cut by orthogonal sets of fractures.

Photo 5.3.7- Deformed quartz veins, sub-parallel to the main foliation in the Cutia mine.

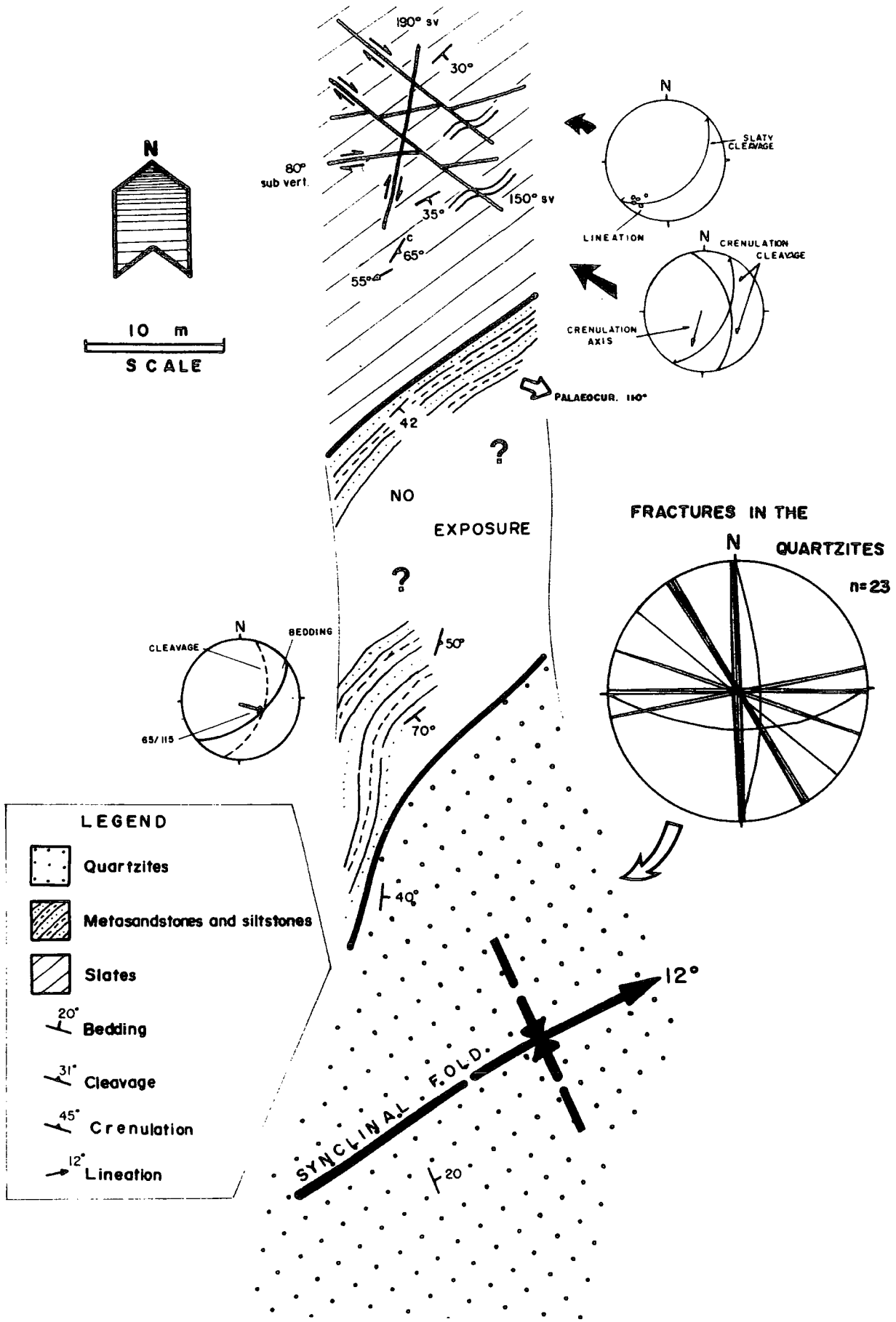

Fig.5.3.7- Map of the quartzite quarry studied in the Serra do Sereno area.

Photo 5.3.8- Concordant contact between siltstones and sandstones observed in the Serra do Sereno quartzite quarry.

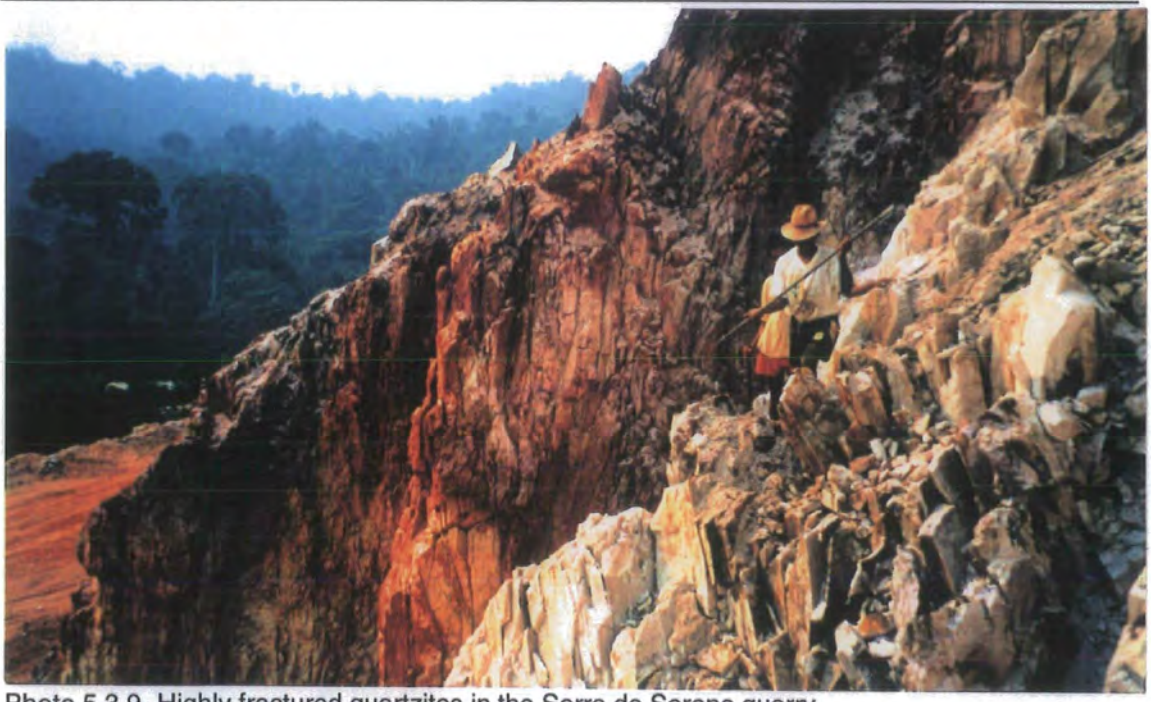

Photo 5.3.9- Highly fractured quartzites in the Serra do Sereno quarry.

of large folds, orientated roughly E-W, in the Serra Pelada and Serra do Sereno areas.

It was demonstrated that the fold axial plane and the broadly coeval slaty cleavage are slightly oblique, defining a transecting cleavage. This geometry can be observed directly in the field or using mean values determined on a stereonet (Fig.5.3.5b).

Transecting cleavages have been described from many locations around the world (e.g. Ramsay, 1963; Powell, 1974; Borradaile, 1978; Treagus and Treagus, 1981; Soper, 1986; Treagus and Treagus, 1992). According to Ramsay (1963), both fold and cleavage may be coeval, but during non-coaxial deformation the cleavage plane (XY) rotates gradually relative to the hinge of the fold during progressive deformation. Borradaile (1978) suggested a small delay between the development of the cleavage relative to the folding in a non-coaxial regime. More recently some authors (e.g. Sanderson *et al.*, 1980; Soper and Hutton, 1984; and Woodcock and Schubert, 1994) have associated transection and transpressional deformations. They suggested that examples of these structures in the Caledonides displaying clockwise transecting cleavage can be related to sinistral transpressional deformation. These ideas have been examined critically by Soper (1986) and Treagus and Treagus (1992) who concluded that a straightforward relationship between transecting cleavage and transpression does not exist and needs to be confirmed by other regional data.

Sinistral transpression has been reported as being responsible for at least one tectonic inversion event along the Itacaiúnas Belt (e.g. Araújo *et al.*,1988; Araújo and Maia, 1990; Costa and Siqueira, 1990). Lab (1992) studying the orientation of quartz C-axes in the quartzites N of the Serra Pelada mine recognised an important sinistral component of deformation coeval with the development of the ductile to brittle-ductile fabrics present in these rocks. Additional evidence for polyphase transtensional and transpressional deformations along the Carajás and Cinzento strike-slip systems has been outlined by Pinheiro and Holdsworth (1997*a*; 1997*b*).

The lack of stretching lineations in many of the rocks in the region e.g. in the pelites of the Serra Pelada mine, suggests that the deformation is in the flattening strain field ($1>K\geq0$). This is consistent with a transpressional deformation according to the strain models of Sanderson and Marchini (1984).

The folds in the Serra do Sereno area plunge ENE-WSW at low angles, following the same orientation as the structures of the Serra Pelada mine area.

The crenulation cleavages observed both in Serra Pelada and Serra do Sereno are orientated E-W and N-S respectively. They probably relate to the main faulting episode observed in the region.

Normal faults in the field follow the trends of the main lineaments visible on satellite images (E-W and NNW-SSE) suggesting that there was an important extensional or transtensional event, post-dating the folds and transecting cleavage. NW-SE lineaments, observed on satellite images, coincide with dextral faults observed in the Serra do Sereno rocks.

E-W and ENE-WSW-trending normal faults may have developed in both the Serra Pelada and the Serra do Sereno rocks during sinistral displacement along the main E-W segment of the Cinzento Strike-Slip System leading to NW-SE transtension in the fault zone terminating splay (Fig.5.3.8).

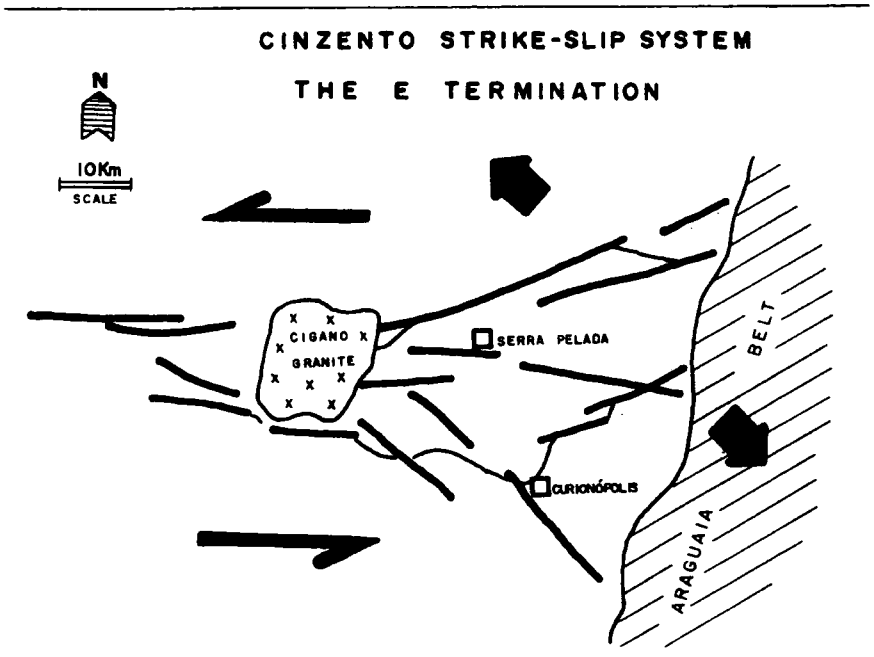

Fig.5.3.8- The termination of the Cinzento Strike-Slip System and transtension during sinistral shearing.

The rocks observed in the Cutia Mine quarry are probably older than those observed in the Serra Pelada and Serra do Sereno areas. The presence of two distinct overprinted foliations in the Cutia mine quarry suggests that at least two main episodes have occurred. The earlier continuous cleavage gives the rocks a phyllonitic aspect. This appears to be associated with a sinistral brittle-ductile episode of shearing associated with hydrothermal alterations. The second disjunctive cleavage is a brittle structure formed sub-parallel to the earlier foliation. An important set of normal faults follows the same trend,

suggesting that they may be geometrically related although they could be formed in a later brittle episode, following planes of weakness along the pre-existing foliation. The slickenlines lineation associated with the latter cleavage appears to be consistent with displacements involving reverse and dextral strike-slip movements.

The metasediments described in these areas are very similar to rocks of the Igarapé Pojuca Group found associated with the Carajás Strike-Slip System (e.g. Bahia Mine region, Itacaiúnas River, Pojuca area) and further west along the Cinzento Strike-Slip System (e.g. Cururú area). They have close petrographic and structural similarities.

The mafic rocks, volcanics, sub-volcanics and intrusives were not studied and a correlation of these rocks is highly problematic. Their massive, rarely deformed, character and low metamorphic grade suggest that they are also most easily assigned to the Igarapé Pojuca Group.

There are no reliable criteria to suggest that these rocks are associated with a greenstone belt sequence.

5.3.7- CONCLUSIONS

1- The E termination of the Cinzento Strike-Slip System is dominated by a strong E-W structural trend defined by sets of faults and folds and in places low temperature brittle-ductile to brittle fabrics.

2- The rocks outcropping in this area are predominantly greenschist facies volcanic mafics and ultramafics, ironstones, pelites, quartzites and sandstones. There is no reliable evidence to suggest that any of these rocks belong to a greenstone belt. They are most readily correlated to the Archaean Igarapé Pojuca Group.

3. The metasedimentary sequences are folded by open to isoclinal structures plunging at low angles WNW or ESE. A clockwise transecting cleavage is developed in these folds together with a sinistral transpressional episode of deformation.

4. The large-scale "horse tail" lineament geometry is strongly reminiscent of a strike-slip fault termination.

5. The superposition of sub-parallel cleavages and fracture sets, originating during different deformations affecting strongly altered basement rocks, clearly suggest that reactivation of older fabrics occurs during later deformation episodes.

6. The predominance of normal fault sets trending E-W to ENE-WSW can be related to later transtension in the fault splay termination during sinistral displacement along the Cinzento Strike-Slip System. Alternatively, they may relate to the regional Middle Proterozoic extensional episode of deformation recognised regionally.

8- Hydrothermal fluids are associated with the deformations profoundly altering host rock mineralogies and controlling ore distribution in the region.

SUMMARY

TECTONOSTRATIGRAPHY

Three groups of rocks are associated with the Salobo Strike-Slip System: (1) gneisses and granitoids representing the Xingu Complex; (2) sequences of schists, quartzites, ironstones, and amphibolites from the Igarapé Salobo Group and (3) metavolcanics and metasedimentary rocks of the Igarapé Pojuca Group (Fig.S5.1 and S5.2).

The Xingu Complex and Igarapé Salobo Group are assigned to the Basement Assemblage, whilst the Igarapé Pojuca Group is thought to represent the lowest unit of the Cover Assemblage. The main difference between these two groups of rocks is the preservation of high temperature deformation fabrics and metamorphism in the Basement Assemblage. In contrast, lower temperatures of deformation and regional metamorphic alteration are seen in the Igarapé Pojuca Group.

The Archaean Old Salobo Granite, has a supposed intrusion age of about 2.5 Ga (Machado *et al.*, 1991) and is emplaced into the Xingu Complex and Igarapé Salobo rocks (Lindenmayer *et al.*, 1994*a*). This granite has been correlated with the Estrela Granite, in the south of the Serra Pelada region (Fig.S.5.1; see section 4.6, Chapter 4). Both the Xingu Complex and the Igarapé Pojuca rocks are also cut by the Cigano Granite, while the Igarapé Salobo rocks are intruded by the Young Salobo Granite. These later intrusive rocks are ca. 1.8 Ga in age.

The geographical distribution of all rocks associated with the Cinzento Strike-Slip System is strongly controlled by the geometry of the main lineaments present in the region and displays a roughly WNW-ESE to E-W trend. The Basement Assemblage occurs both outside and inside the strike-slip system. The rocks of this assemblage are predominantly high grade metamorphic orthogneisses, migmatites and amphibolites. These rocks display high temperature mylonitic foliations in the schists and granitoid rocks and banding in the gneisses.

The schists, quartzites and ironstones of the Igarapé Salobo Group also show evidence of having been deformed and metamorphosed at high temperatures. The presence of hornblende, hastingsite and andesine in the

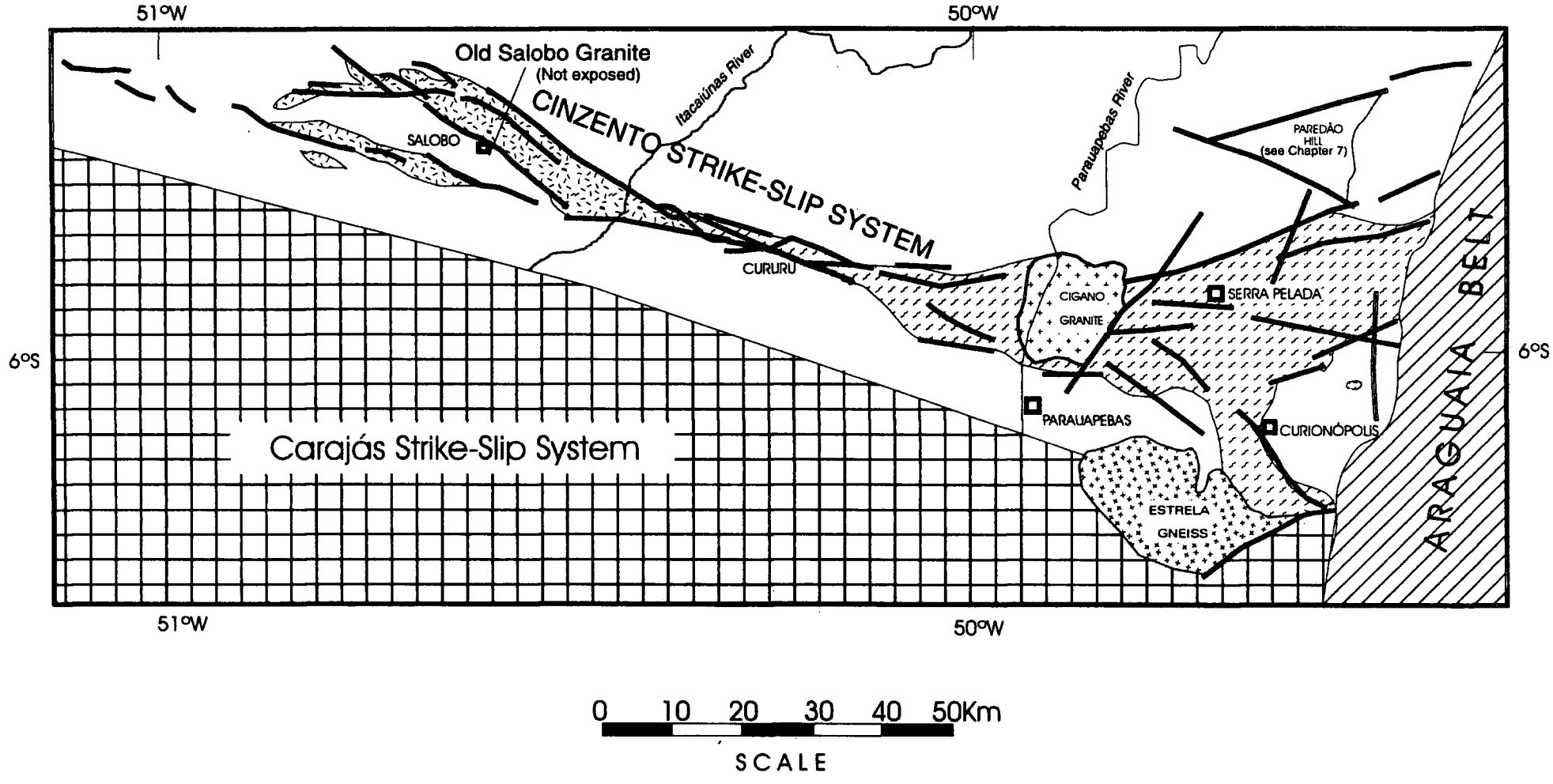

Fig.S5.1- Geological map of the Cinzento Strike-Slip System (modified after Siqueira, 1990; Costa *et al.*, 1990 and Lab, 1992).

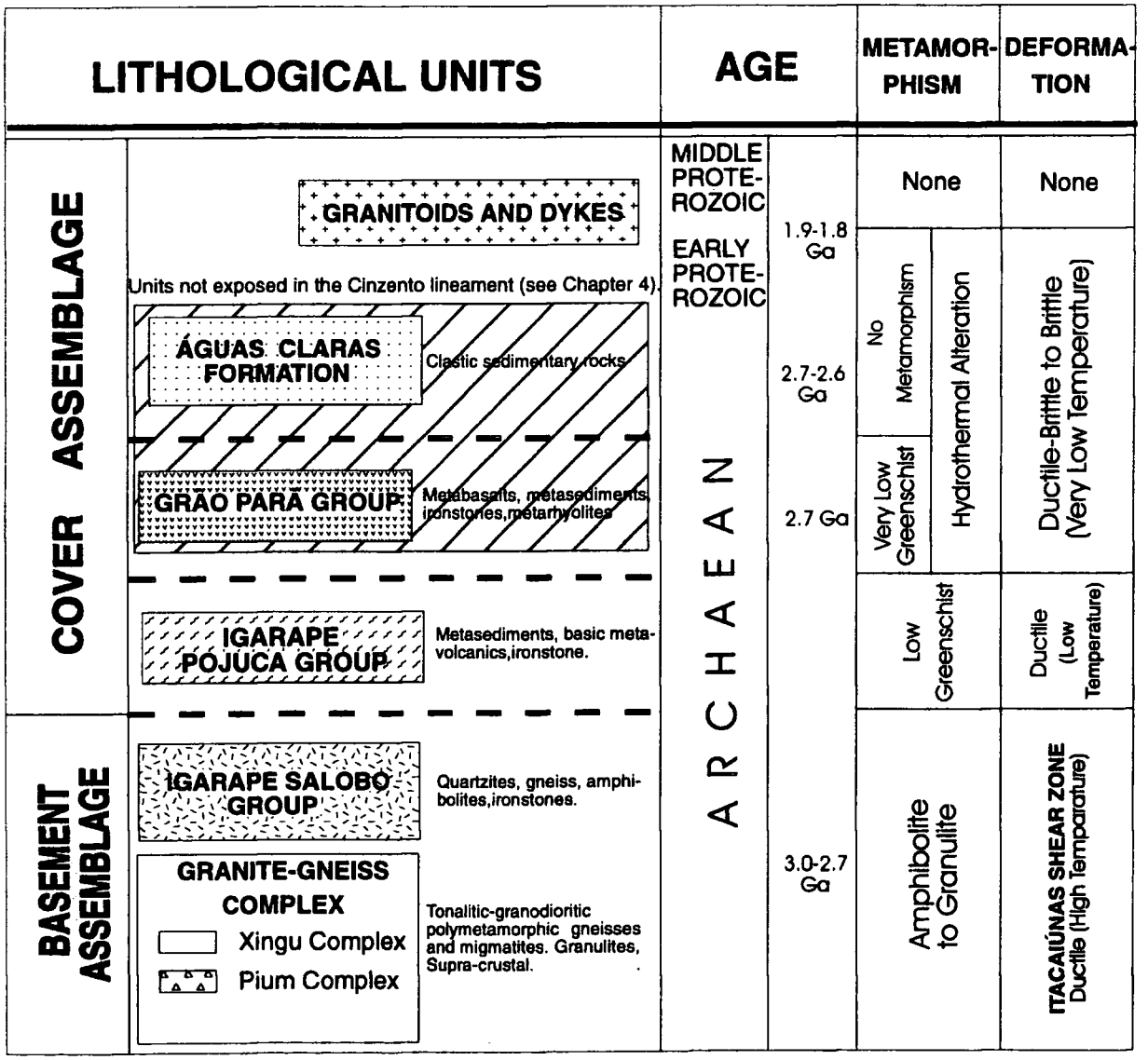

Fig. S5.2- Tectonostratigraphic column for the Cinzento Strike-Slip System. See Fig.S5.1.

ironstones, hornblende-plagioclase-orthoclase in the amphibolites, and sillimanite in the quartzites are indicative of high metamorphic temperatures.

The age of this event lies somewhere between 2851±4 Ma and 2761±3 Ma, according to existing radiometric data (U/Pb, zircon) published by Machado *et al.* (1988 and 1991). The amphibolite metamorphic facies present in these rocks is supposed to be overprinted by at least two later metasomatic and/or hydrothermal alterations (Siqueira, 1990; Lindenmayer, 1990). The Old Salobo Granite was intruded and deformed at 2573±2 Ma (Machado *et al.*, 1991), suggesting that ductile deformation associated with the Itacaiúnas Shear Zone was long-lived continuing for almost 300 Ma.

Based on drill-core rock samples collected from the SE part of the Salobo region (3.5Km x 1.0km), Lindenmayer (1990) suggested that an early high temperature low pressure thermal metamorphism (750°C; 2-3 Kbar) was followed by two consecutive episodes of hydrothermal alteration that reached the amphibolite (650°-550°C; 2.6 Kbar) and greenschist facies (370°C) respectively. According to this author the mylonitic fabric is associated with the (hydrothermal) amphibolite facies, while the (hydrothermal) greenschist facies is related to the development of a latter brittle structure fabric. Conversely, Siqueira (1990) suggests that the mylonitic fabrics formed during a later mylonitic deformation coeval with greenschist hydrothermal alteration. This author interpreted the strongly recrystallized nature of the fabrics as being due to dynamic recovery during deformation. Field observations and thin section studies carried out during the present research, strongly support the idea that the high temperature mylonitic fabric is closely associated to regional upper amphibolite facies metamorphism.

The effects of greenschist facies metamorphism and hydrothermal alteration, were observed affecting rocks within ductile shear zones in the quartzites of the Amethyst Mine (Cururu) and also in the retrogressed gneisses of the Cutia Mine in the Serra Pelada region. A still later episode of hydrothermal alteration is also clearly associated with the brittle reactivation of the early fabrics, as observed by the presence of hydrothermal veins (chlorite+epidote) filling fractures seen all over the region.

The rocks assigned here to the Igarapé Pojuca Group, in the Cinzento Strike-Slip System, cover a large area around the Cururu and Serra do Rabo regions. They are mostly metasedimentary rocks, ironstones, metavolcanics and ultramafics. Field separation of rocks belonging to the Igarapé Salobo and Igarapé Pojuca groups is problematic as lithologies are similar. In some lithologies (e.g. quartzite) the presence of sillimanite is diagnostic of the Igarapé

Salobo Group; this mineral is absent in the Igarapé Pojuca rocks. There are however no reliable criteria established to distinguish ironstones associated with the Igarapé Pojuca and Igarapé Salobo groups. This illustrates that separation of the two groups is often a serious problem in the field.

The correlation of the volcanics of the Grão Pará Group, and the volcanically-derived amphibolites of the Igarapé Salobo Group, as proposed by Hutchinson (1979) and Lindenmayer (1990), seems unlikely as the Grão Pará rocks only ever display very low greenschist metamorphism and low temperature deformation conditions (see section 4.5 Chapter 4).

The tectonic environment for the deposition of the Igarapé Salobo, the Igarapé Pojuca and the Grão Pará groups, is most likely to be the extensional continental crust, in agreement to Hutchinson (1979), Wirth (1986) and Lindenmayer (1990).

STRUCTURAL GEOLOGY

The Cinzento Strike-slip System forms a 170 Km long lineament, orientated roughly WNW-ESE and cross-cut by the Araguaia Belt in its E termination (Fig.S5.3).

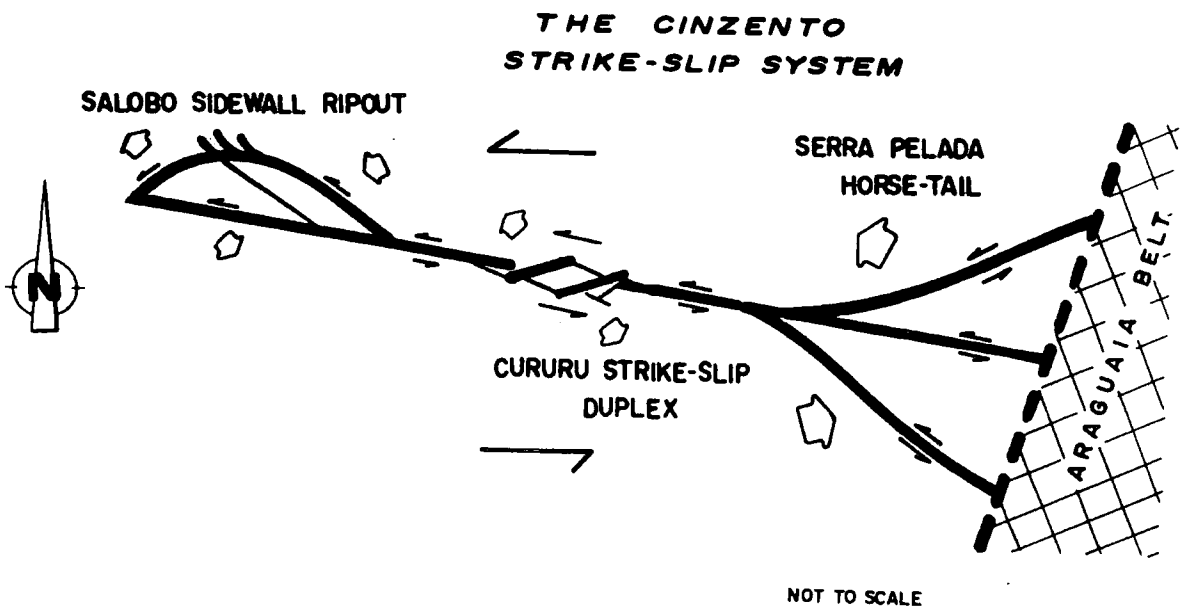

Fig.S5.3- Sketch of the Cinzento Strike-Slip System representing its main structural features.

A sub-vertical mylonitic foliation forms the main ductile fabric observed in the Basement Assemblage in the Salobo and Serra Pelada regions and this fabric is strongly orientated NW-SE to E-W; significant variations in dip occur in the Serra Pelada region (60°-90°).

A linear fabric is associated with the mylonitic foliation in most of the rocks present in the Salobo area, both in the Xingu Complex rocks and in the Igarapé Salobo Group rocks. It is mostly defined by both micaceous and prismatic minerals orientated and elongated into the stretching direction. The orientation of this lineation is variable. It plunges at low angles towards the NW and SE in the Salobo area, whilst a more variable plunge is observed in the Serra Pelada region it always is associated with oblique kinematic indicators suggesting both reverse and sinistral strike-slip displacements.

The high temperature mylonitic fabrics are overprinted by low temperature predominantly planar fabrics which are best seen in the Igarapé Pojuca Group rocks outcropping in the Cururu and Serra Pelada areas. The orientation of these fabrics in these areas follows the general trend of the earlier structures. In the Serra Pelada area, where these structures are associated with folds, they show a transecting relation to the axial surfaces denoting angles of about 10° (clockwise). The clockwise position is consistent with sinistral transpression, as are the crystallographic orientations of C-axes in deformed quartzites (Lab, 1992) and the lack of a penetrative linear fabric suggesting a flattening deformation ($1>K \geq 0$). The transected folds are formed in rocks of the Igarapé Pojuca Group in the Serra Pelada region, and typically plunge shallowly WNW or ESE. Probably the age of folding and transecting cleavage development is between ca. 2.8-2.7 Ga, i.e. post-dating the high temperature mylonitic fabric in the Basement Assemblage rocks, and pre-dating deposition of the Grão Pará Group (see Chapter 4).

High and low temperature ductile fabrics in the Xingu Complex, Igarapé Salobo and Igarapé Pojuca groups were reactivated during later mainly brittle regional episodes of deformation ca. 2.6 Ga and 1.9 Ga, i.e. following emplacement of gabbroic sills in the Águas Claras Formation and before the ca. 1.9 Ga anorogenic granites (see section 4.1, Chapter 4, and Chapter 6).

Brittle deformation was associated with the influx of large volumes of hydrothermal fluids as seen, for example in the Cutia and Cururu mines. Similar alteration has also been described in rocks of the Salobo region (Costa and Siqueira, 1990; Siqueira, 1990).

The brittle deformation along the Cinzento Strike-Slip System has formed three major structural features (Fig.S5.3): (1) the Salobo sidewall ripout;

(2) the Cururu strike-slip duplex; and (3) the Serra Pelada horse-tail structure. All these structures are thought to have formed during sinistral strike-slip displacement although additional vertical components of movement may be important. The Salobo and Cururu structures are brittle features that are clearly defined in satellite images, whilst earlier ductile fabric domains clearly extend beyond the limits of these features. This suggests that the ductile strike-slip duplex models of previous authors (e.g. Costa and Siqueira, 1990; Siqueira, 1990) are untenable. The Cururu structure forms a rhomb-shaped structure formed by R and P fractures (Fig.S5.4). These lineaments are arranged in en echelon pattern, overprinting sub-parallel early low temperature mylonitic fabrics in the metasedimentary rocks of the Igarapé Pojuca Group. The sense of displacement during the formation of this structure is not easy to predict.

Two kinematic interpretations can be suggested by swapping the orientation of R and P fractures: sinistral and dextral (Fig.S5.4A). There are no field data to support either alternative, since most of the fractures and faults observed in the field belong to another later set of fractures with a N-S trend. An extensional jog original geometry is assumed based on the presence of Lower Sequence rocks internally. A sinistral displacement model (Fig.S5.4B)fits the regional history better, since the Salobo structure, to the W, and the Serra Pelada, to the E, clearly originated during left lateral movements.

The Serra Pelada Horse-Tail structure represents the E termination of the Cinzento Strike-Slip System. Once again, brittle deformation is probably responsible for the development of the major lineaments observed in satellite and radar images. This set of structures reactivates early low temperature ductile fabric present in the Igarapé Pojuca rocks and high temperature ductile fabrics in the Basement Assemblage rocks. The predominance of extensional brittle faults displacements suggests that the Serra Pelada Horse-Tail structure developed during sinistral strike-slip movements (see Fig.5.3.8 in this Chapter).

In conclusion, it is proposed here that the Cinzento Strike-Slip System corresponds to a major brittle fault system in rocks of the Basement Assemblage and the Igarapé Pojuca Group of the Cover sequence, reactivating older fabrics present in these rocks. The Cinzento Strike-Slip System was formed probably during regional sinistral strike-slip kinematics. It is proposed that this event is contemporaneous with the sinistral transpression that took place along the Carajás Strike-Slip System at some time between ca. 2.6 Ga and 1.9 Ga. Vertical components of displacement may be responsible in part for the preservation of the main stratigraphic units of the Cover sequence along this structure.

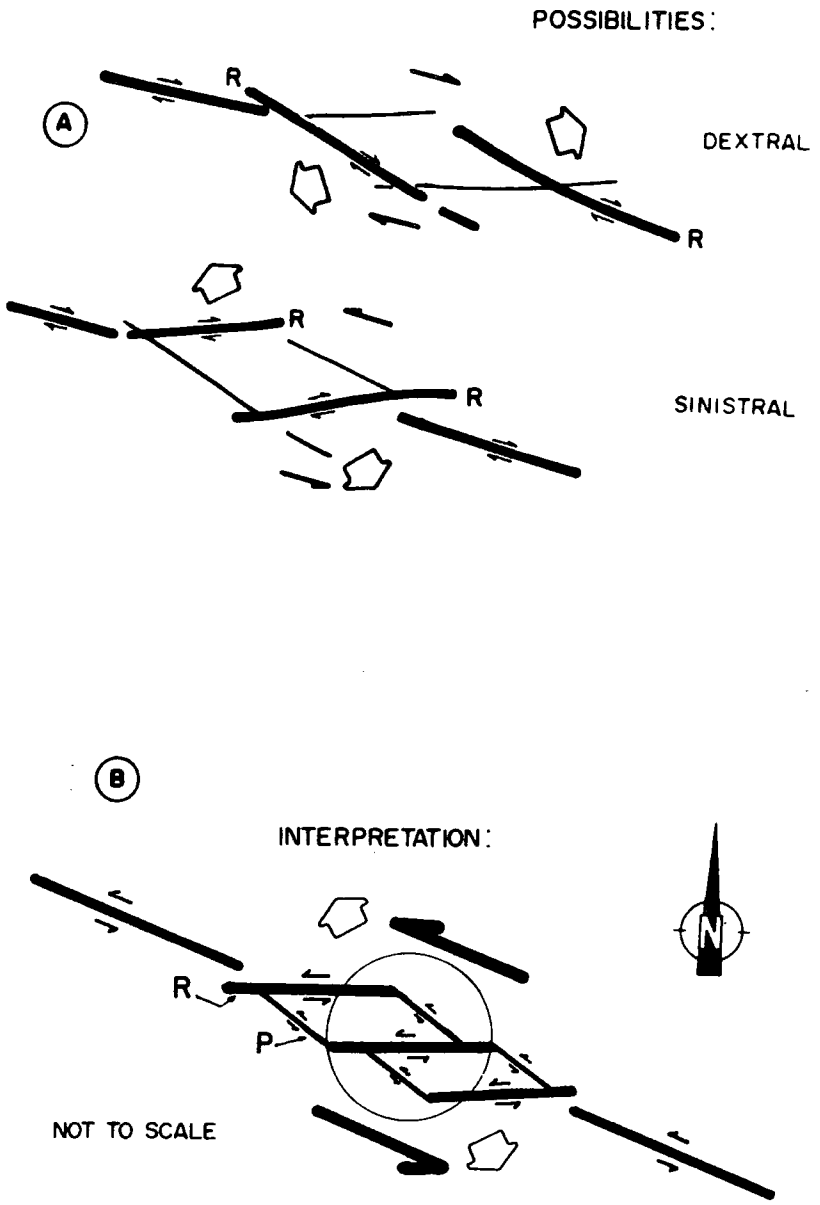

Fig.S5.4- The lineaments forming the Cururu structure, observed in satellite images, could be formed during dextral or sinistral kinematics(A). The sinistral interpretation is supported here, based on regional data (B). See text for more explanations.

CHAPTER 6
GRANITES & DYKES - PROTEROZOIC INTRUSIONS

6.1- INTRODUCTION

The Early-Middle Proterozoic magmatism in the Carajás Region is marked by several important granitic intrusions which occur throughout the E of the area (Fig.6.1). This magmatism was also accompanied by the emplacement of mafic dyke swarms (Fig.6.2) and later, deposition of immature sediments into small fault-bounded basins. Four granitic plutons were studied in the field (Fig.6.1): (1) the Central Carajás Granite; (2) the Cigano Granite; (3) the Itacaiúnas Granite and (4) the Rancho Alegre Granite. Additional information concerning the Young Salobo Granite was obtained from published works. Several other poorly known granitic bodies are mentioned in the literature and most are clearly seen on remote sensing images. Most are in the Serra do Rabo region (Fig.6.1).

Mafic dykes form relatively dense swarms, seen on satellite images (Photo 6.1), and are concentrated in the central area of the Carajás Strike-Slip System (Fig.6.2). The study of these minor intrusions in the field has been restricted to the Águas Claras road section.

Plutons and dyke emplacement were not coeval. No dykes were observed cutting the granites, whilst field relationships suggest that the granites are later in relation to the dykes. Both features however, are strongly controlled by earlier faults and fractures. Later brittle deformation affects both granites and dykes.

Deposition of immature sediments, thought to be related to this Proterozoic extensional episode (Gorotire Formation), are described in sections 4.5 and 4.6, Chapter 4, in this thesis.

6.2- REGIONAL GEOLOGICAL SETTING.

The Middle Proterozoic in the Amazonian Craton is generally considered to have undergone a regional extensional event responsible for widespread magmatism, deposition of sedimentary and volcanic rocks in small extensional

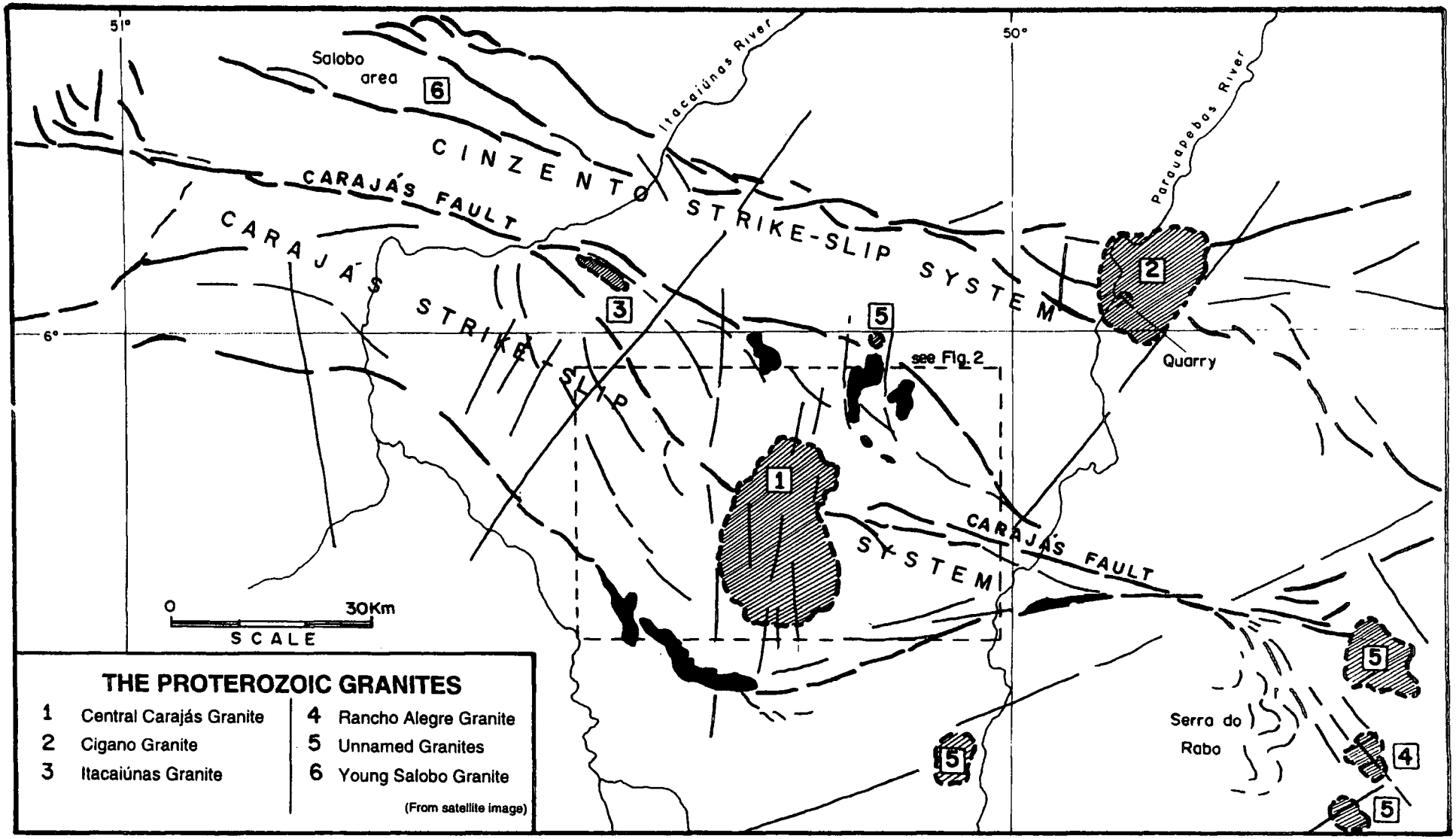

Fig.6.1- Map of plutons in the Carajás area based on interpretation of satellite images and field mapping. Heavy lines correspond to faults. The area enclosed by the dashed box is enlarged in Fig.6.2.

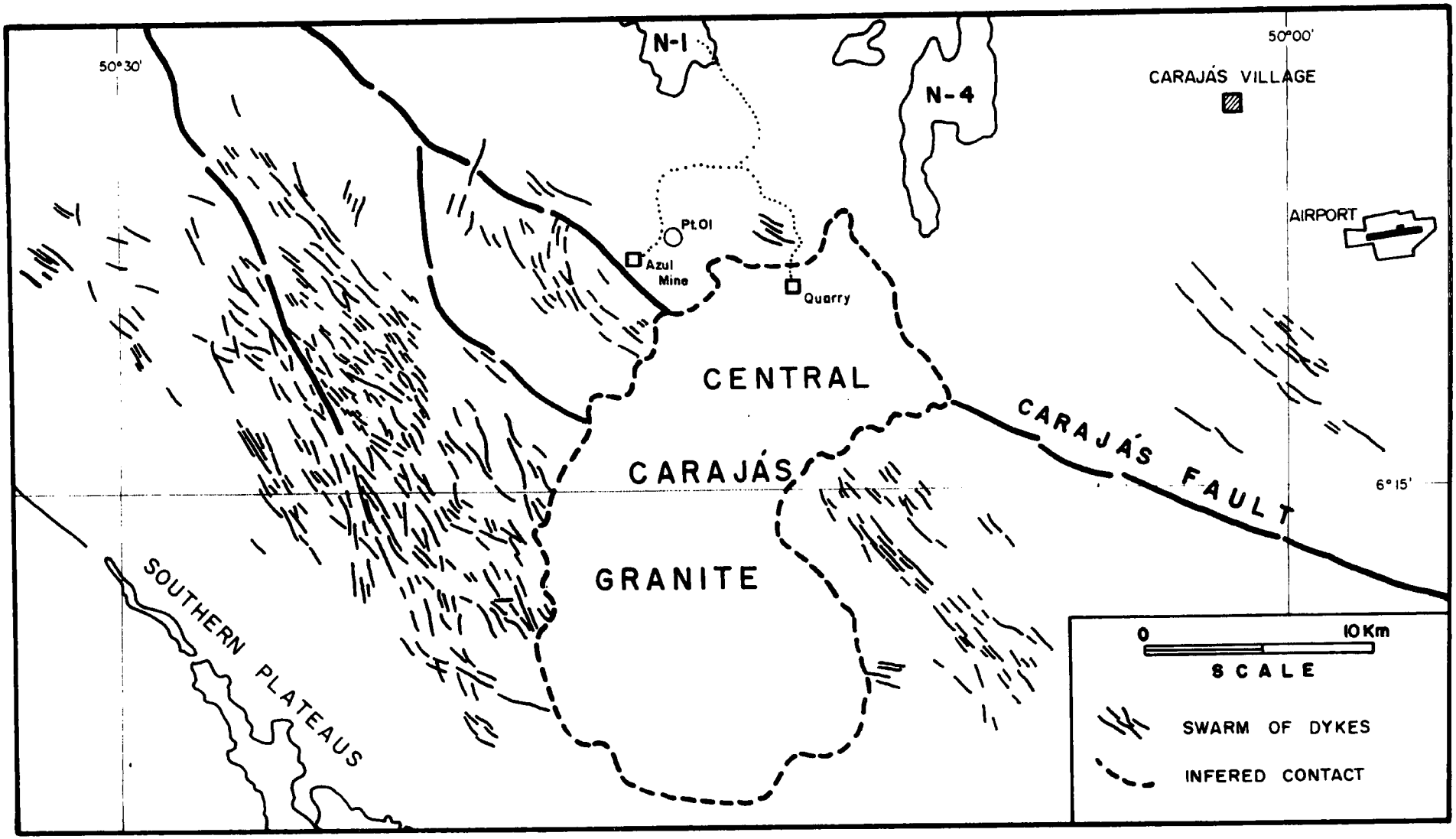

Fig.6.2- Detailed interpretation of satellite image enlarged in Photo 6.1, showing the central area of the Carajás Strike-Slip System highlighting the swarm of dykes and main fault traces observed around the Central Carajás Granite. The Central Carajás Granite quarry is marked by a square in the north of the pluton and the Pt.01 represents the location of the dykes carrying brecciatted xenoliths found along the road to the Azul Mine.

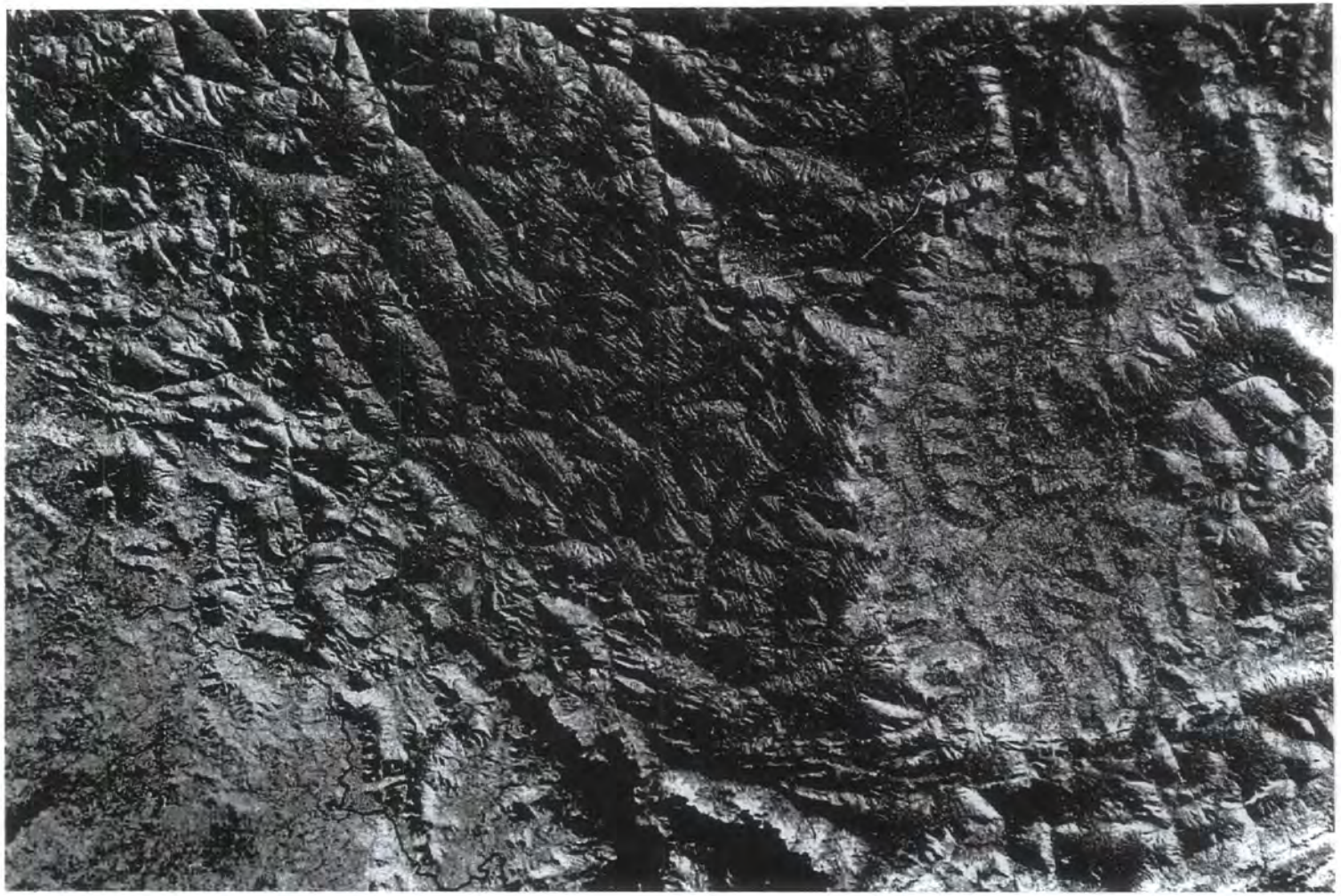

Photo 6.1- Satellite image, from LANDSAT, of the central area of the Carajás Strike-Slip System. Swarms of dykes are observed to the W of the Central Carajás Granite, marked by a large rounded pale area.

basins, and development/reactivation of fault systems (Issler *et al.*,1985; Dall'Agnol *et al.*,1986; Neves, 1986; Sial *et al.*,1987; Teixeira, 1990; Costa *et al.*, 1991; Costa and Hasui, 1991; Neves, 1992; Costa and Hasui, 1992). Extension has been reported as being responsible for the development of sets of NE-SW and NW-SE faults currently observed in the Brazil Central Shield (Costa and Hasui, 1991; Costa and Hasui, 1992; Neves, 1992). The NE-SW set have been interpreted as transfer faults displaying dextral and sinistral displacements whilst the NW-SE set corresponds to normal faults associated with graben in which rocks of the Rio Fresco Formation (Barbosa *et al.*, 1966), the Gorotire Formation (Andrade Ramos, 1954; Barbosa *et al.*,1966), and the Uatumã Group (Silva *et al.*,1974) were deposited (Costa *et al.*, 1991; Costa and Hasui, 1992). Based on the volume of sedimentary and volcanic rocks filling the basins, the coefficient of lithospheric stretching (β) during extension should be $2<\beta<5$ (Costa *et al.*,1991; Costa and Hasui, 1992). Costa and Hasui (op. cit.) suggest that all Middle Proterozoic faults are reactivated older structures, and that many were later reactivated as thrusts during Late Proterozoic tectonic inversion.

The plutonism related to this episode of extension has been referred to as "post-Transamazonian", "anorogenic", "A-type", "intracratonic" and "intraplate" (e.g. Isller *et al.*, 1985; Dall'Agnol *et al.*,1986; Neves, 1986). Dall'Agnol *et al.* (1987) divided the "anorogenic granites" into two sets: (1) Alkaline granites similar to A-type and, (2) Magnetite-series granites with I-type affinities. The A-type granites are predominant in the Central Amazonian Province while I-types are dominant in the Juruena and Rondonian Mobile Belts (Fig.3.4, Chapter 3).

Four different magmatic episodes, based on radiometric evidence, have been recognised in the Amazonian Middle Proterozoic: (1) 1.9-1-8 Ga; (2) 1.7 Ga; (3) 1.6-1.4 Ga, and (4) 1.1-1.0 Ga (Neves, 1986). Using magnetic susceptibility data, Dall'Agnol *et al.* (1988) separated two main groups of Middle Proterozoic granites: (1) "High magnetic susceptibility value granites" (e.g. Jamon, Água Branca - both in the Granite Greenstone Terrain); (2) "Low magnetic susceptibility value granites" (e.g. Central Carajás Granite, Cigano Granite, etc.).

Mafic dyke swarms in the Amazonian Craton are of predominantly Middle Proterozoic age, but Archaean, Lower Proterozoic and Phanerozoic examples are also present (Sial *et al.*,1987). Teixeira (1990) recognised three peaks of dyke emplacement activity around the Middle Proterozoic in the Amazonian Craton: (1) 1.9-1.8 Ga - mainly in the Guyana Shield; (2) ca.1.6 Ga

- the Avanaveiro suite of the Guyana Shield, and probably correlated with the Uatumã volcanism that took place in the Central Brazil Shield, and (3) 1.5-0.9 Ga, present all over the Amazonian Craton. Most of the dykes swarms are orientated NE or NW and have a tholeiitic composition typical of intraplate activity within stable cratonic areas (Sial *et al.*, 1987).

According to Choudhuri *et al.* (1990), there has been basaltic activity in the Amazon Craton since the Early Proterozoic and as the crust was probably weak in the Middle Proterozoic, this led to rifting and also the development of widespread felsic volcanism represented by the Uatumã Group rocks. This process is supposed to have been active till ca.1.0 Ga, or later (Almeida and Hasui, 1984).

6.3- THE CENTRAL CARAJÁS GRANITE

The Central Carajás Granite is the largest pluton present in the Carajás region, covering an area of about 380 Km^2 in the central part of the Carajás Strike-Slip System (Fig.6.1). Its radiometric age of about 1.8 Ga puts it in the group of granites emplaced during the beginning of the Middle Proterozoic. It is one of the most studied granitic plutons in Carajás. The data presented here concern mainly the internal and external structures observed in the field and on satellite images. The pluton is well exposed in the field at just one point in the north, in a quarry a few kilometres from its contact with the Águas Claras Formation (Fig.6.2; Photo 6.1). Access to other possible outcrops of this pluton is very difficult because of the dense rain forest.

a) Previous work: The Central Carajás Granite has been known since CVRD/CMN (1972) and Beisiegel *et al.* (1973) published the first petrographic descriptions and described the pluton as being emplaced into clastic sedimentary rocks.

The name Central Carajás Granite is applied here following Meireles *et al.* (1984) and DOCEGEO (1988) but the pluton has received several other similar names including: "Central Granite" (e.g. Knup, 1971), "Serra dos Carajás Granite" (e.g. Hirata *et al.*, 1982), "Serra dos Carajás Massif" (e.g. Dall'Agnol, 1982), and "Carajás Granite" (Araújo and Maia, 1991). Silva *et al.* (1974) used the term "Serra dos Carajás-type" granites to refer to several

plutons of similar granites outcropping in the region, while Hirata *et al.* (1982) suggested the name "Serra dos Carajás Suite".

Four different facies have been described in the northern part of the pluton (Rios, 1991): (1) biotite-amphibole-syenogranite (dominant in the NW); (2) porphyritic amphibole-biotite-monzogranite (in the NE); (3) microgranites and (4) pegmatites. Geochemical studies of these rocks were carried out by Almeida (1980) and by several others (e.g. Dall'Agnol, 1982; Araújo and Maia, 1991). They recognised an alkaline and hyperaluminous trend in these rocks.

Most of the Central Carajás Granite is emplaced into clastic sedimentary rocks previously assigned to the Rio Fresco Formation or Group, presently referred to the Águas Claras Formation (Nogueira *et al.*,1995). It also cuts volcanics of the Grão Pará Group along its NNE border forming hornfels in basalts belonging to this unit (Rios, 1991). Xenoliths of Águas Claras sandstones are preserved close to the borders (Wirth, 1986; Macambira *et al.*,1990) and apophyses of granites occur in the sandstones (Macambira *et al.*, 1990; Rios,1991). Rotation of beds close to the granite border have been described (Santos, 1978 in Rios, 1991) whilst the effects of contact metamorphism and hornfels are widespread (Almeida, 1980; Macambira *et al.*,1990; Rios, 1991). Dall'Agnol (1982) interprets this granite as being emplaced at high crustal level.

The age of pluton emplacement is thought to be around 1.8-1.9 Ga based on the results of several radiometric studies: 1824 Ma (K/Ar, amphibole, Gomes *et al.*,1971); 1828±90 Ma (K-Ar, amphibole; Beisiegel *et al.*,1973); 1820 ±49 Ma (U/Pb, zircon; Wirth *et al.*,1986); 1880±2 Ma (U/Pb, zircon; Machado *et al.*,1988).

Studies along the northern border, both in the granite and in its wall-rock, reveal a strong influence of late-magmatic fluids. Widespread alteration has occurred in the sandstones and volcanics and hydrothermal veins and greisens are developed within and outside the pluton (Rios,1991, Barros *et al.*,1994*b* and Silva,1996).

b) Shape of the pluton and contacts: The Central Carajás Granite forms a N-S elongated ellipsoidal body, measuring approximately 30 Km x 15 Km, slightly indented in its middle portion (Fig.6.2; Photo 6.1). The borders of this pluton appear to be smoothly curved and slightly irregular, especially along the W, NW and N sides where a series of small apophyses are evident on both satellite and radar images (Photo 6.1). Geophysical data from the Projeto Geofísico Brasil-Canadá (1975 and 1976) highlight the shape of the pluton using iso-

radiometric contours (total Th and U in cps) as shown in the Fig.6.3; the 850 contours correspond approximately to the border of the pluton. This map shows clearly the presence of some few NW-SE orientated apophyses in the NW part of the body. These follow the trend of the Carajás Fault trace which are cut by the granite (Figs.6.1 and 6.2).

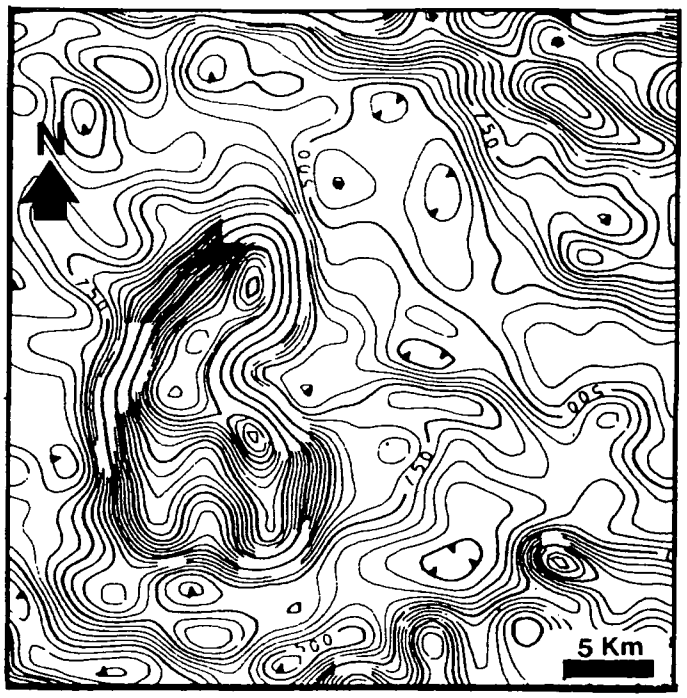

Fig.6.3- Map of iso-radiometric contours (total Th and U in cps) around the Central Carajás Granite (after Araújo and Maia, 1991).

A road diversion, opened about 1.5 Km NW of the contact with the granite and sandstones of the Águas Claras Formation (Pt.01 on Fig.6.2), exposes massive outcrops of sandstone breccias and microbreccia (fragments 5 cm to 0.1 cm) with randomly orientated clasts set in a red-pink aplitic matrix (20% to 40%; Photo 6.2). Xenoliths are mostly dark laminated pelites and other very altered fragments of the country rock (Photo 6.2). Under the microscope these xenoliths comprise mainly quartz (fine-microcrystalline crystals) together with lesser amounts of muscovite, chlorite, epidote and opaque minerals. Anhedral porphyroblasts of andalusite and cordierite occur in the quartz-rich matrix, occasionally altering to mica and pinite. Muscovite and opaques are more abundant in xenoliths of very fine rocks. The texture of the xenoliths is predominantly subheudral granular with fine quartz crystals showing straight

contacts forming a granoblastic-polygonal texture with typical 120° triple-junctions. These rocks are thought to be explosion breccias that form as large dyke-like bodies broadly synchronous with granite intrusions. These dyke-like bodies may be relatively large as these rocks outcrop persistently for at least 300m at different points along the road.

Photo 6.2- Typical explosion breccia formed by centimetre-scale fragments of sandstones and mudstones xenoliths in a very fine quartzo-feldspathic matrix (north border of the Central Carajás Granite.

c) Structures in and around the pluton:

Fluvial sandstones belonging to the Águas Claras Formation are exposed along the secondary road linking the granite quarry to the Azul-N-4 road. The bedding in these sandstones is overturned ca.500m from the granite contact (Fig.6.4) but by 1 Km from the contact, it is the right way up and others parallel to its regional N-S orientation. This suggests that any syn-emplacement deformation affects a relatively narrow zone of rocks (< 750m) adjacent to the granite pluton.

The granite in the quarry is predominantly a homogeneous red, coarse-grained granite with porphyritic variations (Dall'Agnol, 1982; Wirth, 1986). Petrographically, it is a coarse amphibole-biotite granite rich in K-feldspar phenocrysts and it displays very coarse grains, with a syenogranitic tendency (Dall'Agnol, 1982; Macambira *et al.*, 1990; Rios, 1991).

In the field, much of the granite is isotropic and magmatic fabrics are often observed due to the predominantly coarse texture. Rios (1991) suggests that a high liquid/crystal ratio existed in the pluton to explain the generally weak magmatic fabric observed. No internal structures in the granite are seen on satellite or radar images (Photo 6.1).

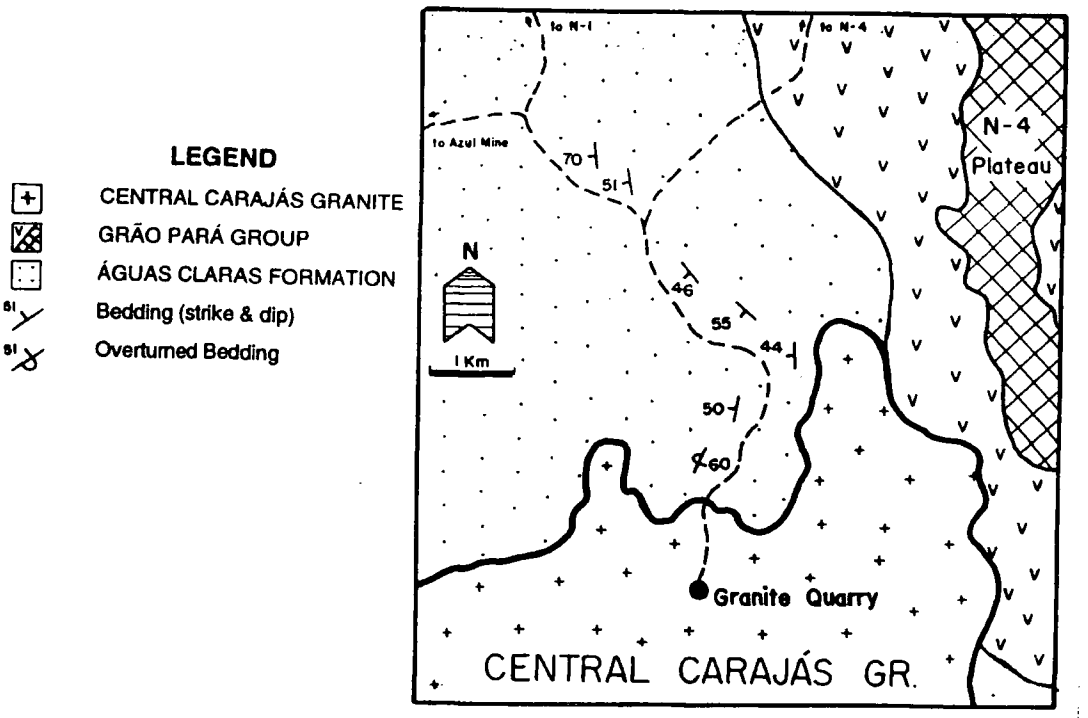

Fig. 6.4- Map of the northern area of the Central Carajás Granite showing the bedding of sandstones outcropping on the border of the granite.

The medium to fine grained facies observed in the quarry, where mafics are relatively abundant, display a good pre-full crystallisation magmatic fabric (Hutton, 1988*b*). This is defined by aligned feldspar and mafic crystals, surrounded by anhedral, undeformed quartz grains or aggregates, with no evidence of plastic deformation or recrystallisation (Photo 6.3). This foliation is orientated mainly NE-SW, dipping at high angles WNW-NW (Fig.6.5A). Contacts observed separating steeply-inclined sheets of coarse-grained and fine-grained granite are roughly orientated subparallel to the magmatic foliation, although they are locally very irregular.

Several microgranite-dykes (<3 cm thick) and pegmatitic veins form slightly later intrusive phases in the quarry (Photo 6.4). The dykes vary from

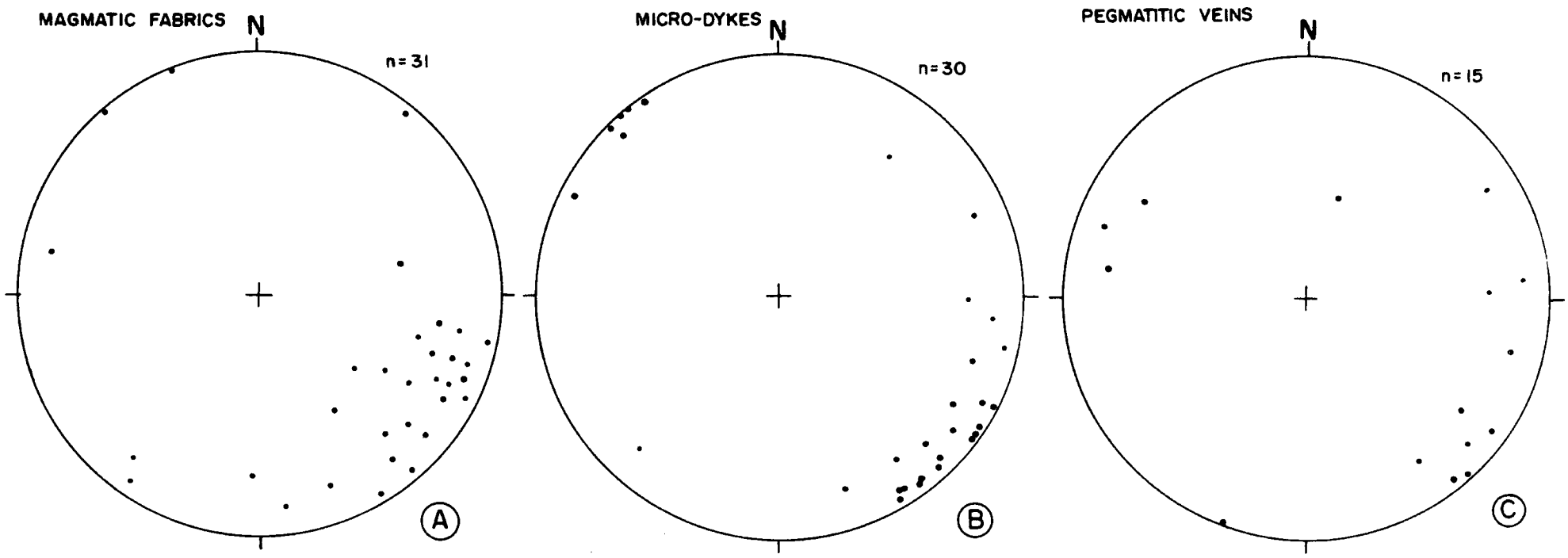

Fig.6.5- Stereonets representing (A) poles of magmatic fabric (magmatic foliation); (B) micro-dykes poles and (C) pole of pegmatitic veins from the Central Carajás Granite outcropping in the north of the pluton. A NE-SW orientation of the structures in the stereonets is remarkable.

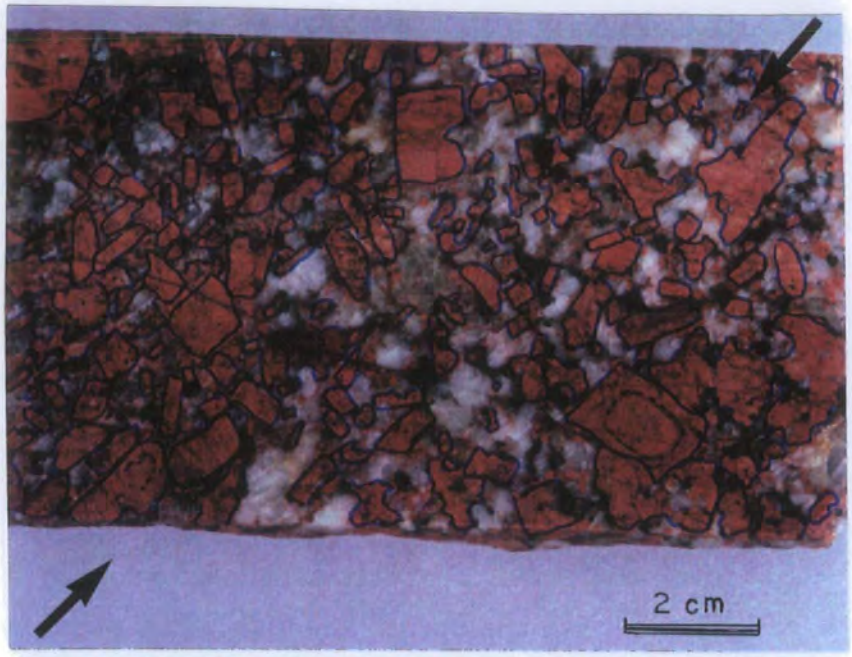

Photo 6.3- The magmatic fabric (magmatic foliation) in the Central Carajás Granite. Tabular feldspar grains are highlighted whilst the arrows indicate the overall trend of the foliation.

Photo 6.4- Close to N-S pegmatitic veins observed in the Central Carajás Granite quarry.

Photo 6.5- Set of N-S fractures concentrated in 30-50 cm zones separated by 1-2 cm of less fractured rocks.

Photo 6.6- Low-angle slickenlines indicating predominant strike-slip displacement along later N-S fractures planes in the Central Carajás Granite.

biotite-rich microgranites to leucomicrogranites. Pegmatitic veins are 0.3 to 1 m thick and most are discontinuous. They display irregular-tabular and curved forms, with bridges, stubs, horns and forks developed (Photo 6.4). A complete petrographic description of these rocks is given by Rios (1991). These structures also lie sub-parallel to the magmatic foliation, with NE-SW strikes and steep NW or SE dip (Figs. 6.5B and C).

A later episode of cataclasis has led to grain-scale microfractures of primary minerals which were later percolated by hydrothermal fluids in several episodes (Rios, 1991). Fractures and faults in the quarry are variable in orientation but N-S (Photo 6.5) and NE-SW orientations are most common (Fig.6.6A). These form 30-50cm fractures zones with a spacing of 1-2m. Slickenlines along some fractures (e.g. Photo 6.6) indicate mainly strike-slip displacements (Fig.6.6B). Kinematic indicators are rare but at least two NE-SW fractures display secondary tension fractures consistent with dextral displacements (Photo 6.7).

Photo 6.7-Steeply dipping NNE-SSW fractures linked by subordinate tension fractures indicating a dextral kinematics for this structures, in the Central Carajás Granite quarry.

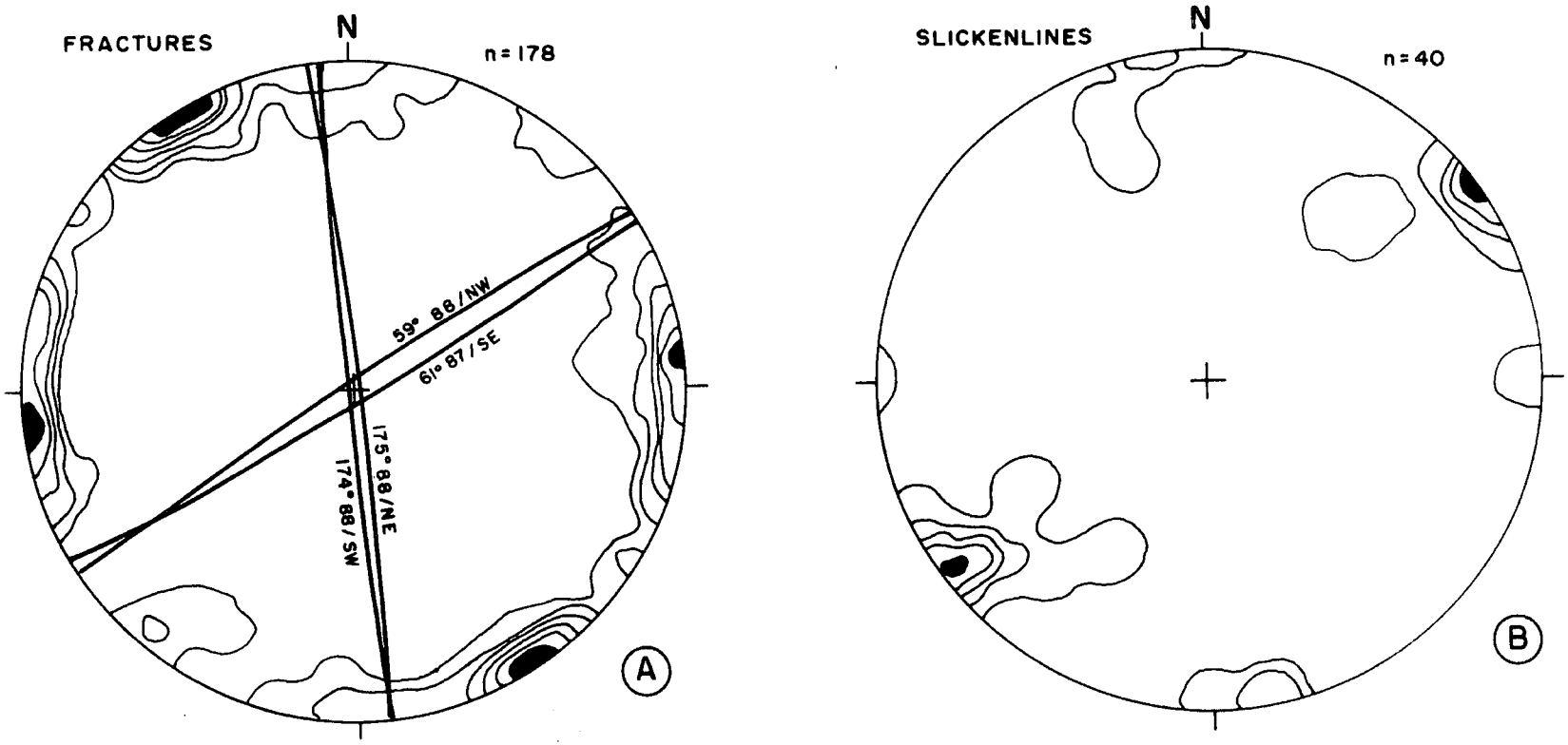

Fig.6.6- Stereonets showing contours of poles to fractures (A) and slikenlines (B) observed in the Central Carajás Granite quarry. A) contours: 2.8/5.1/7.4/9.6/12.0/14.2% to a total of 178 poles. B) 6.6/ 10.0/13.3/16.6% to a total of 40 lines.

6.4- THE CIGANO GRANITE

The Cigano Granite forms the second largest granite pluton in the Carajás region (Fig.6.1), and is emplaced along the eastern part of the Cinzento Strike-Slip System. It occupies an area of approximate 200 Km^2 and cuts rocks of the Xingu Complex and Igarapé Pojuca Group.

The structural data presented here were collected in a quarry located in the central southern region of the pluton, along the margins of the Carajás railway.

a) Previous work: The Cigano Granite was first referred to by Hirata *et al.* (1982). Dall'Agnol *et al.* (1986) presented the first petrographic and petrological description of the pluton. These authors suggested that the regional faults strongly influenced the pattern of hydrothermal alteration. Two different textural facies were recognised: (1) a coarse-grained to porphyritic granite; and (2) mainly in the centre of the pluton, microgranites to aplites. Later work suggested it was an A-type granite, similar to other plutons in the region (Dall'Agnol *et al.*, 1987). Gonçalez *et al.* (1988) published a detailed study of this pluton, which is considered to be the most complete account. They suggested that it is a relatively homogeneous body in which monzogranites, associated with syenogranites are the predominant rock type (Gonçalez *et al.*, 1988). Five distinctive facies were defined: (1) amphibole-biotite-monzogranites; (2) porphyritic amphibole-biotite-monzogranites; (3) biotite monzo- to syenogranite; (4) altered monzogranites; and (5) microgranites (see Gonçalez *et al.*,1988 for further details). The pluton is described as being isotropic with no evidence of internal structures (Gonçalez *et al.*, 1988).

The age of crystallisation of this intrusion is well established from U/Pb (zircon) radiometric dating which gives an age of 1883±2 Ma (Machado *et al.*, 1988); this is similar to the dated granites in the region.

b) Shape of the pluton and contacts: The Cigano Granite has an approximately semi-circular shape in plan view (Fig.6.1). The NE, S and SE borders of the pluton are well defined in remote sensing images. Granite contacts have not been observed in the field due to a lack of outcrops and access to the border areas. According to DOCEGEO (1988), Costa *et al.* (1990) and Matta and Teixeira, (1990), the N part of the pluton is in contact with

tonalitic and granitic gneisses of the Xingu Complex. Elsewhere granite is emplaced into banded iron formations, amphibolites, metavolcanic, metagrabbos, schists and quartzites of the Igarapé Pojuca Group. Contact metamorphism associated with this pluton has been reported by the development of hornfels (hornblende hornfels and pyroxene hornfels facies) along the S and SE margin of the granite (Gonçalez *et al.*, 1988).

c) Structures in and around the pluton: Detailed mapping in the quarry, located along the Carajás railway, reveals that a weak magmatic fabric is present in the granites (Fig.6.7). This fabric (pre-full crystallisation fabric), as in the Central Carajás Granite, is best defined in medium to fine granites with porphyritic texture, or in places where mafic minerals are relatively more concentrated. Alignments of K-feldspar and amphibole crystals mainly define the fabric. Although locally visible in orientation, the magmatic foliation is predominantly NE-SW orientated, dipping at high angles toward SE, with a steeply dipping secondary NNW-SSE fabric also present (Fig.7B).

Steeply-dipping contacts between coarse-grained and medium-to-fine granites can be mapped in many parts of the quarry (Fig.6.7). Most contacts are N-S orientated (Fig.6.7C) but some are approximately E-W. Locally, fine and coarse granite may be found intersheeted on a centimetre-scale with contacts orientated NW-SE (Photo 6.8). Centimetre-scale to metre-scale pegmatitic veins (Photo 6.9) display N-S, NE-SW, and NW-SE orientations, but most are not tabular and it is hard to define preferred orientations.

Faults and fractures are abundant in the quarry. Although locally variable most trend N-S or NNE-SSW. Slickenlines are rare and the few observed plunge at low angles suggesting mainly strike-slip displacements. Local conjugate fracture sets in the quarry (Fig.6.7) suggest a probable NNE-SSW to NE-SW direction to σ_1 (maximum principal stress) during shear fracture development.

6.5- THE ITACAIÚNAS GRANITE

The Itacaiúnas Granite forms an E-W elongated pluton located about 10 Km east of the Itacaiúnas River and about 10Km west of the Igarapé Pojuca Base Camp (Fig.6.1). It lies close to the north border of the Carajás Strike-Slip System, sub-parallel to the trace of the Carajás Fault.

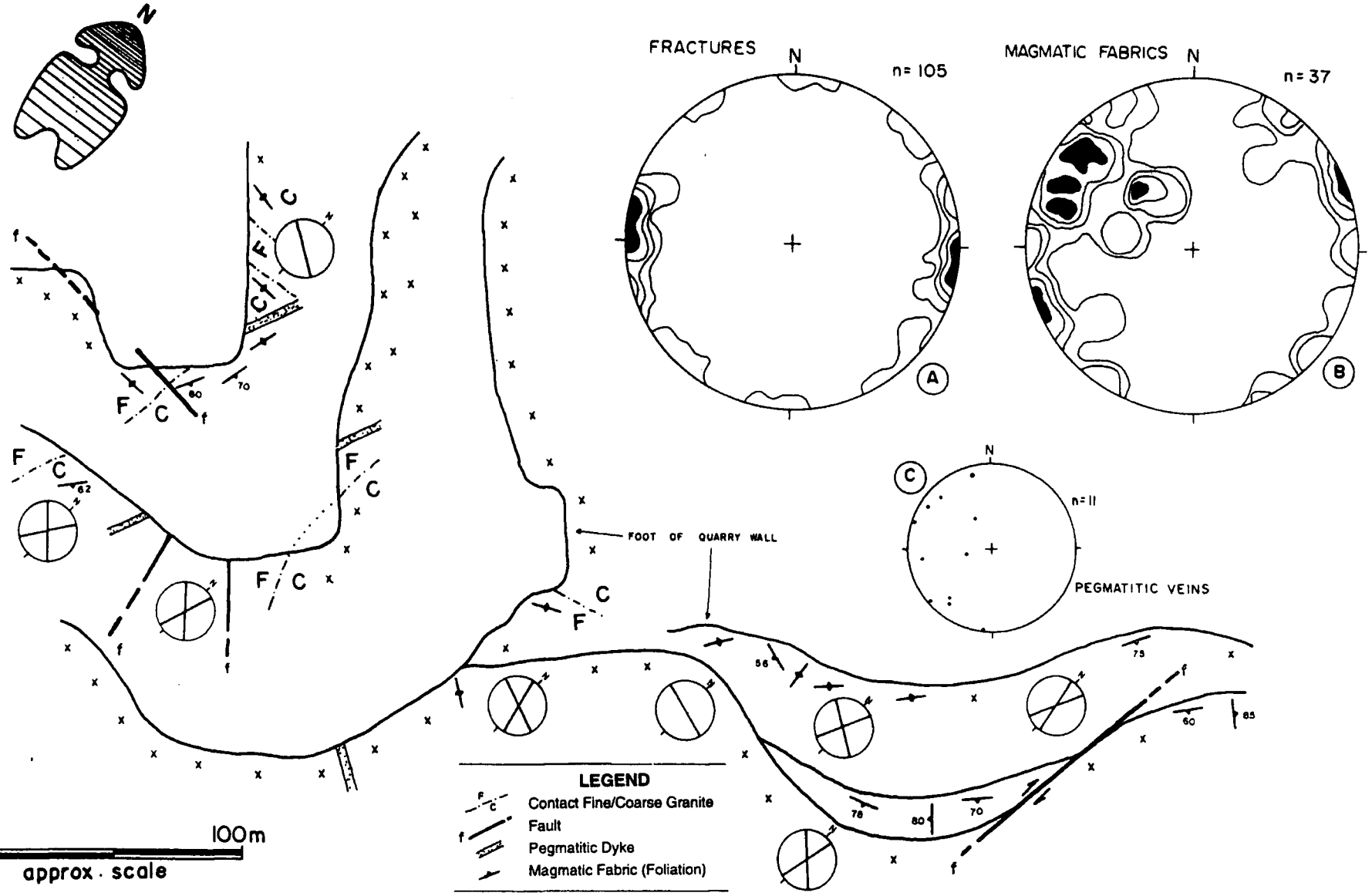

Fig.6.7- Map of main internal structures observed in the Cigano Granite quarry. Stereonets show (A) contours to poles of fractures (1.9/7.8/13.7/19.6% to a total of 105 poles); B) contours of magmatic fabrics (Magmatic foliation): 2.7/8.1/10.8/13.5% to a total of 37 poles; and C) poles of pegmatitic veins. Small stereonets shown around the quarry represent sets of main observed fractures.

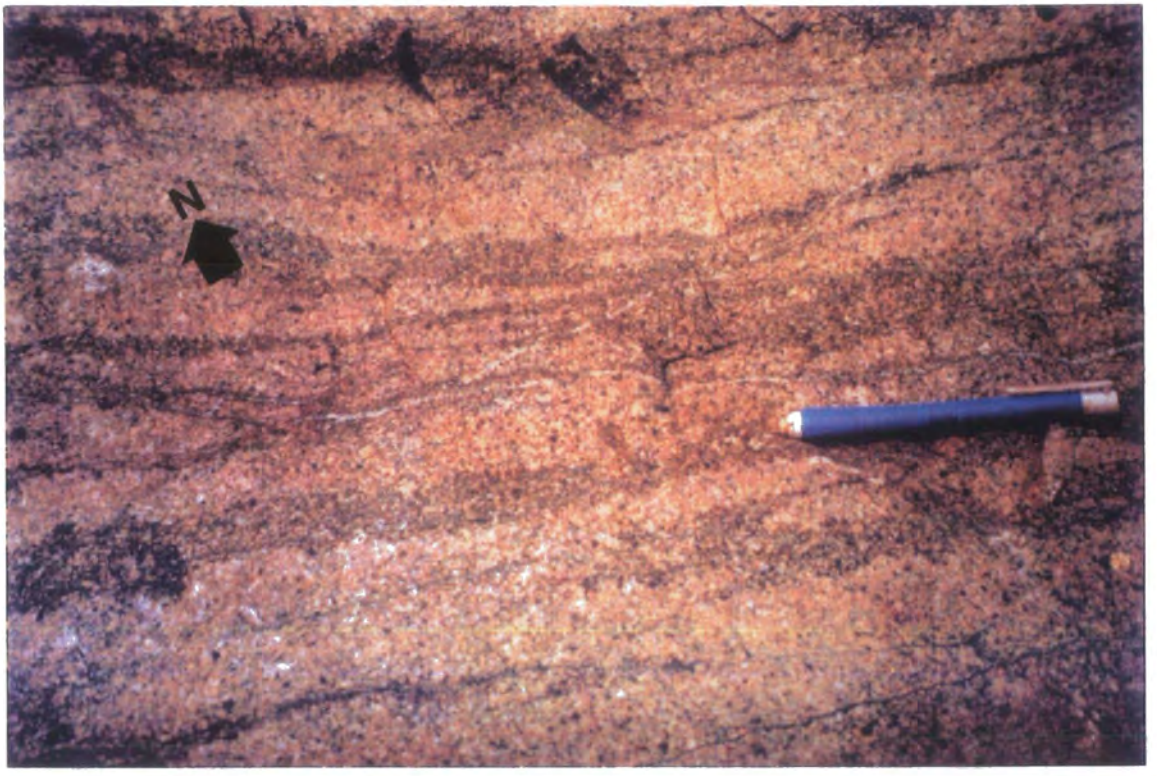

Photo 6.8- NE-SW intersheeted granite observed in the Cigano Granite quarry.

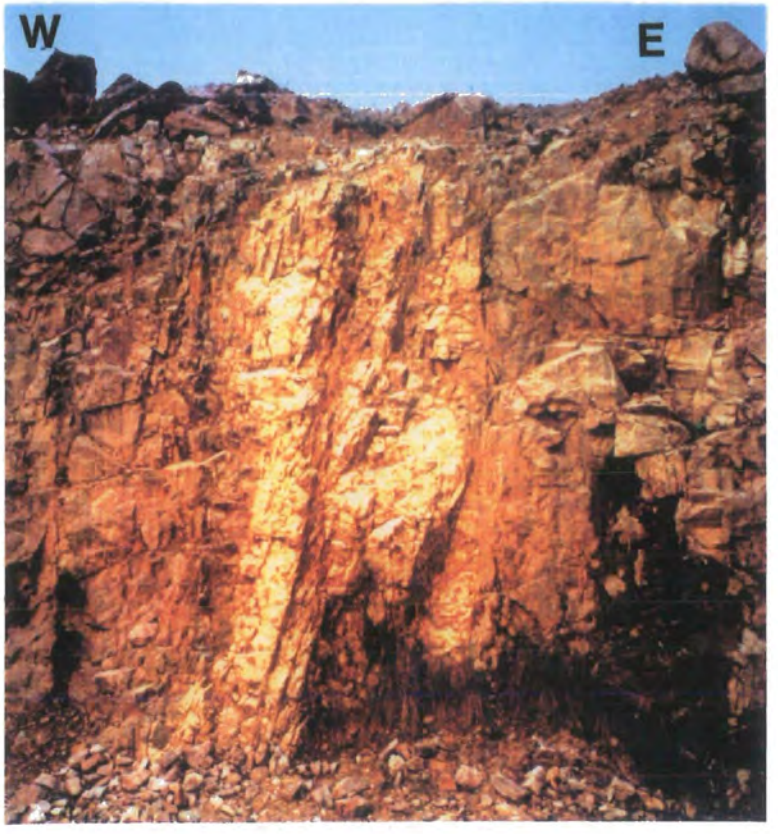

Photo 6.9- Metre-scale, subvertical quartzo-feldspathic pegmatitic vein observed in the Cigano Granite quary (N-S oriented).

The granite is very poorly known as it is exposed only in small outcrops along the road linking the Bahia Mine to the Igarapé Pojuca Base Camp and in boulders along small rivers. In September-October/1994 a new quarry was due to open, located about 700m from the road between the Salobo Base Camp and N-1 Base Camp, about 11 Km from the Itacaiúnas river, to supply materials for new buildings in the Salobo Base Camp. The data presented here was collected mainly at this location.

a) Previous work: The granite has been known since mineral exploration began around the Igarapé Pojuca Base Camp in the 1980's but there are few published references. DOCEGEO (1988) refers to the "Pojuca Granite" which they include in the "Serra dos Carajás Suite", but do not present any further description. Machado *et al.* (1988) obtained a Pb/U zircon radiometric age of 1874±2 Ma for the crystallisation of this pluton. The only published field data was presented by Macambira *et al.*(1990) who mapped the pluton at 1:40000 scale. They used the name "Itacaiúnas Granite" which is adopted here.

Macambira *et al.* (1990) suggested that the pluton is intruded into metavolcanics and metasedimentary rocks of the Igarapé Pojuca Group. Similar granite has been found in several drill holes made by DOCEGEO during ore prospection in places up to 10 Km from the outcropping pluton (Geol. J.B Siqueira, personal communication).

The outcropping rocks are medium- to coarse-grained grey -red granite, with local pegmatitic facies. Quartz and microcline crystals occur up to 4mm in size and the only mafic mineral is biotite in relatively low percentage (Macambira *et al.*, 1990). There are some important differences between the Itacaiúnas Granite and the Central Carajás Granite. The Itacaiúnas Granite does not carry amphibole or pyroxene; it has microcline as K-feldspar; and contains tourmaline as an accessory. The relative percentage of microcline has been reported to increase at the E and W terminations of the pluton.

b) Structures in the pluton: Very few observations were taken as the exposures of this pluton were visited before the opening of the quarry. Pegmatitic veins here are approximately tabular, 10-15 cm wide, oriented around 100°-150°, dipping 80°-85° NE or SW. Millimetre-scale mineralised veins are orientated about 130°-170° dipping steeply (>80°) SW.

Fractures are relatively abundant with the main set trending 115°-150° with dips varying from 80° to sub-vertical. They can be spaced about 2mm-100mm, orientated sub-parallel to the main set of fractures.

6.6- THE RANCHO ALEGRE GRANITE

One of the plutons that crops out along the eastern termination of the Carajás Strike-Slip Fault in the Serra do Rabo region, was studied in two outcrops and named "Rancho Alegre Granite" (Fig.6.1). Numerous boulders are also preserved along secondary roads close to the pluton. In situ, outcrops form distinctive hills up to 100m high. The Rancho Alegre Granite is a rather irregular sub-circular pluton, approximately 5 Km in diameter, slightly elongated NW-SE.

a) Previous work: The pluton forms part of a set of several small granitic bodies first mentioned by Hirata *et al.* (1982), later, followed by other authors (e.g. Dall'Agnol, 1982: Dall'Agnol *et al.*, 1987). DOCEGEO (1988) refers to them as part of the "Borrachudo Granite" which was assigned to the "Post-Tectonic or Anorogenic Granites" (Early Proterozoic). In the DOCEGEO's map, they are shown emplaced into the sedimentary rocks of the Rio Fresco Group and high grade rocks of the Xingu Complex. In Fig.6.1, the shape of these plutons is based on Araújo and Maia (1991), adjusted to the best shape seen on the satellite images.

b) Field data on the rock types: The present work indicates that this small granite is emplaced, at least along its W and SW borders, into metavolcanics of the Grão Pará Group and probably into metasediments belonging to the Igarapé Pojuca Group. Purplish-grey arkosic wacke sandstones and polymictic conglomerates, correlated to the Gorotire Formation, outcrop in several places not far from this pluton, but its relation to the granite is unknown. More accurate geological maps are needed for a better understanding of the geology in this region.

The outcrops in the SW of the pluton reveal a red-grey typical medium to coarse granite with variations to granodiorite, comprising mainly K-feldspar (orthoclase), quartz, plagioclase and hornblende. In many parts the amphibole

is relatively abundant (>20%). The texture observed in thin-sections is a typical hypidiomorphic inequigranular, apparently rather homogeneous. Facies with fine texture are not uncommon and very few veins are observed. A magmatic fabric is relatively well developed and is defined by alignments of euhedral crystals of K-feldspars and mafics (pre-full crystallisation fabric). Measurements in the SW part of the body show a dominance of NW-SE and NE-SW strikes, dipping at high angles (70° to sub-vertical; Fig.6.8A). Fractures are relatively common and most strike NW-SE dipping steeply NE (Fig.6.8B), filled by hydrothermal minerals.

6.7- OTHER PLUTONS.

Several other similar small plutons are present in the Carajás region, most being apparent on remotely sensed data and not yet studied in the field. They occur mainly in the Serra do Rabo region, at the E termination of the Carajás Fault, and in the region south of the Carajás Strike-Slip System (Fig.6.1).

A small 1 Km x 2 Km granitic pluton was described by Macambira *et al.* (1990) as intruded into the mafic rocks of the Grão Pará Group about 3 Km north of the N-4 plateau, close to the northern border of the Carajás Strike-Slip System (Fig.6.1). According to Macambira *et al.* (1990) the pluton has petrological affinities with the Itacaiúnas Granite.

A granitic rock named "Young Salobo Granite" was studied by Lindenmayer (1990) in the Salobo area (Fig.6.1). This rock does not outcrop and is referred to as a NNW oriented 50m-thick sill hosted by gneisses of the Basement Assemblage producing a contact-metamorphic aureole. It corresponds to an isotropic, pink, porphyritic alkali-feldspar quartz-syenitic rock. According to Lindenmayer (1990) and Lindenmayer *et al.* (1994*a*) the Young Salobo Granite is an undeformed A-type plutonic unit that is affected by late hydrothermal alteration. It is thought to correlate with the Central Carajás Granite.

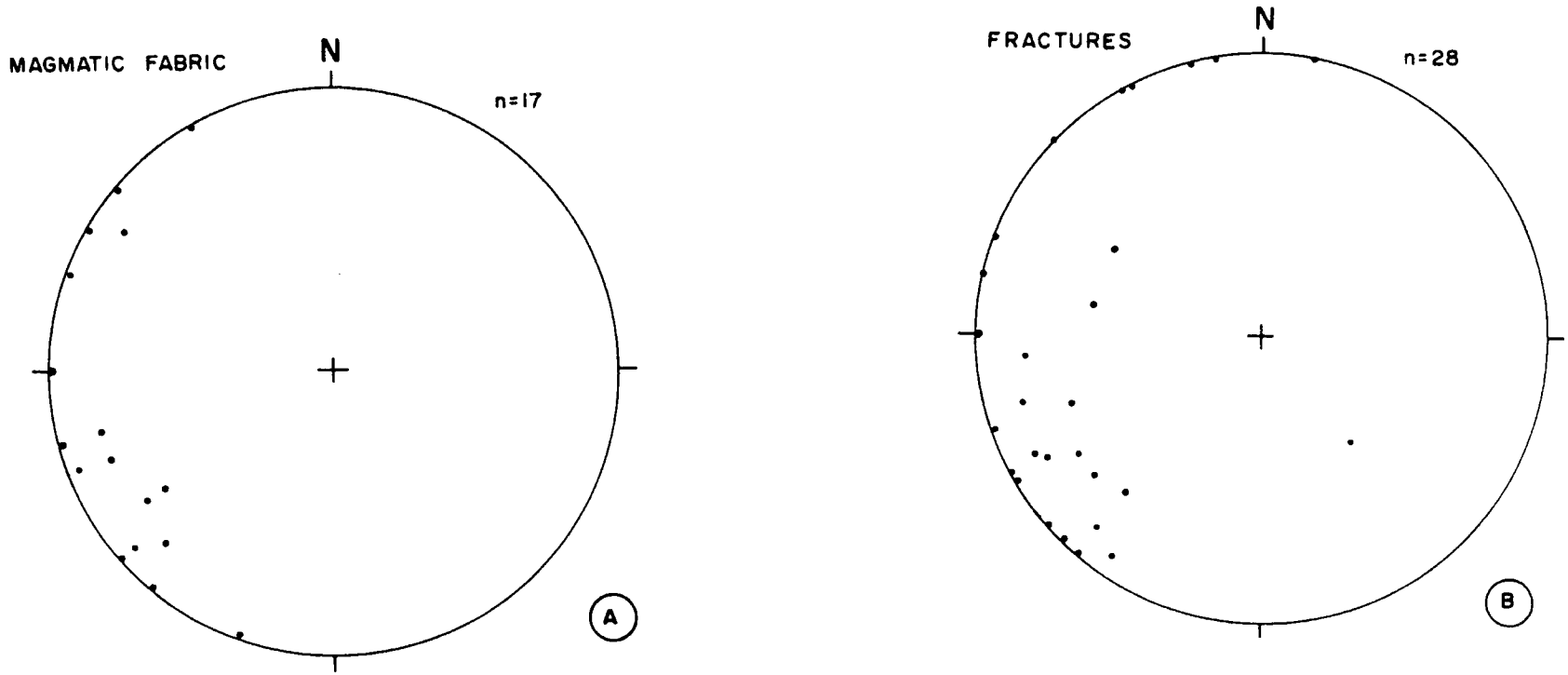

Fig.6.8- Stereonets to magmatic fabric (A) and fractures (B) observed in the Rancho Alegre Granite. NW-SE and NE-SW planes are predominant to both structures.

6.8- DYKES

In the Carajás region dykes represent very important features since they occur on several scales and are widespread throughout the region. They are emplaced into both Basement and Cover assemblages.

Rivalenti *et al.* (1992) have suggested that dykes orientated NE-SW together with sills, are tholeiitic and andesitic basalts, whilst those with NW-SE and N-S trends are predominantly "transitional" basalts. Barros *et al.* (1994*a*) and (Soares *et al.*, 1994) determined tholeiitic compositions from gabbroic sills intruding the Águas Claras Formation and also included data about the effects of later hydrothermal alteration present in these rocks.

Swarms of dykes are observed concentrated in particular areas notably in the central region of the Carajás Strike-Slip System, covering an area of about >240 Km^2, and cut by the Central Carajás Granite (Fig.6.2; Photo 6.1).

The area adjacent to the Central Carajás Granite, when observed using satellite or radar images, presents an unusual textural pattern defined by sets of anastomosing interrupted lines, strongly orientated NW-SE, concordant with the main lineaments interpreted as being related to the Carajás Fault branches (Fig.6.2; Photo 6.1). The outcropping pattern defines a dense anastomosing geometry with a sigmoidal arrangement. En echelon and stepping patterns are also observed. Both straight and curved segments are present. The maximum length of these fine lines in satellite images is around 3 Km. This pattern, corresponding to belts of positive relief, is also present, although less visible, in the area to the E of the Central Carajás Granite and south of the Carajás Fault trace (Photo 6.1). Previously these features have been interpreted as set of "faults or joints" or "mylonitic foliation traces" (Araújo and Maia, 1991), or even "S-C shear bands" (Veneziani *et al.*, 1995). The geological significance of these lines has become much clearer following the opening of the road linking the Azul Mine road to the Bahia Mine, crossing the Águas Claras river. Sets of NW-SE, NE-SW and NNE-SSW dykes with different volumes and widths are exposed in the road-cuts and appear to correspond to those features seen on the remotely sensed images.

In the Águas Claras region (see section 4.1, Chapter 4), dykes display thickness varying from <10m to >200m, with most being 10-15m thick. They intrude sedimentary rocks of the Águas Claras Formation.

Many dykes are severely altered by weathering making it impossible to recognise lithologies. They are dark-red or yellow, with colours changing in zones subparallel to the borders reflecting both different degrees of alteration

and original internal zonation (flow or compositional layers?). In less altered dykes, spheroidal weathering is common.

The anatomy of these dykes in the field is quite variable. Most are tabular to sub-tabular in vertical section, specially those with a thickness <10m. Others are more irregular, displaying a variety of subordinate characteristics such as horns, steps and forks. There are also sills, laccoliths and some more irregular bodies. Offshoots of dyke material may be found invading the country rocks. Sometimes country rock xenoliths, with variable sizes (<1m x 0.3m), are seen engulfed by the dykes. Almost all show some internal features such as columns and a thermal metamorphic aureole that can vary from few millimetres to centimetres wide.

A common structure observed in the margins of these dykes are lineations or striations thought by some authors (e.g. Nogueira, 1995) to be produced by fault reactivation along the dyke. The slickenlines post-date dyke emplacement and display random orientations, with lines varying from sub-horizontal to sub-vertical, along single dyke margins. They are interpreted here as "fingers and grooves" (Baer and Reches, 1987, in Rickwood, 1990), or flow lineations (Roberts and Sanderson, 1971) and are associated with millimetre-scale devitrified selvedges observed in some dyke walls. According to Roberts and Sanderson (1971) the orientation of this flow lineation is a function of dyke margin shape and the dyke geometry.

The age of the dykes present in the region is uncertain as different sets have yielded different ages. Rb/Sr and K/Ar whole rock and mineral ages were the main radiometric techniques used to study these rocks. At least three different phases of dyke emplacement can be recognised: (1) Middle Proterozoic (Tassinari *et al.*, 1982; Cordani *et al.*,1984; Cunha *et al.*,1984); (2) Middle to Late Proterozoic (Teixeira,1978; Gomes *et al.*,1971, 1975); (3) ?Palaeozoic (Gomes *et al.*, 1975; Lindenmayer, 1990). An Rb/Sr age of 198 Ma was obtained by Meireles *et al.*(1982) from dykes in the Serra Pelada area (see section 5.3, Chapter 5). The Middle Proterozoic dykes are thought to be the most abundant in the region (e.g. Choudhuri *et al.*,1990).

Dias *et al.* (1996*a*) dated metagabbro sills emplaced into the Águas Claras Formation as Archaean (2.645±12 Ma, Pb/Pb zircon). This suggests that some intrusions may be older than Middle Proterozoic. The spatial and temporal relationship between the sills dated by Dias *et al.* (op cit) and the dykes are not well established, but both are emplaced into the Archaean Águas Claras Formation.

6.9- DISCUSSION.

The shape of the plutons, their internal structure, wall rock relationships, and orientation of pre-full crystallisation fabrics suggest that the Carajás region granites are emplaced at shallow levels.

All plutons have sharp discordant contacts with wall rocks, whose structures are truncated by the pluton. The irregular semi-circular shapes are predominant in most plutons and although some of them are elongated, they clearly follow the orientation of local or regional structures. Xenoliths are present in most of the plutons, close to their contacts. Thermal metamorphism is also developed around most plutons.

The **Central Carajás Granite** is emplaced into clastic sedimentary rocks of the Águas Claras Formation and also into the Grão Pará Group. These rocks display a local strong NW-SE to WNW-ESE foliation trend. The pluton is N-S elongate. The main trace of the Carajás Fault and several other subsidiary faults are truncated by the pluton, as are dyke swarms. The magmatic structures (magmatic foliation, contacts between facies, veins, etc.) observed in the northern part of this pluton are NNE-SSW orientated and sub-vertical, suggesting a local WNW-ESE sub-horizontal stretching direction sub-parallel to the Carajás Fault (Fig.6.9). NNE-SSW fractures and faults are supposed to be post-crystallisation structures, in addition to micro-fractures affecting these rocks (Rios, 1991). The assemblage of quartz-muscovite-andalusite-cordierite found in the wall rocks adjacent to the plutons suggests hornblende hornfels metamorphic facies. The pluton intrusion deforms wall-rocks only close to the contact, so that, in the northern area for example, overturned bedding is found up to 500m from the contact.

The **Cigano Granite** is a roughly circular pluton bounded by E-W and NE-SW regional faults. It is emplaced into rocks of the Xingu Complex and Igarapé Pojuca Group that follow the regional E-W trend. Magmatic fabrics observed around the central part of the pluton are steeply dipping striking predominantly NE-SW with local swings into a NW-SE orientation. These data suggest a local WNW-ESE sub-horizontal extension together with a secondary NE-SW direction (Fig.6.9).

The **Rancho Alegre Granite** shows an irregular equidimensional map shape. The wall-rocks appear to belong to the Grão Pará and Xingu Complex. Its relation to the adjacent Gorotire Formation rocks is not well established. Magmatic fabrics weakly preserved in the SW part of this pluton point to

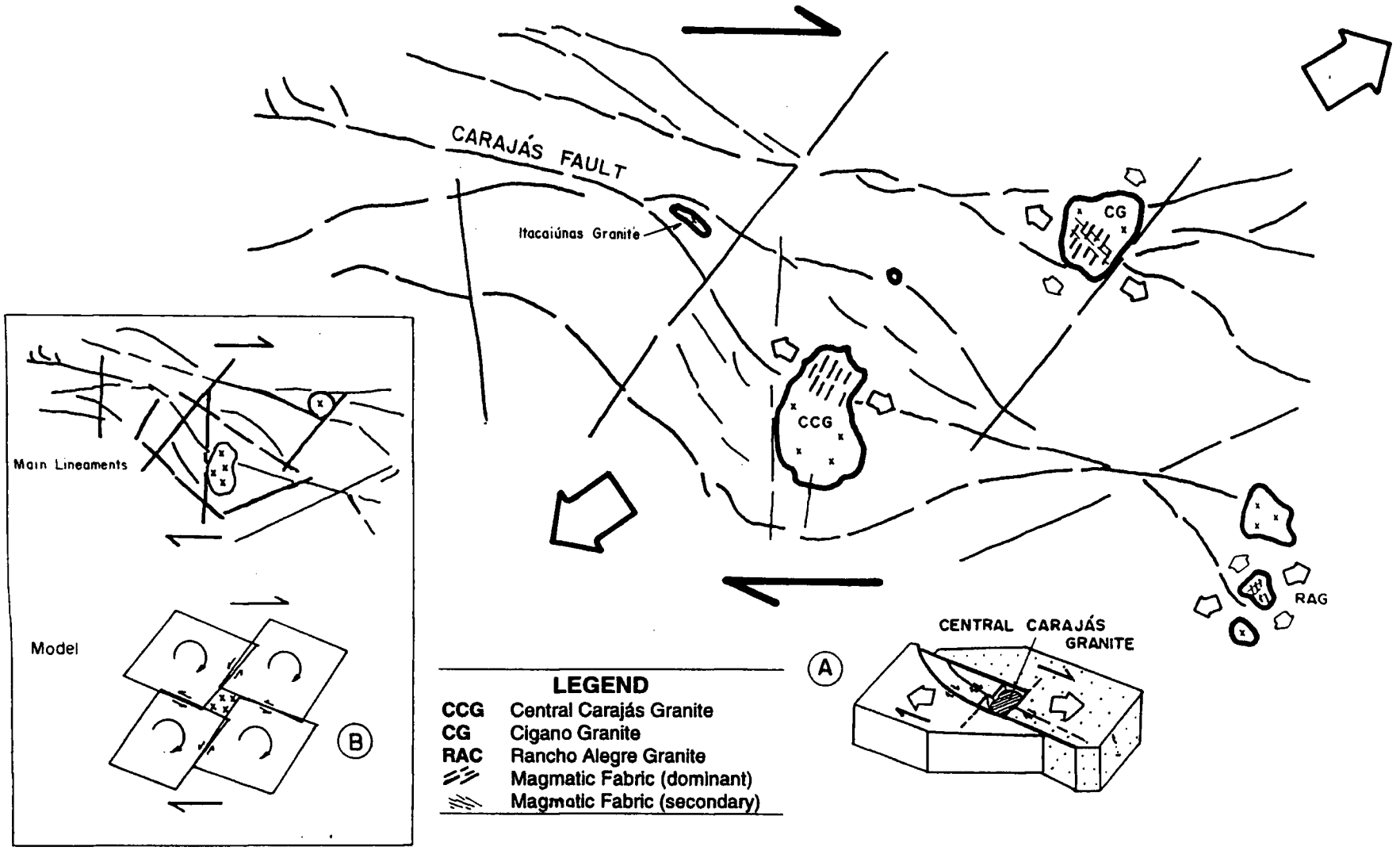

Fig.6.9- Interpretation of probable stretching orientation (small arrows) for individual plutons in the Carajás area. A) sketch diagram showing possible space creation along pull-apart structures in the Central Carajás Granite. B) model showing possible space opening by clockwise rotations of blocks separated by faults, induced by regional dextral kinematic in the Carajás region.

probable WSW-ENE and secondary NNW-SSE sub-horizontal directions of extension during emplacement (Fig.6.9).

The **Itacaiúnas Granite** forms a NW-SE elongate shape, sub-parallel to the trace of the Carajás Fault and the lineaments on the northern border of the Carajás Strike-Slip System.

The end Early Proterozoic and the Middle Proterozoic structures in the Amazonian Craton are thought to have been formed during NE-SW extension (e.g. Costa *et al.*,1991; Costa and Hasui, 1991; Costa and Hasui, 1992; Neves, 1992; Costa *et al.*,1995). It is suggested that few new structures were formed at this time with most displacements accommodated by brittle reactivation of pre-existing faults and fractures.

Magma emplacement at such shallow crustal depths is likely to occur by brittle wall rock deformation processes with stoping, cauldron subsidence and dyking. This is supported by the occurrence of country rock xenoliths, sheeted granite contacts and xenolith breccias.

According to Hutton (1988*b*) movements along complex networks of faults can generate tectonic cavities (e.g. pull-aparts, releasing bends, tension gashes, shear zone terminations, ramp-flat geometries). This, in association with magma buoyancy forces can drive the siting and emplacement of plutons in a extensional or transtensional tectonic regime. The sub-parallelism of magmatic foliations (pre-full crystallisation) and sheet contacts can be explained by the action of magma buoyancy forces acting against sheeted boundaries during tensile emplacement (Hutton, 1988*b*; McErlean, 1993).

It is suggested, therefore, that NE-SW regional extension was accommodated by dextral shearing along the main pre-existing E-W Carajás and Cinzento lineaments. Granites were then emplaced into pull-apart zones in local dilation zones (e.g. Central Carajás; Fig.6.9A). Extension perpendicular to the main lineaments in the E termination of the Carajás Fault may have created space for the Rancho Alegre Granite to be placed. A similar process may explain intrusion of the Itacaiúnas Granite (Fig.6.9). The variable open directions in the Cigano and Rancho Alegre plutons may be explained if small clockwise rotations of pre-existing fault blocks occurred in a manner similar to that envisaged by Thomas (1974) and Jacques and Reavy (1994; Fig.6.9B).

The presence of granitic dykes with brecciated xenoliths injected in the thermally metamorphosed wall rocks, close to the northern margin of the Central Carajás Granite, is evidence of high fluid pressures associated with the pluton emplacement. These dykes are interpreted as post-failure fluid discharges along faulted channelways suggesting fault-valve behaviour (e.g.

Sibson, 1987; 1994). This may have helped induce or facilitate fault reactivation, even in cases where the orientation of the fault is not particularly in a favorable orientation relative to the stress field (Sibson, 1992). Faults adjacent to the magmatic reservoirs may form a highly permeable channelway, allowing episodic fluid discharge leading to changes in the local fluid pressure gradient.

A post-intrusion brittle deformation took place in the region and is responsible for the occurrence of sets of NNE-SSW and N-S fractures observed in the granites and others rocks on all scales.

Dyke swarms in Carajás are arranged in characteristic NW-SE anastomosing, en echelon or stepping patterns, suggesting emplacement during regional NE-SW extension. The dykes are sub-parallel to some fault branches linked to the main Carajás Fault. As mentioned before, these faults are likely to have been reactivated probably as strike-slip (dextral) oblique-slip normal faults during this regional episode.

6.10- CONCLUSIONS.

1) The emplacement of the granitic plutons studied is thought to be related to the well known Early to Middle Proterozoic regional extension that took place all over the Amazonian Craton. This extension initiated before ca.1.9 Ga and may have occurred in several pulses with the location and emplacement of magmatism being determined by reactivation of existing faults.

2) The granitic plutons in the Carajás region are anorogenic (A-type), intruded at shallow crustal depths and emplaced in fairly permissive manner. Stoping, cauldron subsidence and dyking are probably the most important mechanisms associated to the pluton emplacements.

3) Pull apart structures controlled by reactivation of overstepping fault segments have controlled pluton emplacement (e.g. Central Carajás Granite). Articulated clockwise fault block rotations during dextral transtension may also facilitate magma emplacement into marginal voids with variable opening directions (e.g. Cigano and Rancho Alegre granites).

4) Fault reactivations may be assisted by fault-valve behaviour induced by increases in fluid pressure due to magmatism. Most of the pre-existing faults

are favourably orientated to be reactivated during NE-SW extension. Partitioned transtension is likely to have been the dominant mechanism of deformation.

5) A later brittle episode of deformation is responsible for regional scale fracturing and development of a brittle foliation affecting rocks on all scales.

6) Swarms of dykes are supposed to have been emplaced mostly during the Early-Middle Proterozoic, before the granite emplacements, filling pre-existing weakness zones and fractures. A similar kinematic setting (i.e. NE-SW extension) seems likely suggesting that dykes and granites may have been emplaced during a single protracted phase of extension affecting the Amazonian Craton.

CHAPTER 7
THE SERRA DO PAREDÃO AREA

The Serra do Paredão forms a series of 400-450m hills located about 20 Km northeast of the Serra Pelada mine and approximately 10 Km north of the E termination of the Cinzento Strike-Slip System.

The hills forming the Serra do Paredão are irregularly orientated in the NE-SW and NW-SE in the north and south of the area respectively, forming a roughly triangular shape in map view, elongated slightly NE-SW (Fig.7.1).

The rocks present in this region comprise conglomerates and sandstones forming a sequence >250m thick lying unconformably upon gneisses and granitoids of the Xingu Complex. The age and stratigraphical position of the sediments are controversial.

7.1- REGIONAL SETTING AND PREVIOUS WORK

The rocks outcropping in the Serra do Paredão area have been studied in some detail by Ramos *et al.* (1984), Figueiras and Villas (1984); Serique and Ramos (1984) and Figueiras *et al.* (1987). These authors have shown that the sedimentary sequence present in this area is not easily correlated with the Archaean Rio Fresco Formation or Group as proposed previously (e.g. Hirata, 1982; DOCEGEO, 1988).

The rocks from the Serra do Paredão have been described as predominantly reddish orthoquartzite sandstones, associated with quartz wackes and lithic wackes, and polymictic conglomerates formed mainly of pebbles of quartz and quartzites that can be more than 20cm across (Serique and Ramos, 1984). Constituent grains, according to Ramos *et al.* (1984), comprise quartz, rock fragments (including ironstones and slates), chert, microcline, plagioclase, muscovite and opaque minerals. Kaolinite and illite are the main minerals found in the matrix. Ripple marks are the most frequent primary structure but cross-bedding is also observed. They have been interpreted as probable fluvial deposits laid down in a tectonically stable continental environment (Ramos *et al.*,1984; Serique and Ramos, 1984). They show no evidence of metamorphism.

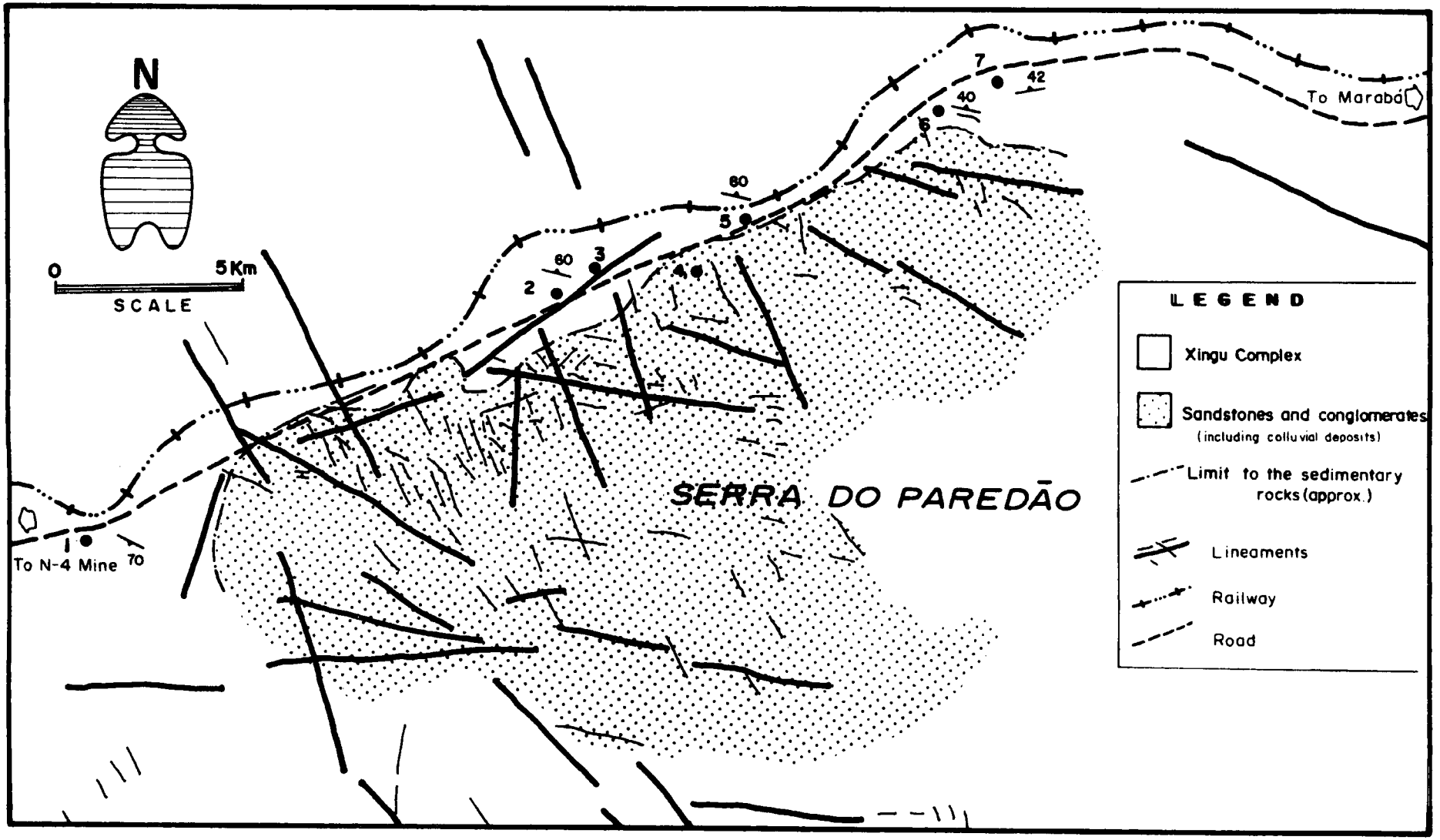

Fig.7.1- Map of the Serra do Paredão area showing main lineaments observed on satellite images and the approximate area covered by sedimentary rocks. Points visited are indicated together with the attitude of the foliation in the Xingu Complex rocks.

Figueiras and Villas, (1984) suggested that these sedimentary rocks may be equivalent to other units outcropping in the Carajás region. They suggested that the Serra do Paredão rocks represent a coarse proximal facies of a widespread unnamed sedimentary sequence with some affinities to the Gorotire Formation.

Figueiras *et al.* (1987) later suggested that the rocks outcropping in the Serra do Paredão area could be correlated with the so-called Rio Fresco Formation, with the Serra do Paredão as a basal sequence to this unit. However, the Rio Fresco Formation or Group, as described to the Serra dos Carajás region, was not well defined. It included at that time both metamorphic and sedimentary rocks now recognised as being part of the Igarapé Pojuca Group, the Águas Claras Formation and also the Gorotire Formation. The age of these rocks was not well defined and several authors mentioned ages ranging from the Archaean to Middle Proterozoic or even Devonian (Ramos *et al.*, 1984).

A more recent publication by Araújo and Costa (1994) suggested an Early to Middle Proterozoic age for the rocks of the Serra do Paredão area and introduced the name Paredão Group.

The basement gneisses underlying the Serra do Paredão sedimentary rocks are consistently referred to as Archaean Xingu Complex, even though they are little studied. Lab (1992) examined basement rocks in the region between Serra Pelada and Serra do Paredão. He reported a predominance of granodioritic and tonalitic gneisses, with lenses of amphibolites and staurolite-cordierite-andalusite-biotite schists. The rocks supposedly carry an important mylonitic foliation formed during a regional high temperature sinistral transpressional event. The unconformity between the basement and the sediments is not exposed.

7.2- FIELD OBSERVATIONS.

Exposures in the Serra do Paredão area were investigated along the small road that follows the railway linking the N-4 Mine to Marabá, 40 Km to 65 Km from Parauapebas (Fig.7.1). Most of the outcrops observed displayed rocks of the Xingu Complex (Basement Assemblage; all points in Fig.7.1, except point 4). A large area around the northern slope of the Serra do Paredão (>2 Km, in places) is covered by colluvial deposits.

a) The basement rocks- The basement rocks were observed at several locations marked on the map (Fig.7.1). The rocks are predominantly fine to coarse grained, dark-grey biotite-quartz gneiss with garnet with a compositional a banding of variable thickness (0.5 cm to >2.5cm; Photo 7.1). Mafic bands are mainly formed by biotite and amphibole in variable proportions. Leucocratic units are formed by quartz, feldspar (plagioclase: albite-oligoclase, microcline in small percentage). Pegmatitic rocks are also present defining quartzo-feldspathic-tourmaline veins sub-parallel to the general orientation of the layering (Photo 7.2) and showing, together with the banding, several deformational features (boudins, pinch-and-swell, asymmetric folds, ptygmatic folds). Aplitic rocks are also observed in veins sub-parallel to the banding. Garnet-rich gneisses form metre-wide zones inside the biotite-hornblende-quartz gneisses (Photo 7.1). Garnets range in size from a few millimetres to 1cm (Photo 7.3). Most rocks are S or LS tectonites, with mineral lineations, where present, defined by alignments of micas and elongate quartz-feldspar aggregates.

Granitoid rocks with a weak planar fabric pass laterally into biotite-quartz-gneisses and hornblende-quartz-gneisses. These rocks are medium to coarse grained, with a typical granitic to granodioritic composition, comprising plagioclase-quartz-microcline-biotite and hornblende.

The Fig.7.2 shows stereonets of the foliation (a), lineation (b) and fractures (c) observed in the Xingu Complex rocks studied. The foliation (a) shows a general NW-SE orientation and the lineation (b) is plunging towards NW, SE and SW. The relation between the foliation and the lineation suggests both strike-slip and reverse displacement. Fractures are N-S, NE-SW and NW-SE, mostly sub-vertical. N-S fractures may display sinistral offsets of up to 30cm (e.g. point 02), whilst NW-SE fractures are mainly normal faults with centimetre-scale displacements (e.g. points 6 and 7). Major folds are occasionally present, plunging shallowly (ca. 20°) northwards (Photo 7.3) .

b) The sedimentary rocks- The sedimentary rocks were studied in only one outcrop (point 3 in the Fig.7.1). Several major colluvial blocks spread across the slopes were also examined. The best outcrops of these rocks are largely inaccessible, in >100m high vertical cliffs.

The rocks observed in point 3 lie on the northern slope of Paredão hill (Fig.7.1), ca. 50m above the railway. They are fine to medium red sandstones, with moderately well-sorted to unsorted grains, mostly sub-rounded. Sub-horizontal beds have a thickness of about 0.5m to >2m. Metre-scale planar

Photo 7.1- Gneiss observed in loose blocks around point 4 (Fig.7.1).

Photo 7.2- Pegmatitic veins with quartzo-feldspar and tourmaline oriented sub-parallel to the foliation in gneisses around the point 5.

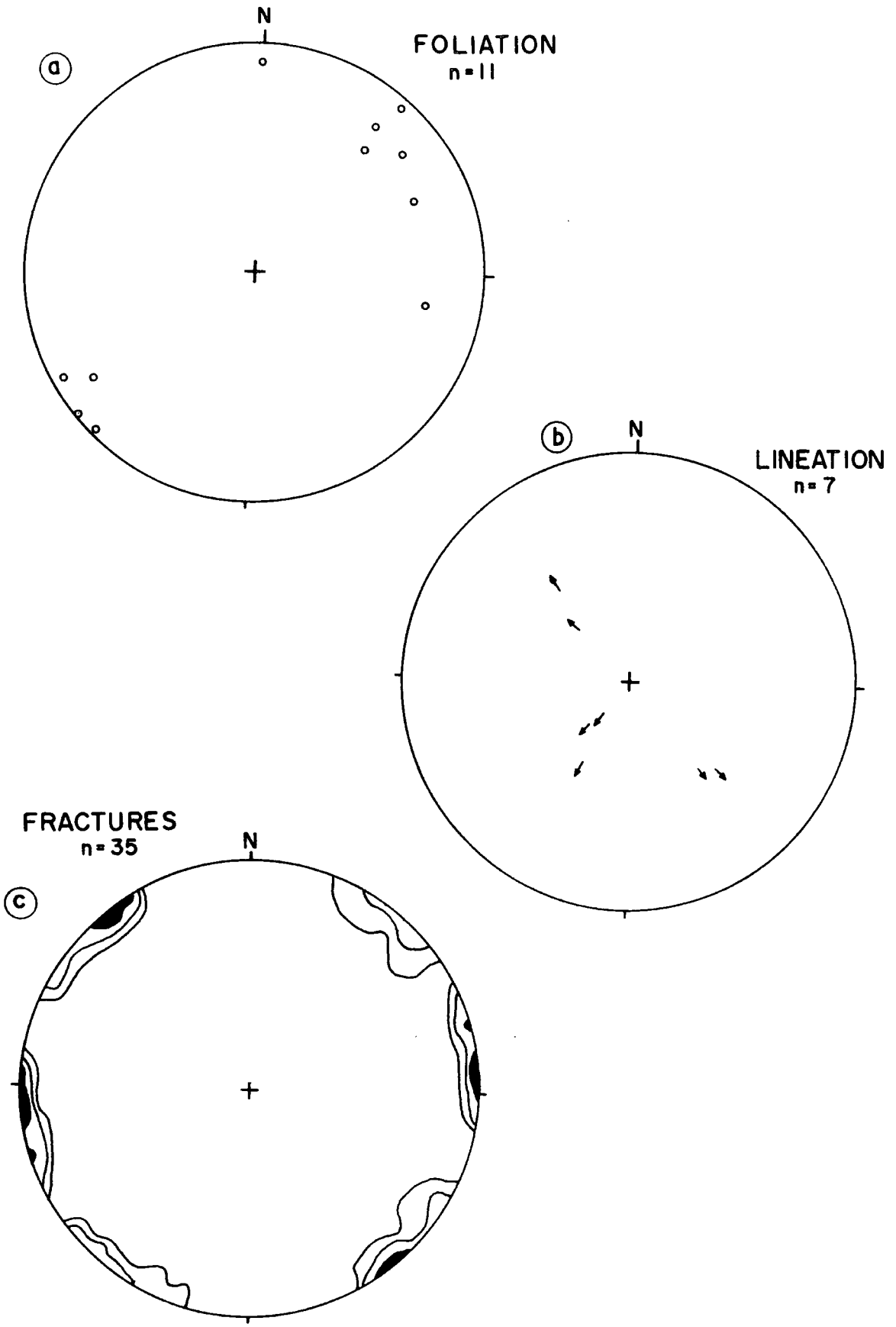

Fig.7.2- Stereonets to the foliation (a); lineation (b) and fractures to the Xingu Complex rocks observed to the north of the Serra do Paredão. Contours in the diagram C correspond to concentration of 3%; 6% and 12% of a total of 35 poles to planes.

cross-stratification (Photo 7.4) preserved with foresets dipping with low angles (<12°). Small-scale normal faults striking about E-W can be found displacing the stratification in the sandstones (Photo 7.5).

Blocks of polymictic conglomerates with unsorted sub-rounded to rounded pebbles of quartz veins and grey-red sandstones up to 10-15cm in diameter were found at the base of the hill (Photo 7.6).

Photo 7.3- Very altered gneisses outcropping in a road-cut around the point 5 (Fig.7.1). A pair of folds is observed in the E corner of the outcrop

c) Major structural features from satellite images- The visual analysis of LANDSAT images, originally in the scale of 1:100.000 (Photo 7.7 and Figs. 7.1 and 7.3), reveals the presence of a few lineaments orientated in three main directions: NNW-SSE; E-W and NE-SW.

The mapping of the Xingu Complex and the sedimentary rock domains, is rather difficult due to the strong anthropogenic influence, reflected in several pale rectilinear features that interfere in any interpretation. The cuesta morphology present in the Serra do Paredão is easily observed in the LANDSAT image (Photo 7.7 and Fig.7.3), with the steep scarp contouring the curved external border of the hills. In contrast a more gentle dip slope lies behind the steep scarp dipping towards the centre of the region of elevated relief, suggesting an apparent synformal structure (Fig.7.3). The possibility of a major fold was first suggested by Figueiras and Villas (1984) but this structure

Photo 7.4- Cross stratification observed in the sandstones of the Serra do Paredão (point 4, Fig.7.1).

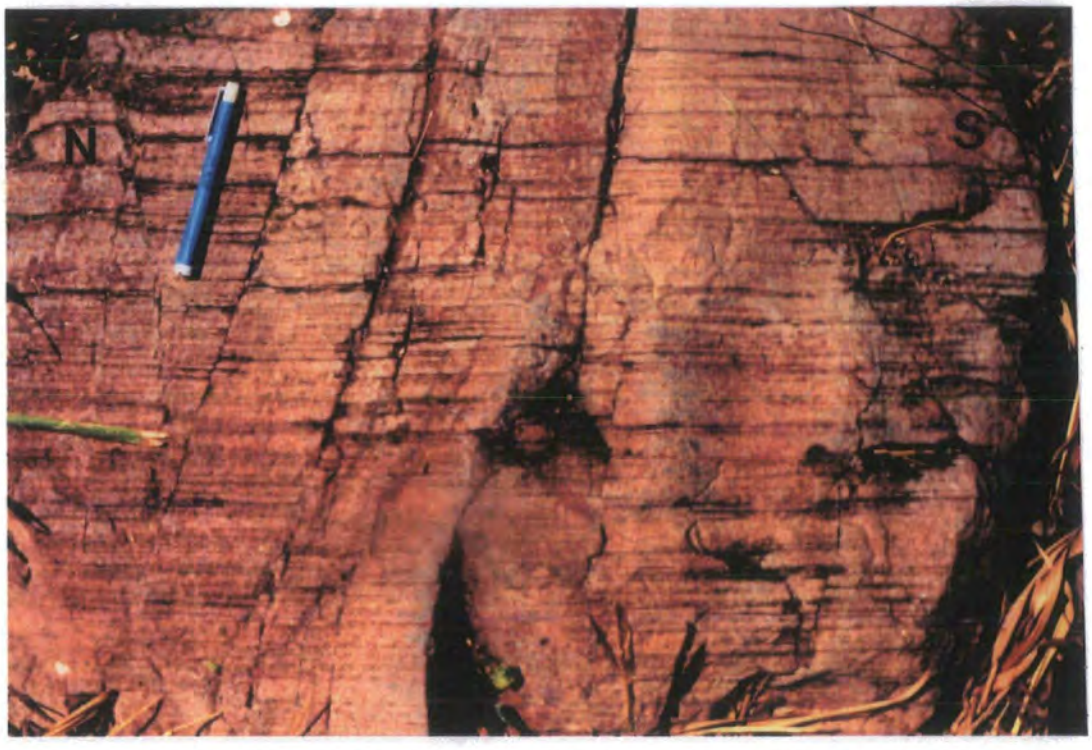

Photo 7.5- Set of small-scale normal faults cutting the stratification observed in sandstones of the Serra do Paredão (point 4, Fig.7.1).

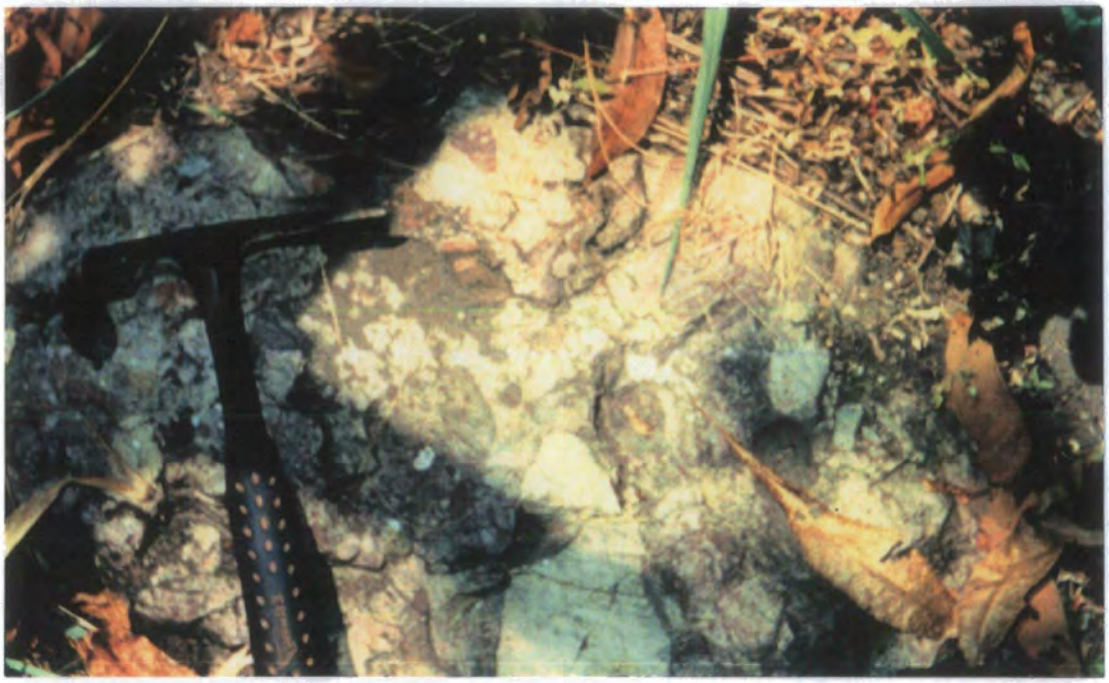

Photo 7.6- Typical conglomerate observed in the Serra do Paredão area (point 4, Fig.7.1).

Photo 7.7- LANDSAT image of the Serra do Paredão region (see scale in the map below).

Fig. 7.3- Contours to the border of the cuestas observed in satellite image to the Serra do Paredão area. Folds are suspected to be present but they were not mapped in field.

has never been locate in the field; if it exists, it is likely to be a very open structure.

7.3- DISCUSSION

Figueiras and Villas (1984) have suggested that the rocks of the Serra do Paredão area were similar to the Gorotire Formation as defined by Andrade Ramos (1954). They are also correlated to the Serra do Paredão rocks with purplish red immature sandstones and polymictic conglomerates which occur in several isolated points in the Carajás Strike-Slip System; these rocks have now been assigned to the Gorotire Formation during the present study (e.g. Itacaiúnas river, Serra do Rabo region).

The similarities observed between the rocks interpreted here as the Gorotire Formation and the rocks of the Serra do Paredão are: (1) they are both immature rocks (textural and mineralogical); (2) in both units there is a predominance of coarse sandstones and polymictic conglomerates. There are, however, many differences:

(1) the conglomerates of the Serra do Paredão are bimodal (Figueiras and Villas, 1984); those from the Gorotire Formation are polymodal; (2) the pebbles of the Gorotire Formation are predominantly formed by locally-derived gneisses, granitoids and volcanics; those from the Serra do Paredão are mostly formed by quartz and sandstone (Serique and Ramos,1984); (3) the sandstones of the Gorotire Formation are predominantly feldspathic; those from the Serra do Paredão are only partially feldspathic; (4) arkosic wackes were found only in the Gorotire formation while the sandstones of the Serra do Paredão are more diversified; (5) Gorotire Formation rocks display predominantly trough cross stratification, whilst ten-metre scale planar cross-sets occur in the Serra do Paredão; (6) both rocks of the Serra do Paredão contain subordinate units of fine sandstone, while such rocks are absent in the Gorotire Formation.

Based on these differences it is suggested that the sedimentary rocks of the Serra do Paredão area cannot be confidently correlated with units previously associated to the Rio Fresco Formation, (i.e. the Águas Claras and Gorotire formations).

Existing sedimentological information (e.g. Figueiras and Villas, 1984) suggests that the rocks of the Serra do Paredão were deposited in a large basin. Palaeozoic sediments of the Parnaíba Intracratonic Basin (see Fig.3-1,

Chapter 3) have been reported to be present in several places in the southeastern border of the Central Brazil Shield preserved in small graben formed during the Mesozoic Gondwana break-up (Silva *et al.*,1974; Mabesoone, 1978; Cunha *et al.*, 1981). Outcrops of Palaeozoic rocks associated with the Parnaíba Basin have been mapped about 20 Km northeast of the Serra do Paredão, (Hirata *et al.* 1982).

The basal unit of the Parnaíba Basin, the Siluro-Ordovician Serra Grande Formation (Fig.7.5; Small, 1914, in Caputo and Lima, 1984) most closely resembles the rocks outcropping in the Serra do Paredão area. Figure 7.4 summarises a comparison of the main characteristics of these two sets of rocks.

The Serra Grande Formation rocks correspond, at the base, to consolidated whitish to yellowish brown conglomerates and conglomeratic sandstones, with pebbles of quartz, slates, sandstones and siltstones with diameters <20cm. This sequence is followed upward by yellowish brown fine to medium coarse sandstones with medium to well sorted grains, corresponding to arkoses and wackes. The top of the unit is dominated by fine sedimentary rocks including sandstones, siltstones and mudstones (Mabesoone, 1977; Mabesoone, 1978; Schobbenhaus *et al.*,1984; Caputo and Lima, 1984). The Silurian age of these rocks was based on palaeontological data from shales of this sequence.

The Serra Grande Group lies unconformably over the basement rocks and is overlain by the Devonian Pimenteiras Formation (Mabesoone, 1977). It was interpreted as being deposited in a fluvial (Kegel, 1953, in Caputo and Lima, 1984), or possibly a shallow marine environment (Bigarella *et al.*, 1965 and Bigarella, 1973, in Caputo and Lima, 1984; Mabesoone, 1978).

It is tentatively suggested that there are sufficient similarities to warrant a possible correlation between at least the lower parts of the sedimentary rocks of the Serra do Paredão region and those of the Serra Grande Group.

Probably the most serious problem concerning this correlation relates to the >240m thickness of the Serra do Paredão sequence (Ramos *et al.*, 1984; Serique and Ramos,1984). The expected thickness for the rocks of the Serra Grande Group rocks in the western border of the Parnaíba Basin should not be <100m according to several authors (e.g. Caputo and Lima,1984). Mabesoone (1978) shows that the nearest outcrop of the Serra Grande Group rocks is about 200 Km SE from the Serra do Paredão region (Fig.7.5).

SERRA DO PAREDÃO ROCKS

Figueiras *et al.* (1987)

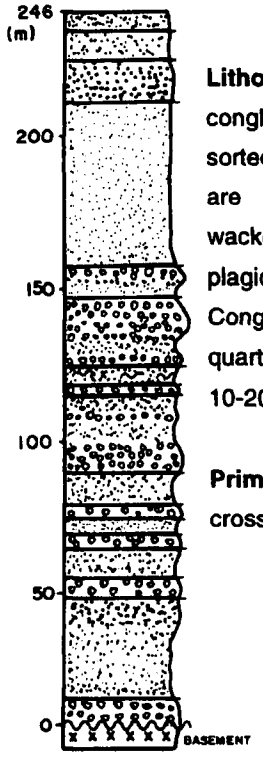

Lithologies: Sandstones and polymictic conglomerates. Sandstones are reddish with well sorted and rounded grains, with little matrix; they are orthoquartzites. quartz wackes and lithic wackes. They are formed by quartz, and plagioclase, microcline in smaller proportions. Conglomerates are polymictic, with pebbles of quartz, silex, sandstones and slates; pebbles with 10-20cm in diameter.

Primary Structures: ripple-marks, stylolites and cross stratification (less common).

THE SERRA GRANDE FORMATION

(Mabesoone, 1978)

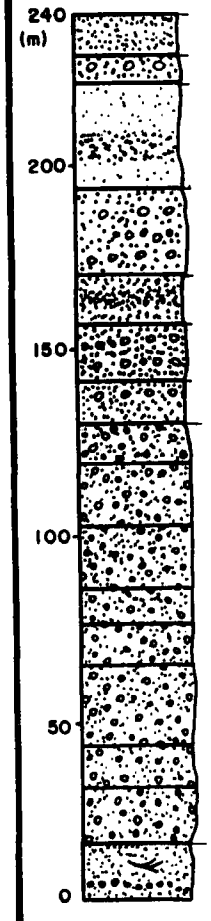

Lithologies: Sandstones and polymictic conglomerates. Sandstones are mostly orthoquartzites, lithic sandstones, and arkoses and greywackes in minor proportions; composed of medium to coarse grained sand fining upwards. Conglomerates are polymictic with quartz and quartzites pebbles being the most common; pebbles with 10 cm in diameter dominate, in a sandy matrix.

Primary Structures: cross-bedding stratification with low angle and decametre-scale sets are predominant. Normal gradational contacts are very common forming major sets separated by abrupt ones.

Palaeoenvironment: coastal to shallow marine (transgressive)

Fig.7.4- Some differences and similarities between the Serra do Paredão and the Serra Grande Formation. See text for details.

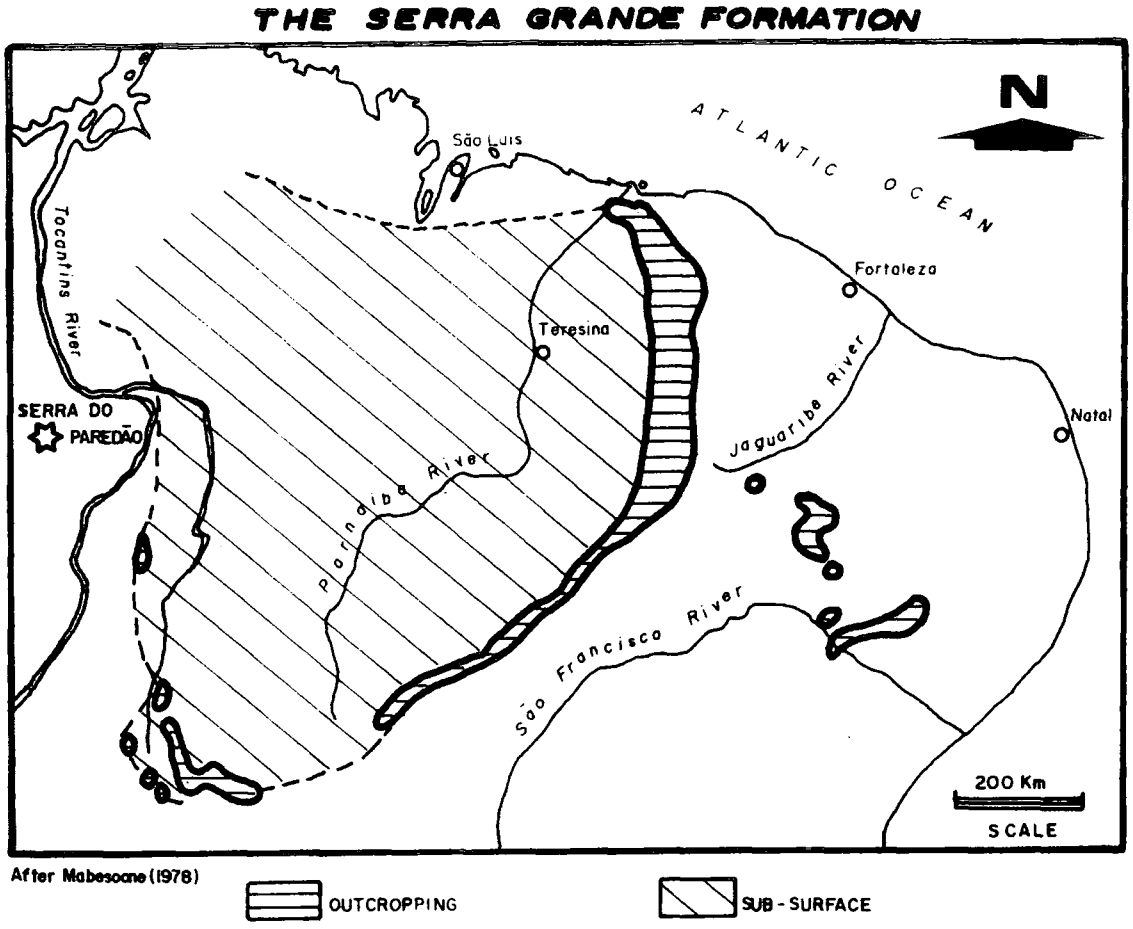

Fig.7.5- Geographic distribution of the Serra Grande Formation according to Mabesoone (1978).

Inspection of the satellite images reveals that the triangular shape of the sedimentary rocks outcrop is defined by lineaments corresponding to major sets of faults. These structures are sub-parallel to the basement ductile fabric and follow the same trend as the Itacaiúnas Shear Zone and the eastern termination of the Cinzento Strike-Slip System (Fig.7.1). The contact between the sedimentary rocks and those from the basement was not observed directly in the field, but a down-faulted graben structure seems to be a reasonable interpretation. Further research is needed to confirm these stratigraphical affinities and the age of these rocks together with their internal structure and setting.

The basement rocks observed near the Serra do Paredão area are typical examples of the Archaean Xingu Complex, as suggested by other

authors (e.g. Araújo and Costa, 1994). They are directly comparable to the Xingu Complex rocks adjacent to the Estrela Granite (see section 4.6, Chapter 4) and in the Itacaiúnas river section (see section 4.1, Chapter 4).

7.4- CONCLUSIONS.

1) The high grade metamorphic rocks of the Serra do Rabo region belong to the Archaean Xingu Complex of the Basement Assemblage. High temperature deformation is complex, involving kinematic and intensity strain partitioning. Sinistral displacements within associated reverse shear sense are predominant.

2) The sedimentary rocks present in the area are probably Phanerozoic and correspond to lower units of Palaeozoic sequences associated with the Parnaíba Intracratonic Basin. A tentative correlation with the Siluro-Devonian Serra Grande Formation is suggested here but further stratigraphical and sedimentological studies are necessary to prove this hypothesis.

3) The sedimentary rocks may be in a graben. The main lineaments thought to represent the faults bounding this structure, are sub-parallel to the trend of the main structures in the basement and the Cinzento Strike-Slip System.

4) The graben may have formed during the Mesozoic opening of the South Atlantic.

"É provável que o falhamento originado no Pré-Cambriano tenha sido reativado durante o Paleozóico e Terciário" *

Knup (1971)

(* Probably the Precambrian faulting has been reactivated during the Palaeozoic and Tertiary)

CHAPTER 8
CONCLUSIONS

8.1- THE CARAJÁS REGION TECTONOSTRATIGRAPHY

The present study has shown that the regional tectonostratigraphy of the ***Itacaiúnas Belt*** can be subdivided based on the geological relationship of units to the main phase of deformation and associated high grade regional metamorphism (Fig.8.1). An Archaean ***Basement Assemblage*** includes an older group of granulite facies orthogneisses (*Pium Complex*; ca. 3.05 Ga; Rodrigues *et al.*, 1992), a younger sequence of upper amphibolite facies orthogneisses including migmatites - the *Xingu Complex* (ca. 2.85 Ga., Machado *et al.*, 1991) and syn-tectonic granitoids (e.g. *Plaquê Suite*; Araújo & Maia, 1991). Collectively, these rocks are here referred to as the **Granite-Gneiss Complex** (Fig.8.1b). In addition, there are geographically isolated occurrences of high grade supracrustal rocks, the most important of which are a volcano-sedimentary sequence known as the **Salobo Group** (ca. 2.76 Ga; Lindenmayer, 1990; Machado *et al.*, 1991; Fig.8.1). All these rocks are deformed in a broad braided zone of steeply-dipping, E-W-trending, ductile shearing, here termed the ***Itacaiúnas Shear Zone*** (Fig.8.1) that formed during high grade regional metamorphism (amphilolite facies or higher).

The Granite-Gneiss complex occupies much of the studied region (ca. 65% by area). The Igarapé Salobo Group outcrops at the western end of the **Cinzento Strike-Slip System**, in kilometre-scale lensoid enclosed by the surrounding Xingu Complex, and bounded by straight and curved lineaments that are thought to be faults (Fig.8.1a). These rocks are inferred to have originally been deposited unconformably upon the Xingu Complex, subsequent to the formation of the Granite-Gneiss Complex, but prior to sinistrally transpressive ductile deformation and amphibolite facies metamorphism associated with the development of the Itacaiúnas Shear Zone (ca. 2.85 Ga). They are quite different to the lower Grão Pará Group and for this reason, should not be correlated with these rocks (see sections 4.3, 4.5, 4.6 and 5.1).

A ***Cover Assemblage*** (Fig.8.1) is represented by low- to very low-grade volcanic and sedimentary rocks that are either known or are inferred to rest unconformably on rocks of the Granite-Gneiss Complex. A deformed Archaean

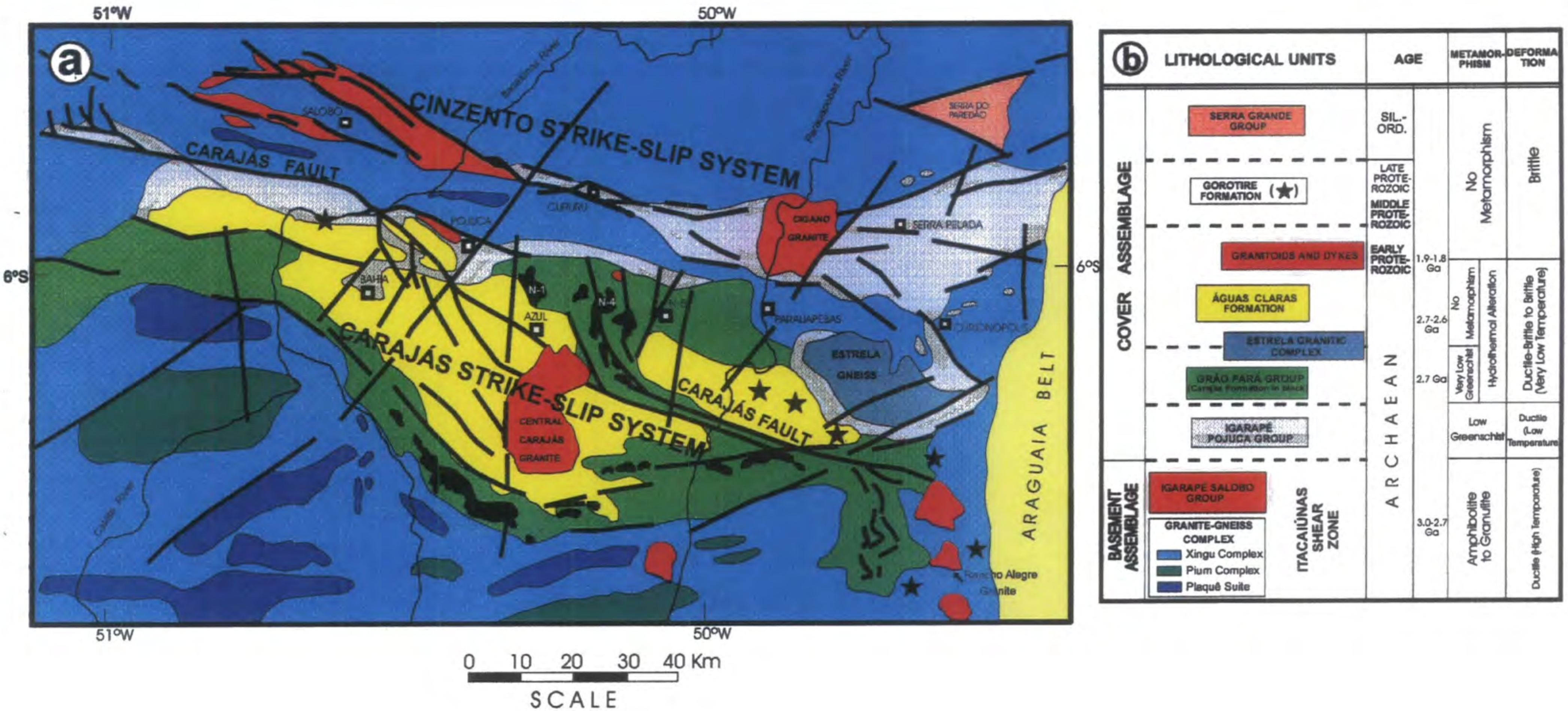

Fig.8.1- (a) Simplified geological map of the Carajás area based on the present work. (b) Table summarising the tectonostratigraphy of the Carajás region and key to the geological map (modified after Hirata *et al*,1982; DOCEGEO, 1988; Siqueira, 1990; Costa *et al.*,1990; Araujo and Maia, 1991 and Lab, 1992).

sequence of greenschist facies clastic sediments (**Igarapé Pojuca Group**; DOCEGEO, 1988) are presumed to be unconformably overlain by less deformed volcanic and ironstone sequences that have suffered only very low grades of regional metamorphism (**Grão Pará Group**; ca. 2.76 Ga; Wirth *et al.*, 1986; Machado *et al.*, 1991). All these rocks are in turn unconformably overlain by an unmetamorphosed sequence of shallow-water marine to fluvial clastic deposits (**Águas Claras Formation**; Nogueira *et al.*, 1995). These rocks are preserved in fault bend and offset regions along the **Carajás Strike-Slip System** and **Cinzento Strike-Slip System** (Fig.8.1a). The metamorphism and deformation affecting these rocks are predominantly low temperature and brittle-ductile to brittle, with the rocks in many cases affected strongly by later hydrothermal alteration.

The Igarapé Pojuca Group outcrops along the northern periphery of the Carajás Strike-Slip System and in the eastern part of the Cinzento Strike-Slip System, in the Igarapé Pojuca, Cururu and Serra Pelada regions (Fig.8.1a). The contact between the Igarapé Pojuca Group and the Xingu Complex is marked by an unconformity that is exposed in the Serra Pelada region (see Chapter 5, section 5.3).

The Grão Pará Group forms a series of ridges following both the southern and northern margins of the Carajás Strike-Slip System (Fig.8.1a) and can be divided into two sub-units: the Carajás Formation comprising a sequence of ironstones (in black in Fig.8.1a), and the Parauapebas Formation composed of basalt flows, mafic breccias, felsic tuffs and rhyolites. The contacts between the Carajás and Parauapebas formations are mostly faults. Dykes and sheets of sub-volcanics are intruded into ironstones and interlayered relationships between these rocks are observed (see Chapter 4, section 4.3). The contact between the Grão Pará and Igarapé Pojuca groups is not seen in the field although it is also presumed to be unconformable based on the obvious difference in metamorphic grade. The contact between the low grade rocks of the Grão Pará Group and the unmetamorphosed Águas Claras Formation is also presumed to be unconformable based on differences in both style of deformation and metamorphic grade, but this contact is not observed in the field (see Chapter 4, sections 4.1 and 4.3).

The Águas Claras Formation is exposed in the central area of the main Carajás structure, overlying the Grão Pará Group and the Igarapé Pojuca Group (see Chapter 4, sections 4.1 and 4.4).

The **Estrela Granitic Complex** (Fig.8.1; Barros & Dall'Agnol, 1993) is an intrusive granitoid emplaced into rocks of the Granite-Gneiss Complex and Grão

Pará Group. The age of emplacement and deformation of this pluton is thought to be ca. 2.5 Ga as it has been correlated by these authors with a dated (ca. 2.57 Ga; U-Pb zircon) small granitoid at Salobo Camp ('Old Salobo Granite': Lindenmayer, 1990; Barros & Dall'Agnol, 1993).

Both Cover and Basement assemblages are intruded by ca. 1.87-1.88 Ga **A-type granitic plutons** and **basic dykes**, including the Central Carajás, the Cigano, the Rancho Alegre and other granites (Fig.8.1; Wirth *et al.*, 1986; Dall'Agnol *et al.*, 1987; Machado *et al.*, 1991). The country rock units described so far are thought to be overlain unconformably by thin, localised sequences of ?Middle Proterozoic (**Gorotire Formation,** Andrade Ramos *et al.*, 1954) and Phanerozoic clastic sedimentary rocks (**Serra Grande Group**; Caputo and Lima 1984; Fig.8.1). Both of these sequences are presumed to post-date intrusions of the ca. 1.87-1.88 Ga plutons on the basis of very similar granitic clast contents; unconformable contacts between these rocks and the plutons were not observed, however.

The Gorotire Formation corresponds to lithic sandstones and polymictic conglomerates that cover areas mainly in and around the Serra do Rabo region, at the eastern end of the Carajás Strike-Slip System and a large area in the northeastern part of the Carajás structure, E of the Parauapebas river (Fig.8.1a; see Chapter 4, sections 4.5 and 4.6). These rocks are not affected by significant deformation and show sub-horizontal bedding. The map distribution of the Gorotire Formation is not well known and further studies are required.

The Serra Grande Formation is suggested to distinguish the sandstones and siltstones outcropping in the Serra do Paredão region (Fig.8.1a) from those of the Águas Claras and Gorotire Formation (see Chapter 7).

The high temperature ductile fabrics in the basement rocks are post-dated by at least three cycles of brittle-ductile reactivation at generally low metamorphic grades, leading to the formation of two major E-W-trending fault zones: the Carajás and Cinzento strike-slip fault systems. The early ductile fabrics in the Basement Assemblage appear to significantly influence the geometry of these fault zones, which in turn control the location of Cover Assemblage outcrops and the distribution of later deformation.

8.2- STRUCTURAL HISTORY

High temperature ductile deformation

The steeply-dipping, generally E-W-trending high temperature mylonitic fabrics defining the Itacaiúnas Shear Zone are thought to have developed under upper amphibolite facies regional metamorphic conditions (e.g. DOCEGEO, 1988; Araújo & Maia, 1991). A series of anastomosing high strain zones enclose lenticular augen of less deformed gneiss on all scales (Fig.8.2). Radiometric dating (Zircon U/Pb) of the shear zone fabrics indicates that the metamorphism and deformation occurred toward the end of the Archaean (ca. 2.90-2.85 Ga, Machado *et al.*, 1988, 1991). According to previous studies, kinematic indicators suggest a regime of sinistral transpression with partitioning of deformation producing linked systems of ductile strike-slip and thrust-dominated shear zones (e.g. Araújo *et al.*, 1988, Araújo & Maia, 1990; Costa *et al.*, 1994*a*). The present work confirms the general geometry of the shear zone fabrics, but suggests that the kinematic history may be more complex than has previously been indicated. One of the most complete sections occurs through part of the Xingu Complex exposed along the Itacaiúnas River (Chapter 4, section 4.5). The foliation in this region shows an overall NW-SE trend, dipping moderately to steeply NE (section 4.5). Deformation is heterogeneous, but it is possible to define a number of domains in which similar fabric intensity, orientation and kinematic patterns are developed. Lineation orientations are highly variable, even within single domains. Both sinistral and dextral shear criteria are preserved, often with one sense dominant in certain domains; all examples display a significant component of top-to-the-SW (i.e. reverse) movement. It was not possible to determine any overprinting relationships or evidence that these dextral and sinistral shears form conjugate arrays. The occurrence of complex foliation and lineation patterns is generally consistent with a transpressional regime (e.g. Strachan *et al.*, 1992; Fossen & Tikoff, 1993; Robin and Cruden, 1994) and, regionally, sinistral shear sense indicators are dominant (e.g. in the relatively well exposed basement regions around Parauapebas-Curionópolis and N of Serra Pelada; Chapter 4, section 4.6 and Chapter 5, section 5.3).

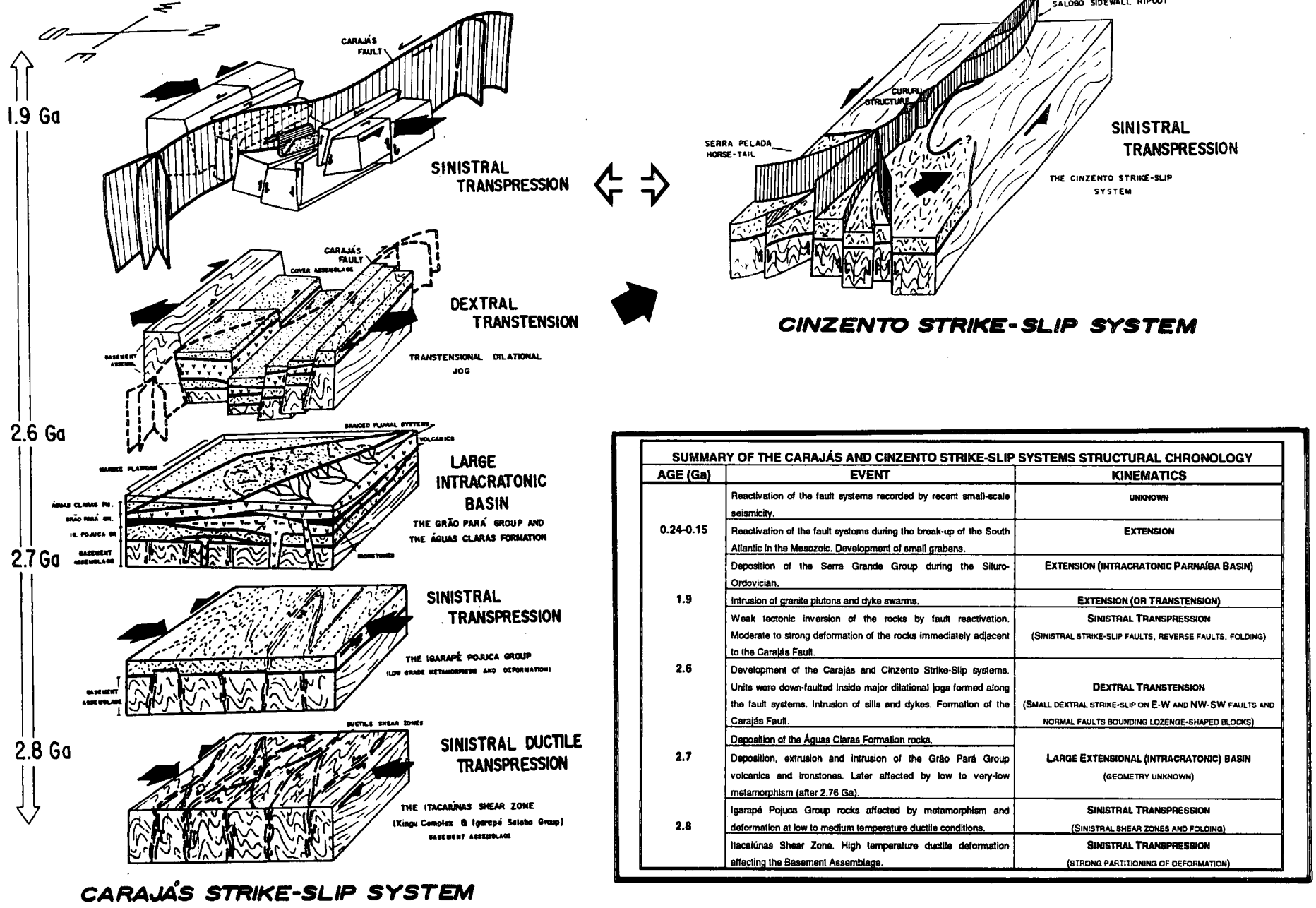

SUMMARY OF THE CARAJÁS AND CINZENTO STRIKE-SLIP SYSTEMS STRUCTURAL CHRONOLOGY

AGE (Ga)	EVENT	KINEMATICS
	Reactivation of the fault systems recorded by recent small-scale seismicity.	UNKNOWN
0.24-0.15	Reactivation of the fault systems during the break-up of the South Atlantic in the Mesozoic. Development of small grabens.	EXTENSION
	Deposition of the Serra Grande Group during the Siluro-Ordovician.	EXTENSION (INTRACRATONIC PARNAÍBA BASIN)
1.9	Intrusion of granite plutons and dyke swarms.	EXTENSION (OR TRANSTENSION)
	Weak tectonic inversion of the rocks by fault reactivation. Moderate to strong deformation of the rocks immediately adjacent to the Carajás Fault.	SINISTRAL TRANSPRESSION (SINISTRAL STRIKE-SLIP FAULTS, REVERSE FAULTS, FOLDING)
2.6	Development of the Carajás and Cinzento Strike-Slip systems. Units were down-faulted inside major dilational jogs formed along the fault systems. Intrusion of sills and dykes. Formation of the Carajás Fault.	DEXTRAL TRANSTENSION (SMALL DEXTRAL STRIKE-SLIP ON E-W AND NW-SW FAULTS AND NORMAL FAULTS BOUNDING LOZENGE-SHAPED BLOCKS)
	Deposition of the Águas Claras Formation rocks.	
2.7	Deposition, extrusion and intrusion of the Grão Pará Group volcanics and ironstones. Later affected by low to very-low metamorphism (after 2.76 Ga).	LARGE EXTENSIONAL (INTRACRATONIC) BASIN (GEOMETRY UNKNOWN)
	Igarapé Pojuca Group rocks affected by metamorphism and deformation at low to medium temperature ductile conditions.	SINISTRAL TRANSPRESSION (SINISTRAL SHEAR ZONES AND FOLDING)
2.8	Itacaiúnas Shear Zone. High temperature ductile deformation affecting the Basement Assemblage.	SINISTRAL TRANSPRESSION (STRONG PARTITIONING OF DEFORMATION)

Fig.8.2- Cartoon summarising the structural history of the Carajás region. See text for details.

Low temperature ductile deformation: The Igarapé Pojuca Group

Clastic metasediments of the Igarapé Pojuca Group crop-out in E-W-trending belts along the eastern part of the Cinzento fault zone and along the northern and western borders of the Carajás Strike-Slip System (Fig.8.1a). These rocks display moderately- to steeply-dipping slaty cleavages in pelitic lithologies (e.g. Bahia Mine, Serra Pelada; Chapters 4 and 5) and low temperature protomylonitic to mylonitic fabrics in arenaceous-to-quartzitic units (e.g. Cururu, Itacaiúnas river; Chapters 4 and 5) and basic metavolcanics (e.g. Igarapé Pojuca Mine, Itacaiúnas river; Fig.8.1a). Deformation textures and mineral assemblages in these rocks are consistent with low greenschist facies regional metamorphic conditions although the effects of hydrothermal alteration are also ubiquitous. The exact relationship between these rocks and those of the Grão Pará Group are uncertain and controversial (e.g. Medeiros Neto & Villas, 1984; Medeiros Neto, 1985; Lindenmayer & Fyfe, 1992) due to a lack of exposed contact relationships. However, as discussed early in this chapter, the two groups are likely to be separated by an unconformity on the basis that the Igarapé Pojuca Group is more pervasively deformed and that it displays consistently higher temperature mineral assemblages and fabrics compared to the Grão Pará Group (e.g. Serra do Rabo region, Chapter 4, section 4.6). Deformation in the Igarapé Pojuca Group has produced close to isoclinal folding of the sequences on all scales and, in well exposed sections (e.g. Serra Pelada; Chapter 5), the folds display a consistent clockwise sense of cleavage transection that appears to be consistent with regional sinistral transpression (Pinheiro & Holdsworth, 1995). This phase of deformation is presumed to be significantly younger than the Itacaiúnas Shear Zone because the temperatures of deformation are lower and the Igarapé Pojuca Group is known to unconformably overlie rocks of the Basement Assemblage (Fig.8.2). Narrow, low temperature ductile shear zones and an associated greenschist facies retrograde metamorphism are widespread in parts of the Granite-Gneiss Complex (e.g. Lindenmayer, 1990; Araújo & Maia, 1991; Lindenmayer & Laux, 1994) and may be the same age as the deformation and metamorphism affecting the Igarapé Pojuca Group.

The Carajás-Cinzento strike-slip fault systems

Later brittle faulting led to the formation of two regional, E-W-trending fault zones that are clearly visible on Landsat and radar images: the Carajás and Cinzento strike-slip systems (Fig.8.1a). These steeply-dipping structures display curved and braided patterns typical of strike-slip fault zones and preserve direct and indirect evidence for several phases of dextral and sinistral movement since ca.2.7 Ga. The fault orientations are strongly controlled by the trend of pre-existing ductile fabrics in the underlying Basement Assemblage. On a small-scale, brittle fracture sets in the basement rocks show variable strikes, but if the N-S and NE-SW-trending sets thought to relate to Later Proterozoic faulting (see below) are removed, the majority of fractures trend sub-parallel to the foliation and outcrop-scale examples of parallelism between the mylonitic fabric and faults are common; shear senses are variable (e.g. Itacaiúnas River, Serra do Rabo region; Chapter 4). On a larger scale, Cover Assemblage rocks are closely associated with the major fault strands and appear to be preserved adjacent to bends, offsets and splays (Fig.8.1a). This has led several authors to suggest that the Cover Assemblage rocks were laid down in a series of small dilational jog or pull apart basins along the Carajás and Cinzento faults during a phase of dextral strike-slip movements (e.g. Araújo *et al.* 1988; Siqueira, 1990; Costa & Siqueira, 1990; Araújo & Maia, 1991; Costa *et al.*, 1994*a*). More recent sedimentological and structural studies (Nogueira, 1995; Nogueira *et al.*, 1995; Pinheiro & Holdsworth (1995, 1997*a*, and 1997*b*) have shown that a pull-apart basin model is inconsistent with the stratigraphy and facies patterns of the Grão Pará Group and Águas Claras Formation. All these rocks appear to have been laid down in sedimentary basins of regional extent *prior* to the onset of dextral strike-slip movements which then faulted down previously deformed (Igarapé Pojuca Group) and undeformed (Grão Pará Group, Águas Claras Formation) cover rocks into the basement in a series of dilational jogs along the major fault strands (Fig.8.1a and 8.2). Significantly, the tholeiitic basalts and associated ironstones of the Grão Pará Group are comparable to rocks found in very large, broadly coeval basins in the Transvaal (South Africa) and Hamersley (Australia) regions (Lindenmayer, 1990). It is difficult to ascribe individual structures in either basement or cover to this dextral event due to subsequent sinistral and dextral reactivations (see below), so it remains to some extent a conjectural episode, based on the distribution of the stratigraphic units in the region.

Sinistral transpression and inversion: the Carajás Fault and the Cinzento Lineament.

Very low temperature brittle-ductile to brittle deformation is highly localised along particular fault strands and pre-existing jogs along major structures, notably the Carajás Fault and the Cinzento Lineament, forming the Salobo Sidewall Ripout (Fig.8.1a and 8.2; see Chapter 4, section 4.1 and Chapter 5, section 5.1). Along the Carajás Fault, a narrow (<2km wide) zone of complex folds and sinistral strike-slip faults (e.g. Águas Claras region, Fig.8.1a) is developed in the otherwise little deformed Águas Claras Formation and Grão Pará Group rocks, adjacent to the main fault strand. Elsewhere (e.g. N-4 Mine, Fig.8.1a) larger scale folding and partitioning of sinistral transpressional strains is associated with inversion of Cover Assemblage rocks buttressed against basement in pre-existing dilational jogs (Pinheiro & Holdsworth, 1997*b*).

Later events

Later faulting movements were associated with the regional emplacement of igneous rocks, including a series of A-type granitoids (e.g. Central Carajás, Cigano, Rancho Alegre plutons; Fig.8.1a). The Central Carajás Granite cuts the Carajás Fault system. A U-Pb Zircon age of ca.1.88 Ga (Machado *et al.*, 1988) is thought to date pluton emplacement, placing an important lower age limit on the age of sinistral transpression (Fig.8.2). The granites carry well defined, mainly N-S-trending magmatic state deformation fabrics and, on the basis of limited exposures, appear to be formed from a series of coalesced N- or NNE-trending sub-vertical sheets (Chapter 6). The form and location of some plutons (e.g. Central Carajás Granite; see Chapter 6) is consistent with emplacement into dilational jogs formed during minor dextral movements along pre-existing major fault strands. Some plutons may be emplaced into marginal voids created during clockwise fault block rotations during dextral transtension (Chapter 6). Prominent N-S- and NE-SW-trending extensional and transtensional fracture sets are found throughout the Basement Assemblage and parts of the Cover Assemblage. These are thought to have formed during the Middle Proterozoic, together with similarly oriented basic dykes (Choudhuri *et al.*, 1990) thought to be related to a regional extensional NE-SW episode recognised throughout the SE part of the Amazonian Craton (Costa *et al.*, 1991; Costa & Hasui, 1992). This correlation would imply that the

pre-existing E-W trending faults in the Carajás region could have accommodated limited dextral displacements acting as oblique transfer structures at this time.

Apparently isolated outcrops of immature sandstones and boulder conglomerates (Gorotire Formation) have been recognised in a number of locations in the Carajás region (marked with " ✱" in Fig.8.1a). They were first recognised by Knup (1971) who correlated these rocks with the Proterozoic Gorotire Formation (Andrade Ramos, 1954). These alluvial fan deposits carry clasts of all earlier rock types found in the region, including granitoids petrographically identical to the ca 1.8 Ga suite of plutons. The poorly sorted, immature character of the deposits may indicate highly localised derivation, possibly due to local faulting and pull-apart basin formation, although further mapping is required to test this hypothesis. Phanerozoic alluvial sandstones and siltstones of the Serra Grande Formation were down-faulted into the basement (e.g. Serra do Paredão; Fig.8.1a; Chapter 7), possibly during the Mesozoic Atlantic opening (e.g. Petri & Fúlfaro, 1983). Minor displacements have continued in the region to the present day as neotectonic activity is recognised along the Cinzento Fault based on the occurrence of recent seismicity (Costa *et al.*, 1993; e.g. Salobo Camp; Geol. J. B. Siqueira, personal communication, 1994) and hot springs (e.g. Cururu area; Fig.8.1a; see Chapter 5, section 5.2).

REACTIVATION AND WEAKENING

There is good circumstantial evidence that the orientation of the regional basement fabrics has controlled the geometry and location of subsequent deformation events, i.e. reactivation. Reliable criteria indicating reactivation in the Carajás region include: the occurrence of inversion geometries in the previously down-faulted cover sequences; the observed parallelism between successively lower temperature deformation fabrics and faults in basement outcrops, often with changes in shear sense; direct and indirect dating of early high temperature and later events using dated cover sequence unconformities and cross-cutting plutons; the occurrence of neotectonic activity along the fault zones.

The protracted reactivation history suggests that long-term weakening has occurred in the Carajás region. In exposures of the Basement Assemblage, later low temperature ductile shear zones and/or brittle fractures are often seen to run parallel to pre-existing basement fabrics, especially in old high strain

zones. This may suggest that geometric or fabric softening have influenced initial reactivation processes, but more obvious weakening effects are associated with the development of later structures. In particular, the low temperature brittle-ductile deformations are associated with the extensive retrogression, phyllonitisation and hydrothermal alteration of rocks along and adjacent to faults and shear zones (Chapter 4, section 4.6; Chapter 5, section 5.2). These processes almost certainly associated with the syn-tectonic influx of fluids and are likely to cause significant and permanent reaction weakening effects; they are also responsible for some of the mineralization (e.g. gold, copper) in the region.

8.3- FINAL DISCUSSION AND SUMMARY

The structural history of the Carajás region, summarised in Fig.8.2, reveals a number of important features concerning the reactivation of Archaean basement terrains:

1) There is an overall decrease in temperature associated with deformation through time that is consistent with progressive exhumation of the crust. Similar embrittlement sequences are recognised in many other long-lived shear zones in Precambrian basement rocks (Grocott, 1977).

2) The regional basement fabrics are steeply-dipping and E-W trending. Subsequent deformations are wrench-dominated events possibly because the foliation orientation favours strike-slip, as opposed to dip-slip reactivation (Etheridge, 1986; Daly *et al.*, 1989).

3) The location of the younger Cover Assemblage rocks is structurally controlled by the strike-slip faults. Most cover sequences occur in dilational jogs or offsets along major reactivated strike-slip fault zones. However, faulting entirely post-dates deposition, in this case illustrating that fault-controlled stratigraphies are not necessarily indicative of fault-controlled sedimentation and basin formation.

4) Strain intensity partitioning during successive events are often controlled by the location and geometry of pre-existing structures. Thus, deformation may be

localised into narrow zones adjacent to major fault strands or into restraining bends or offsets. These local transpression zones may also display kinematic partitioning of strains due to basement buttressing effects or accommodation of different displacement components along differently oriented pre-existing fault sets.

5) The intensity of later deformations appears to progressively decrease and the development of widespread 'new' fracture orientations during the 1.8-1.0 Ga episode is consistent with a decrease in the influence of the pre-existing basement architecture with time. As a result, the structural control exerted by earlier fabrics may not always be immediately obvious in all exposures of basement rocks as later, cross-cutting brittle fracture arrays are also present. However, it is possible to filter-out these later fracture sets as they are also seen to cut across earlier structures and cover sequences, especially on Landsat and radar images. Once removed, the earlier influence of the basement fabric during reactivation is much more obvious.

6) These observations suggest that the Archaean rocks of the Carajás region preserve evidence for over 2.8 Ga of deformational activity during which time the original high temperature basement fabric has been reactivated thereby exerting a strong influence over the distribution, geometry and kinematic patterns of later deformations. The influence of the basement architecture and the intensity of later reactivations appears to wane after a time period of ~1.0 Ga following initial high temperature deformation in the basement. This may indicate the existence of a weakening effect on a lithospheric-scale with a finite life span, possibly originating in the underlying lower crust or mantle. Similar reactivation time-limits may exist in other Precambrian basement terrains.

REFERENCES

Ab'SABER, A. N., 1986. Geomorfologia da Região. In *Carajás, desafio político, ecologia e desenvolvimento*, (ed. Almeida Jr., J.M.G. de). CNPq-Editora Brasiliense, São Paulo, 88-124, 633pp.

ADAMS, A.E.; MacKENZIE, W.S. and GUILFORD, C., 1984. Atlas of Sedimentary rocks under the microscope. Longman Scientific & Technical. 104pp.

ALMEIDA, F.F.M. and HASUI, Y., 1984. *O Pré-Cambriano do Brasil.* Ed. Edgard Blücher Ltda., São Paulo, 378pp.

ALMEIDA, F.F.M. de; HASUI, Y.; NEVES, B.B. de B., 1976. The Upper Precambrian of South America. *Boletim do Instituto de Geociências, USP.* **7**(45), 45-80.

ALMEIDA, F.F.M. de; HASUI, Y.; NEVES, B.B. de B. and FUCK, R.A., 1977. Províncias estruturais brasileiras. *Actas VII Simpósio de Geologia do Nordeste*, Campina Grande, **6**, 363-391.

ALMEIDA, F.F.M. de; HASUI, Y.; NEVES, B.B. de B. and FUCK, R.A., 1981. Brazilian Structural Provinces: an introduction. *Earth-Sciences Reviews*, **17**, 1-29.

ALMEIDA, R.C.C., 1980. *Contribuição à petrologia do Granito Central da Serra dos Carajás.* Unpublished MSc. dissertation, Curso de Pós-Graduação em Ciências Geofísicas e Geológicas, Belém, 84pp.

ALTHOFF, A.M.R.; VILLAS, R.N. and GIULIANI, G., 1994. A mineralização cuprífera da área Bahia, Serra dos Carajás (PA): evolução dos fluidos hidrotermais e modelo metalogenético. *Geochimica Brasiliensis*, **8**(2), 135-155.

AMARAL, G., 1974. *Geologia pré-cambriana da região Amazônica.* Unpublished dissertation, Universidade de São Paulo, Instituto de Geociências, 212pp.

AMBRASEYS, N.N., 1970. Some characteristic features of the Anatolian fault zone. *Tectonophysics*, **9**, 143-165.

ANAISSE Jr., J. and TRUCKENBRODT, W., 1995. *Petrologia dos arenitos da Formação Águas Claras, Pré-Cambriano, Serra dos Carajás.* Universidade Federal do Pará, Departamento de Geologia, CNPq, unpublished report, Belém, 11pp.

ANDERSON, W.L.; DYER, R.C. and TORRES, D.D., 1974. Ocorrências de manganês na bacia do Rio Itacaiúnas, centro-leste do Estado do Pará. *Anais XXVIII Congresso Brasileiro de Geologia*, Porto Alegre, **6**, 149-164.

ANDRADE, W.O.; MACHESKY, M.L. and ROSE, A.W., 1991. Gold distribution and mobility in the surficial environment, Carajás region, Brazil. *Journal of Geochemical Exploration*, **40**, 95-114.

ANDRADE RAMOS, J.R. de, 1954. O carvão do Rio Fresco, afluente do Xingu. *Engenharia, Mineração e Metalurgia*, **19**(114). Rio de Janeiro, 259pp.

ARAÚJO, O.J.B. de and COSTA J.B.S., 1994. Correlações entre as principais unidades rochosas da região nordeste do Pará na área do Programa Grande Carajás. *Anais 38º Congresso Brasileiro de Geologia,* Balneário de Camboriú, 65-67.

ARAÚJO, O.J.B. de; COSTA, J.B.S.; PINHEIRO, R.V.L.; MAIA, R.G.N.M.; MACAMBIRA, E.M.B.; VALE, A.G.; SIQUEIRA, J.B. and JORGE JOÃO, X. da S., 1992. Arcabouço estrutural do complexo de bacias transcorrentes arqueanas da região de Serra dos Carajás. *37º Congresso Brasileiro de Geologia*, Boletim de Resumos Expandidos, São Paulo,1 , 547-548.

ARAÚJO, O.J.B. de; MACAMBIRA, E.M.B.; VALE, A.G.; OLIVEIRA, J.R. de; SILVA NETO, C.S.; COSTA, E.J. de S.; SANTOS, A. dos; PENA FILHO, J.I. de C.; NEVES, A.P.; JORGE JOÃO, X. da S. and COSTA, J.B.S., 1994. Primeira integração das investigações geológicas do Programa Grande Carajás na região SSE do Estado do Pará. *IV Simpósio de Geologia da Amazônia*, Boletim de Resumos Expandidos, Belém, 229-301.

ARAÚJO, O.J.B. de, and MAIA, R.G.N., 1991. *Projeto especial mapas de recursos minerais, de solos e de vegetação para a área do Programa Grande Carajás; Subprojeto Recursos Minerais; Folha SB.22-Z-A Serra dos Carajás - Estado do Pará.* DNPM/CPRM, Brasilia, 136pp.

ARAÚJO, O.J.B. de; MAIA, R.G.N.; JORGE JOÃO, X. da S. and COSTA, J.B.S., 1988. A megaestruturação arqueana da Folha Serra dos Carajás. *Anais VII Congresso Latino-Americano de Geologia*, Belém, **1**, 324-338.

ASSAD, R. and BEISIEGEL, V. de R., 1978. Depósito de bauxita na Serra dos Carajás. *Anais XXX Congresso Brasileiro de Geologia,* Recife, **4**, 1385-1391.

AVELAR, V. G.de; LAFON, J.M.; SCHELLER, T.; ARAÚJO, O.J.B. de and MACAMBIRA, E.M.B., 1994. Geocronologia Pb/Pb por evaporação de zircão e Rb/Sr em rocha total do Granito Seringa, Província Mineral de Carajás. *Anais 38º Congresso Brasileiro de Geologia,* Balneário de Camboriú, 387-388.

BAER, G. and BEYTH, M., 1990. A mechanism of dyke segmentation in fractured host rock. In *Mafic Dykes and Emplacement Mechanisms*, (ed. Parker, Rickwood and Tucker), Balkema, Rotterdam, 3-11.

BALLANCE, P.F. and READING, H.G., 1980. Sedimentation in oblique-slip mobile zones: an introduction. In *Sedimentation in oblique-slip mobile zones,* (ed. Ballance, P.F. and Reading, H.G.), 265pp. International Association of Sedimentologist, Special Publication **4**,1-5.

BARBOSA, O.; RAMOS, J.R.de A.; GOMES, F. de A. and HELMBOLD, R., 1966. *Geologia estratigráfica, estrutural e econômica da área do "Projeto Araguaia".* Monografia da DGM, unpublished, Rio de Janeiro, 94pp.

BARD, J.P., 1980. *Microtextures of Igneous and Metamorphic Rocks.* D.Reidel Publishing Company, 264pp.

BARKER, A.J., 1989. *Introduction to Metamorphic Textures and Microstructures.* Blackie Ed., 162pp.

BARROS, C.E. de M., 1991. *Evolução petrológica e estrutural do Gnaisse Estrela, Curionópolis, PA.* Unpublished MSc. dissertation, Universidade Federal do Pará, Curso de Pós-Graduação em Geociências, Belém, 134pp.

BARROS, C.E. de M. and DALL'AGNOL, R., 1993. Deformação de rochas granitóides em regime dúctil: o exemplo do Gnaisse Estrela, região de Carajás. *Revista Brasileira de Geociências*, **23**(2), (in press).

BARROS, C.E. de M.; DALL'AGNOL, R.; BARBEY, P. and BOULLIER, A.M., 1997 - Geochemistry of the Estrela Gneiss, Carajás Region, Brazil: an example of Archaean A-type granitoid. *Journal of South American Earth Sciences* (in press).

BARROS, C.E. de M.; DALL'AGNOL, R.; LAFON, J.M.; TEIXEIRA, N.P.; RIBEIRO, J.W., 1992*a*. Geologia e Geocronologia Rb-Sr do Gnaisse Estrela, Curionópolis, PA. *Boletim do Museu Paraense Emílio Goeldi, Série Ciências da Terra*, **4**(85),85-104.

BARROS, C.E. de M.; DALL'AGNOL, R.; SOARES, A.D.V. and DIAS, G.S., 1994*a*. Metagabros de Águas Claras, Serra dos Carajás: petrologia, geoquímica e transformações metamórficas. *Acta Geológica Leopoldensia*, **40**(XVII), 31-70.

BARROS, C.E. de M.; DALL'AGNOL R.; TEIXEIRA, N.P. and RIBEIRO, J.R., 1992*b*. Evolução estrutural do Gnaisse Estrela, Curionópolis-PA. *37º Congresso Brasileiro de Geologia*, Boletim de Resumos Expandidos, São Paulo, **1** ,333-335.

BARROS, C.E. de M.; DALL'AGNOL; VIEIRA, E.A.P and MAGALHÃES, M.S. de, 1994*b*. Granito Serra dos Carajás: uma discussão sobre o seu potencial metalogenético para estanho com base em estudos na borda oeste do corpo. *IV Simpósio de Geologia da Amazônia*, Boletim de Resumos Expandidos, Belém, 307-309.

BARTLETT, W.L.; FRIENDMAN, M. and LOGAN, J.M., 1981. Experimental folding and faulting of rocks under confining pressure. Part IX. Wrench faults in limestone layers. *Tectonophysics*, **79**, 255-277.

BECKWICTH, R.H., 1941. Trace-slip faults. *American Association of Petroleum Geologist Bulletin*, **25**, 2181-2193.

BEISIEGEL, V. de R., 1982. Distrito ferrífero da Serra dos Carajás. *Anais I Simpósio de Geologia da Amazônia*, anexo, Belém, 21-46.

BEISIEGEL, V. de R.; BERNARDELLI, A.L.; DRUMMOND, N.F.; RUFF, A.W. and TREMAINE, J.W., 1973. Geologia e recursos minerais da Serra dos Carajás. *Revista Brasileira de Geociências*, **3**, 215-242.

BELL, A.M., 1881. Vergence: an evaluation. *Journal of Structural Geology*, **3**(3), 197-202.

BEMERGUY, R. L. and COSTA, J.B.S., 1991. Considerações sobre a evolução do sistema de drenagem da Amazônia e sua relação com o arcabouço tectônico-estrutural. *Boletim do Museu Paraense Emílio Goeldi, Série Ciências da Terra*, **3**, 75-97.

BERNARDELLI, A.L., 1982. Jazida de manganês do Azul. *Anais I Simpósio de Geologia da Amazônia*, anexo, Belém, 47- 59.

BERNARDELLI, A.L. and BEISIEGEL, V.de R., 1978. Geologia econômica da jazida de manganês do Azul. *Anais XXX Congresso Brasileiro de Geologia,* Recife, **4**, 1431-1444.

BERTHÉ, D.CHOUKROUNE, P. and JEGOUZO, P., 1979. Orthogneiss, mylonite and non-coaxial deformation in granites: the example from South Armorican Shear Zone. *Journal of Structural Geology,* **1**, 31-42.

BORRADAILE, G.J., 1978. Transected folds: a study illustrated with examples from Canada and Scotland. *Geological Society of America Bulletin,* **89**, 481-491.

BURCHFIEL, B.C. and STEWARD, J.H., 1966. "Pull-Apart" origin of the Central Segment of Death Valley, California. *Geological Society of America Bulletin,* **77**, 439-442.

BURKE, K. and SENGÖR, A.M.C., 1986. Tectonic scape in the evolution of the continental crust. In *Reflection seismology: the continental crust,* (ed. Barazangi, M. and Brown, L.D.), American Geophysic Union, Geodynamics Series, **14**, 41-53.

BUTLER, C.A., 1995. *Basement fault reactivation: the kinematic evolution of the Outer Hebrides Fault Zone, Scotland.* Unpublished D. Phil. thesis, University of Durham, England, 363pp.

BUTLER, R.W.H., 1989. The influence of pre-existing basin structures on thrust system evolution in the Western Alps. In *Inversion Tectonics* (ed. Cooper M.A. and William G.D.) Geological Society Special Publication, Classics, 1993, 105-122.

CAPUTO, M.V. and LIMA, E.C., 1984. Estratigrafia, idade e correlação do Grupo Serra Grande - Bacia do Parnaíba. *XXXIII Congresso Brasileiro de Geologia,* Anais, Rio de Janeiro, **VIII**, 740-753.

CAPUTO, M.V.; RODRIGUES, R. and VASCONCELOS, D.N.N. de, 1971. Litoestratigrafia da Bacia do Amazonas. PETROBRAS, unpublished report 641-A, Belém.

CHINNERY, M. A., 1966*a*. Secondary faulting. I- Theoretical aspects. *Canadian Journal of Earth Sciences,* **3**, 163-174.

CHINNERY, M. A., 1966*b*. Secondary faulting. II- Geological aspects. *Canadian Journal of Earth Sciences,* **3**, 175-190.

CHRISTIE-BLICK, N. and BIDDLE, K.T., 1985. Deformation and basin formation along strike-slip faults. In *Strike-slip deformation, basin formation and sedimentation,* (ed. Biddle K.T. and Christie-Blick, N.), Society of Economic Paleontology and Mineralogy, Special Publication, **37**, 1-34.

CHOUDHURI, A.; SIAL, A.N. and OLIVEIRA, E.P., 1990. Unmetamorphosed Proterozoic tholeiit dykes from the northern Amazon Craton, Guyana, the evolution of basaltic magmatism. In *Mafic Dykes and Emplacement Mechanisms* (ed. Parker, Rickwood and Tucker), Balkema, Rotterdam, 275-282.

COLLISON, J.D. and THOMPSON, D.B., 1989. *Sedimentary Structures.* Unwin Hyman Ed., 2nd edition, London, 207pp.

CORDANI, U.G., 1980. *Comentários a respeito das datações efetuadas para a região da Serra dos Carajás.* DOCEGEO unpublished report, 3pp.

CORDANI, U.G. and NEVES, B.B. de B., 1982. Geologic evolution of South America during the Archean and Early Proterozoic. *Revista Brasileira de Geociências*, **12**(1-3), 79-88.

CORDANI, U.G.; TASSINARI, C.G. and KAWASHITA, K., 1984. A Serra dos Carajás como região limítrofe entre províncias tectônicas. *Ciências da Terra*, **9**, 6-11.

CORDANI. U.; TASSIANARI, C.G.; TEIXEIRA,W.; BASEI, M.A.S. and KAWASHITA, K., 1979. Evolução tectônica da Amazonia com base em dados geocronológicos. *2º Congresso Geologico Chileno*, Actas, J137-J148.

CORDEIRO, A.C.; ALVES, C.A. and FONSECA, L.R. da, 1982. Geologia da região de Serra dos Gradaús. *Anais I Simpósio de Geologia da Amazônia*, Belém, 50-58.

COSTA, J.B.S.; ARAÚJO, O.J.B. de; JORGE JOÃO, X. da S.; MAIA, R.G.N.N.; MACAMBIRA, E.M.B.; VALE, A.G.; SANTOS, A. dos; PENA FILHO, J.I.de C. and NEVES, A.P., 1994*a*. Panorama tectono-estrutural da região sudeste do Estado do Pará. *IV Simpósio de Geologia da Amazônia*, Boletim de Resumos Expandidos, Belém, 314-317.

COSTA, J.B.S; ARAÚJO, O.J.B. de; SANTOS, A. dos; JORGE JOÃO, X. da S.; MACAMBIRA, M.J.B. and LAFON, J.M., 1995. A Província Mineral de Carajás: aspectos tectono-estruturais, estratigráficos e geocronológicos. *Boletim do Museu Paraense Emílio Goeldi, Série Ciências da Terra*, 7,199-235.

COSTA J.B.S. and HASUI, Y., 1991. O quadro geral da evolução tectônica da Amazônia. *Boletim 3º Simpósio Nacional de Estudos Tectônicos*, Rio Claro, 142-145.

COSTA J.B.S. and HASUI, Y., 1992. Aspectos tectônicos fundamentais do Proterozóico Médio na Amazônia brasileira. *Revista Brasileira de Geociências*, **22**(4), 487-492.

COSTA, J.B.S.; HASUI, Y.; BEMERGUY,R.L.; BORGES, M. da S.; COSTA, A.R.; TRAVASSOS, W.; MIOTO, J.A. and IGREJA, H.L.S. da, 1993*a*. Aspectos fundamentais da neotectônica na Amazônia Brasileira. *I Simpósio Internacional do Quaternário da Amazônia*, Resumos e Contribuições Científicas, Manaus, 103-106.

COSTA, J.B.S.; HASUI, Y.; BORGES, M. da S.; BEMERGUY, R.L.; SAADI, A. and COSTA JÚNIOR, P.S.da C., 1994*b*. Arcabouço tectônico Meso-Cenozóico da região da calha do Rio Amazonas. *IV Simpósio de Geologia da Amazônia*, Resumos Expandidos, Belém, 47-50.

COSTA, J.B.S.; MACAMBIRA, E.M.B.; VALE, A.G.; ARAÚJO, O.J.B. de and PINHEIRO, R.V.L., 1992. Geologia estrutural da Folha São Félix do Xingú (SB.22-Y-B), Serra dos Carajás. *37º Congresso Brasileiro de Geologia*, Boletim de Resumos Expandidos, São Paulo, **1** ,332-333.

COSTA. J.B.S.; MACAMBIRA, E.M.B.; VALE, A.G.; ARAÚJO, O.J.B.;de PINHEIRO, R.V.L. and JOÃO, X.S.J., 1993*b*. Geologia estrutural da folha São Félix do Xingu, Serra dos Carajás. *Revista Brasileira de Geociências*, **23**, 315-332.

COSTA, J.B.S.; PINHEIRO, R.V.L.; JORGE JOÃO, X. da S. and ARAÚJO, O.J.B. de, 1991. Esboço estrutural do Proterozóico Médio da Amazônia Oriental. *Boletim do Museu Paraense Emílio Goeldi, Série Ciências da Terra*, **3**, 9-24.

COSTA, J.B.S. and SIQUEIRA J.B., 1990. Transtração e transpressão ao longo do Lineamento Cinzento (Região de Serra dos Carajás). *Revista Brasileira de Geociências*, **20**, 234-238.

COSTA, J.B.S.; TEIXEIRA, N.P.; PINHEIRO, R.V.L. and BEMERGUY, R.L., 1990. Os sistemas estruturais transcorrentes do Cinturão Itacaiúnas na região de Curionópolis, leste do Estado do Pará. *Anais 36º Congresso Brasileiro de Geologia,* Natal, **5**, 2345-57.

CROWELL, J. C., 1974*a*. Origin of Late Cenozoic basins in South California. In *Tectonics and Sedimentation,* (ed. W. R. Dickinson). Society of Economic Paleontologists and Mineralogists, Special Publication **22**, 190-204.

CROWELL, J. C., 1974*b*. Sedimentation along the San Andreas Fault, California. In *Modern and Ancient Geosynclinal Sedimentation,* (ed. R. H. Dott, and R. H. Shaver). Society of Economic Paleontologists and Mineralogists Special Publication **19**, 292-303.

CROWELL, J.C. 1979. The San Andreas fault system through time*: Geological Society of London Quarterly Journal*, **136**, 293-302.

CROWELL, J.C. and SYLVESTER, A.G., 1979. Introduction to the San Andreas Salton Trough juncture. In *Tectonics of the juncture between the San Andreas fault and the Salton Trough, southeastern California - A guidebook,* (ed. Crowell, J.C. and Sylvester, A.G.) Department of Geological Sciences, University of California, 1-14.

CUNHA, B.C.C. da: POTIGUAR, L.A.T.; IANHEZ, A.C.; BEZERRA, P.E.L.; PITTHAN, J.H.L.; SOUZA Jr., J.J. de: MONTALVÃO, R.M.G. de; SOUSA, A.M.S. de; HILDRED, P.R. and TASSINARI, C.C.G., 1981. *Projeto RADAMBRASIL; Folha SC.22 Tocantins; geologia, geomorfologia, solos e uso potencial da terra,* Levantamento de Recursos Naturais (2), Rio de Janeiro, 196pp.

CUNHA, B.C.C. da; SANTOS, D.B. dos and PRADO, P., 1984. Contribuição ao estudo da estratigrafia da região dos Gradaús com ênfase no Grupo Rio Fresco. *Anais 33º Congresso Brasileiro de Geologia*, Rio de Janeiro, **2**, 873-885.

CVRD-CMM, 1972. Distrito Ferrífero da Serra dos Carajás. *Anais XXVI Congresso Brasileiro de Geologia*, Resumo das Comunicações, Belém, **2**, 78-80.

DAHLSTROM, C.D.A., 1970. Structural geology in the eastern margin of the Canadian Rocky Mountains. *Bulletin of the Canadian Petroleum Geology*, **18**, 332-406.

D'LEMOS, R.S.; BROWN, M.; STRACHAN, R.A., 1992. Granite generation, ascent and emplacement within a transpressional orogen. *Journal of the Geological Society, London*, **149**(4), 487-490.

DALL'AGNOL, R., 1982. Estudo comparativo de alguns maçicos graníticos pós-Transamazônicos da Amazônia Oriental. *Anais XXXII Congresso Brasileiro de Geologia,* Salvador, **2**, 500-513.

DALL'AGNOL, R.; BETTENCOURT, J.S.; JOÃO, X. da S.J.; MEDEIROS, H. de; COSTI, H.T. and MACAMBIRA, M.J.B., 1987. Granitogenesis in northern Brazilian region: a review. *Revista Brasileira de Geologia*, **17**(4), 382-403.

DALL'AGNOL, R.; SAUCK, W.A. and GONÇALEZ, M. das G.B., 1988. Suscetibilidade magnética em granitóides da Amazônia: um estudo preliminar. *Anais XXXV Congresso Brasileiro de Geologia,* Belém, **3**, 1164-1173.

DALL'AGNOL, R.; VIERA, E.A. de P.; SÁ, C.E.S.; MEDEIROS, H. de ; GASTAL, M.do C.P. and TEIXEIRA, N.P., 1986. Estado atual do conhecimento sobre as rochas granitóides da porção sul da Amazônia Oriental. *Revista Brasileira de Geociências*, **16**(1), 11-23.

DALY, M.C.; CHOROWICZ, J. and FAIRHEAD, J.D., 1989. Rift basin evolution in Africa: the influence of reactivated steep basement shear zones. In *Inversion Tectonics* (ed. Cooper, M.A. and Williams, G.D.), Special Publication of the Geological Society of London, **150**, 309-334.

DEEKS, N.R. and THOMAS, S.A., 1995. Basin inversion in a strike-slip regime: the Tonquist Zone, southern Baltic Sea. In *Basin Inversion* (ed. Buchanan, J.G. and Buchanan, P.G.) Geological Society Special Publication, **88**, 319-338.

de SITTER, L.U., 1958. Boudins and parasitic folds in relation to cleavage and folding. *Geol. en Mijnb.* **20**, 277-286.

DIAS, G.S.; MACAMBIRA, M.J.B.; DALL'AGNOL, R.; SOARES, A.D.V. and BARROS, C.E. de, 1996*a*. Datação de zircões de sill de metagabro: comprovação da idade arqueana da Formação Águas Claras, Carajás - Pará. *V Simpósio de Geologia da Amazônia,* SBG-NO, Boletim de Resumos Expadidos, Belém, 376-379.

DIAS, G.S.; SOARES, J.E.B.; DALL'AGNOL, R.; BARROS, C.E.M.; SOARES, A.D.V. and MAGALHÃES, M.S., 1996*b*. Metagabros de Águas Claras: novos dados petrográficos e estudos de susceptibilidade magnética e minerais opacos. *V Simpósio de Geologia da Amazônia,* SBG-NO, Boletim de Resumos Expandidos, Belém, 60-63.

DIBBLE JR, T. W., 1977. Strike-slip tectonics of the San Andreas Fault and its role in Cenozoic Basin evolvement. Late Mesozoic and Cenozoic Sedimentation and Tectonics in California. In *Wrench fault tectonics* (ed. Sylvester, A.G.), 374pp. Americam Association of Petroleum Geologists, 1985, reprinted series, **28**, 26-38.

DOCEGEO, 1986. Lithostratigraphic review of the Carajás District and southern Pará - Brazil. In IGCP Project 204. Final meeting of the working group. Extended Abstract, Carajás, 11-19.

DOCEGEO, 1988. Revisão litoestratigráfica da Província Mineral de Carajás. *Anais XXXV Congresso Brasileiro de Geologia*, anexo, Belém, 10-54.

DOOT, R.H., 1964. Wacke, greywacke and matrix - what approach to inmature sandstone classification. *Journal of Sedimentary Petrology*, **34**, 625-636.

ETHERIDGE, M.A., 1986. On reactivation of extensional fault systems. *Philosophical Transactions of the Royal Society of London,* **A317**, 179-194.

EYAL, Y. and EYAL, M., 1986. The origin of the Bir Zreir rhomb-shaped graben, eastern Sinai. *Tectonics*, **5**(2), 267-277.

FARIAS, N.F.; SANTOS, A.B.S.; BIAGINI, D. de O.; VIEIRA, E.A.P.; MARTINS, L.P.B. and SAUERESSIG, R., 1984. Jazidas de Cu e Zn da área Pojuca, Serra dos Carajás - PA. *Anais 33º Congresso Brasileiro de Geologia,* Rio de Janeiro, **8**, 3658-3668.

FARIAS, N.F. and SAUERESSIG, R., 1982. Jazida de cobre Salobo 3A. *Anais I Simpósio de Geologia da Amazônia,* anexo, Belém, 61-73.

FERREIRA FILHO, C.F.; CORDANI, U.G.; TEIXEIRA, W.; DANNI, J.C.M., 1987. Geochronology of the Bahia Prospect copper deposit - Carajás Province - Brazil. *Final Meeting of the Working Group IUGS-UNESCO,* Extended Abstracts, Carajás, 32-39.

FERREIRA FILHO, C.F. and DANNI, J.C.M., 1985. Petrologia e mineralizações sulfetadas do Prospecto Bahia - Carajás. *Anais II Simpósio de Geologia da Amazônia,* Belém, **3**, 34-47.

FERREIRA JR. C.A.P., 1993. *Relações estruturais entre o Terreno Granito-Greenstone do Sul do Pará e o Cinturão de Cisalhamento Itacaiúnas na região de Xinguara, sudeste do estado do Pará.* Unpublished 'Trabalho de Conclusão de Curso', Universidade Federal do Pará, Departamento de Geologia, Belém, 116pp.

FIGUEIRAS, A.J.M.; MACAMBIRA, J.B. and VILLAS, R.N.N., 1987. Contribuição ao estudo paleoambiental da Formação Rio Fresco na região de Carajás - PA. *Anais Simpósio sobre Sistemas Deposicionais no Pré-Cambriano,* Ouro Preto, 17-30.

FIGUEIRAS, A.J.M. and VILLAS, R.N.N., 1984. Estudo petrológico e sedimentológico da sequência clástica (Pós-Grupo Grão Pará) da Serra dos Carajás, Estado do Pará. *Anais XXX Congresso Brasileiro de Geologia*, Rio de Janeiro, **2**, 832-846.

FLINN, D., 1962. On folding during three-dimensional progressive deformation. *Journal of the Geological Society, London,* **118**, 385-433.

FONSECA, L.R. da; RIGON, J.C. and GONÇALEZ, R., 1984. Descoberta de cobre na Formação Rio Fresco, Igarapé Bahia-Serra dos Carajás, PA. *Actas 2º Simposium Amazônico,* Manaus, 355-357.

FOSSEN, H. and TIKOFF, B., 1993. The deformation matrix for simultaneous simple shearing, pure shearing and volume change, and its application to transpression-transtension tectonics. *Journal of Structural Geology,* **15**(2-5), 413-422.

FREUND, R., 1970. Rotation of strike slip faults in Sistan, Southeast Iran. *Journal of Geology,* **78**, 188-200.

FREUND, R., 1971. The Hope Fault: A strike slip fault in New Zealand. *New Zealand Journal of Geological Survey,* **86**, 49pp.

FREUND, R., 1974. Kinematics of transform and transcurrent faults. *Tectonophysycs,* **21**, 93-134.

GAMOND, J.F., 1987. Bridge structures as sense of displacement criteria in brittle fault zones. *Journal of Structural Geology,* **9**(5/6), 609-620.

GARFUNKEL, Z. and RON, H., 1985. Block rotation and deformation by strike-slip faults 2. The properties of a type of macroscopic discontinuous deformation. *Journal of Geophysical Research,* **90**(B10), 8589-8602.

GATTO, L.C.S., 1991. Região Norte, Relevo. In *Geografia do Brasil, Região Norte*, Vol.3, Ministério da Economia, Fazenda e Planejamento. Fundação Instituto Brasileiro de Geografia e Estatística, IBGE, Diretoria de Geociências, Rio de Janeiro, 47-60.

GAUDETTE, H.E. and OLSZEWSKI JR., W., 1985. Geochronology of the basement rocks, Amazonas Territory, Venezuela, and the tectonic evolution of the western Guyana Shield. *Geol. Mijnb.*, **64**, 131-144.

GAWTHORPE, R.L. and HURST, J.M., 1993. Transfer zones in extensional basins: their structural style and influence on drainage development and stratigraphy. *Journal of the Geological Society, London,* **150**, 1137-1152.

GIBBS, A. D., 1984. Structural evolution of extensional basin margins. *Journal of the Geological Society, London,* **141**, 609-620.

GIBBS, A.K. and BARRON, C.N., 1983. The Guyana Shield reviewed. *Episodes*, **23**,7-14.

GIBBS, A.K. and WIRTH, K.R., 1990. Geologic setting of the Serra dos Carajás iron deposits, Brazil. In *Ancient Banded Iron Formation, Regional Presentations*, (ed. Chauvel, J.J.; Yuqi, C.; El Shazly, E.M.; Gross, G.A.; Laajoki, K.; Markov, M.S.; Rai, K.L.; Stulchikov, V.A. and Augustithis, S.S.).Theophrastus Publication, Greece, 342pp

GIBBS, A.K.; WIRTH, K.R.; HIRATA, W.K. and OLSZEWSKI Jr., W.J., 1986. Age and composition of the Grão Pará Group volcanics, Serra dos Carajás. *Revista Brasileira de Geociências*, **16**(2), 201-211.

GOMES, C.B.; AMARAL, G.; KAWASHITA, K., 1971. Geocronologia da área dos Carajás, PA. *Anais XXV Congresso Brasileiro de Geologia*, Resumo das Comunicações, São Paulo, 162-163.

GOMES, C.B.; CORDANI, U.G. and BASEI, M.A.S., 1975. Radiometric ages from the Serra dos Carajás Area, northern Brazil. *Geological Society of American Bulletin*, **86**, 939-942.

GONÇALEZ, M. das G.B.; DALL'AGNOL, R.; VIEIRA, E.A. de P.; MACAMBIRA,M.J.B. and SENTA, N.D., 1988. Geologia do maçico anorogênico Cigano. Vale do rio Parauapebas-PA. *Anais XXXV Congresso Brasileiro de Geologia*, Belém, **3**, 1132-1146.

GOODWIN, L.B. and WILLIAMS, P.F., 1996. Deformation path partitioning within a transpressive shear zone, Marble Cove, Newfoundland. *Journal of Structural Geology*, **18**(8), 975-990.

GOUVÊA, J.L., 1990. *Técnicas de sensoriamento remoto aplicadas em pesquisas geológicas na Amazônia (Região de Carajás).* Unpublished MSc. dissertation, Universidade Federal do Pará, Curso de Pós-graduação em Geociências, Belém, 93pp.

GROCOTT, J., 1977. The relationship between Precambrian shear belts and modern fault systems. *Journal of the Geological Society, London,* **133**(3), 257-261.

GROSS, G.A., 1983. Tectonic systems and the deposition of iron-formation. *Precambrian Research*, **20**,171-187.

GUINEBERTEAU, B.; BOUCHEZ, JEAN-LUC and VIGNERESSE, JEAN-LOUIS, 1987. The Mortagne granite pluton (France) emplaced by pull-apart along a shear zone: structural and

gravimetric arguments and regional implication. *Geological Society of America Bulletin*, **99**, 763-770.

HARDING, T.P., 1985. Seismic characteristics and identification of negative flower structure, positive flower structure, and positive structural inversion. *The American Association of Petroleum Geologist Bulletin*, **69**(4), 582-600.

HARDING, T.P. and LOWELL, J.D., 1979. Structural style, their plate-tectonic habitats, and hydrocarbon traps in petroleum provinces. *American Association of Petroleum Geologist Bulletin*, **63**, 1016-1058.

HARLAND, W.B., 1971. Tectonic transpression in Caledonian Spitsbergen. *Geological Magazine*, **108**(1), 27.42.

HASUI, Y.; ABREU, F.A.M.; COSTA, J.B.S. and SILVA, J.M.R., 1981. A Faixa de Dobramento Araguaia, estado de conhecimento. *Simpósio de Geologia do Centro-Oeste*, Acta, Goiânia, 177-195.

HASUI, Y. and COSTA, J.B.S., 1990. O Cinturão Araguaia: um novo enfoque estrutural-estratigráfico. *Anais 36º Congresso Brasileiro de Geologia*, Natal, **5**, 2535-2549.

HASUI, Y.; HARALYI, N.L.E. and COSTA, J.B.S., 1992 - Megaestruturação Pré-Cambriana do território brasileiro baseada em dados geofísicos e geológicos. *Revista Brasileira de Geociências*, 07-13.

HASUI, Y.; HARALYI, N.L.E. and SCHOBBENHAUS, C., 1984. Elementos geofísicos e geológicos da região amazônica: subsídios para o modelo geotectônico. *Actas 2º Simposium Amazônico*, Manaus, 129-145.

HAYWARD, A.B. and GRAHAM, R.H., 1989. Some geometrical characteristics of inversion. In *Inversion Tectonics* (ed. Cooper M.A. and William G.D.), Geological Society Special Publication, Classics, (2nd. edition), 17-39.

HERZ, N.; HASUI, Y.; COSTA, J.B.S.and MATTA, M.A.da S., 1989. The Araguaia Fold Belt, Brazil: a reactivated Brasiliano-Pan-African cycle (550 Ma) geosuture. *Precambrian Research*, **42**, 371-386.

HILLS, E.S., 1946. Some aspects of the tectonics of Australia. *Proceedings of the Royal Society of New South Wales*, **79**, 67-91.

HIRATA, W.K.; RIGON, J.C.; CORDEIRO, A.A.C. and MEIRELES, E. de M., 1982. Geologia regional da Província Mineral de Carajás. *Anais I Simpósio de Geologia da Amazônia*, Belém, 100-108.

HOLDSWORTH, R.E., 1988. The stereographic analysis of facing. *Journal of Structural Geology*, **10**(2), 219-223.

HOLDSWORTH, R.E., 1994. Structural evolution of the Gander-Avalon terrane boundary: a reactivated transpression zone in the NE Newfoundland Appalachians. *Journal of the Geological Society, London*, **151**, 629-646.

HOLDSWORTH, R.E.; BUTLER, C.A. and ROBERTS, A.M., 1997. The recognition of reactivation during continental deformation. *Journal of the Geological Society, London* (in press).

HOLDSWORTH, R.E. and STRACHAN, R.A., 1991. Interlinked system of ductile strike slip and thrusting formed by Caledonian sinistral transpression in northeastern Greenland. *Geology*, **19**, 510-513.

HOPPE, A.; SCHOBBENHAUS, C. and WALDE, D.H.G., 1987. Precambrian Iron Formation in Brazil. In *Precambrian Iron-Formation*, (ed. Appel, P.W.W. and LaBerge, G.), Theophrastus Publication, Greece, 347-390

HUHN, S.R.B.; SANTOS, A.B.S.; AMARAL, A.F. do; LEDSHAM, E.J.; GOUVEA, J.L.; MARTINS, L.P.B.; MONTALVÃO, R.G.M. de and COSTA, V.G., 1988. O Terreno "Granito Greenstone" da região de Rio Maria - sul do Pará. *Anais XXXV Congresso Brasileiro de Geologia*, Belém, **3**, 1438-1452.

HUTCHINSON, R.W., 1979. *MM1-Salobo e suas relações geológicas regionais. Relatório sobre o Projeto Cobre-DOCEGEO.* DOCEGEO, Distrito Amazônia, unpublished report (translated by Santos, B., 1982), Belém, 21pp.

HUTTON, D.H.W., 1988*a*. Igneous emplacement in a shear-zone termination: the biotite granite at Strontian, Scotland. *Geological Society of America Bulletin,* **100**, 1392-1399.

HUTTON, D.H.W., 1988*b*. Granite emplacement mechanisms and tectonic controls: inferences from deformation studies. *Transaction of the Royal Society of Edinburgh, Earth Sciences,* **79**, 245-255.

HUTTON, D.H.W., 1992. - Granite sheeted complex: evidence for the dyking ascent mechanism. *Transaction of the Royal Society of Edinburgh, Earth Sciences*, **83**, 377-382.

HUTTON, D.H.W. and REAVY, R.J., 1992. Strike-slip tectonics and granite petrogeneses. *Tectonics*, **11**(5), 960-967.

IDESP, 1971. *Programa de pesquisa de carvão mineral na bacia do rio Fresco, afluente do rio Xingu, Estado do Pará.* Instituto de Desenvolvimento Econônico e Social da Pará. Unpublished report **2**, 19pp.

ISSLER, R.S.; FREIRE, F. de A. and SANTOS, R.O.B. dos, 1985. O plutonismo intra-placa do Cráton Amazônico no intervalo de tempo de 1800 a 900 M.A. *Anais II Simpósio de Geologia da Amazônia,* Belém, **2**, 53-72.

JACQUES, J.M. and REAVY, R.J., 1994. Caledonian plutonism and major lineaments in the SW Scottish Highlands. *Journal of the Geological Society, London.* **151**(6), 955-970.

JOHNSON, T.E., 1991. Nomenclature and geometric classification of cleavage-transected folds. *Journal of Structural Geology,* **12**, 261-274.

JONES, R.R. and TANNER, P.W.G., 1995. Strain partitioning in transpression zones. *Journal of Structural Geology,* **17**(6), 793-802.

JORGE JOÃO, X. da S. and ARAÚJO, O.J.B. de, 1992. Magmatismo granítico sin-cisalhamento Itacaiúnas no sudoeste do Estado do Pará. *37° Congresso Brasileiro de Geologia*, Boletim de Resumos Expandidos, São Paulo, **1**, 36-38.

JORGE JOÃO, X. da S.; NEVES, A.P. and LEAL, J.W.L., 1982. Ouro de Serra Pelada - Aspectos da Geologia e Garimpagem. *Anais I Simpósio de Geologia da Amazônia*, Belém, **2**, 52-61.

KELLER, E.A.; BONKOWSKI, M.S.; KORSCH, R.J. and SHLEMON, R.J., 1982. Tectonic geomorphology of the San Andreas Fault zone in the southern Indio Hills, Conchella Valley, California. *Geological Society of America Bulletin*, **93**, 46-56.

KINGMA, J.T., 1958. Possible origin of piercement structures, local unconformities, and secondary basins in the Eastern Geosyncline, New Zealand. *New Zealand Journal of Geology and Geophysics*, **1**, 269-274.

KNUP, P.E., 1971. Reconhecimento geológico na região dos rios Itacaiúnas e Tocantins, Estado do Pará. *Anais XXV Congresso Brasileiro de Geologia*, Resumo das Comunicações, São Paulo, 61-62.

KODAMA, K.; TAKEUCHI, T. and OZAWA, T., 1993. Clockwise tectonic rotation of Tertiary sedimentary basins in central Hokkaido, northern Japan. *Geology*, **21**, 431-434.

LAB, K. L., 1992. *Considerações lito-estruturais sobre o Duplex Transpressivo Serra Pelada.* Unpublished MSc. dissertation, Universidade Federal do Pará, Curso de Pós-graduação em Geociências, Belém, 109pp.

LAB, K.L. and COSTA, J.B.S., 1992. Evolução lito-estrutural do Duplex Serra Pelada. *37º Congresso de Geologia,* Boletim de Resumos Expandidos, São Paulo,**1**, 350-351.

LADEIRA, E.A. and CORDEIRO, J.R.C.A., 1988. Jazida N4E: reavaliação dos corpos de hematita dura e jaspelitos. *35º Congresso Brasileiro de Geologia,* Anexo Anais, Belém, 55-69.

LAFON, J.M. and MACAMBIRA, M.J.B., 1992. Evolução da Província Mineral de Carajás com base em novos dados geocronológicos. *37° Congresso Brasileiro de Geologia,* Boletim de Resumos Expandidos, São Paulo, **2**, 174-175.

LEITE, A. da S. and DALL'AGNOL, R., 1994. Estratigrafia e aspectos geológicos da região de ocorrência do Granito Xinguara (SE do Pará). *IV Simpósio de Geologia da Amazônia*, Boletim de Resumos Expandidos, Belém, 325-327.

LE MAITRE, R.W.; BATEMAN, P.; DUDEK, A.; KELLER, J.; LAMEYRE,J.; LA BAS, M.J.; SABINE, P.A.; SCHMID, R.; SØRENSEN, STRECKEISEN, A.; WOOLLEY, A.R. and ZANETTIN, B., 1989. *A classification of the International Union of Geological Sciences subcommision on the Systematics of igneous rocks.* Blackwell, Oxford, 193pp.

LIANDRAT, E., 1972. Reconhecimento ao longo dos rios Itacaiúnas e Parauapebas, município de Marabá, estado do Pará. *Revista Brasileira de Geografia*, **34**(1), 165-184.

LIMA, M.I.C. de, 1994. Província Estrutural Amazônia. *Anais* 38º *Congresso Brasileiro de Geologia* , Balneário de Camboriú, 410-411.

LINDENMAYER, Z.G., 1990. *Salobo Sequence, Carajás, Brazil: geology, geochemistry and metamorphism.* Unpublished D. Phil. thesis, University of Western Ontario, Canada, 407pp.

LINDENMAYER, Z.G., 1993. Descoberto fóssil com 2.7 bilhões de anos. *Jornal do Brasil*, Rio de Janeiro, 21, março, 93, p.28.

LINDENMAYER, Z.G. and FYFE, W.S., 1992. Comparação preliminar entre os metabasaltos dos grupos Parauapebas e Salobo da Bacia de Carajás, Estado do Pará. *37° Congresso Brasileiro de Geologia*, Boletim de Resumos Expandidos, São Paulo, **2**, 33-34.

LINDENMAYER, Z.G.; FYFE, W.S. and BOCALON, V.L.S., 1994*a*. Nota preliminar sobre as intrusões granitóides do depósito de cobre do Salobo, Carajás. *Acta Geológica Leopoldensia*, **40**(XVIII)84.

LINDENMAYER, Z.G.; FYFE, W.S. and LAUX, J.H., 1994*b*. Contribuição à petrologia dos metabasaltos do Grupo Salobo, Carajás, Pará. *Acta Geológica Leopoldensia*, **40**(XVII),115-152.

LINDENMAYER, Z.G. and LAUX, J.H., 1994. O papel da alteração hidrotermal nas rochas da Bacia de Carajás. *IV Simpósio de Geologia da Amazônia*, Boletim de Resumos Expandidos, Belém, 328-330.

LISLE, R.J., 1993. Strike-slip motion in the Minches, NW Scotland, deduced from the trends of the Scourie Dyke swarm. *Journal of the Geological Society, London,* **150**, 653-656.

MABESOONE, J.M., 1977. Paleozoic-Mesozoic deposits of the Piauí-Maranhão syneclise (Brazil): geological history of a sedimentary basin. *Sedimentary Geology,* **19**, 7-38.

MABESOONE, J.M., 1978. Origem dos conglomerados da Formação Serra Grande e unidades equivalentes (Siluriano Superior Devoniano Inferior, Nordeste do Brasil). *XXX Congresso Brasileiro de Geologia,* Anais, Recife, **2**, 799-808.

MACAMBIRA, E.M.B.; JORGE JOÃO, X. da S.; LAFON, J.M. and PEREIRA, E.D., 1992. Aspectos geológicos e geomorfológicos do Granito Parauari no domínio da Folha São Félix do Xingú (SB.22-Y-B) - Sul do Pará. *37° Congresso Brasileiro de Geologia,* Boletim de Resumos Expandidos, São Paulo, **1**, 171-173.

MACAMBIRA, E.M.B.; VALE, A.G.; JORGE JOÃO, X. da S. and COSTA, J.B.S., 1994. O quadro geológico da Folha São Félix do Xingu (SB.22-Y-B), SE do estado do Pará. *Anais 38º Congresso Brasileiro de Geologia,* Balneário de Camboriú, 111-112.

MACAMBIRA, J.B.; RAMOS, J.F. da F.; ASSIS, J.F.P. and FIGUEIRAS, A.J.M., 1990. *Mapeamento geológico. Projeto Serra Norte/Projeto Pojuca.* SEPLAN/DOCEGEO/UFPa e DNPM/DOCEGEO/UFPa, unpublished report, Belém, 150pp.

MACAMBIRA, J.B. and SILVA, V.F., 1994. Estruturas primárias e diagenéticas preservadas na Formação Carajás - Pará. *IV Simpósio de Geologia da Amazônia,* Resumos Expandidos, Belém, 335-338.

MACAMBIRA, M.J.B. and LAFON, J.M., 1994. Geocronologia da Província Mineral de Carajás; síntese dos dados e novos desafios. *IV Simpósio de Geologia da Amazônia,* Boletim de Resumos Expandidos, Belém, 339-342.

MACAMBIRA, M.J.B. and LANCELOT, J., 1992. Idade U-Pb em zircões de metavulcânica do Greenstone do Supergrupo Andorinhas; Delimitante da estratigrafia arqueana de Carajás, Estado do Pará. *37° Congresso Brasileiro de Geologia,* Boletim de Resumos Expandidos, São Paulo, **2**, p.188.

MACHADO, W.; LINDENMAYER, Z.; KROGH, T.E. and LINDENMAYER, D., 1991. U-Pb geochronology of Archean magmatism and basement reactivation in the Carajás area, Amazon shield, Brazil. *Precambrian Research*, **49**, 329-354.

MACHADO, N.; LINDENMAYER, D. and LINDENMAYER, Z., 1988, Geocronologia U-Pb da Província Metalogenética de Carajás, Pará: resultados preliminares. *Anais VII Congresso Latino Americano de Geologia*, Belém, **1**, 339-347.

MacKENZIE, W.S.; DONALDSON, C.H. and GUILFORD C., 1995. *Atlas of igneous rocks and their textures*. Longman Scientific & Technical, England, sixth edition, 148pp.

MacKENZIE, W.S. and GUILFORD, C., 1988. *Atlas of rock-forming minerals in thin section*. Longman Scientific & Technical, England, sixth edition, 98pp.

MANN, P.; HEMPTON, M.; BRADLEY, D. C. and BURKE, K., 1983. Development of pull-apart basins. *Journal of Geology*, **91**, 529-554.

MARÇAL, M. dos S., 1991. *Aspectos lito-estruturais das minas de Ferro N4E e Manganês do Azul, Serra dos Carajás (PA)*. Unpublished MSc. dissertation. Universidade Federal do Pará, Curso de Pós-Graduação em Geociências, Belém, 135pp.

MARÇAL, M. dos S. ; COSTA, J.B.S.; HASUI, Y. and EBERT H.D., 1992. A estruturação da Serra Norte, com ênfase na área da Mina N4E, Serra dos Carajás. *37° Congresso Brasileiro de Geologia*, Boletim de Resumos Expandidos, São Paulo, **2**, 330-331.

MARINHO, P.A. da C., 1973. *Projeto Xingu-Araguaia: relatório preliminar*. CPRM- Agência/BE, unpublished report, Belém, 34pp.

MARTINS, R.C. and ARAÚJO, O.J.B. de, 1979. *Projeto integração geológico geofísica Sul do Pará*. DNPM/CPRM, unpublished report, Belém, **1**, 322pp.

MATTA, M.A. da S.; TEIXEIRA, N.P., 1990. Mapeamento e análise estrutural das unidades lito-estruturais aflorantes na região do platô N-5, Serra Norte-Carajás, Estado do Pará. *Anais* 36º *Congresso Brasileiro de Geologia*, Natal, **5**, 2309-2320.

McCAFFREY, K.J.W., 1992. Igneous emplacement in the transpressive shear zone: Ox Mountains igneous complex. *Journal of the Geological Society, London*, **149**(2), 221-235.

McCLAY, K., 1987. *The Mapping of Geological Structures*. Geological Society of London Handbook, Handbook Series (ed. Cox, K.), John Wiley & Sons, Chichester,161pp.

McERLEAN. M, 1993. *Granitoid emplacement and deformation: a case study of the Thorr Pluton, Ireland, with contrasting examples from Scotland*. Unpublished Ph.D. dissertation, University of Durham, England, 344pp.

MEDEIROS NETO, F.A. de, 1985. *Estudos geológicos, geoquímicos e microtermométricos da Jazida de Sulfeto de Cu-Zn do Corpo 4-E/Pojuca, Serra dos Carajás*. Unpublished MsC. dissertation, Universidade Federal do Pará, Curso de Pós-Graduação em Geociências, Belém, p.168.

MEDEIROS NETO, F.A. de and VILLAS, R.N., 1984. Caracterização lito-estrutural da sequência Salobo-Pojuca e sua correlação com o Grupo Grão Pará, Serra dos Carajás. *Resumos da 36ª Reunião Anual da SBPC*, São Paulo, 676pp.

MEIRELES, E. de M.; HIRATA, W.K.; AMARAL, A.F. do; MEDEIROS FILHO, C.A. and GATO, W. da C., 1984. Geologia das Folhas Carajás e Rio Verde, Província Mineral dos Carajás, Estado do Pará. *Anais XXXI Congresso Brasileiro de Geologia*, Rio de Janeiro, **5**, 2164-2174.

MEIRELES, E. de M. and TEIXEIRA, J.T., 1982. Geologia do depósito de ouro de Serra Pelada. *I Simpósio de Geologia da Amazônia*, anexo, Belém, 75-85.

MEIRELES, E. de M. TEIXEIRA, J.T. and MEDEIROS FILHO, C.A., 1982. Geologia preliminar do depósito de ouro de Serra Pelada. *Anais I Simpósio de Geologia da Amazônia*, Belém, **2**, 74-83.

MENEZES, N. R., 1970. *Projeto Cobre-Pará, relatório final.* DNPM, 5º Distrito. Unpublished report, Belém.

MEYER, D.J.K., 1980. *Exploração geológica-geoquímica-geofísica da área Xingu-Araguaia, Projeto Aquiri - AOC-9.* Unpublished DOCEGEO report, Belém, Pará, 2 vols.

MEYER, D.J.K. and FARIAS. N.F., 1980. O depósito de cobre Salobo 3-Alfa, Serra dos Carajás. *31º Congresso Brasileiro de Geologia*, Resumo das Comunicações, Camboriú, **2**, p.382.

MIALL, A.D., 1984. *Principles of Sedimentary Basin Analysis.* Spring-Verlag, New York, 490pp.

MOLNAR, P., 1992. Brace-Goetze strength-profiles, the partitioning of strike-slip and thrust faults at zones of oblique convergences and the stress-heat flow paradox of the San Andreas Fault. In: *Fault Mechanism and Transport Propriety of Rocks* (ed. by Evans, B. & Wong, T.F.). Academic Press. New York. 435-459.

MORRIS, G.A. and HUTTON, D.H.W., 1993. Evidence for sinistral shear associated with the emplacement of the early Devonian Etive dyke swarm. *Scottish Journal of Geology*, **29**(1), 69-72.

NAYLOR, M.A.; MANDL, G. and SIJPESTEIJN, C.H.K., 1986. Fault geometries in basement-induced wrench faulting under different initial stress state. *Journal of Structural Geology*, **8**(7), 737-752.

NEUGEBAUER, J., 1994. Closing-up structures, alternatives to pull-apart basins; the effect of bends in the North Anatolian Fault, Turkey. *Terra Nova*, **6**, 359-365.

NEVES, B.B.de B., 1986. Tectonic regimes in the Proterozoic of Brazil. *Actas XII Simpósio de Geologia do Nordeste*, João Pessoa, 235-251.

NEVES, B.B. de B., 1992. O Proterozóico Médio no Brasil: Ensaio do conhecimento e seus problemas. *Revista Brasileira de Geociências*, **22**(4), 449-461.

NIMER, E., 1991. Região Norte, Clima. In *Geografia do Brasil, Região Norte*, Vol.3, Ministério da Economia, Fazenda e Planejamento. Fundação Instituto Brasileiro de Geografia e Estatística, IBGE, Diretoria de Geociências, Rio de Janeiro, 61-71.

NOGUEIRA, A.C.R., 1995. *Análise faciológica e aspectos estruturais da Formação Águas Claras, Região Central da Serra dos Carajás - Pará.* Unpublished MSc. dissertation, Universidade Federal do Pará, Curso de Pós-Graduação em Geociências, Belém, 167pp.

NOGUEIRA, A.C.R. and TRUCKENBRODT, W., 1994. Evidências de maré e tempestades na Formação Águas Claras, Pré-Cambriano, Serra dos Carajás. *Acta Geológica Leopoldensia*, **40**(XVII), 7-30.

NOGUEIRA, A.C.R.; TRUCKENBRODT, W.; COSTA, J.B.S. and PINHEIRO, R.V.L., 1994. Análise faciológica e estrutural da Formação Águas Claras, Pré-Cambriano da Serra dos Carajás. *IV Simpósio de Geologia da Amazônia*, Boletim de Resumos Expandidos, Belém, 363-364.

NOGUEIRA, A.C.R.; TRUCKENBRODT, W. and PINHEIRO, R.V.L., 1995. Formação Águas Claras, Pré-Cambriano da Serra dos Carajás. Redescrição e redefinição. *Boletim do Museu Paraense Emílio Goeldi, Série Ciências da Terra*, **7**, 177-197.

NOGUEIRA, A.C.R.; TRUCKENBRODT; W.; PINHEIRO, R.V.L. and COSTA, J.B.S., 1992. Estudo Faciológico e Tectônico de sedimentos Pré-Cambrianos na região do Igarapé Águas Claras, Serra dos Carajás-PA. *37° Congresso Brasileiro de Geologia*, Boletim de Resumos Expandidos, São Paulo, **2**, 443-444.

NUR, A., 1978. Nonuniform friction as a physical basis for earthquake mechanics. *Pure Applied Geophysics*, **116**, 964-991.

NUR, A; RON, H. and SCOTTI, O., 1989. Kinematics and mechanism of tectonic block rotations. In: *Slow Deformation and Transmission of Stress in the Earth* (Ed. Cohen and Vanícek), IUGG, **4**, Geophysical Monograph **49**, 31-46.

ODONNE, F. and VIALON, P., 1983. Analogue model of folds above a wrench fault. *Tectonophysycs*, **99**, 31-46.

OLIVEIRA, E.P. and TARNEY, J., 1990. Geochemistry of the Mesozoic Amapa and Jari Dyke Swarms, northern Brazil: Plume-related magmatism during the opening of the central Atlantic. In *Mafic Dykes and Emplacement Mechanisms*, (ed. Parker, Rickwood and Tucker), Balkema, Rotterdam, 173-183

OLIVEIRA, G.P. de, 1991. *Aspectos lito-estruturais de um pequeno segmento da extremidade leste da estrutura em flor positiva da Serra dos Carajás.* Unpublished Trabalho de Conclusão de Curso, Universidade Federal do Pará, Departamento de Geologia, Belém, 77pp.

OLIVEIRA, G.P. de and COSTA, J.B.S., 1992. Aspectos estruturais de um pequeno segmento da extremidade leste da estrutura em flor positiva da Serra dos Carajás. *37° Congresso Brasileiro de Geologia*, Boletim de Resumos Expandidos, São Paulo, **2** , 347-348.

OLIVER, D.,1987. The development of structural patterns above reactivated basement faults. Unpublished D. Phil. Thesis, University of London, England, 291pp.

OLSZEWSKI, W.Jr.; WIRTH, K.R.; GIBBS, A.K. and GAUDETTE, H.E., 1989. The age, origin, and tectonic of the Grão Pará Group and associated rocks, Serra dos Carajás, Brazil: Archean continental volcanism and rifting. *Precambrian Research*, **42**, 229-254.

PASSCHIER, C.W.; MYERS, J.S. and KRÖNER, A., 1990. *Field Geology of High-Grade Gneiss Terrains.* Springer-Verlag Berlin Heidelberg, 188pp.

PEACOCK, D.C.P. and SANDERSON, D.J., 1995. Pull-aparts, shear fractures and pressure solution. *Tectonophysycs*, **241**, 1-13.

PETRI, S. and FÚLFARO, V.J., 1983. *Geologia do Brasil, Fanerozoico.* Editora da Universidade de São Paulo, São Paulo, 631pp.

PETTIJOHN, F.J.; POTTER, P.E. and SIEVER,R., 1972. *Sand and sandstones.* New York; Springer-Verlag, 632pp.

PIMENTEL, M.M. and MACHADO, N., 1994. Geocronologia U-Pb dos terrenos Granito-Greenstone de Rio Maria, Pará. *Anais* 38º *Congresso Brasileiro de Geologia,* Balneário de Camboriú, 390-391.

PINHEIRO, M.M. and JORGE JOÃO, X. da S., 1970. *Relatório da 2ª etapa do Projeto Cobre-Pará.* DNPM/ 5º Distrito, ATDGM nº 312, unpublished report, 19pp.

PINHEIRO; R.V.L.; NOGUEIRA, A.C.R. and COSTA, J.B.S., 1991. Superposição de transpressão na Serra dos Carajás - PA. *Boletim 3° Simpósio Nacional de Estudos Tectônicos*, Rio Claro, 44-46.

PINHEIRO, R.V.L. and HOLDSWORTH, R.E., 1995. Significado tectônico da clivagem transversa (transecting cleavage) em dobras na Mina de Serra Pelada, Pará. *Boletim do Museu Paraense Emílio Goeldi, Série Ciências da Terra*, **7**, 259-278.

PINHEIRO, R.V.L. and HOLDSWORTH, R.E., 1997*a*. Reactivation of Archaean strike-slip fault systems, Amazon region, Brazil. *Journal of the Geological Society, London* (in press).

PINHEIRO, R.V.L. and HOLDSWORTH, R.E., 1997*b*. The structure of the Carajás N-4 ironstone deposit and associated rocks: relationship to Archaean strike-slip tectonics and basement reactivation in the Amazon region, Brazil. *Journal of South American Earth Sciences* (in press).

PLAT, J.P., 1984. Secondary cleavages in ductile shear zones. *Journal of Structural Geology,* **6**, 439-442.

PLUMB, K.A., 1991. New Precambrian Time Scale. *Episodes*, **14**(2), 139-140.

PONCE DE LEON, M.I. and CHOUKROUNE, P., 1980. Shear zones in the Iberian Arc. *Journal of Structural Geology,* **2**,63-68.

POWELL, C. McA., 1974. Timing of slaty cleavage during folding of Precambrian rocks, Northwest Tasmania. *Geological Society of America Bulletin*, **85**, 1043-1060.

PRICE, N.J. AND COSGROVE, J.W., 1994. *Analysis of Geological Structures.* Cambridge University Press, Cambridge, 502.

PRIOR, D.J.; KNIPE, R.J.; BATES, M.P.; GRANT, N.T.; LAW, R.D.; LLOYD, G.E.; WELBON, A.; AGAR, S.M.; BRODIE, K.H.; MADDOCK, R.H.; RUTTER, E.H.; WHITE, S.H.; BELL, T.H.; FERGUSON, C.C. and WHEELER, J., 1987. Orientation of specimens: essential data for all fields of geology. *Geology*, **15**,824.

PRUCHA, J.J., 1992. Zone of weakness concept: a review and evaluation. In *Basement Tectonics 8: Characterization and comparison of ancient and Mesozoic continental margins. Proceedings of the Eighth International Conference on Basement Tectonics held in Buttle, Montana, USA, August 1988,* (ed. Bartholomew, M.J.; Hyndman, D.W. and Mason,R.), Kluwer Academic Publishers, Netherlands, 83-92.

PUTY, C.O.F.; MARTINS, R.C.; MONTALVÃO, R.M.G.; JORGE JOÃO, X.S.; CARREIRA.J.M.; SILVA, G.H.; NEVES, A.P. GILFFONI, L.E.; LOURENÇO, R.S. and FRIZZO, S.J., 1972. *Projeto Marabá.* DNPM/CPRM, unpublished report, Belém, **1**, 124pp.

RAMOS, J.F. da F.; MELO, C.F.; SERIQUE, J.S.B.; PEREIRA, J.L. and RODRIGUES, M.D.R., 1983. *Mapeamento geológico - Projeto Parauapebas*, Convênio SUDAM-UFPa-FADESP, unpublished report, Belém, 66pp.

RAMOS, J.F. da F.; MOURA, C.A.V.; MELO, C.F.de; PEREIRA, J.L.; SERIQUE, J.S.C.; and RODRIGUES, R.M., 1984. Uma discussão sobre sequências sedimentares tidas como Formação Rio Fresco, Sudeste do Pará. *Anais 33º Congresso Brasileiro de Geologia*, Rio de Janeiro, **2**, 862-872.

RAMSAY, J.G., 1963. Structural investigations in the Barberton Mountains Land, Eastern Transvaal. *Transactions Geological Society of South Africa*, **66**, 353-401.

RAMSAY, J.G., 1967. *Folding and fracturing of rocks.* McGraw-Hill, New York, 568pp.

RAMSAY, J.G. and HUBER, M.I., 1987. *The techniques of Modern Structural Geology, Vol.2: Folds and Fractures.* Academic Press, London, New York, 700pp.

READING, H.G., 1980. Characteristics and recognition of strike-slip fault systems. In *Sedimentation in oblique-slip mobile zones,* (ed. Ballance,P.F. and Reading,H.G.). International Association of Sedimentologist, Special publication, **4**, 7-26.

RÊGO, L.F. de M., 1933. Notas geográficas e geológicas sobre o Rio Tocantins. *Boletim do Museu Emilio Goeldi da Historia Natural e Etnografia*, Belém, **9**, 272-288.

REID, H.F.; DAVIS, W.M.; LAWSON, A.C. and RANSOME, F.L., 1913. Report of the Committee on the nomenclature of faults. Geological Society of America Bulletin, **24**, 163-186.

RICKWOOD, P. C., 1990. The anatomy of a dyke and the determination of propagation and magma flow directions. In *Mafic Dykes and Emplacement Mechanisms*, (ed. Parker, Rickwood and Tucker), . Balkema, Rotterdam, 81-100

RIOS, F.J., 1991. *O Granito Central da Serra dos Carajás: fácies petrográficas e alteração hidrotermal do setor norte.* Unpublished MSc. dissertation, Universidade Federal do Pará, Curso de Pós-Graduação em Geociências, Belém, 152pp.

RIVALENTE, G.; GIRARDI, V.A.V.; MAZZUCHELLI, C.T.;CORREIA,M.; MOLESINI, M. and FINNATI, M.C., 1992. Mafic magmatism in the Carajás region: a petrological reconnaissance. *Anais 37º Congresso Brasileiro de Geologia*, São Paulo,**1**, 481-487.

RIVERAU, J.C., 1972. Notas de aula do curso de fotointerpretação. *Anais Semana de Estudos da Sociedade de Intercâmbio Cultural e Estudos Geológicos*, **11**, Ouro Preto,1-30.

ROBERTS, J.L. and SANDERSON, D.J., 1971. The intrusive form of some basalt dykes showing flow lineation. *Geological Magazine*, 108 (**6**), 489-499.

ROBIN, P.Y.F. and CRUDEN, A.R., 1994. Strain and vorticity patterns in ideally ductile transpression zones. *Journal of Structural Geology*, **16**(4), 447-466.

RODRIGUES, E.S.; LAFON, J.M. SCHELLER, T., 1992. Geocronologia Pb-Pb da Província Mineral de Carajás: primeiros resultados. *37º Congresso Brasileiro de Geologia*, Boletim de Resumos Expandidos, São Paulo, **2**, 183-184.

RON, H., FREUND, R., GARFUNKEL, Z. and NUR, A., 1984. Block rotation by strike-slip faulting: structural and paleomagnetic evidence. *Journal of Geophysical Research*, **89**, 6256-6270.

ROYDEN, L. H., 1985. The Vienna Basin: a thin-skinned pull-apart basin. In *Strike Slip Deformation, Basin Formation and Sedimentation* (ed. Biddle, K.T. and Christie-Blick, N.). The Society of Economic Paleontologist and Mineralogist, Especial Publication **37**, 319-338.

SACHS, L.L.B.; BATISTA, J.J.; CHOUDHURI, A. and MORAIS, S.M.M., 1992. Dados preliminares sobre o magmatismo básico do Igarapé Bahia - Carajás, Pará - Brasil. *37° Congresso Brasileiro de Geologia*, Boletim de Resumos Expandidos, São Paulo, **2**, 79-80.

SANDERSON, D.J. and MARCHINI, W.R.D., 1984. Transpression. *Journal of Structural Geology*, **6**(5), 444-458.

SANDERSON, D.J.; ANDREWS, J.R.; PHILLIPS, W.E.A. and HUTTON, D.H.W., 1980. Deformation studies in the Irish Caledonides. *Journal of Structural Geology*, **137**, 289-302.

SANTOS, A. dos, 1986. *As águas da região.* In: *Carajás, desafio político, ecologia e desenvolvimento*, (ed. Almeida Jr., J.M.G. de), 633pp. CNPq-Editora Brasiliense, São Paulo, 156-183.

SCHOBBENHAUS, C.; CAMPOS, D.A.; DERZE, G.R. and ASMUS, H.E., 1984. *Geologia do Brasil.* DNPM, Brasilia, 501pp.

SEGALL, P. and POLLARD, D. D., 1980. Mechanics of discontinuous faults. *Journal of Geophysical Research*, **85**(B8), 4337-4370.

SEGALL, P. and POLLARD, D. D., 1983. Nucleation and growth of strike slip faults in granite. *Journal of Geophysical Research*, **88**(B1), 555-568.

SERIQUE, J.S.C.B. and RAMOS, J.F. da F., 1984. Aspectos petrográficos dos sedimentos pré-cambrianos da Serra do Paredão. *Anais 33º Congresso Brasileiro de Geologia*, Rio de Janeiro, **2**, 886-893.

SHACKLETON. R.M., 1957. Downward-facing structures of the Highland Border. *Quaternary Journal of the Geological Society of London*, **113**, 361-392.

SIAL, A.N.; OLIVEIRA, E.P. CHOUDHURI, A., 1987. Mafic Dyke Swarms of Brazil. *Geological Association of Canada*, Special Paper **34**, 467-481.

SIBSON, R.H., 1977. Fault rocks of the Moine Thrust Zone. Texture and microstructures. *Journal of the Geological Society, London*, **133**, 191-213.

SIBSON, R.H., 1987. Earthquake rupturing as a hydrothermal agent. *Geology*, **13**, 701-704.

SIBSON, R.H., 1992. Earthquake faulting, inducing fluid flow, and fault-hosted gold-quartz mineralization. In *Basement Tectonics 8, Characterization and Comparation of Ancient and Mesozoic Continental Margins. Proceedings of the Eighth International Conference on Basement Tectonics, Montana, USA, August 1988.* (ed. Bartholomew; M.J. Hyndman, D.W.; Mogk, D.W. and Mason, R.), Kluwer Academic Publisher, 603-614.

SIBSON, R.H., 1994. Crustal stress, faulting and fluid flow. In *Geofluids: origin, migration and evolution of fluids in sedimentary basins*, (Ed. Parnell, J.), Geological Society Special Publication, **78**, 69-84.

SIBSON, R.H., 1996. Structural permeability of fluid-driven fault-fracture meshes. *Journal of Structural Geology*, **18**(8), 1031-1042.

SILVA, A.R.B. da, 1984. *Geologia, mineralização e produção aurífera de Serra Pelada*. MME-DNPM-5º Distrito, unpublished report, Belém, 24pp.

SILVA, C.M.G. da, 1996. *O Prospecto Águas Claras, Serra dos Carajás (PA): Alteração hidrotermal e mineralização de sulfeto associada*. Unpublished MSc. dissertation, Curso de Pós-Graduação em Geociências, Belém, 130pp.

SILVA, G.G.; LIMA, M.J.C.; ANDRADE, A.R.F.; ISSLER, R.S. and GUIMARÃES, G., 1974. Geologia das folhas SB-22 Araguaia e parte SC-22 Tocantins, *Projeto RADAMBRASIL, geologia, geomorfologia, solos e uso potencial da terra,* Levantamento de Recursos Naturais (4), Rio de Janeiro, 143pp.

SILVA J.L. da, 1988. Mina de Manganês do Azul. *XXV Congresso Brasileiro de Geologia*, anexo, 73-94.

SIQUEIRA, J.B., 1990. *Organização lito-estrutural do duplex Salobo-Mirim, Serra dos Carajás*. Unpublished MSc. dissertation, Universidade Federal do Pará, Curso de Pós-Graduação em Geociências, Belém, 125pp.

SIQUEIRA, J.B. and COSTA, J.B.S., 1991. O Duplex Salobo-Mirim, Serra dos Carajás. *Boletim 3° Simpósio Nacional de Estudos Tectônicos*, Rio Claro, 47-48

SMITH, J.V. and DURNEY, D.W., 1992. Experimental formation of brittle and element mobility in the development of ultramylonites. *Geology*, **14**, 883-886.

SMITH, J.V. and YAMAUCHI, S., 1994. Kinematic interpretation of remnant en-echelon rift segments of the southwestern Japan Sea. *Tectonophysycs*, **230**, 143-150.

SMITH, V.S., 1993. Kinematics of secondary synthetic ("P") faults in wrench systems. *Tectonophysycs*, **223**, 439-443.

SOARES, A.V.; SANTOS, A.B.; VIEIRA, E.A.; BELLA, V.M. and MARTINS, L.P.B., 1994. Área Águas Claras contexto geológico e mineralizações. *IV Simpósio de Geologia da Amazônia*, Boletim de Resumos Expandidos, Belém, 379-382.

SOARES, P.C. and FIORI, A.P., 1976. Lógica e siatemática na análise e interpretação de fotografias aéreas em Geologia. *Notas Geomorfológicas* **16** (32), Campinas, 71-104.

SOPER, N.J., 1986. Geometry of transecting, anastomosing solution cleavage in transpression zones. *Journal of Structural Geology*, **8**, 937-940.

SOPER, N.J. and HUTTON, D.H.W., 1984. Late Caledonian sinistral displacement in Britain: implications for a three-plate collision model. *Tectonics*, **3**, 781-794.

SOUZA, Z.S. de; MEDEIROS, H.; ALTHOFF, F.J. and DALL'AGNOL, R., 1990. Geologia do Terreno "Granito-Greenstone" da região de Rio Maria, sudeste do Pará. *36º Congresso Brasileiro de Geologia*, Anais, Natal, **6**, 2913-2928.

SPÖRLI, K.B.,1980. New Zealand and oblique-slip margins: tectonic development up to and during the Cainozoic. In: *Sedimentation in oblique-slip mobile zones* (ed. Ballance, P.F. and Reading, H.G.), Special Publication, **4**, 147-170.

STRACHAN, R.A.; HOLDSWORTH, R.E.; FRIDERECHSEN, J.D. and JEPSEN, H.F., 1992. Regional Caledonian structure within an oblique convergent zone, Dronning Loise Land, NE Greenland. *Journal of the Geological Society, London*, **149**, 359-371.

SUDAM, 1972. Pesquisa Mineral do Tapajós/Jamanxin, relatório preliminar, Superintendência do Desenvolvimento da Amazônia, unpublished report, Belém, 172pp.

SUITA, M.T.F. and NILSON, A.A., 1988. Geologia do Complexo Máfico-Ultramáfico Luanga (Província de Carajás, Pará) e das unidades encaixantes. *Anais XXXV Congresso Brasileiro de Geologia*, Belém, **6**, 2813-2823.

SUSZCZYNSKI, E., 1972. A origem vulcânica do minério de ferro primário Serra dos Carajás - Estado do Pará - Região Amazônica. *Anais XXVI Congresso Brasileiro de Geologia* Belém, **1**, 103-120.

SWANSON, M.T., 1988. Pseudotachylyte-bearing strike-slip duplex structures in the Fort Foster Brittle Zone, S. Maine. *Journal of Structural Geology*, **10**(8), 813-828.

SWANSON, M.T., 1989. Sidewall ripouts in strike-slip faults. *Journal of Structural Geology*, **11**, 933-948.

SYLVESTER, A. G., 1984. Wrench fault tectonics. Introduction. In *Wrench Fault Tectonics*. The American Association of Petroleum Geologists Bulletin, Reprint Series, **28**, 374pp.

SYLVESTER, A.G., 1988. Strike-slip faults. *Geological Society of American Bulletin*, **100**, 1666-1703.

SYLVESTER, A. G. and SMITH, R. R., 1976. Tectonic transpression and basement-controlled deformation in San Andreas Fault Zone, Salton Trough, California. *The American Association of Petroleum Geologist Bulletin*, **30**, 2981-2102.

TASSINARI, C.C.G.; HIRATA, W.K. and KAWASHITA, K., 1982. Geologic evolution of the Serra dos Carajás, Pará, Brazil. *Revista Brasileira de Geociências*, **12**(1-3), 263-267.

TASSINARI, C.C.G.; TEIXEIRA, W.; SIGA Jr.,O.; KAWASHITA, K. and CORDANI, U.G., 1987. Geological Evolution and evaluation of recent geochronological data in Amazonian Craton. *Final Meeting of the Working Group-Project 204, IUGS-UNESCO*, Extended Abstracts, 20-31.

TCHALENKO, J. S., 1970. Similarities between shear zones of different magnitudes. *Geological Society of America Bulletin*, **81**, 1625-1640.

TCHALENKO, J.S. and AMBRASEYS, N.N., 1970. Structural analysis of the Dasht-e Baýaz (Iran) earthquake fractures. *Geological Society of America Bulletin*, **81**, 41-60.

TEIXEIRA, J.B.G. and EGGLER, D.H., 1994. Petrology, geochemistry, and tectonic setting of the Archean basaltic and dioritic rocks from the N-4 Iron deposit, Serra dos Carajás, Pará, Brazil. *Acta Geológica Leopoldensia*, **40**(XVII), 71-114.

TEIXEIRA, W., 1978. Significação tectônica do magmatismo anorogênico pré-cambriano básico e alcalino na região amazônica. *Anais XXX Congresso Brasileiro de Geologia*, Recife, **1**, 491-505.

TEIXEIRA, W., 1990. The Proterozoic mafic dyke swarms and alkaline intrusions in the Amazonian Craton, South America, and their tectonic evolution based on Rb-Sr, K-Ar and 40Ar-39Ar geochronology. In *Mafic Dykes and Emplacement Mechanisms*, (ed. Parker, Rickwood and Tucker), Balkema, Rotterdam, 285-293

TEIXEIRA, W.; TASSINARI, C.C.G.; CORDANI, U.G. and KAWASHITA, K., 1986. A geochronological review of the Amazon Craton. *99th Geological Society of America Annual Meeting*, Abstract, San Antonio, TX, **18**, 770.

TEIXEIRA, W.; TASSINARI, C.C.G.; CORDANI, U.G. and KAWASHITA, K., 1989. A review of the geochronology of the Amazonian Craton: tectonic implications. *Precambrian Research*, **42**, 213-227.

TEYSSIER, C.; TIKOFF, B. and MARKLEY, M., 1995. Oblique plate motion and continental tectonics. *Geology*, **23**(5), 447-450.

THOMAS, G.E., 1974. Lineament-block tectonics: Williston-Blood Creek Basin. *The American Association of Petroleum Geologist Bulletin*, **58**, 7, 1305-1322.

TIKOFF, B. and TEYSSIER, C., 1994. Strain modelling of displacement-field partitioning in transpressional orogens. *Journal of Structural Geology*, **16**(11), 1575-1588.

TOLBERT, G.E.; SANTOS, B.A. dos ; ALMEIDA, E.B. de and RITTER, J.E., 1968. Recente descoberta de ocorrências de minério de ferro no Estado do Pará. *Mineração e Metalurgia*, **XLVIII** (288), 253-256.

TOLBERT, G.E.; TREMAINE, J.W.; MELCHER, G.C. and GOMES, C.B., 1971. The recently discovered Serra dos Carajás Iron Deposits, Northern Brazil. *Economic Geology and the Bulletin of the Society of Economic Geology*, **66**(7), 985-994.

TREAGUS J.E. and TREAGUS, S.H.,1981. Folds and the strain ellipsoid: a general model. *Journal of Structural Geology*, **3**(1), 1-17.

TREAGUS, S.H. and TREAGUS, J.E., 1992. Transected folds and transpression: how are they associated?. *Journal of Structural Geology*, **14**(3), 361-367.

TRUCKENBRODT, W.; ANAISSE Jr., J. and NOGUEIRA, A.C.R., 1996. Contribuição à petrografia dos arenitos da Formação Águas Claras, Pré-Cambriano, Serra dos Carajás. *V Simpósio de Geologia da Amazônia*, SBG-NO, Boletim de Resumos Expadidos, Belém, 217-219.

TWISS, R.J. and MOORE, E.M., 1992. *Structural Geology*. Freeman & Company, New York, 532pp.

VALARELLI, J.V.; BERNARDELI, A. and BEISIEGEL, W.R., 1978. Aspectos genéticos do Minério de manganês do Azul. *Anais XXX Congresso Brasileiro de Geologia*, Recife, **4**, 1670-79.

VENEZIANI, P. and DOS ANJOS, C.E., 1982. *Metodologia de interpretação de dados de sensoriamento remoto e aplicação em geologia*. INPE-2227-MD/014, São José dos Campos, 14pp.

VENEZIANI, P.; SANTOS, A.R.; PARADELLA, W.R.; CHIANG, L.C. and BIGNELLI, P.A., 1995. Reconhecimento de zonas de cisalhamento transcorrentes (ZCTs) na região de Serra dos Carajás (PA), em produtos de sensoriamento remoto. *V Simpósio Nacional de Estudos Tectônicos,* Boletim de Resumos Expandidos, 106-108.

VIEIRA, E.A.P.; SAUERESSIG, R; SIQUEIRA, J.B.; SILVA, E.R.P.; REGO, J.L. do, and CASTRO, F.D.C. de, 1988. Caracterização geológica da jazida polimetálica do Salobo 3A, reavaliação. *Anais, 35º Congresso Brasileiro de Geologia,* Belém, 97-111.

VIDAL, L.., 1986. A questão indígena. In: *Carajás, desafio político, ecologia e desenvolvimento,* (ed. Almeida Jr., J.M.G. de), CNPq-Editora Brasiliense, São Paulo, 222-264

VILLAS BOAS, J.M.; QUARESMA, J.B. and JORGE JOÃO, X.S., 1980. *Projeto Prospecção de Carvão Energético nas Áreas de Ocoreência da Formação Rio Fresco.* DNPM/CPRM, Belém, unpublished report, 36pp.

WATTERSON, J., 1975. Proterozoic intraplate deformation in the light of South-east Asian neotectonics. *Nature,* **273**, 636-40.

WEBER, K., 1981. Kinematic and metamorphic aspects of cleavage formation in very low grade metamorphic slates. *Tectonophysics,* **78**, 291-306.

WERNICK, E., 1981. The Archean of Brazil. *Earth-Science Reviews,* **17**, 31-48.

WHITE, S.H.; BRETAN, P.G. and RUTTER, E.H., 1986. Fault zone reactivation. Kinematic and mechanism. *Philosophical Transactions of the Royal Society,* **A**(317), 81-97.

WILCOX, R.E.; HARDING, T.P. and SEELY, D. R., 1973. Basic wrench tectonics. *The American Association of Petroleum Geologist Bulletin,* **57**(1), 74-96.

WILLIS, G.F. and TOSDAL, R.M., 1992. Formation of gold veins and breccias during dextral strike-slip faulting in the Mesquite Mining District, Southeastern California. *Economic Geology,* **78**, 2002-2022.

WILSON, T. J., 1965. A new class of faults and their bearing on continental drift. *Nature,* **4995**, 343-347.

WIRTH, K.R., 1986. *The geology and geochemistry of the Grão Pará Group, Serra dos Carajás, Pará, Brazil.* Unpublished MSc. dissertation, Cornell, Ithaca, New York, 284pp.

WIRTH, K.R.; GIBBS, A.K. and OLSZEWSKI Jr., 1986. U-Pb ages of zircons from the Grão-Pará Group and Serra dos Carajás Granite, Pará, Brazil. *Revista Brasileira de Geociências,* **16**(2), 195-200.

WISE, D. V.; DUNN, D.E.; ENGELDER, J.T.; GEISER, P.A.; HATCHER, R.D.; KISH, S.A.; ODOM, S.A. and SCHAMEL, S., 1984. Fault related rocks: suggestion for terminology. *Geology,* **12**, 391-394.

WOODCOCK, N.H., 1986. The role of strike-slip fault systems at plate boundaries. *Philosophical Transaction of the Royal Society, London,* **A**(317), 13-29.

WOODCOCK, N.H., 1987. Kinematics of strike-slip faulting, Builth Inlier, Mid-Wales. *Journal of Structural Geology,* **9**, 353-363.

WOODCOCK, N.H. and FISCHER, M., 1986. Strike-slip duplexes. *Journal of Structural Geology,* **8**(7), 725-735.

WOODCOCK, N.H. and SCHUBERT, C., 1994. Continental Strike-Slip Tectonics. In *Continental Deformation,* (ed. Hancock, P.), Pergamon Press, London, 251-263

YARDLEY, B.W.D.; MacKENZIE, W.S. and GUILFORD, C., 1990. *Atlas of Metamorphic rocks and their textures.* Longman Scientific & Technical, England, 120pp.

ZANG, W. and FYFE, W.S., 1993. A three-stage genetic model for the Igarapé Bahia lateritic gold deposit, Carajás, Brazil. *Economic Geology,* **88**, 1768-1779.

ZOLNAI, G., 1991. *Continental Wrench-Tectonics and Hydrocarbon-Habitat.* The American Association of Petroleum Geologist, Continuing Education Course Note Series, **30** (2nd edition), 152pp.